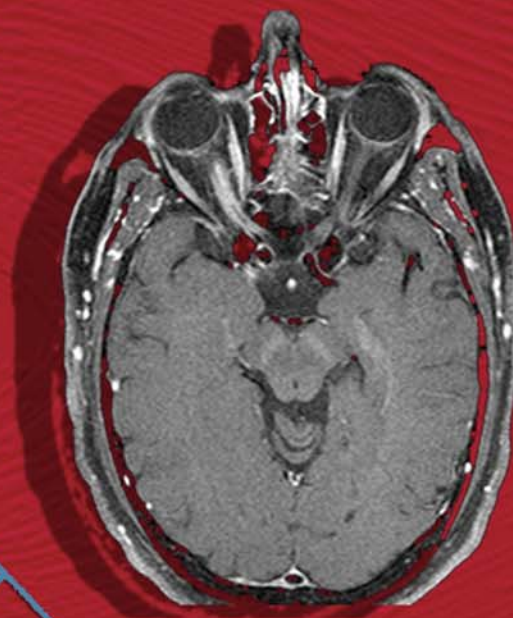
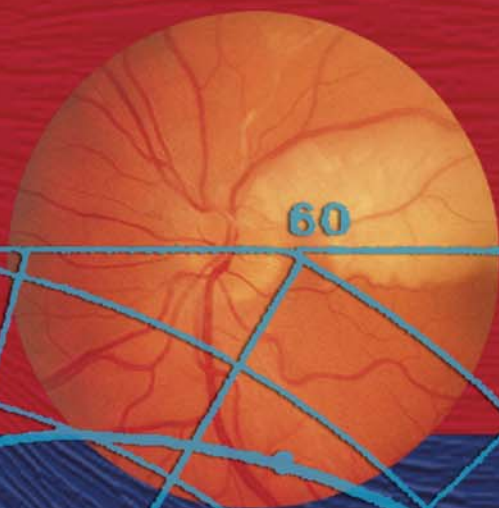


FIELD OF VISION

A MANUAL AND ATLAS OF
PERIMETRY



Jason J. S. Barton, MD, PhD, FRCP(C)

Michael Benatar, MBChB, DPhil

 HUMANA PRESS

FIELD OF VISION

CURRENT CLINICAL NEUROLOGY

Daniel Tarsy, MD, *Series Editor*

Field of Vision: A Manual and Atlas of Perimetry, by Jason J. S. Barton, MD, PhD and Michael Benatar, MBChB, DPhil, 2003

Surgical Treatment of Parkinson's Disease and Other Movement Disorders, edited by Daniel Tarsy, MD, Jerrold L. Vitek, MD, PhD, and Andres M. Lozano, MD, PhD, 2003

Myasthenia Gravis and Related Disorders, edited by Henry J. Kaminsky, 2003

Seizures: Medical Causes and Management, edited by Norman Delanty, MB, FRCPI, 2001

Clinical Evaluation and Management of Spasticity, edited by David A. Gelber, MD, and Douglas R. Jeffery, MD, PhD, 2001

Early Diagnosis of Alzheimer's Disease, edited by Leonard F. M. Scinto, PhD and Kirk R. Daffner, MD, 2000

Sexual and Reproductive Neurorehabilitation, edited by Mindy Aisen, MD, 1997

FIELD OF VISION

A Manual and Atlas of Perimetry

By

JASON J. S. BARTON, MD, PhD, FRCP(C)

*Departments of Neurology and Ophthalmology
Beth Israel-Deaconess Medical Center,
Harvard Medical School and Department of Bioengineering,
Boston University, Boston, MA*

and

MICHAEL BENATAR, MBChB, DPhil

*Department of Neurology
Beth Israel-Deaconess Medical Center,
Harvard Medical School, Boston, MA*

Foreword by

MARTIN A. SAMUELS, MD

*Neurologist-in-Chief
Brigham and Women's Hospital,
Boston, MA*



HUMANA PRESS
TOTOWA, NEW JERSEY

© 2003 Humana Press Inc.
999 Riverview Drive, Suite 208
Totowa, New Jersey 07512

www.humanapress.com

For additional copies, pricing for bulk purchases, and/or information about other Humana titles, contact Humana at the above address or at any of the following numbers: Tel.: 973-256-1699; Fax: 973-256-8341; E-mail: humana@humanapr.com; Website: <http://humanapress.com>

All rights reserved.

No part of this book may be reproduced, stored in a retrieval system, or transmitted in any form or by any means, electronic, mechanical, photocopying, microfilming, recording, or otherwise without written permission from the Publisher.

Due diligence has been taken by the publishers, editors, and authors of this book to assure the accuracy of the information published and to describe generally accepted practices. The contributors herein have carefully checked to ensure that the drug selections and dosages set forth in this text are accurate and in accord with the standards accepted at the time of publication. Notwithstanding, as new research, changes in government regulations, and knowledge from clinical experience relating to drug therapy and drug reactions constantly occurs, the reader is advised to check the product information provided by the manufacturer of each drug for any change in dosages or for additional warnings and contraindications. This is of utmost importance when the recommended drug herein is a new or infrequently used drug. It is the responsibility of the treating physician to determine dosages and treatment strategies for individual patients. Further it is the responsibility of the health care provider to ascertain the Food and Drug Administration status of each drug or device used in their clinical practice. The publisher, editors, and authors are not responsible for errors or omissions or for any consequences from the application of the information presented in this book and make no warranty, express or implied, with respect to the contents in this publication.

Cover design and illustration by Jason J. S. Barton, MD, PhD, FRCP(C)

This publication is printed on acid-free paper. 
ANSI Z39.48-1984 (American National Standards Institute) Permanence of Paper for Printed Library Materials.

Photocopy Authorization Policy:

Authorization to photocopy items for internal or personal use, or the internal or personal use of specific clients, is granted by Humana Press Inc., provided that the base fee of US \$20.00 per copy is paid directly to the Copyright Clearance Center at 222 Rosewood Drive, Danvers, MA 01923. For those organizations that have been granted a photocopy license from the CCC, a separate system of payment has been arranged and is acceptable to Humana Press Inc. The fee code for users of the Transactional Reporting Service is: [1-58829-175-8/03 \$20.00].

Printed in the United States of America. 10 9 8 7 6 5 4 3 2 1

Library of Congress Cataloging-in-Publication Data

Barton, Jason, J. S.

Field of vision: a manual and atlas of perimetry / by Jason J. S. Barton and Michael Benatar
p.;cm.-(Current clinical neurology)

Includes bibliographical references and index.

ISBN 1-58829-175-8 (alk. paper) eISBN 1-59259-355-0

1. Perimetry. 2. Visual fields. I. Benatar, Michael. II. Title. III. Series.

[DNLN: 1. Perimetry--methods--Atlases. 2. Visual Fields--Atlases. WW 17 B293v 2002]

RE79.P4 B37 2002

617.7'15--dc21

2002068919

SERIES EDITOR'S INTRODUCTION

Among the medical specialties, clinical neurology remains one of the last bastions of the careful history and physical examination. A subspecialty of both neurology and ophthalmology, neuro-ophthalmology is the epitome of a clinical discipline in which skillful examination and the interpretation of physical findings are essential steps towards diagnosis. In particular, the detection of patterns of visual field defects is key to identifying and localizing lesions in the visual pathways between the retina and occipital cortex.

Evaluation of the visual field poses the twin challenges of how to measure that field and how to interpret the results. This book provides the reader with the necessary tools to meet these challenges. The neurologist will hone his technique of confrontation testing and acquire an understanding of how manual and automated perimetry are performed, as well as how this perimetric data should be interpreted. The ophthalmologist, better acquainted with computerized perimetry, will be reintroduced to the value of the simple bedside examination and the still important role of manual perimetry, and acquire the knowledge of neuroanatomy and neuropathology critical to understanding the patterns of visual field defects.

Most neurologists and ophthalmologists have seen and can recognize the cartoons of visual defects that tend to be reproduced in standard textbooks. However, in the real world, visual field abnormalities are not stereotyped cartoons, but vary from patient to patient in extent, severity, and shape. Repeated experience with abnormal fields is necessary to develop a feel for the key features of different defects on a perimetric plot. To this end, the heart of *Field of Vision: A Manual and Atlas of Perimetry* is a perimetric atlas that provides many representative cases drawn from a large clinical experience. They are arranged in order from retina to visual cortex and are shown as they appear in the real world of perimetry. Each case is further enhanced by detailed clinical descriptions, images of lesions, and discussion of relevant clinical issues, bringing the field back to its proper setting—the care of the patient. The superb integration here of clinical and technical material will make this work a valuable teaching reference for all those involved in the management of visual disorders.

Daniel Tarsy, MD

FOREWORD

When television arrived in the early 1950s many predicted the end of the motion pictures, but in time it became clear that the richness and complexity of the theater experience could not be reproduced by TV. Paradoxically exposure to TV from an early age even heightened the allure of the much more challenging, enthralling and engaging theater experience. When the CT scan arrived in the mid 1970s, the same group predicted the end of clinical neurology, but as the last 30 years have clearly demonstrated, the development of brain imaging has only enhanced the challenge of clinical neurology. Now my own practice consists largely of using the history and neurological examination (the basic blocking and tackling of clinical neurology) to put into perspective and often explain away irrelevant findings on CT, MRI, SPECT, and PET studies.

Clinical neurology is very challenging. The best practitioners learn to use every bit of evidence, no matter how small, to give them clues to the complex manifestations of nervous system disease. All of the components of the history and examination are important, but the single most useful, particularly for central nervous system problems, is the examination of the eyes. The eye movements, pupils, fundusoscopic examination, lid function, and vision very often provide the most salient clues to the underlying problem. Of these the examination of the visual pathways is the portion that is most foreign to the ophthalmologist and neurologist alike. In a sense this important area falls in a gap between the two fields. The art and science of examining the visual fields and interpreting the results of automated perimetry is mastered only by a tiny number of neuro-ophthalmologists with a special interest in this area. This is a shame in that every doctor who sees a neurological patient (emergency physician, internist, family physician, neurosurgeon, neurologist, or ophthalmologist) could benefit greatly from a working knowledge of visual field testing.

Field of Vision: A Manual and Atlas of Perimetry is written by Jason J.S. Barton, a neurologist/neuro-ophthalmologist and Michael Benatar, a clinical neurologist, in response to a correctly perceived need. The book begins with a chapter on the importance and principles of perimetry and the normal visual field. This is followed by chapters on the functional anatomy of the visual system and the techniques for performing perimetry in the office and at the bedside. The final two didactic chapters detail the use of the two most important instruments: the Goldmann perimeter and the Humphrey automated field analyzer. After the five didactic chapters, there is an impressive 120 case atlas complete with relevant histories, neuroimaging, and detailed explanations of the pathophysiology of the visual field disturbances. All of the major disorders that cause visual field disturbances are covered by this beautiful atlas.

Overall, *Field of Vision: A Manual and Atlas of Perimetry* will be a welcome addition to the basic texts for all those who practice clinical neurology, as well as those training in the area. Neurologists, ophthalmologists and neurosurgeons are the most relevant, but all others who are called upon to evaluate people with neurological problems would find this book useful. I enjoyed reading it from beginning to end and will undoubtedly refer back to it frequently in the future.

Martin A. Samuels, MD
Neurologist-in-Chief
Brigham and Women's Hospital
Boston, MA

PREFACE

Evaluating the visual field poses two challenges. The first is how to measure the visual field and the second is how to interpret the results. *Field of Vision: A Manual and Atlas of Perimetry* provides the reader with the tools to meet both challenges. Through the joint venture of a neuro-ophthalmologist (JB) and a general neurologist (MB), the result is a text in which the expertise of the specialist is made accessible to the generalist.

Visual field testing at the bedside or in the clinic is a neglected art, often performed cursorily, leaving the clinician uncertain about the true extent of defects or, worse yet, whether defects are present at all. These days formal perimetry supplements bedside testing, but all of these procedures still need guidance from the examiner, and the best results require knowledge of both neuroanatomy and the pathologic patterns of disease. Many neurologists have such knowledge, but do not know how to operate perimeters. On the other hand, many ophthalmologists and optometrists have experience with perimeters, but do not have the neurologic information needed for truly expert perimetry. The goal of the first half of this book—the “manual”—is to give both groups the background they need to test visual fields, and to do it well.

We begin with two general chapters on perimetric concepts and visual anatomy. These are followed by specific chapters on the procedures and interpretive strategies used in bedside, manual, and automated perimetry. The focus is upon clinically relevant points, with enough detail for the examiner to understand what is actually happening to the patient during perimetry. More technical material is deferred to an appendix for readers interested in the principles behind visual testing. At the end of this first section the clinician should be able to sit down at a perimeter and test a patient.

The second challenge, the interpretation of perimetric data, requires experience. We are all familiar with cartoons of the visual field where black areas represent visual loss and white areas preserved vision. Perimetric data seldom looks like that. Borders of defects can be complex and irregular and there are often zones of partial loss. The resulting patterns on perimetric plots can bewilder the novice. In the second half of the book—the “atlas”—we present examples of real perimetric data aimed at developing the reader’s skills in recognizing these patterns.

The first part of the atlas contains 100 cases arranged in an anatomic progression from retina to striate cortex. The cases are presented in a form that will allow the reader to practice interpretation in a clinical context, by placing a brief clinical vignette with a visual field on one page, and the description of the field and the causal lesion on the reverse side. We provide the results of bedside testing so that the reader may acquire a feel for the correlation between bedside and formal perimetry. The accompanying discussion addresses the nuances of the field, considers some of the relevant clinical issues, and provides images of the lesions responsible wherever possible. We believe that these latter additions are particularly useful to ophthalmologists and optometrists, who may not be familiar with neuro-imaging or the clinical implications of the underlying diseases.

Last is a section of 20 visual fields arranged in random order. This is meant to provide a reader who has toiled through the preceding 100 cases a chance to practice their new expertise before heading for the clinic. If our readers find that they can detect the relevant abnormalities in these 20 fields, describe them, localize the lesions, and make a reasonable guess at pathology given the history, this book will have succeeded.

Jason J. S. Barton, MD, PhD, FRCP(C)
Michael Benatar, MBChB, DPhil

ACKNOWLEDGMENTS

Many of the visual fields in this book were performed by JB, but many others were done by perimetrists at Toronto Western Hospital, the University of Iowa Hospitals and Clinics, and Beth Israel Deaconess Medical Center, whose help and skill we acknowledge. Felix Tyndel assisted us with collecting data from the Toronto Western Hospital, and Chun Lim with photography of the perimeters. Mark Kuperwaser generously contributed some of the fields of the glaucoma patients. We also thank Rick Calderone for his ultrasound work. Finally we thank our patients, whose cooperation, endurance, and effort made this collection possible, and the many colleagues who referred them to us.

DEDICATIONS

JB: to the family that raised me (Maurice, Violet, Sharon, and Rachel) and the family I am raising (Hannah, Alistair, and Caroline).

MB: to my grandmothers, and in memory of my grandfathers

CONTENTS

<i>Series Editor's Introduction</i>	v
<i>Foreword</i>	vii
<i>Preface</i>	ix
1 <i>An Introduction to Perimetry and the Normal Visual Field</i>	1
2 <i>Functional Visual Anatomy</i>	7
3 <i>Perimetry at the Bedside and Clinic</i>	21
4 <i>Goldmann Perimetry</i>	31
5 <i>Automated Perimetry (Humphrey Field Analyzer)</i>	45
6 <i>Atlas</i>	71
<i>Color Plates of Selected Cases Follows</i>	180
<i>Appendix</i>	319
<i>Index</i>	325

1 An Introduction to Perimetry and the Normal Visual Field

The analysis of the visual field is an important part of the neurologic and ophthalmologic examination. The eye exists to see, and more than 40% of the human brain is involved in visual processing in some fashion. Not surprisingly, many diseases of these two structures affect vision. Assessing the visual field is often helpful in localizing, diagnosing, and following the course and efficacy of treatment of these diseases.

The diagnostic value of the visual field is highest in neuroophthalmologic problems. Most other ophthalmic diseases that affect vision have visible signs on slit-lamp examination or funduscopy, and, hence, diagnosis relies on the vision of the ophthalmologist rather than the visual field of the patient. By contrast, with the exception of the optic disc and the retinal nerve fiber layer, neurologic structures are unseen, and their integrity must be deduced from the report and behavior of the patient. The pattern of visual field disturbance in these patients has high localizing value, information that can raise or lower the suspicion of ominous disease and guide the investigative process. On the other hand, the greatest impact of visual fields on the management of disease is in glaucoma, in which the progress and extent of visual loss is the key determinant in medical and surgical therapeutic decisions. Much of the drive behind the development and standardization of automated perimetry has been from the field of glaucoma, and much of current perimetric research continues to be devoted to this disease.

All of the visual fields displayed in this volume were obtained with a perimetric device. One of the main aims of this work is to help the reader learn to interpret the outputs of these devices. However, it is possible in many patients to obtain a reasonable assessment of the visual field “by hand” in the clinic or at the bedside. To this end, Chapter 3 discusses the methods and value of simple confrontation testing, and it is hoped that the reader will also try to envision how the defects portrayed would be reflected in bedside testing.

1. WHY DO PERIMETRY?

Formal perimetry requires more effort, time, cost, and equipment than confrontation testing. To justify any procedure, clinicians must know what they hope to gain from subjecting a patient to it.

Formal perimetry is *more sensitive* to subtle defects. This is especially true with damage to the anterior optic pathway. These defects are often relative depressions, rather than absolute losses, and may not have sharp borders along much of their extent. When these occur in the periphery, rather than the center of the visual field, as with arcuate defects and nasal steps, they can be asymptomatic and difficult to find at the bedside. The data reviewed in Chapter 3 show how insensitive confrontation testing is compared to formal perimetry, even when colored targets are used. Detection of mild optic neuropathy in the early stages of processes such as glaucoma or the papilledema of idiopathic intracranial hypertension (IIH) cannot rely on confrontation testing but requires formal perimetry.

Perimetry provides a *more standardized* assessment of the visual field. The examiner in confrontation testing has limited control over the background behind the target or lighting conditions, and the targets themselves—fingers, colored objects, and so forth—will differ between examiners. Perimetry controls all these factors.

The most important benefit of standardization is *reproducibility*. That is, repeated assessments in the same patient can be compared over time, to determine whether there has been any change in a finding. In addition, standardization across instruments means that fields obtained in one location are theoretically comparable with fields obtained in a different office, town, or country. This cross-institution reproducibility has its limits, though, particularly for techniques whose testing procedures depend heavily on the judgment of the operator, as is the case for Goldmann perimetry.

Standardization also makes it possible to *compare one subject with another*. However, there are many reasons why subjects differ from each other in the way that they perform a test, not all of them directly related to vision. The importance of comparisons of patients with other subjects is limited to a few specialized circumstances, such as the detection of generalized constriction from retinal disease. Most of the time, ocular or neurologic diseases cause relative defects in one part of the field compared with another, and these qualitative distortions from the normal pattern of vision are more important than quantitative deviations from some mean normal sensitivity.

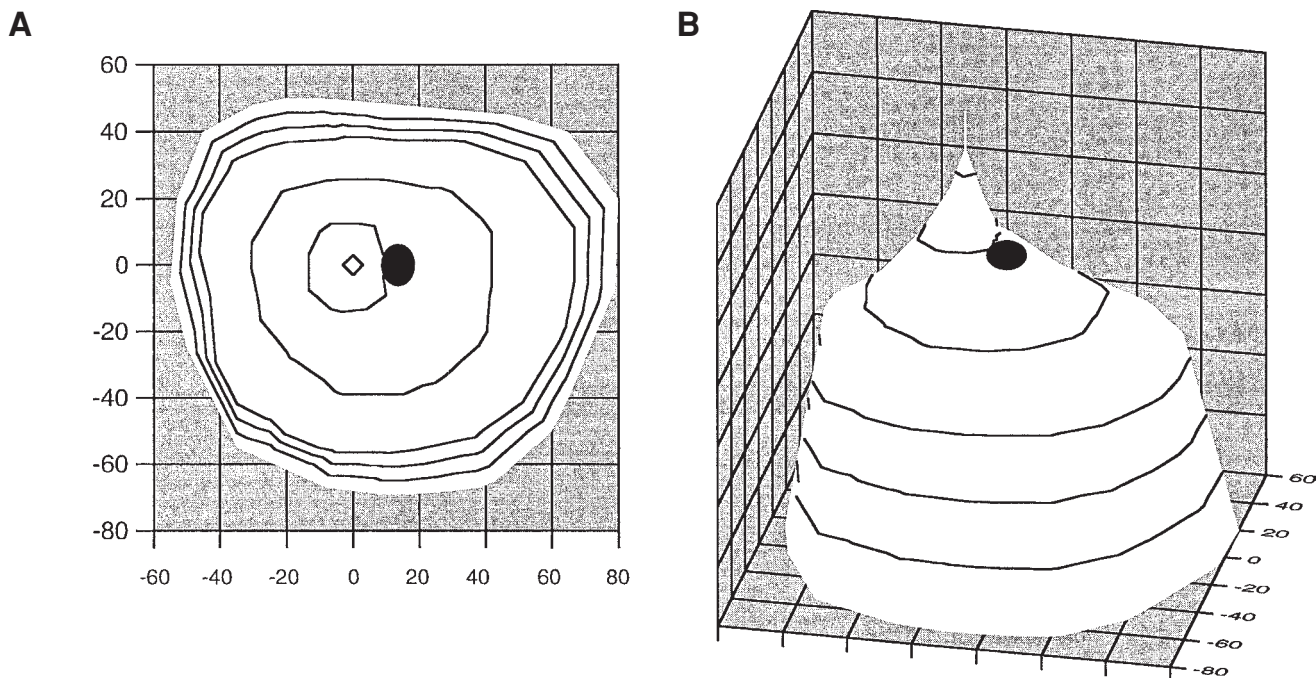


Fig. 1. Island of Traquair: data generated from normal eye of patient in Case 24. (A) x - y plot of a set of isopters extrapolated from four measured isopters of this case; (B) rotation of this plot in three dimensions, so that the z -axis plots the sensitivity of each isopter. It is easy to see the utility of the analogy of an island/hill of vision arising out of a sea of darkness. Note that the slope is steeper at the edges and at the central peak.

Most perimetric techniques generate a *permanent record* of the visual field. Although rough impressions of the results of confrontation field testing can be sketched, following changes in field loss is difficult without a formal perimetric record.

2. THE NORMAL VISUAL FIELD

The normal visual field has an absolute extent and a pattern of varying sensitivity with which the perimetrist must become completely familiar. A most useful pictorial concept that has stood the test of time is Traquair's "island of vision in a sea of darkness." Like an island arising out of the ocean, there is a shore that marks the absolute limit of vision. Just as an island rises from the shore to some inland prominence or hill, visual sensitivity increases as one proceeds from the peripheral boundary of vision to a peak at the fovea (Fig. 1). In this sense the island of vision is also a "hill of vision." The rate of rise is not linear but a bit steeper at the outer boundary and within the central 30° , with a particularly sharp incline within the central 10° . The only focal disturbance in this topography is the physiologic blind spot, a deep well marking the location of the optic disc, which has no overlying photoreceptors. This spot, centered at 15° eccentric on the temporal meridian, has a horizontal width of 6 – 10° and extends radially 15 – 20° on either side of the vertical meridian. The boundaries of vision differ by direction. The superior and nasal fields are least extensive, ending at about 60° eccentricity, and the inferior and temporal fields the most. (In fact, the extreme limit of temporal vision is actually slightly beyond the 90° limit of the Goldmann perimeter.) The result is an oval, somewhat egg-shaped island.

The analogy with geographic topography is apt because of the way visual sensitivity is depicted on Goldmann kinetic perimetry. A target is used to define spots with the same threshold for

differential light sensitivity (see Appendix), and these spots are joined by an interpolated line drawn by the perimetrist to estimate a zone of shared or equal sensitivity, the "isopter." The process is repeated for fainter or smaller targets, and the result is a series of rings that resemble the elevation lines on a topographic map (Fig. 1). If one understands such maps, one understands Goldmann perimetry. For automated perimetry, the analogy still holds with respect to the sensitivity plot, but the results are shown a bit differently. Rather than interpolated isopters, the program shades areas of predicted equal sensitivity the same gray, with lighter grays for more sensitive regions.

The absolute size of any given isopter or, put another way, the absolute light sensitivity at any given point in the retina, varies considerably among subjects, even those in the peak years of young adulthood. Besides age, there are several factors that influence perimetry, including pupil size (1); refractive error; and, particularly for automated perimetry, learning and fatigue (2,3).

2.1. EFFECTS OF NORMAL AGING

All studies have shown that sensitivity declines with age throughout the visual field. Reports using Goldmann perimetry show an age-related shrinkage of isopters in all quadrants (4–6), in both the central and peripheral fields (5). On automated perimetry, age raises thresholds for static targets (7) in all regions of the field, but perhaps slightly more so outside of the central 10° (8). Automated thresholds also become more variable, especially in the periphery beyond 24° (9).

In most studies, the effect of age on sensitivity appears to be a constant steady decline in all decades beyond age 20 (5–7) (Fig. 2). However, others argue that there is a steeper loss after the sixth decade (4) (Fig. 3).

There are four main reasons for a decline in luminance sensitivity with age: changes in the ocular media, linear reduction in pupil

diameter (10), decrease in the absorbance efficiency of photopigments, and neural losses in both the retina and the retino-geniculostriate pathway. Some investigators have minimized the impact of the ocular media and pupil by using yellow targets, brighter backgrounds, and mydriatic drops in all subjects (5,8). These have still found declines of about 0.8 dB per decade (8), which have therefore been attributed to neuronal losses. High-resolution perimetry, which is thought to more accurately assess elements at or above the retinal ganglion cell level, has estimated the loss of neural channels funneling information from the retina to cortex at about 9000/yr, or about 1/hr (11)—a very sobering thought.

Tables can be drawn from samples of the normal population, but, ultimately, the main message to clinicians is that with a few exceptions, size does not matter. It is the pattern of the visual field that counts. Deviations from the normal pattern are far more reliable indicators of disease than absolute size or sensitivity.

3. THE TWO TYPES OF PERIMETRY

There are two broad classes of perimetry: manual and automated (computerized). Both have an appropriate setting and, in some circumstances, can complement each other. To make the appropriate choice, the strengths and weaknesses of each class must be appreciated.

Manual techniques require an operator to present each target, monitor the patient's fixation, and record the patient's response. These requirements have several advantages. Because the operator is monitoring fixation, responses made when the patient was not looking straight ahead can be discarded, improving the validity of the remaining results. The operator can also provide periodic feedback to the patient to encourage better fixation and improve the test. Because the operator chooses the locations to probe, each test can be groomed to the type of problem suspected from history or confrontation testing. Likewise, unexpected findings that emerge during perimetry can be probed in more detail to confirm the validity of the defect.

However, because the operator does all these functions, manual perimetry is highly dependent on the skill and judgment of that person. An inexperienced operator with little knowledge of anatomy or the types of field defects associated with different diseases will produce perimetric maps with limited and potentially misleading information. The rise of automated perimetry with its commercial appeal has made it hard to find ophthalmic technicians with the requisite skill for manual perimetry. Nevertheless, most manual perimetry has simple instrumentation and is easy to perform. With a little familiarity with perimetric maps and a basic knowledge of anatomy and disease, all residents and practitioners of neurology, optometry, and ophthalmology should be able to do their own Goldmann perimetry when needed.

Automated perimetry asks for less skill and time from the clinic staff, but it demands more time and attentional resources from the patient. This makes it difficult to obtain useful information from young children or adults with inattention or impaired cognitive skills. Although the computer does present a few options for the region of visual field on which to focus the test, it does not have the flexibility to pursue individual strategies for a specific defect or to reformulate its strategy when an unexpected defect is encountered during the test. Nevertheless, automated perimetry is more highly standardized and provides a sophisticated statistical analysis that is grounded in age-related normative data. It also provides estimates of the reliability and response bias of the patient, issues

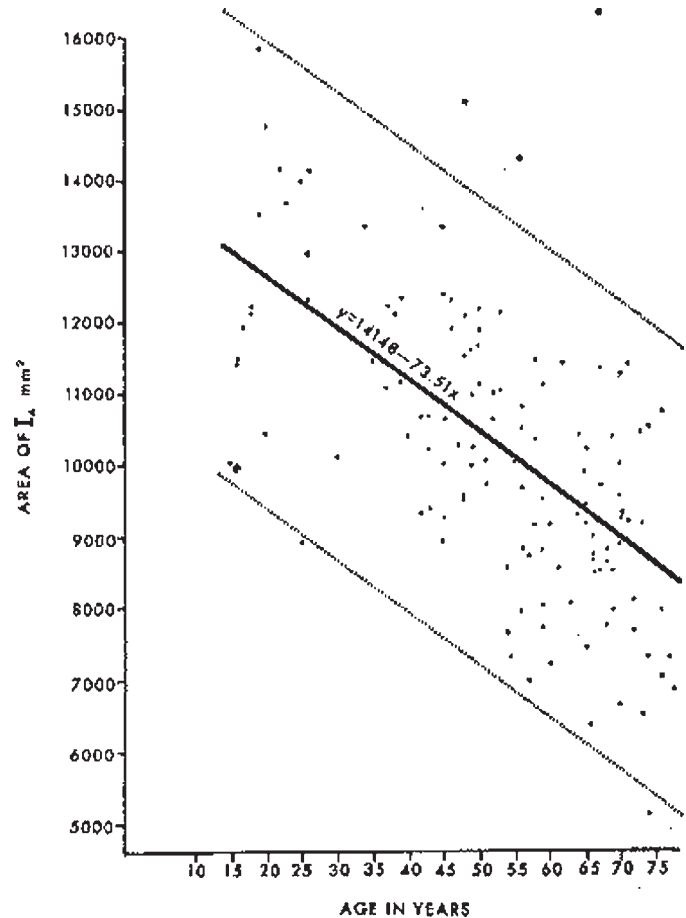


Fig. 2. Age and kinetic perimetry. Despite considerable scatter, the area encompassed by the I4 stimulus can be seen to decline linearly with age, even through young adulthood. (From ref. 5 with permission.)

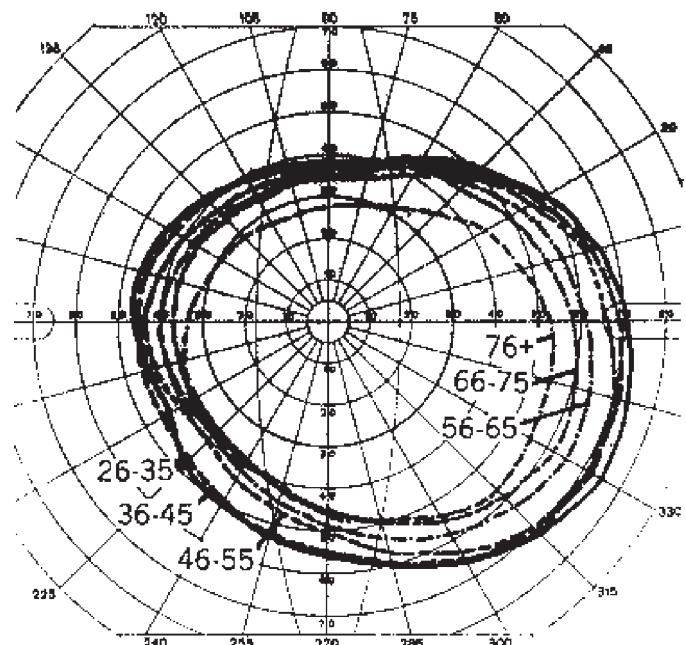


Fig. 3. Age and kinetic perimetry showing gradual shrinkage of a size II Goldmann target with age, with a suggestion of accelerated decrease after the age of 55. (From ref. 4 with permission.)

at which the Goldmann perimetrist can only guess (though the guess of an experienced examiner may be quite accurate).

3.1. WHICH PERIMETRIC METHOD TO CHOOSE

Although automated perimetry has become more popular, there are still situations in which Goldmann perimetry is preferable.

1. *Inattentive patients who do not maintain fixation well:* These do far better with manual perimetry. The test can be completed more rapidly, there is an interactive component between two people, the examiner can omit or redo points where fixation was lost, and the test can be interrupted more easily to reinforce the concept of fixation.
2. *Defects extending outside the central 30°:* Peripheral defects are not so well captured by automated perimetry, which presents the examiner with an awkward choice when large areas of visual field need to be tested. The examiner either uses a less informative but rapid suprathreshold strategy or spends exhausting amounts of time and effort performing threshold perimetry in two or more sessions, taxing the patient's powers of concentration, endurance, and patience.
3. *Residual islands of vision:* Sometimes the examiner finds a patient who claims some residual glimmer of vision in an otherwise blind hemifield. Finding this region may be difficult with automated perimetry, which only samples at intervals (usually 6°). It is much faster and thorough to search for a small island by sweeping a large V4e target back and forth through the suspected location to see if a consistent island of conscious vision can be detected. A negative result with this technique is more likely to be true than a negative report from static perimetry.
4. *Functional visual loss:* Automated perimetry is useless in this setting. It requires guidance and encouragement beyond the algorithms driving automated perimetry, and patterns that stamp a field as functional are more obvious on manual perimetry (see Case 98).

Automated perimetry is preferred for the following circumstances:

1. *Subtle relative defects in central or paracentral vision:* Goldmann perimetry is poor at characterizing even severe defects within the central 5°. In the central 10°, the ability of the automated perimeter to produce a fine-grain map of this region alone is a major advantage. Manual perimetry does detect many arcuate defects, but subtle ones are most easily found with automated perimetry, for which a major drive in design was the reliable detection of the arcuate defects produced by glaucoma. A general rule is that if a suspected central or paracentral defect cannot be detected on confrontation testing, the best hope of finding it lies with automated perimetry.
2. *Sequential monitoring:* When repeated assessments are going to guide therapeutic decisions, automated perimetry has an advantage, because it is standardized, its normal inter-test variability is better characterized, and it matters much less if a different perimetrist supervises the second exam.

4. FUTURE DIRECTIONS

Although the aim of this volume is to provide clinicians with a working knowledge for performing and interpreting current

perimetry, it would be amiss not to mention briefly a few of the perimetric methods under development. Some may eventually find a place in our battery of commonly used clinical tests, while others will remain experimental tools. The utility of any proposed advance can be judged by its ability to answer positively to one of the following three questions:

1. *Is it more practical?* Does the new test produce comparable results faster, or results that are more reliable and reproducible across subjects, between repeated tests over time (inter-test variability), or more consistent within a single test (intra-test variability)?
2. *Is it more discriminative?* Does the new technique detect subtler deficits that would escape detection with conventional perimetry? To be truly more powerful, this increased sensitivity should not come with the price of increased rates of false positives (see Signal Detection Theory section in appendix).
3. *Is it more selective?* Some new strategies have been designed with physiologic rationales that they may target certain neuronal populations (currently the focus is on different subtypes of retinal ganglion cells). The hope is that they might detect deficits earlier than conventional perimetry, whose stimuli are probably detected by most if not all cell types. There are two reasons why this might happen. One is that some diseases may affect certain neuronal subtypes earlier or more severely. For example, glaucoma is said to affect large-diameter axons preferentially (12,13). The physiologic interpretation of this anatomic finding is that glaucoma may affect magnocellular and/or koniocellular ganglion cells first. The other reason is that, even if the diseases are not selective, it may be better to use a stimulus to which some retinal ganglion cells are blind than to use stimuli that all cells detect. This revolves around an issue of redundancy. Because any area in the retina is covered by the overlapping receptive fields of multiple retinal ganglion cells from the different classes, early nonselective loss of one retinal ganglion cell in that area may not impair stimulus detection if other ganglion cell types there are still functioning. More selective stimuli may avoid this redundancy and therefore detect defects at an earlier stage (14). In general, these tests are touted not as differentiating between pathologies—though that may come—but as more sensitive markers and prognostic indicators in the early stages of specific diseases—most often glaucoma.

The following is a small sample of recent research.

4.1. SHORT-WAVELENGTH AUTOMATED PERIMETRY

Short-wavelength automated perimetry (SWAP) tests the detection of a large blue stimulus against a yellow background. The targets are retinal ganglion cells with blue-yellow color opponency, which account for 1% of the total population. These blue-yellow ganglion cells form a specific class that project to the intralaminar-koniocellular layers of the lateral geniculate nucleus (15). They have large dendritic fields and axons, nearly as large as those of the magnocellular cells, and may thus number among the large fibers preferentially lost in pathologic studies of glaucomatous damage to the optic nerve.

A number of studies have shown that SWAP detects glaucomatous defects earlier than conventional perimetry (14). How-

ever, it may be more variable between tests, and its thresholds may be adversely affected by posterior subcapsular cataracts.

The latest models of automated perimeters have the capability of performing SWAP perimetry, so this technique is already a clinical reality.

4.2. HIGH-PASS RESOLUTION PERIMETRY

The stimulus in high-pass resolution perimetry is a bright ring (25 candles [cd]/m²) sandwiched by two dark rings (15 cd/m²), a pattern that can be obtained by high-pass spatial filtering of a single luminant ring (Fig. 4). The luminance averaged over all rings is the same as the background; hence, contrast rather than brightness is being used to define the target. Instead of varying contrast, the test varies the size of the ring, to find the smallest detectable ring in a given region. The special feature of these stimuli is that the threshold for detection is close to the threshold for resolution, which is the ability to perceive the two dark lines as separate elements. Thus, the width of the bright ring is the key feature in detection (16). There are good theoretical grounds and empiric evidence that perceiving this fine spatial detail depends on the parvocellular ganglion cell population (17,18).

High-pass resolution perimetry appears to be as good as conventional automated perimetry at detecting glaucomatous defects, but not any better (19–21). A similar conclusion is probably valid for neuroophthalmologic conditions (22). The clinical appeal of this new perimetry lies in some practical advantages. It takes 50% less time, patients seem to feel more comfortable with it, and it has less intra-test variability (22,23). Age, stimulus location, and pupil diameter also do not adversely affect variability (24), but the results may be more vulnerable to poor focus from inadequate refraction or cataract (16). A commercial system is available but requires its own hardware.

4.3. MOTION PERIMETRY

Two main strategies of motion perimetry have been used. One is to determine for a single spot or line the smallest position shift that is detectable as stimulus motion (minimum displacement threshold) (25). The second is to present a swarm of moving dots. Some, belonging to a noise pool, move randomly; others, in a signal pool, move in a common direction. The threshold is the lowest ratio of signal-to-noise dots at which the subject can accurately guess the signal direction (26). Motion is thought to be processed more by magnocellular than parvocellular cells, though this selectivity does not likely mean exclusivity.

Studies of patients with glaucoma or ocular hypertension suggest that motion perimetry might be more sensitive than conventional perimetry for nerve fiber bundle defects in these conditions (25–28). However, stimulus size and duration may be critical variables in determining the sensitivity of the technique (28). There is a similar suggestion of better sensitivity to arcuate defects in IIIH (29), which may share with glaucoma a pathologic effect of increased pressure at the optic nerve head. Although there are some claims of immunity to the effects of refractive blur and cataracts, defocus does affect foveal motion thresholds in complex ways that depend on stimulus displacement and velocity (30).

4.4. FREQUENCY DOUBLING PERIMETRY

This unique type of perimetry actually tests for an illusion. When a low spatial frequency (<1 cycle/°) sinusoidal grating is rapidly flickered (>15 Hz) in counterphase (meaning that the white peaks become the dark troughs and vice versa), there is an illusion

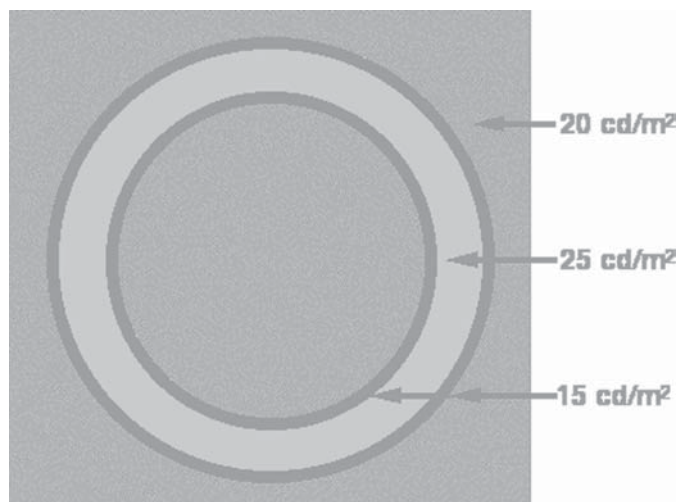


Fig. 4. High-pass resolution perimetry: display of a typical target, showing rings of brightness and darkness, which, averaged together, equal background luminance of 20 cd/m². (Reprinted with permission of the Kresge Eye Institute.)

that there are twice as many dark and light bars. In other words, the perceived spatial frequency is doubled. Because human vision is more sensitive to contrast at the spatial frequency of the illusion than at that of the actual stimulus, perception of the grating at faint contrast levels depends on the ability to generate the illusion. It is believed that this illusion is mediated by M-gamma cells, which make up 25% of magnocellular neurons and have the largest-diameter axons in this population (31,32).

This stimulus requires fairly sizable patches, about 10° in width, and therefore cannot assess the spatial distribution of visual loss in fine detail. Only a few target locations are tested, generally about 17. The advantages are that this test is not affected much by refractive error of up to 6 diopters (33), the machinery is cheap, and training needs are minimal for patients and technicians. Because only a few points are tested, a screen can be completed in 90 s (34). The target disease is again glaucoma. Most studies compare frequency doubling perimetry against the “gold standard” of Humphrey automated perimetry, which means that one cannot determine whether it is better than conventional perimetry, only whether it is as good as the current test. (If a defect shows up on the new test but not the conventional one, it would be considered a false positive, whereas in truth the defect might be real and the new test better at detecting it.) Nevertheless, recent studies suggest that frequency doubling perimetry performs as well as conventional perimetry in detecting glaucoma (32,34,35), and it has some practical advantages. Whether it is as good at following progression is not yet clear.

Small, inexpensive frequency doubling perimeters are available and are cropping up in many optometry practices as rapid screening devices.

REFERENCES

1. Lindenmuth K, Skuta G, Rabbani R, Musch D. Effects of pupillary constriction on automated perimetry in normal eyes. *Ophthalmology* 1989;96:1298–1301.
2. Autzen T, Work K. The effect of learning and age on short-term fluctuation and mean sensitivity of automated static perimetry. *Acta Ophthalmol (Copenh)* 1990;68:327–330.

3. Stewart WC, Hunt HH. Threshold variation in automated perimetry. *Surv Ophthalmol* 1993;37:353–361.
4. Wolf E, Nadraski AS. Extent of the visual field: changes with age and oxygen tension. *Arch Ophthalmol* 1971;86:637–642.
5. Drance SM, Berry V, Hughes A. Studies on the effects of age on the central and peripheral isopters of the visual field in normal subjects. *Am J Ophthalmol* 1967;63:1667–1672.
6. Drance SM, Berry V, Hughes A. The effects of age on the central isopter of the normal visual field. *Can J Ophthalmol* 1967;2:79–82.
7. Haas A, Flammer J, Schneider U. Influence of age on the visual fields of normal subjects. *Am J Ophthalmol* 1986;101:199–203.
8. Johnson CA, Adams AJ, Lewis RA. Evidence for a neural basis of age-related visual field loss in normal observers. *Invest Ophthalmol Vis Sci* 1989;30:2056–2064.
9. Katz J, Sommer A. Asymmetry and the normal hill of vision. *Arch Ophthalmol* 1986;104:65–68.
10. Loewenfeld I. Pupillary changes related to age. In: Thompson H, Daroff R, Frisén L, Glaser J, Sanders M, eds. *Topics in Neuro-ophthalmology*. Baltimore: Williams & Wilkins, 1979:124–150.
11. Frisen L. High-pass resolution perimetry and age-related loss of visual pathway neurons. *Acta Ophthalmol (Copenh)* 1991;69:511–515.
12. Quigley H, Sanchez R, Dunkelberger G, L'Hernault N, Baginski T. Chronic glaucoma selectively damages large optic nerve fibers. *Invest Ophthalmol Vis Sci* 1987;28:913–920.
13. Quigley H, Dunkelberger G, Baginski T, Green W. Chronic human glaucoma causes selectively greater loss of large optic nerve fibers. *Ophthalmology* 1988;95:357–363.
14. Sample PA, Bosworth CF, Weinreb RN. Short-wavelength automated perimetry and motion automated perimetry in patients with glaucoma. *Arch Ophthalmol* 1997;115:1129–1133.
15. Casagrande V. A third parallel visual pathway to primate area V1. *Trends Neurosci* 1994;17:305–310.
16. Frisen L, Nikolajeff F. Properties of high-pass resolution perimetry targets. *Acta Ophthalmol (Copenh)* 1993;71:320–326.
17. Frisen L. High-pass resolution perimetry: central-field neuroretinal correlates. *Vision Res* 1995;35:293–301.
18. Frisén L. High-pass resolution perimetry: evidence for parvocellular channel dependence. *Neuro-ophthalmology* 1992;12:257–264.
19. Sample PA, Ahn DS, Lee PC, Weinreb RN. High-pass resolution perimetry in eyes with ocular hypertension and primary open-angle glaucoma. *Am J Ophthalmol* 1992;113:309–316.
20. Iester M, Capris P, Altieri M, Zingirian M, Traverso CE. Correlation between high-pass resolution perimetry and standard threshold perimetry in subjects with glaucoma and ocular hypertension. *Int Ophthalmol* 1999;23:99–103.
21. Martinez GA, Sample PA, Weinreb RN. Comparison of high-pass resolution perimetry and standard automated perimetry in glaucoma. *Am J Ophthalmol* 1995;119:195–201.
22. Lindblom B, Hoyt WF. High-pass resolution perimetry in neuro-ophthalmology: clinical impressions. *Ophthalmology* 1992;99:700–705.
23. Chauhan BC, House PH. Intra-test variability in conventional and high-pass resolution perimetry. *Ophthalmology* 1991;98:79–83.
24. Martin-Boglund L, Graves A, Wanger P. The effect of topical antiglaucoma drugs on the results of high-pass resolution perimetry. *Am J Ophthalmol* 1991;111:711–715.
25. Westcott MC, Fitzke FW, Hitchings RA. Abnormal motion displacement thresholds are associated with fine scale luminance sensitivity loss in glaucoma. *Vision Res* 1998;38:3171–3180.
26. Wall M, Ketoff KM. Random dot motion perimetry in patients with glaucoma and in normal subjects. *Am J Ophthalmol* 1995;120:587–596.
27. Wall M, Jennisch CS, Munden PM. Motion perimetry identifies nerve fiber bundle-like defects in ocular hypertension. *Arch Ophthalmol* 1997;115:26–33.
28. Bosworth CF, Sample PA, Gupta N, Bathija R, Weinreb RN. Motion automated perimetry identifies early glaucomatous field defects. *Arch Ophthalmol* 1998;116:1153–1158.
29. Wall M, Montgomery EB. Using motion perimetry to detect visual field defects in patients with idiopathic intracranial hypertension: a comparison with conventional automated perimetry. *Neurology* 1995;45:1169–1175.
30. Barton J, Rizzo M, Nawrot M, Simpson T. Optical blur and the perception of global coherent motion in random dot cinematograms. *Vision Res* 1996;36:3051–3059.
31. Maddess T, Henry G. Performance of non-linear visual units in ocular hypertension and glaucoma. *Clin Vision Sci* 1992;7:371–383.
32. Cello K, Nelson-Quigg J, Johnson C. Frequency doubling technology perimetry for detection of glaucomatous visual field loss. *Am J Ophthalmol* 2000;129:314–322.
33. Alward WL. Frequency doubling technology perimetry for the detection of glaucomatous visual field loss [editorial]. *Am J Ophthalmol* 2000;129:376–378.
34. Patel S, Friedman D, Varadkar P, Robin A. Algorithm for interpreting the results of frequency doubling perimetry. *Am J Ophthalmol* 2000;129:323–327.
35. Burnstein Y, Elish N, Magbalon M, Higginbottom E. Comparison of frequency doubling perimetry with Humphrey visual field analysis in a glaucoma practice. *Am J Ophthalmol* 2000;129:328–333.

2 Functional Visual Anatomy

A basic knowledge of how the visual field is represented at different levels of the neuraxis is fundamental to the performance of perimetry. Without this knowledge, it is impossible to intelligently select a perimetric program, decide among perimetric techniques, or appropriately guide the exploration of the field during manual perimetry.

A couple of general rules deserve statement up front. The first is that the optics of the eye, like those of any camera, create an inverted retinal image, such that the superior visual field is projected onto the inferior retina and the nasal field onto the temporal retina. The second is that the topographic arrangement of the retina tends to be preserved throughout much of the visual pathway, with the superior retina placed in the superior or dorsal aspect, and the left portions of the retina on the left side of various structures. The exceptions are the distal optic tract and lateral geniculate nucleus (LGN), where the map tilts 90°, and in its horizontal arrangement at the striate cortex, where the periphery-to-center topography turns to assume an anterior-posterior dimension, with the central field posterior and the peripheral field anterior.

1. RETINA

There are two classes of photoreceptors: rods and cones. The rhodopsin protein of the rods is highly sensitive to light, with each rod able to respond to a single photon, and a mere five to eight photon detections needed to reach the threshold for perception of light in darkness (scotopic conditions) (1). However, in bright light (photopic conditions) the rods lose visual sensitivity, and perception in this setting depends on cones. Normal subjects have three cone types that differ in their opsin pigments. These differences cause different peaks of sensitivity along the spectrum of light, with designations of short (S, sometimes colloquially referred to as “blue”), medium (M, or green), and long (L, or red) wavelength cones. The retinal ganglion cells compare the activity of the different cones to determine what wavelengths of light are impinging on the retina. Color perception also requires participation of extrastriate cortex, in part to adjust for the type of lighting in a scene, to achieve constancy of colors despite variations in such lighting (2,3).

Cones are more numerous than rods in the fovea, while rods are more numerous than cones outside the central 5°. Around

From: *Current Clinical Neurology: Field of Vision: A Manual and Atlas of Perimetry*
By J. J. S. Barton and M. Benatar © Humana Press Inc., Totowa, NJ

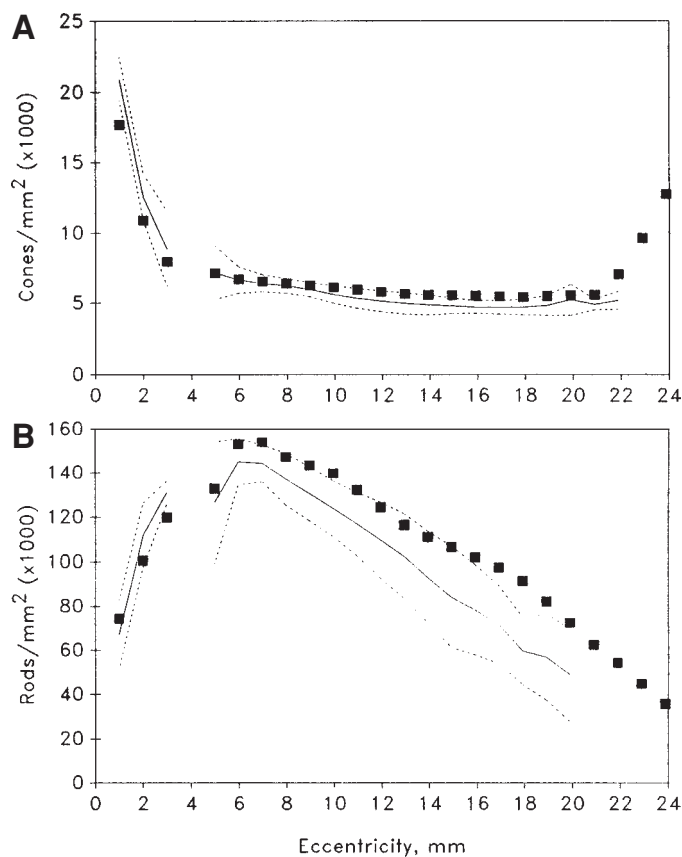


Fig. 1. Distribution of (A) cones and (B) rods. Photoreceptor density is plotted on the y-axis against retinal eccentricity on the x-axis. (From ref. 49 with permission.)

50% of cones are concentrated in the central 30°, with a steep decline in density from center to 3°, followed by a shallower, fairly linear rate of decrease with increasing eccentricity (Fig. 1). This decline in density with eccentricity is true of almost all retinal elements with the exception of rods, which are not found at the fovea, but rather are maximally dense at an eccentricity of about 6–8°, followed again by a gradual decline with increasing eccentricity (Fig. 1).

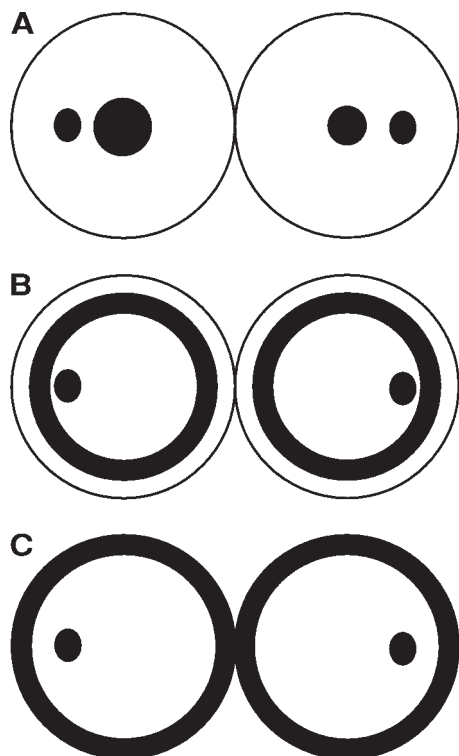


Fig 2. Illustrations of retinal patterns of visual loss: (A) macular or cone disease, causing central scotomata; (B) rod disease, such as retinitis pigmentosa, causing ring scotomata; (C) generalized constriction. The temporal ovals are the physiologic blind spots, and the right eye is on the right, with fields plotted from the patient's view, with right hemifield on the right.

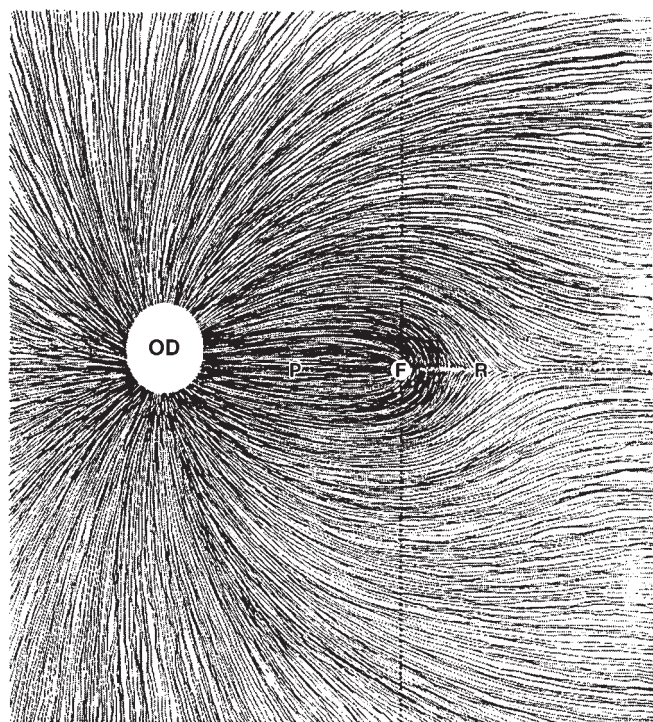


Fig. 3. Retinal nerve axons in the retina. The optic disc (OD) is the white disc, which is left of the fovea (F), in this view of a left eye. The course of the nerve fibers toward the optic disc is shown. The temporal retina lies to the right of the vertical dotted line. P = papillomacular bundle, R = raphe. (From ref. 49 with permission.)

The consequence of the distribution pattern of cones and rods is that retinal disorders that preferentially affect cones (e.g., cone dystrophies) will tend to affect central vision first (Fig. 2). Disorders that are specific to rods (e.g., retinitis pigmentosa) will tend to affect the midperiphery of vision more, sparing both central vision and color vision. Otherwise, there are no specific anatomic issues regarding the distribution of retinal elements that are reflected in the topography of the field defects of retinal disease. Some conditions present simply with generalized constriction. Examples include the toxic effects of vigabatrin and mild background diabetic retinopathy (4). Others present with defects that correspond to the location of retinal damage and, hence, are related more to issues of preferential pathology than anatomy. Examples include macular degeneration, retinal detachments, and congenital defects such as staphylomata. Most retinal lesions that produce focal defects in the visual field are visible on fundoscopy, and perimetry does not add much to the diagnostic process.

1.1. VASCULAR SUPPLY

The main supply of the outer retina, where the photoreceptor layer lies, is the posterior ciliary arteries, which, like the central retinal artery, are terminal branches of the ophthalmic artery, the first major branch of the internal carotid artery within the cavernous sinus.

2. RETINAL NERVE FIBER LAYER

The axons of the retinal ganglion cells project to the optic disc, where they form the optic nerve. Because the optic disc is situated in the nasal retina, rather than in the center of the field, there are asymmetries in the paths followed by the axons to reach it. The organization of these axons is key not only to understanding disturbances of the inner retinal layer, as with retinal arterial disease, but also to understanding the field defects in optic neuropathy, as this topography is maintained within the optic nerve.

The most important feature of nerve fiber layer topography is the papillomacular bundle (Fig. 3). The large concentration of retinal ganglion cells at the fovea gives rise to a sheaf of axons that projects directly to the optic disc. Those from the temporal side of the fovea must arch around the large group of fibers from the nasal fovea and thus divide into superior and inferior groups divided by a raphe along the horizontal meridian. This division continues into the peripheral temporal retina; all of these fibers must arch around the massive papillomacular bundle to reach the optic disc, which they enter supero- and inferotemporally. By contrast, fibers from the superior, inferior, and nasal retina are not obstructed by the papillomacular bundle and project in direct radial lines toward the optic disc.

Consequently, there are three classic field defects found with disorders of the optic nerve (Fig. 4):

1. A lesion of the *papillomacular bundle* causes a central scotoma or, if more extensive, a cecocentral scotoma, in which the central defect is continuous with the physiologic blind spot.
2. A lesion of the *temporal retinal fibers* arching around the papillomacular bundle will cause a nasal arcuate defect in either the superior or inferior field. This will come to an abrupt halt at the horizontal meridian in the nasal field. If more extensive, it will follow a curved path around the central macular region and point toward the

blind spot marking the location of the optic disc. A more subtle arcuate defect may have a paracentral scotoma along this path.

3. A lesion of the *nasal retinal fibers* will cause a temporal wedge defect. This will rarely have a border that is aligned along the temporal meridian, as there is no anatomic divide between the upper and lower fibers in the nasal retina.

Combinations of these exist. A superior altitudinal defect, for example, combines damage to the inferior temporal arcuate fibers and the inferior nasal radial fibers. The result is loss of the upper half of vision with a sharp horizontal border nasally and a variable border temporally, which can spare some of the upper temporal field or involve part of the lower temporal field. The macular region can be spared or involved with extension into the lower field, depending on the degree of involvement of the papillomacular bundle. Altitudinal defects are not uncommon with ischemic damage to the optic nerve.

The 1.25 million retinal ganglion cells in each human eye are not a homogeneous group, but divisible into at least 22 different subtypes. Three major types are the parvocellular, magnocellular, and koniocellular groups, which constitute 70%, 8–10%, and 1–10% of the total population, respectively. The parvocellular (P, midget) neurons have small dendritic fields, somas, and axonal diameters and physiologically respond with sustained bursts to light, have color opponency, and conduct information at moderate speeds. Because of these characteristics, they are said to be specialized for stimuli with fine spatial detail (high spatial frequencies) and color (5). Magnocellular (M, parasol) cells have large dendritic fields, somas, and axonal diameters. They respond transiently to the onset and offset of lights, lack color opponency, and have rapid conduction. They are specialized for rapidly changing stimuli (high temporal frequencies) and are poor at fine spatial detail (5). Koniocellular cells receive input from blue-cone bipolar cells and have blue-yellow opponency. The clinical relevance of these subtypes is still being determined (6), but these subtypes are guiding much of the development of newer perimetric strategies (see Chapter 1).

2.1. VASCULAR SUPPLY

The inner retina, which contains the retinal ganglion cells and their axons in the nerve fiber layer, is supplied by the central retinal artery, an end branch of the ophthalmic artery.

3. OPTIC NERVE

At the optic disc the arrangement of the axons of the retinal ganglion cells is much as expected from the above discussion about the nerve fiber layer. The papillomacular bundle occupies about the central third of the temporal half of the optic disc (7). Beside it the superior and inferior arcuate fibers from the nasal field enter the superotemporal and inferotemporal disc. The rest of the disc is straightforward, with nasal retina (temporal field) flowing into the nasal optic disc, superior retina (inferior field) into the superior aspect, and inferior retina into the inferior disc. For each of these latter regions, the more peripheral fibers occupy the periphery of the optic disc (8–10).

As the optic nerve progresses through the orbit and enters the cranium through the optic canal, just medial to the superior orbital fissure, the retinotopy gradually shifts so that the macular fibers occupy the center of the optic nerve. The approximate arrangement mirrors the origin in the retina, with superior retinal axons

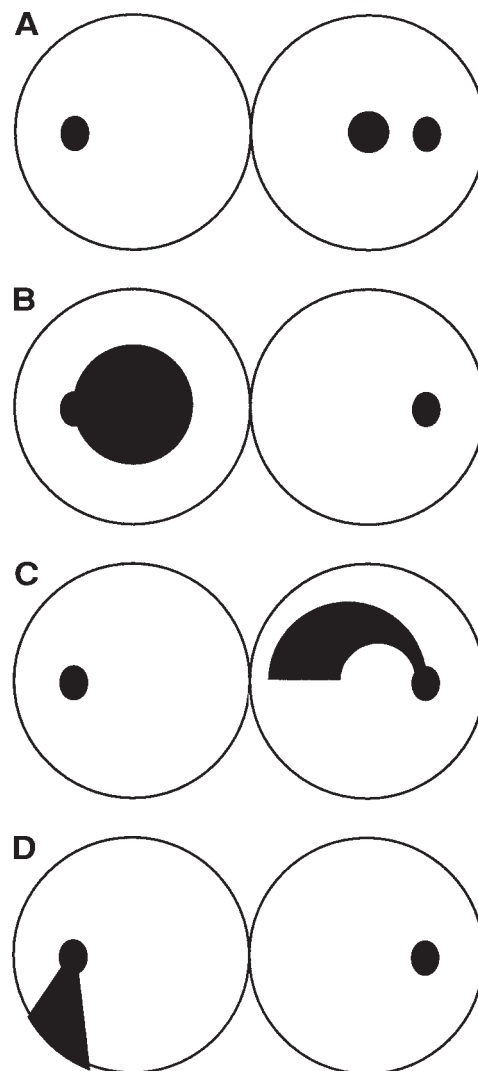


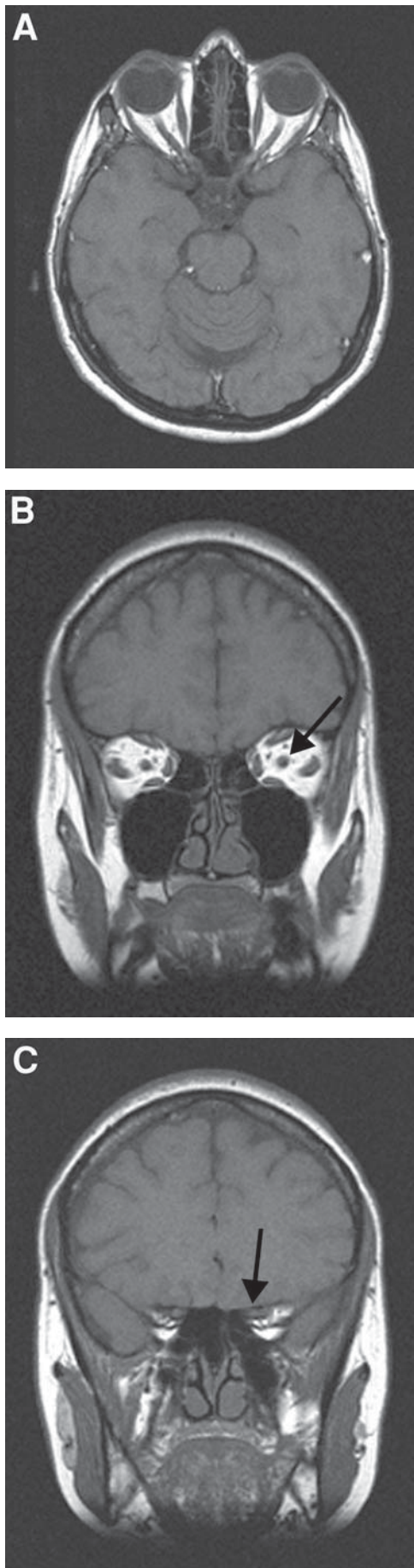
Fig. 4. Illustrations of retinal nerve fiber bundle and optic neuropathic patterns of visual loss: (A) central scotoma; (B) cecentral scotoma; (C) nasal arcuate defect; (D) temporal wedge defect.

located superiorly, nasal retinal axons nasally, and peripheral axons peripherally.

3.1. NEIGHBORHOOD AND VASCULAR SUPPLY

Within the orbit the optic nerve lies within a cone of extraocular muscles that proceeds from the apex of the orbit to insert on the circumference of the globe (Fig. 5). Large mass lesions within the cone cause proptosis but tend not to displace the eye in any particular direction. The optic canal through which the nerve passes is bordered medially by the ethmoid sinuses, and pathology here such as aspergillus infection or Wegener's disease may affect the optic nerve. Laterally lies the superior orbital fissure, which contains cranial nerves III, IV, the first division of V, and VI. A lesion here may cause visual loss with ophthalmoparesis and numbness of the forehead.

The intraorbital optic nerve is supplied by branches of the ophthalmic artery. The optic disc is supplied by the posterior ciliary artery.



4. OPTIC CHIASM

The fibers of the nasal retina decussate in the chiasm, while the temporal retinal fibers do not. Amazingly, this anatomic fact may have been first proposed by Isaac Newton in 1704 (11). The result is that the axons of the temporal field of the contralateral eye join the axons of the nasal field of the ipsilateral eye to form the optic tract, which leaves the chiasm. The hallmark of all visual field defects at or beyond the chiasm is the hard anatomic divide between the left and right visual fields at the vertical meridian.

One clinical point of note about the junction of the optic nerve and the optic chiasm is Wilbrand's knee (12). This is a hypothesized loop of decussating axons from the superior temporal field, in the inferior aspect of the chiasm, which is said to project slightly into the contralateral optic nerve. A lesion here causes a junctional scotoma, which is the combination of an optic neuropathy in the ipsilateral eye with a superotemporal field defect in the other eye that respects the vertical meridian (Fig. 6C). However, more recent studies have suggested that Wilbrand's knee is a myth, an artifact of fixation (13). Rather, junctional scotomata may result from compression of both the intracranial optic nerve and the adjacent optic chiasm by an inferior mass, a not uncommon type of pathology in this region. Regardless of the explanation, the localizing value of a superotemporal field defect in the eye opposite to one with optic neuropathy remains unchallenged. Its clinical importance is that it shifts the etiologic differential diagnosis from the large and varied list associated with optic neuropathy to that of perichiasmatal pathology, which implies a mass lesion until proven otherwise.

Because the nasal retina is larger than the temporal retina, slightly more optic nerve fibers (about 53%) decussate than remain uncrossed (14). The macular crossing fibers are diffusely scattered throughout the chiasm, with a slight concentration toward its central and posterior aspects (15). Again, axons from the inferior and superior retina tend to retain the same inferior and superior relations in the chiasm. Beyond this, though, there is much uncertainty on the topography of the chiasm, particularly in humans.

Lesions of the decussating fibers in the optic chiasm cause bitemporal field defects (Fig. 6A). Because the majority of the mass lesions in this region compress the chiasm from below, the superior and central fields are particularly vulnerable. Compression of the lateral aspect of the chiasm can, on rare occasions (16), produce an ipsilateral nasal hemifield defect respecting the vertical meridian (unlike the nasal arcuate defects of optic neuropathy) (Fig. 6B). Lateral compression is more likely from masses in the region of the cavernous sinus, such as giant intracavernous aneurysm, than from pituitary tumors. It is even claimed that bilateral lateral compression might cause binasal field defects. However, nasal field defects in both eyes are far more likely to represent bilateral optic neuropathies than chiasmatal lesions, and one would have to make certain that any vertical meridian effect in such a case was not an artifact of perimetry, before embarking on neuroimaging of the sella.

Fig. 5. Magnetic resonance imaging (MRI) of optic nerve, showing orbital T1-weighted images: (A) axial view showing optic nerves from globe to chiasm; two coronal views, one (B) anterior through orbit, showing optic nerves (arrow) within cone of extraocular muscles, and (C) one at the level of optic canal (arrow).

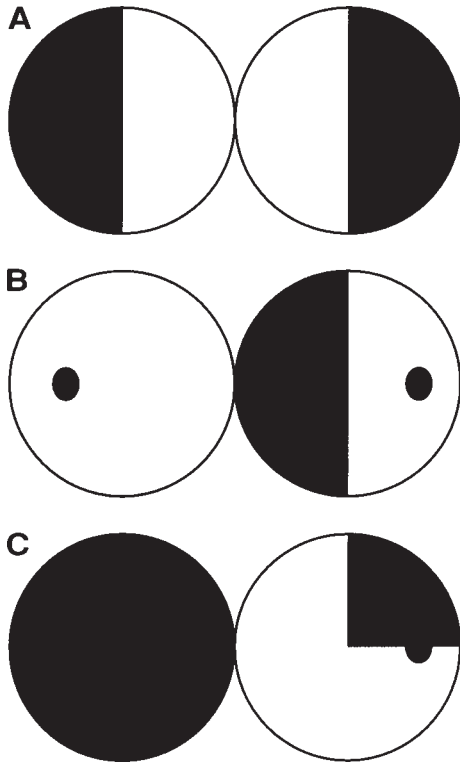


Fig. 6. Illustrations of optic chiasm patterns of visual loss: (A) bitemporal hemianopia; (B) unilateral nasal hemianopia; (C) junctional scotoma.

Long-standing severe lesions of the optic chiasm will be associated with optic atrophy, as the axons degenerate in retrograde fashion. Loss of the fibers from the nasal retina leads to a characteristic pattern of atrophy. The nasal optic disc will be affected because of loss of fibers from the peripheral nasal retina, as will the temporal optic disc, because this contains axons from the central nasal retina, which lies between the blind spot and the fovea. The superior and inferior aspects of the optic disc, which are occupied by the arcuate fibers coming from the temporal retina, are spared, however. The result is a pattern called “bowtie” or “band” optic atrophy (17) (see Case 65).

4.1. NEIGHBORHOOD AND VASCULAR SUPPLY

The optic chiasm lies superior to the pituitary gland, and inferior to the hypothalamus (Figs. 7 and 8). It is supplied by perforating branches originating from the anterior communicating artery and the A1 segments of both anterior cerebral arteries (18).

5. OPTIC TRACT

The visual pathway leaving the optic chiasm is no longer organized as separate structures for each eye (the optic nerves) but as separate structures for each homonymous hemifield. There are two key features about the retinotopy within the optic tract. One is that the correspondence of the retinal map of one eye with that of

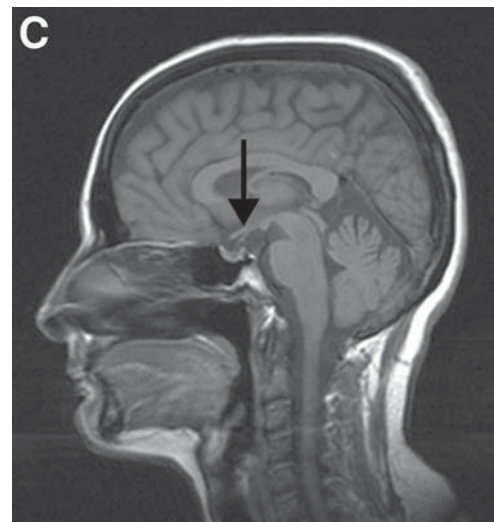
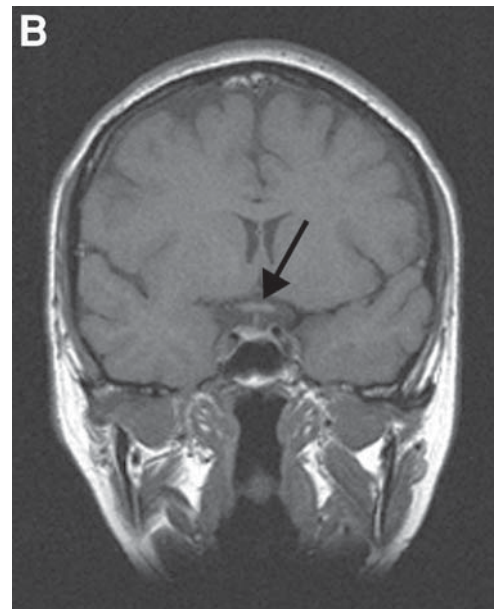
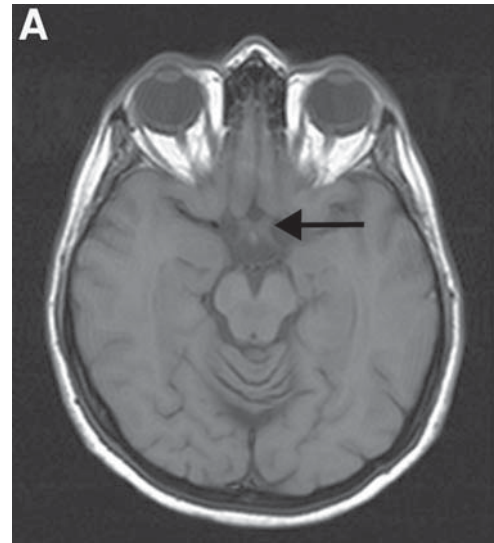


Fig. 7. MRI of optic chiasm showing sella T1-weighted images: (A) axial view showing chiasm (arrow) as X-shaped structure just anterior to infundibulum of pituitary gland; (B) coronal view showing the flat chiasm (arrow) in suprasellar cistern, just above infundibu-

lum, together forming a “T”; (C) midline sagittal view showing chiasm (arrow) just above sella and infundibulum, which slopes down to the pituitary gland.



Fig. 8. Pathology specimen, ventral surface of brain, with temporal lobe removed on right side of image. N = optic nerve, C = optic chiasm, T = optic tract.

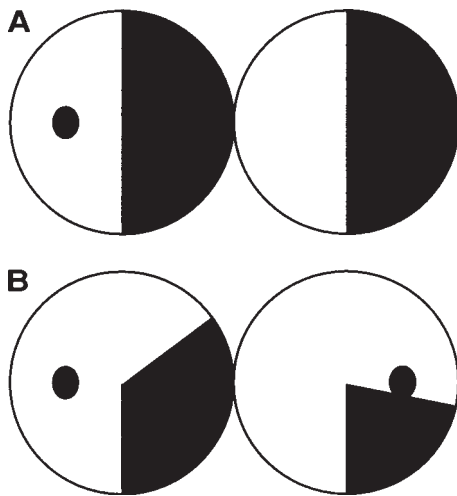


Fig. 9. Illustrations of optic tract patterns of visual loss: (A) complete hemianopia; (B) incongruous partial hemianopia.

the other is only approximate. Hence, partial tract lesions will cause incomplete hemianopias that are quite different in one eye compared with the other (Fig. 9). Although homonymous, in that the defects of the two eyes are in the same hemifield, they are thus incongruous. In general, congruity increases gradually as one proceeds from the chiasm to striate cortex, with a milder degree of incongruity occurring with optic radiation lesions and high congruity typical of striate lesions.

The second feature is a gradual rotation of the retinal map as the tract approaches its termination in the lateral geniculate

nucleus. The superior retina (inferior field) ends up in the dorsomedial tract, the inferior retina in the ventrolateral aspect, and the central field in a dorsolateral position. In addition to this retinotopy, recent data suggest a segregation of magnocellular and parvocellular axons in the tract also, with the magnocellular axons located more ventrally (19).

Because the fibers of the optic tracts are still the axons of the retinal ganglion cells, there will be optic atrophy with long-standing lesions (see Case 69). The eye with temporal field loss may have a bowtie or band optic atrophy (17), as described for chiasmal lesions. The eye with nasal field loss will have more diffuse atrophy, affecting the superior, inferior, and temporal disc, with relative sparing of the nasal disc.

Fibers for the pupillary light reflex also travel in the optic tract, leaving it just prior to the tract's termination in the lateral geniculate nucleus to project to the pretectal nucleus. Asymmetries in field loss from partial tract lesions will thus be associated with a relative afferent pupillary defect in the eye with more profound visual loss. Even with complete tract hemianopia, there will be a relative afferent pupillary defect in the eye with temporal field loss (20–22). Because the temporal field is larger than the nasal field, and the uncrossed nasal field fibers represent 47% of the optic nerve whereas the decussating temporal field fibers constitute 53%, there is more loss of visual input from the eye with temporal hemianopia than from the eye with nasal hemianopia. A relative afferent pupillary defect in the absence of optic atrophy may be the only clue that a homonymous hemianopia stems from optic tract dysfunction (21).

As is true for all homonymous hemifield defects, from the optic tract to striate cortex, visual acuity is not affected unless there is either bilateral damage or additional involvement of the optic chiasm or optic nerves (22,23). One surviving hemifovea is sufficient to support good central spatial resolution.

5.1. NEIGHBORHOOD AND VASCULAR SUPPLY

The optic tract travels medial to the anterior temporal lobe and inferolateral to the hypothalamus (Fig. 10). The main arterial supply of the optic tract is the anterior choroidal artery.

6. PARASELLAR LESIONS

A word about the impact of mass lesions in the vicinity of the optic chiasm is important. Most practitioners are aware, from the early days of their training, of how lesions such as pituitary macroadenomas compress the optic chiasm and produce bitemporal hemianopia. However, the anatomic position of the optic chiasm with relation to the pituitary fossa is variable (24,25). In some cases, the chiasm is situated anterior to the fossa. A pituitary mass in a patient with such a "prefixed" chiasm may present with homonymous hemianopia rather than bitemporal hemianopia, because the compression may affect one of the optic tracts more than the optic chiasm. Other patients may have a "post-fixed" chiasm situated posterior to the pituitary fossa. In this situation, a mass may present with compressive intracranial optic neuropathy, with or without a junctional scotoma.

7. LATERAL GENICULATE NUCLEUS

The LGN, a hat-shaped structure, is located in the ventro-posterolateral thalamus. It is the terminus of the axons of the retinal ganglion cells and contains the cell bodies of the next (and last) neurons in the relay of visual information to striate cortex. In

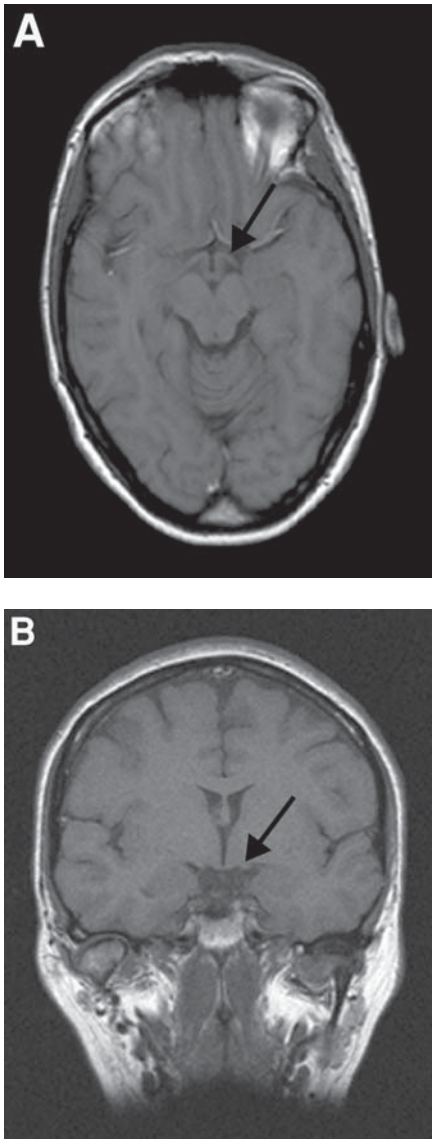


Fig. 10. MRI of optic tract showing T1-weighted images: (A) axial view showing tracts projecting posterolaterally (arrow), anterior to cerebral peduncles and paired medially positioned mammillary bodies; (B) coronal view showing tracts on undersurface of thalami, just superior to hippocampi (arrow).

addition to being a relay station, there is substantial modulation of visual responses in the LGN (26), which involves feed-back and feed-forward projections from extraretinal sources, including superior colliculus, striate cortex, and midbrain nuclei such as the locus ceruleus and dorsal raphe nucleus.

The LGN contains six main horizontal layers (Fig. 11), with each eye providing a segregated innervation to three, in an approximately alternating order (the contralateral eye projects to layers 1, 4, and 6). The ventral two are the magnocellular layers, with the dorsal four being the parvocellular layers. These names derive from the histology of the neuronal cell bodies in these layers. Functionally, the retinal ganglion cells that project to these two different types of layers differ (5). The magnocellular layer receives input from cells with large receptive fields and

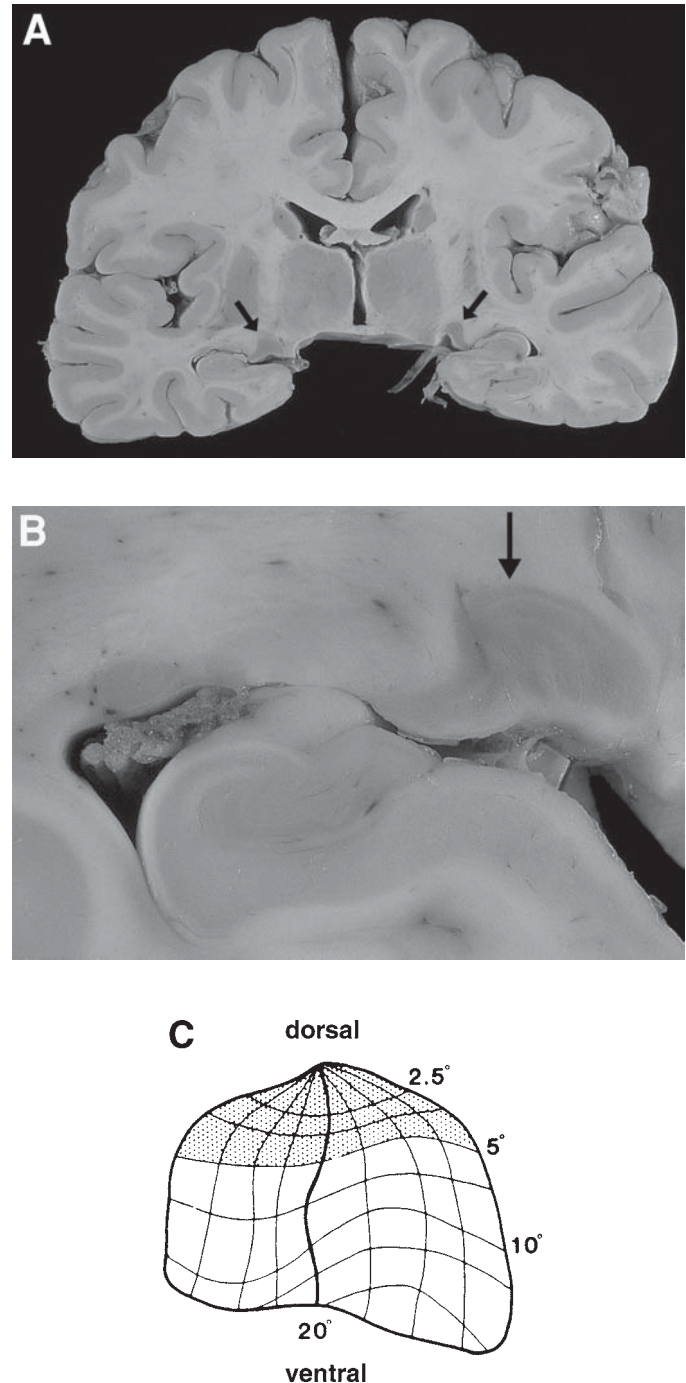


Fig. 11. LGN: (A) pathologic specimen of LGN, coronal section; (B) close-up shows layering; (C) diagram of retinotopy of LGN. Here horizontal layering is shown for retinal eccentricity, not by cell type. (Modified from ref. 49 with permission.)

transient responses to either the onset or offset of light stimuli, whose axons are larger and conduct at a fast rate. The parvocellular layer receives input from neurons with smaller receptive fields, color opponent organization, sustained responses to light and slower conduction along its axons (see Retinal Nerve Fiber Layer, p. 8).

In coronal section the representation of the visual field is an approximate continuation of that found in the terminal optic tract.

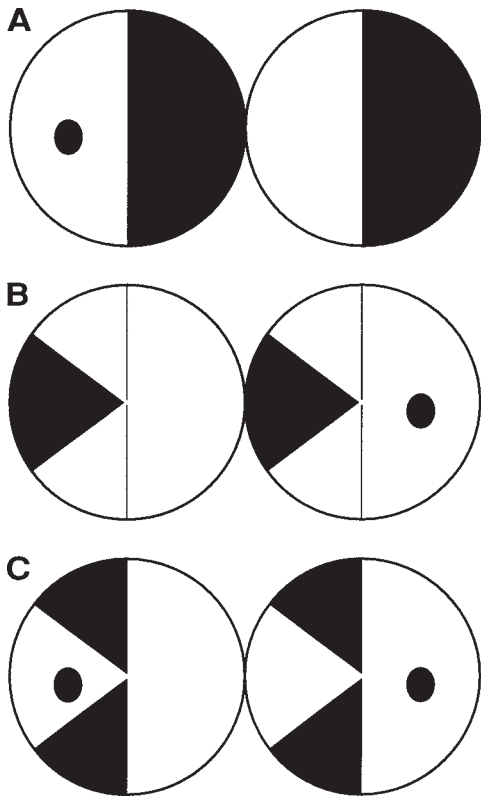


Fig. 12. Illustrations of LGN patterns of visual loss: (A) complete hemianopia; (B) horizontal sectoranopia, from damage to midzone; (C) vertical sectoranopias from lesion sparing midzone.

That is, the macular region occupies a large portion of the dorsal aspect of the nucleus (27), with the periphery located in the broader ventral surface, proceeding from the inferior visual field medially to the superior field laterally (28,29) (Fig. 11C).

The clinical importance of the retinotopy of the LGN derives from lesions that can preferentially affect parts of this structure and spare others. The classic example is an ischemic insult to the LGN. The midzone of the LGN is supplied by the posterior (lateral) choroidal artery, whereas the lateral and medial zones are supplied by the anterior choroidal artery. Infarcts in one or the other zone cause sectoranopias (Fig. 12). In the case of the posterior choroidal artery, the result is a homonymous sector of visual loss straddling the horizontal meridian from the center to the periphery (30). In the case of the anterior choroidal artery, the field defect is the reverse: a hemianopia sparing a wedge straddling the horizontal meridian (31). Incongruity of these hemifield patterns is also the rule with LGN lesions.

Optic atrophy often accompanies LGN lesions. Complete LGN destruction will lead to the same combination of contralateral bowtie atrophy and ipsilateral diffuse atrophy seen with optic tract lesions. The partial damage with sectorial hemianopias causes more subtle optic atrophy restricted to the relevant disc sectors (30,31). Because the afferent fibers subserving the pupillary light reflex have already left the optic tract, there is no relative afferent pupillary defect (RAPD). With incongruous hemianopia and optic atrophy, this is the only feature that distinguishes optic tract from LGN lesions.

7.1. NEIGHBORHOOD AND VASCULAR SUPPLY

Nearby thalamic subnuclei include the medial geniculate nucleus ventromedially, the ventral posterior nucleus dorso-medially, and the pulvinar superiorly and dorsally. The medial geniculate nucleus, a relay nucleus in the auditory pathway, gives rise to the acoustic radiations, which pass by the dorsomedial aspect of the LGN on their way to the auditory cortex in the temporal lobe. The optic radiations arise from the dorsolateral surface of the LGN. Ventrally, the hippocampus and parahippocampal gyrus face the LGN across the ambient cistern and the inferior horn of the lateral ventricle. The dual blood supply to the LGN has been discussed already.

8. OPTIC RADIATIONS

Optic radiations contain the axons from the LGN to the ipsilateral striate cortex. There may also be direct projections to extrastriate cortex, which may support residual covert or unconscious perception (“blindsight”) within the homonymous field defects of striate lesions.

The radiations leave the LGN as a compact bundle. These quickly fan out and pass as a wedge-shaped stream of axons coursing through the white matter of the temporal and parietal lobes to their destination in striate cortex. This fan preserves the topography, with the superior (dorsal, or parietal) radiations representing the superior retina and the inferior (ventral, or temporal) radiations representing the inferior retina. The central field is spread over the lateral surface of the radiations.

One important anatomic feature is the displacement of the temporal radiations anteriorly by the growth of the lateral ventricle during embryogenesis. Thus, this half of the radiations, representing the superior visual field and known as Meyer’s loop, projects anterolaterally from the LGN to pass superior to the temporal ventricular horn, deep in the anterior temporal lobe (Fig. 13). Although there is some individual variability, the most forward extent of the radiations is to within about 5 cm of the anterior tip of the temporal lobe. Temporal lobectomies for complex partial seizures do not cause visual loss if they are limited to the most anterior 4 cm of the lobe. The first portion of the field to be affected with lobectomies that proceed a little farther posteriorly is the region adjacent to the vertical meridian (32). With more daring resections, the field defects expand down toward the horizontal meridian, becoming larger pie-shaped wedges. Lesions extending more than 8 cm posterior to the temporal lobe tip start to affect the inferior visual field also. Parietal white matter lesions are most likely to affect the superior optic radiations in isolation. Lesions may also affect the central portion, causing a sectoranopia (33) (Fig. 14).

With damage to the visual pathway distal to the LGN, there is rarely optic atrophy or relative afferent pupillary defects. The only exceptions are long-standing, generally congenital lesions that presumably have been followed by transsynaptic retrograde degeneration.

8.1. NEIGHBORHOOD AND VASCULAR SUPPLY

Nearby relations are essentially the cerebral lobes through which the radiations pass. Meyer’s loop is close to the hippocampus, and the superior and inferior parietal lobules are lateral to the parietal optic radiations. Thus, associated signs of cerebral damage are frequent with lesions of the optic radiations. Superior quadrantic defects may be associated with complex partial seizures, memory disturbances, or a fluent aphasia if the domi-

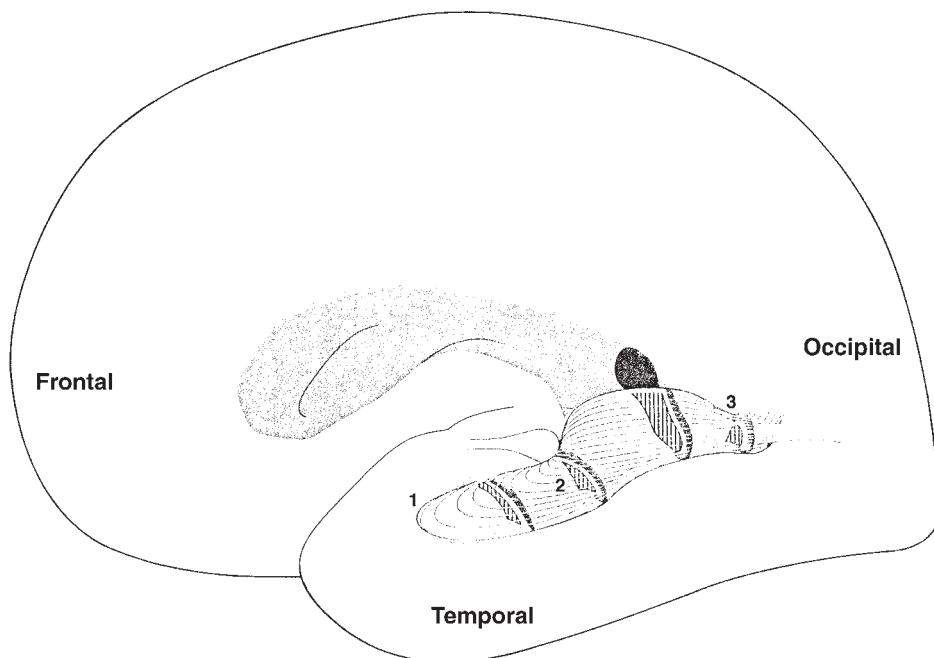


Fig. 13. Diagram of optic radiations showing how radiations loop around anterior temporal horn of lateral ventricle. 1 = temporal optic radiations (Meyer's loop); 2 = central bundle; 3 = upper (parietal) bundle, representing inferior visual field. (From ref. 50 with permission.)

nant (usually left) temporal lobe is involved. Inferior quadrantic defects may be associated with somatosensory disturbances in the contralateral hand, or impaired smooth pursuit eye movements for targets moving toward the side of the lesion. Dominant hemisphere lesions may have Gerstmann syndrome (acalculia, finger anomia, right-left disorientation, and agraphia), fluent or global aphasia, or alexia with or without agraphia.

The blood supply to the optic radiations is primarily the middle cerebral artery. The terminal portion enters into the territory of the posterior cerebral artery, and the portion just exiting from the LGN is supplied by the anterior choroidal artery.

9. STRIATE CORTEX

Striate cortex is the primary visual cortical area ("visual area 1" or V1, also known as calcarine cortex or Brodmann area 17) and the termination of the optic radiation and the retino-geniculocalcarine relay. It occupies the depths and upper and lower banks of the calcarine fissure, running anteroposteriorly along the medial surface of the occipital lobe, approximately parallel to the cerebellar tentorium (Figs. 15 and 16). The parietooccipital fissure forms a reasonably reliable marker of the anterior extent of striate cortex. The posterior limit is more variable, extending from the medial occipital surface over the first 1 or 2 cm of the superficial posterior surface of the occipital pole.

The retinotopic map proceeds from the fovea posteriorly at the occipital pole to the far periphery anteriorly at the parieto-occipital fissure (34,35). The superior bank of the calcarine fissure corresponds to the superior retina, and hence the inferior visual field,

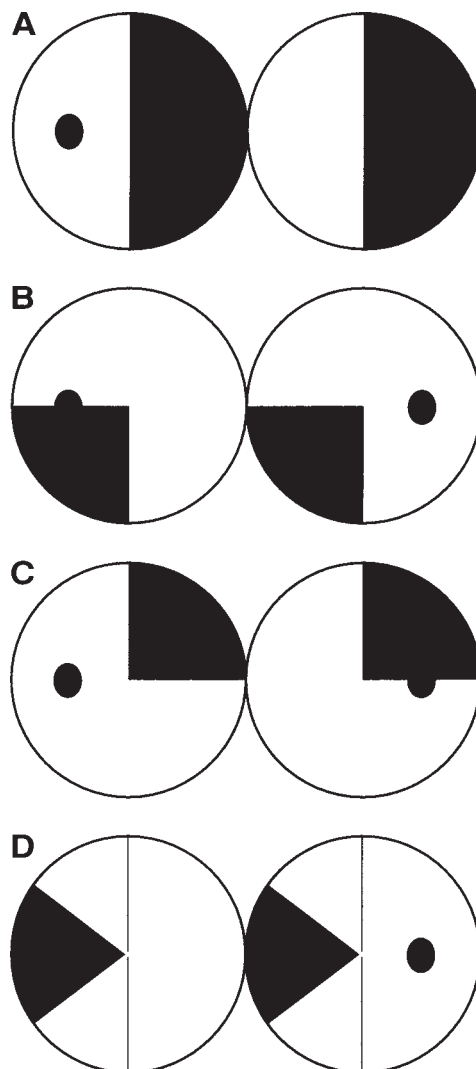
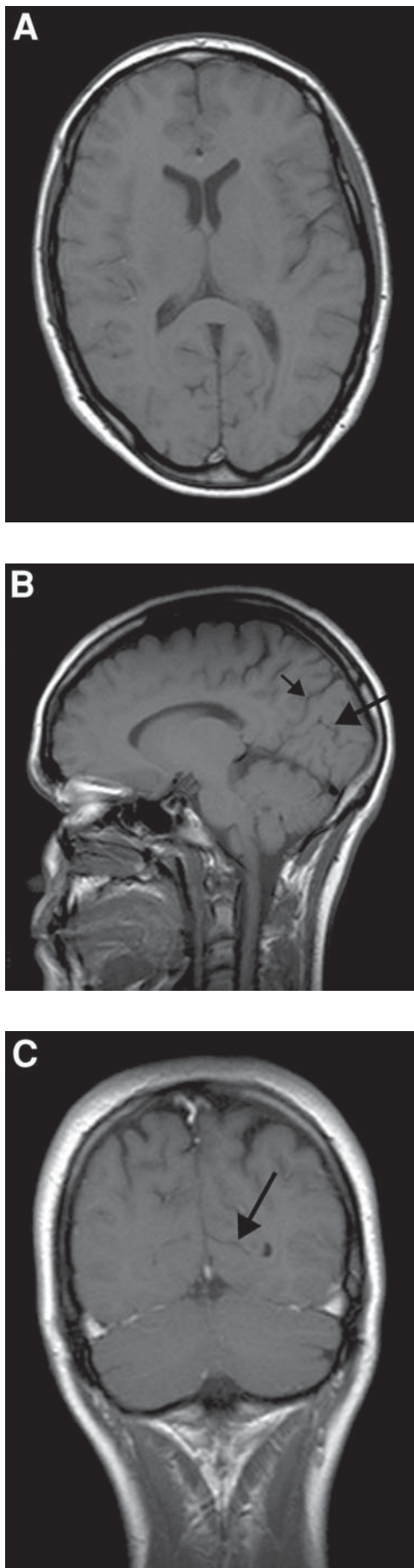


Fig. 14. Illustrations of optic radiation patterns of visual loss: (A) complete hemianopia; (B) lower quadrantanopia, from parietal optic radiation damage; (C) upper quadrantanopia, from temporal optic radiation damage; (D) sectoranopia, from damage to midzone of combined parietal and temporal optic radiations.



while the inferior bank represents the inferior retina and superior visual field (Fig. 16). The most anterior part of striate cortex corresponds to the monocular temporal crescent, the temporal region in the contralateral eye that lies beyond the nasal limits (60°) of the ipsilateral eye. As in most of the visual system, there is a gradient of decreasing neuronal resources as one proceeds more peripherally in the field. The “cortical magnification factor” is a value in an equation that captures this relation (36,37). Over half of striate cortex is devoted to the central 10° (38,39). The striate cortex contains a mix of monocular and binocular cells in ocular dominance columns, and the retinal maps of the two eyes are closely registered with each other, resulting in high congruity of the various field defects from lesions there (Fig. 17).

9.1. NEIGHBORHOOD AND VASCULAR SUPPLY

The striate cortex is supplied by branches of the posterior cerebral artery (40). A parieto-occipital branch supplies the superior calcarine bank, a posterior temporal branch supplies the inferior bank, and a calcarine branch supplies the central region posteriorly. The most important variation among individuals is the location of the watershed between the posterior and middle cerebral arteries at the occipital pole, with respect to where the foveal representation lies. In some individuals, a good portion of the fovea may be supplied by the middle cerebral artery, whereas in others the posterior cerebral artery supplies all striate cortex (40). The result is that some individuals with posterior cerebral arterial infarcts will have hemianopia with sparing of the fovea, while others will have complete hemianopia.

Structures anterior to striate cortex in the medial occipital lobe include the lingual and fusiform gyri, and farther afield the hippocampus; all of these are supplied by the posterior cerebral artery and not uncommonly are damaged along with striate cortex during infarction. Variable degree of memory impairment, dyschromatopsia, and rarely visual agnosia may result.

10. EXTRASTRIATE CORTEX

Beyond the striate cortex the stream of visual information changes drastically. Instead of a serial relay with information modulation at each stage, perceptual data now fan out into a large array of cortical regions, each specialized for a particular type of visual function. This array is organized in a loose hierarchy, with feed-forward inputs, back projections, and interconnections among many regions (41). The retinal topography of these areas is much coarser than that in striate cortex and the preceding elements of the visual pathway, and it is gradually lost further up the hierarchy, as the receptive fields of neurons become larger and larger, with some eventually spanning the entire ipsilateral and contralateral visual field. Instead, visual processing becomes more and more specialized, with regions selective for faces, colors, and motion, for example. This selectivity can be grouped approximately into a dorsal stream through occipitoparietal cortical regions that is dedicated to visuospatial analysis (the “Where” path) and a ventral stream through medial occipitotemporal

Fig. 15. MRI of striate cortex. (A) The axial view shows the more convoluted sulci and gyri of striate cortex on the medial surface of the occipital lobe. Locating striate cortex is easier on (B) the sagittal view, where the calcarine fissure (long arrow) runs parallel to the tentorium, and (C) the coronal view, where this fissure is easily seen on the medial occipital lobe (arrow). Short arrow shows parieto-occipital fissure in (B).

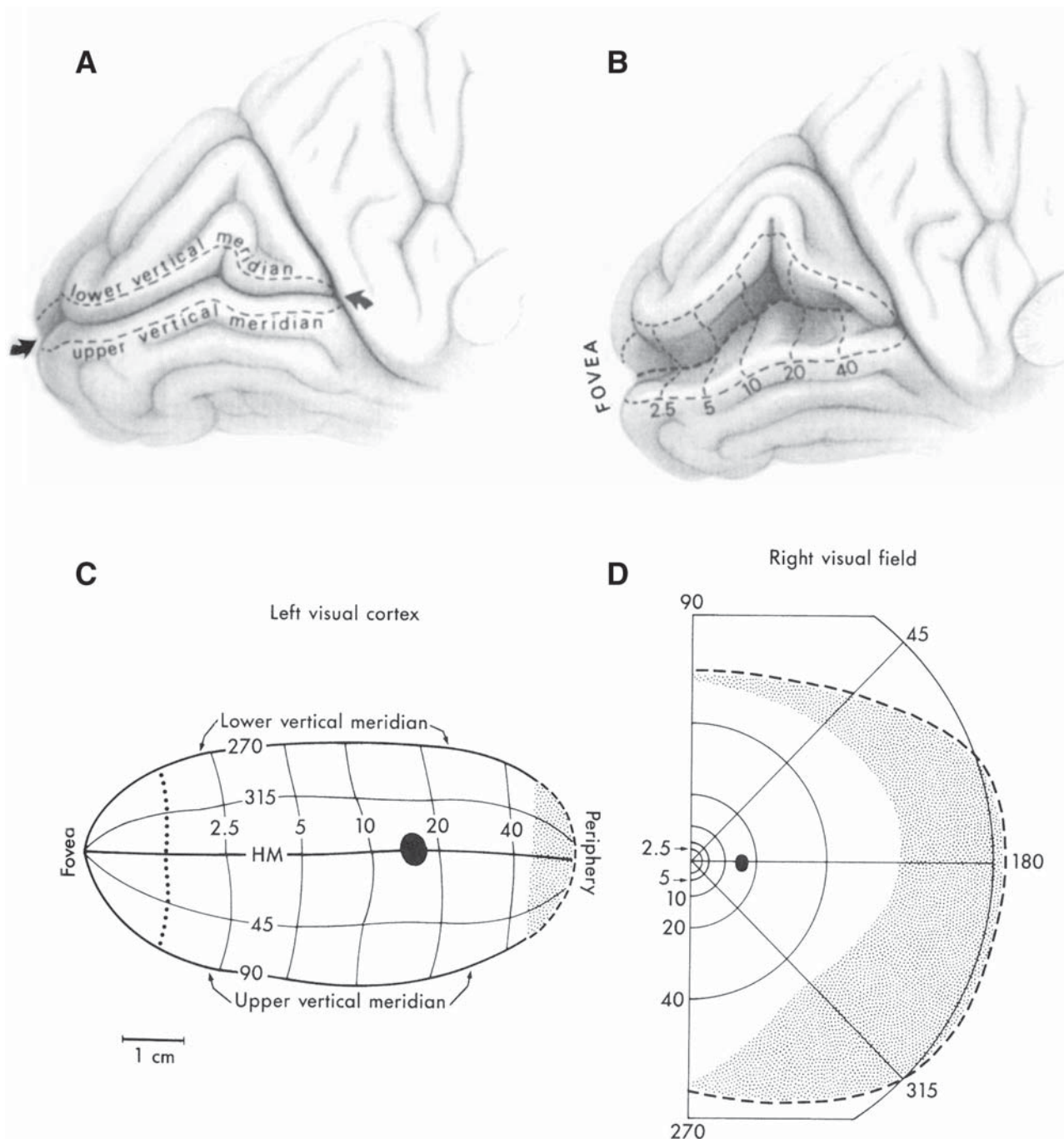


Fig. 16. Representation of vision in striate cortex showing views of striate cortex with occipital pole, or posterior aspect, at left side (A,B) and flat maps of topography of visual cortex (C) and corresponding visual field (D). HM = horizontal meridian (180°). Grey stipple is the monocular temporal crescent. (From ref. 38 with permission.)

regions that focuses on object recognition (the “What” path) (42). Lesions of these regions are typified not so much by field defects as by interesting highly selective defects, such as achromatopsia, the loss of color discrimination, and prosopagnosia, the inability to recognize familiar faces.

Do lesions of extrastriate cortex ever lead to visual field defects? It has been proposed that quadrantic defects may arise from V2 lesions (43); however, this remains a point of contention, and is not supported by data from nonhuman primate studies. Areas V4 and V5 do have a coarser retinotopic map, and lesions in these

regions may generate visual dysfunction limited to one hemifield or even one contralateral quadrant. However, these hemifield defects are selective, in that they affect some types of vision but spare others. Lesions of the fusiform gyri, which contain a human region specialized for color perception, cause hemiachromatopsia, the impaired discrimination of hue in the contralateral hemifield (44,45). Lesions of the lateral occipitotemporal cortex, which likely contains a human homolog of area V5, can cause a hemiakinetopsia, in which the perception of complex motion patterns is degraded in the contralateral field (46,47).

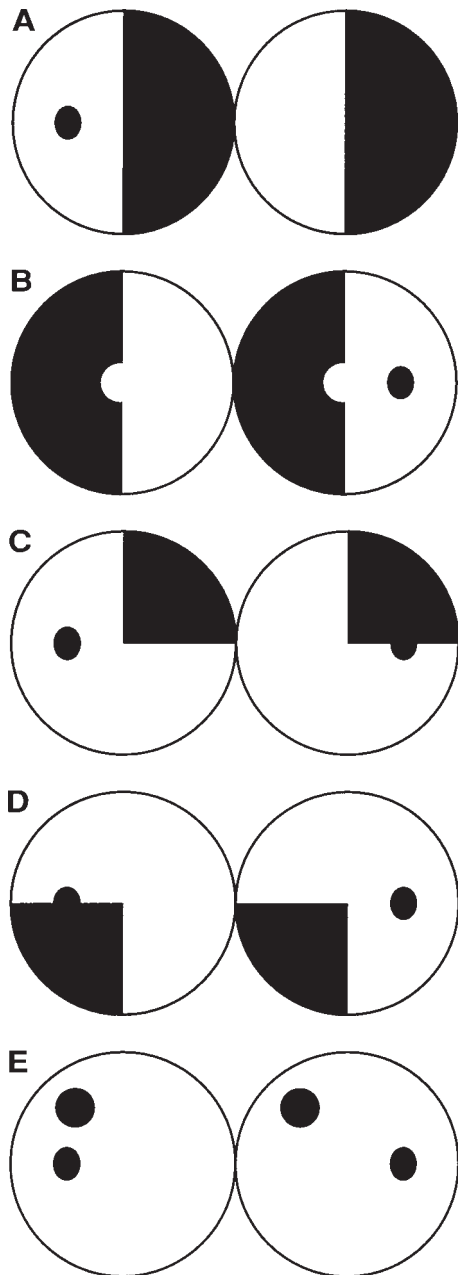


Fig. 17. Illustrations of striate patterns of visual loss. (A) complete macula-splitting hemianopia; (B) macula-sparing hemianopia, from sparing of occipital pole; (C) upper quadrantanopia, from lesion of inferior calcarine bank; (D) lower quadrantanopia, from lesion of superior calcarine bank; (E) congruous hemifield scotomata, from lesion of midzone of inferior calcarine bank.

Current perimetric devices are not designed to pick up these selective hemifield deficits. Adequate testing for such problems requires specialized software or equipment, not commonly found in most clinics or standardized for clinic use.

REFERENCES

1. Hecht S, Shlaer S, Pirenne M. Energy, quanta and vision. *J Gen Physiol* 1942;224:665–699.
2. Land E. Recent advances in retinex theory. *Vision Res* 1986; 26:7–21.
3. Zeki SM. A century of cerebral achromatopsia. *Brain* 1990;113: 1721–1777.
4. Trick G, Trick L, Kilo C. Visual field defects in patients with insulin-dependent and noninsulin-dependent diabetes. *Ophthalmology* 1990;97:475–482.
5. Schiller P, Logothetis N. The color-opponent and broad-based channels of the primate visual system. *Trends Neurosci* 1990;11:392.
6. Sample PA. What does functional testing tell us about optic nerve damage? *Surv Ophthalmol* 2001; 45(Suppl. 3):S319–S324.
7. Radius R, Anderson D. The course of axons through the retina and optic nerve head. *Arch Ophthalmol* 1979;97:1154–1158.
8. Wolff E, Penman G. The position occupied by the peripheral retinal fibers in the nerve fiber layer and at the nerve head. *Trans Ophthalmol Soc UK* 1950;70:35.
9. Hoyt W, Luis O. Visual fiber anatomy in the infrageniculate pathway of the primate: uncrossed and crossed retinal quadrant fiber projections studied with Nauta silver stain. *Arch Ophthalmol* 1962; 68:94–106.
10. Minckler D. The organization of nerve fiber bundles in the primate optic nerve head. *Arch Ophthalmol* 1980;98:1630–1636.
11. Brewster D. *Memoirs of the Life, Writings and Discoveries of Sir Isaac Newton*. Vol. 1. Edinburgh: Thomas Constable and Co., 1855:426.
12. Wilbrand H. Schema des Verlaufs der Sehnervenfasern durch das Chiasma. *Z Augenheilkd* 1926;59:135–144.
13. Horton J. Wilbrand's knee of the primate optic chiasm is an artefact of monocular enucleation. *Trans Am Ophthalmol Soc* 1997; 95: 579–609.
14. Kupfer C, Chumbley L, Downer JDC. Quantitative histology of optic nerve, optic tract, and lateral geniculate nucleus of man. *J Anat* 1967;101:393–401.
15. Hoyt W, Luis O. The primate chiasm: details of visual fiber organization studied by silver impregnation techniques. *Arch Ophthalmol* 1963;70:69–85.
16. Cox T, Corbett J, Thompson H, Kassell N. Unilateral nasal hemianopia as a sign of intracranial optic nerve compression. *Am J Ophthalmol* 1981;92:230–232.
17. Unsöld R, Hoyt WF. Band atrophy of the optic nerve: the histology of temporal hemianopia. *Arch Ophthalmol* 1980;98:1637–1638.
18. Perlmutter D, Rhoton A. Microsurgical anterior cerebral-anterior communicating-recurrent artery complex. *J Neurosurg* 1976;45:259–272.
19. Tassinari G, Campara D, Balercia G, Chilosi M, Martignoni G. Magno- and parvocellular pathways are segregated in the human optic tract. *Neuroreport* 1994;5:1425–1428.
20. Bell R, Thompson H. Relative afferent pupillary defect in optic tract hemianopias. *Am J Ophthalmol* 1978;85:538–540.
21. O'Connor P, Mein C, Hughes J, Dorwart RH, Shacklett DE. The Marcus Gunn pupil in incomplete optic tract hemianopias. *J Clin Neuroophthalmol* 1982;2:227–234.
22. Newman S, Miller N. Optic tract syndrome: neuro-ophthalmologic considerations. *Arch Ophthalmol* 1983;101:1241–1250.
23. Frisén L. The neurology of visual acuity. *Brain* 1980;103:639–670.
24. Renn W, Rhoton AJ. Microsurgical anatomy of the sellar region. *J Neurosurg* 1975;43:288–298.
25. Rhoton A, Harris F, Renn W. Microsurgical anatomy of the sellar region and cavernous sinus. *Clin Neurosurg* 1977;24:54–85.
26. Sillito A, Murphy P. The modulation of the retinal relay to the cortex in the dorsal lateral geniculate nucleus. *Eye* 1988;2(Suppl.): S221–S232.
27. Kupfer C. The projection of the macula in the lateral geniculate nucleus of man. *Am J Ophthalmol* 1962;54:597–609.
28. Shacklett DE, O'Connor PS, Dorwart RH, Linn D, Carter JE. Congruous and incongruous sectoral visual field defects with lesions of the lateral geniculate nucleus. *Am J Ophthalmol* 1984;98:283–290.
29. Connolly M, van Essen D. The representation of the visual field in parvocellular and magnocellular layers of the lateral geniculate nucleus in the monkey. *J Comp Neurol* 1984;226:544–564.
30. Frisén L, Holmegaard L, Rosenkrantz M. Sectoral optic atrophy and homonymous horizontal sectoranopia: a lateral choroidal artery syndrome? *J Neurol Neurosurg Psychiatry* 1978;41:374–380.

31. Fris en L. Quadruple sectoranopia and sectorial optic atrophy: a syndrome of the distal anterior choroidal artery. *J Neurol Neurosurg Psychiatry* 1979;42:590–594.
32. Jacobson D. The localizing value of a quadrantanopia. *Arch Neurol* 1997;54:401–404.
33. Carter J, O’Connor P, Shacklett D, Rosenberg M. Lesions of the optic radiations mimicking lateral geniculate nucleus visual field defects. *J Neurol Neurosurg Psychiatry* 1985;48:982–988.
34. Inouye T. *Die Sehstorungen bei Schussverletzungen der kortikalen Seshphare*. Leipzig: Engelmann, 1909.
35. Holmes G, Lister W. Disturbances of vision from cerebral lesions with special reference to the cortical representation of the macula. *Brain* 1916;39:34–73.
36. Rovamo J, Virsu V. An estimation and application of the human cortical magnification factor. *Exp Brain Res* 1979;37:495–510.
37. Tolhurst D, Ling L. Magnification factors and the organization of the human striate cortex. *Hum Neurobiol* 1988;6:247–254.
38. Horton J, Hoyt W. The representation of the visual field in human striate cortex: a revision of the classic Holmes map. *Arch Ophthalmol* 1991;109:816.
39. McFadzean R, Brosnahan D, Hadley D, Mutlukan E. Representation of the visual field in the occipital striate cortex. *Br J Ophthalmol* 1994;78:185–190.
40. Smith C, Richardson W. The course and distribution of the arteries supplying the visual (striate) cortex. *Am J Ophthalmol* 1966; 61:1391–1396.
41. Felleman D, Van Essen D. Distributed hierarchical processing in the primate cerebral cortex. *Cereb Cortex* 1991;1:1–47.
42. Ungerleider L, Mishkin M. Two cortical visual systems. In: Ingle DJ, Mansfield RJW, Goodale MS, eds. *The Analysis of Visual Behaviour*. Cambridge, MA: MIT Press, 1982:549–586.
43. Horton JC, Hoyt WF. Quadrantic visual field defects: a hallmark of lesions in extrastriate (V2/V3) cortex. *Brain* 1991;114:1703–1718.
44. K lme HW. Pure homonymous hemiachromatopsia: findings with neuroophthalmologic examination and imaging procedures. *Eur Arch Psychiatr Neurol Sci* 1988;237:237.
45. Paulson HL, Galetta SL, Grossman M, Alavi A. Hemichromatopsia of unilateral occipitotemporal infarcts. *Am J Ophthalmol* 1994; 118:518.
46. Greenlee M, Lang H, Mergner T, Seeger W. Visual short-term memory of stimulus velocity in patients with unilateral posterior brain damage. *J Neurosci* 1995;15:2287–2300.
47. Plant G, Laxer K, Barbaro N, Schiffman J, Nakayama K. Impaired visual motion perception in the contralateral hemifield following unilateral posterior cerebral lesions in humans. *Brain* 1993;116: 1303–1335.
48. Curcio C, Sloan K, Kalina R. Human photoreceptor topography. *J Comp Neurol* 1990;292:497–523.
49. Miller N, Newman N. *Walsh and Hoyt’s Clinical Neuro-ophthalmology*. Baltimore: Williams & Wilkins, 1998.
50. Ebeling U, Reulen H-J. Neurosurgical topography of the optic radiation in the temporal lobe. *Acta Neurochir (Wien)* 1988;92:29–36.

3 Perimetry at the Bedside and Clinic

While all of the visual field diagrams in this volume were obtained with a perimetric device, many of the defects they illustrate were detected on clinical examination. There are several reasons why it is worth developing the skill and confidence to probe for field defects with little more than the contents of one's pocket:

1. One does not always have immediate *access* to perimetric instruments. This is particularly the case in the emergency room and in most neurology clinics at present. In the urgent setting, one often has to make decisions about neuroimaging and other investigations before formal perimetry can be obtained.
2. Perimetry is reserved for *selected patients*. For patients not suspected of having a visual field defect, confrontation testing will be the only test of the visual field they will have. A good screening examination of the visual fields must be part of every routine neurologic or ophthalmologic examination. Because people are less attuned to their peripheral than central vision, such screening will occasionally uncover an asymptomatic peripheral field defect.
3. The choice of perimetric device and perimetric strategy should be *guided* by the suspicions aroused by the clinical examination and history. It is pointless to order automated perimetry of the central 24° of vision if one suspects a defect beyond 30°. A small defect within the central 10° of vision is better assessed by automated than Goldmann perimetry. Suspicion of a problem at the optic chiasm can guide the Goldmann perimetrist to concentrate testing around the vertical meridian.

The following is a distillation of clinical practice. Most of it is based on our experience and that of other clinicians; there are only a few studies that have attempted to validate confrontation testing, in contrast to the burgeoning literature on automated perimetry. Nevertheless, we recommend that each clinician perusing the case studies in the Atlas section think about the confrontation strategy that he or she might use to test for each defect depicted.

1. STIMULI

Theoretically, any object can be used for testing. In practice, a series of objects of increasing subtlety are used, approximating a

rough quantification of the severity of the defect and the true probability of a defect existing. A crude hierarchy is as follows:

1. *Hand motion*: The examiner holds a hand within a quadrant and waves it, taking care not to move the forearm or elbow (which are situated in the lower quadrant when testing the upper quadrant). Patients report when they see something moving.
2. *Finger motion*: The examiner holds up a hand within a quadrant and wiggles the index finger rather than the entire hand.
3. *Finger counting/mimicking*: The examiner holds his closed fist in a quadrant, then raises one or two fingers briefly. Patients report whether they see one or two fingers, or mimic with their own fingers what they see if there is some doubt about the reliability of their verbal report, as with children or patients with expressive aphasia. More than two fingers in a quadrant should not be used.
4. *Hand/face comparison*: The examiner holds up two hands in two different quadrants, equidistant from fixation, and asks if one hand appears dim, faded, or blurred compared with the other. If a difference is found, the examiner explores the size of the defect by moving the abnormal hand until it reaches a region where it appears normal. For central vision, the patient fixates the examiner's nose and reports whether some part of the face is blurred, darker, or even missing compared with the rest of the face.
5. *Color comparison*: The examiner uses bright red targets as stimuli. If two are used, quadrants can be contrasted as for hand/face comparison. A response that one target is faded, less intense, or duller is useful. It is hard to know how to interpret a claim that one target is "darker red:" this could mean that the darker target is dimmer or that the other target is faded. If a difference is found, the examiner then moves the defective target in a circle equidistant from fixation until it appears the same as the normal target. If only a single red target is available, this can still be used to determine whether there is a difference across the vertical and nasal horizontal meridians. The examiner moves the target across each meridian repeatedly and asks the patient if they notice any sudden change in the color as the target crosses from the right to left or the upper to lower hemifield.

In general, a larger stimulus will be more easily seen than a small one, a brighter one more than a dimmer one, and a moving one more than a stationary one. As one proceeds down the list, the ability to detect subtle relative defects increases. Thus, a patient may have a superior arcuate defect in which one can still see movement of a hand and count fingers, but note that a hand in the superonasal quadrant is darker than one in the inferonasal field. The patient may also state that a downward moving red target becomes suddenly brighter as it crosses the nasal horizontal meridian.

The price for this increasing sensitivity is a higher false-positive rate (*I*). Variations in ambient lighting and the room background behind the examiner's targets can affect more subtle stimulus comparisons. Overly introspective normal subjects may note subtle variations between quadrants or hemifields. It is useful to ask the patient if there is a sudden change as the stimulus in question moves slowly from the apparently defective area. Many true defects have a sharp border, and this is particularly true at the vertical or nasal horizontal meridians in neurologic disease. A gradual increase in stimulus brightness or color is more in keeping with regional variations in lighting or background.

The type of stimulus chosen will depend on several factors. One factor is how much the examiner suspects the presence of a subtle defect—the “pretest probability.” Another factor is where the suspected field defect is thought to lie. Color testing is not useful for a scotoma in the far periphery, but is excellent for a paracentral one. A third factor is the alertness, attentiveness, and cooperation of the patient. Comparisons of hand or color are not helpful in someone who will not or cannot play the game. On the other hand, a patient who obsesses over details and checks all items on a review-of-systems questionnaire is almost always going to report some difference in color when none exists. A good clue to this patient is that the response to the question about a difference in color is prefaced with a pause, followed by “Um . . .” The experienced examiner realizes when to move on.

2. STRATEGY

Two key points must be stressed at the outset. First, fields are always tested one eye at a time. Monocular defects will not be apparent with both eyes open, and binocular defects that do not overlap will be missed that way too. Testing one eye at a time also means checking carefully that the covered eye is truly covered, with the patch or occluder snug to the nose. Not infrequently a patient will inadvertently peek around the edge of a patch without realizing it. Second, testing is not complete until both eyes are checked. The presence of a second defect in the other eye radically changes the diagnosis (see Case 89).

Almost all students are taught to place themselves 1 m from the patient, have the patient look at their eye, place their hand midway between the patient and themselves, and then march their wiggling finger in from the periphery until the patient responds that he or she sees it. Students are to be reassured if this also matches the point at which they themselves see it.

There are several reasons why this is bad technique. First, and most important, the neural machinery for vision does not emphasize the far periphery. Since 90% of striate neurons (2,3) and retinal ganglion cells are concentrated within the central 30° of vision, it is inefficient to be spending time checking the field at 50–70°. Second, this technique is bound to pick up constrictions related to aging and refractive abnormalities such as dense cata-

acts, which are seldom indications for perimetry. Third, a key mistake sometimes committed with this technique is to forget to check the field within the borders defined by the wiggling fingers. The result is failure to detect paracentral scotomata or arcuate defects. Fourth, it is impossible to check the temporal extent of the field in this manner, unless one places one's hand at or behind the patient's ear. Finally, there is no guarantee that the examiner's own field is normal. (It certainly raises an interesting question of what should be done if the patient sees the target before the examiner.)

A better strategy is to concentrate on comparing quadrants within the central 30°. This can be done both for the central 5–10° and for the remaining paracentral vision.

2.1. CENTRAL VISION

The human face is about 15 cm wide and 20 cm high. At a viewing distance of 1 m, the examiner's face thus spans about 9 by 11°, covering the central 5° (radius) of vision if the patient is fixating on the examiner's nose. Central vision can first be tested by having the patient do this and then asking if any regions of the examiner's face are missing, blurry, or darker than the other parts. If this reveals a defect, or a central defect is strongly suspected even though the patient denies any problem, the test can be supplemented by comparison tests at increased viewing distance (4). The increased area spanned by a given degree of viewing angle at a farther distance allows more room for exploring central defects. Tests at increased distance can use the same colored stimuli and hand or finger presentations employed in testing the paracentral field. With the increased viewing distance, these same targets have smaller retinal images and thus become more effective probes of relative defects. Colored stimuli in particular have been considered useful for central field defects (5).

Although comparison between facial sectors has been considered highly sensitive for defects of macular vision, less observant subjects may deny noting any difference despite severe focal central defects. For example, it is not uncommon for subjects with macular-splitting hemianopia to claim that they see no difference between the left and right sides of the face. In some cases, this is due to an unconscious shift of fixation into the blind hemifield (6), but in others it is not. Vision is driven as much by expectations of what we should see as what we actually do, and a highly stereotyped stimulus such as the face is prone to predictive “filling in,” or the “completion effect” (7).

If the entire central field is depressed, as with central or cecentral scotomata, the entire face may be blurred or dimmed in all regions. A diffuse central defect can be revealed by comparison with the other eye, if the process is monocular, or by comparison with the adjacent paracentral field. To do the latter, examiners can hold one stimulus over their own face and another about 20–30 cm away and ask which is clearer (Fig. 1). Another way is to start a stimulus near the nose and move it slowly outward, to see if it brightens at some point. Both of these methods may be easier to implement at an increased viewing distance. All objects are naturally clearer and brighter at the center of vision than when seen off to the side. Any response that it is easier to see an object in the periphery than at the center is definitely abnormal. However, a subtle central defect may not be sufficient to reverse the inherent physiologic superiority of the macula over the paracentral field. Such subtle defects may be better appreciated by comparison with the other eye.

2.2. PARACENTRAL VISION

Since the width of an extended hand is about the same as a face, a hand 1 m from a patient covers about 10° . Three handwidths on each side of the vertical meridian will cover the central 30° , where 90% of the neurons lie.

Once a defect has been identified in one or more quadrants, the boundaries of the abnormal field must be mapped. This is done by moving targets from within the defective region toward normal quadrants or zones, moving methodically in all directions in sequence. Particular borders have neurologic import.

The nerve fiber layer in the temporal retina is divided along a horizontal raphe (see Chapter 2). Hence, the effect of many lesions of the optic nerve on the nasal field of vision will stop sharply along the horizontal meridian. A desaturated red target or dim hand will suddenly appear more vivid to the patient as it is moved vertically from the defective field to the intact one. This is known as a *nasal step*. When monocular or heteronymous (affecting different hemifields in the two eyes), it always implies a lesion of the retinal ganglion cells or optic nerve, and not a photoreceptor problem.

At the optic chiasm, the visual input of each eye is divided into hemifields, with each hemifield leaving to project to the opposite striate cortex. A hallmark of the vast majority of lesions at or behind the optic chiasm is a sharp border at the vertical meridian. This does not occur with retinopathy or optic neuropathy.

These horizontal and vertical anatomic divides are rigid and cause sharp, abrupt changes in visual sensitivity when there is pathology. The contrast between normal and abnormal vision is especially stark to the patient. By contrast, pathologic borders not located at anatomic divides are shallower and less precise, particularly in the acute stage. Examples are the horizontal flanks of cerebral quadrantanopias and the curving banks of arcuate defects. These types of borders are generated by the regional extent of varied pathologic processes such as ischemia, edema, hemorrhage, tumor infiltration, and diffusion of toxins, which themselves do not have sharp margins in tissue.

After mapping, the defect of one eye always has to be compared with the field of the other eye. Defects in both eyes are incongruous if they affect different regions of the visual field. Bilateral arcuate defects from bilateral optic neuropathy are an example. Heteronymous defects affect different (nonoverlapping) hemifields in the two eyes, as mentioned above. Bitemporal defects from chiasmal lesions are the classic case. Homonymous defects affect the same hemifield in both eyes and usually indicate a retrochiasmal problem. Incongruity of homonymous defects is more typical of lesions of the optic tract, whereas striate lesions cause virtually identical, and hence highly congruous, field defects.

2.3. PLOTTING THE RESULTS

A drawing of the results from confrontation testing in the chart is a helpful supplement to any verbal description. The results can be plotted in two concentric circles, one representing the central field and the other the surrounding paracentral field, both divided into quadrants (Fig. 2). The convention is to plot from the patient's point of view, with the right hemifield and the right eye on the right side. The borders of any defect are drawn, and it should be indicated what it is that can or cannot be seen within the defect.

3. VALIDATION OF THE CLINICAL EXAMINATION

How good are these techniques once properly mastered? There are actually a few studies comparing the results of bedside



Fig. 1. Detecting a central scotoma. The examiner's face is shown, with the central scotoma of the patient overlaid as a region of blurred, darkened vision, when the patient is fixating on the examiner's nose. The examiner places one index finger adjacent to the nose and the other in the paracentral field. The patient reports that the finger near the nose is actually seen less well than the one on the more peripheral hand.

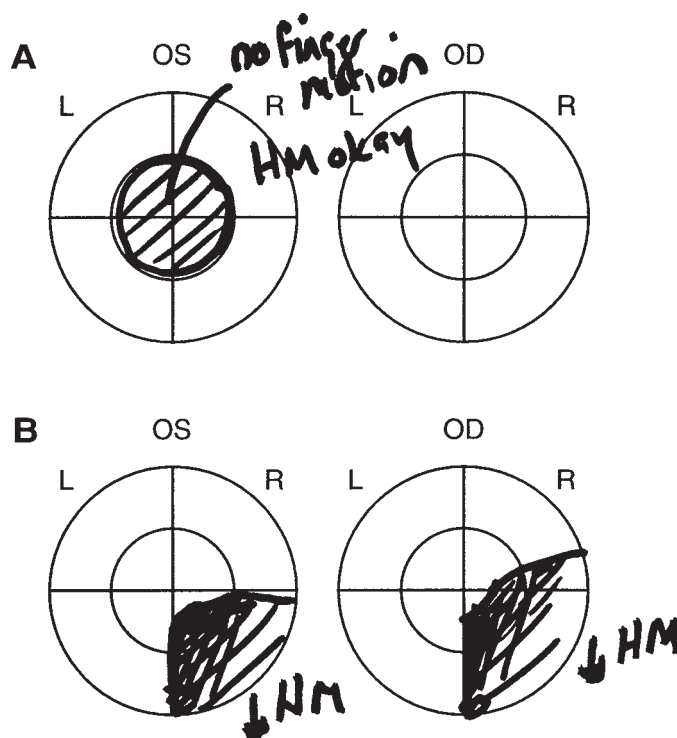


Fig. 2. Plot of confrontation results. Circles represent central and paracentral fields. (A) Example of a relative central scotoma in the left eye, in which hand motion (HM) but not finger motion can be seen. (B) Example of an incongruous homonymous right quadrantanopia.

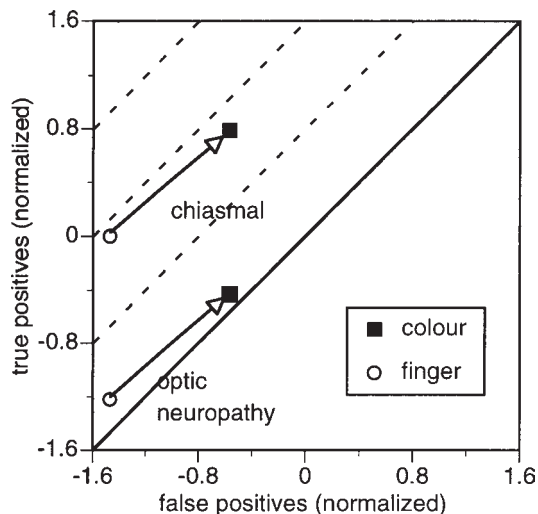


Fig. 3. Detection theory analysis comparing finger to color testing. The true positive rate (y -axis) is plotted against the false positive rate (x -axis) in z -transformed or normalized space. The diagonal lines indicate curves of equal discriminative power. The solid line intersecting the origin in the center is a line with $d' = 0$, i.e., no discriminative power. For either retrochiasmal lesions or optic neuropathies, the switch to colored targets results in a shift that is parallel to the diagonal lines, indicating that one does not gain in discriminative power but is merely shifting the criterion for a positive result (see Appendix, Fig. 5).

examination to the current “gold standards,” automated and manual perimetry.

Not unexpectedly, the data show that the sensitivity depends on the type of defect one is trying to detect. Finger motion and face comparison detects about 75–90% of homonymous hemifield defects on automated static perimetry (8,9). With disease at or anterior to the optic chiasm, sensitivities are highly variable. Altitudinal defects and central scotomata are detected 80–100% of the time, but arcuate defects, paracentral scotomata, and constrictions are detected only 20–50% of the time (8,9). In another study anchored to Goldmann perimetry, “optic nerve defects” were detected only 10% of the time by any finger test, whether motion, counting, or comparison (1).

Presumably, the reduced sensitivity to optic neuropathic defects relates to the size of the affected area as well as the severity of the visual loss. Both will often be less than that seen with hemifield defects from cerebral lesions. In a quadrant, the mean reduction in sensitivity on automated perimetry associated with a 50% probability of detection by finger motion confrontation testing was estimated at about 20 dB, a 100-fold reduction in normal threshold intensity (9).

Surprisingly, only 50% of bitemporal defects on automated or Goldmann perimetry are found with either finger motion, finger counting, or hand comparison, without much difference among the three (1,8). Color confrontation tests involving comparisons between two stimuli or a single moving target were both more sensitive, detecting 78% of chiasmal defects.

False positives to finger motion occur in only about 3–6% of eyes normal on automated static perimetry (8,9). In another study comparing the bedside clinical examination to Goldmann perimetry, none of 14 normal fields were classified as abnormal by

confrontation with finger motion, comparison, or counting, but 4 of 14 were false positives on color confrontation fields (1).

What does a more sensitive test like color confrontation really mean for the examiner? Since there are also more false positives, it is not clear whether color testing really discriminates more accurately between the normal and the abnormal eye. Signal detection theory (see appendix) offers us a means to answer this problem. In normalized plots of true positive rates (sensitivity) vs false positive rates ($1 - \text{specificity}$), if the false positive rate increases at the same rate as the true positive rate, then there is no real increase in discriminative power (d'). Rather, this would represent a shift in the criterion used by the subject. A proportionate increase would indicate that the subject is relaxing his or her internal rules for deciding what constitutes a positive (abnormal) event.

If we plot the data from Trobe et al. (1), this is precisely what is happening when one moves from tests based on finger comparison to color comparison or kinetic color testing (Fig. 3). While it is true that color comparison picks up more defects, the false-positive rate increases at the same rate, indicating a criterion shift. While d' is greater for chiasmal than optic neuropathic defects, this does not change between finger and color testing (d' for optic neuropathy = 1.22 for both color and finger; d' for chiasmal defects = 1.47 for finger and 1.36 for color).

Although the numbers from Trobe et al. (1) are small, this has certain implications. The examiner is not really using a “better” test with color testing over finger counting. The patient is simply shifting to a looser criterion for what constitutes a positive response. It is akin to adjusting the level that indicates a positive response on a laboratory test. A strict criterion (finger motion) is good for a diagnostic test, in which a positive result is highly indicative of disease, though a negative result is meaningless. A looser criterion (color comparison) is better for a screening test, in which a negative result more effectively excludes disease, but at the price of more false positives that will need further evaluation.

The one area where color tests come into their own is the central field. Color vision is much better and reliable in central regions, where small defects may be difficult to test with large stimuli such as fingers and hands. A strategy of moving the target in circular paths at constant distance from fixation has been reported to be as highly sensitive and is also specific to many pre- and postchiasmal defects as Goldmann perimetry (5).

4. CLINICAL ADJUNCTS TO CONFRONTATIONAL TESTING

4.1. CENTRAL VISION: THE AMSLER GRID

The Amsler grid is a rectangle of chart paper with a fixation spot at the center of the rectangle (Fig. 4). When held at about 28 cm (11 in.) away from the subject, each 0.5-cm grid square spans 1° . The examiner shows the grid to the patient, so that the patient appreciates that these are straight vertical and horizontal lines on the paper. The patient is then told to keep looking at the fixation spot, while the examiner watches to see that the patient understands and complies, and to report if any region of the grid is missing or distorted. If so, the patient is asked to outline with a finger or a pen the region that is abnormal.

While the Amsler grid was designed with the aim of delineating the defects associated with macular disease, it is useful for central scotomata of any origin, from optic neuropathy to striate lesions. One important differentiating point between retinal disease and

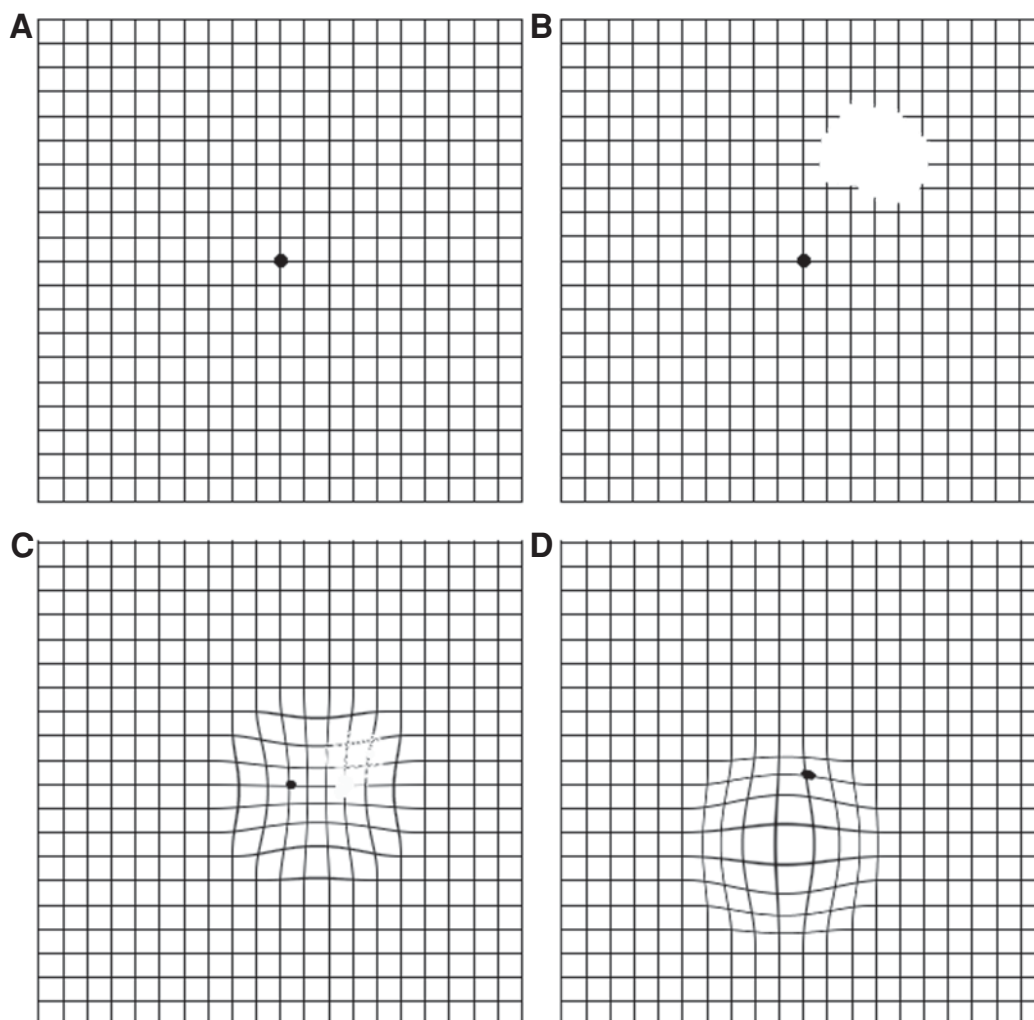


Fig. 4. The Amsler grid. (A) shows an example of the sheet. (B) shows how it might appear to someone with a parafoveal scotoma. (C) shows micropsic distortion due to macular edema, because the photoreceptors become more widely spaced. There may also be zones where lines are fragmented or disappear. (D) shows retinal macropsia related to chronic retraction and retinal scarring, reducing the spacing between photoreceptors. Both of these distortions indicate retinopathy, whereas scotomata occur with either retinopathy or neuropathy at any level.

neuropathic disease is the report of distortion or local curving of the grid (10–12). Macular edema will increase the separation between photoreceptors; thus, there will be fewer photoreceptors than normal between the images of two lines cast on this retinal region. The result is that the two lines will appear closer together in this region than they do elsewhere. On the other hand, macular scarring can reduce the distance between photoreceptors, causing lines to bow outward rather than inward. Such distortions do not occur with central scotomata from optic neuropathy.

4.2. PARACENTRAL VISION: TANGENT (BJERRUM) SCREEN PERIMETRY

The tangent screen is actually a type of perimetry—in fact, the cheapest and easiest of techniques—but can be considered a clinical adjunct because it can be run in any examining room. Typically, a black felt screen is placed on a wall. The patient sits at a fixed distance from the screen, so that the examiner knows how many centimeters on the screen correspond to how many degrees of visual field. If one is designing one's own screen, a useful number to remember is 57 cm, because at this viewing distance 1° of

visual angle would equal 1 cm on the screen, since $1/\tan(\pi/180 \text{ radians}) = 57.3$. At a screen distance of 1.14 m, 1° equals about 2 cm on the screen. Most commercial tangent screen preparations are designed for testing at 1 m, at which distance 1° equals 1.7 cm. (Of course, since these are flat screens rather than bowls, angles farther away from fixation occupy more space on the screen than angles near fixation.)

The examiner stands beside the screen, holding a black wand with a white target at its tip, which can be exchanged for targets of different size. A kinetic strategy similar to that described for Goldmann perimetry is used to explore the field. Twisting the wand to hide then reveal the white target can mimic a static presentation.

Although this is certainly an advance on confrontation testing, tangent screen perimetry has its limits compared with Goldmann perimetry:

1. It is difficult for a single examiner to monitor both patient fixation and the location of the target on the screen. From a stance beside the screen, the examiner can look at the patient's eyes or the screen, but not both.

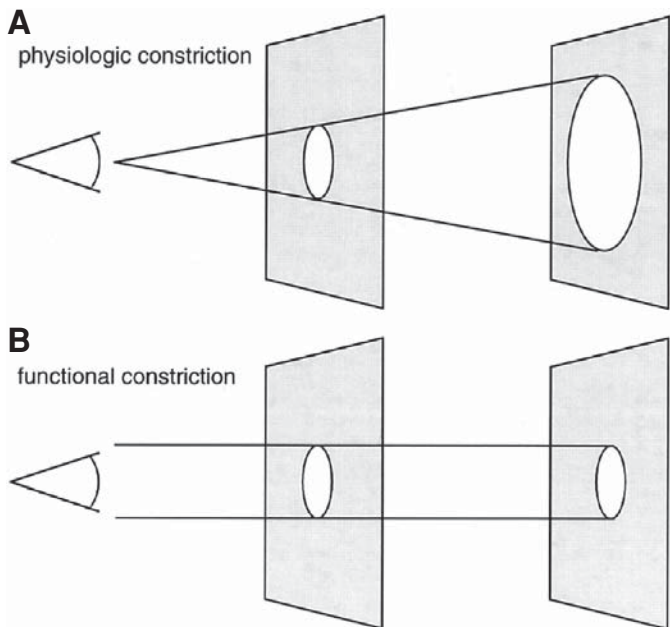


Fig 5. Functional vs physiologic constriction. True constriction (A) is a cone that encompasses progressively larger areas at increasing viewing distance. Functional constriction (B) is a cylinder, in which the remaining circle of vision does not vary with viewing distance.

2. Lack of control over, or calibration of clinic room lighting makes tangent screen testing incompletely standardized.
3. The procedure does not generate a formal record during the test.
4. Because the screen is a flat surface and not a bowl, the examiner cannot test very far into the peripheral field. To test at 80° in the peripheral visual field would require presenting a very large target more than 3 m away from the center of the screen. This last point is not necessarily a major drawback, though, since many defects of interest are within the central 30° .

A modified version of tangent perimetry can even be performed at the bedside of an inpatient, using the wall of the room as the screen and dark rather than light targets. Overall, however, if more formal perimetry is desired, Goldmann perimetry has benefits that outweigh the convenience of tangent screen perimetry.

5. SPECIAL CLINICAL PROBLEMS

5.1. FUNCTIONAL VISUAL LOSS

The most common functional field complaint is diffuse constriction. There are two major goals of any examination of functional defects. The first is to show that the deficit does not conform to physiologic patterns. The second is to prove what the real level of function is behind the factitious claim.

The functional constriction pattern does not display any vertical or nasal horizontal meridian effects, unlike constriction from optic neuropathy or bilateral cerebral disease. Most patients are also not sophisticated enough to realize that the angle of vision that they claim to possess should cover a larger area in the distance than up closer. Hence, their pattern of constriction resembles a cylindrical tunnel rather than a cone—a “tunnel rather than a funnel” (Fig. 5) (13). That is, patients report that

they have only a 1-m-diameter circle of vision left no matter whether the examiner is testing them at a distance of 1 or 3 m. If the constriction is physiologic, the 1-m circle found at a distance of 1 m should expand to 3 m at a distance of 3 m. To be strictly correct, the size of the target should be increased proportionally as well, but with coarse large stimuli such as moving hands, this is not a significant issue.

One means of proving the true extent of peripheral vision in these patients is to move the target toward them, rather than moving farther away. Most people have the expectation that the closer a target is, the easier it is to see it. Yet if a target is moving toward a subject parallel to the line of sight, it is actually moving farther into the peripheral field. It is not uncommon for subjects to finally respond that they see the target when it is about a foot away from them, at which point it is about $50\text{--}60^\circ$ in their periphery. This is strong evidence that the patient actually has fairly extensive peripheral vision. One caveat, though, is that a mid-peripheral scotoma could also mimic this pattern. The classic example is the patient with sparing of the monocular temporal crescent. However, this should have been detected with the standard confrontation examination at a fixed distance from the subject and can be verified with the Goldmann perimeter.

On occasion, the examiner faces a functional hemianopia. Most of these patients do not realize that the visual fields of the two eyes overlap, and that a true hemianopia that respects the vertical meridian affects both eyes (see Case 99). Rather, they usually claim that the temporal half of one eye alone is affected. Hence, with a purported left hemianopia, the examiner may find a hemianopia with the left eye viewing and also with both eyes viewing, but not when the right eye views alone (14). The contradiction between right eye and binocular fields is evident. This is one of the few situations in which testing fields with both eyes open is useful.

5.2. VISUAL TESTING IN INATTENTIVE OR APHASIC ADULTS

Patients who cannot understand or cooperate pose a special challenge to any sensory testing, which usually depends on some self-report of perceptual experience. Self-report requires that the patient comprehend instructions and communicate back; hence, dementia, confusional states, and aphasia are limiting factors in testing sensation.

Vision is no exception. The examiner cannot expect to find subtle relative field defects in such patients. However, a severe reduction in vision in one quadrant or hemifield should be detectable.

The first difficulty is to have the subject maintain steady fixation. Confused subjects are often distractible and may not fixate on one point for more than a few seconds at a time, and the examiner must catch whatever opportunity brings. Usually a steady gaze at a patient's eyes can arrest their gaze on the examiner's face for a few moments.

If the subject has sufficient language and attention to hold a conversation, finger counting in each quadrant may be tried. The fingers must be flashed briefly, since inattentive or confused patients invariably look toward the moving fingers. This in itself can be taken as an index of perception, though researchers in blindsight argue that saccadic localization of targets can occur in patients with striate lesions (in general, blindsight saccadic localization is very inaccurate compared with normal saccades to consciously appreciated targets). If the patient can understand the test but has an expressive aphasia, or does not speak the

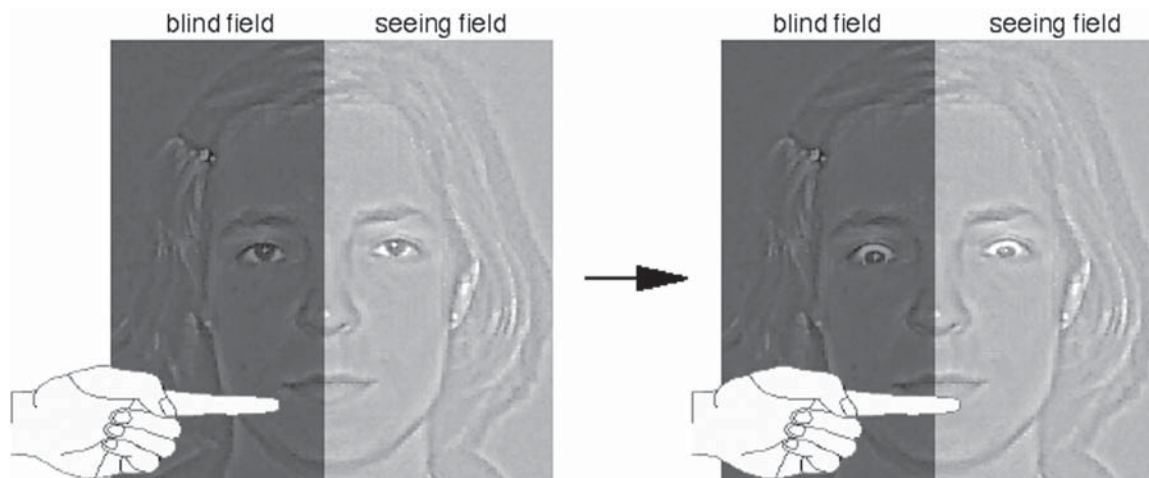


Fig. 6. The “looking test” in hemianopia. The patient is depicted looking at the examiner’s face. The examiner surreptitiously moves their finger from the blind hemifield toward the seeing one. As the finger crosses the vertical meridian, it appears suddenly to the patient, who reflexively looks toward it. This can be done in both the upper and lower fields.

examiner’s language, the patient may still be able to mimic the number of fingers held up.

If the patient is too aphasic or confused to understand and follow instructions, looking toward a suddenly moving or appearing target is the best index. A classic sign of hemianopia in the uncommunicative patient can be elicited by bringing a moving finger or hand from the blind field toward the seeing field. As the moving object crosses the vertical meridian, its sudden appearance in the seeing field often elicits a vertical saccade toward it. Consistent reproduction of this sign is solid evidence of hemianopia (Fig. 6).

Examination in the stuporous or comatose patient is even more problematic. Blinking to threat is treated as a sign of preserved vision, yet whether it truly reflects preserved pathways for conscious vision is not clear. Nevertheless, some examiners try to determine whether blinking is asymmetric between the right and left hemifields. Care must be taken not to stimulate the cornea with a sudden puff of air, which can elicit a corneal reflex. Overall, we have been less impressed by either the utility or the reliability of this technique in the comatose patient.

5.3. VISUAL TESTING IN CHILDREN

Many of the same issues that vex the perimetrist with inattentive adults occur with children who are too young to understand perimetry or persist with what can turn into a long, boring experience. Most children older than 8 yr of age can cooperate with all adult testing and even perform perimetry. Between the ages of 5 and 8 they can count one or two fingers. Younger than age 5, mimicking the number of fingers held up is possible. Younger than age 3, saccades toward a suddenly moving target with some appeal (but no noise) is most reliable. It is even possible to do reasonable perimetry in young children based on this looking principle (15).

5.4. MACULA SPARING OR MACULA SPLITTING?

Some patients with hemianopia seem to have a small zone of spared vision surrounding fixation. Hence, they respond to a target moving toward fixation just before the target reaches it. Sparing of the central 5° of vision is termed macula sparing and is considered pathognomonic of a striate lesion (Chapter 2). As with all central field issues, this is best demonstrated by increasing the viewing distance, having the patient fixate on the narrow tip of some object

such as a pen or finger, and then moving a small precise object such as a finger toward that tip.

Macula-splitting hemianopia has less localizing value, because it can occur with a lesion anywhere from the optic tract to striate cortex. However, some patients with hemianopia may give a false appearance of macula sparing. Many adapt to their severe defect by shifting fixation slightly into the hemianopic side of space (16), thus placing more of a fixated object in their seeing hemifield. Some do this constantly; others make repeated small horizontal saccades around fixation, much like square-wave jerks. Both will also respond to a moving finger just before it reaches the tip of the other finger that they are fixating. To differentiate true macula sparing from pseudo-sparing due to fixation shift, the examiner must then test at the vertical meridian above and below the macula. In true macula sparing, the hemianopia will terminate exactly at the vertical meridian when tested outside of the macula. In pseudo-sparing, the hemianopic boundary outside the macula will also fall just short of the vertical meridian.

A clever strategy for demonstrating this simultaneously is to use three objects on a vertically held stick, one object above another (Fig. 7). The objects should be large enough that they are easily visible in the midperiphery. The stick is advanced from the blind field toward the seeing field, with the middle object traveling along the horizontal meridian. In true macula-sparing the middle object will be seen first, with the others following shortly after. In macula-splitting hemianopia with fixation shift, all objects will appear at the same time.

5.5. NEGLECT OR HEMIANOPIA?

For patients who have a story of bumping into objects on one side, a frequent question is: Is it neglect or hemianopia? This is especially relevant to patients with lesions of the right or non-dominant cerebral hemisphere, because contralateral hemineglect of the left side is far more common than right hemineglect after left-sided lesions (17). Hemineglect is a defect in attention that has a horizontal bias, being worse for the (contralateral) left side. This can have multiple frames of reference. Patients may ignore the objects on the left side of space, or the left side of objects, even those in right hemisphere (18). With text, for example, they may fail

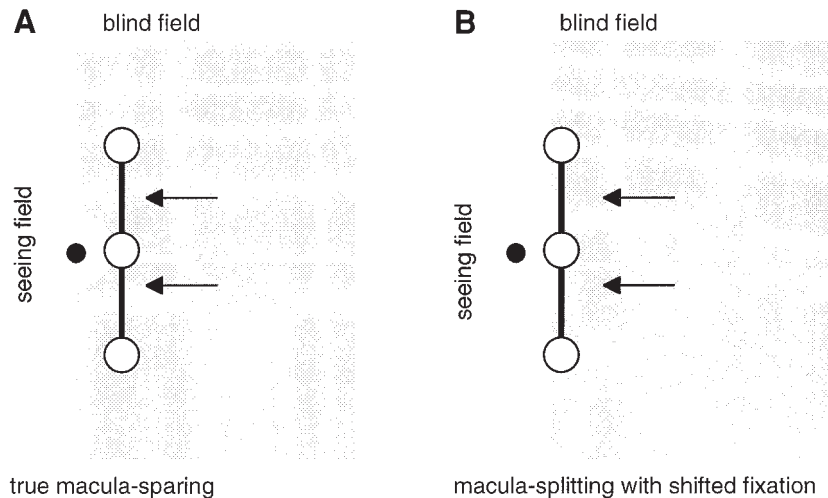


Fig. 7. A test for macula sparing. The patient is supposed to be fixating on the black spot. Three objects more than 5° apart and vertically aligned are advanced from the blind to the good hemifield, with the center object moving along the horizontal meridian. In true macular sparing (A), this central object is seen before the other two discs. In macula-splitting hemianopia with fixation shifted into the blind field (B), all three objects are seen simultaneously.

Table 1
Neglect vs Hemianopia

	<i>Hemianopia</i>	<i>Hemineglect</i>
1. Detection of stimuli		
Awareness of defect	Yes	No
Modality	Visual only	Often multimodal
Extinction	Unusual	Common (also with two targets in the ipsilesional hemifield!)
Contralateral cueing	Ineffective	Improves neglect
2. Performance of neglect tests		
Line bisection bias	None or contralesional	Ipsilesional
Drawing (e.g., clocks)	Normal	Lack of contralesional details
3. Exploration of space		
Contralesional saccades	Increased (chronically)	Decreased
Object search tests	Contralesional emphasis	Contralesional neglect
4. Lesions		
Hemisphere	Right or left	More often right

to read the left side of lines, starting midway on the page, and also omit or alter the left side of the words that they do detect on the right side (19,20). This left neglect can also affect their reading of the Snellen acuity charts.

Patients with acute onset of hemianopia can display similar omissions, especially when the hemianopia involves the macula. If a subject does not report an object in left space, how can the examiner determine whether this is neglect or hemianopia? There are several key differences (21) (see Table 1).

First, hemineglect is a gradient of inattention spanning all of space (22). If an ignored item on the left is moved slowly toward the right, the point at which it is eventually detected is quite variable (23). This will depend on the salience of the object, the presence of other distracters, the use of cueing toward contralateral space (24), and other nonspecific factors such as fatigue and arousal level. It may also vary within the examination. By contrast, hemianopia always has a sharp demarcation at the vertical meridian for objects of any size or salience, and cueing does not help.

Second, the frame of reference for hemineglect may not be retinotopic. The space that is ignored may be anchored to the object (object centered), the head (craniotopic), the body center (somatotopic), or the environment (25). If the field assessment is repeated with the eyes in right gaze, the patient may now report objects in the left hemifield of vision, which has now been displaced by gaze into the right hemispace (Fig. 8).

Third, a frequent part of the hemineglect syndrome is the failure to explore the hemispace contralateral to the lesion. Patients with hemianopia who have been aware of their defect for some time learn to explore the side of space in their blind field. In particular, they use eye movements to compensate, and they are less likely to miss items on the left side, if given enough time to search. In fact, patients with hemianopia explore the contralateral space more than normal subjects (26,27). Thus, they have an adaptive gradient of attention that stresses exploration of the contralateral (blind) side, in contrast to the pathologic gradient in neglect that ignores the contralateral side. The examiner can

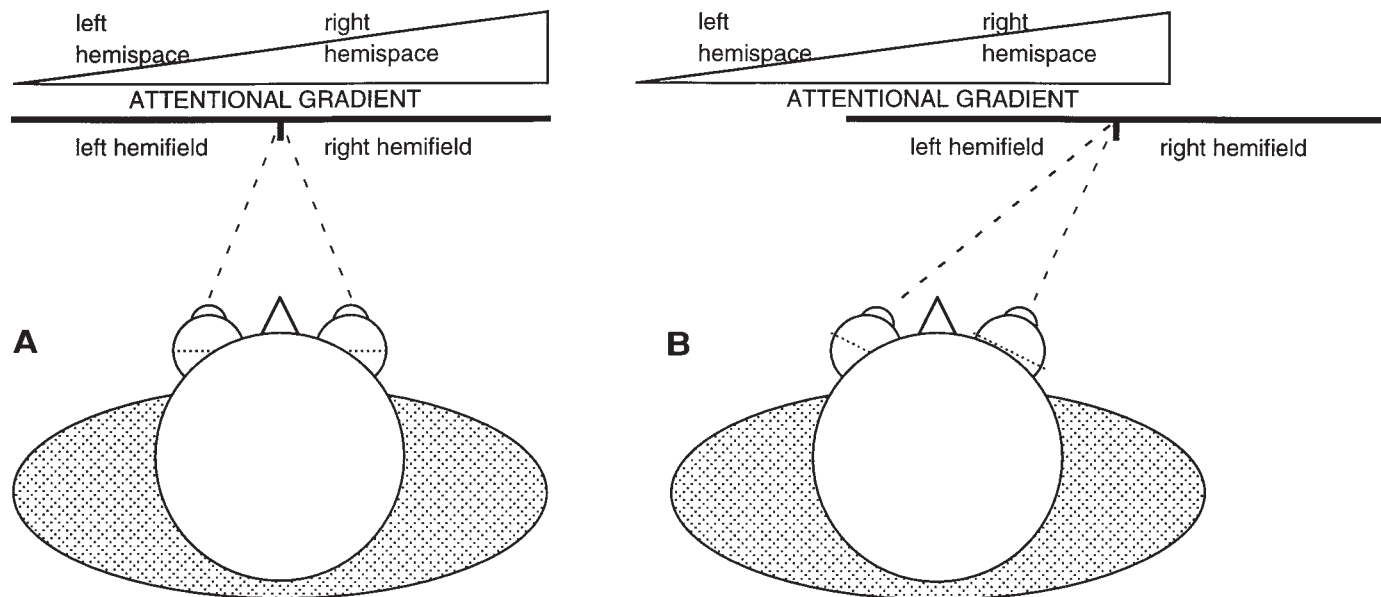


Fig. 8. Neglect vs hemianopia. (A) Unlike hemianopia, which has a sharp demarcation at the midline, hemineglect is a gradient across space, and neglected targets will not suddenly enter awareness at the midline consistently. (B) While the hemifields will always move in space as the eyes move, neglect often is referenced to the hemispace, not the hemifield. Restesting the patient with the eyes turned right will show that, in hemianopia, objects will still not be seen until they cross the vertical meridian in the visual field. However, with neglect, objects may be easier to see in the left hemifield because they are now actually in the right hemispace.

observe this difference in either their eye movements (26,27) or their results in tasks in which they have to scan a page searching for objects, such as line cancellation. When asked to indicate the midposition of a horizontal line (line bisection), left hemineglect patients place their mark toward the right end of the line, whereas patients with left macula-splitting hemianopia actually place their mark slightly toward the left end (28).

Fourth, neglect is often multimodal. Hence, patients may also ignore sounds on the left or touch on the left side of the body.

Extinction refers to the finding in which a patient reports an item in the contralateral hemifield when it is shown alone, but fails to see it when it is presented simultaneously with another object in the ipsilateral hemifield. It is often used as evidence of neglect, but a subtle relative field defect may also show the same phenomenon.

Despite these differences, it remains to be said that many patients with left hemineglect from right parietal lesions can have left hemianopic defects from damage to the optic radiations. The prognosis for rehabilitation of hemianopia is worse when it is accompanied by persistent hemineglect, because such patients are often unaware (anosognosic) of the visual loss. This interferes with the learning of adaptive strategies to use eye movements to scan contralateral space.

5.6. HEMIACHROMATOPSIA

Beyond the striate cortex, visual processing fans out into a large array of extrastriate visual cortex (29). These regions become progressively more specialized for the types of visual input that they process, and less specific for the area of visual field represented. Thus, areas selective for face processing will respond to faces regardless of the region of visual field that they occupy. Early levels of the extrastriate hierarchy do have

some retinotopic organization, though, and it is possible to find deficits for color and motion perception confined to one hemifield or one quadrant.

Hemiakinetopsia occurs with lesions of the V5 (middle temporal, or MT) area in monkeys, and the human homolog of this region is located in lateral occipitotemporal cortex. However, testing for this defect remains a research endeavor requiring specialized software (30,31).

Hemiachromatopsia, on the other hand, can be detected at the bedside (see Case 76). It is the result of a lesion of the fusiform and lingual gyri (32). Patients with hemiachromatopsia will still detect colored stimuli in the hemifield contralateral to their lesion, as long as these differ in brightness from the background and are not placed in a dense hemifield defect. (An associated superior quadrantanopia is common, from damage to the inferior calcarine bank or optic radiations.) However, they cannot discriminate the hue or saturation of these objects and may not be able to name their colors (33,34). This should be contrasted with their ability in a mirror region of similar eccentricity in the ipsilateral hemifield to ensure that the targets are not too far in the retinal periphery, where color vision is naturally poor.

Most commercial color tests are designed for testing central vision. These are designed so that with the approved lighting—usually illuminant C, mimicking natural daylight—the targets differ only in hue or saturation, not in brightness. Holmgren wool strands have been used to test peripheral color vision (33). Chips from the Farnsworth-Munsell 100-hue test or the D15 could also be used. Without these, the examiner can resort to colored bottle caps or strips of colored paper (35), even though they will vary in brightness. As long as the patient does not know ahead of time which color is the brighter, this will not matter. Hence, the impaired field should be tested first.

REFERENCES

1. Trobe JD, Acosta PC, Krischer JP, Trick GL. Confrontation visual field techniques in the detection of anterior visual pathway lesions. *Ann Neurol* 1981;10:28–34.
2. Horton J, Hoyt W. The representation of the visual field in human striate cortex: a revision of the classic Holmes map. *Arch Ophthalmol* 1991;109:816–824.
3. McFadzean R, Brosnahan D, Hadley D, Mutlukan E. Representation of the visual field in the occipital striate cortex. *Br J Ophthalmol* 1994;78:185–190.
4. Kodsi SR, Younge BR. The four-meter confrontation visual field test. *J Clin Neuroophthalmol* 1993;13:40–43.
5. Frisen L. A versatile color confrontation test for the central visual field: a comparison with quantitative perimetry. *Arch Ophthalmol* 1973;89:3–9.
6. Gassel M, Williams D. Visual function in patients with homonymous hemianopia III. The completion phenomenon: insight and attitude to the defect; and functional efficiency. *Brain* 1963;86:229–260.
7. Gassel M, Williams D. Visual function in patients with homonymous hemianopia II. Oculomotor mechanisms. *Brain* 1963;86:1–36.
8. Johnson LN, Baloh FG. The accuracy of confrontation visual field test in comparison with automated perimetry. *J Natl Med Assoc* 1991;83:895–898.
9. Shahinfar S, Johnson LN, Madsen RW. Confrontation visual field loss as a function of decibel sensitivity loss on automated static perimetry: implications on the accuracy of confrontation visual field testing. *Ophthalmology* 1995;102:872–877.
10. Frisèn L, Frisèn M. Micropsia and visual acuity in macular edema: a study of the neuro-retinal basis of visual acuity. *Albrecht von Graefe's Arch Klin Exp Ophthalmol* 1979;210:69–77.
11. Sjostrand J, Anderson C. Micropsia and metamorphopsia in the re-attached macula following retinal detachment. *Acta Ophthalmol* 1986;64:425–432.
12. Enoch J, Schwartz A, Chang D, Hirose H. Aniseikonia, metamorphopsia and perceived entoptic pattern: some effects of a macular epiretinal membrane, and the subsequent spontaneous separation of the membrane. *Ophthalmic Physiol Opt* 1995;15:339–343.
13. Bose S, Kupersmith M. Neuro-ophthalmologic presentations of functional visual disorders. *Neurol Clin* 1995;13:321–339.
14. Keane J. Hysterical hemianopia: the “missing” half field defect. *Arch Ophthalmol* 1979;97:865–866.
15. Dobson V, Brown AM, Harvey EM, Narter DB. Visual field extent in children 3.5–30 months of age tested with a double-arc LED perimeter. *Vision Res* 1998;38:2743–2760.
16. Bischoff P, Lang J, Huber A. Macular sparing as a perimetric artifact. *Am J Ophthalmol* 1995;119:72–80.
17. Weintraub S, Mesulam M-M. Right cerebral dominance in spatial attention. *Arch Neurol* 1987;44:621–625.
18. Chatterjee A. Picturing unilateral spatial neglect: viewer versus object centered reference frames. *J Neurol Neurosurg Psychiatry* 1994;57:1236–1240.
19. Behrmann M, Moscovitch M, Black S, Mozer M. Perceptual and conceptual factors in neglect dyslexia: two contrasting case studies. *Brain* 1990;113:1163–1183.
20. Karnath H-O, Huber W. Abnormal eye movement behaviour during text reading in neglect syndrome: a case study. *Neuropsychologia* 1992;30:593–598.
21. Kerkhoff G, Schindler I. Hemineglect versus Hemianopsie. *Hinweise zur Differentialdiagnose. Fortschr Neurol Psychiat* 1997;65:278–289.
22. Kinsbourne M. Mechanisms of unilateral neglect. In: Jeannerod M, ed. *Neurophysiological and Neuropsychological Aspects of Spatial Neglect*. Amsterdam: Elsevier, 1987:69–86.
23. Gainotti G. The dilemma of unilateral spatial neglect. *Neuropsychol Rehab* 1994;4:127–132.
24. Riddoch M, Humphreys G. The effect of cueing on unilateral neglect. *Neuropsychologia* 1983;21:589–599.
25. Karnath H-O, Fetter M, Niemeier M. Disentangling gravitational, environmental and egocentric reference frames in spatial neglect. *J Cogn Neurosci* 1998;10:680–690.
26. Behrmann M, Watt S, Black S, Barton J. Impaired visual search in patients with unilateral neglect: an oculographic analysis. *Neuropsychologia* 1997;35:1445–1458.
27. Barton J, Behrmann M, Black S. Ocular search during line bisection: the effects of hemineglect and hemianopia. *Brain* 1998;121:1117–1131.
28. Barton J, Black S. Line bisection in hemianopia. *J Neurol Neurosurg Psychiatry* 1998;64:660–662.
29. Felleman D, Van Essen D. Distributed hierarchical processing in the primate cerebral cortex. *Cereb Cortex* 1991;1:1–47.
30. Greenlee M, Lang H, Mergner T, Seeger W. Visual short-term memory of stimulus velocity in patients with unilateral posterior brain damage. *J Neurosci* 1995;15:2287–2300.
31. Plant G, Laxer K, Barbaro N, Schiffman J, Nakayama K. Impaired visual motion perception in the contralateral hemifield following unilateral posterior cerebral lesions in humans. *Brain* 1993;116:1303–1335.
32. Damasio A, Yamada T, Damasio H, Corbett J, McKee J. Central achromatopsia: behavioral, anatomic and physiologic aspects. *Neurology* 1980;30:1064–1071.
33. Kölmel HW. Pure homonymous hemiachromatopsia: findings with neuroophthalmologic examination and imaging procedures. *Eur Arch Psychiatr Neurol Sci* 1988;237:237–243.
34. Paulson HL, Galetta SL, Grossman M, Alavi A. Hemiachromatopsia of unilateral occipitotemporal infarcts. *Am J Ophthalmol* 1994;118:518–523.
35. Albert ML, Reches A, Silverberg R. Hemianopic color blindness. *J Neurol Neurosurg Psychiatry* 1975;38:546–549.

4 Goldmann Perimetry

The Goldmann perimeter is the most common device providing standardized manual exploration of the peripheral visual field in clinical practice. It presents targets on a bowl set 33 cm away from the cornea of the patient, with a background illumination of 31.5 apostilbs (asb). The choice of target size and brightness and its presentation are under the moment-to-moment command of the perimetrist.

1. PREPARATION FOR GOLDMANN PERIMETRY

1.1 CALIBRATION OF THE PERIMETER

Calibration of the perimeter should be a routine morning task for machines in daily use. The exact procedure differs among machines of different vintage and manufacture but is generally simple and outlined in a page or two in the manuals provided with each perimeter. Both the target luminance and the background luminance need to be calibrated.

1.2. "CALIBRATION" OF THE PATIENT

Calibration of the patient requires that the patient wear corrective lenses appropriate for near viewing, when testing in the central 20–30°. If the patient is wearing contact lenses that provide suitable near correction, so much the better. In fact, for aphakic patients or those with high myopia, contact lenses may provide a more accurate rendition of both peripheral and central fields. Otherwise, the perimeter provides a lens holder in which a lens can be placed if correction is needed. Although it is possible to do perimetry with a patient's own reading glasses, the variety in the shape of frames makes it difficult to know where different frames obscure the field of vision. At least with the lens holder, the location of the holder artifact is standardized.

Correction does not make much of a difference for large targets detected outside of the central 20°, but poorly focused small targets have diffused fainter images that create an artifactual shrinkage of central isopters. One essentially has to climb higher on Traquair's island to perceive a blurred point. With visual defects, this sometimes causes not just a generalized constriction for that isopter, but also an apparent qualitative change in the shape of the isopter, just as isopters for different targets will have different shapes in relative field loss. When following a patient's field loss over time, a refractive change may thus create the appearance of

Table 1
Lens Correction by Age

<i>Age (yr)</i>	<i>Add to distance glasses (diopters)</i>
30–39	+1.00
40–44	+1.50
45–49	+2.00
50–54	+2.50
55–59	+3.00
>60, aphakia	+3.25

a qualitative change. The clue that this has occurred will be a general constriction of the isopter as well as the alteration in shape (see Fig. 14).

There is an approximate guide for how many plus diopters need to be added to a patient's distance correction for suitable near refraction, given their age (Table 1). This can be used when patients are not aware of their reading prescription.

Is near correction always necessary? For neurologists, it is difficult to access a lensometer to measure the strength of a patient's correction, and few patients know the power of the lenses in their glasses. For a single diagnostic assessment, correction can be omitted or patients can be tested with their own reading glasses (but not bifocals, which will distort the field in strange ways). Whatever is done should be noted on the perimetric record. Most of the time the examiner is not interested in how absolutely sensitive the visual field is, but whether there are distortions in one part of the field relative to another, and this should be apparent with either a blurred or a finely focused target. Following the visual field over a few weeks or months will not be hampered by lack of correction either, because the refractive power of most subjects is stable over the short term. Problems are more likely to occur when following subjects over months to years in their early forties, when presbyopia is incipient and reading power is changing. Older subjects are at risk for cataracts, which sometimes develop with surprising speed. These can be associated with a change in reading correction too, generally a hyperopic shift, but a good part of the blur will be the light-scattering effect of the opacification and will not be correctable by lenses anyway.

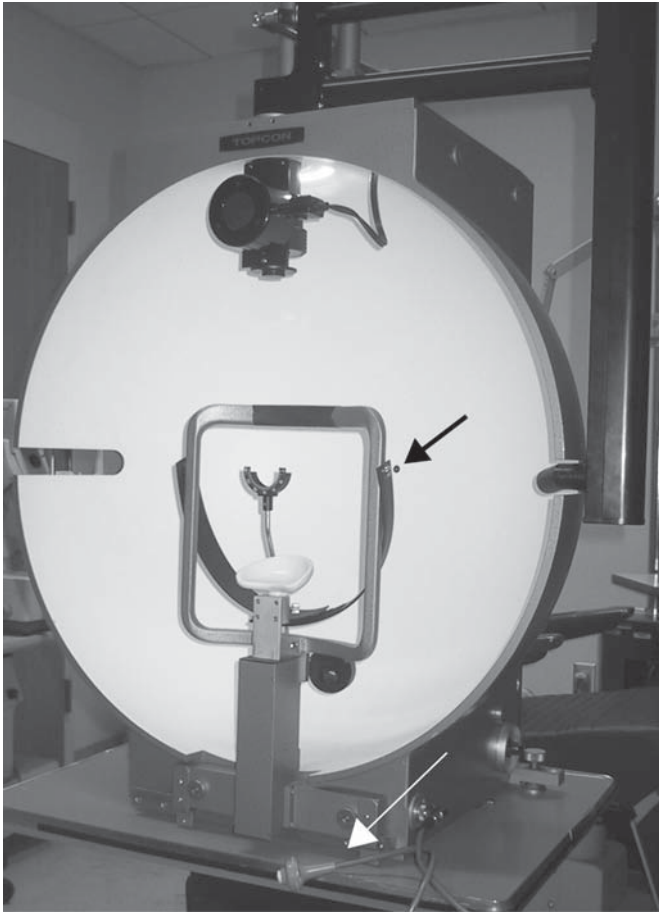


Fig. 1. Patient's side of Goldmann perimeter depicting chin rest and forehead strap. The long rod for holding a lens is shown in place, but it is easily removable. The black telescope aperture is visible in the center of the white bowl. The white fixation target is situated in the middle of the aperture (short black arrow). The button press is attached to the right-hand side of the perimeter (long white arrow).

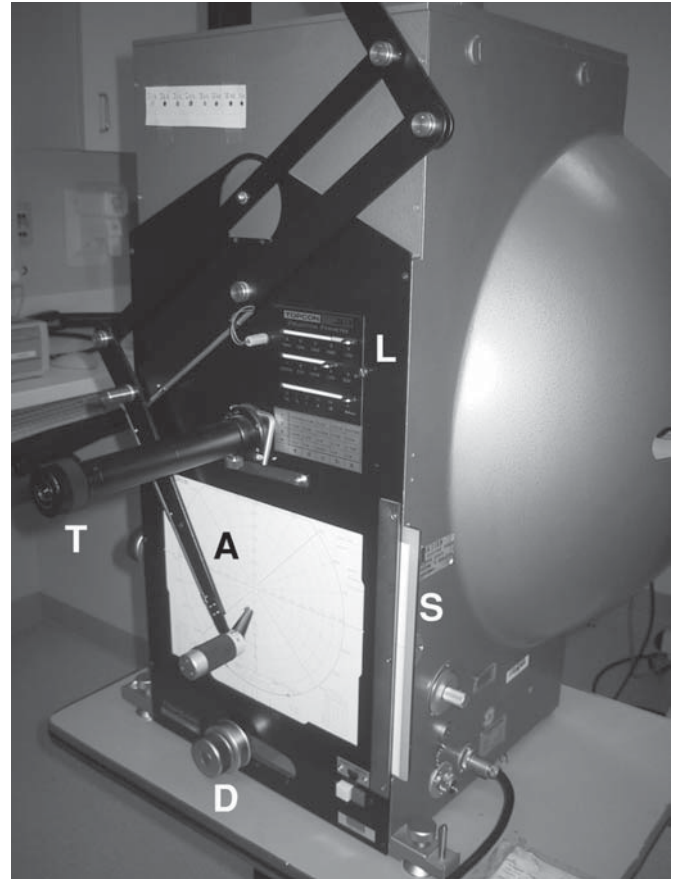


Fig. 2. Examiner's side of Goldmann perimeter. The chart paper is inserted in the slot (S) on the right of the drawing area. The dials (D) for adjusting the patient's vertical and horizontal position are below this area. The levers (L) for altering target size and brightness are above and right of this area. The arm (A) that moves the target ends in a cylinder that the examiner holds to guide the target, with a stylus pointing to current target location on the paper. The long black tube is the telescope (T) through which the examiner monitors the patient's eye fixation.

1.3. PLACEMENT OF THE SUBJECT

If one eye is probably normal, it is best to test it first, especially if this is the first time the patient has had perimetry. Otherwise, the right eye is usually tested first.

The patient has one eye occluded with a snug patch in contact with the nose and lateral cheek. The patch should not protrude so that it obscures the nasal field of the viewing eye. The patient sits with their chin on the chin rest and forehead resting on the forehead bar (Fig. 1). The chin rest is adjusted horizontally and vertically (Fig. 2) until the patient's viewing eye is centered in the crosshairs of the telescope, so that fixation is easily monitored during the test. The entire perimeter or the patient's chair is then adjusted vertically for comfort. Back or neck pain will distract patients during the test, and it is preferable that patients not leave the clinic with more problems than when they entered. Finally, the button press is placed in the patients' hand and they are shown how to operate it. If they cannot press the button because of hand weakness, a variety of other responses could be used, such as a finger tap or saying "yes" aloud, with the examiner then marking the location of the response on the perimetric record.

The "mental placement" of the patient is also crucial. The black disc marking the telescope's window on the subject contains a small white fixation spot. This should be pointed out to the patient. The importance of maintaining constant fixation on this point must be stressed, as well as the fact that the examiner will be watching through a telescope, in order to assist the patient by pointing out occasions when he or she looks away from the center. Awareness that they are under surveillance reinforces fixation in some patients. Next, it is explained that this is a test of the patient's "side vision," a point that also often improves fixation. The V4e target is shown to the patient as an example of what the patient will be looking for. We usually jiggle it a bit to make the point that it will be a moving target. Patients are then told that these targets will be moved from far in the periphery, where they can't see it, toward the center, and that at some point it will become visible. At that point, patients should indicate that they see it. It is stressed that they are not expected to see the target clearly, and that they should not be waiting for a sharp, crisp view of it before indicating that they see it. Rather, they should press the button as soon as



Fig. 3. Close-up from Fig. 2 showing levers for target selection. The levers are set for a V4e target. Note the chart indicating the brightness for various letter and arabic numeral lever combinations, measured in thousands of apostilbs (i.e., 4e = 1.00 = 1000 asb). The area (mm^2) of each target size designated by Roman numerals is also shown under the lowest lever (see Table 2).

Table 2
Goldman Target Sizes

Name	Diameter (mm)	Area (mm^2)	Diameter ($^\circ$)
V	9.03	64	3.44
IV	4.51	16	1.72
III	2.26	4	0.86
II	1.13	1	0.43
I	0.56	0.25	0.22
0	0.28	0.0625	0.11

they have a faint glimmer of light. Also, they should not turn their eyes to look at the target but stay looking at the middle, at the fixation spot. Once their vision has been mapped with a large target, a few smaller or fainter targets will then be used.

The duration of the test varies. A normal field in an attentive patient usually takes no more than a few minutes with an experienced examiner. Perimetry will take longer with a complex field defect or an inattentive patient.

2. STRATEGY FOR GOLDMANN PERIMETRY

2.1. THE TARGETS

The Goldman perimeter has manual controls (Fig. 3) that change the size or brightness of the target being projected on the bowl located 33 cm away from the subject. There are six different target sizes, ranging from 0.28 to 9.03 mm in diameter (Table 2). These are denoted by the prefixes 0, I, II, III, IV, and V, with a doubling of diameter from one size to the next. Brightness is controlled by levers marked by letters or Arabic numerals. The lever with Arabic numerals changes brightness by 5 dB for each shift, and the letter lever changes it by finer 1-dB steps (Chapter 5, Table 1). The various combinations of target size and bright-

ness provide the perimetrist with a fairly wide range of targets to use. The target sizes and brightness on the Goldman perimeter were designed to overlap seamlessly in a simple fashion. Increasing the size of the target is theoretically equivalent in effect to increasing the brightness by 5 dB. Thus, a II4e should equal a III3e or a IV2e, and a I2d should be the same as an 03d or a II1d. Put another way, targets sharing the same letter designation are supposed to be equally visible if the sum of their Roman and Arabic numerals is the same (i.e., II + 4 = III + 3). This theoretical simplicity does not always work out exactly in practice, though. For example, it is our frequent experience that an 03e target gives a slightly smaller isopter than an I2e target, implying that the 0.2- mm^2 reduction in target area outweighs the 5-dB increase in brightness.

2.2. CHOICE OF TARGETS

Usually at least three different isopters are mapped (Fig. 4). The general aim is to map the farthest extent of the field with the largest, brightest target (the V4e), and use a faint target that is only perceived at or just within the central 30°, and another that produces an isopter lying intermediate to these (Fig. 4). By tradition, the latter two are often the I2e and I4e targets. However, there is nothing magical about the I2e and I4e targets. It is more important to pick targets that cover the regions one wishes to examine. In young people, the I2e may lie outside of the central 30°, and a fainter target may be required. The opposite may be true in older subjects with cataracts, who may not be able to see the I2e target. Some subjects can see the I4e target very close to where they see the V4e target, so mapping with the I4e will be redundant. The I3e is a better choice in this situation.

Further targets or alternative choices can be made according to the situation. If a defect is thought to involve the paracentral or central field, an 03e isopter can be added. If a defect is visible on the I2e but not the I4e, the region between these two can be filled in with an I3e target. One can experiment with targets in a patient to find the right one to cover a certain region of the field. Again, knowledge of what one is looking for is invaluable in guiding the exploratory strategy.

2.3. TARGET PRESENTATION

There are two main types of target presentation: static (stationary) and kinetic (moving) (Fig. 5). With *kinetic* targets the procedure is to move a target from a region where it is not visible toward a location where it is, and to mark the point where the patient first reports seeing it. The speed of movement should be about 2 to 3°/s. This is repeated at spaced intervals, more finely in areas under suspicion, and at the end an interpolated line is drawn to connect all these points, which are deemed to share a common kinetic threshold. This line is the kinetic isopter, marking the zone at which a given target first becomes visible, and is the chief feature of manual perimetry.

Static presentations also can be done with manual perimetry. *Static thresholds* are obtained by holding a target too dim to be seen (the 01a is the extreme) in one spot and gradually increasing the brightness until it is perceived. This is, however, too time-consuming to be used for the entire field. Rather, a *static suprathreshold* strategy tends to be used, in the following manner. With a given target, a kinetic strategy is first used to define an isopter. Because of the increase in sensitivity as one approaches the center of vision, that target should normally be visible at all points within that isopter, with the exception of the physiologic

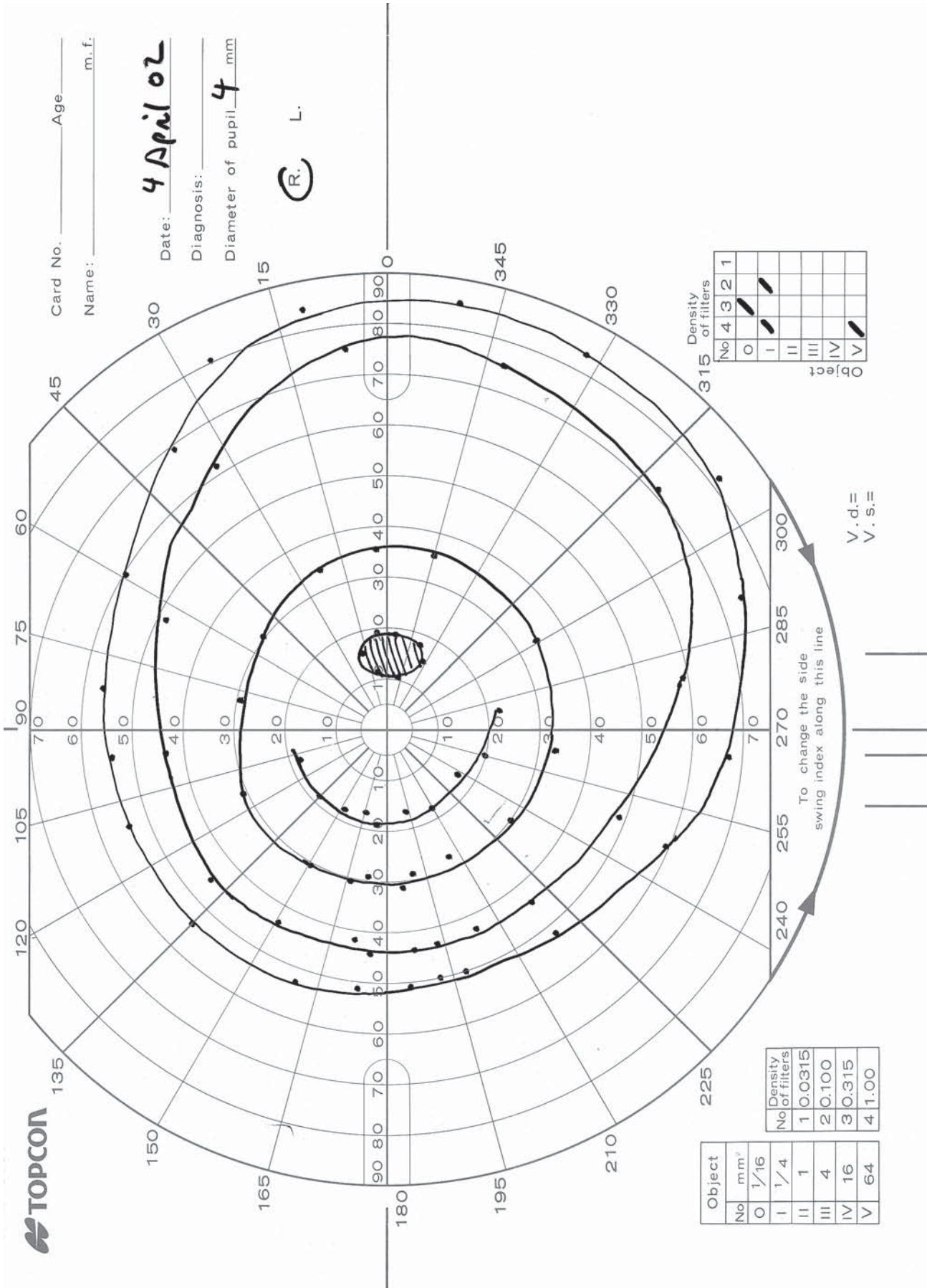


Fig. 4. Normal Goldmann visual field, right eye. Note the greater extent temporally than nasally, and inferiorly than superiorly. The physiologic blind spot lies between 10 and 20° eccentricity. The targets used are indicated in the box in the lower right corner; the legend to target size and filters for brightness is in the lower left corner.

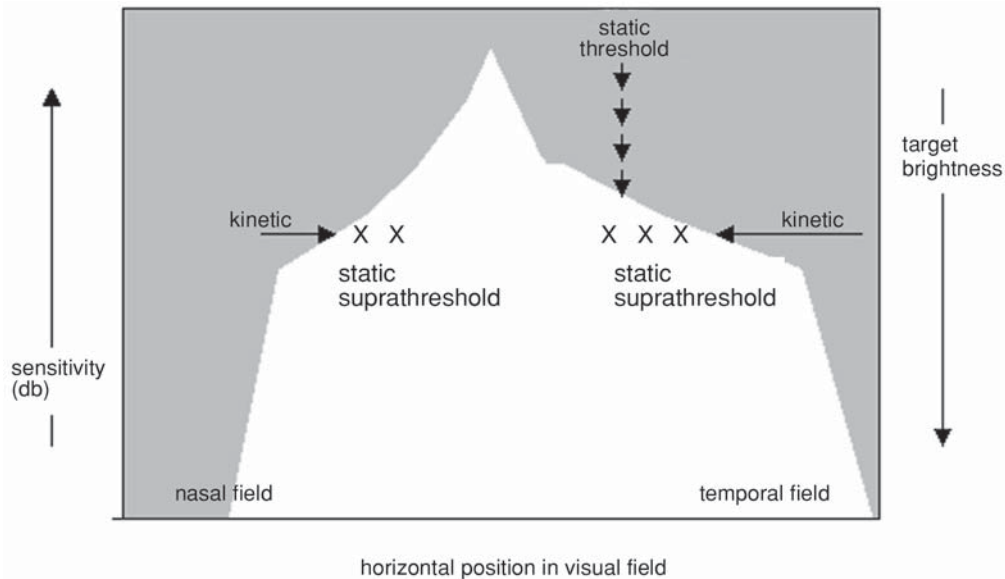


Fig. 5. Kinetic vs static strategies. A section through a hill of vision is shown. Sensitivity increases going up on the y-axis, and target brightness decreases. Points above the hill (gray area) are not visible to the observer, whereas targets whose brightness lies within the hill are seen. A kinetic presentation involves moving a target of constant brightness horizontally, from where it is not visible, toward center until it intersects with the hill of vision (horizontal arrows). A static threshold involves keeping the target steady and increasing its brightness until it is seen (vertical series of arrowheads). One static suprathreshold strategy (“x” symbols) involves flashing a target within its kinetic boundary to ensure that there are no “holes” in vision.

blind spot. Therefore the target should be visible if it is flashed anywhere within that isopter. If there are locations within the isopter where the patient cannot see this target, there is a scotoma that requires further exploration. This suprathreshold technique may miss subtle central or paracentral defects, particularly if too large a target is chosen for the suprathreshold static survey.

An alternative static suprathreshold strategy is to define in one region the static threshold, then to increase the brightness of the target slightly above this threshold by about 2 dB (increase of two letters, i.e., II2b to II2d) and test other points of equal eccentricity (see Text Box, p 36). This is reasonable in the central field, where the isopters are more circular, but less reliable in the periphery, where the quadrants start to differ significantly from each other.

In general, kinetic presentations are the chief manual technique. They are the most rapid means of generating the isopter lines that mimic the topographic lines on maps. Static presentations are used secondarily as probes for depressions or holes (scotomata) within a kinetic contour, or to confirm or reveal distortions of a kinetic contour (see Fig. 6). Static suprathreshold strategies are best for probing for scotomata in the central 15°, where kinetic isopters are difficult to implement. Once a static presentation has identified a defect, though, one usually switches back to a kinetic strategy, moving the previously static target within the defect to find the boundaries of the distortion or scotoma, linking these to form yet another isopter line.

2.4. MAPPING AN ISOPTER: A “GENERAL” STRATEGY

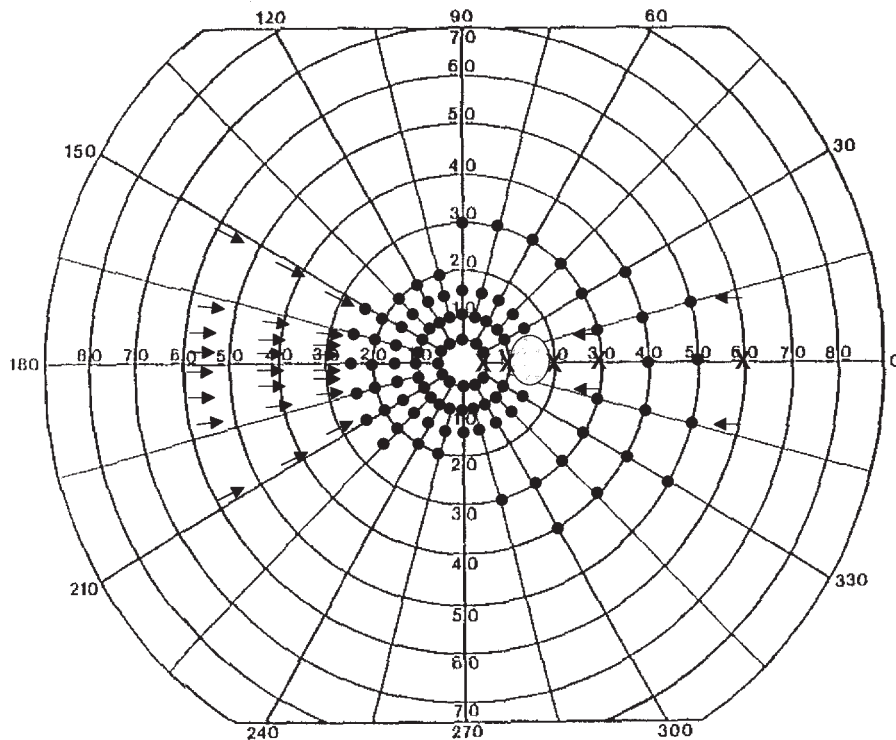
For an essentially normal eye, one can pick three targets as above and for each use a kinetic strategy with a similar number of locations in each quadrant to map each isopter. At each location, one could simply move the target along a radial path heading toward the center where the patient is fixating. How many locations is enough? That depends on one’s suspicions and the coop-

eration of the patient. Four or five per quadrant can be regarded as minimum figures. Following the mapping of kinetic isopters, the smallest kinetic target can be flashed within the central 10°, once in each of the quadrants, as a static suprathreshold strategy to exclude a significant central defect. In the region between isopters, the target used to map the more peripheral and larger isopter can be flashed as a similar suprathreshold strategy, but this is generally a bit of overkill in a general screen.

Plotting of the physiologic blind spot is important and generally uses the I-size target, usually the I4e or I2e target. Larger targets occupy too much area to permit accurate determination of the size of the blind spot. The technique is straightforward. While monitoring the patient’s fixation, the target is turned off, placed at 15° temporally on the horizontal meridian (in the middle of the usual location of the blind spot) and then turned on. If the patient reports seeing it, the target is turned off, moved laterally or vertically a few degrees, and presented again, checking to make sure that fixation is true. Once the patient fails to see the target, it is in the blind spot. The target is moved until the patient sees it, then placed back in the blind location and moved in another direction until the patient sees it there too, and so on, until the vertical and horizontal extent of the spot has been determined. Eight evenly spaced directions are recommended if the size of the blind spot is of particular interest. Inability to plot the blind spot is a sign of poor fixation by the patient. The blind spot normally extends from 10 to 20° along the horizontal meridian and extends to between the 15 and 30° radial lines above and below the meridian (Fig. 4).

Of course, there really is no such thing as a general strategy. Perimetry is done on people who have suspected problems. Even an apparently asymptomatic eye must be tested with a mind to the clinical context. For example, with a unilateral optic neuropathy, might there be subclinical optic neuropathy in the other eye? Or a subtle temporal hemifield defect that would localize the other eye’s

ARMALY-DRANCE SCREENING TECHNIQUE—ONE VERSION



A version of the Armaly–Drance Screening Technique. Arrows are kinetic test points, dots are static suprathreshold test points, and X indicates locations where static thresholds are measured to determine the targets suitable for suprathreshold testing.

1. Suprathreshold static screen of the central field. After plotting the blind spot, static thresholds are first determined at 5, 10, and 20° along the horizontal meridian in the temporal field. This is done by starting with the I1a target and increasing brightness gradually until the target is just seen, then repeating this at the next location. A target 2 dB larger than the 5° threshold (i.e., if threshold is I2a, increase by two letters to I2c) is then used to check points every 15° apart in the circle at 5° eccentricity. The same is done with a target 2 dB above the 10° threshold for 10° eccentricity. A target 2 dB brighter than the 20° threshold is used to check the circle at 15° eccentricity, the 20° semicircle in the nasal hemifield, and the 25° quarter circle flanking the nasal meridian.
2. Kinetic plotting of a nasal isopter. This is done within the central 30°, usually the I2e target, and for several peripheral isopters, usually the I4e and V4e targets (these without the lens correction). This is restricted to the sections 30° above and below the nasal horizontal meridian. This kinetic testing probes for nasal steps.
3. Suprathreshold screen of the temporal field. Static thresholds are determined for the 30 and 60° location on the horizontal meridian in the temporal field. As above, a 2-dB brighter target is used to test the 30° semicircle in the temporal field. The 60° threshold target is used without change to test locations flanking the temporal meridian at 40 and 50° eccentricity.
4. Kinetic probe of the temporal field. Targets are chosen to be detected at around 25 and around 55° eccentricity in the temporal field, above and below the meridian.

neuropathy to the suprasellar region? The point is, all clinical perimetry is done to answer questions, and the test is not adequately done if it does not address the pertinent issues.

2.5. LOCATION-SPECIFIC MAPPING STRATEGIES

2.5.1. Mapping Retinal Disease

The anatomic pattern of disorders of the retina is guided by what one sees on funduscopy and the type of pathology. Macular diseases such as central serous retinopathy, macular degeneration, and cone dystrophies mandate careful testing of the central 20°, mainly with suprathreshold methods, and it is probably best done by automated perimetry. Retinitis pigmentosa redirects one to the

midperiphery. Retinal arterial occlusions produce defects similar to optic neuropathy and require similar approaches.

2.5.2. Mapping Optic Neuropathy

The most frequent defects from optic nerve disease are arcuate defects and central scotomata. Therefore, the key regions to concentrate on are the central 20° and the nasal meridian.

The central 20° should be explored with a hybrid kinetic and static method. Suprathreshold presentations, several per quadrant, can be made in the central 10° until a region of abnormality is discovered. At this point, the same target can then be moved to map the borders of the *central scotoma*. If the outer limit cannot be located, it may be that the target being used is too close to thresh-

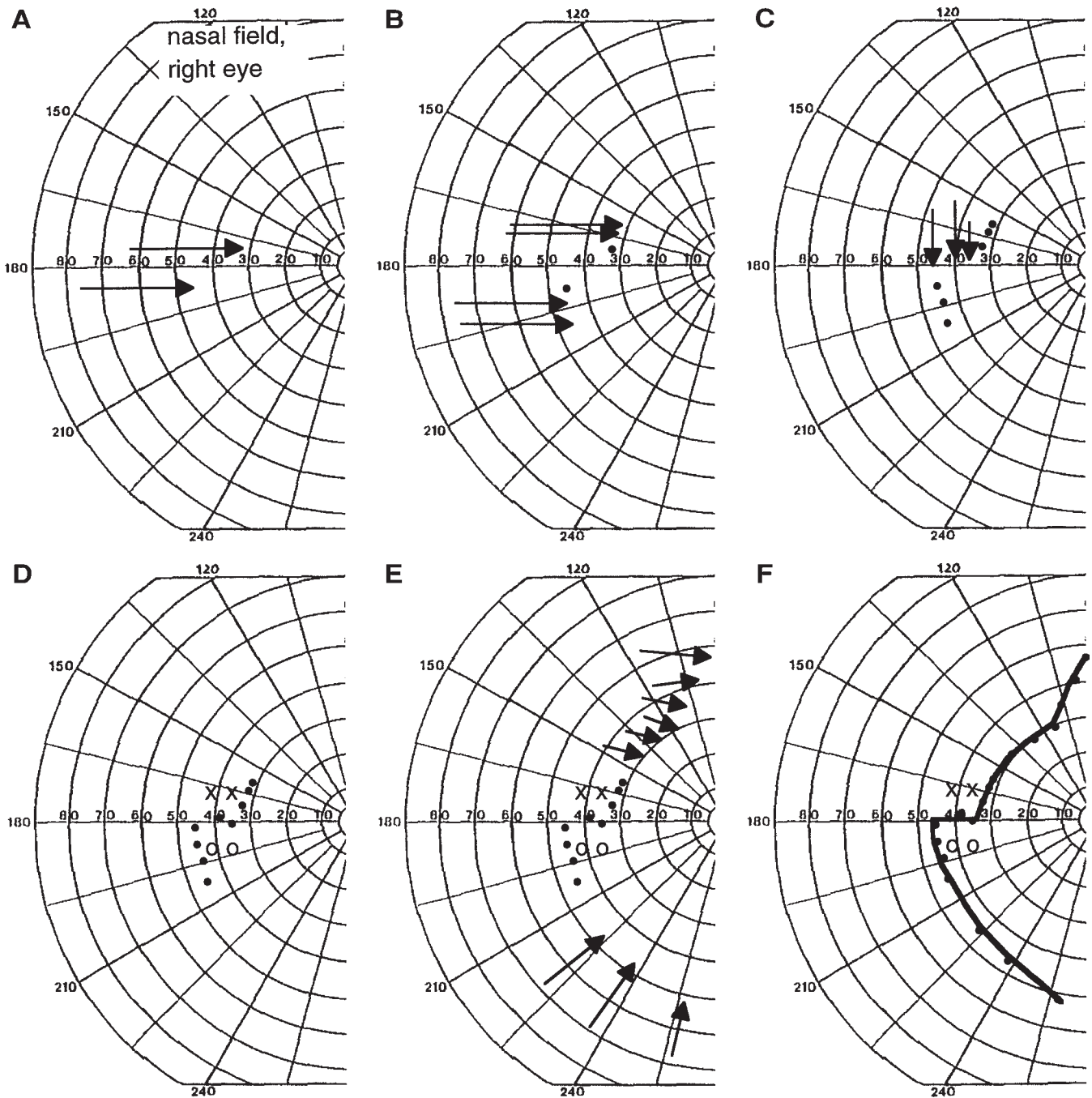


Fig. 6. Plotting a superior nasal step, right eye. A single target size and brightness are used in these diagrams. Arrows are kinetic presentations, with the tip located where the target is seen, represented in succeeding frames as black dots. **X** and **O** are static presentations of the same target, with **O** marking locations where the target was seen and **X** where it was not. (A) The target is moved horizontally above and below the meridian, and a discrepancy is noted. (B) The target motion is repeated to verify the consistency of this discrepancy. (C) Kinetic targets moving perpendicular to the suspected nasal step are made from the defective area toward the meridian. This is done at several points to verify that this is a horizontal step. (D) Static presentations of the same target are made on either side of the meridian, to confirm that the target is seen on one side but not the other. (E) Points away from the meridian are tested, with more detailed exploration of the superonasal defective area, showing the arching nature of the loss. (F) The kinetic isopter is drawn.

old, and a brighter one should be substituted, as long as it too is unseen in the depths of the scotoma. The depth or severity of the scotoma is estimated by placing a static target at its center and increasing its brightness until the subject reports that he or she can see it. The slope of the scotoma's edges can be estimated by repeat-

ing kinetic perimetry with several different targets of less intensity than this last perceived target.

The *nasal horizontal meridian* is explored by moving targets centripetally both above and below the meridian several times and seeing if there is a discrepancy between the upper and lower field

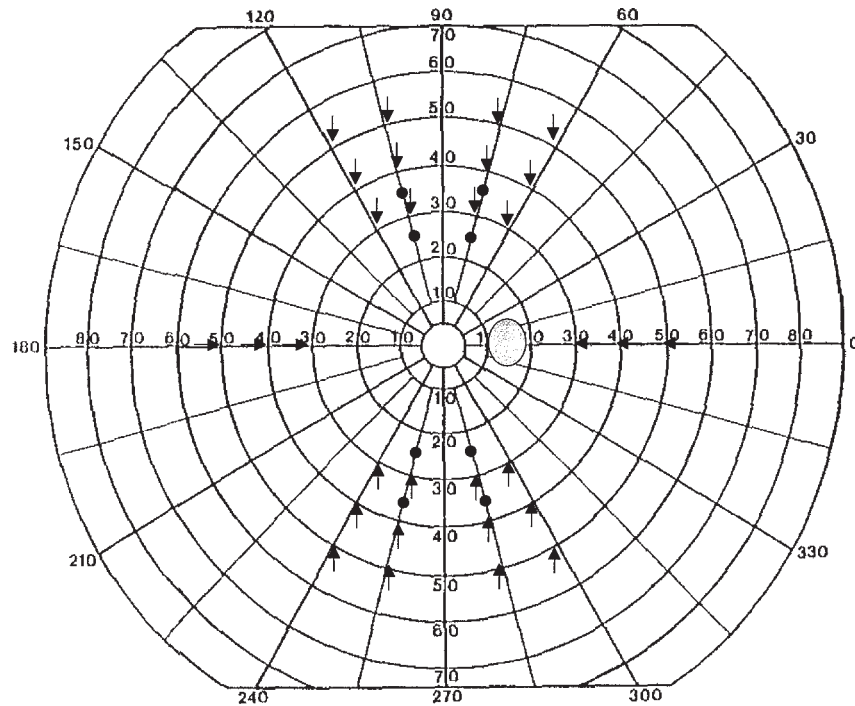


Fig. 7. Trobe et al.'s (1) version of testing for vertical meridians. Kinetic perimetry is done with three vertically moving targets, chosen to reveal isopters at 30, 40, and 50° eccentricity, as indicated by the arrows, which flank the vertical meridian. The kinetic data can then be corroborated by a static suprathreshold technique as in Fig. 6. The essential idea is to take the same target used to mark the kinetic isopter and flash it just within the isopter, comparing responses on either side of the vertical meridian (indicated by the dots). This method should be supplemented by testing within the central 30°.

(Fig. 6). If so, this should then be confirmed by moving the target perpendicular to the meridian from the supposed defect, to see if the target suddenly becomes visible as it crosses the meridian. Further confirmation can be obtained by static flashing of the same target at equal eccentricities on either side of the meridian, within and across from the defect. The non-meridian margins of the nasal step defect are then explored, with the examiner particularly noting if they follow an arching course curving toward the blind spot. The rest of the isopter in the superior, inferior, and temporal regions is mapped with a general strategy as above. This process is repeated for several isopters, in both the central and peripheral field, since the presence of a similar defect in more than one isopter is more reliable evidence of disease.

Some optic neuropathies produce almost exclusively central defects, including metabolic problems such as B₁₂ deficiency and Leber's hereditary optic neuropathy. Others such as primary open-angle glaucoma, branch retinal arterial occlusion, and papilledema produce almost exclusively nasal steps and arcuate defects, particularly in early stages. Other conditions such as optic neuritis and ischemic optic neuropathy can produce either central or arcuate defects.

The Armary-Drance screening technique has evolved as an attempt to standardize the documentation of arcuate defects, nasal steps, and other defects in glaucoma (see Text Box, p 36). This is not an unreasonable strategy for other optic neuropathies as well. While the need for standardized kinetic perimetry has been largely superseded by the advent of automated perimetry, a review of this technique is useful in demonstrating the regions of interest that should be tested in some fashion when optic neuropathy is in question.

2.5.3. Mapping Vertical Meridians

Diseases at or behind the optic chiasm are typified in the majority of cases by a marked change at the vertical meridian. Documenting this utilizes a strategy similar to that used for detecting nasal steps at the horizontal meridian, only now rotated 90°. A screening method limited to this strategy has been reported and studied for chiasmal lesions, and has been found to have good sensitivity (Fig. 7) (1).

2.6. COMMENTARY

Finally, it is sometimes useful to write comments on the field. If the patient is inattentive, responds slowly, or fixates poorly, these should be noted. Areas where the patient gives highly variable responses should be marked in some fashion. Because there is no printout of reliability measures by a Goldmann perimeter, the examiner has to provide a subjective sense of this on the examination results.

3. INTERPRETATION OF GOLDMANN PERIMETRY

The principles that guide how a Goldmann field is performed are the same that guide how one looks at the plot. Determining whether these guidelines have been followed is important, particularly when reviewing a perimetric examination done by another clinician. One should not simply look at the isopter lines drawn, as these are secondary interpolations from the actual data obtained, which are the dots on the map. Has the examiner concentrated kinetic test points in the appropriate regions, thus displaying knowledge of both visual anatomy and the patient's presenting problem? If not, the examination may not be sensitive enough to

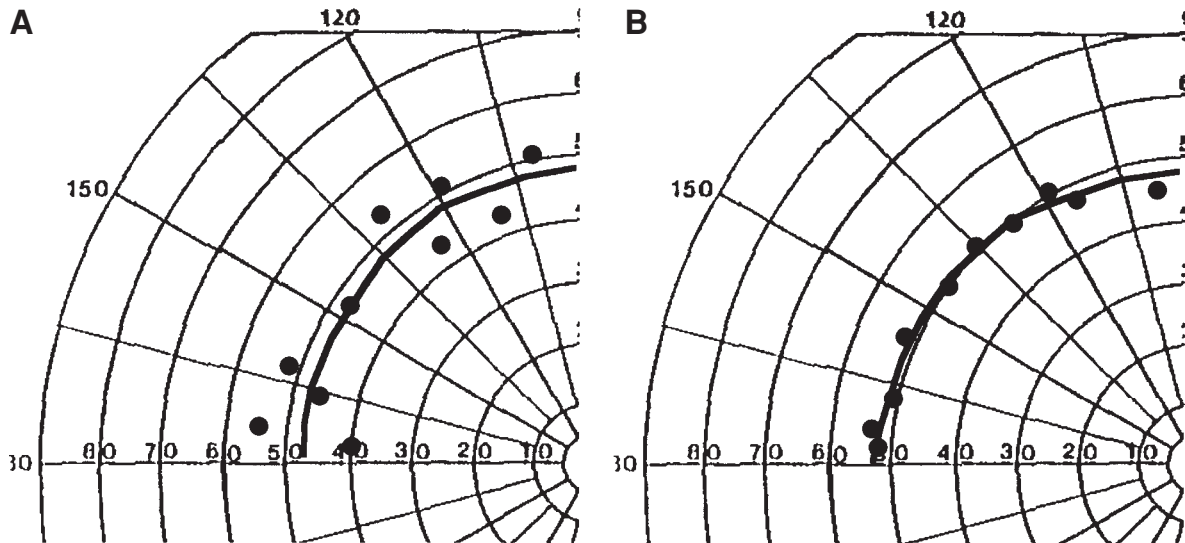


Fig. 8. Patient variability: (A) highly variable patient, showing significant scatter of 10 kinetic detection points around isopter line; (B) very consistent patient, showing that the 10 points align well along isopter line.

exclude the field defect in question. Has the examiner presented static targets within kinetic isopters where suspected holes may be hidden? Have they “connected the dots” in an appropriate manner, reflecting the physiology and anatomy of the visual system? In most regions, it is not appropriate to connect points directly, but to interpolate a smooth curve through them. On the other hand, in regions where sharp discontinuities occur with pathology (e.g., nasal and vertical meridian steps), smoothly interpolating through the points will obscure small defects.

Once satisfied that the perimetrist did an adequate job of obtaining and presenting data, one should determine the consistency of the patient. To a large part this will have to be gleaned from the comments written by the perimetrist. However, one can obtain an approximate feel for the variability of the patient by looking at test points for the same target that were spaced closely together. If these tend to be quite scattered around the mean isopter line, the patient may be inattentive or a poor fixator (Fig. 8). (Scatter, however, can be expected at pathologic boundaries in an otherwise consistently performing patient. This is akin to the increased short-term fluctuation in automated perimetry.) Many real defects will produce similar effects on more than one isopter, particularly closely spaced ones. A small deviation on one isopter alone, involving only one or two kinetic points, is more likely due to inattention or variability on the part of the patient. The defect should be confirmed with more data points with the same target and other ones along a neighboring isopter.

If confident that the fields are of value, one proceeds to evaluating the pattern of the field. Here, a mental picture of the hill of vision (see Chapter 1, Fig. 1) is invaluable (Fig. 9). Trying to envision how the patient’s field deviates from the smooth increase to peak sensitivity at the fovea, with hill-like elevations and valley-like depressions, is the goal of interpretation. Teaching the patterns of defects in visual disease is the aim of Chapter 6 (the Atlas section) of this book. A few broad questions are worth mentioning here as a general approach for any perusal of fields:

1. Could the abnormality be an artifact?
2. Is this a monocular or a binocular problem? Never evaluate one eye without seeing the field of the other.

3. If monocular, which part of the field is affected most, central or peripheral? If peripheral and nasal, does it respect the horizontal meridian?
4. If binocular, do the defects in both eyes resemble each other or are they radically different? Are they limited to one hemifield? Do they respect the vertical meridian?

3.1. ARTIFACTS

The rationale behind the last three questions listed is detailed in Chapter 2, and examples of their application are in Chapter 6. It is worth reviewing some examples of the first question (artifacts) here. Classic artifacts include the following:

1. *Lens rim artifact*: If the lens holder is used, it is important to know where the lens rim artifact will fall on the field (Fig. 10). This is easier with the Goldmann perimeter than the Humphrey automated perimeter, because the lens holder of the former is not adjustable.
2. *Lid artifact*: Patients with ptosis, blepharochalasis, or just naturally droopy lids may have a constricted superior field. This may show a sharp drop with overlapping isopters. Repeating perimetry while they consciously raise their lids by contracting their frontalis muscle (“raise your eyebrows and lids”) will expand their fields (Fig. 11)—probably the only immediate cure of visual loss the examiner will ever effect. Taping the lid up will do the same in patients who cannot maintain a wide palpebral fissure on their own.
3. *General constriction*: Although sometimes resulting from disease, constriction has many artifactual causes, ranging from small pupils and bad refractive correction (more of a problem for the central than the peripheral field), to inattention, high internal criterion bias (which can be overcome with encouragement and instruction), and functional performance. If the examiner moves the target too fast, the marker will have moved beyond the point where the target was seen by the time the patient responds. The same effect will occur with normal target speed movement but abnormally slow responses on the part of a patient with dementia, retardation, or parkinsonism (Fig. 12).

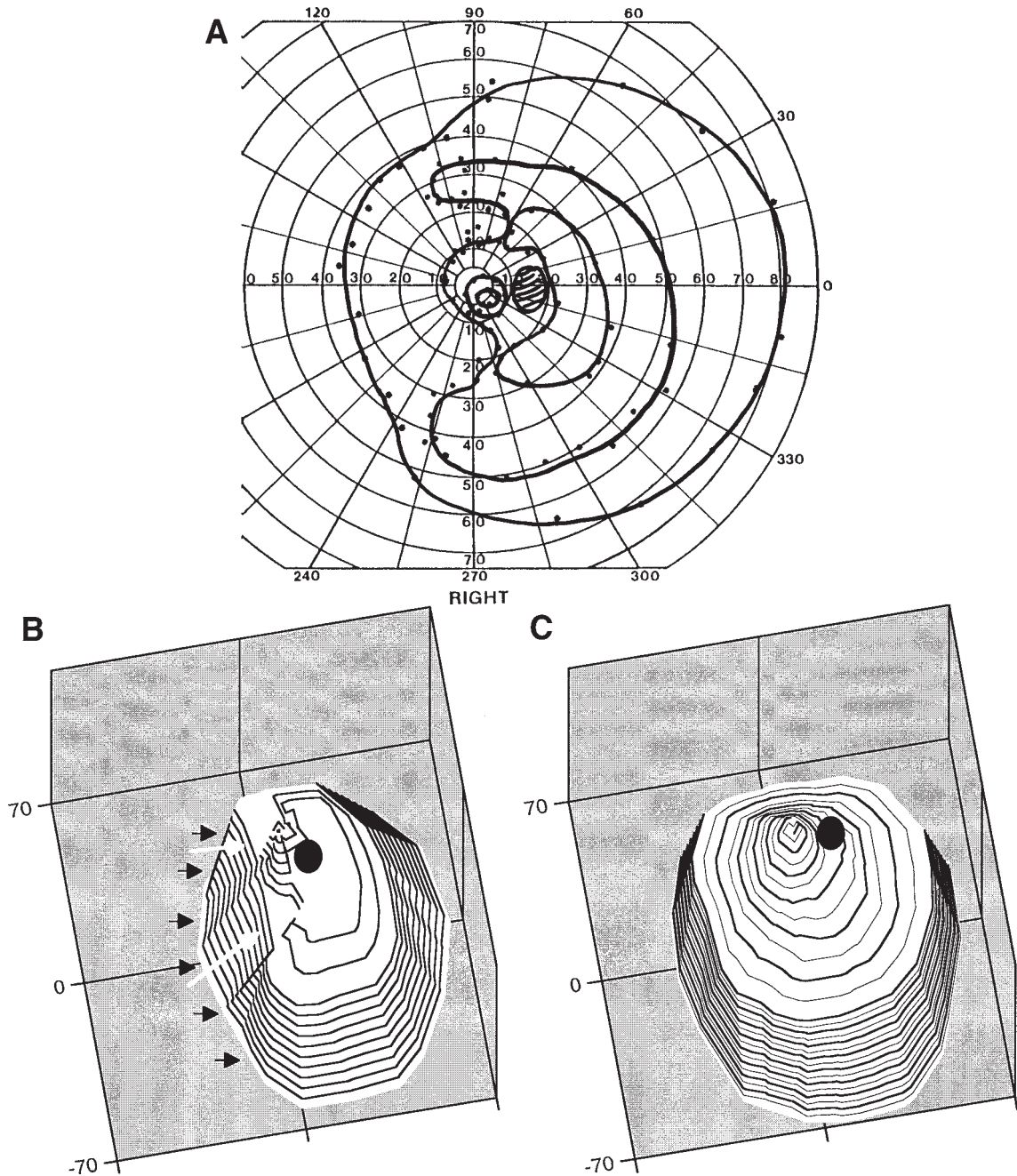


Fig. 9. Envisioning the hill of vision: (A) complex Goldmann plot showing superior and inferior arcuate defects arching around a peak of residual central sensitivity, with constriction of nasal field; (B) three-dimensional plot of hill of vision represented in this Goldmann plot, with a normal plot for comparison (C). Note the arcuate defects (white arrows) and nasal constriction (black arrowheads).

4. *Solitary wobble*: Not uncommonly one finds fields with a slight indentation of an isopter somewhere along its course. Some, like the slight indentation in the inferonasal field caused by the nose, are so well known to experienced perimetrists that they do not merit comment. Others may be due to momentary inattention on the part of the patient or the perimetrist. Occasionally, these occur in anatomically plausible locations, such as the horizontal nasal meridian, raising suspicion of disease. Their credibility is strengthened if their shape conforms with pathologic anatomy, if they can be reproduced in a repeated examina-

tion or in a different isopter in the same examination. In general, one should be cautious about interpreting a non-specific defect in a single isopter.

5. *Baring of the blind spot*: Because the superior field is less sensitive than the inferior field, isopters that approach the blind spot might merge with it superiorly but not inferiorly, giving rise to the appearance of an arcuate or wedge defect arising out of the blind spot. Pathologic defects have either a more prominent temporal shoulder that defines the wedge's edge, or a nasal step that reveals the termination of the arcuate defect (Fig. 13).

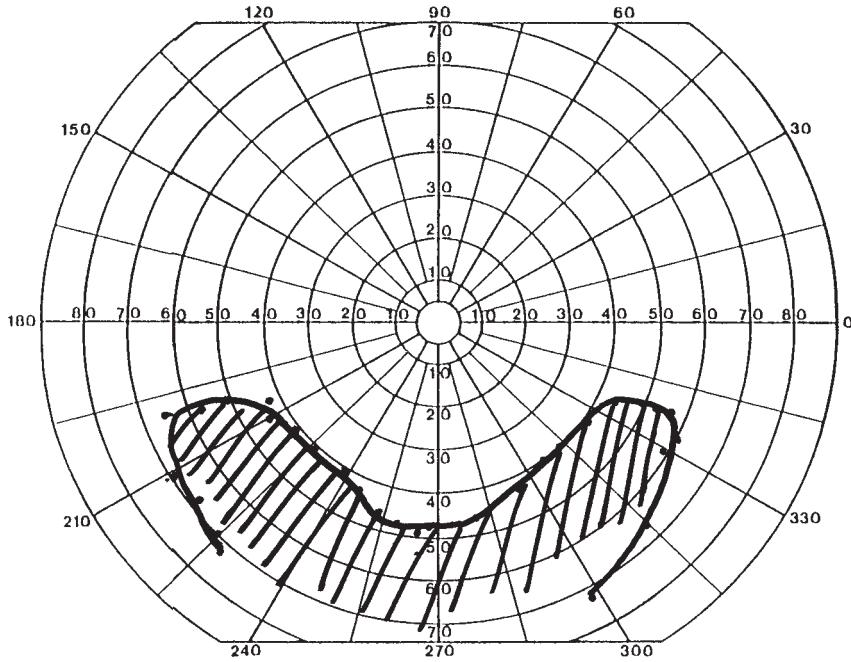


Fig. 10. Location of lens rim artifact. This demonstrates why lenses are only used for testing within the central 30° of vision.

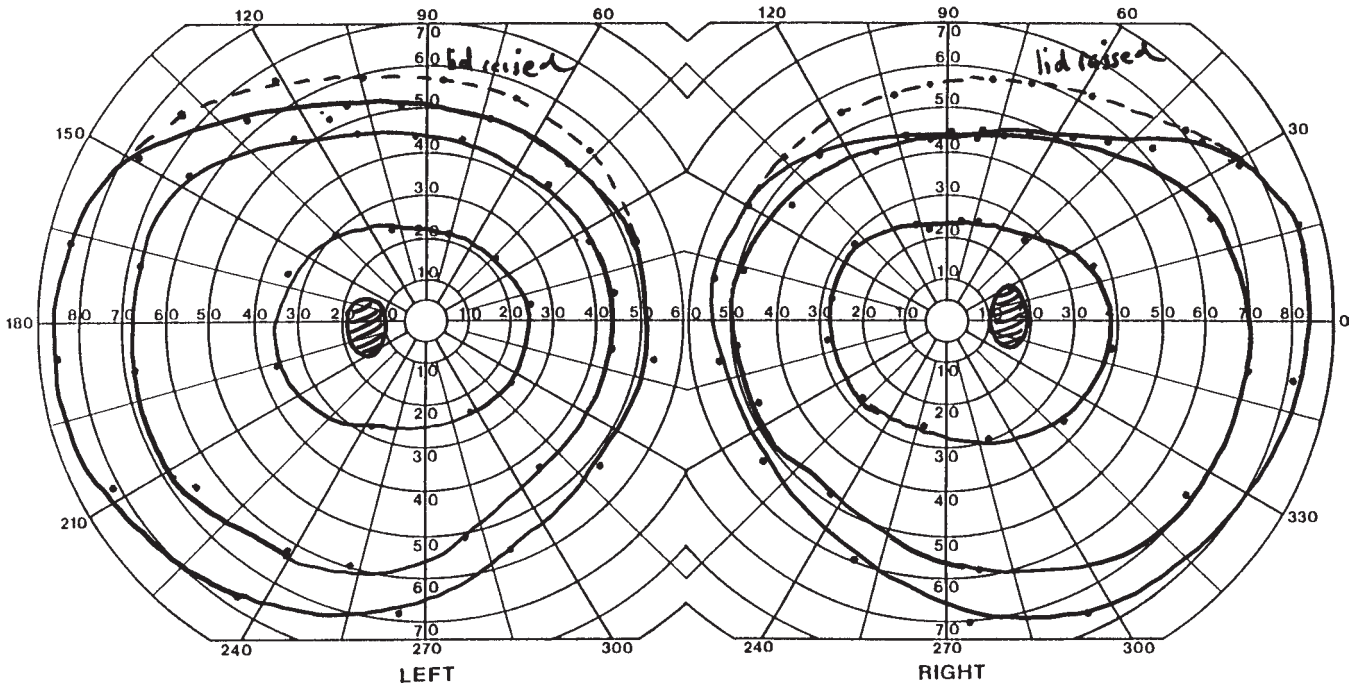


Fig 11. Lid artifact. A 35-yr-old man was referred for reduced peripheral vision. His fields are actually fine except in the superior periphery. However, note that in the right eye the 14e and V4e isopters merge for a significant distance, a suspiciously nonphysiologic finding. His lids tend to a low position, though, and when he is asked to actively raise his eyebrows and lids, the V4e isopter expands to a normal position in both eyes.

3.2. NOMENCLATURE

Describing what one sees is an important part of the visual field evaluation, a theme that will be repeatedly emphasized in Chapter 6. There are two main features of any field defect: its location and its shape.

3.2.1. Location

In terms of eccentricity, location can be broadly divided into central and peripheral sites. The central field can be considered synonymous with the macular region, which measures 5.5 mm, or a central disc with a radius of about 9° of visual field. Essen-

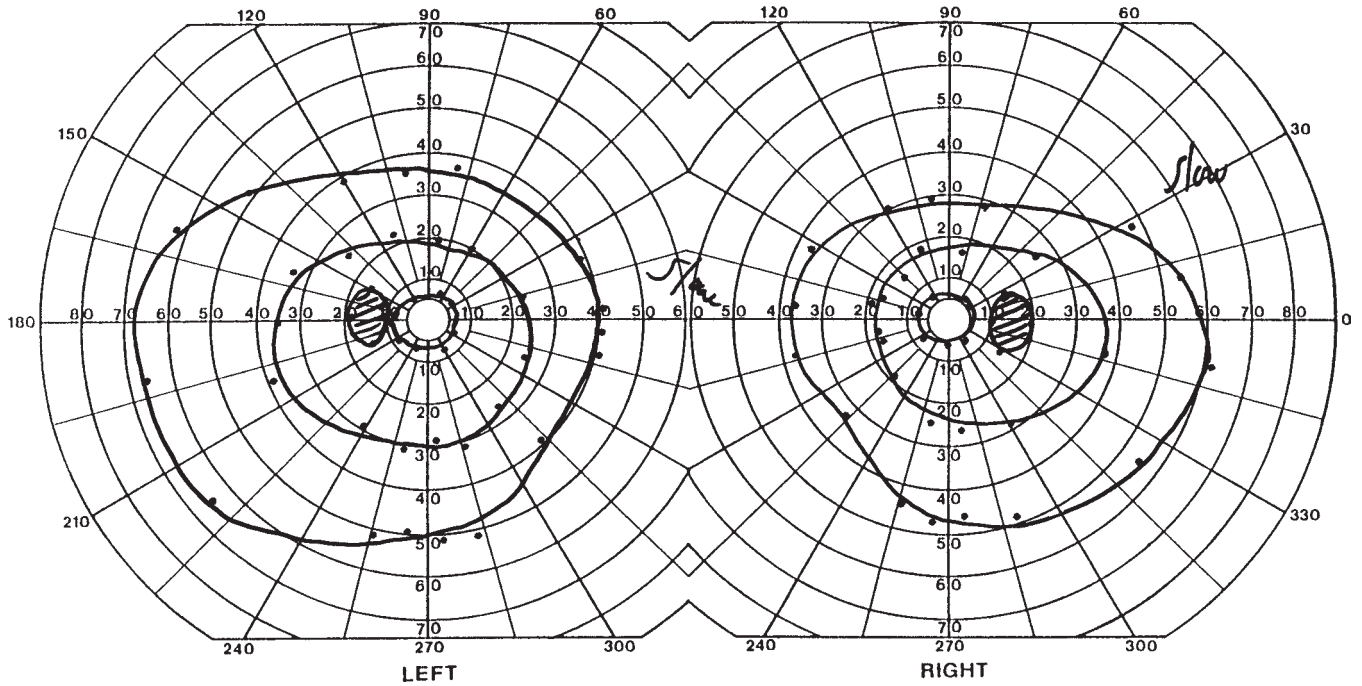


Fig 12. Factitious general constriction: perimetry in a 44-yr-old man with a progressive dementia. Note the perimetrist's remark that the patient is "slow." The constriction is due to the fact that by the time the patient eventually signals that he saw a target, it has moved a significant distance from the point of perception.

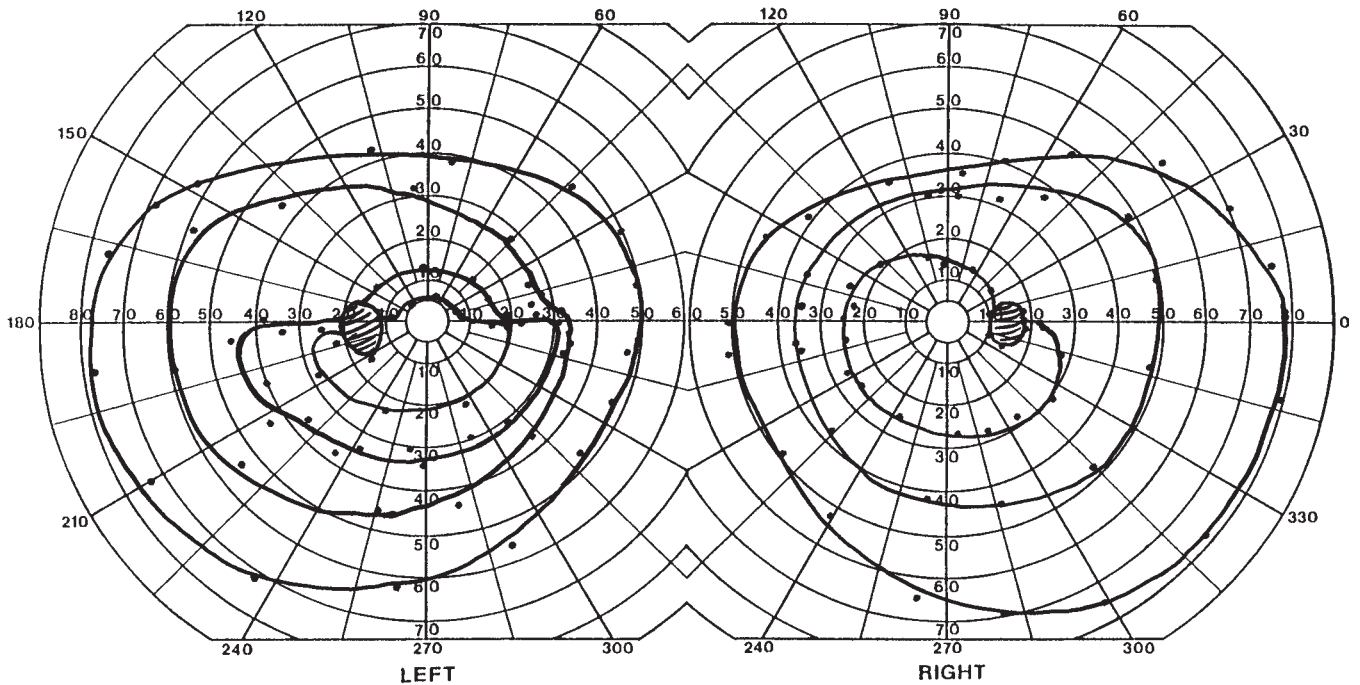


Fig. 13. Baring of physiologic blind spot: perimetry in a 70-yr-old woman. Both eyes show baring, but that in the right eye is normal whereas that in the left eye is pathologic. The clue is the associated nasal step defect on the left, marking this as an arcuate defect, in her case due to anterior ischemic optic neuropathy.

tially, this is all the retina that is less eccentric than the physiologic blind spot, whose inner edge lies at about 10° . This central macular region has subdivisions. The fovea covers the central 3° , the parafoveal area from 3 to about 5° , and the perifoveal area

from 5 to 9° . For practical purposes dividing this region into the central 5° (foveal) and from 5 to 10° (perifoveal) is sufficient, because fine distinctions within the central 5° are not achievable with Goldmann perimetry.

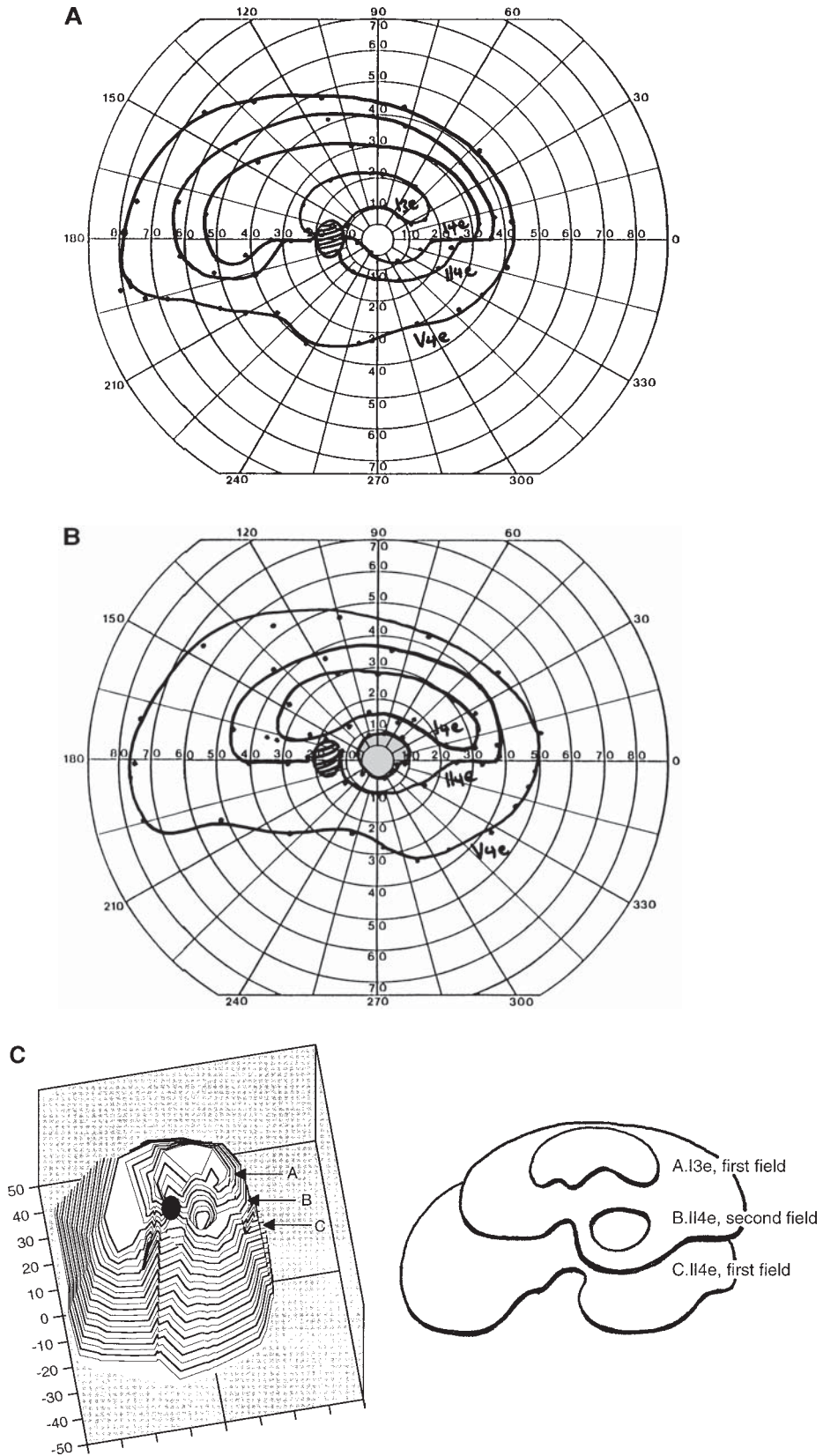


Fig. 14. Effect of progressive cataract on abnormal field. This patient was followed for ischemic optic neuropathy. Her initial field (A) shows an inferior altitudinal defect with relative depression of central vision. Another field 6 mo later (B) shows an apparent worsening of the central defect. However, note that the isopters in the superior field are generally constricted compared with the initial field. The new I4e isopter looks more like the old I3e (note that she no longer sees the I3e in the new field), and the new II4e like the old I4e. Thus, everything is diffusely submerged, in addition to her old altitudinal defect, which probably has not changed. A three-dimensional reconstruction of her hill of vision (C) shows where different isopters on the different visits intersected the hill.

Outside of this central region is a zone from 10 to 20–25° that contains the blind spot in the temporal field. This is known as the Bjerrum area and is a ring where glaucomatous field defects are often found. This can be considered the *paracentral* field. Beyond 25° is the *peripheral* visual field. Thus, location in terms of eccentricity has four main possibilities: foveal, perifoveal, paracentral, and peripheral.

Besides eccentric location, the side involved is also important. For monocular defects, the best terminology is nasal vs temporal. For bilateral homonymous defects, right or left is preferred. Upper- or lower-field location should also be noted.

3.2.2. Shape

While there are infinite possibilities, recognizing the general pattern of a defect is key. Monocular defects have five main possibilities:

1. *Scotomata*, holes in the visual field, of variable contour.
2. *Arcuate defects*, which begin at the nasal horizontal meridian then form a progressively narrowing arch that aims or ends at the blind spot.
3. *Nasal steps*, which are sharp discontinuities between the upper and lower fields along the horizontal meridian and are a minimal expression of an arcuate defect.
4. *Wedges*, which are shaped like slices of a pie, with their narrow apex pointing toward the blind spot.
5. *Altitudinal defects*, in which either the upper or lower half of the visual field has been obliterated, with variable degrees of sparing or spread around the meridian in the central or temporal field.

Defects affecting both eyes from disease at or behind the chiasm will have hemifield defects. These have four main patterns:

1. *Hemianopia*, in which most of the upper and lower field is affected, with at most minor degrees of sparing, perhaps of the macula region or the monocular temporal crescent.
2. *Quadrantanopia*, which may be *partial*, with some sparing in the quadrant, usually around the horizontal meridian, or a *quadrantanopia plus*, with some involvement of the other quadrant in the same hemifield.
3. *Sectoranopia*, in which wedge-shaped defects are present in both eyes.
4. *Homonymous scotomata*, in which a small hole is present in the same location in both eyes.

3.3. FOLLOWING SEQUENTIAL FIELDS

One can use Goldmann visual fields to follow the course of a patient's visual field defect. It is not necessarily easy to decide whether a change in a patient's field is the result of variability in performance from one day to another (long-term inter-test variability) or the result of a pathologic change.

First, one needs to guard against artifacts and errors by paying attention to a few specific issues:

1. Check the *name* to ensure that one is examining the right patient! Many clinicians have known the embarrassment of having to halt the delivery of a grim prognosis because of the sudden realization that the field or mag-

netic resonance images in their hands belong to a different patient.

2. Check which *targets* were used, so that one knows that the isopters being compared are the same targets. This also means checking that factors that alter retinal illumination or focus have not changed either, since they will alter the effective isopter too. If the patient was tested with a different *lens*, make sure that this was because the patient's refraction had changed and not because of an error. Could the patient's *pupil size* have changed drastically? This usually means being tested with drops on one occasion but not on another; do not forget the possibility of a patient discontinuing miotic medication for glaucoma, as well as the more obvious case of mydriatic drops applied in the clinic. Do the clinic notes suggest that the patient may have had progression of a *cataract* in the interim (Fig. 14)?
3. Check that the patient did not differ in *attention or arousal* between tests. It is hoped that the perimetrist has noted this on the chart. Further investigation may reveal that the patient was on a sedating medication on one occasion.

Fortunately, almost all of these factors will alter sensitivity globally rather than focally. For example, a cataract makes a target fainter and blurred, which can make an I3e target appear more like the I2e target when there had been no cataract. The result is a general constriction of isopters, as if the target had been moved up the hill of vision. However, sometimes a global change can alter the appearance of the isopters in a patient with an abnormal field. If the hill has a complex shape, moving the target up the hill of vision might place it in a region with a different shape from the prior isopter, *even though no change in the shape of the hill had occurred* (Fig. 14). A clue that one or the other of these global factors is operating on a complex field is that the isopters (using the same targets) are also constricted in the otherwise normal sectors of the visual field.

Changes from pathology are often obvious if they involve the addition of a second focal defect. Consider a patient with multiple sclerosis and an old central scotoma from optic neuritis in the right eye who now develops a homonymous superior quadrantanopia from a demyelinating plaque in the optic radiations. This is not going to be confused with long-term variability or artifact.

More difficult is the issue of progression of the original defect. Is a nasal step or arcuate defect worsening in a patient with idiopathic intracranial hypertension or glaucoma? Therapeutic decisions often hinge on such questions. One must consider all the factors, whether a global reduction from some other irrelevant factor is creating a "pseudo-progression," and whether the patient's current or past performance was too unreliable and variable on which to rely. In situations of uncertainty it is best to have the patient return for another perimetric examination or two. Continued persistence or consistent progression over several fields is less likely to be due to inter-test variability than one-time discrepancy between a single pair of fields.

REFERENCE

1. Trobe J, Acosta P, Krischer J. A screening method for chiasmal visual-field defects. *Arch Ophthalmol* 1981;99:264–271.

5 Automated Perimetry (Humphrey Field Analyzer)

The Humphrey field analyzer is the dominant automated perimetric device in clinical practice. There are other devices, though, including the Octopus, Topcon, and Dicon perimeters. While the printouts of the reports differ in format, they all measure the same differential light sensitivity threshold, and the principles of analyses are fairly similar and often translate from one device to another.

The Humphrey perimeter was designed to mimic the conditions of the Goldmann perimeter. Thus, it has the same viewing distance (33 cm), same background luminance (31.5 asb), same size targets with the same designations (I–V), and its intensity can be converted easily to that of the Goldmann targets with a table (Table 1). The range of target luminances possible is greater than that of the Goldmann device. However, automated perimetric programs generally do not switch among different target sizes, so that this restricts the testing range in a different way. The standard or default target test size is the III target (diameter = 2.3 mm). With this size III target, the brightest target ($S = 0$ dB, $I = 10,000$ asb) is perceptually equivalent to the V4e Goldmann target.

In contrast to manual Goldmann perimetry, the mainstay of automated perimetry is the static rather than kinetic mode of target presentation. The Humphrey Field Analyzer flashes targets for 200 ms at predetermined locations arranged in a grid (Fig. 1). The pattern of the field is interpolated from these separated locations. It is important to remember that the field is not actually tested at locations between these grids, so small scotomata (or, conversely, small islands of vision in a large defect) may be missed if the grid of the test selected is too coarse. Newer models of the Humphrey Field Analyzer do offer an automated kinetic program, but it is not clear how useful this will prove in practice. The flexibility to tailor an examination to a patient's defect on the fly, using the judgment of a human operator, is an advantage to a manual technique that is hard for a machine to match, whether the target moves or not.

1. PERFORMANCE OF PERIMETRY

1.1. CALIBRATION

As with the Goldmann perimeter, calibration of the background and target is important. Unlike the Goldmann perimeter, this is done automatically by the Humphrey Field Analyzer. As

Table 1
Relation of Intensity (I), Humphrey Sensitivity (S), and Goldmann Target Brightness

I (asb)	$\log(I, \text{asb})$	S (dB)	Goldmann
10,000	4	0	
6310	3.8	2	
3981	3.6	4	
2512	3.4	6	
1585	3.2	8	
1000	3	10	4e
794	2.9	11	4d
631	2.8	12	4c
501	2.7	13	4b
398	2.6	14	4a
316	2.5	15	3e
251	2.4	16	3d
200	2.3	17	3c
158	2.2	18	3b
126	2.1	19	3a
100	2	20	2e
79	1.9	21	2d
63	1.8	22	2c
50	1.7	23	2b
40	1.6	24	2a
32	1.5	25	1e
25	1.4	26	1d
20	1.3	27	1c
16	1.2	28	1b
13	1.1	29	1a
10	1	30	
6	0.8	32	
4	0.6	34	
3	0.4	36	
2	0.2	38	

with all perimetry, the room should be dark and without visual or auditory distraction.

Patients should have an appropriate near correction for most tests, since the vast majority of tests are devoted to the central 30° or less, where refraction affects thresholds. If their near correction is not known, a table of approximate age-appropriate additions to their far prescription is available in the device's manual.

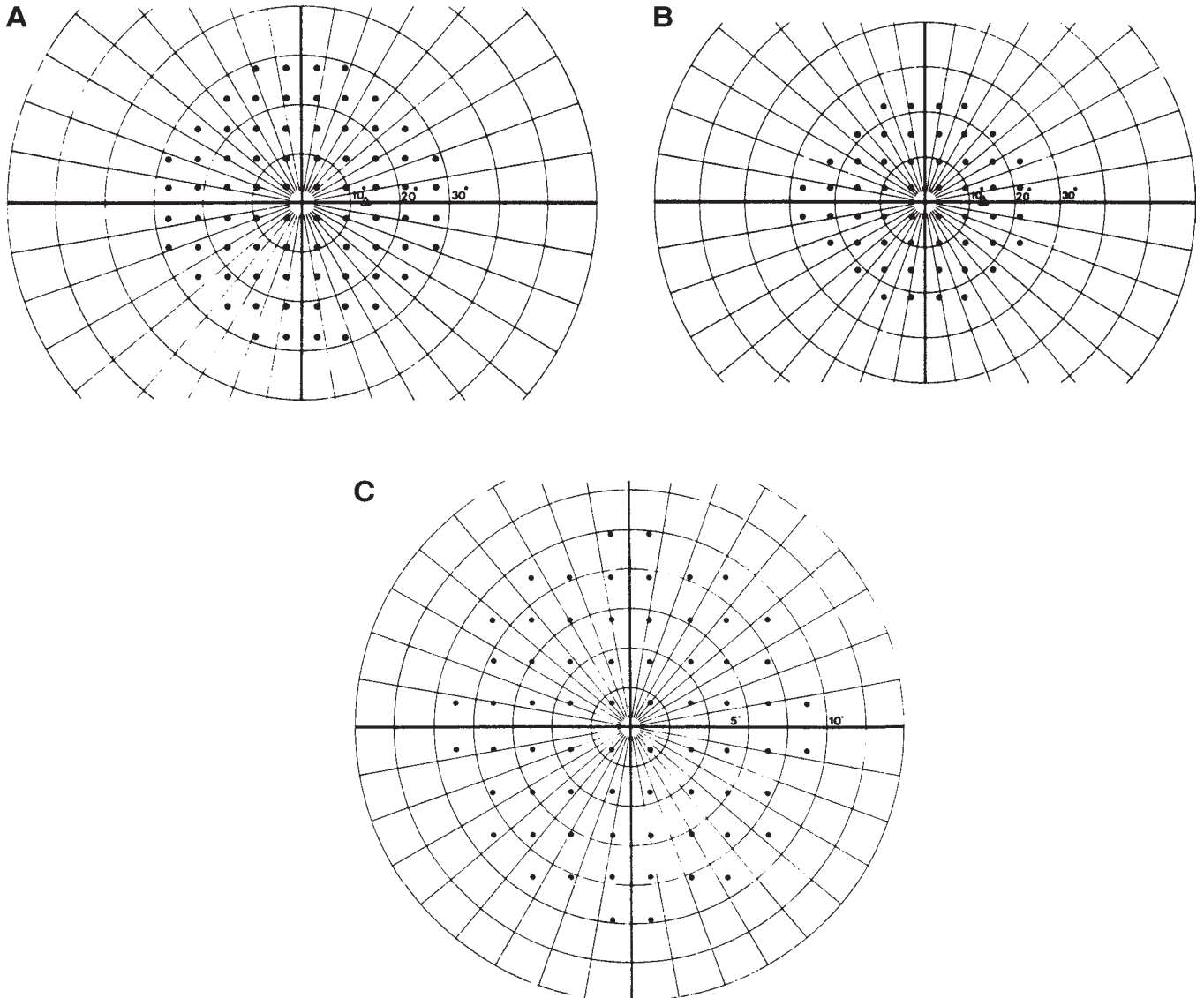


Fig. 1. Grids of test points: (A) 30-2; (B) 24-2; (C) 10-2. (From the Humphrey Field Analyzer manual.)

1.2. DATA ENTRY

Date entry is required as a preliminary step, under "Main menu" (Fig. 2). The following entries are included:

1. *Date, time:* These may be automatically entered by the computer.
2. *Patient name, identification number, and birth date:* If the examiner wishes to have the perimeter print out a sequential analysis of several fields done over time in the same patient, the name must be entered exactly the same on all fields. Numbers and birth dates differentiate patients with the same name.
3. *Visual acuity, pupil diameter (in clinic), and refractive correction used during perimetry:* Again, if comparisons over time are to be made, the examiner needs to know if these factors are changing. A decrease in pupil diameter from 4 to 2 mm will reduce sensitivity by about 0.7 dB (1). Refractive blur will also increase thresholds diffusely.

4. *The type of test and eye being tested:* Finally, on the next screen (Fig. 3), the type of test to be performed is chosen (see below), following which the eye being tested is indicated. After this a screen appears with a display of the locations that will be tested in the field, along with reliability indices that will be completed and some menu options (Fig. 4). Among these is one to display the eye position monitor, a videocamera view of the patient's eye for online monitoring of fixation. This should be chosen. The screen remains visible during the test.

1.3. PATIENT PLACEMENT

One eye is occluded with the patch flush to the nose but not protruding to obscure the vision of the viewing eye. The buzzer is placed in the patient's hand. The chair or perimeter is adjusted for the patient's height. Discomfort from poor posture maintained over 10 min will distract the patient and degrade performance. The chin holder is adjusted vertically and horizontally by means of

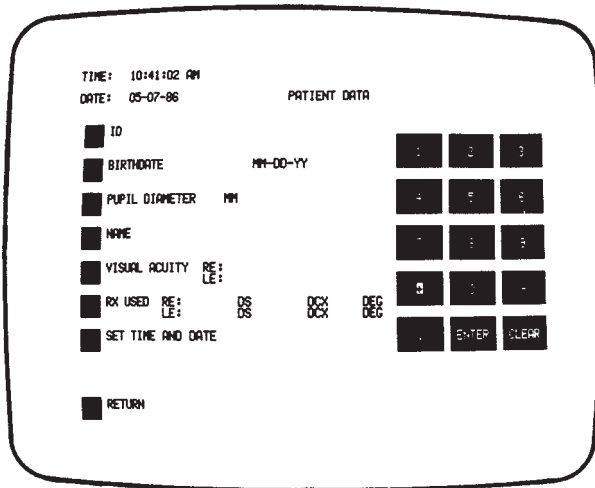


Fig. 2. Screen for data entry. The item to be entered is selected by touching the squares on the left. New models also have a keyboard option. (From the Humphrey Field Analyzer manual.)

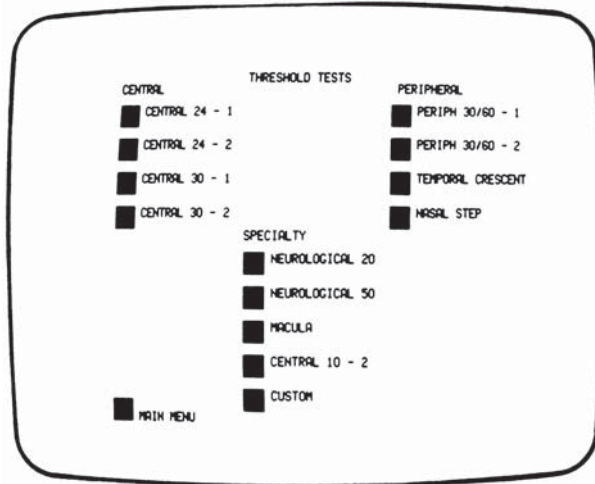


Fig. 3. Screen menu for threshold tests. (From the Humphrey Field Analyzer manual.)

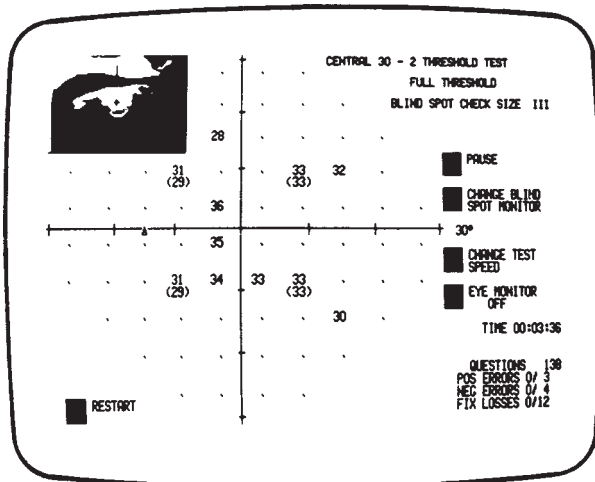


Fig. 4. Screen during test. A video of the patient's eye is displayed in the top left corner. Dots are gradually replaced by threshold values as they are measured. (From the Humphrey Field Analyzer manual.)

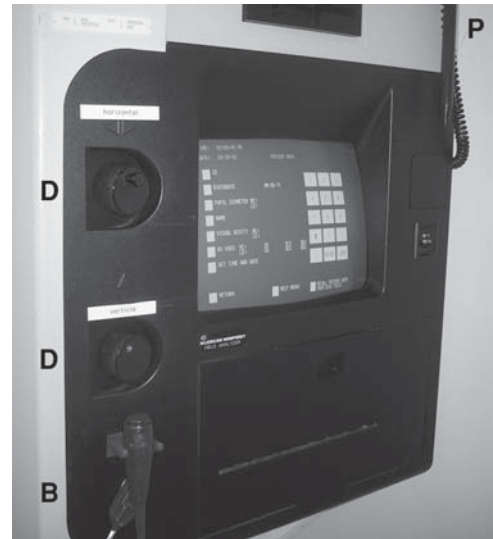


Fig. 5. Operator's end of machine. The touchpen (P) used to enter data on the screen is at the top right, the buzzer (B) used by the patient is stored at the bottom left, and the dials (D) for adjusting the chin rest are to the left of the screen.



Fig. 6. Patient's end of machine showing a view through chin rest with lens holder in position. The small fixation spot is visible just right of the lens.

dials on the side of the machine (Fig. 5) until the eye being tested is centered in the crosshairs of the eye position monitor. Final adjustments of the chair are made for comfort. The lens holder is adjusted to place the lens as close to the patient's eye as possible, without touching the lashes (Fig. 6). A lens holder far from the patient will occlude the patient's view of the test area and cause an artifactual scotoma. If the patient does not need a lens, the lens holder is flipped out of the way.

1.4. INSTRUCTIONS TO THE PATIENT

Giving instructions to patients is critical, particularly in patients new to the test. A few minutes here greatly increases the likelihood of obtaining useful data. The following key points must be stressed to patients:

1. They should always look at the steady yellow light at center, no matter how boring this is. Only when patients are looking at the yellow light do we know where the test lights flash on their retina. If they are looking away, we have no idea where they were, and if this happens too often the test becomes meaningless.
2. While they fix on the yellow light, the computer will flash small spots of light at random locations in their side vision. Their job is to press the button in their hand every time they are aware that something flashed.
3. If this is a threshold test, the perimeter is trying to determine at each location the boundary between the visible and the invisible. This has two consequences. The first is that there will always be some very faint lights that they do not see, no matter how good their vision is, but this does not mean that they are going blind. The test must show them some unseen lights to know where that boundary lies. The second is that lights very close to the boundary will be quite dim and they will feel uncertain of their presence. They should do their best, realizing this, and simply signal if they are aware that something has flashed, no matter how dim.
4. They should not feel afraid to blink from time to time. The best plan is to blink just after they see a target, since there is always a short interval between one target and the next.
5. A typical threshold test will take about 10 min for each eye.
6. It is best if a technician monitors the test, providing feedback on fixation via the eye monitor, but patients should not talk to the technician unless there is a problem.

On the screen displayed during the test (Fig. 4), the perimeter initially provides the option of a short demonstration. The lights should be dimmed and this demo should be shown so that (1) the patient can see examples of the flashes that are the targets, and (2) the examiner can see that the patient understands the concept of fixation. It is useful to remind the patient at this point to keep their eye on the yellow spot and press the button when they see the small white flashes. Once the operator is confident that the patient can comply with fixation and respond to flashes with a button press, the test can be started.

After completion of the first eye's test, the occluder is removed and the lights turned on so that the occluded eye recovers from its dark-adapted state before it is tested.

1.5. PROGRAM CHOICE: MODE OF TARGET PRESENTATION

1.5.1. Screening Strategies

Screening strategies are meant to save time, screen for the presence of a defect, and roughly localize it. They are best reserved for new patients in whom the index of suspicion of a deficit is low, or in whom one wishes to get a screen of the whole field but cannot access a Goldmann perimeter. Detailed quantitative assessment of the full field is better done with the Goldmann, and detailed central perimetry should use threshold strategies. Three different screening strategies are available, in the following order of sophistication:

1. *Single intensity*: This is what it says. One value of brightness—by default 24 decibels (dB), but easily altered—is presented at all points tested (Fig. 7). However, because of the natural decline in sensitivity with eccentricity, a central

defect would have to be much greater than a peripheral defect to be detected by this strategy.

2. *Threshold related*: This attempts to make the degree to which the screening target exceeds expected threshold the same across the visual field. It measures a central threshold and a peripheral threshold and fashions an expected normal hill of vision for that eye from these two values. (If the subject fails to exceed a threshold of 26 dB at either locale, this value will be used as a default.) It then presents a series of suprathreshold targets 6 dB above the threshold predicted at each test location.
3. *Three zone*: This takes the threshold-related screen one step further. If the suprathreshold target is missed, the spot is retested later with a maximum intensity target of 0 dB (10,000 asb). The three zones of results are: normal (saw suprathreshold target), relative defect (missed suprathreshold but saw maximum intensity target), absolute defect (did not see even the maximum intensity target).

1.5.2. Threshold Strategies

Threshold strategies quantify the degree of reduction of sensitivity at all tested points. They are most useful in following defects over time, and providing a detailed map of each eye's deficit. Although more time-consuming than screening protocols, these are the method of choice for the diagnostic fields required in neuro-ophthalmology. There are three strategies here also:

1. *Full threshold* (Fig. 8): Each point in the field is subjected to the staircase method of threshold determination (see Appendix). The computer first determines the threshold at one "primary point" per quadrant (9° away from the vertical meridian and 9° away from the horizontal meridian for a 30-2 program). This threshold is then used to determine the starting point for the staircase at neighboring locations, as a time-saving maneuver. These thresholds then feed into the staircase onsets of their neighbors, and so on. All staircases consist of 4 dB decrements in light intensity until the patient fails to respond (first reversal), then 2 dB increments until the patient sees the light again (second reversal). This final level is the sensitivity printed (Fig. 9). The primary points have their thresholds estimated twice, as do points that deviate more than 4 dB from an expected threshold based on their neighbors' results. These second estimates appear in parentheses on the sensitivity plot.
2. *Full threshold from prior data*: The starting point of each staircase sequence is adjusted on the basis of performance at that location on a previous test. Obviously, this time-saving maneuver can only be used when there is a prior field in the computer, with the patient's name entered precisely the same way.
3. *Fast threshold*: Baseline data from prior fields are also used, and a full threshold strategy implemented only at spots where there is a deviation from the baseline. The major drawback here is the ineligibility of these results for statistical analysis, since there are no real sensitivity numbers for the points that have not changed from the prior test.

1.6. PROGRAM CHOICE: THE ALGORITHM

Full threshold perimetry is tedious for any subject. The average time per eye for a 30-2 field is more than 12 min for normal subjects (2). It is even longer for patients, in whom the visual fields are more complex; for example, the test takes a mean of

EYE: LEFT

FULL FIELD 120 POINT SCREENING TEST

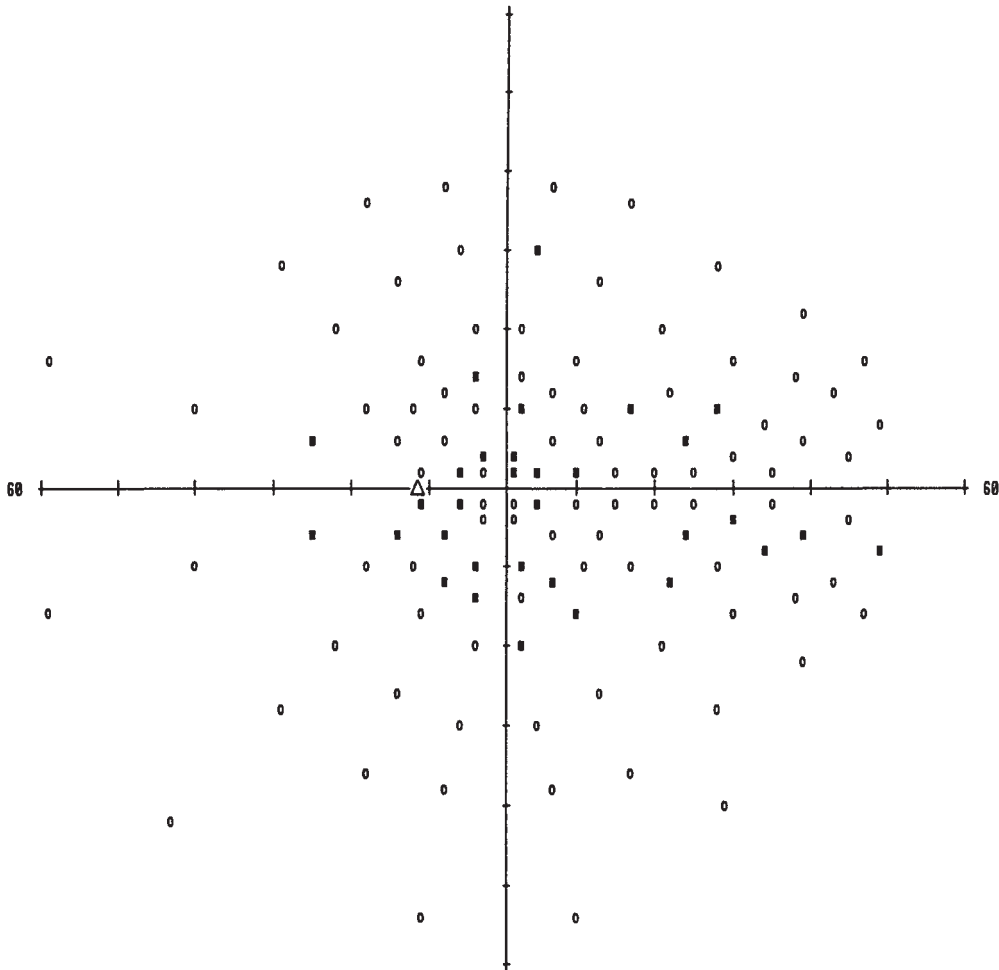
FIXATION MONITOR: BLINDSPOT
 FIXATION TARGET: CENTRAL
 FIXATION LOSSES: 13/17 XX
 FALSE POS ERRORS: 7/15 XX
 FALSE NEG ERRORS: 5/14 XX
 TEST DURATION: 09:27

STIMULUS: III, WHITE
 BACKGROUND: 31.5 ASB
 STRATEGY: TWO ZONE
 TEST MODE: AGE CORRECTED

PUPIL DIAMETER:
 VISUAL ACUITY:
 RX: DS DC X

DATE: 02-05-2002
 TIME: 11:59 AM
 AGE: 37

CENTRAL REFERENCE: 34 DB
 PERIPHERAL REFERENCE: 34 DB



○ SEEN 80/120
 ■ NOT SEEN 32/120
 △ BLINDSPOT

Fig. 7. Example of 120-point screening test. Points are scored as either seen (circles) or not seen (solid squares). There is a suggestion of a central defect, but all the reliability indices are terrible. Nothing can be concluded about this patient's field.

CENTRAL 30 - 2 THRESHOLD TEST

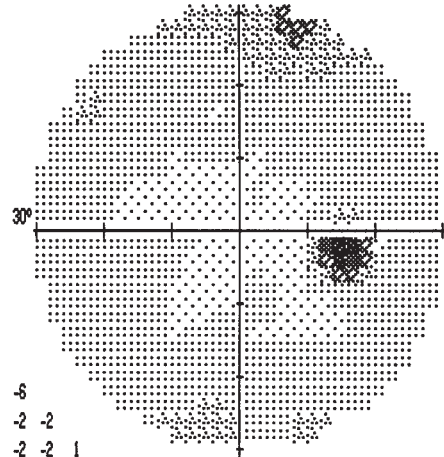
DATE 01-28-02

STIMULUS III, WHITE, BCKGND 31.5 ASB BLIND SPOT CHECK SIZE III
 STRATEGY FULL THRESHOLD
 FASTPAC

FIXATION TARGET CENTRAL
 RX USED +1 DS DCX DEG PUPIL DIAMETER 3.0 MM VA 20/20
 TIME 03:37:14 PM

RIGHT

AGE	35	25	28	28	28	26	26	26	26	26
FIXATION LOSSES	1/16	25	30	28	31	26	31	28	30	30
FALSE POS ERRORS	0/4	27	29	29	31	30	31	29	28	27
FALSE NEG ERRORS	0/7	30	30	33	31	35	30	27	28	28
QUESTIONS ASKED	252	29	29	29	30	34	33	31	32	28
TEST TIME	00:07:31	29	29	29	28	36	29	34	30	29
HFA S/N	630-4943	28	30	31	29	31	31	33	26	26
		27	29	27	29	29	31	28		



	-1	-1	-3	-6						
	0	0	0	-2	-2	-2				
	-3	0	-2	1	-4	-2	-2	1		
	-1	-1	-2	-1	-2	-1	-3	-2	-2	-2
	2	0	1	-2	2	-3	2	-3	-2	
	0	-2	-3	-3	-1	0	-1	1	-3	
	1	-1	-3	-2	0	-3	0	-1	-2	-2
	-1	-2	0	-3	-1	-1	0	-5		
	-2	-1	-3	-2	-2	-1				
TOTAL DEVIATION	-3	-5	1	-5						

	-1	-1	-4	-6						
	0	-1	-1	-3	-2	-2				
	-4	0	-3	0	-4	-2	-2	1		
	-1	-1	-2	-1	-2	-1	-4	-2	-2	-3
	1	0	1	-2	2	-3	2	-3	-3	
	0	-2	-4	-4	-1	-1	-2	0	-3	
	0	-2	-3	-2	0	-4	0	-2	-2	-3
	-2	-3	-1	-3	-1	-1	0	-5		
	-3	-1	-4	-2	-2	-1				
PATTERN DEVIATION	-3	-5	0	-5						

PROBABILITY SYMBOLS
 :: P < 5%
 ◐ P < 2%
 ◑ P < 1%
 ■ P < 0.5%

MD -1.34 DB
 PSD 1.77 DB
 SF 2.63 DB
 CPSD 0.00 DB

	GRAYTONE SYMBOLS									REV BG
SYM										
ASB	.8	2.5	8	25	79	251	794	2512	7943	≥
	.1	1	3.2	10	32	100	316	1000	3162	10000
DB	41	36	31	26	21	16	11	6	1	≤0
	50	40	35	30	25	20	15	10	5	≤0

BETH ISRAEL HOSPITAL
 330 BROOKLINE AVENUE
 BOSTON, MA. 02215

HUMPHREY SYSTEMS

Fig. 8. Example of normal 30-2 full-threshold test. There is excellent reliability and the global indices are all normal. The total deviation map shows only one spot with a slight <5% deviation from normal, and the pattern deviation is clean.

14.5 min in those with glaucoma (3). Fatigue and boredom can become confounding factors. If there are no prior data for the subject to help speed up the test, there are still other means of shortening the ordeal.

The FASTPAC option accepts a less accurate estimate of threshold in exchange for shorter test times, with savings of about 40%. It uses 3-dB steps and terminates at a single change in response (i.e., from seeing to not seeing), rather than reversing

direction to find a second change in response (Fig. 9). This reduces testing time by 30-36% in patients with glaucoma, at the expense of greater short-term fluctuations (4,5). This slightly greater variability may make it less effective than the standard full-threshold technique in following defects serially.

SITA (Swedish Interactive Threshold Algorithms) methodology has been introduced more recently into clinical practice. This technique starts with similar threshold determinations for

Table 2
Field Location Options for Humphrey Automated Perimetry

Zone	Screening test	Threshold test	Area of field covered
Central field only		Macula	0–4°
		Central 10-2	0–10°
	Central 40pt, or	Central 24-1	0–24°
	Central 80pt	Central 24-2	0–24°
	Central 76pt, or	Central 30-1	0–30°
	Central 166pt	Central 30-2	0–30°
Peripheral field only	Peripheral 68pt	Peripheral 30/60-1	30–60°
		Peripheral 30/60-2	30–60°
Full field	Full field 120pt, or Full field 246pt		0–60°
			0–60°
Special designs	Glaucoma/optic neuropathy	Armaly central	0–15°, plus nasal wedge to 25°
		Armaly full field	0–15°, plus nasal wedge to 60°
	Nasal step	Nasal step	Nasal field only, 30–50°
Neurologic		Temporal crescent	Temporal field only, 60–80°
		Neurologic 20	Vertical meridian only, 0–20°
		Neurologic 50	Vertical meridian only, 0–50°

Bold type indicates most frequently used programs.

the four primary points in the quadrants, again using these to generate the starting levels for thresholds at neighboring points. However, as the test proceeds, sophisticated statistical analyses are applied, using knowledge of typical probability functions for this frequency-of-seeing task in both age-corrected normal and abnormal populations (6). This generates with each response of the patient a best guess of the threshold, called the *maximum posterior estimate*, as well as an estimate of the measurement error for that value. When this error estimate is less than a pre-determined limit (the error-related factor), testing at that location is stopped; otherwise, the strategy continues until two staircase reversals occur, as in the traditional full-threshold strategy. Additional tweaks to the process involve incorporating data from neighboring points in modeling responses and using the patient's reaction times to determine an optimal response-time window, during which responses to the stimuli are accepted by the computer. False positives are calculated from anticipatory responses (button presses made too quickly after a light flash to be considered a response to the stimulus) rather than the formal catch trials used in full-threshold perimetry.

There are now also SITA Standard and SITA Fast options. The latter uses a more lax error-related factor to terminate threshold estimates, again buying speed at the sacrifice of some accuracy.

The end result of the SITA modifications is a test that is quicker yet comparable in accuracy to traditional methods. In normal subjects, a single field takes 6 min to complete with the SITA Standard program, compared with 7 min for FASTPAC and 12 min for Full Threshold. In glaucoma, average test times of one field are 5 min for SITA Fast and 8 min for SITA Standard, compared with 9.5 min for FASTPAC and 14.5 min for Full Threshold (3,7). The results appear to be equivalent in accuracy, with SITA estimates

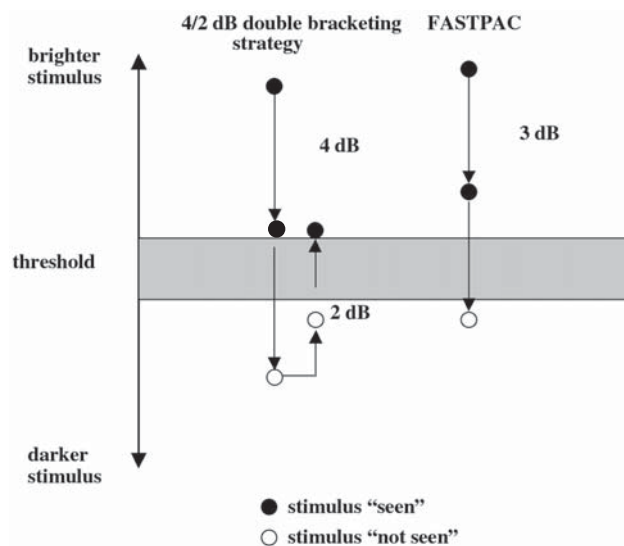


Fig. 9. Staircase strategies. A comparison between standard full-threshold technique (left) and FASTPAC option (right). The standard technique requires two response reversals (from "seen" to "not seen" in 4-dB steps, then back to "seen" again with 2-dB steps), whereas the FASTPAC option uses 3-dB steps to a single response reversal. (From ref. 4, with permission.)

of threshold slightly higher than those of conventional perimetry, and consistently reproducible across repeated testing, an important point in following progression (3). SITA also produces results comparable with the Full Threshold method in optic neuropathies and hemifield defects (8). SITA will likely supplant Full Threshold programs in the near future.

A

SINGLE FIELD ANALYSIS

EYE: LEFT

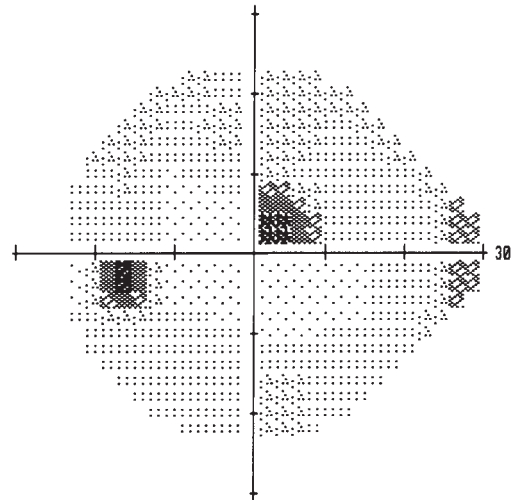
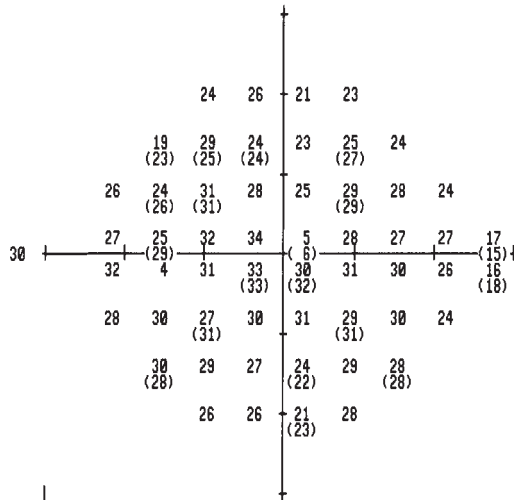
CENTRAL 24-2 THRESHOLD TEST

FIXATION MONITOR: BLINDSPOT
 FIXATION TARGET: CENTRAL
 FIXATION LOSSES: 0/21
 FALSE POS ERRORS: 0/9
 FALSE NEG ERRORS: 0/9
 TEST DURATION: 11:28
 FCOVER: OFF

STIMULUS: III, WHITE
 BACKGROUND: 31.5 ASB
 STRATEGY: FULL THRESHOLD

PUPIL DIAMETER:
 VISUAL ACUITY:
 RX: +3.25 DS DC X

DATE: 05-22-2001
 TIME: 12:54 PM
 AGE: 70



TOTAL DEVIATION

0	2	-4	-2
-5	1	-3	-4
0	-2	3	-1
-1	3	3	-26
4	1	2	0
0	1	-1	0
1	0	-2	-6
-2	-2	-5	1

PATTERN DEVIATION

-1	0	-5	-3
-6	-1	-4	-6
-2	-4	2	-2
-2	1	2	-27
3	0	1	-2
-1	0	-2	-2
-1	-1	-3	-7
-3	-3	-7	0

GHT
 OUTSIDE NORMAL LIMITS

MD -1.44 DB
 PSD 5.41 DB P < 1%
 SF 1.50 DB
 CPSD 5.17 DB P < 0.5%

:: < 5%
 ☒ < 2%
 ☒ < 1%
 ■ < 0.5%

JOSLIN DIABETES CENTER
 ONE JOSLIN PLACE
 BOSTON, MA 02215
 617-732-2400

Fig. 10. Comparison of 10-2 and 24-2 threshold test of a patient with a small perfoveal scotoma. (A) This causes a single abnormal spot on the 24-2 test. (B) Note the greater detail on the 10-2 test. (Fig. 10B continued on next page.)

B

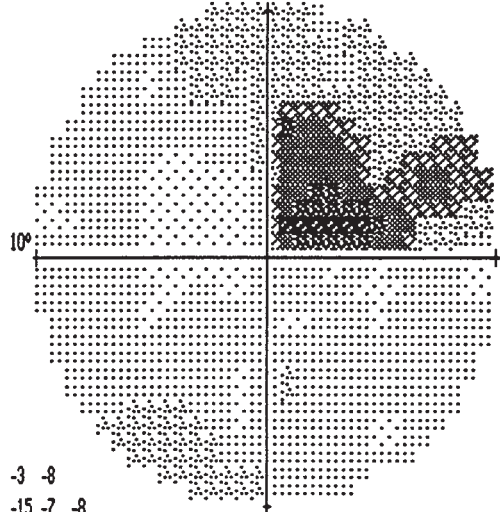
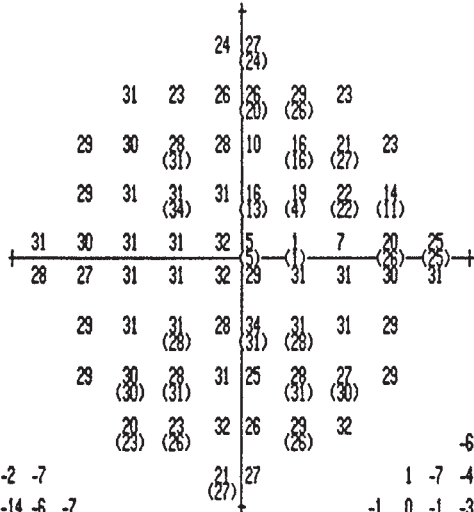
CENTRAL 10 - 2 THRESHOLD TEST

DATE 10-25-01

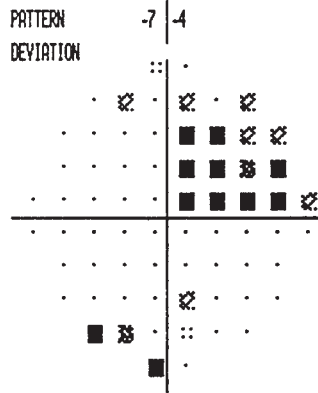
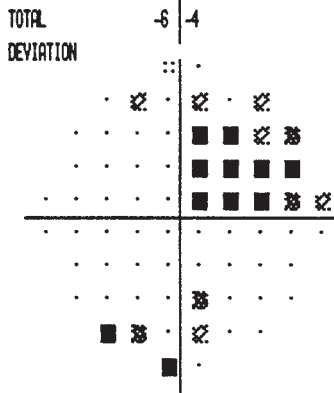
STIMULUS III, WHITE, BCKGND 31.5 ASB BLIND SPOT CHECK SIZE III
 STRATEGY FULL THRESHOLD
 FASTPAC

FIXATION TARGET CENTRAL
 RX USED +3.25 DS DCX DEC PUPIL DIAMETER VA
 TIME 12:27:03 PM

LEFT
 AGE 71
 FIXATION LOSSES 0/18
 FALSE POS ERRORS 0/4
 FALSE NEG ERRORS 0/7
 QUESTIONS ASKED 301
 TEST TIME 00:09:28
 SF 3.79 DB
 HFA S/N 630-4943



		-5	-4							
	2	-7	-4	-7	-2	-7				
	0	1	-1	-2	-20	-14	-6	-7		
	-1	1	2	0	-16	-19	-9	-18		
	2	0	1	0	1	-26	-30	-24	-8	-6
	-2	-3	1	0	1	-2	0	0	-1	0
	-1	0	-2	-3		2	-2	0	-2	
	-1	-1	-1	0		-6	-1	-2	-2	
	-9	-6	2			-5	-3	1		



PROBABILITY SYMBOLS
 :: P < 5%
 ☒ P < 2%
 ☒☒ P < 1%
 ■ P < 0.5%

Fig. 10. (continued)

**1.7. PROGRAM CHOICE:
 ZONE OF TARGET PRESENTATION.**

Once the method of target presentation has been selected, the locations to be tested must also be chosen (Table 2). There are three major zones—central, peripheral, and full field—in addition to specialized zones.

1. *Central zone:* This region has the most choice. The most common region to test is the central 30° or the central 24°, the latter used more in the setting of glaucoma. The screening menu in these two regions offers both a standard screen and a more detailed screen with more test locations in a finer grid. Thus, both the central 76-point and central 166-point screens cover the central 30°, but

the latter tests 166 points as opposed to the 76 of the former. (The central 76-point screen tests the same locations as the 30-2 threshold program.) The threshold menu in these two regions also offers two versions. These are marked by the suffixes -1 and -2. Both space their locations 6° apart, but the -1 versions start their points on the horizontal and vertical meridians, whereas the -2 versions place test locations flanking the meridians. The flanking design of the -2 versions is better suited for determining nasal and hemianopic steps, and for this reason is always to be preferred. More fine-grained tests of the central 10° or 4° (macula) are useful for subjects with very small central field defects (Fig. 10) that would be

- poorly characterized by the coarse spacing of the grids used in the 24-2 and 30-2 programs (Fig. 1).
2. *Peripheral zone*: Mapping of the field only between 30 and 60° is also available. Generally, this is meant to supplement a central field examination when a more extensive defect is suspected. It is seldom used, because such defects are better diverted to Goldmann perimetry.
 3. *Full field*: Threshold strategies are not available for the full-field programs because they would take far too long to accomplish. The full-field 120-point screen is the most commonly used (Fig. 7). Again, if one is seeking a detailed evaluation of the periphery, the Goldmann perimeter should be used.
 4. *Specialized*: These are designed to save time by concentrating on a region specific to some disease process that the clinician has already identified. For glaucoma, the central 15° and the nasal meridian are the vulnerable zones, and the Armaly screening programs concentrate on these two regions. Probes for nasal steps alone are also available. For neurologic defects at or beyond the chiasm, there are neurologic programs that test flanking pairs of points along the vertical meridian. There is also a program to test the temporal crescent, but to arrive at this point one has presumably already used a central and a peripheral threshold examination. Far better to do one Goldmann field in 10 min than three Humphrey fields in 40.

1.8. PRINTING RESULTS

One of the highlights of automated threshold perimetry is the availability of statistical analysis of the patient's results. When the patient has completed testing, there is a choice of three types of printout: single field analysis, change analysis, and overview. The latter two are meant to aid the interpretation of multiple fields obtained at different times.

2. THRESHOLD PERIMETRY ANALYSIS

2.1. THE SINGLE-FIELD ANALYSIS

Always check a few simple things first. The name, to ensure that it is the right patient; the date; and the refraction used. The latter is important when comparing one field with another in follow-up. An apparent global decrease in sensitivity may merely reflect a difference in lenses used, with presumably improper refraction on one occasion.

2.1.1. Reliability Indices

Can you trust what you see or is it junk? These indices will help you:

1. *Fixation loss (FL)*: The perimeter periodically flashes a target in the physiologic blind spot, which it maps early in the course of the test. If the patient is not looking at the yellow fixation light, he or she will see the flash and press the button. The denominator tells how many times the perimeter tested for this in the test, and the numerator the number of times the patient fell for it. Frequent FLs cast doubt on the sensitivity of the test to find subtle defects; the location and margins of these will be degraded by a roving eye. Caution is required when interpreting seemingly low fixation loss indices in patients with blind spots that are enlarged or fall within larger field defects (such as a temporal hemianopia). These patients may still not see the target probing for FL even if they are making large movements with their eyes.

This means of monitoring fixation is known as the Heijl-Krakau method. The disadvantage is that the results cannot be modified by fixation data. Other automated devices monitor actual eye position with video or infrared technology and either halt testing or exclude trials with improper eye position. The newer Humphrey Field Analyzers also monitor eye position with a video system but do not use the data to modify data on-line, except to exclude trials in the case of blinks. Rather, a small graph is made to provide one with a sense of eye stability during the test, to augment the FL index.

2. *False positives (FPs)*: Occasionally there are intervals during which the machine makes a soft click but shows no target. An overly sensitive subject will have a high FP error rate, pressing the button during these intervals. This too will lead to underestimation of the severity and extent of a defect. As mentioned, the SITA strategy does not use these "catch trials" but, rather, counts the number of anticipatory responses, made too soon after a flash to be a response to the light (6).
3. *False negatives (FNs)*: A fairly bright suprathreshold target is flashed in a region previously tested with fainter targets. If the patient fails to indicate its presence, this is an FN error. A high FN rate usually implies inattention or fatigue and will be accompanied by a field with scattered factitious elevations of threshold.

For all these reliability indices, the Humphrey Field Analyzer suggests that more than 20% error rate is a warning of poor reliability. This will be indicated by an "xx" beside the aberrant value and a printed statement of "low patient reliability," in the upper left corner.

4. *Number of questions asked and time taken to do the test*: These are not usually that important, but if the patient's reliability was poor, it may be because the test took a long time and presented a lot of trials, leading to fatigue. The problem can also work in the other direction. An unreliable patient will confuse the machine's algorithms and not allow it to use its statistical shortcuts, leading to longer test times. Patients with complex field defects generally take longer to test than those with normal fields.

2.1.2. Maps

There are three maps printed in any single-field analysis, each represented by a number plot and an accompanying pictorial representation. The three maps are visual sensitivity, total deviation, and pattern deviation. The visual sensitivity map and its gray scale counterpart plot decibel values, whereas the graphs of the latter two are sometimes referred to as *probability maps*, because they plot a statistical analysis of the deviation of the patient's performance from a normal reference.

1. *Visual sensitivity*: The large plot of numbers, which are numeric (decibel) results, contains the actual estimates of sensitivity at each point tested (to find out what threshold luminance is implied by the decibel results, see Table 1). Some of these numbers have other numbers in brackets below them—these are locations where the threshold has been estimated twice. If the two estimates are close together, there is little fluctuation, and the results are consistent. The gray scale result is a pictorial rendition of these numbers, in which darker shades represent lower sensitivities, and the shading is interpolated for the areas

between the actual points tested. The pictorial code is shown at the bottom as “gray tone symbols.” In a sense, the gray scale gives the misleading impression of what has really been measured, since only a small region of the field within the depicted circle has actually had light shone on it.

2. *Total deviation*: Are those sensitivities normal or not? The perimeter has a bank of normative age-matched data, to which each point is compared. The total deviation takes the patient’s sensitivity at point A, subtracts the mean sensitivity of the normal group at that location, and assigns this difference to point A. A negative value means that the patient is less sensitive than the normal group. To determine whether this is significant, one also needs to take into account the variance of the normal group. This is what the pictorial graph for total deviation does. It plots the probability that the measured deviation is significantly different from the group, essentially using a *t*-test. The more deviant, the darker the symbol, as is indicated by the code “probability symbols” printed on each field analysis.
3. *Pattern deviation*: The normal pattern of vision is the hill, with a peak central sensitivity that gradually decays with increasing eccentricity in all directions. Deviations from this hill are characteristic of many pathologic field defects. By contrast, effects of pupil size and refractive errors tend to cause global reductions, without a change in the normal pattern of vision. To remove the impact of diffuse reductions, the perimeter finds the 51 most sensitive locations in the field, estimates what the normal hill of vision should be from these, and then determines how much of a deviation from this theoretical hill is present at each tested point. Again, a probability map is presented that estimates the significance of each deviation. This pictorial map is the most important one in determining whether a pathologic defect is present or not.

2.1.3. GLOBAL INDICES

Global indices are meant to provide some grand summary that captures something about the field in a single number. While this may seem a bit futile, these indices can be useful in sequential follow-up. All are printed as sensitivity measures in decibels, along with the (*p*-value) probability that these are abnormal.

1. *Mean deviation (MD)*: This is simply the mean of all the values in the total deviation map. Obviously, the deviation in the localized defects common to neuro-ophthalmologic problems will be diluted by the lack of deviation in regions without defects. On the other hand, MD will be strongly affected by refractive factors that globally depress sensitivity, such as cataracts or incorrect refractive correction. Nevertheless, MD can be moderately useful in the following the change in a field over time, as long as global refractive issues are taken into account. The latter should be obvious from the total deviation probability plots.
2. *Pattern standard deviation (PSD)*: This is the mean of the values in the pattern deviation plot. PSD advances on mean deviation in that the effects of global depression should be filtered out.
3. *Short-term fluctuation (SF)*: How consistent is the patient from moment to moment (intra-test variability)? This can be checked from the points that were measured twice.

The mean of each pair is taken as the best guess of the true sensitivity, and the square of the deviation of the points of the pair from the mean is the variance. Thus, readings of 30 and 36 at one location give an estimated mean of 33, and a variance of $(30 - 33)^2 + (36 - 33)^2 = 18$. The mean of the variances of all points tested twice is calculated, and the square root of this is the SF. A value of < 2 dB indicates consistent performance. Higher fluctuation may occur with a variably attentive subject. Such subjects should also have a high FN error rate. A low FN error rate with high SF is characteristic of subtle relative defects, particularly with optic neuropathies, in which the visual function in slightly impaired regions or borders can be variable and tenuous.

4. *Corrected pattern standard deviation (CPSD)*: The pattern deviation can be adversely affected by a high SF, since moment-to-moment variability may cause a patient to fail to respond sensitively in a particular region, generating a local depression. The CPSD adjusts pattern deviation downward using the SF measure.

2.1.4. Interpreting the Field

What is the best way to integrate all the complex information presented in a routine plot and arrive at some decision about what is happening to a patient’s vision?

In general, most analyses rest on the pictures, since few of us are adept at creating a mental image of the patient’s fields from the numerical plots. However, before looking at the plots, one should recall the problem being investigated. This will direct one’s attention in reviewing the plots and also guide one’s assessment of whether the field done is the best way of answering the clinical problem. A well-performed perimetric test will still be inconclusive if it was poorly matched to the area of suspected abnormality.

The gray scale automatically draws our attention because it is large and obvious. It provides a direct representation of the patient’s hill of vision, much as the Goldmann perimeter does. Instead of “topographic elevation” rings, it presents a shaded topographic map, with lighter shades for higher elevations of the hill of vision. The gray scale and the numbers in the visual sensitivity plot are useful in gauging how severe a defect is, since both are more finely graded than the probability maps.

However, the gray scale should not be relied on alone to indicate abnormality. Rather, the total deviation and pattern deviation maps need to be consulted to see which areas are statistically abnormally depressed. Discrepancies between the appearance of the gray scale and the probability plots are not uncommon. For example, sensitivity in the superior field is fairly variable in normal subjects and not uncommonly lower than that of the inferior field. This may generate a dark superior rim on the gray scale of sensitivity, yet the probability plots will be normal in this area, indicating that this is within the normal range of variation (Fig. 11). On the other hand, a subtle central defect may still have a fairly high sensitivity. Thus, it will not create a dark appearance on the gray scale, but the probability plots will show that the center is statistically abnormal, not only in total deviation but also in pattern deviation (Fig. 12).

When evaluating probability maps, it is useful to remember some basic statistical principles. A *p* value of < 0.05 at a single point means that the chance that a normal subject would have a sensitivity at or below that value there is at or below 1 in 20. With 76 points being tested, there are 76 statistical tests being applied

CENTRAL 30 - 2 THRESHOLD TEST

DATE 03-14-02

STIMULUS III, WHITE, BCKGND 31.5 ASB BLIND SPOT CHECK SIZE III
 STRATEGY FULL THRESHOLD
 FASTPAC

FIXATION TARGET CENTRAL
 RX USED +1 DS DCX DEG

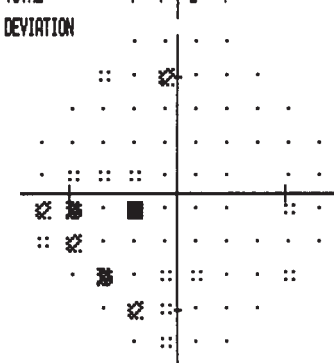
TIME 03:51:28 PM
 PUPIL DIAMETER 3.0 MM VA 20/20

RIGHT
 AGE 44
 FIXATION LOSSES 1/19
 FALSE POS ERRORS 1/8
 FALSE NEG ERRORS 0/8
 QUESTIONS ASKED 312

TEST TIME 00:10:48

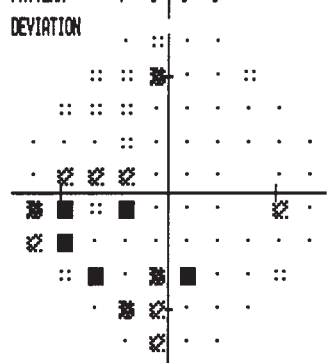
HFA S/N

0	-9	-4	-5
-8	-6	-12	0
-6	-5	-5	-2
-3	0	-1	-3
-4	-5	-4	-4
-8	-7	-3	-7
-7	-6	-2	-1
-3	-7	-3	-5
0	-8	-6	-2
TOTAL	-4	-7	-2

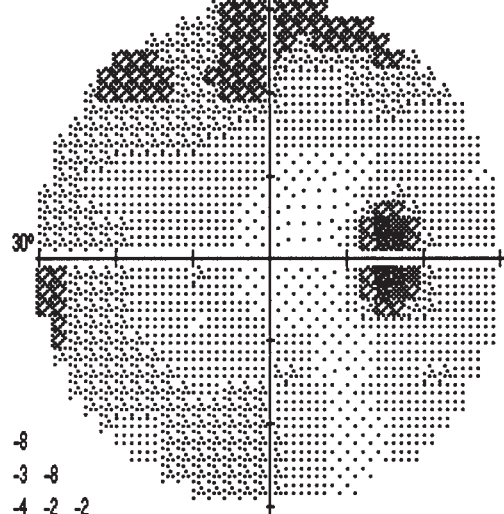


		28	16	20	17	
		(22)		(20)		
	19	22	16	27	27	21
		(18)				
	22	24	25	28	27	29
		(25)		(30)	(28)	(28)
	24	29	28	30	35	37
		(29)		(28)	(40)	(30)
	24	24	27	28	32	40
		(26)		(27)	(34)	(32)
	20	29	24	31	32	36
		(26)		(34)		(31)
	20	23	29	31	31	34
			(31)		(34)	
	25	21	28	26	27	36
		(24)		(24)		(26)
	28	20	24	28	31	31
		(23)		(28)		
	23	21	26	32		

-2	-12	-7	-8
-10	-8	-14	-3
-8	-8	-7	-4
-5	-2	-4	-6
-6	-8	-7	-7
-10	-9	-5	-10
-10	-9	-4	-4
-6	-10	-5	-8
-3	-10	-8	-5
PATTERN	-7	-9	-5



PROBABILITY SYMBOLS
 :: P < 5%
 ☼ P < 2%
 ☼☼ P < 1%
 ■ P < 0.5%



MD -2.03 DB
 PSD 4.21 DB P < 5%
 SF 1.53 DB
 CPSD 3.83 DB P < 2%

	GRAYTONE SYMBOLS					REV BG				
SYM										
ASB	.8	2.5	8	25	79	251	794	2512	7943	≥
	.1	1	3.2	10	32	100	316	1000	3162	10000
DB	50	40	35	30	25	20	15	10	5	≤0

BETH ISRAEL HOSPITAL
 330 BROOKLINE AVENUE
 BOSTON, MA. 02215

HUMPHREY SYSTEMS

Fig. 11. Field with pseudo-superior defect. Note that the most salient depression on the gray scale (top right) is a superior darkening. However, the total deviation plots tell us that this decline in sensitivity superiorly is normal; rather, a more subtle arcuate depression in the inferonasal region is the real defect.

CENTRAL 30 - 2 THRESHOLD TEST

DATE 01-16-97

STIMULUS III, WHITE, BCKGND 31.5 ASB BLIND SPOT CHECK SIZE III
 STRATEGY FULL THRESHOLD
 FASTPAC

FIXATION TARGET CENTRAL
 RX USED DS DCX DEG PUPIL DIAMETER 4.0 MM VA 20/25
 TIME 02:46:42 PM

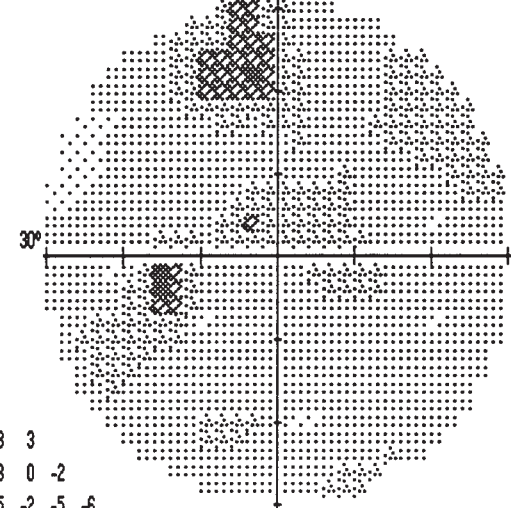
LEFT
 AGE 34
 FIXATION LOSSES 0/18
 FALSE POS ERRORS 0/6
 FALSE NEG ERRORS 0/9
 QUESTIONS ASKED 322

TEST TIME 00:10:23

HFA S/N 630-4943

	-2	-6	2	2					
	-1	-10	-13	-4	0	-3			
	2	-1	-2	-3	-5	-2	-6	-6	
	5	-1	-1	-2	-6	-5	-7	-2	-4
	-1	-1	-6	-12	-10	-8	-3	2	-2
	-1	0	-5	-6	-6	-11	-5	-4	1
	-3	-9	-8	-1	-6	-5	-3	-5	1
	-6	-2	-2	-2	-2	-2	-1	-3	
	-1	-6	-6	1	0	-3			
TOTAL	-3	0	-1	-4					
DEVIATION									

				23	19	28	28						
				27	18 (18)	15 (15)	25	28	25				
				31	29	26 (29)	27	25	28	24	22		
				34	29	30	28 (31)	26	30 (24)	28 (22)	26	27 (21)	
				29	30	28	26	19 (22)	23	25	30 (27)	30 (33)	27
				30 (30)	31 (31)	12	27	26 (29)	28 (26)	19 (25)	27	27	30 (30)
				27 (27)	22	23 (23)	31 (31)	25 (28)	28	28 (31)	27	33 (30)	30 (24)
				25	29 (28)	30	30	30	29	31 (28)	26		
					34 (25)	25	25	-31	30	26			
					26	29 (28)	28	21 (27)					



	-2	-6	3	3					
	-1	-10	-13	-3	0	-2			
	2	0	-2	-3	-5	-2	-5	-6	
	5	-1	0	-1	-5	-5	-7	-2	-3
	-1	-1	-6	-12	-10	-7	-3	2	-1
	0	0	-5	-5	-5	-11	-5	-3	2
	-3	-9	-8	-1	-5	-4	-3	-4	2
	-5	-2	-1	-1	-1	-2	-1	-3	
	0	-6	-6	1	0	-3			
PATTERN	-3	0	0	-4					
DEVIATION									

MD -3.75 DB P < 5%
 PSD 3.73 DB P < 5%
 SF 2.15 DB
 CPSD 2.82 DB P < 5%

PROBABILITY SYMBOLS
 :: P < 5%
 ☼ P < 2%
 ☼ P < 1%
 ■ P < 0.5%

GRAYTONE SYMBOLS

REV BE

SYM										
ASB	.8	2.5	8	25	79	251	794	2512	7943	≥
DB	41	36	31	26	21	16	11	6	1	≤0
	50	40	35	30	25	20	15	10	5	≤0

BETH ISRAEL HOSPITAL
 330 BROOKLINE AVENUE
 BOSTON, MA. 02215

HUMPHREY INSTRUMENTS
 A CARL ZEISS COMPANY

Fig. 12. Field with subtle central scotoma of 33-year-old man with a retrobulbar optic neuritis OS, with acuity of 20/25, reduced color vision of 10/14 plates, and a left relative afferent pupillary defect. The gray-scale plot at the top right does not look very impressive, apart from some probably normal variability in the upper field. The probability plots, however, reveal the relative central scotoma.

in each probability map, and at each of the 76 points there is a 1 in 20 chance of a normal subject getting a low score. Theoretically, if the odds at each point were independent—which they are not really, since they come from the same subject under similar conditions—the odds of getting every single point within 95% normal limits would be $(0.95)^{76}$, or a mere 2%. Thus, it is highly likely that just by chance a normal subject will get a few low scores. If we make the criteria more stringent, and look only at points marked with black squares ($p < 0.005$), there is still a 31% chance of a normal subject getting one or more abnormal points.

The point is that a few abnormal scores do not make a story. Rather, one seeks patterns. A normal subject may have some points flagged as abnormal, but these will be randomly scattered. By contrast, the abnormal points of a subtle defect will be clustered in a pattern consistent with the clinical suspicion. On occasion, this may be a single point—as with enlargement of the blind spot—but most of the time it will be a cluster of several spots. If only a single spot is defective, one should be cautious about conclusions of either normality or pathology. A single point near fixation is more likely to be abnormal than one in the periphery, where performance is always more variable, but even so this indicates that a more finely grained central field such as a 10-2 might have been a better choice of test.

To evaluate the patterns in the probability, the same questions posed in the last chapter apply, with the same reliance on knowledge of anatomy and disease. These questions are not recapitulated here. However, the appearance of artifact on automated perimetry will differ from that in manual perimetry. The following examples should be considered:

1. *“High responder”*: Some subjects are determined to see every possible light (Fig. 13). In the parlance of signal detection theory (see appendix), they will have a criterion bias that is shifted toward low signal values. Anything that suggests the hint of a light will trigger a response. Thus, these patients have elevated FP rates, their MD is a positive value, and they have locations with improbably high thresholds. They will often also show FLs, because their drive to see will lead them to look for targets with eye movements.
2. *“Low responder”*: Other subjects feel that they should be cautious and not respond unless they are certain that a target was present (Fig. 14). This is not uncommon among patients doing automated perimetry for the first time, especially if poorly instructed. The result is a criterion bias opposite to that of high responders. Interestingly, this shift tends to affect the peripheral more than the central field, so that there is often the appearance of a concentric constriction. This can lead to problems if the patient is being investigated for just such a defect. The examination should be repeated with more detailed instructions about the need to respond to very faint lights. It can also be helpful to supplement the test with Goldmann perimetry, which is less prone to such problems.
3. *Lens holder artifact*: This is more variable than in Goldmann perimetry, because the lens holder is adjustable. The typical pattern is a severe reduction in the peripheral lower field (Fig. 15). (The holder does not have an upper part, so the upper field is spared, unless one errs by using a trial lens with a large rim.) This can mimic an

inferior arcuate defect, but two points can help to differentiate the two. First, lens rim artifact may not respect the nasal horizontal meridian (see the examples, Fig. 15). Second, arcuate defects will “point” to the blind spot, whereas rim artifacts will often circle around it. This will be particularly evident with the 30-2 program, which provides a 10° margin between the blind spot and the edge of the tested field. However, at times it can be hard to tell the difference (Fig. 16), and one should repeat perimetry without a lens holder or with more careful attention to it.

4. *Lid artifact*: This sometimes crops up on automated perimetry, just as it does with manual perimetry (Fig. 17). The appearance is not much different, a shade over the superior field with variable slant. Perimetry can be repeated with the lids taped up (it is too much to ask patients to voluntarily elevate their lids for the whole time it takes to do automated perimetry), or a quick check with Goldmann perimetry can confirm or deny the defect.

2.2. SEQUENTIAL ANALYSES OF FIELDS

As with Goldmann perimetry, one of the key issues is detecting change over time. The difficulty again is differentiating true change in pathology from the variable performance of a patient with a stable, unchanging defect. Even normal subjects will not produce identical perimetric results from two different sessions. This is known as *long-term fluctuation*, or inter-test variability. Unlike SF, there is no simple way of assessing the degree of long-term fluctuation in a given patient, although studies show that it is quite variable in normal subjects. The advantage of an automated collection of numerical data is that it is possible to apply statistical analysis to the problem of detecting or depicting change.

Local changes or changes in the pattern of the field are best captured on the overview printout (Fig. 18). This plots the gray scale and pictorial probability maps for each session in one row, with subsequent sessions added one below the other. Each also has a listing of the reliability indices, global indices, pupil size, and acuity. The progression over time is more easily appreciated, but no statistical analysis is provided. As with Goldmann perimetry, a new defect superimposed on an old defect can be easy to spot (see Case 25). On the other hand, progression in the severity of a pre-existing defect is more difficult to judge with confidence (see Case 43). Again, repeating the assessment several times to check for persistence or continued decline across a number of fields is the best strategy if doubt lingers about the stability of the field loss.

The change analysis program of the Humphrey automated perimeter is a convenient way of looking at the progression of some overall summary variables (Fig. 19). This printout first displays a box plot for each date of testing. This simply masses all the threshold values obtained in a test, irrespective of location, and determines the median (center stripe in the box), the 15th and 85th percentiles (the top and bottom of the box, meaning that the box thus contains 70% of all data points), and the least and most sensitive thresholds (indicated by the extent of the arms). Next are four plots for the four global indices. Points obtained from tests with poor reliability indices are flagged with an “x” rather than an “o”. These plots show the 5 and 1% limits of normative data. If five or more fields are used in the change program, it will also indicate whether the slope of the linear regression is significantly different from zero.

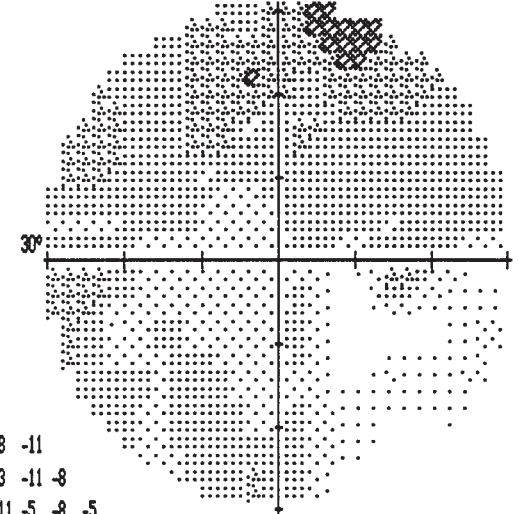
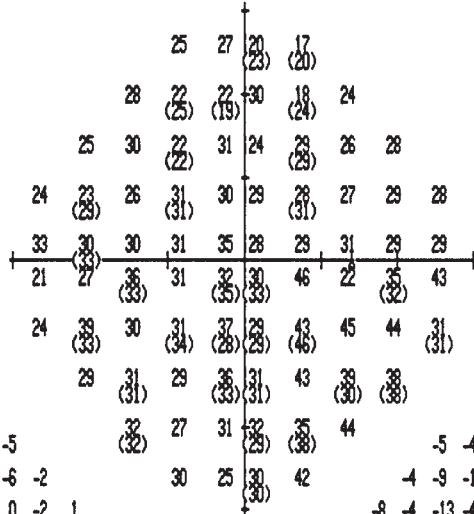
CENTRAL 30 - 2 THRESHOLD TEST

DATE 07-12-99

STIMULUS III, WHITE, BCKGND 31.5 ASB BLIND SPOT CHECK SIZE III
 STRATEGY FULL THRESHOLD
 FASTPAC
 LOW PATIENT RELIABILITY

FIXATION TARGET CENTRAL
 RX USED +1.75 DS DCX DEC PUPIL DIAMETER 4.0 MM VA 20/30
 TIME 01:44:15 PM

RIGHT
 AGE 48
 FIXATION LOSSES 8/19 xx
 FALSE POS ERRORS 3/9 xx
 FALSE NEG ERRORS 2/10
 QUESTIONS ASKED 330
 TEST TIME 00:10:47
 HFA S/N



	1	2	-2	-5					
	1	-4	-7	-3	-6	-2			
	-2	1	-7	2	-5	0	-2	1	
	-2	-2	-4	0	-1	-2	0	-2	0
	6	3	-1	-1	3	-4	-2	-1	0
	-6	-3	3	-1	1	-1	15	4	14
	-3	7	-1	1	1	-3	13	15	14
	1	2	-1	4	1	12	4	9	
	4	-2	2	1	7	15			
TOTAL	3	-2	2	14					

			-5	-4	-8	-11			
			-4	-9	-13	-3	-11	-8	
			-8	-4	-13	-4	-11	-5	-8
			-8	-8	-10	-6	-7	-6	-6
			0	-3	-7	-7	-3	-10	-8
			-12	-8	-3	-7	-5	-7	9
			-9	1	-6	-5	-5	-8	8
			-5	-4	-7	-2	-5	7	-1
			-2	-8	-4	-5	1	9	
			-3	-8	-4	8			

PROBABILITY SYMBOLS
 :: P < 5%
 ☼ P < 2%
 ☼☼ P < 1%
 ■ P < 0.5%

MD +1.27 DB
 PSD 5.44 DB P < 2%
 SF 2.51 DB
 CPSD 4.64 DB P < 1%

	GRAYTONE SYMBOLS				REV BE					
SYM										
ASB	.8 - .1	2.5 - 1	8 - 3.2	25 - 10	79 - 32	251 - 100	794 - 316	2512 - 1000	7943 - 3162	≥ 10000
DB	41 50	36 40	31 35	26 30	21 25	16 20	11 15	6 10	1 5	≤0

BETH ISRAEL HOSPITAL
 330 BROOKLINE AVENUE
 BOSTON, MA. 02215

HUMPHREY INSTRUMENTS
 A CARL ZEISS COMPANY

Fig. 13. High responder: 48-yr-old man doing perimetry for the first time. Note frequent FLs, high FP error rate, positive MD, and a scatter of impossibly high thresholds ranging from 35 to 45(!) in the lower temporal quadrant. These high thresholds serve to make the more normal areas of his field appear depressed on the pattern deviation plots. Note also the flag (top left) "low patient reliability."

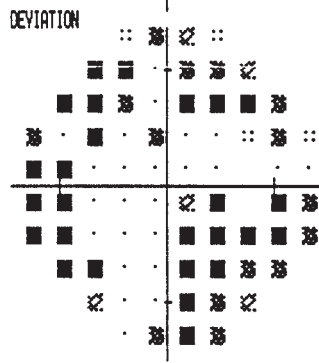
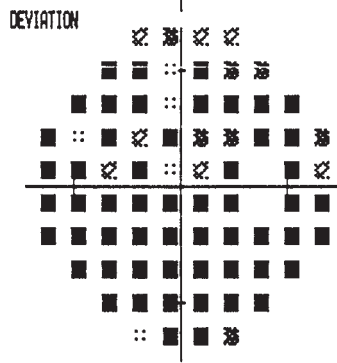
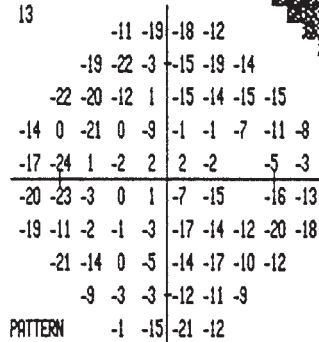
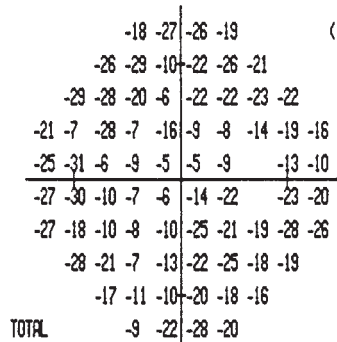
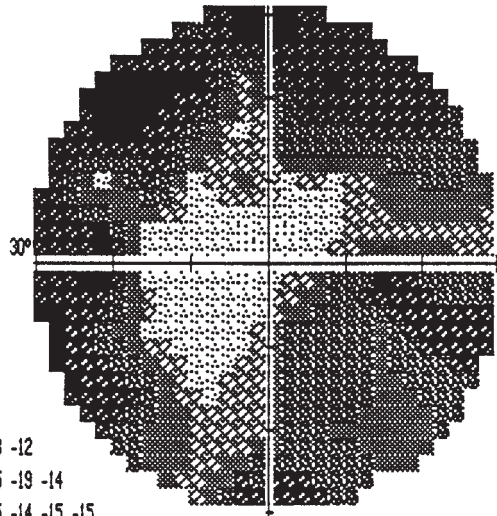
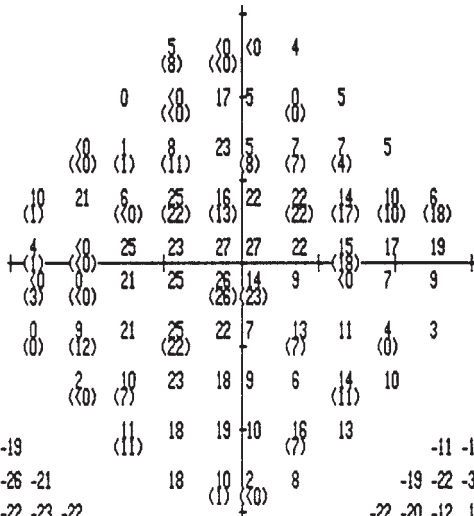
CENTRAL 30 - 2 THRESHOLD TEST

DATE 04-29-99

STIMULUS III, WHITE, BCKGND 31.5 ASB BLIND SPOT CHECK SIZE III
 STRATEGY FULL THRESHOLD
 FASTPAC

FIXATION TARGET CENTRAL
 RX USED +2 DS OCX DEG PUPIL DIAMETER 3.0 MM VA 20/20

RIGHT
 AGE 50
 FIXATION LOSSES 0/22
 FALSE POS ERRORS 0/14
 FALSE NEG ERRORS 3/11
 QUESTIONS ASKED 416
 TEST TIME 00:13:41
 HFA S/N



PROBABILITY SYMBOLS
 :: P < 5%
 ☒ P < 2%
 ☒ P < 1%
 ■ P < 0.5%

MD -16.10 DB P < 0.5%
 PSD 8.70 DB P < 0.5%
 SF 2.93 DB P < 10%
 CPSD 8.04 DB P < 0.5%

	GRAYTONE SYMBOLS					REV BE				
SYM										
ASB	.8	2.5	8	25	79	251	794	2512	7943	≥
	.1	1	3.2	10	32	100	316	1000	3162	10000
DB	41	36	31	26	21	16	11	6	1	≤0
	50	40	35	30	25	20	15	10	5	

BETH ISRAEL HOSPITAL
 330 BROOKLINE AVENUE
 BOSTON, MA. 02215

HUMPHREY INSTRUMENTS
 A CARL ZEISS COMPANY

Fig. 14. Low responder: 50-yr-old woman doing perimetry for the first time. All points are depressed on the total deviation plot, but the gray scale and pattern deviation plots show that the depression is more pronounced peripherally, creating a tubular constriction. There are also FN errors, and the SF is high. With some encouragement, she performs better on Goldmann perimetry.

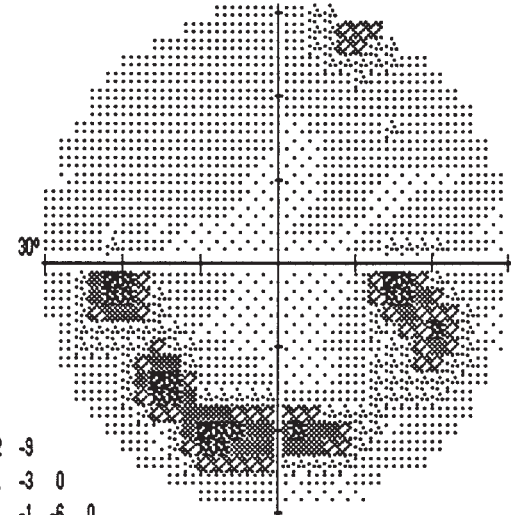
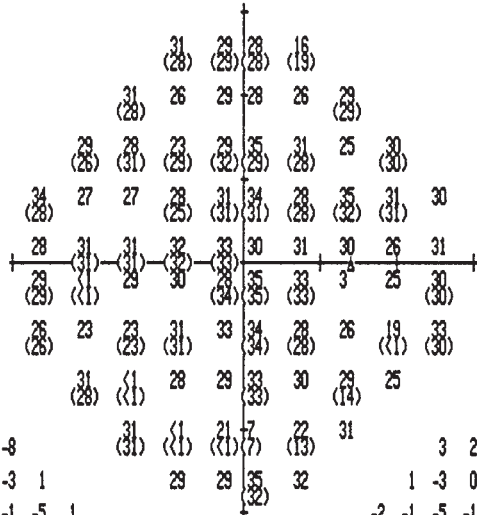
B CENTRAL 30 - 2 THRESHOLD TEST

DATE 07-06-01

STIMULUS III, WHITE, BCKGND 31.5 ASB BLIND SPOT CHECK SIZE III
 STRATEGY FULL THRESHOLD
 FASTPAC
 LOW PATIENT RELIABILITY

FIXATION TARGET CENTRAL
 RX USED - 0.50 DS DCX DEG PUPIL DIAMETER VA

RIGHT
 AGE 30
 FIXATION LOSSES 7/23 xx
 FALSE POS ERRORS 0/15
 FALSE NEG ERRORS 1/12
 QUESTIONS ASKED 440
 TEST TIME 00:14:06
 HFA S/N 630-4943



	3	3	2	-8						
	1	-3	0	-1	-3	1				
	-1	-1	-5	0	2	-1	-5	1		
	3	-3	-4	-6	-1	1	-3	3	1	0
	-1	1	-1	-1	0	-3	-1	-5	0	
	0	-32	-4	-3	-3	2	0	-7	-1	
	-3	-8	-9	-2	0	1	-4	-6	-22	1
	0	-32	-4	-3	1	-2	-10	-6		
	1	-31	-21	-24	-14	0				
TOTAL		1	0	4	3					
DEVIATION										

	3	2	2	-9						
	1	-3	0	-1	-3	0				
	-2	-1	-5	-1	1	-1	-6	0		
	2	-4	-5	-7	-2	0	-4	2	0	0
	-2	0	-2	-2	-1	-4	-2	-6	0	
	-1	-33	-4	-4	-3	1	0	-7	-2	
	-3	-8	-10	-3	-1	1	-5	-6	-23	0
	-1	-33	-4	-4	1	-3	-11	-7		
	1	-32	-21	-25	-14	0				
PATTERN		0	-1	3	2					
DEVIATION										

PROBABILITY SYMBOLS
 :: P < 5%
 ☒ P < 2%
 ☒ P < 1%
 ■ P < 0.5%

MD -4.14 DB P < 5%
 PSD 8.82 DB P < 0.5%
 SF 4.24 DB P < 2%
 CPSD 7.40 DB P < 0.5%

	GRAYTONE SYMBOLS					REV BG				
SYM										
ASB	.8	2.5	8	25	79	251	794	2512	7943	≥
	.1	1	3.2	10	32	100	316	1000	3162	10000
DB	41	36	31	26	21	16	11	6	1	≤0
	50	40	35	30	25	20	15	10	5	≤0

BETH ISRAEL HOSPITAL
 330 BROOKLINE AVENUE
 BOSTON, MA. 02215

HUMPHREY SYSTEMS

Fig. 15. (Continued) (B) Right eye in a 30-yr-old woman. The rim was farther away from her eye than in the previous patient and the artifact forms a circle at 20-25° eccentricity. (Figure 15C continued on next page.)

C

CENTRAL 30 - 2 THRESHOLD TEST

DATE 07-18-01

STIMULUS III, WHITE, BCKGND 31.5 ASB BLIND SPOT CHECK SIZE III
 STRATEGY FULL THRESHOLD
 FASTPAC

FIXATION TARGET CENTRAL
 RX USED DS DCX DEG PUPIL DIAMETER 4.0 MM VA 20/20
 TIME 08:19:02 AM

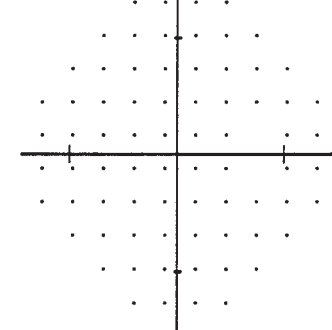
RIGHT
 AGE 30
 FIXATION LOSSES 0/15
 FALSE POS ERRORS 0/4
 FALSE NEG ERRORS 0/7
 QUESTIONS ASKED 244

TEST TIME 00:06:56

HFA S/N 630-4943

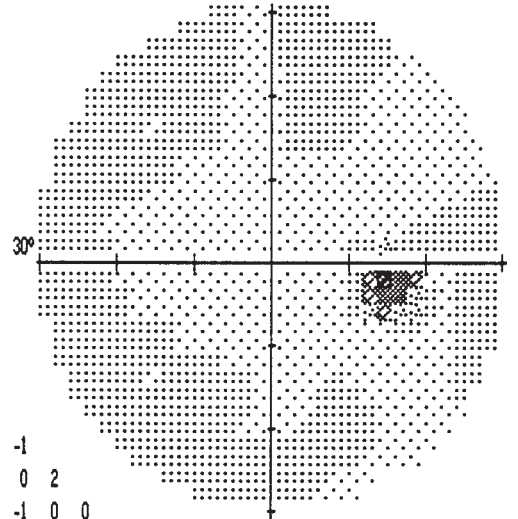
	1	6	3	1						
	-2	0	3	1	2	4				
	-3	1	-2	1	0	0	2	2		
	0	0	-1	0	-1	0	1	2	2	1
	-1	1	2	-1	0	1	0	-1	-2	
	-2	-1	0	2	0	0	0	-1	-1	
	1	-1	-2	-1	1	1	2	0	0	-1
	-1	0	-3	-2	1	-2	2	0		
	-2	0	0	0	-3	0				
TOTAL	2	-1	-1	3						

DEVIATION



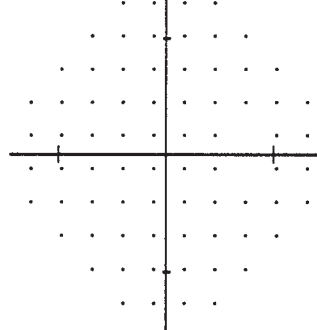
PROBABILITY SYMBOLS

- ∴ P < 5%
- ⊗ P < 2%
- ⊗ P < 1%
- P < 0.5%



		0	4	2	-1					
	-4	-1	2	0	0	2				
	-4	-1	-3	0	-2	-1	0	0		
	-2	-2	-3	-2	-3	-2	-1	0	0	0
	-3	-1	0	-3	-2	-1	-2	-3	-3	
	-4	-3	-1	1	-2	-2	-1	-2	-3	
	0	-2	-4	-2	-1	0	0	-1	-2	-2
	-3	-2	-4	-4	-1	-4	0	-2		
	-3	-2	-1	-2	-5	-1				
PATTERN	0	-3	-2	1						

DEVIATION



MD +0.02 DB
 PSD 1.58 DB
 SF 1.81 DB
 CPSD 0.00 DB

GRAYTONE SYMBOLS

REV BG

SYM										
ASB	.8	2.5	8	25	79	251	794	2512	7943	∞
	1	1	3.2	10	32	100	316	1000	3162	10000
DB	50	41	36	31	26	21	16	11	6	1
	50	40	35	30	25	20	15	10	5	≤0

BETH ISRAEL HOSPITAL
 330 BROOKLINE AVENUE
 BOSTON, MA. 02215

HUMPHREY SYSTEMS

Fig. 15. (Continued) (C) Repeat field in the same woman 12 d later, without use of a lens, showing a normal field.

A

CENTRAL 30 - 2 THRESHOLD TEST

DATE 02-28-02

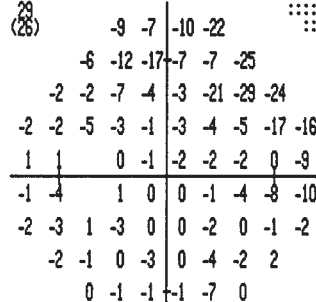
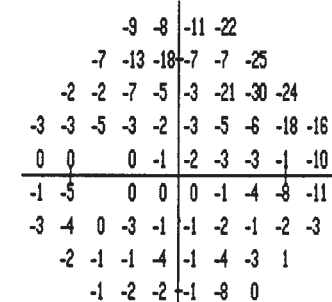
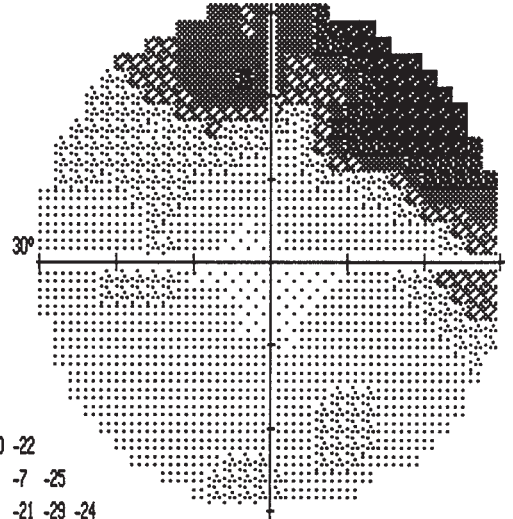
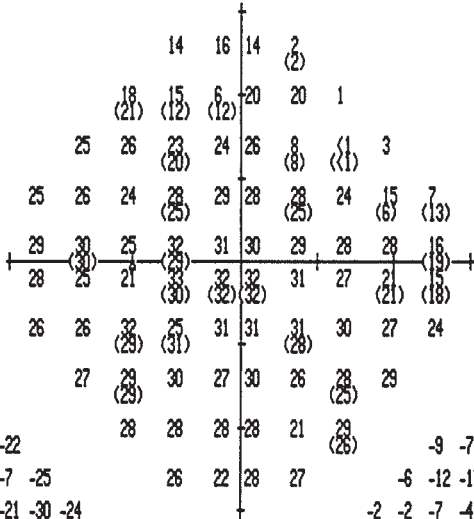
STIMULUS III, WHITE, BCKND 31.5 ASB BLIND SPOT CHECK SIZE III
 STRATEGY FULL THRESHOLD
 FASTPAC

FIXATION TARGET CENTRAL
 RX USED + 1.50 DS DCX DEG PUPIL DIAMETER 6.0 MM YA 20/20

LEFT
 AGE 50
 FIXATION LOSSES 0/19
 FALSE POS ERRORS 0/12
 FALSE NEG ERRORS 0/10
 QUESTIONS ASKED 322

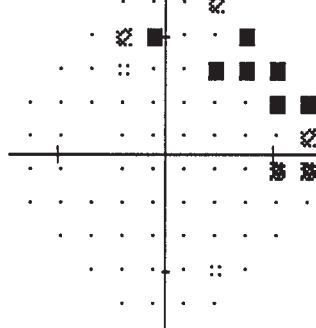
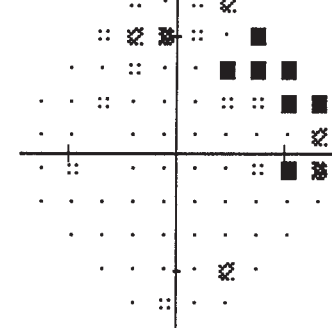
TEST TIME 00:10:08

HFA S/N 630-4943



TOTAL DEVIATION

PATTERN DEVIATION



PROBABILITY SYMBOLS
 :: P < 5%
 ☼ P < 2%
 ☼ P < 1%
 ■ P < 0.5%

MD -4.13 DB P < 5%
 PSD 6.34 DB P < 1%
 SF 1.91 DB
 CPSD 5.96 DB P < 0.5%

GRAYTONE SYMBOLS

REV BG

SYM									
ASB	.8	2.5	8	25	79	251	794	2512	7943
	.1	1	3.2	10	32	100	316	1000	3162
DB	50	40	35	30	25	20	15	10	5
									≤0

BETH ISRAEL HOSPITAL
 330 BROOKLINE AVENUE
 BOSTON, MA. 02215

HUMPHREY SYSTEMS

Fig. 17. Lid artifact. (A,B) This 49-year-old man with lymphomatous orbital infiltration causing bilateral ptosis approaching the pupil margins and intraorbital fullness has reduced sensitivities superiorly. These even appear more significant in the right hemifield. (Figure 15B,C continued on next page.)

B

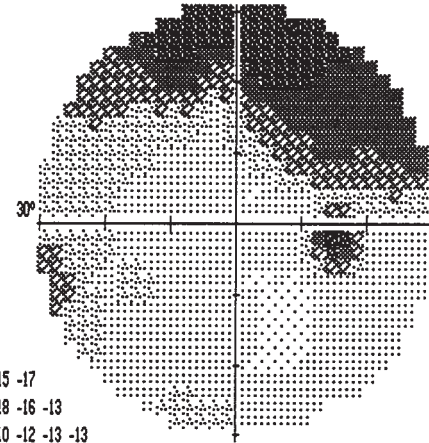
CENTRAL 30 - 2 THRESHOLD TEST

DATE 02-28-02

STIMULUS III, WHITE, BCKGRD 31.5 ASB BLIND SPOT CHECK SIZE III
 STRATEGY FULL THRESHOLD
 FASTPAC

FIXATION TARGET CENTRAL
 RX USED +1.75 DS DCX DEG PUPIL DIAMETER 5.5 MM VA 20/30
 TIME 10:30:49 AM

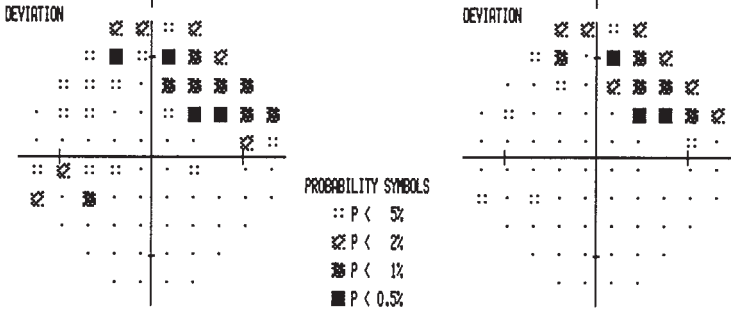
			5	7	8	5			
RIGHT			17	14	20	8	9	12	
AGE 50			(8)	(8)			(14)		
FIXATION LOSSES 0/16		20	22	23	26	18	17	14	13
FALSE POS ERRORS 0/8			(20)	(20)		(18)	(18)		
FALSE NEG ERRORS 0/7		22	21	24	31	29	26	19	15
QUESTIONS ASKED 269			(28)	(28)	(23)	(23)	(16)	(16)	
		22	25	28	29	30	31	29	24
									(21)
		21	24	27	28	29	31	29	27
									(20)
TEST TIME 00:08:41		18	27	24	31	28	31	29	28
					(28)	(28)	(31)	(28)	(28)
HFA S/N 630-4943			25	31	29	27	30	33	29
				(25)				(29)	27
			29	27	28	31	31	28	



	-18	-18	-16	-18					
	-9	-16	-7	-19	-17	-14			
	-7	-7	-8	-3	-11	-13	-14	-14	
	-4	-7	-6	-2	-3	-6	-12	-14	-15
	-5	-4	-3	-3	-2	-1	-2	-7	-7
	-6	-5	-4	-4	-3	-3	-4	-2	-2
	-9	-2	-7	-2	-4	-1	0	-1	-2
	-3	-1	-1	-4	-1	2	1	-2	
	1	-2	-1	-1	1	1	-1		
TOTAL	-3	-2	-2	1					
DEVIATION									

	-17	-17	-15	-17					
	-8	-15	-6	-18	-16	-13			
	-6	-6	-7	-2	-10	-12	-13	-13	
	-3	-6	-5	-1	-2	-5	-11	-13	-14
	-4	-3	-2	-2	-1	0	-1	-6	-6
	-5	-4	-3	-3	-2	-2	-3	-1	-1
	-8	-1	-6	-1	-3	1	1	0	-1
	-2	0	0	-3	1	3	0	-1	
	2	-1	0	2	2	0			
PATTERN	-2	-1	-1	2					
DEVIATION									

MD -4.54 DB P < 2%
 PSD 5.05 DB P < 2%
 SF 2.00 DB
 CPSD 4.52 DB P < 1%



C

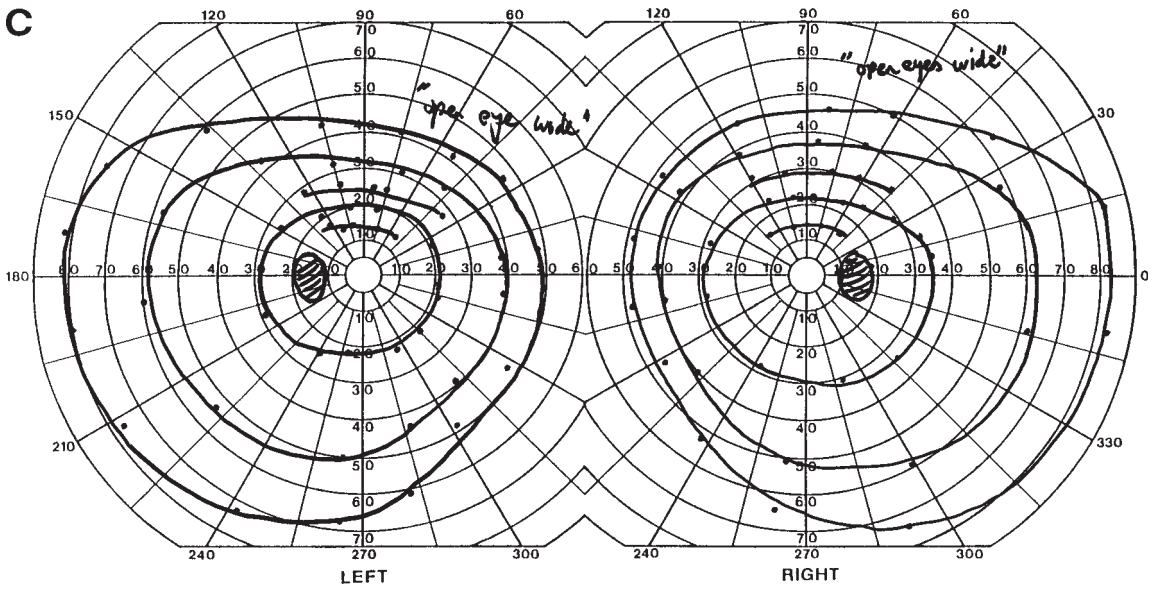


Fig. 17. (continued) (C) Goldmann perimetry with instructions to keep the eyes open wide and detailed testing of the upper region showed normal superior fields, without a step defect at the vertical meridian.

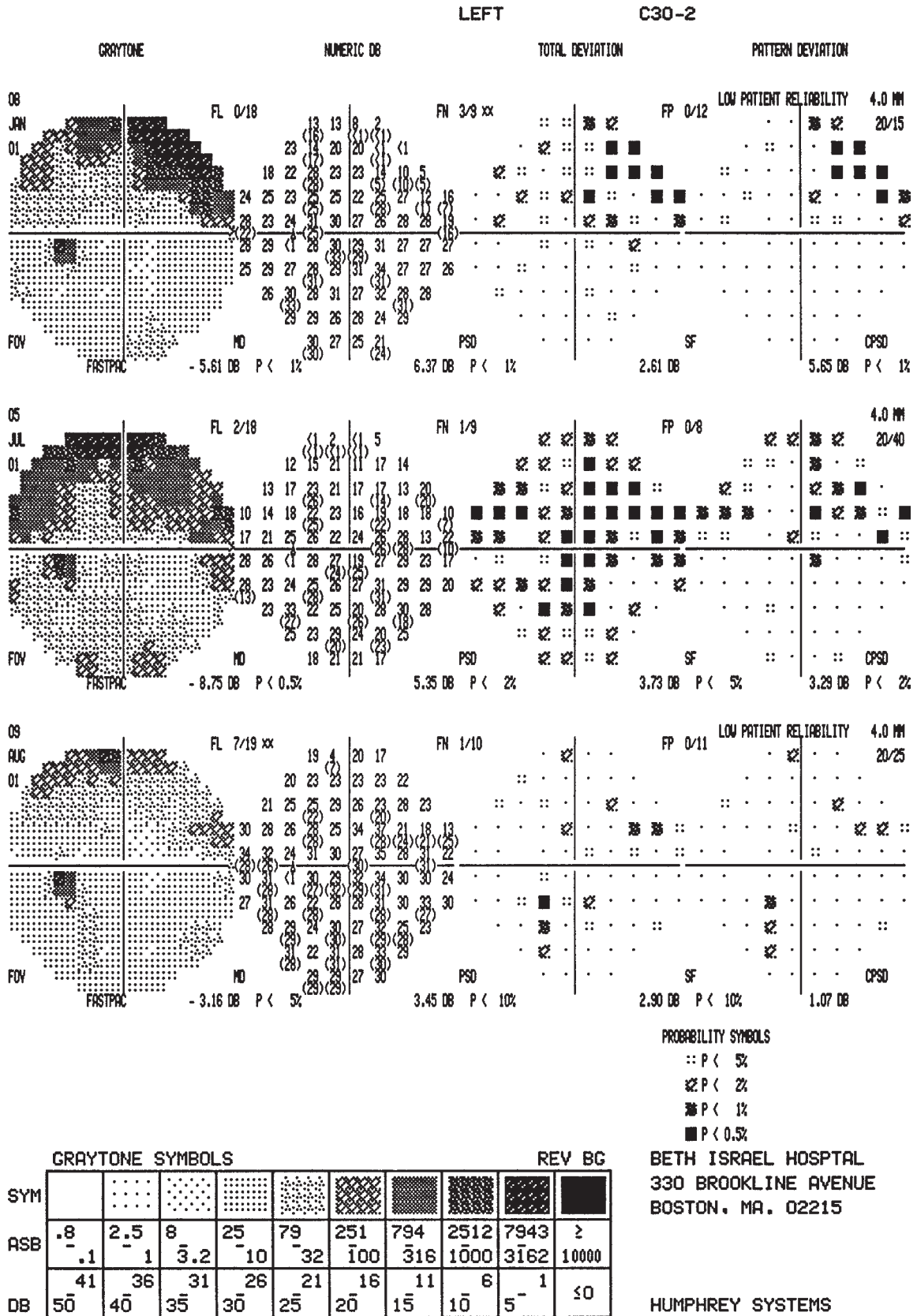


Fig. 18. Overview of a 33-year-old woman with multiple sclerosis who had an episode of optic neuritis in the left eye in January 2001 and again in July 2001, the latter with a reduced acuity of 20/40. The initial episode presented with a superior arcuate defect. The second had a central depression in addition to apparent persistence of the superior defect. One month later, both the central and superior deficits had cleared, suggesting that the superior arcuate defect had actually recurred rather than persisted. Note the listing of reliability indices (FL, FN, FP) and global indices (MD, PSD, SF, CPSD).

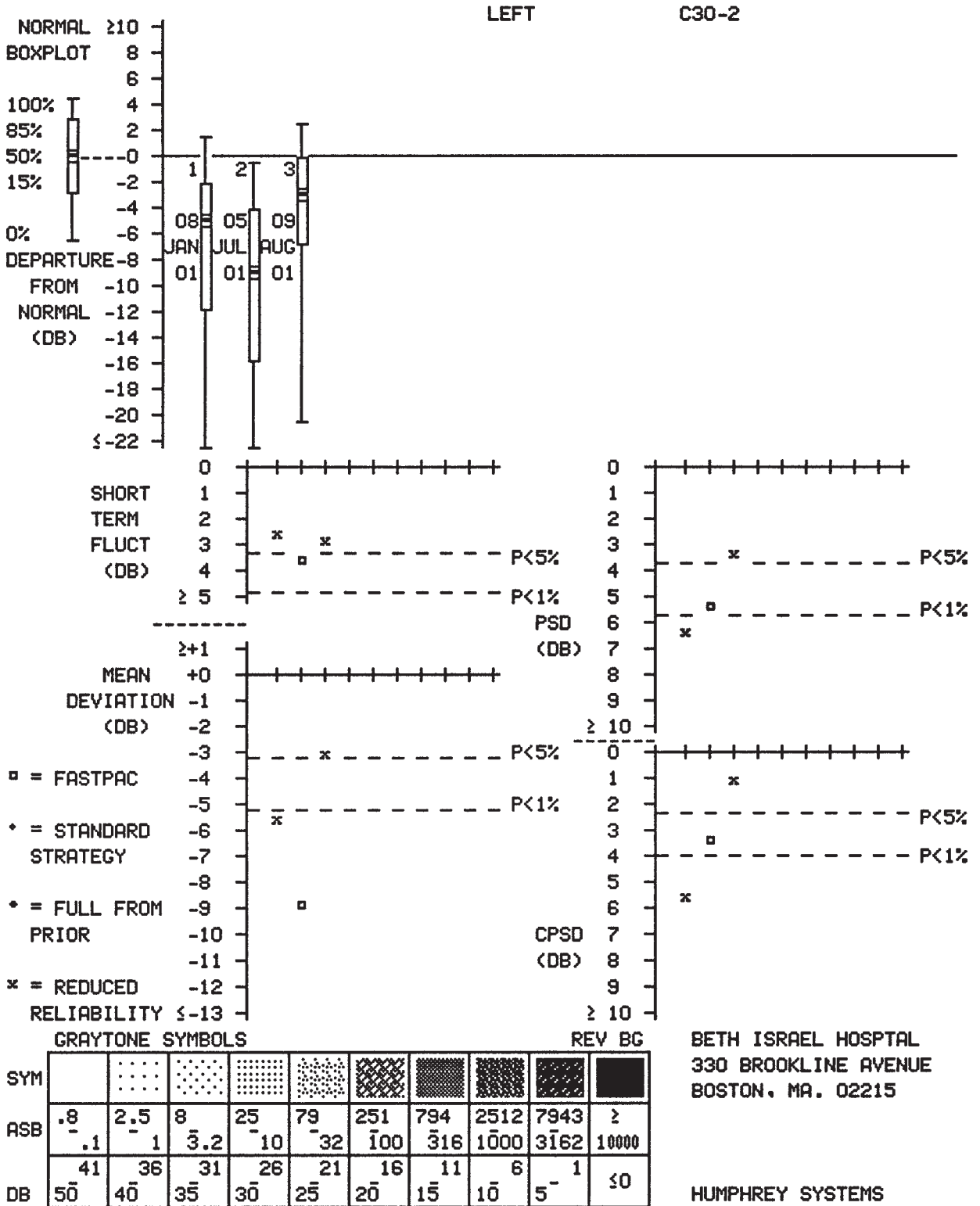


Fig. 19. Change analysis of same patient as Fig. 18. Box plot (top) shows depression in January 2001, worsening in July 2001, with recovery in August 2001. Short-term fluctuation (SF) increased slightly in July 2001, as expected with any optic neuropathy. Mean deviation (MD) was dramatically worse in July 2001, but pattern deviation (PSD, CPSD) was worse in January 2001, when the defect was confined to a more focal area of the field. In August 2001, with resolution of the second attack, all indices had normalized.

These change analyses are a convenient way of viewing overall trends, although they do not capture local changes as effectively as the overview; these local effects will be diluted by the normal portions of the field, which ideally should not change. Newer software does try to identify significant regressions for individual points.

REFERENCES

1. Lindenmuth K, Skuta G, Rabbani R, Musch D. Effects of pupillary constriction on automated perimetry in normal eyes. *Ophthalmology* 1989;96:1298.
2. Bengtsson B, Heijl A, Olsson J. Evaluation of a new threshold visual field strategy, SITA, in normal subjects. Swedish Interactive Thresholding Algorithm. *Acta Ophthalmol Scand* 1998;76:165–169.
3. Bengtsson B, Heijl A. Evaluation of a new perimetric threshold strategy, SITA, in patients with manifest and suspect glaucoma. *Acta Ophthalmol Scand* 1998;76:268–272.
4. Schaumberger M, Schäfer B, Lachenmayr B. Glaucomatous visual fields. FASTPAC versus full threshold strategy of the Humphrey visual field analyzer. *Invest Ophthalmol Visual Sci* 1995;36:1390–1397.
5. Flanagan J, Wild J, Trope G. Evaluation of FASTPAC, a new strategy for threshold estimation with the Humphrey field analyzer, in a glaucomatous population. *Ophthalmology* 1993;100:949–954.
6. Bengtsson B, Olsson J, Heijl A, Rootzen H. A new generation of algorithms for computerized threshold perimetry, SITA. *Acta Ophthalmol Scand* 1997;75:368–375.
7. Bengtsson B, Heijl A. SITA Fast, a new rapid perimetric threshold test: description of methods and evaluation in patients with manifest and suspect glaucoma. *Acta Ophthalmol Scand* 1998;76:431–437.
8. Wall M, Punke SG, Stickney TL, Brito CF, Withrow KR, Kardon RH. SITA standard in optic neuropathies and hemianopias: a comparison with full threshold testing. *Invest Ophthalmol Vis Sci* 2001;42:528–537.

INTRODUCTION TO THE ATLAS

Armed with the information from the last two chapters on perimetric technique and interpretation, the reader is presented now with a selection of 120 cases gathered over 12 years. This section is meant not only as a demonstration but also as an exercise, a chance to hone interpretative skills. Each case is presented on two pages.

The first page shows the fields of patient with a brief clinical description. The reader should engage in three tasks. First, they should verbally describe the fields. (How would you communicate the deficit over the phone?) Second, they should estimate the likely location of the lesion. Third, they should consider the clinical history, evolution, and location to arrive at a possible cause of the defect.

The second page, hidden on the reverse side, describes the features of each case, beginning with those three aspects. The fields are discussed in further detail, and relevant points stressed. We also mention what confrontation field testing showed in most cases, so that the reader may obtain a sense of which defects are detectable and which are likely to be missed in the clinic or at the bedside. Photographs, further fields or imaging are provided to illustrate the clinical problem. We also provide a brief discussion about clinical points related to the case. All fields belong to patients with problems. Since we expect that most of the readers of this work are engaged in the clinical care of these patients, we believe that the diagnostic and management issues that arise from these fields should be of interest to the audience.

The first hundred cases are given in anatomic order, beginning with retinal conditions and ending with striate lesions. The last twenty cases are placed in random order within a short “quiz” section. The aim of the quiz is to provide the reader a chance to practice the skills in field analysis and localization that we hope they acquire by reading this book.

GOLDMANN CONVENTIONS:

First, we clarify a few points on our drawing notation with the Goldmann fields. Dots represent points where the patient stated they first saw a moving target. Small ‘x’ marks note where they said they saw a static target. For ease of reading, scotomata are shaded. When there are two shades, the darker, usually inner shade represents a deeper depression of sensitivity than the lighter. In the belief that it is the pattern rather than the actual isopter that is important, we do not label the isopters, except where this may help clarify certain issues. On selected fields there may be dotted lines as well as solid lines. These indicate where an isopter was measured again with the patient using a different lens. The size of that lens in diopters (negative or positive) will be written next to the dashed line.

HISTORY AND EXAM

This 80-yr-old man complained of a hazy line located just left of center in the vision of the left eye, gradually increasing in width over the last 10 years. The haze did not distort vision and he could read through it. Earlier medical history was significant for coronary artery disease, peripheral vascular disease, and hypertension. There was no history

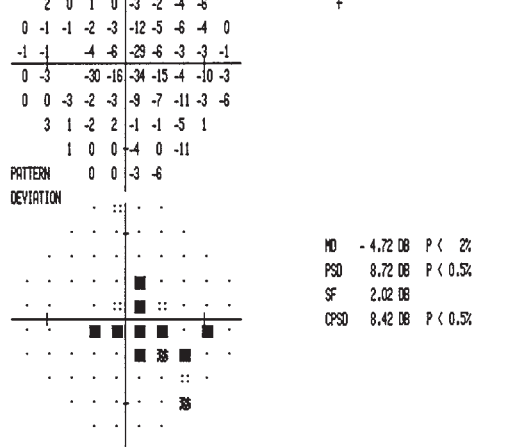
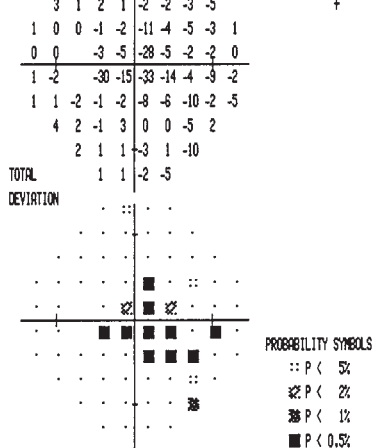
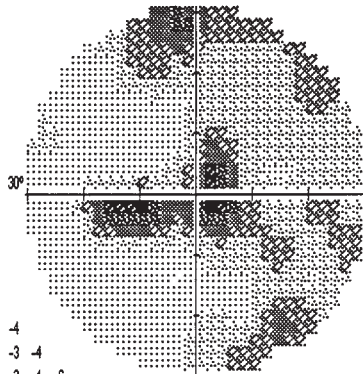
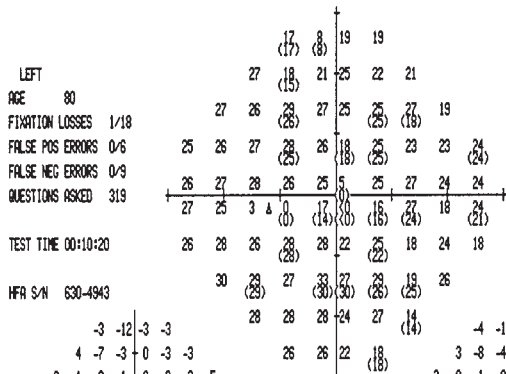
of smoking. Visual acuity was 20/20 OD and 20/30 OS, not improving with pinhole. Ishihara color plates were 12/14 OD and 1/14 OS. There was no relative afferent pupillary defect (RAPD).

CENTRAL 30 - 2 THRESHOLD TEST

DATE 12-12-96

STIMULUS III, WHITE, BCKGD 31.5 ASB BLIND SPOT CHECK SIZE III
 STRATEGY FULL THRESHOLD
 FASTPAC

FIXATION TARGET CENTRAL TIME 10:34:41 AM
 RX USED +3 DS DCX DEG PUPIL DIAMETER 3.0 MM VA 20/30

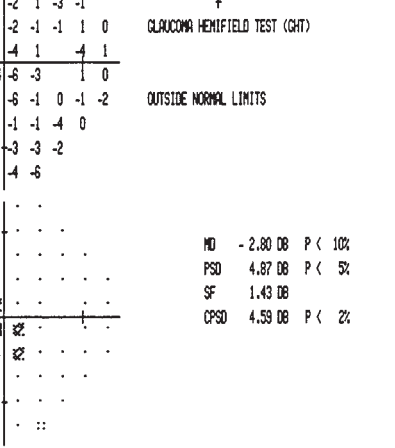
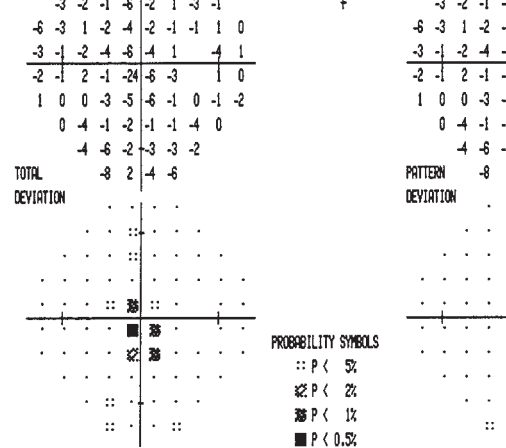
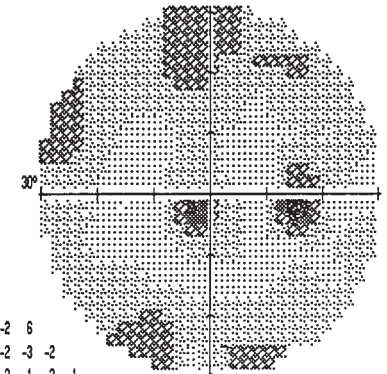
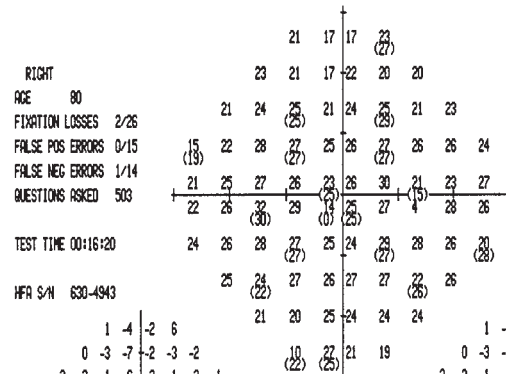


CENTRAL 30 - 2 THRESHOLD TEST

DATE 12-12-96

STIMULUS III, WHITE, BCKGD 31.5 ASB BLIND SPOT CHECK SIZE III
 STRATEGY FULL THRESHOLD

FIXATION TARGET CENTRAL TIME 10:21:17 AM
 RX USED +3 DS DCX DEG PUPIL DIAMETER 3.0 MM VA 20/20



DISCUSSION

Field description: Incongruous relative central scotomata OU.

Localization: Bilateral macula.

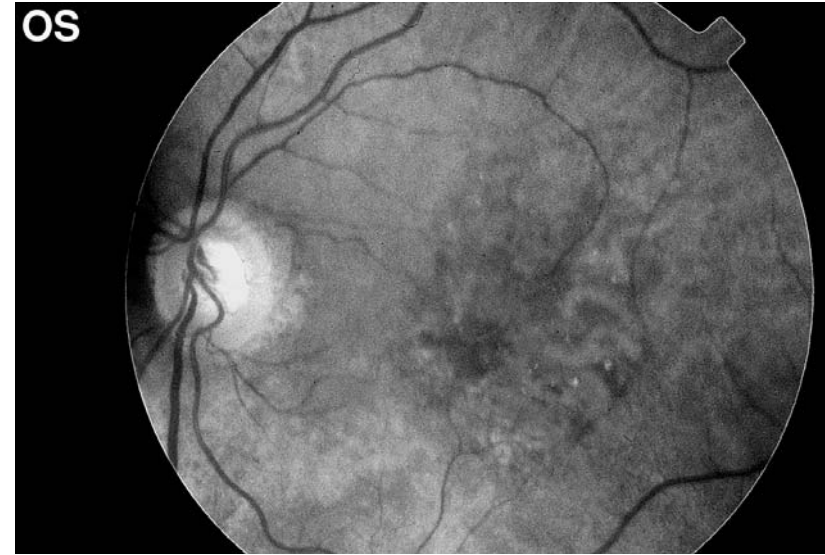
Pathology: Age-related macular degeneration, late atrophic form.

Confrontation testing was normal OU, but tangent screen perimetry showed small areas of haze centrally OU.

The patient has central defects OU, larger OS, where the defect extends to the blind spot. Bilateral central defects can occur at any level of the visual system. The incongruity and lack of a step at the vertical meridian are against bilateral occipital lesions. Instead, bilateral optic neuropathy (see Case 38) or bilateral maculopathy are most likely. Fundoscopy showed macular pigmentary changes, making the diagnosis of age-related macular degeneration.

Age-related macular degeneration causes progressive loss of acuity, central holes in vision, and metamorphopsia, or distorted vision, caused by fluid and scarring in the retina

(1). This latter complaint is best shown on Amsler grid. These central defects impair the fine spatial resolution needed for tasks such as reading, face recognition, and driving, although patients can walk without help because of their good peripheral vision. Macular changes are subtle in the early stage, consisting mainly of drusen and mild pigmentary changes. The late stage is associated with visual loss and has two forms (2). In “dry” macular degeneration, there is atrophy of the photoreceptors, retinal pigment epithelium, and choriocapillaris, in a patchy “geographic” arrangement, as here. Acuity tends to be about 20/40 or better. In “wet” macular degeneration, there is serous or hemorrhagic detachment of the retinal pigment epithelium with choroidal neovascularization, leakage, and scarring, with more severe loss of acuity, sometimes abrupt. Smoking and a diet low in antioxidant vitamins and zinc are identified risk factors that can be modified. Progression is usually slow. There is no known treatment, but laser photocoagulation and photodynamic therapy are being evaluated (2).



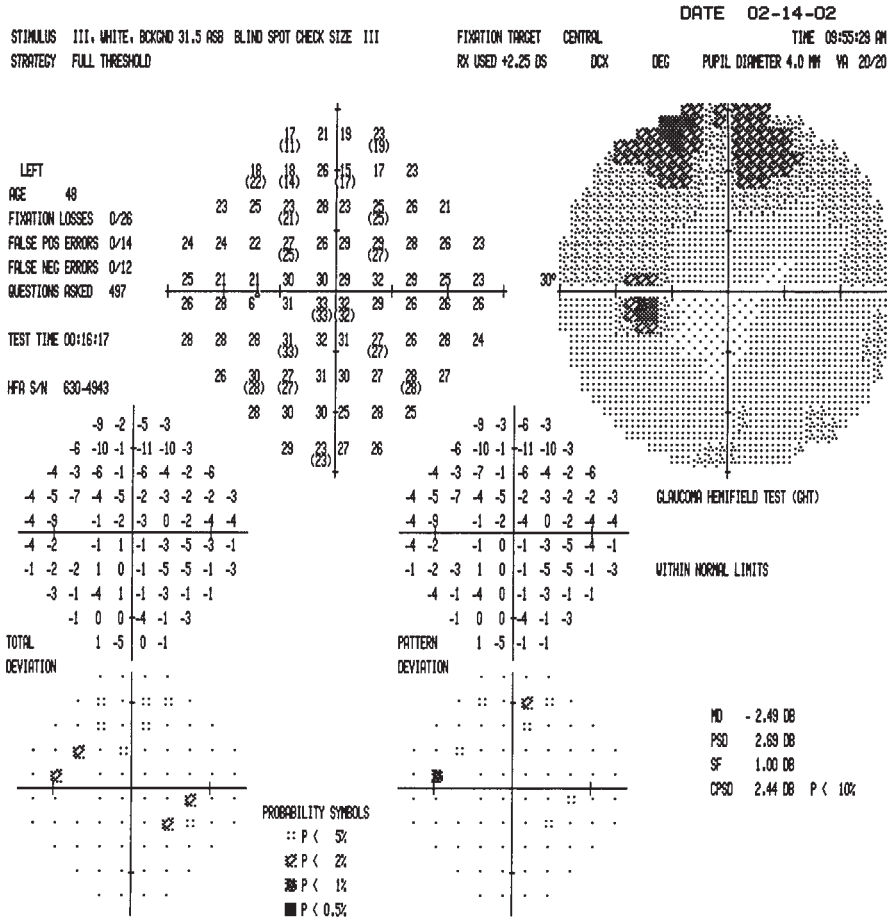
See Color Plate after page 180

HISTORY AND EXAM

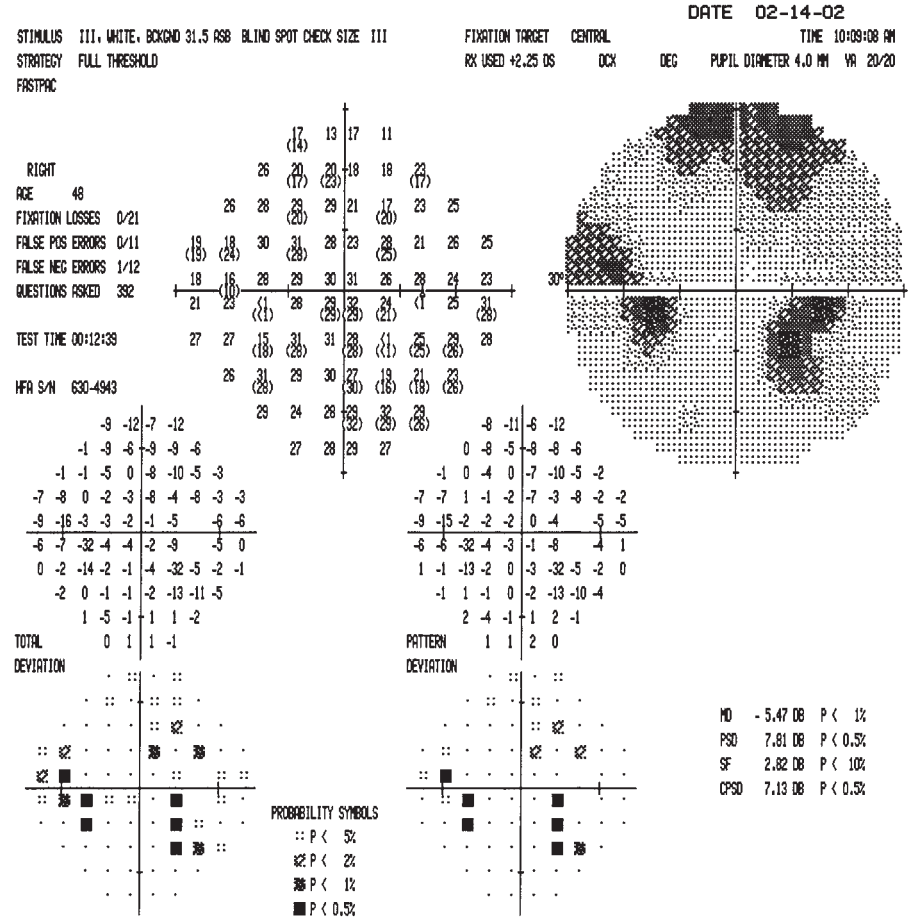
This 47-yr-old man had central dimming of vision OD 7 years earlier, resolving over a few months. Since then he has had four recurrences, the most pronounced episode 2 years earlier, which lasted 5 months. In between episodes he notes micropsia, in that when he looks at people's heads with his right eye only they are quite a bit smaller than either

their bodies or their heads viewed with his other eye. For 8 months he was also aware of small holes in his vision just nasal and temporal to fixation. These were stable. Visual acuity was 20/20 OU but the photostress test was prolonged OD, being more than 2 min compared with 60 s OS. There was no RAPD.

CENTRAL 30 - 2 THRESHOLD TEST



CENTRAL 30 - 2 THRESHOLD TEST



DISCUSSION

Field description: Scotomata adjacent to inferior aspect of blind spot and in nasal field, not respecting the meridian, OD.

Localization: Retina.

Pathology: Central serous retinopathy (choroidopathy).

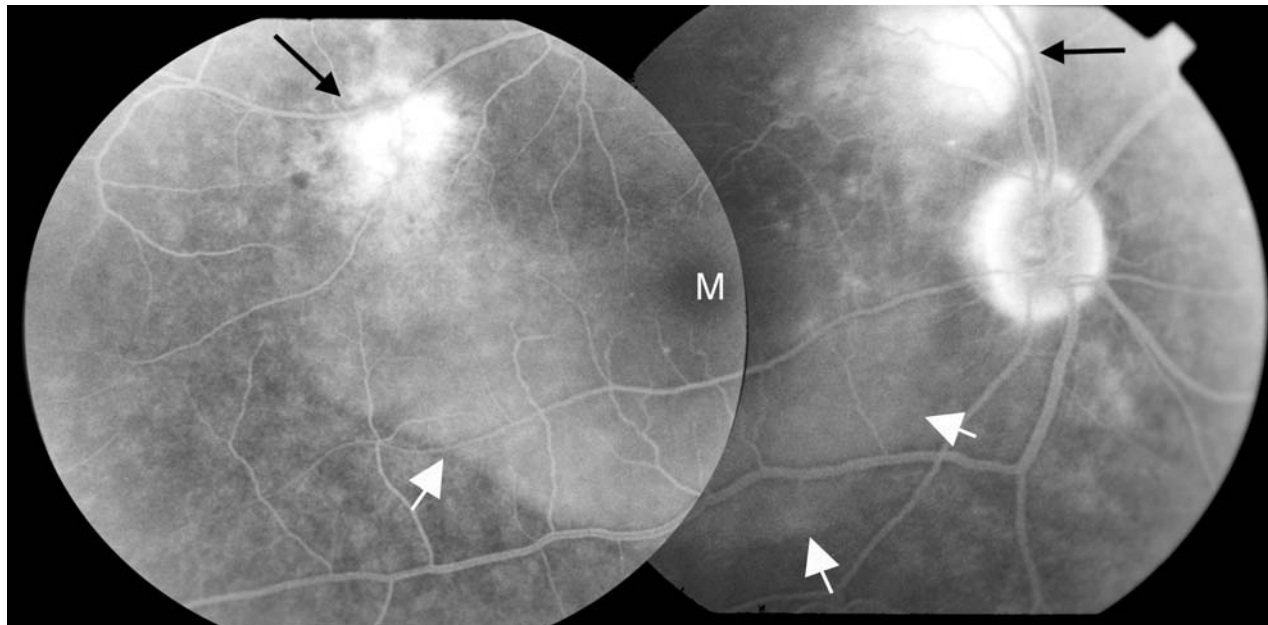
Amsler grid showed an area of distortion inferotemporal to the blind spot.

The patient's scotomata bear some resemblance to an arcuate defect, with depression near the horizontal meridian and near the blind spot; however, the presence of defects above the meridian argue against this. The location of these defects correlates with sites of retinal pigmentary epithelial changes, shown on fluorescein angiogram from a earlier attack as hyperfluorescent regions (black arrows), rather than with the more extensive zone of subretinal fluid present at that time (white arrows).

The photostress test measures how long visual acuity takes to recover after the retina is bleached by having the patient look at a bright light (4). It is prolonged in macular disease but not optic neuropathy.

The patient's story of recurrent attacks with resolution might suggest an optic neuritis, although the number of attacks and their long duration are unusual for this condition. Central serous retinopathy is a condition that is easily confused with optic neuritis, since it also causes central field depressions and color defects, affects mainly young people, and its ophthalmoscopic findings are subtle. It can even prolong latencies on visual evoked potentials. However, there is often no or minimal RAPD, compared with optic neuropathy (5). If suspected, a dilated retinal examination and fluorescein angiogram are helpful. The latter shows small hyperfluorescent defects of the retinal pigmentary epithelium, with slow leakage of fluid subretinally behind the neurosensory detachment. Visual defects tend to disappear as the fluid resolves over several months. However, a few patients have a recurrent or chronic central serous retinopathy, as did this patient. Persistent and more severe focal field defects tend to correlate with sites of retinal pigmentary epithelial changes (6).

The cause of this condition remains a mystery. Laser treatment is indicated in those with prolonged serous detachments and permanent visual loss.



DISCUSSION

Field description: Field A: mild generalized depression; field B: cecocentral scotoma with enlargement of the blind spot OD.

Localization: Retina.

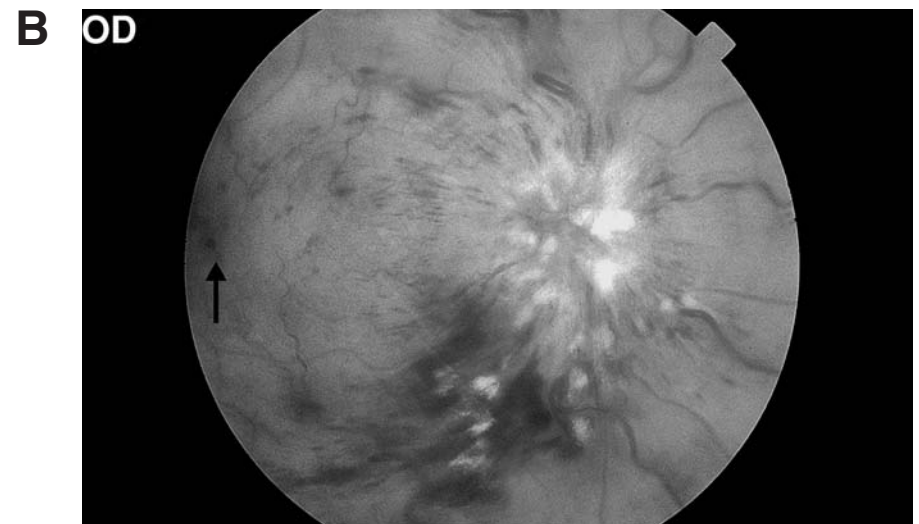
Pathology: Central retinal vein occlusion (CRVO), ischemic, with macular edema.

Confrontation testing showed no abnormality at the initial examination.

The initial field shows mild changes characteristic of nonischemic CRVO, a diagnosis suggested by painless, progressive visual loss with disc edema, dilated tortuous veins, and flame hemorrhages, as in fundus A here. By the patient's return, however, funduscopy (B, this page) showed ischemic exudative changes, more hemorrhage, and macular edema

(arrow), indicating a change to ischemic CRVO. On his second field the blind spot is larger, and now, thanks to the macular edema, he has a definite central scotoma with a marked decline in visual acuity.

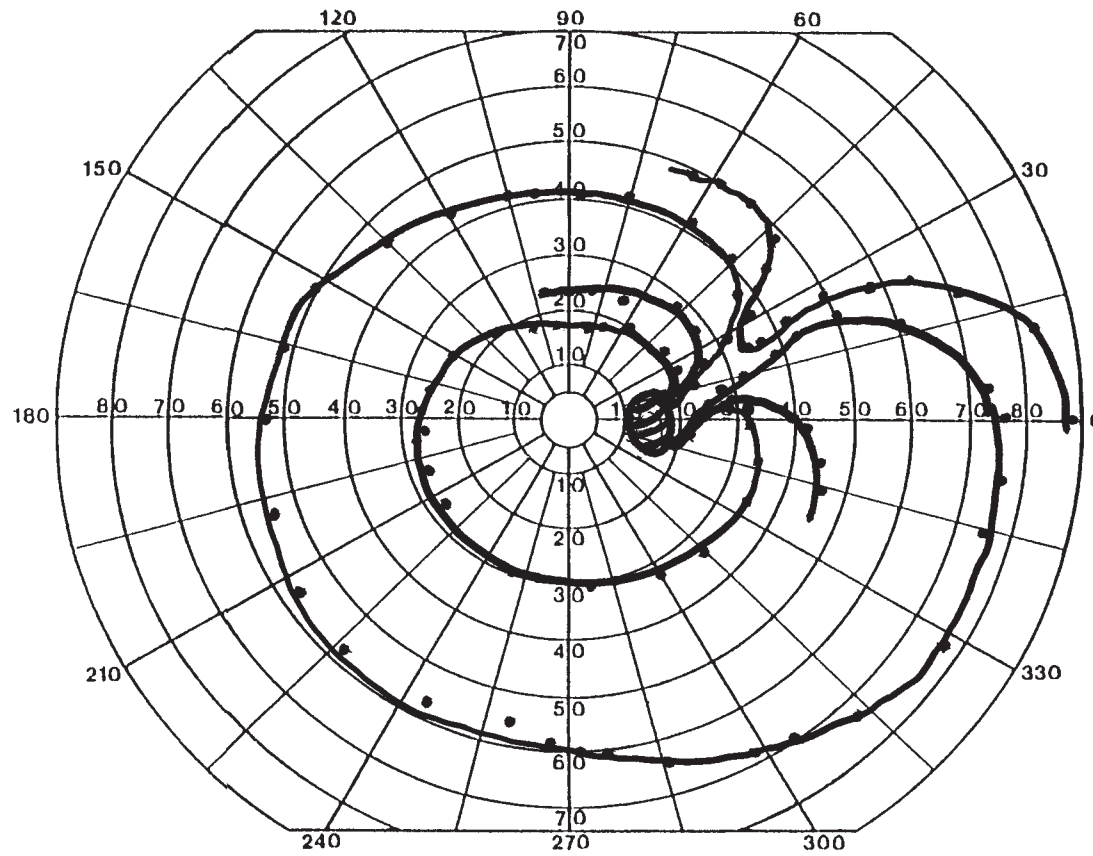
A number of mechanisms may underlie CRVO, including external compression of the vein; venous stasis from hypoperfusion due to systemic hypotension or carotid arterial stenosis; and degeneration of the venous endothelium, as in patients with diabetes mellitus. There is no recognized treatment of this disorder other than treatment of any underlying disease to prevent a similar occurrence in the fellow eye. Experimental surgical therapies are being investigated for ischemic forms of CRVO, none with proven efficacy yet.



See Color Plate after page 180

DISCUSSION

This 57-yr-old Iowan woman was referred for an anomalous optic disc with a temporal field defect OD. She had no symptoms. Her corrected visual acuity was 20/15 OU and color scores were 13.5/14 OD and 14/14 OS. There was a small RAPD OD.



Right eye

DISCUSSION

Field description: Temporal wedge defect extending from the blind spot OD.

Localization: Retinal nerve fiber layer.

Pathology: Presumed ocular histoplasmosis (POHS).

The defect is a narrow wedge that points straight from the temporal periphery to the blind spot, much as the nerve fiber bundle in this area travels. The other eye's field was normal.

The patient's fluorescein angiogram (figure) demonstrates the fundoscopic combination of peripapillary and peripheral chorioretinal atrophic scars typical of POHS, as well as mild raised inferonasal gliotic scar of the optic disc. This condition is highly endemic in the Mississippi and Missouri river basins, as well as central America and many river

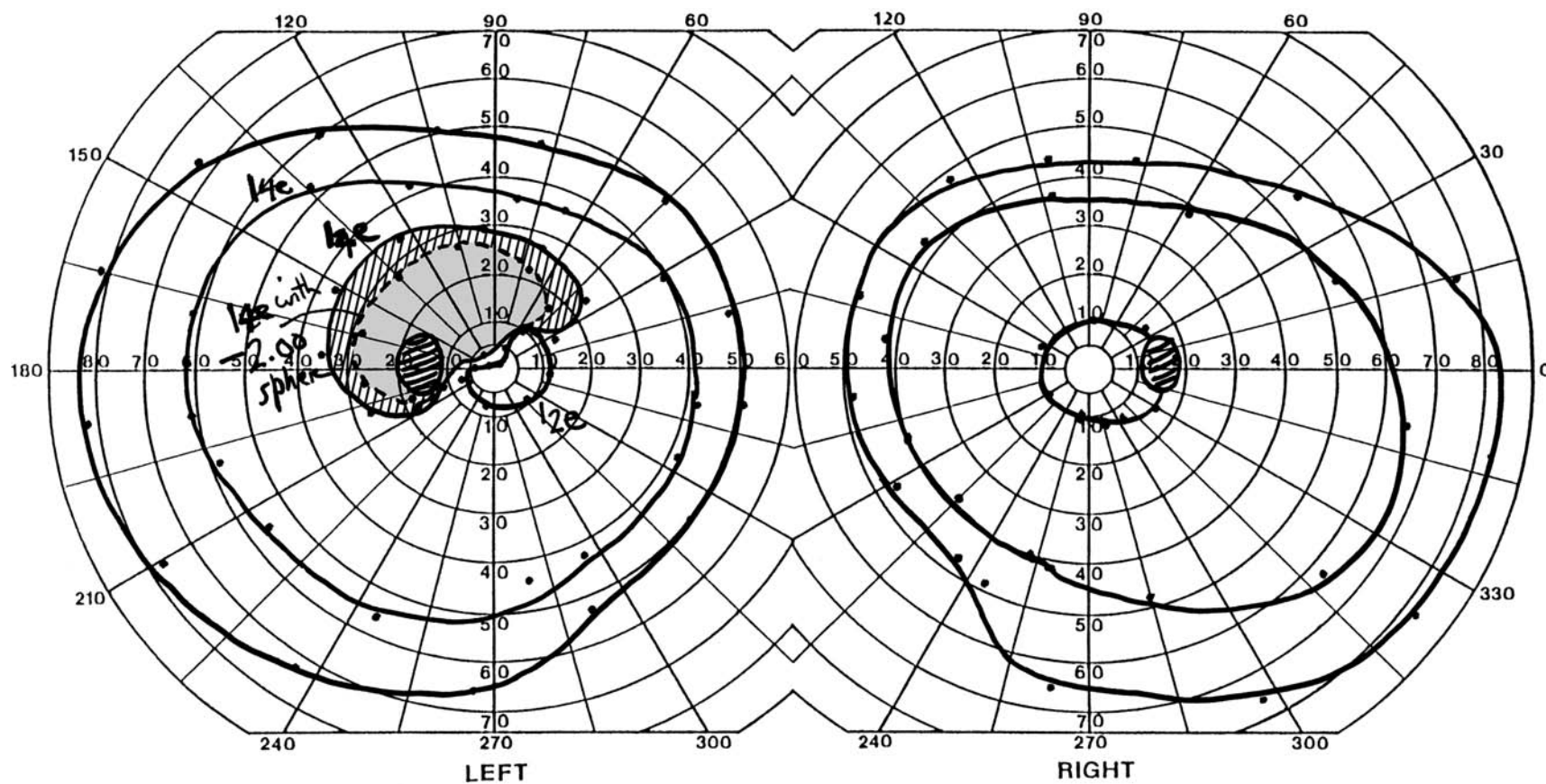
basins of South America. The organism *Histoplasma capsulatum* is a fungus found in soil that generates airborne spores that are inhaled. This can lead to an acute or chronic pulmonary condition, and rarely a serious disseminated form that can involve the central nervous system, with meningitis, encephalitis, or myelitis. Patients with POHS often lack systemic or neurologic symptoms, but chest X-ray or serologic testing may reveal signs of earlier infection (7). Whether the ocular signs are a secondary immunologic event or a primary ocular infection is a matter of debate. Most often POHS is discovered incidentally in an inactive stage and does not require treatment. Choroidal or subretinal neovascularization in the macular region may occur and requires photocoagulation to preserve vision. Acute neuroretinitis or papillitis is rarely seen but responds to steroids (8).



HISTORY AND EXAM

This 66-yr-old woman was seen for headache and periorbital pain. Angle closure glaucoma was found 12 years previously. Visual acuity was 20/30 OD and 20/50 OS, with mild cataracts OU. She saw 14/14 Ishihara plates OD and 12/14 OS. There was no RAPD.

Her refraction was quite asymmetric: +2.00 sphere with $-1.25 \times 70^\circ$ OD and -1.75 sphere with $-1.00 \times 50^\circ$ OS.



DISCUSSION

Field description: Dense superior paracentral scotoma OS.

Localization: Retina.

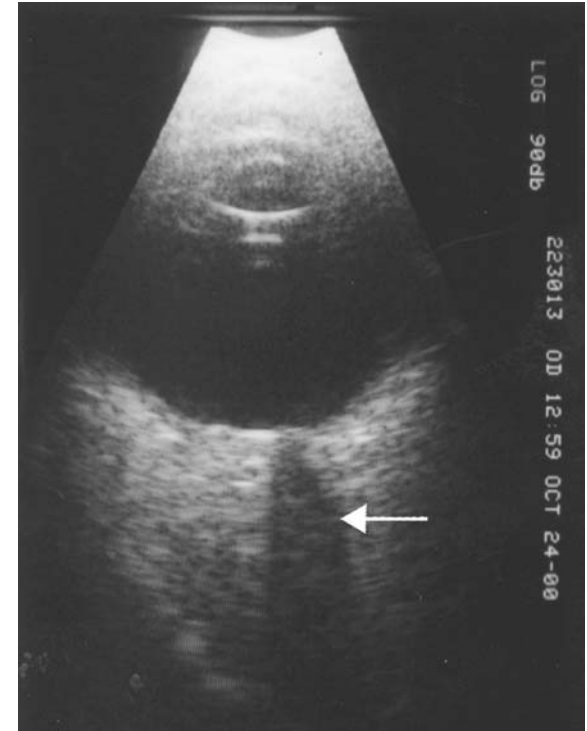
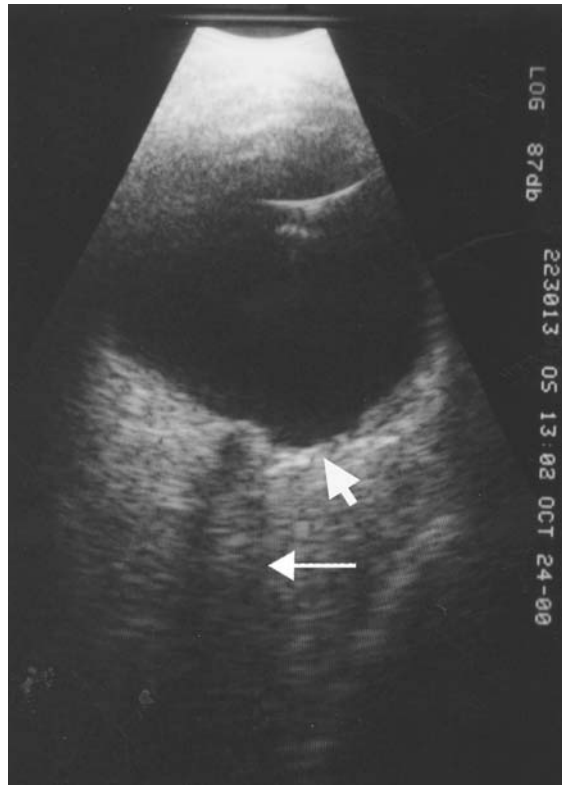
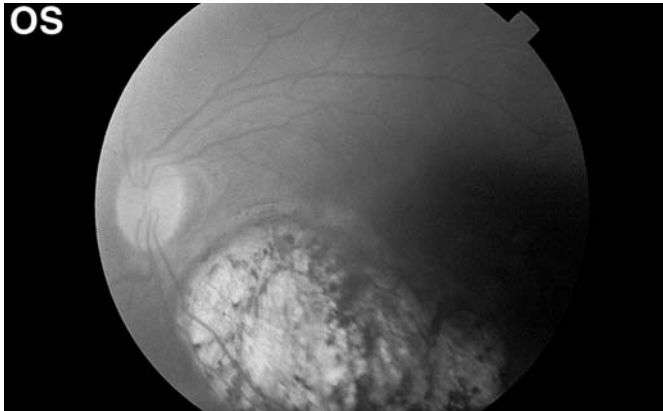
Pathology: Posterior staphyloma.

Confrontation testing showed decreased red but normal finger comparison in the superior paracentral field OS.

The defect superficially resembles an arcuate defect, but though large it does not reach the horizontal meridian. It also has a fairly extensive relative enlargement of the blind spot, unusual for arcuate defect unless associated with disc edema. The effect of adding a -2.00 spherical lens shrinks the edges of the scotoma, leaving a small area of absolute loss

(the smaller shaded region). Fundoscopy shows the staphyloma that caused the scotoma, which is also evident on ultrasound as a posterior bulge (arrow) of the globe just lateral to the optic nerve (long arrows) in the left eye (left image), compared with the normal eye (right image).

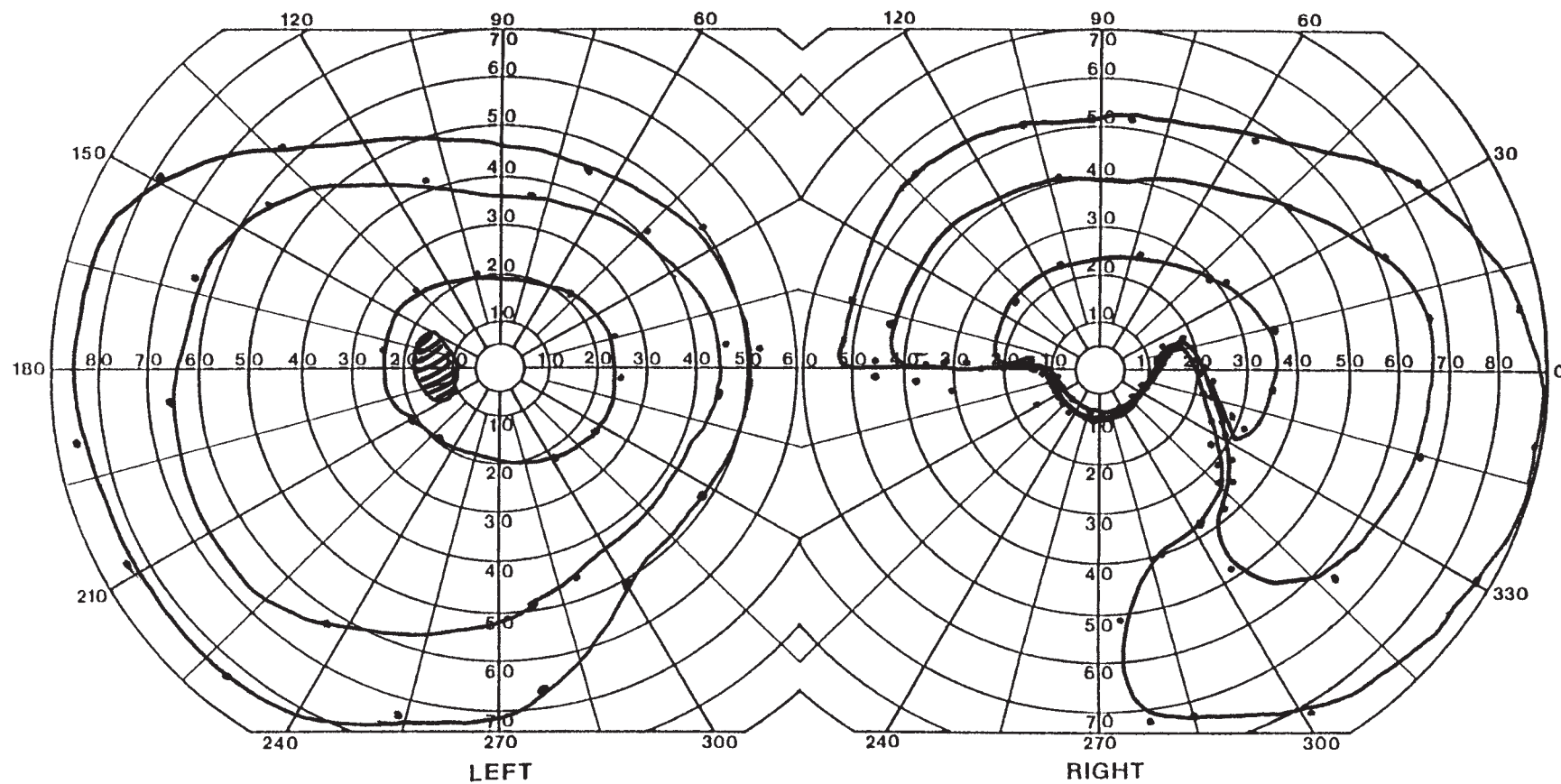
Staphylomas are congenital bulgings of the uvea into a focally thinned sclera. They can be located around the ciliary body or in the posterior retina, usually in a peripapillary location, as in this case. Posterior staphylomata have associated choroidal atrophy, and the posterior bulge is often associated with myopia. The cause is unknown. The main differential is a coloboma, which is a developmental failure of closure of the optic vesicle. Both are static nonprogressive conditions.



HISTORY AND EXAM

This 60-yr-old woman had new photopsias in the left eye that were due to a posterior vitreous detachment. Twenty-five years earlier she had had visual loss in the right eye, diagnosed as an optic neuritis, and was treated with monthly steroids for at least several

months, with partial improvement. Visual acuity was 20/20 OU, and Ishihara color scores were 11/14 OD and 14/14 OS, with a small RAPD OD.



DISCUSSION

Field description: Large inferior arcuate defect OD.

Localization: Nerve fiber layer.

Pathology: Old chorioretinitis, presumably from toxoplasmosis.

Confrontation fields showed an inferonasal step OD to hand motion.

The patient's arcuate defect looks much like any number of arcuate defects from glaucoma or other optic neuropathies shown later in this atlas (see Case 23). The resemblance is not coincidental. Fundoscopy showed a focal retinal lesion in the superior peripapillary region, which presumably has disrupted the nerve fiber bundle arching in from the temporal retina. These retinal ganglion cell axons are in the innermost layer of the retina and

can be vulnerable to certain retinal diseases as well as optic neuropathy. Such retinal lesions are usually visible on fundoscopy.

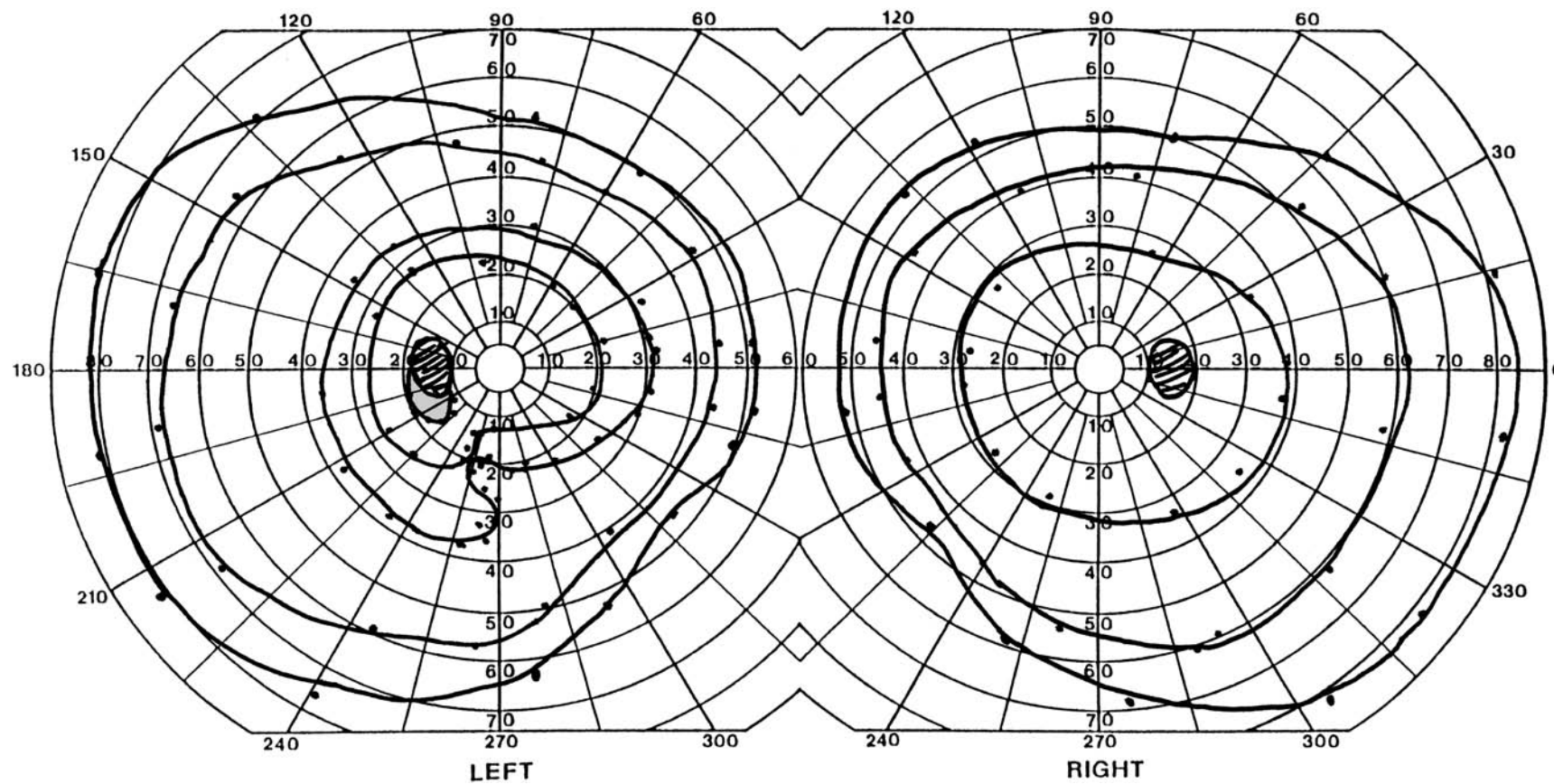
Toxoplasmosis is a common cause of chorioretinitis, caused by an obligate intracellular parasite carried by cats and transmitted to humans. Acute lesions are yellowish and associated with a marked vitritis, creating a hazy fundoscopic view. Serologic tests are available and treatment is with sulfadiazine and pyrimethamine. Old healed lesions typically have a highly pigmented chorioretinal scar, as seen here. Congenital toxoplasmosis, spread from the mother to the fetus, can cause cerebral and ocular complications; in the eye the congenital form tends to affect the macula (9).



HISTORY AND EXAM

This 54-yr-old woman noted inferior nasal blurring in the left eye. This had begun to improve by the time she presented a month later. She had no headache, eye pain, or systemic symptoms. Visual acuity was 20/15 OU and color vision was normal. There was no

RAPD. There was slight blurring of the nasal disc OS with a peripapillary flame hemorrhage and a cotton wool spot (soft exudate) at the superonasal disc margin. The remainder of the examination was normal.



DISCUSSION

Field description: Inferior arcuate defect with inferiorly enlarged blind spot OS.

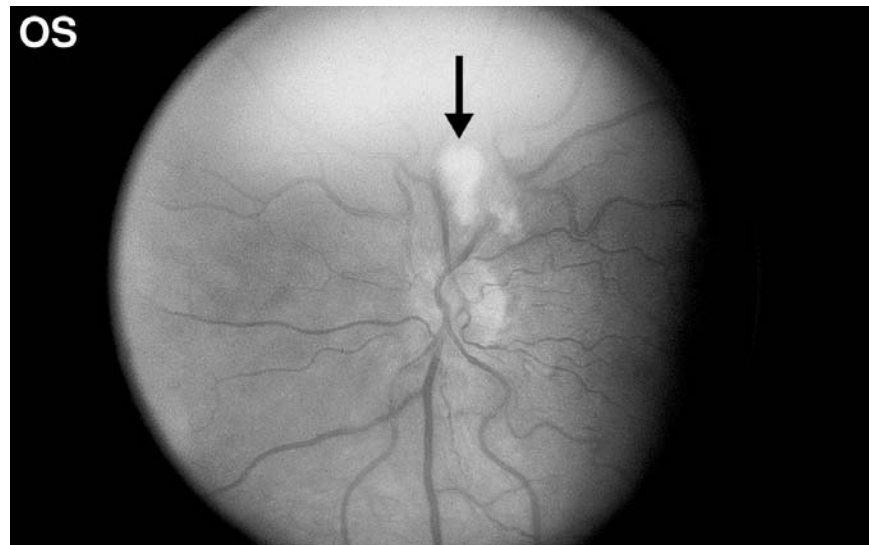
Localization: Optic nerve.

Pathology: Optic disc vasculitis.

Confrontation fields were normal.

Fluorescein angiography confirmed mild disc edema with late disc leakage. Together with the cotton wool spot and nerve fiber layer hemorrhage, this suggested an optic disc vasculitis. The arcuate defect is the result of focal ischemia of the nerve fiber layer at the location of the cotton wool spot (arrow), which corresponds to the site of the inferior enlargement of the blind spot.

The features of optic disc vasculitis are the sudden onset of unilateral mild visual impairment in a relatively young adult, with relatively preserved acuity despite optic disc edema and enlarged retinal veins. The patient would correspond to what Hayreh has called "type 1" optic disc vasculitis, with exudates on the disc or peripapillary retina and minor degrees of nerve fiber layer hemorrhages (10). Other terms used for this include *papillophlebitis*, or *benign retinal vasculitis*. The cause is unclear. Mononuclear cell infiltrates within the wall of the central retinal artery and surrounding the central retinal vein were identified in one case (11). Usually no underlying systemic inflammatory disorder is found. Steroids are recommended by some, but the course is benign with recovery over many months (10). With time and without specific treatment, this patient's signs gradually resolved and her visual field defect improved over the next year..



See Color Plate after page 180

HISTORY AND EXAM

This 41-yr-old man with hypertension suddenly noted an inferotemporal blind spot OS while watching TV. Visual acuity was 20/20 OD and 20/25 OS, with an RAPD OS. He read 14/14 Ishihara plates OU. His neurologic examination was normal.

CENTRAL 30 - 2 THRESHOLD TEST

DATE 02-14-02

STIMULUS III, WHITE, BKGND 31.5 ASB BLIND SPOT CHECK SIZE III
 STRATEGY FULL THRESHOLD
 FASTPAC
 LOW PATIENT RELIABILITY

FIXATION TARGET CENTRAL TIME 12:03:19 PM
 RX USED +1.75 DS DCX DEG PUPIL DIAMETER 4.0 MM VA 20/20

LEFT	26	26	22	24	25	25				
AGE 43	24	28	22	23	25	27	25			
FIXATION LOSSES 6/19 xx	27	28	29	31	28	28	28	23	24	
FALSE POS ERRORS 0/10	28	32	25	28	33	32	31	30	30	27
FALSE NEG ERRORS 0/9	28	29	13	28	(1)	(1)	(15)	2	2	(1)
QUESTIONS ASKED 314	31	29	30	31	(1)	9	10	5	5	5

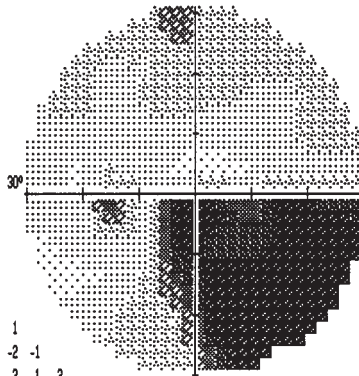
TEST TIME 00:10:37
 HFA S/N 630-4943

-2	-5	0	0						
-1	-1	-5	-4	-3	-2				
-4	-1	-4	-6	-5	-3	-2	-3		
-1	-1	-1	-2	-3	-2	-4	-1	-6	-3
-2	2	-3	1	-1	-1	-1	1	-1	
-2	-2	-4	-31	-34	-18	-30	-28	-21	
2	-1	-1	-2	-33	-23	-25	-26	-25	-22
2	-1	-6	-18	-30	-27	-27	-30		
-4	-7	-4	-31	-30	-29				
TOTAL	-4	-5	-16	-28					

-1	-5	1	1						
0	0	-5	-3	-2	-1				
-3	0	-4	-6	-4	-2	-1	-2		
-1	-1	0	-2	-2	-1	-3	-1	-5	-2
-1	3	-3	1	0	-1	-1	1	0	
-1	-1	-3	-31	-33	-17	-29	-27	-21	
2	-1	0	-1	-32	-22	-25	-25	-24	-22
3	0	-5	-17	-29	-26	-26	-29		
-3	-6	-4	-30	-30	-29				
PATTERN	-4	-4	-16	-28					

MD -11.56 DB P < 0.5%
 PSD 13.73 DB P < 0.5%
 SF 2.99 DB P < 10%
 CPSD 13.30 DB P < 0.5%

PROBABILITY SYMBOLS
 :: P < 5%
 ⌘ P < 2%
 ⌘ P < 1%
 ■ P < 0.5%



CENTRAL 30 - 2 THRESHOLD TEST

DATE 02-14-02

STIMULUS III, WHITE, BKGND 31.5 ASB BLIND SPOT CHECK SIZE III
 STRATEGY FULL THRESHOLD
 FASTPAC

FIXATION TARGET CENTRAL TIME 11:40:49 AM
 RX USED +1.75 DS DCX DEG PUPIL DIAMETER 4.0 MM VA 20/20

RIGHT	26	26	26	23	26	20				
AGE 43	26	28	26	26	25	25	24			
FIXATION LOSSES 3/17	19	24	27	31	28	28	29	28	27	
FALSE POS ERRORS 0/6	28	25	31	29	36	30	31	24	29	31
FALSE NEG ERRORS 0/6	28	29	32	33	(28)	(33)	28	4	(28)	(32)
QUESTIONS ASKED 263	26	29	29	31	30	32	31	30	32	28

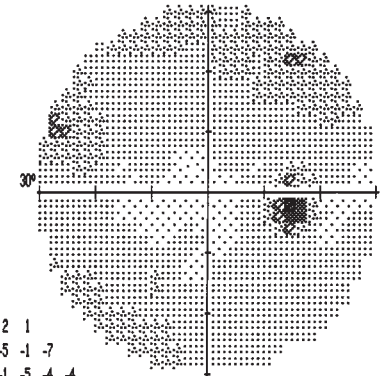
TEST TIME 00:10:33
 HFA S/N 630-4943

-2	-2	2	1						
-1	-2	1	-4	-1	-7				
-2	-1	-4	-4	0	-4	-4			
-8	-5	-3	-2	-4	-3	-2	-1	-3	-1
0	-4	0	-3	4	-2	0	-1	2	
-2	-1	0	0	-2	0	-4	3	1	
-1	-1	-2	-1	-2	0	-2	-1	2	-1
-4	-1	-6	1	-3	-3	-4	-4		
-3	-3	-3	-4	-1	-4				
TOTAL	-4	-1	-2	-1					

-2	-2	2	1						
-1	-2	1	-5	-1	-7				
-2	-1	-4	-4	-1	-5	-4	-4		
-8	-5	-4	-2	-4	-3	-1	-3	-2	
0	-5	-1	-4	3	-3	-1	-2	1	
-2	-1	0	0	-2	0	-4	3	1	
-2	-1	-2	-2	-2	0	-2	-1	2	-2
-4	-2	-6	1	-3	-3	-4	-4		
-4	-4	-3	-5	-1	-4				
PATTERN	-5	-1	-2	-2					

MD -1.79 DB
 PSD 2.27 DB
 SF 1.86 DB
 CPSD 0.85 DB

PROBABILITY SYMBOLS
 :: P < 5%
 ⌘ P < 2%
 ⌘ P < 1%
 ■ P < 0.5%



DISCUSSION

Field description: Dense inferior arcuate defect OS.

Localization: Retina.

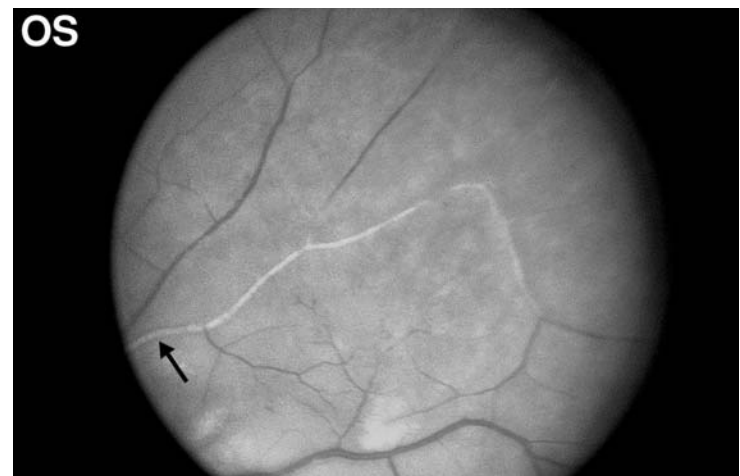
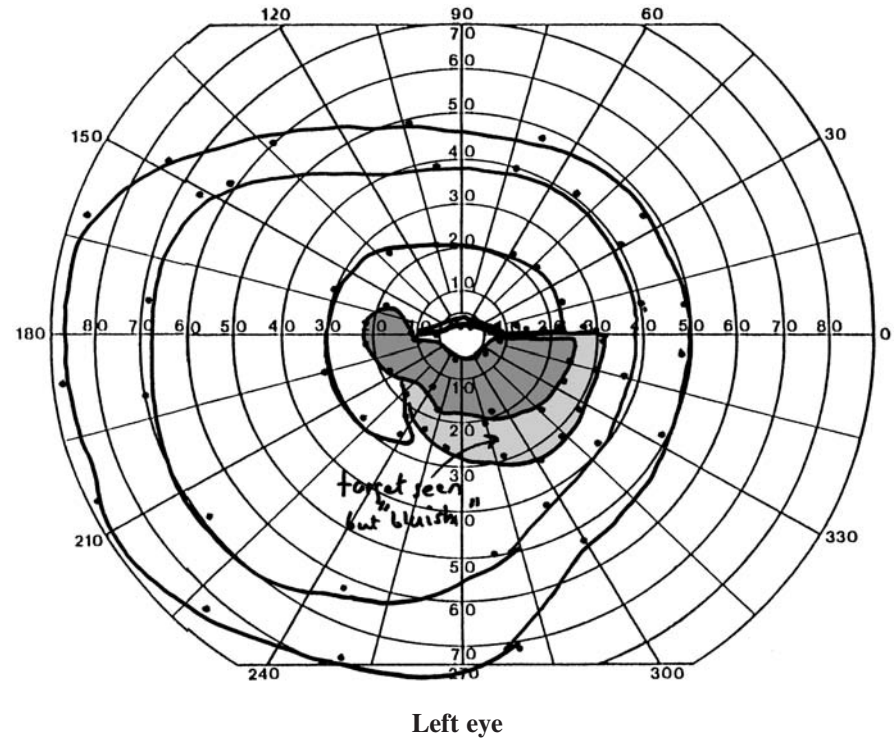
Pathology: Branch retinal arterial occlusion.

Confrontation testing showed an inferior paracentral defect to finger motion OS.

Although the patient's defect on Humphrey 30-2 perimetry extends to the edge of the test area, Goldmann perimetry (this page) showed that his defect is confined to the central 30°. Fundoscopy showed a central stripe of pale retina superior to the fovea, consistent with his field defect. In addition, an artery above this zone is pale, a "ghost vessel" (arrows).

Retinal arterial occlusions cause sudden painless loss of vision. This can affect a branch (branch retinal arterial occlusion [BRAO]), one of the two divisions of the central retinal artery that emerge at the optic disc (hemi-central retinal artery occlusion), or the whole central retinal artery (CRAO). The main causes are emboli from the heart or atherosclerotic carotid arteries. Giant cell arteritis is a less common cause in the elderly. In patients 40 years or younger, echocardiography reveals a cardiac source in a third. In the remainder, a coagulopathy must be excluded (12), with platelet count and tests for lupus anticoagulant, antithrombin III, proteins S and C, plasminogen activator, fibrinogen, and homocysteine. Cocaine and carotid dissection are other causes of stroke in younger individuals. In this patient, transesophageal echocardiogram, carotid ultrasound, and coagulation studies were normal. He was started on ASA.

There is no proven treatment for retinal artery occlusion. Thrombolysis studies are ongoing. The prognosis for visual recovery is poor if loss persists for more than 3 h. There is increased risk of future strokes, about 18% over 5 years in the elderly (13).



HISTORY AND EXAM

For 10 months this 49-yr-old man had noted swirling black-and-white patterns in his lower right field, even with eyes closed. His left eye also had an area of decreased vision in this region and just to the left of fixation, which shrank in size over several months.

Acuity was 20/15 OU, with normal Ishihara color scores of 14/14 OU. There was no RAPD.

CENTRAL 30 - 2 THRESHOLD TEST

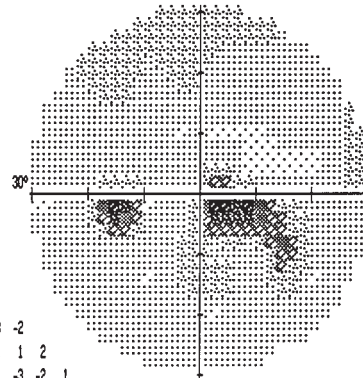
DATE 10-22-01

STIMULUS III, WHITE, BCKGND 31.5 ASB BLIND SPOT CHECK SIZE III
 STRATEGY FULL THRESHOLD
 FASTPAC

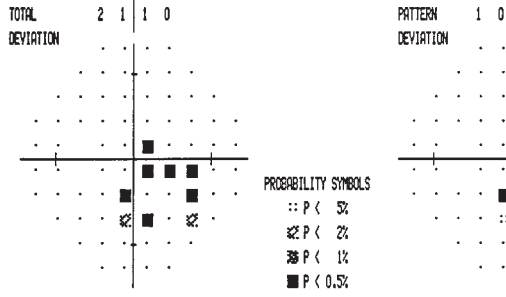
FIXATION TARGET CENTRAL TIME 11:01:11 AM
 RX USED +2.75 DS DCX DEG PUPIL DIAMETER 4.0 MM VA 20/20

LEFT

AGE	49
FIXATION LOSSES	1/18
FALSE POS ERRORS	0/10
FALSE NEG ERRORS	0/7
QUESTIONS ASKED	295
TEST TIME	00:09:20
HFA S/N	630-4943



-1	-2	-2	-1
-3	1	4	2
0	-3	1	-3
-1	-1	0	-2
-1	-1	-3	-2
2	-1	-1	-2
-1	-1	0	-2
0	0	0	-6
0	-1	-1	2
2	1	1	0



MD -3.30 DB P < 5%
 PSD 8.12 DB P < 0.5%
 SF 2.22 DB
 CPSD 7.72 DB P < 0.5%

CENTRAL 30 - 2 THRESHOLD TEST

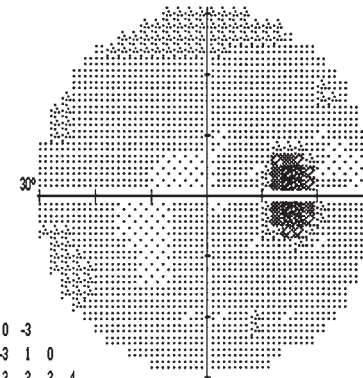
DATE 10-22-01

STIMULUS III, WHITE, BCKGND 31.5 ASB BLIND SPOT CHECK SIZE III
 STRATEGY FULL THRESHOLD
 FASTPAC

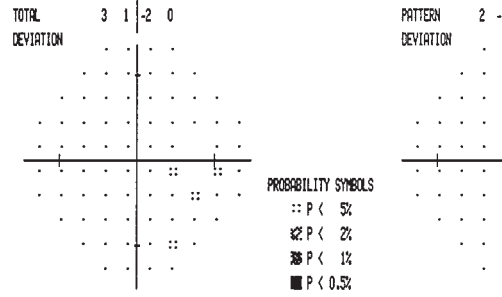
FIXATION TARGET CENTRAL TIME 10:48:40 AM
 RX USED +2.75 DS DCX DEG PUPIL DIAMETER 4.0 MM VA 20/20

RIGHT

AGE	49
FIXATION LOSSES	0/17
FALSE POS ERRORS	0/11
FALSE NEG ERRORS	0/7
QUESTIONS ASKED	291
TEST TIME	00:08:46
HFA S/N	630-4943



-1	-2	1	-1
-1	-1	-1	-1
-1	-1	-3	-3
-1	-1	0	-2
1	-1	-3	0
0	-3	2	-1
-3	-2	-1	4
-3	0	2	4
1	-2	2	1
3	1	-2	0



MD -0.78 DB
 PSD 2.21 DB
 SF 1.91 DB
 CPSD 0.41 DB

DISCUSSION

Field description: Inferior perifoveal scotoma OS.

Localization: Retina.

Pathology: Branch retinal arterial occlusion.

Confrontation testing showed a perifoveal scotoma OS to red targets, also apparent on the Amsler grid.

The patient has a defect within the central 5°, but acuity is normal, hence the fovea is spared, making this a central perifoveal defect. The defect is clearly monocular, and only partly respects the horizontal meridian, in the more peripheral extent of the defect. It is an

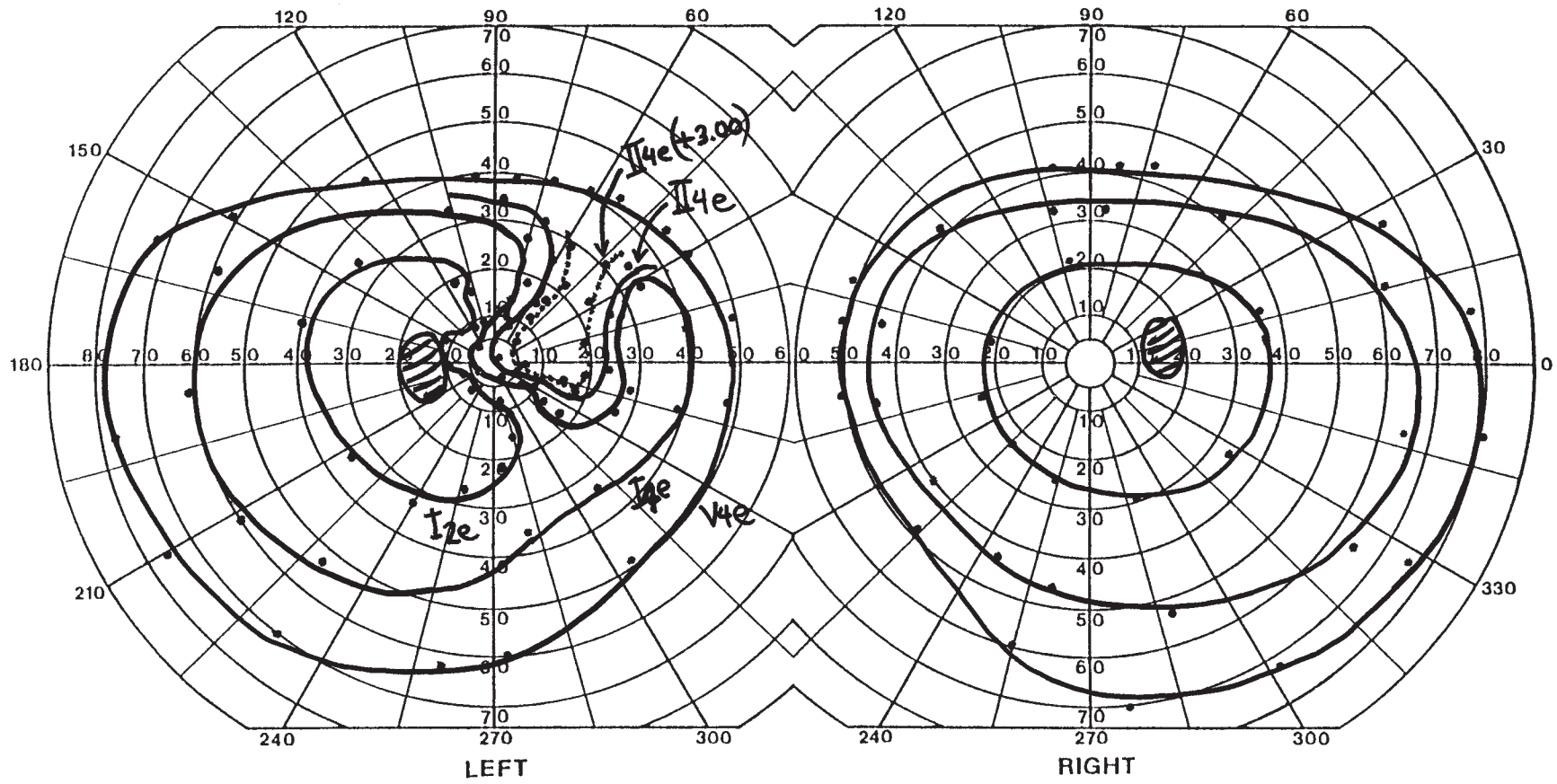
unusual defect and an unusual presentation for a retinal artery occlusion, but funduscopy clearly showed a small plaque at the terminus of an arteriole in the region of the abnormality. Focal electroretinography confirmed a zone of nonfunctioning retina in this region also. Investigations for young stroke were done (see Case 9), with negative results. Field defects associated with hallucinations suggest a release phenomenon, but release requires that an area of the field have lost visual input from both eyes. This is clearly not the case here. One can speculate that his hallucinations may be due to some retinal instability in surviving neuronal elements, possibly more likely given the relatively minimal nature of his ischemic defect.



HISTORY AND EXAM

This 44-yr-old man had an 18-year history of non-Hodgkin lymphoma involving the abdomen, pelvis, and cervical nodes, and, in the prior year, pulmonary involvement. For 2 weeks he had unusual frontal headaches daily and for 3 days painless blurred vision OS.

Visual acuity was 20/20 OD and 20/30 OS. Color vision was normal. There was no RAPD. Fundoscopy showed a few pale raised choroidal lesions in the left eye in the temporal retina.



DISCUSSION

Field description: Relative nasal scotoma OS, partially refractive.

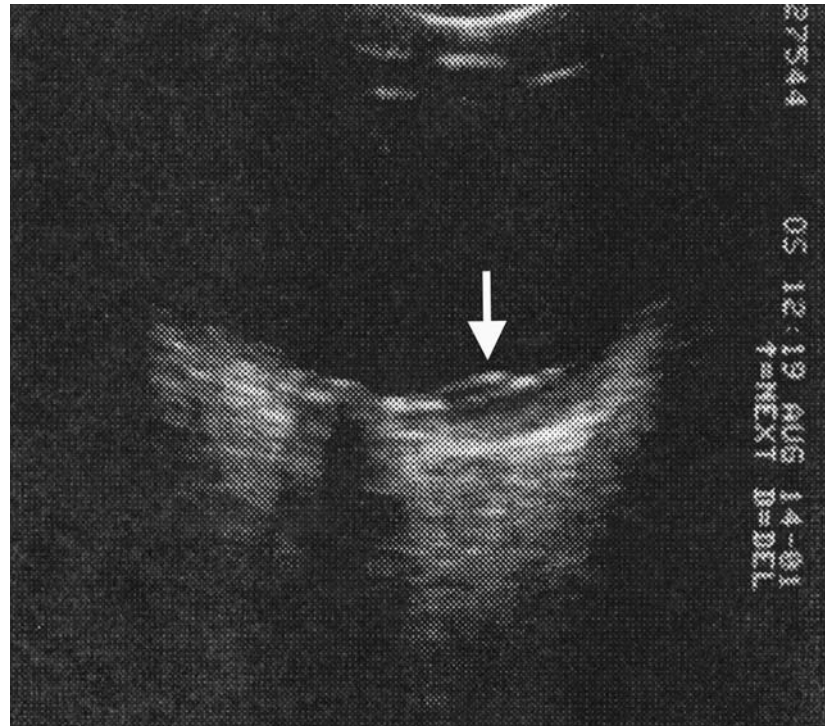
Localization: Retina/choroid.

Pathology: Choroidal metastasis from lymphoma.

Confrontation testing showed nasal blurring for hand comparison, but red targets appeared normal in this region.

Note that the patient's nasal field defect does not respect the horizontal meridian or appear arcuate in shape. This points away from the optic nerve, which can be involved by lymphoma. Part of the defect shrinks with use of a +3.00 sphere, indicating that some of it is refractive in origin, from elevation of the retina out of the plane of focus. Choroidal metastasis was confirmed with an orbital ultrasound, which shows this elevation (arrow).

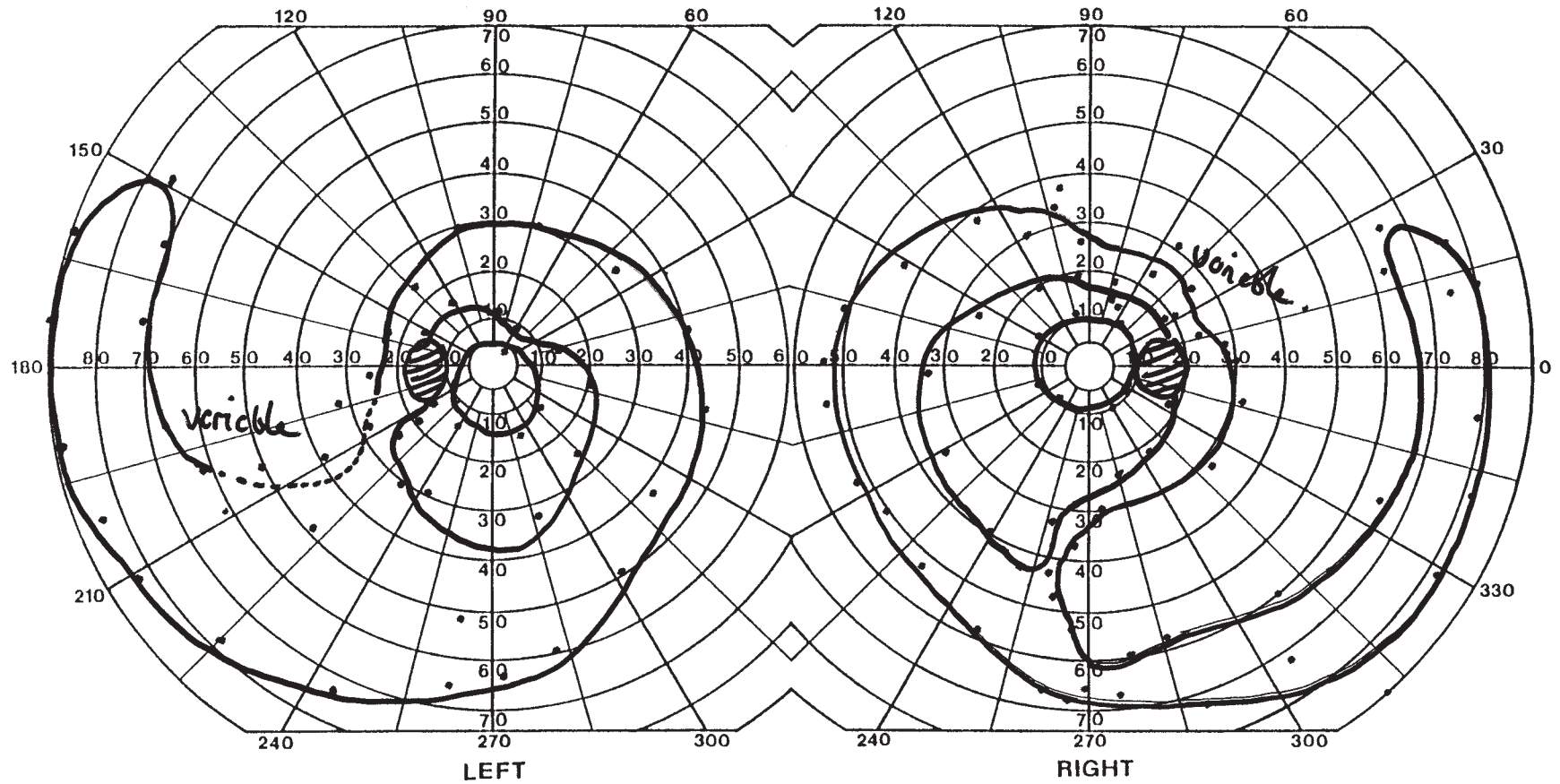
The choroid may be involved by metastatic non-Hodgkin lymphoma as well as primary central nervous system (CNS) lymphoma (14). With metastatic non-Hodgkin lymphoma, there is typically concurrent involvement of the brain parenchyma, though not present in this patient. The lymphoma initially involves the space between the choroid and the retinal pigment epithelium and the vitreous becomes cloudy, being filled with inflammatory and neoplastic cells. Definitive diagnosis of choroidal lymphoma can be made by cytologic examination of a vitreous aspiration. This procedure is particularly useful when primary CNS lymphoma is suspected, but there is no focal lesion amenable to biopsy and lumbar puncture fails to reveal malignant cells. With combined involvement of the brain parenchyma and the choroid, treatment consists of whole brain and ocular irradiation. If isolated to the eye, ocular irradiation is the treatment of choice.



HISTORY AND EXAM

This 53-yr-old man described a 25-year history of episodes of flashes of light lasting 10–15 seconds occurring on awakening and with transition between light and dark environments. These had become gradually more frequent over a few years. He also noted

some diminution of his peripheral vision, especially at night, and a periodic flickering sensation in his peripheral vision. There was no relevant family history. Visual acuity was 20/20 OD and 20/25 OS. Ishihara color plates were 13/14 OU.



DISCUSSION

Field description: Bilateral hemi-ring scotomata predominantly in the temporal fields.

Localization: Retina.

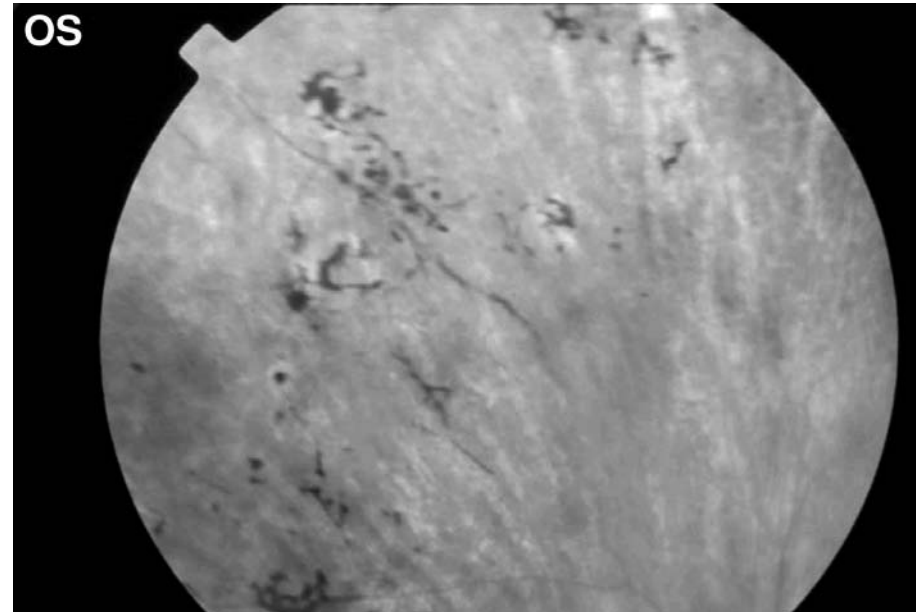
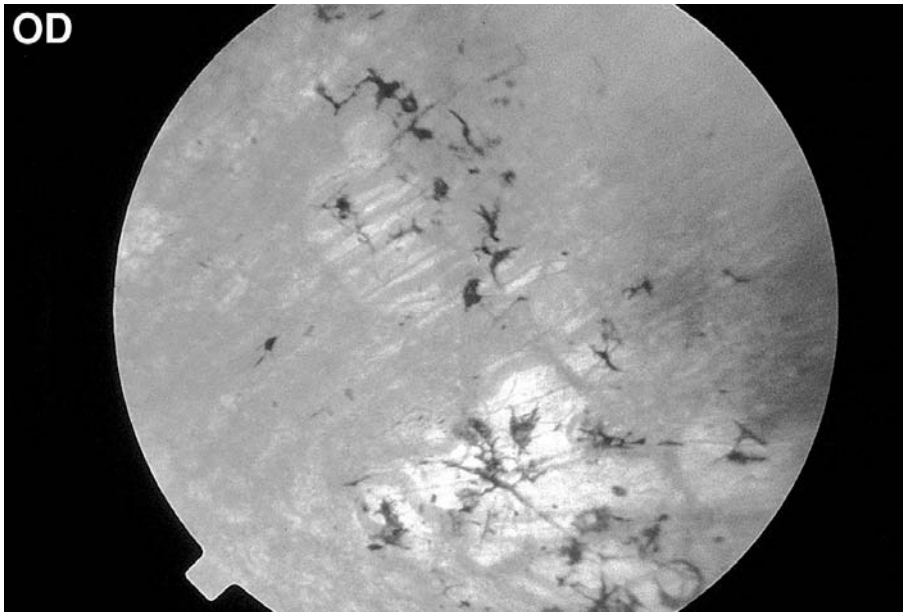
Pathology: Retinitis pigmentosa.

Confrontation fields showed decreased finger counting in the temporal fields.

Note that these temporal field deficits do not respect the vertical meridian (cf. Case 65) and spare the far periphery. Fundoscopy (shown here) showed spicules of pigment and attenuated arterioles in the retinal periphery. Full-field electroretinograms (ERGs) were reduced OU, consistent with the diagnosis of retinitis pigmentosa.

Retinitis pigmentosa is a term that encompasses a range of genetically heterogeneous diffuse photoreceptor-retinal pigment epithelial disorders. The inheritance pattern is vari-

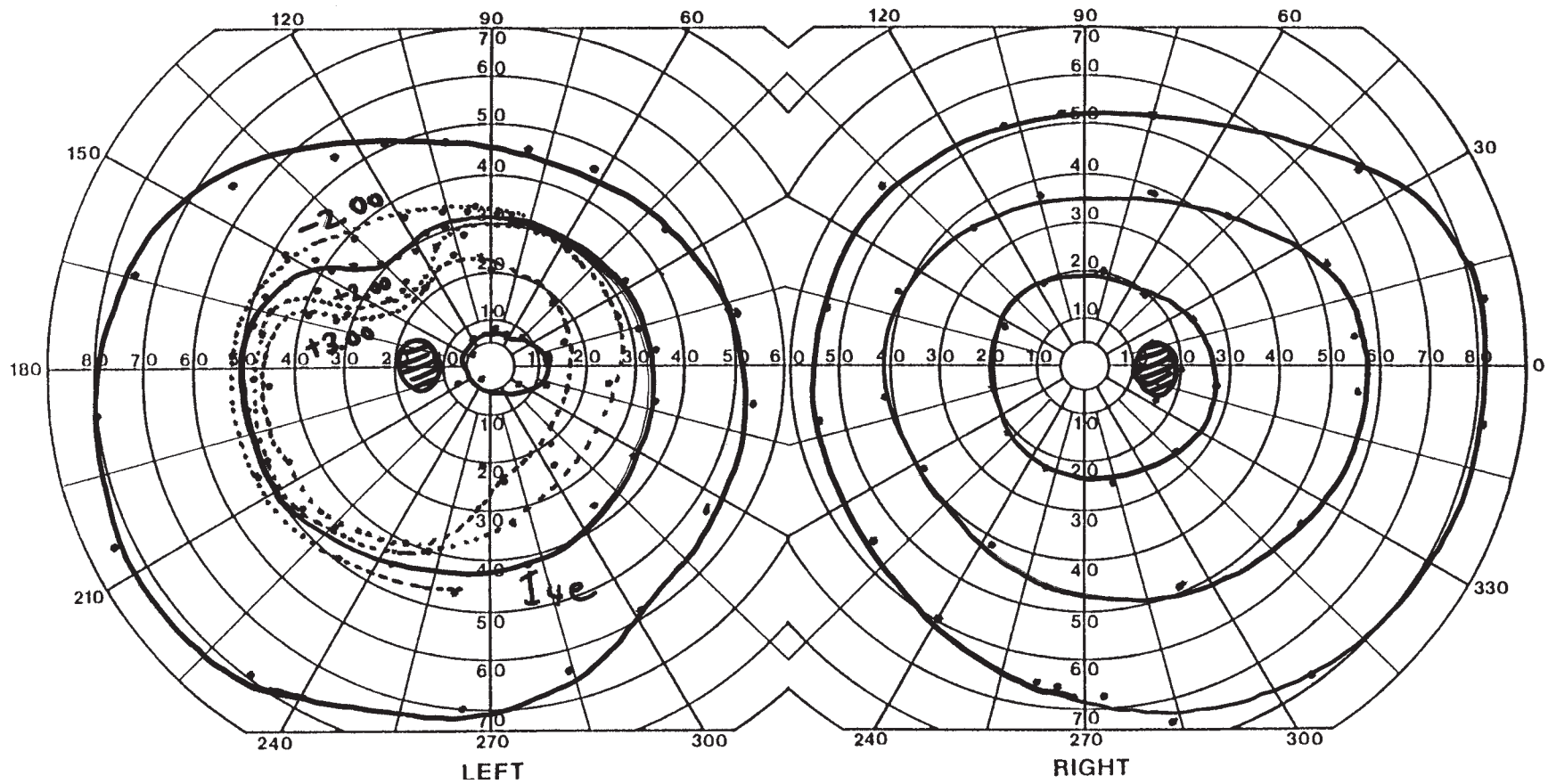
able, with autosomal dominant, autosomal recessive, and X-linked patterns (15). Some forms are due to mutations in the rhodopsin gene (16). The rod photoreceptors usually bear the brunt of the early degenerative changes, and initial symptoms typically include slowly progressive binocular loss of dark adaptation and night vision (nyctalopia). Fields show ring scotomata, typically between 20 and 40° eccentricity initially. Some forms are more focal; in this case, selective pigmentary degeneration of the nasal retina resulted in a field defect that mimicked bitemporal hemianopia. The onset of symptoms varies from infancy to middle age and tends to occur earliest in the X-linked variety and latest in autosomal dominant forms (15). With advanced disease, the visual fields may become markedly constricted with relative sparing of central vision.



HISTORY AND EXAM

This 62-yr-old woman had a superotemporal field defect OS discovered incidentally 15 years prior at a visit for chronic headache. Magnetic resonance imaging (MRI) then

showed a foramen magnum meningioma. Visual acuity was 20/20 OD and 20/25 OS, and color plates were normal OU. There was no RAPD.



DISCUSSION

Field description: Superotemporal depression OS, minimized by negative lenses.

Localization: Globe/local refractive.

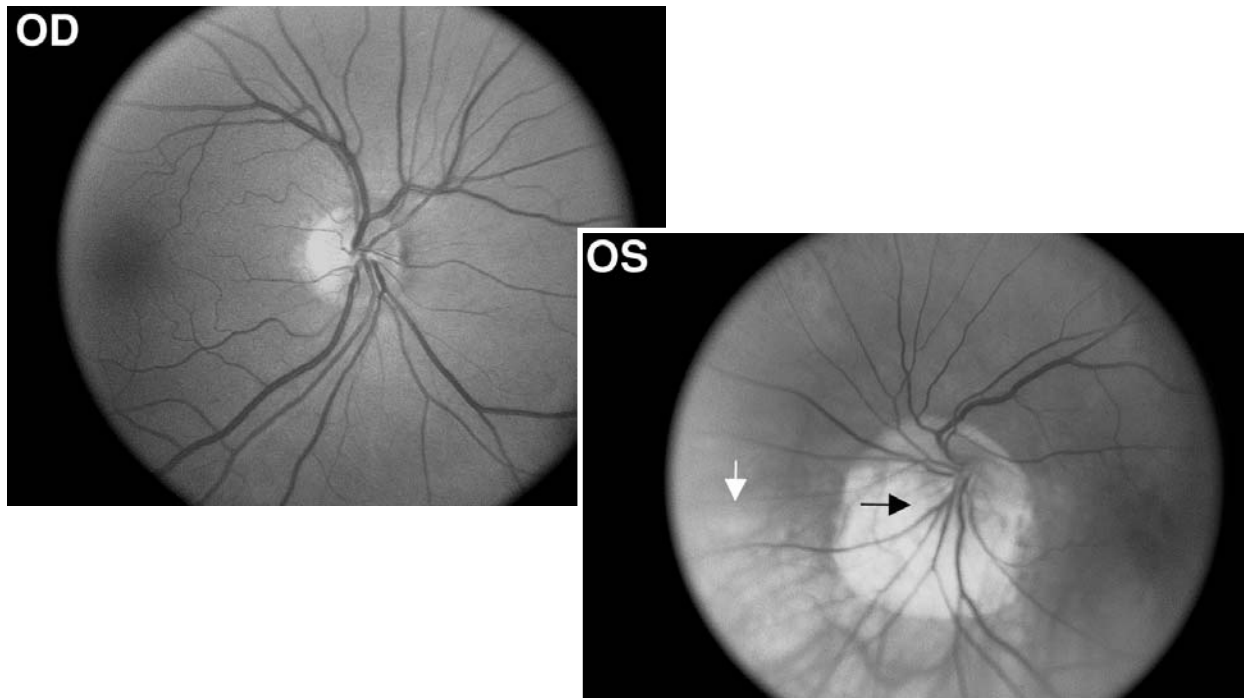
Pathology: Nasal fundus ectasia, tilted disc syndrome.

Confrontation testing with red targets but not other stimuli showed a subtle superotemporal field defect OS.

The field shows a mild superotemporal depression of the I4e isopter, and also of the I2e temporally. The temporal defect does not respect the vertical meridian or point in a wedge toward the optic disc. The I4e defect is accentuated by viewing with plus lenses (which shorten the focal length) and eradicated by viewing with minus lenses. This suggests a local elongation of the globe in the inferonasal region. Fundus pictures show a nasally tilted disc (black arrow) with peripapillary atrophy and hypopigmented inferior nasal retina (white arrow) OS. T2-weighted axial MRI confirms elongation of the nasal globe

(compare with right eye, shown here), and also shows anomalous tilted entry of the optic nerve to the globe (not shown).

Nasal fundus ectasia is a developmental anomaly in which the globe nasal to the optic disc is elongated—hence, the reversal of the normal tilt of the disc so that it now faces nasally (17). In 25% of individuals, the ectasia is unilateral. In 65%, the globe anomaly is associated with a nasal tilt of the disc—“tilted disc syndrome”—as here. The retina in the ectatic fundal zone is posterior to the plane of focus of the rest of the eye—essentially, a region of high myopia. The defocus creates a region of relative depression of visual sensitivity that is only present for the smaller targets (which are more dependent on precise focusing) and can be corrected or reduced by adding high negative diopter lenses. If bilateral, this condition may be mistaken for bitemporal hemianopia from compression of the optic chiasm. The lack of a vertical step defect at the meridian and the fundoscopic appearance are key to avoiding this confusion.

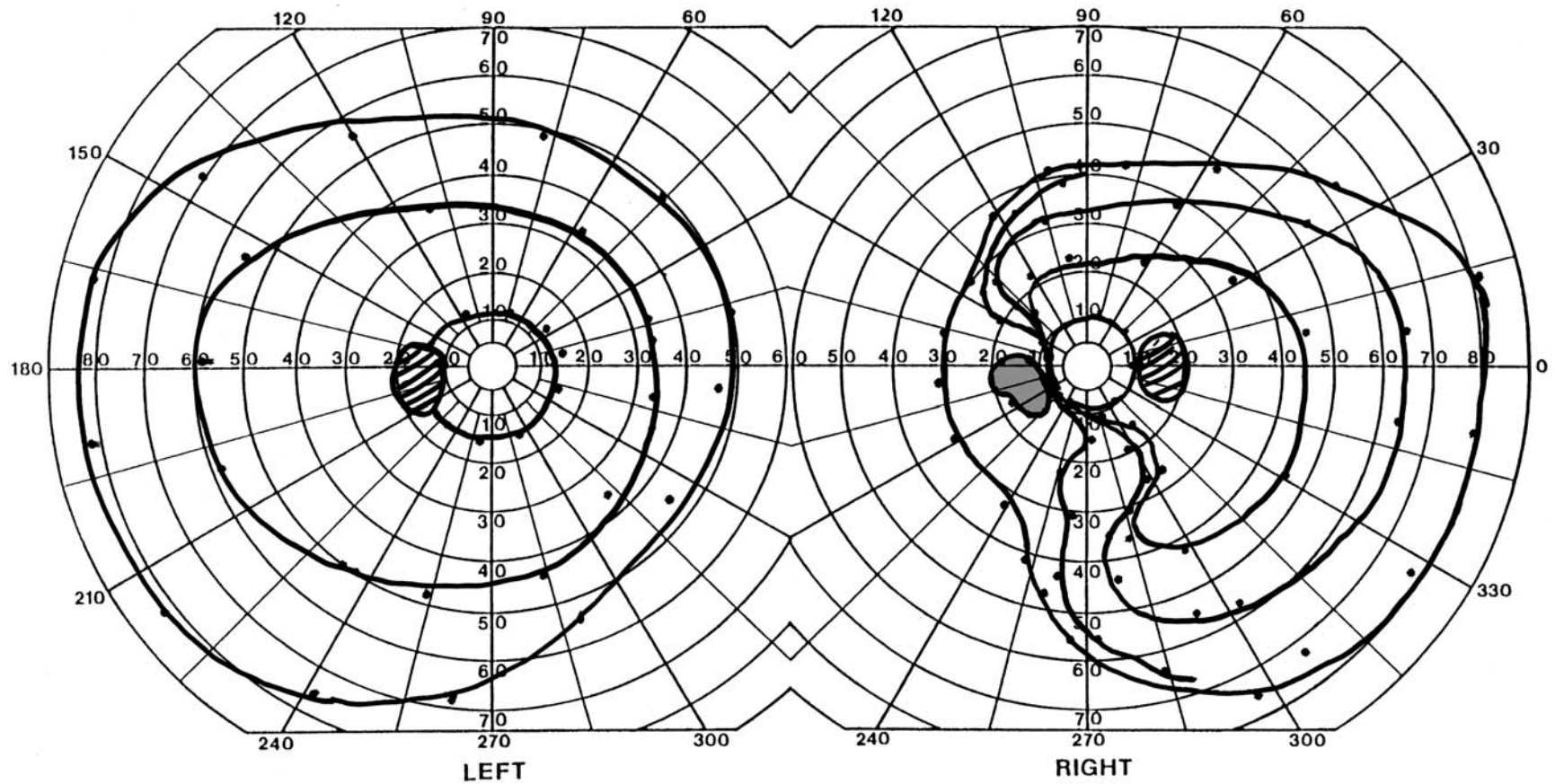


See Color Plate after page 180

HISTORY AND EXAM

This 42-yr-old man was referred for evaluation of congenital nystagmus. However, he also reported a history of a retinal detachment OD 6 years earlier. Visual acuity was 20/60

OD and 20/20 OS and color scores were 11/14 OU. There was no RAPD. Fundoscopy showed the double-ring sign of optic nerve hypoplasia OU.



DISCUSSION

Field description: Nasal constriction OD, worse inferiorly, with a small dense hole.

Localization: Retina.

Pathology: Retinal detachment.

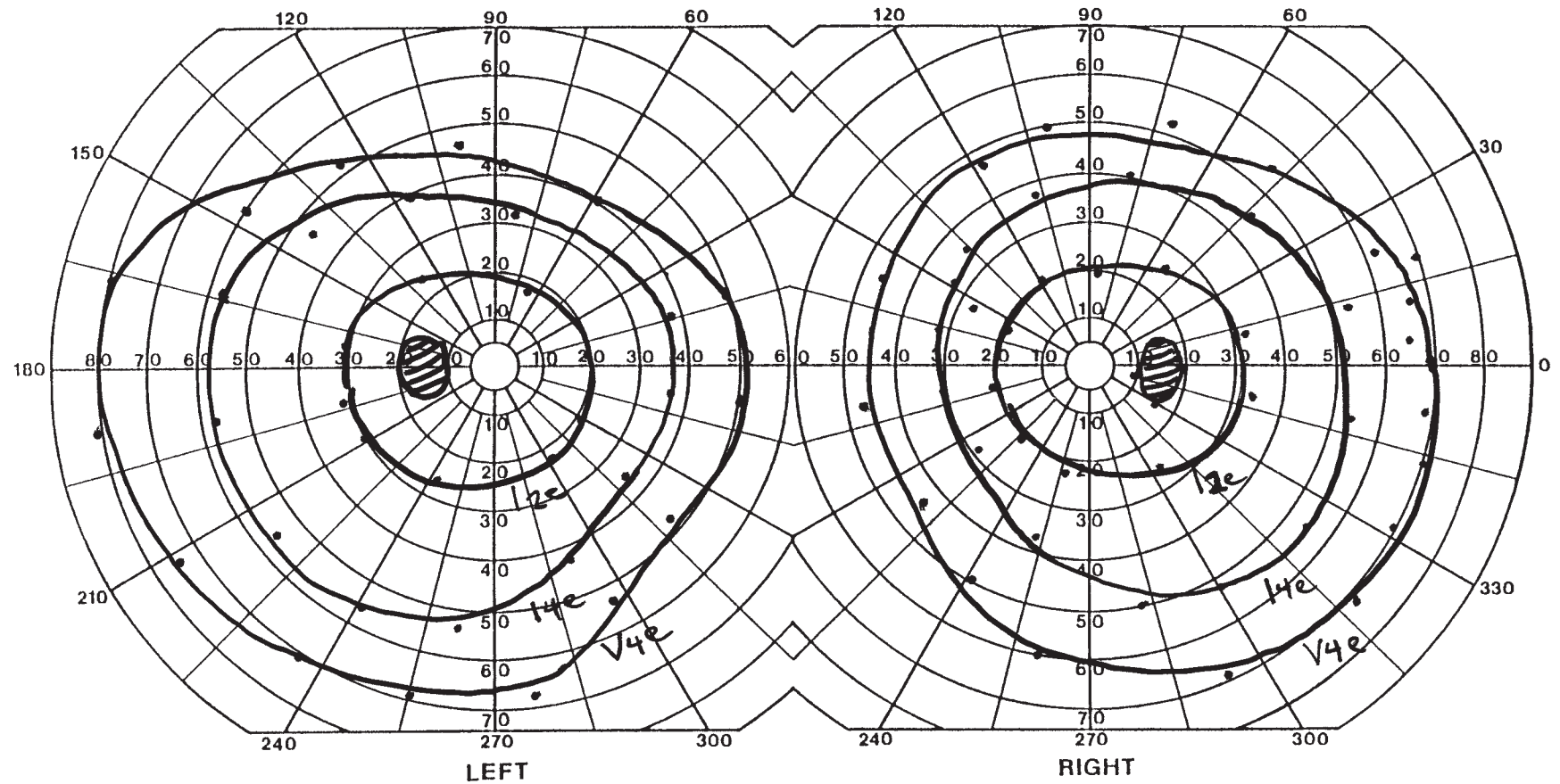
Confrontation fields showed a peripheral inferior quadrantic scotoma that did not approach either the horizontal or vertical meridians.

The patient has a nasal defect with shallow sloping borders that is more marked inferiorly, but that crosses both nasal horizontal and inferior vertical meridians without a step

defect. This makes it unlikely to represent optic neuropathy, and suggests retinal origin. Retinal detachment causes relative depression of vision in the area where the retina has detached from the underlying choroid. Detachment typically begins in the anterior retina (peripheral visual field) and extends posteriorly (into the central field) as the retinal detachment becomes more extensive. The defect tends to have a gradual sloping border with relative depression. This contrasts with retinoschisis, a separation within the layers of the retina itself that disrupts the connections between the inner and outer retina. Retinoschisis causes a dense absolute scotoma with sharp borders in the affected region.

HISTORY AND EXAM

This 16-yr-old man with long-standing complex partial seizures was referred for visual field testing because he had been using vigabatrin for 7 years. He had no visual symptoms. Acuity at far with correction was 20/20 OD and 20/15 OS, and Ishihara color plates were 14/14 OU. There was no RAPD. Fundoscopy was normal.



DISCUSSION

Field description: Relative peripheral depression bilaterally, more marked on the right.

Localization: Retina.

Pathology: Vigabatrin toxicity.

Confrontation testing was normal OU.

At first glance, little appears to be abnormal about the patient's field. However, for his age, the isopters are constricted in both eyes (see Chapter 4). ERG revealed that photopic (cone) *b-wave* amplitudes were reduced for single-flash stimuli and for 30-Hz flicker. Such abnormalities correlate strongly with the visual field constriction in vigabatrin toxicity (18).

Visual field defects are present in a proportion of patients taking vigabatrin. The most characteristic defect is a concentric narrowing of the field with preservation of central acuity and color vision. Most patients report no visual symptoms and the defect may be detected only with formal perimetry. Manual kinetic perimetry is most sensitive for demonstrating subtle peripheral depressions and contractions. Some investigators have observed a correlation between the presence of a visual defect and both the total dose and duration of therapy (19). Although cone function may improve following discontinuation of vigabatrin (shown by increased *b-wave* amplitudes under photopic conditions), it remains unclear whether the visual field defect is similarly reversible (20).

HISTORY AND EXAM

This 76-yr-old African-American woman had a 12-year history of primary open-angle glaucoma (POAG), currently being treated with topical latanaprost (a prostaglandin F_{2α} analog that increases aqueous humor outflow) and dorzolamide (a carbonic anhydrase inhibitor that decreases aqueous humor production). She had also had bilateral cataract

extractions. Her visual acuity was 20/25 OD and 20/30 OS. Ishihara color scores were 13/14 OD and 14/14 OS. She had pale discs with moderate cupping OU. Intraocular pressures most recently were 27 mmHg OU, despite compliance with treatment. Over the previous 3 years they had ranged from 21 to 23 mmHg.

CENTRAL 30 - 2 THRESHOLD TEST

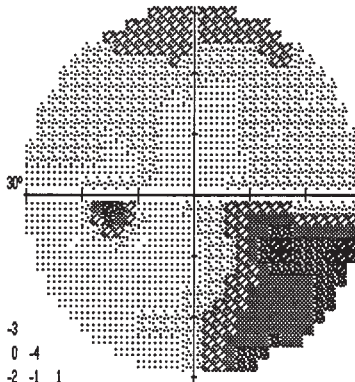
DATE 06-15-00

STIMULUS III, WHITE, BCKGND 31.5 ASB BLIND SPOT CHECK SIZE III
 STRATEGY FULL THRESHOLD
 FASTPAC

FIXATION TARGET CENTRAL
 RX USED +1.50 OS -1.50 DCX 108 DEG
 PUPIL DIAMETER 3.0 MM VA

TIME 02:09:36 PM

LEFT
 AGE 76
 FIXATION LOSSES 3/18
 FALSE POS ERRORS 0/5
 FALSE NEG ERRORS 1/8
 QUESTIONS ASKED 305
 TEST TIME 00:09:45
 HFA S/N 630-4943



4	0	-3	-3						
-1	-1	4	0	0	4				
0	-3	-1	1	-2	-1	1			
-4	-4	-1	-3	-1	-2	-4	-2	-3	0
2	-1	-4	-3	-2	-4	-5	-3	-1	
1	2	-3	-5	-6	-15	-13	-3	-1	
1	4	-2	2	-2	-5	-10	-30	-17	-25
2	1	-2	-2	-3	-11	-12	-14		
2	-2	-3	-8	-11	-14				
TOTAL	1	0	4	-15					
DEVIATION

4	0	-3	-3						
-1	-1	4	0	0	4				
0	-3	-1	1	-2	-1	1			
-4	-4	-1	-3	-1	-2	-4	-2	-3	0
2	-1	-4	-3	-2	-4	-5	-3	-1	
1	2	-3	-5	-6	-15	-13	-3	-1	
1	4	-2	2	-2	-5	-10	-30	-17	-25
2	1	-2	-2	-3	-11	-12	-14		
2	-2	-3	-8	-11	-14				
PATTERN	1	0	4	-15					
DEVIATION

MD -4.80 DB P < 2%
 PSD 7.07 DB P < 0.5%
 SF 3.75 DB P < 5%
 CPSD 5.65 DB P < 1%

PROBABILITY SYMBOLS
 :: P < 5%
 ☼ P < 2%
 ☼☼ P < 1%
 ■ P < 0.5%

CENTRAL 30 - 2 THRESHOLD TEST

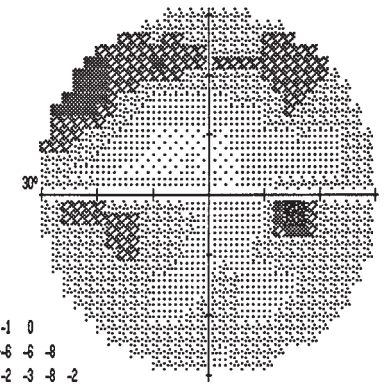
DATE 06-15-00

STIMULUS III, WHITE, BCKGND 31.5 ASB BLIND SPOT CHECK SIZE III
 STRATEGY FULL THRESHOLD
 FASTPAC

FIXATION TARGET CENTRAL
 RX USED +1.50 OS -2.00 DCX 80 DEG
 PUPIL DIAMETER 3.0 MM VA

TIME 01:57:33 PM

RIGHT
 AGE 76
 FIXATION LOSSES 2/18
 FALSE POS ERRORS 1/3
 FALSE NEG ERRORS 0/3
 QUESTIONS ASKED 302
 TEST TIME 00:09:00
 HFA S/N 630-4943



1	-1	1	2						
-7	-11	-5	-4	-4	-6				
-12	-4	2	-1	-1	-6	0			
-6	-2	-1	3	2	2	0	-1	2	-1
0	1	2	2	-1	3	-1	-1	-1	
-4	-8	-8	-5	0	-3	-3	-2		
-3	-1	-11	-7	-4	-2	-5	-5	-2	-2
-3	-2	-2	-2	-5	-2	-2	-1		
-3	1	-2	-3	-1	-1				
TOTAL	-3	0	0	-2					
DEVIATION

1	-1	1	2						
-7	-11	-5	-4	-4	-6				
-12	-4	2	-1	-1	-6	0			
-6	-2	-1	3	2	2	0	-1	2	-1
0	1	2	2	-1	3	-1	-1	-1	
-4	-8	-8	-5	0	-3	-3	-2		
-3	-1	-11	-7	-4	-2	-5	-5	-2	-2
-3	-2	-2	-2	-5	-2	-2	-1		
-3	1	-2	-3	-1	-1				
PATTERN	-5	-2	-2	-4					
DEVIATION

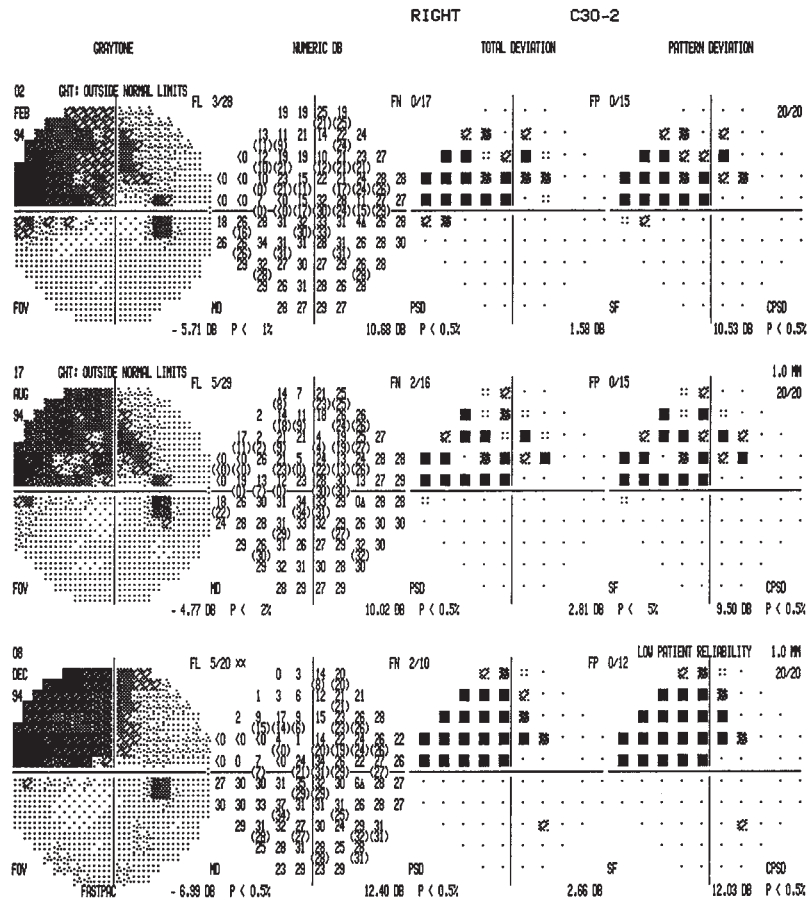
MD -2.29 DB
 PSD 3.88 DB P < 5%
 SF 1.68 DB
 CPSD 3.37 DB P < 2%

PROBABILITY SYMBOLS
 :: P < 5%
 ☼ P < 2%
 ☼☼ P < 1%
 ■ P < 0.5%

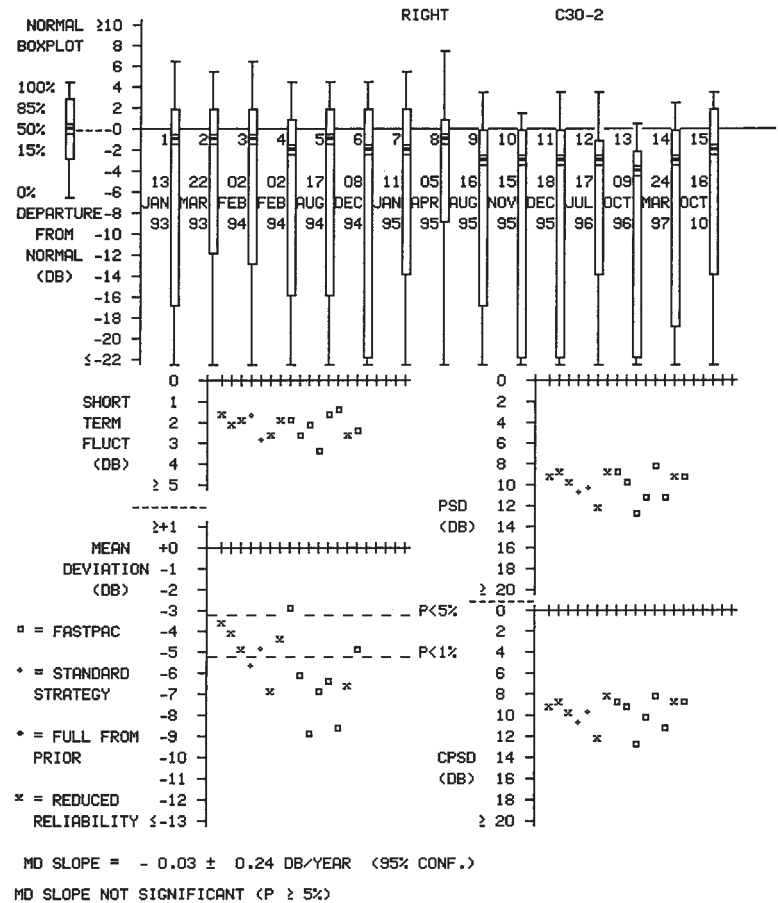
HISTORY AND EXAM

This 67-yr-old man was diagnosed with POAG at age 49. His mother had the same condition, with severe visual loss. His intraocular pressures were asymmetric early in the course of disease, being higher on the right, often in the low 20s (mmHg). He had been treated with timolol and pilocarpine eye drops for many years. His acuity throughout had

remained good, at 20/20 OU, with an RAPD OD. His optic discs showed pallor and cupping of the optic disc OD, with normal disc OS. Intraocular pressures on treatment have stabilized around 16 mmHg OU.



Overview



Change analysis

DISCUSSION

Field description: Superior arcuate defect with nasal step OD.

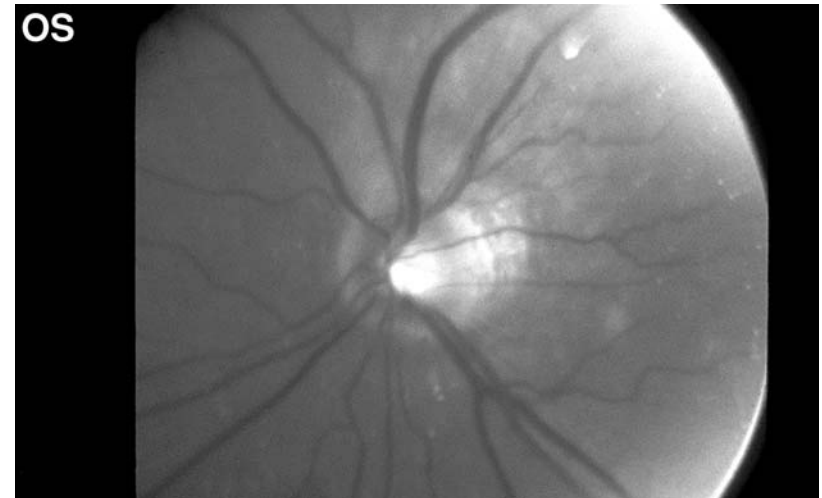
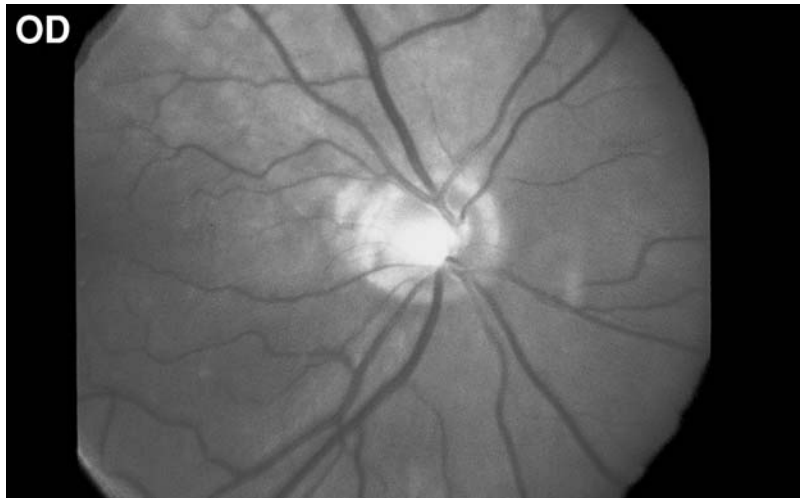
Localization: Optic nerve.

Pathology: Primary Open Angle Glaucoma (POAG).

The overview shows gradual progression of the severity of the superonasal defect, with worsening of thresholds within the depths of the defect. The first and second fields show one arcuate defect at about 10° eccentricity, within the Bjerrum area, as well as a more peripheral superonasal depression. These merge by the time of the third field. The change analysis is drawn from many fields over a longer time span. The linear regression of the mean deviation against time (MD SLOPE, at bottom) shows a declining slope of -0.03 dB/yr, which is not significant because of the scatter of the points and the reduced reliability of some data points. Despite this, inspection of the plot of MD against time does suggest a slow decline over this 8-year period, even though the patient's intraocular pressures have been reasonably controlled.

The visual field of his left eye has remained normal over this period. His optic discs show an asymmetry that corresponds with his visual fields. The left disc has a normal cup and a healthy rim, whereas the right eye has a larger cup with more disc pallor.

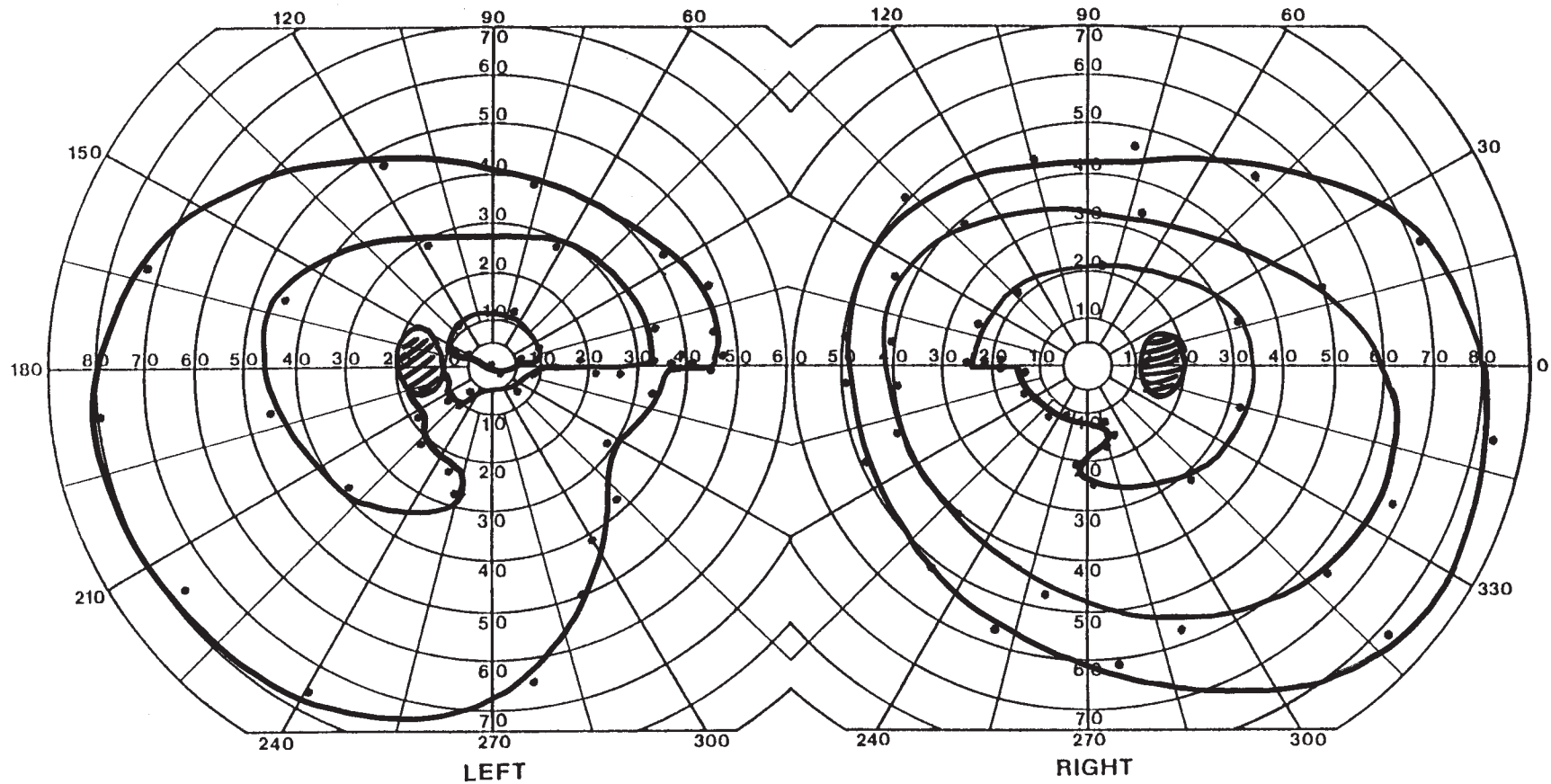
Intraocular pressure normally ranges from 10 to 22 mmHg. Glaucoma is often defined as a triad of elevated intraocular pressure, optic atrophy with cupping, and nerve fiber bundle defects in the visual field. Increased intraocular pressure alone is variably labeled "glaucoma suspect" or "ocular hypertension." Acute angle-closure glaucoma is a dramatic form attributable to impaired outflow of the aqueous humor through Schlemm's canal (24). It presents with high intraocular pressures, ocular inflammation, and corneal edema. POAG, which accounts for 70% of glaucoma (25), is more insidious. As many as 17% of patients with POAG never have high intraocular pressures, despite typical glaucomatous discs and field loss, suggesting that the definition should not include elevated intraocular pressure (25). The pathophysiology of "normal tension" POAG is unclear. The optic nerves of these patients may have a vulnerability, perhaps of a vascular nature, that makes normal ranges of intraocular pressure damaging.



HISTORY AND EXAM

This 69-yr-old African-American man noted poor vision in his peripheral field for about a year, which had not progressed much. He was unsure of the tempo of onset. Visual acuity was 20/20 OU, Ishihara color scores were 12/14 OD and 7/14 OS, and there was

an RAPD OS. Optic discs showed significant cupping OU, with mild superior disc pallor OS. Intraocular pressures were monitored and found to be consistently elevated, in the range of 24–26 mmHg. Other investigations for optic neuropathy were negative.



DISCUSSION

Field description: Bilateral inferior arcuate defects.

Localization: Bilateral optic nerve.

Pathology: Primary Open Angle Glaucoma (POAG).

Confrontation testing showed an inferonasal step defect OS to red targets and finger counting.

The patient has bilateral arcuate defects, more extensive OS, where the defect marches from the blind spot to the nasal meridian. Glaucoma is among the most common causes of bilateral arcuate defects. However, many other bilateral optic neuropathies could cause similar loss, particularly ischemic or inflammatory conditions (but not toxic/metabolic ones, which cause central scotomata almost exclusively). Without clearer information about the onset, it is difficult to definitively exclude these.

Automated perimetry has assumed the dominant role in the evaluation of glaucomatous visual field defects. Nevertheless, in up to 25% of patients with glaucoma, Goldmann

perimetry of the more peripheral field can show defects when automated assessments of the central 24° are normal or equivocal (26). Generalized constriction, a nasal step, or a temporal sector (wedge) defect are the most frequent findings. General constriction may be an early finding, but it is hard to differentiate from other nonspecific causes of constriction. A more focal constriction of nasal isopters is helpful, even if no nasal step is evident. This may represent equivalent damage to both upper and lower arcuate fibers, whereas a step defect always means more severe damage to one arcuate bundle or the other. One last interesting defect is the “hemianopic offset,” a peripheral wedge in the nasal field adjacent to the vertical meridian. This can be confused with a retrochiasmal hemifield defect, except that it is seldom bilateral or homonymous.

The three major risk factors for POAG are age over 70, being African American, and elevated intraocular pressures. Several genetic loci have also been identified recently for POAG (24).

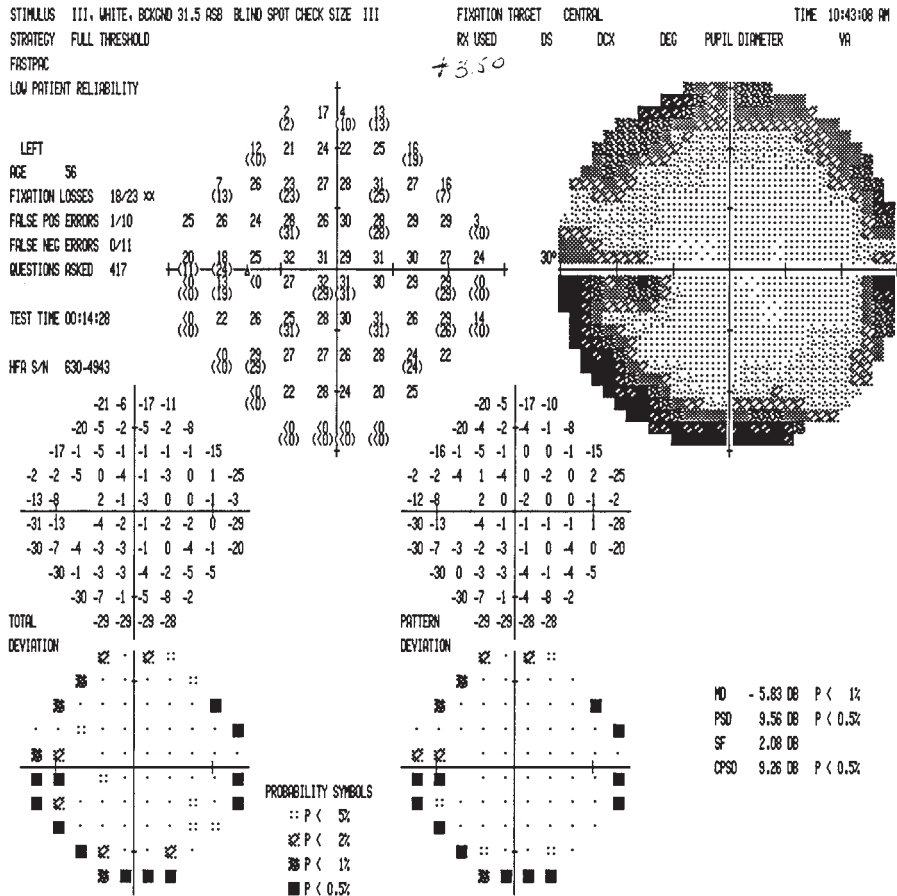
HISTORY AND EXAM

This 56-yr-old woman presented with a painful right IV nerve palsy. Two months later she developed a fluctuating partial right III nerve palsy with tingling in the right forehead and vertex. Over the next month her right lid swelled and the eye reddened. Acuity was 20/25 OD and 20/15 OS. Ishihara color scores were 11/14 OU and there was no RAPD.

Optic discs were normal. There was a mild anisocoria, with the right pupil larger in light, and periorbital and lid swelling OD. There was 4-mm proptosis OD, and scleral and conjunctival vessels were dilated. There were partial right III and VI nerve palsies.

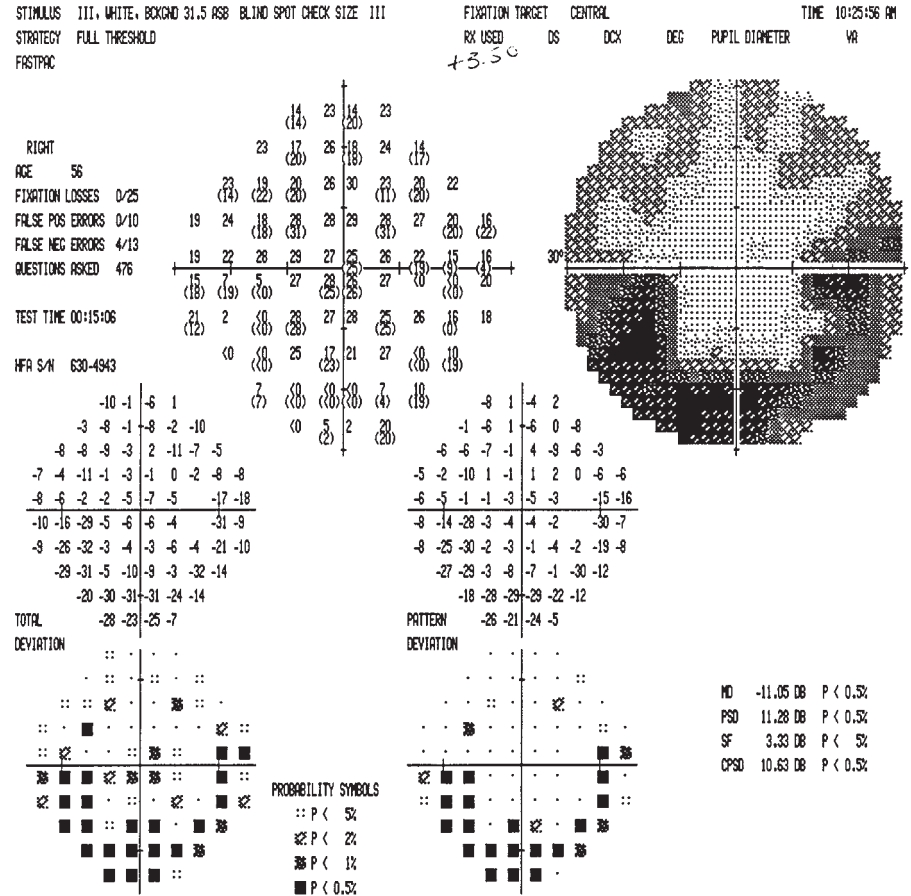
CENTRAL 30 - 2 THRESHOLD TEST

DATE 05-10-00



CENTRAL 30 - 2 THRESHOLD TEST

DATE 05-10-00



DISCUSSION

Field description: Inferior arcuate defect with nasal step OD, mild rim depression OS (possibly lens holder artifact).

Localization: Nerve fiber layer, optic disc.

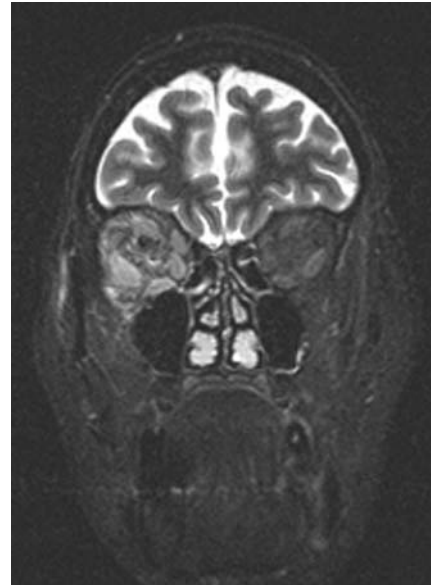
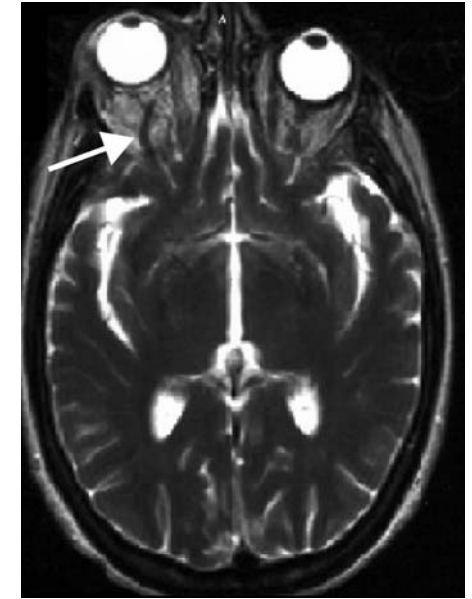
Pathology: Secondary glaucoma; spontaneous (low-flow) carotid-cavernous fistula.

Confrontation fields were full OU.

Note the difference in the peripheral defects in the two eyes. On the right, the arcuate defect emerges from the blind spot and stops sharply at the nasal horizontal meridian. On the left, the rim artifact runs temporal to the blind spot and stays at the outermost points, slightly petering out inferonasally.

The patient had signs involving multiple ocular motor nerves, which led some clinicians to consider myasthenia gravis. However, this was excluded once trigeminal tingling, proptosis, periorbital swelling, and red eye were apparent. Magnetic resonance angiography (MRA) confirmed a dural carotid-cavernous fistula: MRA source films (top left) show bright signal in the right cavernous sinus, indicating arterial flow in this venous structure (arrow). The axial T2-weighted MRI (top right) shows a dilated superior ophthalmic vein on the right (arrow), and coronal views show the edematous extraocular muscles OD (bottom left). Formal angiogram (bottom right) also shows the arterial blood in the cavernous sinus and superior ophthalmic vein, on this lateral view (arrow). The patient had coil placement with resolution of her field defect and all signs apart from a mild right VI nerve palsy.

Arterial shunting into the cavernous sinus increases the venous pressure in the superior ophthalmic vein, which drains into the sinus. Besides congesting the superficial veins of the eye, this increases intraocular pressure, causing secondary glaucoma. Her pressures were 31 mmHg OD and 15 mmHg OS, and she was treated with topical timolol. Control of glaucoma can be difficult if the fistula does not close spontaneously or with treatment.



DISCUSSION

Field description: Cecocentral scotoma OD.

Localization: Retrobulbar optic nerve.

Pathology: Retrobulbar optic neuritis, demyelinating.

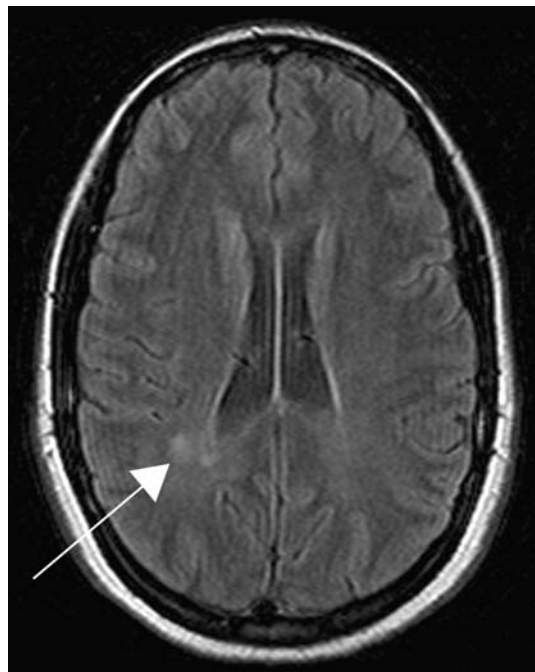
Confrontation fields showed a blurry region just temporal to fixation, when viewing the examiner's face. On Amsler grid there was a fading of lines in the same region.

Central defects have traditionally been considered the classic field defect of optic neuritis (27). If the abnormal central area is large enough to merge with the normal blind spot, this is termed a *cecocentral scotoma*. If not, it is just a central scotoma. Because central vision is so heavily used in daily life, virtually all patients notice their loss. Testing almost always shows reduced acuity and/or color vision. Sometimes with very subtle loss, or more frequently as a residue of earlier optic neuritis, there might be a central scotoma with normal acuity. In such cases, contrast sensitivity testing may reveal impaired vision for faint gray stimuli on white backgrounds (i.e., low contrast), compared to the typical Snellen letters, which are black symbols on white backgrounds (i.e., high contrast) (28).

Why might central vision be vulnerable to optic neuritis? Some argue that it is simply

the odds. Since so many retinal ganglion axons are devoted to central vision, even a random pattern of pathologic hits would tend to create a large proportion of central defects. Others claim that the papillomacular bundle (see Chapter 2) that serves the cecocentral zone has some special, still undefined Achilles heel to demyelination. Yet others suggest that since there are so many parvocellular (P-cells, see Chapter 2) retinal ganglion cells in central vision, where color vision and spatial acuity are at their peak, optic neuritis might be a P-cell disease (29). However, while this issue was being debated, it became clear that small, isolated central scotomata actually comprise only about 15% of the focal field patterns in optic neuritis (30,31). Perhaps the “random hit” answer is the correct one after all.

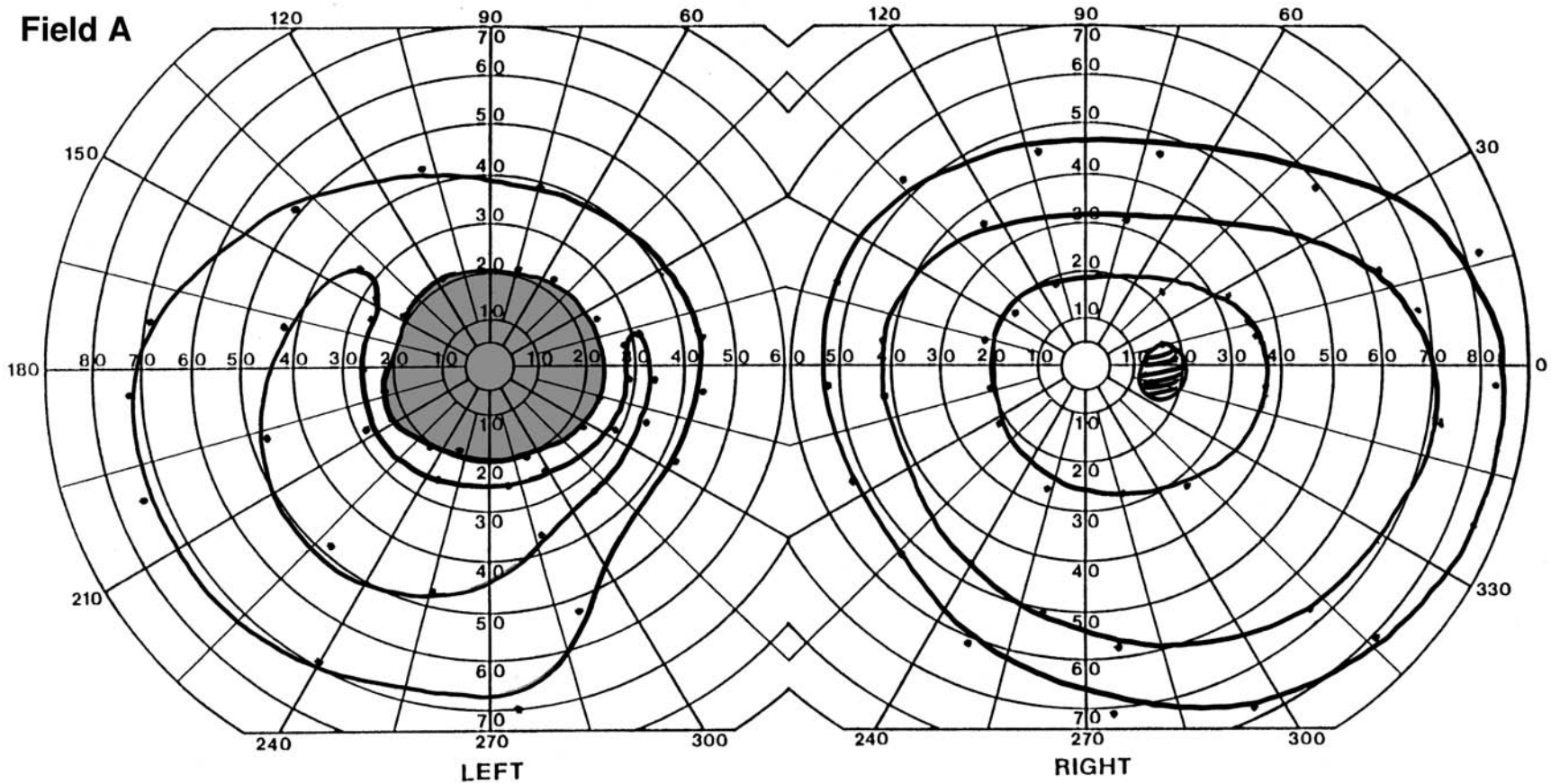
This patient's vision returned to normal 2 months later. Her normal MRI and negative neurologic examination and earlier history place her in a low-risk group for developing future attacks of multiple sclerosis (MS) over the next 5 years (see Case 22). However, she developed leg numbness and bladder incontinence 1 year later, with white matter lesions on MRI of her cervical cord and brain (axial FLAIR image shown, see arrow). She started β -interferon treatment at this point.



HISTORY AND EXAM

This 26-yr-old woman noticed a small white area in the center of vision of the left eye, which grew over 5–6 day into a dense “faded” central region, with frontal headache and pain with eye movements. Visual acuity was 20/20 OD and count fingers at 4' OS. There was a large RAPD OS, but fundoscopy was normal OU. The remainder of the neurologic examination was normal. The initial visual field is shown in field A. Over the next month

her vision improved to 20/25 OS. About 6 months later, however, she returned with blurred vision OS, imbalance, and vertical diplopia. Visual acuity was 20/30 OD and 20/60 OS, with Ishihara color scores of 14/14 OD and 7/14 OS. She had an RAPD OS and normal optic discs. She had a skew deviation and mild gait ataxia. Visual fields from this next visit are shown in field B (next page).



DISCUSSION

Field description: (A) Large cecocentral scotoma OS; (B) inferior arcuate defect OD and superior paracentral scotoma OS.

Localization: Retrobulbar optic nerve.

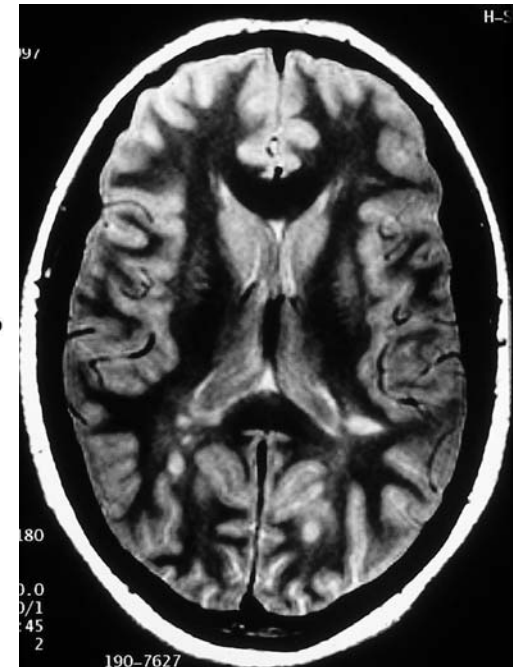
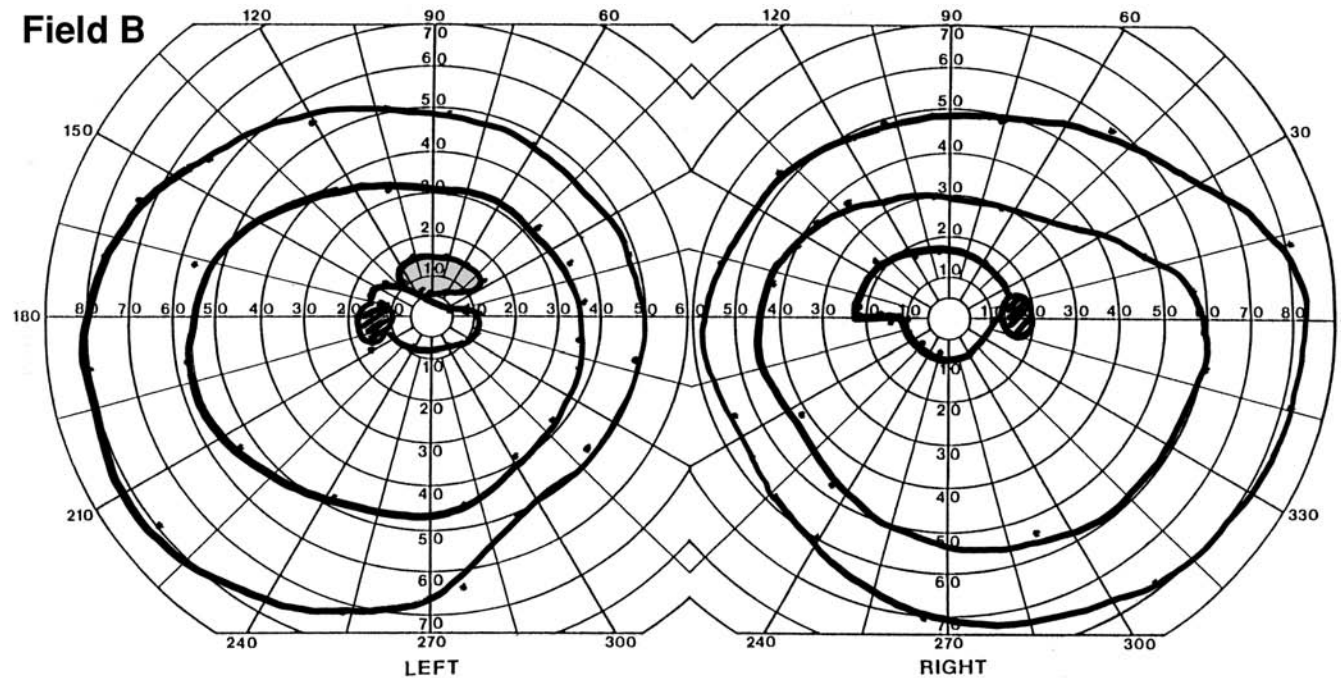
Pathology: Retrobulbar optic neuritis.

Confrontation testing with hand motions easily showed the large central defect at first examination.

In field A, there is a large hole OD in which the patient cannot see even the largest V4e target. This defect also eliminates most vision for the I4e target superiorly, so that it is mainly seen inferiorly, because vision is normally more sensitive eccentrically in the inferior field. In field B, there are more subtle bilateral defects that conform to nerve fiber defects around the central zone.

The patient's initial presentation is a more severe version of Case 21, with a larger cen-

tral defect yet still normal-appearing disc. Isolated retrobulbar optic neuritis without antecedent neurologic history is the scenario, proven by the anticipated recovery of vision a few weeks later. The key question in this setting is, What is her risk of MS? The single most informative prognostic tool during an attack is MRI of the brain (not the orbit, since we already know that she has optic neuritis and numerous studies have shown that imaging the orbit in typical cases is a waste of time). In the Optic Neuritis Treatment Trial (ONTT), the cumulative probability of a second demyelinate attack over the next 5 years increased from 16% in those with no white matter lesions to 51% in those with three or more lesions of 3 mm or more in diameter (32). Unfortunately, her MRI showed numerous lesions, illustrated on a T2 axial slice, and within 6 months she had the second attack mentioned, involving not just both eyes but also her brain stem and cerebellar pathways. (Of note, bilateral sequential optic neuritis, as she has, is itself a high risk factor for MS, in contrast to bilateral simultaneous optic neuritis, as in Case 30.)



HISTORY AND EXAM

This 44-yr-old woman had 1 week of blurred vision nasally in the left eye, which worsened slightly 6 days after onset, when there was also some pain with eye movement.

Acuity was 20/20 OU, and Ishihara color scores were 14/14 OU. There was an RAPD OS. There was also mild disc edema OS.

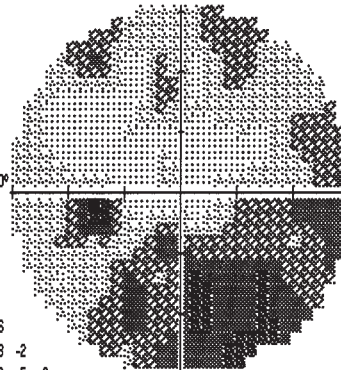
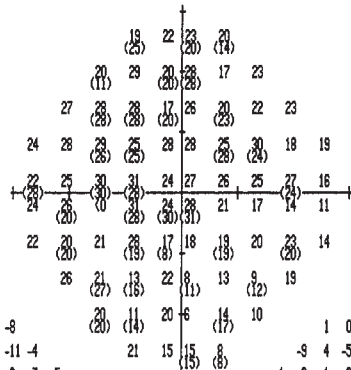
CENTRAL 30 - 2 THRESHOLD TEST

DATE 04-26-99

STIMULUS III, WHITE, BCKGND 31.5 ASB BLIND SPOT CHECK SIZE III
 STRATEGY FULL THRESHOLD
 FASTPAC

FIXATION TARGET CENTRAL
 RX USED +2 DS DCX DEG
 PUPIL DIAMETER 3.0 MM VA 20/20

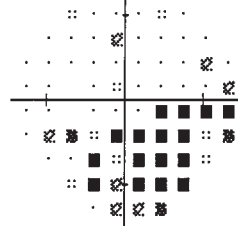
LEFT
 AGE 44
 FIXATION LOSSES 1/20
 FALSE POS ERRORS 1/8
 FALSE NEG ERRORS 1/10
 QUESTIONS ASKED 347



TEST TIME 00:11:15
 HFA S/N

-2	-2	-4	-8
-11	2	-7	0
-1	-1	-1	-11
-4	-1	-2	-5
-4	-5	-2	-8
-6	-7	-2	-6
-7	-10	-10	-8
-4	-7	-17	-9
-9	-18	-10	-14
-7	-13	-13	-19

PATTERN DEVIATION



MD -0.96 DB P < 0.5%
 PSD 6.38 DB P < 1%
 SF 3.03 DB P < 10%
 CPSD 5.38 DB P < 1%

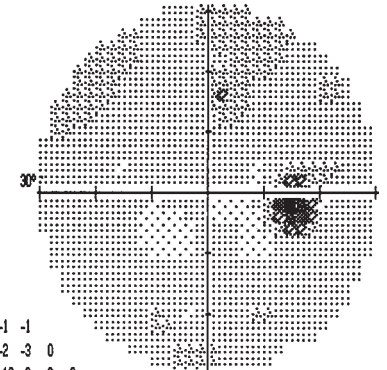
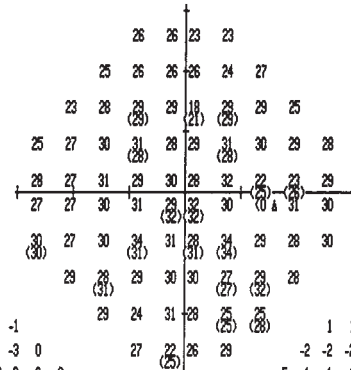
PROBABILITY SYMBOLS
 :: P < 5%
 ☒ P < 2%
 ☐ P < 1%
 ■ P < 0.5%

DATE 04-26-99

STIMULUS III, WHITE, BCKGND 31.5 ASB BLIND SPOT CHECK SIZE III
 STRATEGY FULL THRESHOLD
 FASTPAC

FIXATION TARGET CENTRAL
 RX USED +2 DS DCX DEG
 PUPIL DIAMETER 3.0 MM VA 20/20

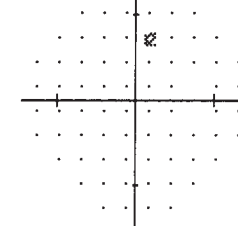
RIGHT
 AGE 44
 FIXATION LOSSES 0/17
 FALSE POS ERRORS 0/10
 FALSE NEG ERRORS 0/9
 QUESTIONS ASKED 287



TEST TIME 00:08:47
 HFA S/N

1	1	-1	-1
-2	-2	-2	-1
-5	-1	-1	-1
-2	-2	0	-2
0	-2	0	-3
-1	-3	-2	-2
3	-2	-1	0
1	0	-2	-1
1	-5	1	-2
0	-4	-2	1

PATTERN DEVIATION



MD -1.41 DB
 PSD 2.06 DB
 SF 1.65 DB
 CPSD 0.87 DB

PROBABILITY SYMBOLS
 :: P < 5%
 ☒ P < 2%
 ☐ P < 1%
 ■ P < 0.5%

DISCUSSION

Field description: Inferior arcuate defect OS.

Localization: Anterior optic nerve.

Pathology: Papillitis OS.

Confrontation fields showed an inferonasal step to color and hand comparison.

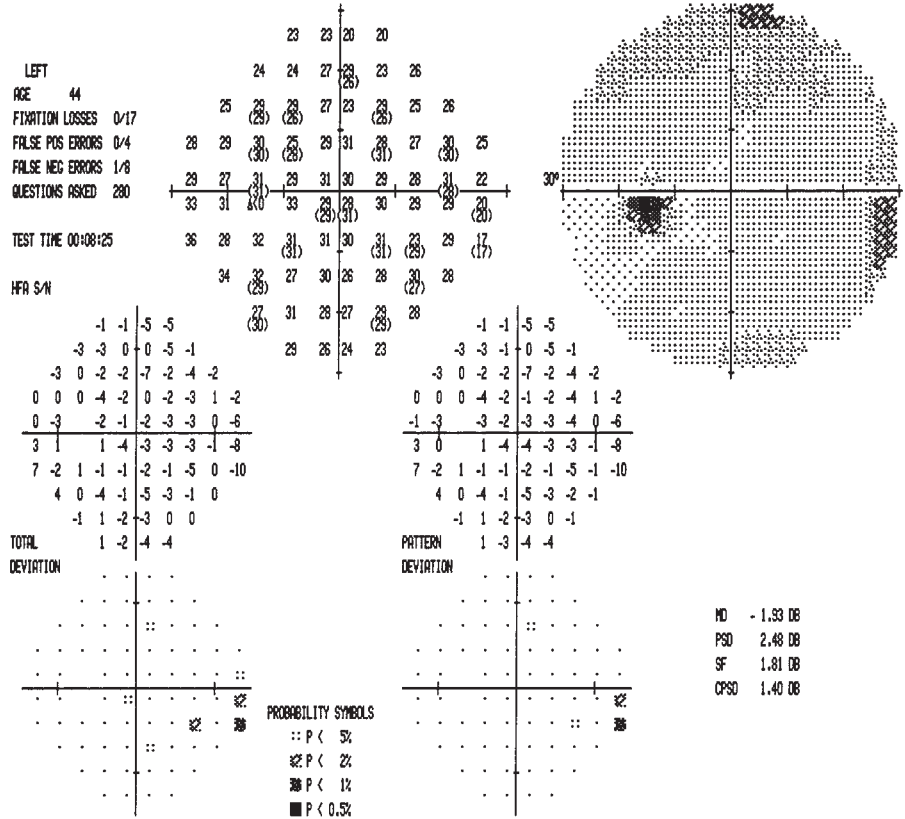
Perimetry shows a wide and dense arching defect that marches out of the blind spot and curves to end at the nasal horizontal meridian. These are the essential features of a complete arcuate defect. While there are a few scattered points of reduced sensitivity in the superior field on the total deviation plots, these drop out on the pattern deviation plot, and inspection of the sensitivity decibel numbers shows a marked drop from the top to the bottom nasal field, from the mid-twenties to mid-teens.

After presentation the patient also noted tingling and numbness in her right leg, which resolved. Her visual defect disappeared over the next 3 weeks (repeat OS field shown this page).

Optic neuritis may affect the optic disc (anterior optic neuritis, or papillitis) or the portion of the optic nerve behind the disc (retrobulbar optic neuritis), in which case the optic disc appears normal in the acute phase of the illness. The retrobulbar form is more common, accounting for about two-thirds of cases (31). Papillitis rarely causes severe disc edema or hemorrhage, and such findings should raise alternative diagnoses, such as ischemia, venous occlusion, asymmetric papilledema, or disc infiltration. In patients without brain lesions on MRI, the risk of developing MS over the next 5 years is about 8% in patients with papillitis, about half the risk in those with retrobulbar optic neuritis (32).

CENTRAL 30 - 2 THRESHOLD TEST

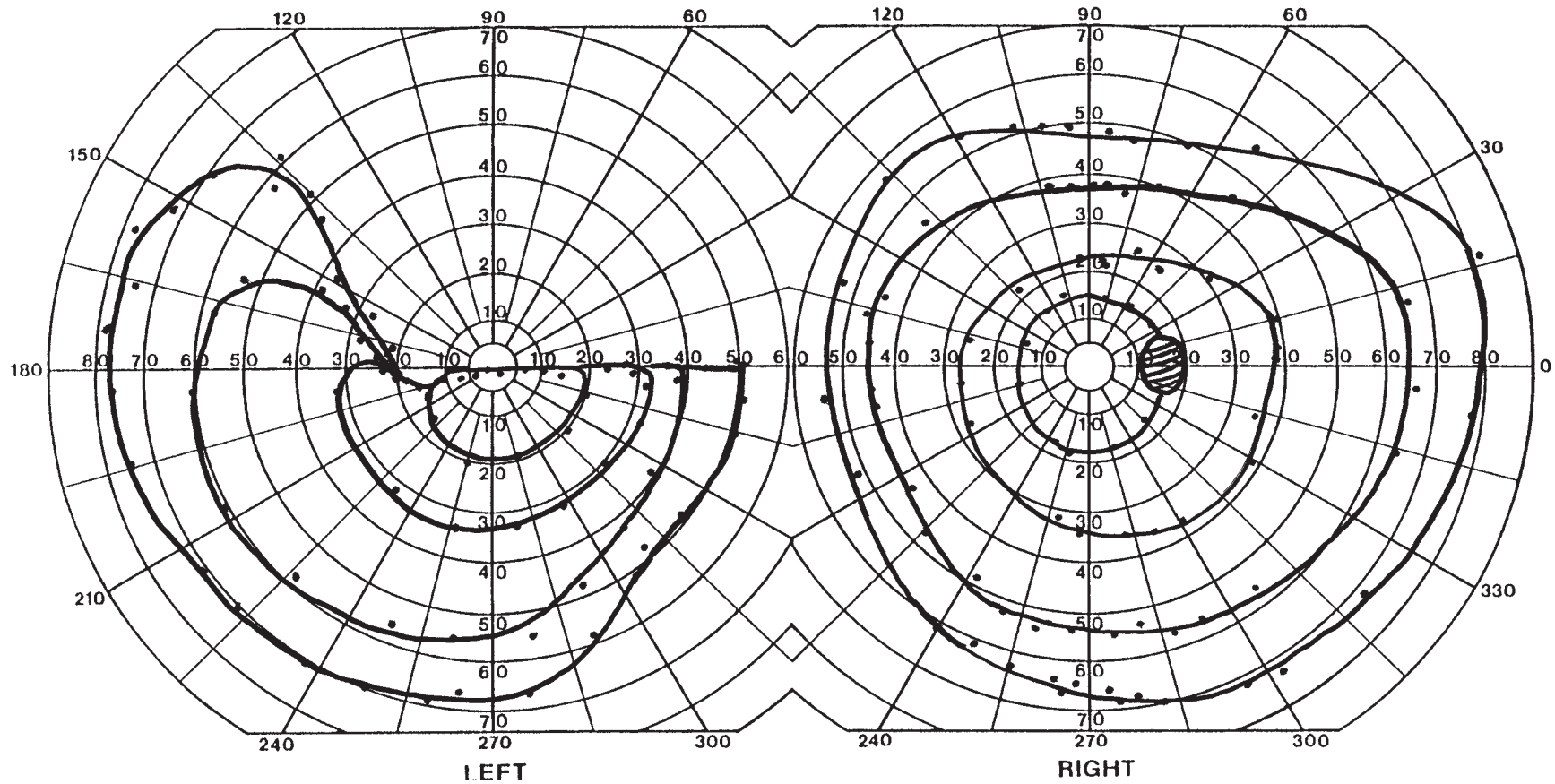
STIMULUS III, WHITE, BCKGND 31.5 ASB BLIND SPOT CHECK SIZE III
 STRATEGY FULL THRESHOLD
 FIXATION TARGET CENTRAL
 RX USED +2 DS DCX DEC
 DATE 05-14-99
 TIME 10:33:08 AM
 PUPIL DIAMETER 3.0 MM VA 20/20
 FASTPAC



HISTORY AND EXAM

This 44-yr-old woman noted decreased vision in the left eye during a cold. Over a few days she realized that she now could not see in the upper field of the left eye. She had no other symptoms. Visual acuity 23 days later was 20/20 OU, and Ishihara color scores

were 13/14 OD and 12/14 OS. There was a large RAPD OS but the optic discs were normal. The remainder of the neurologic examination was normal.



DISCUSSION

Field description: Incomplete superior altitudinal defect, bisecting the macula, OS.

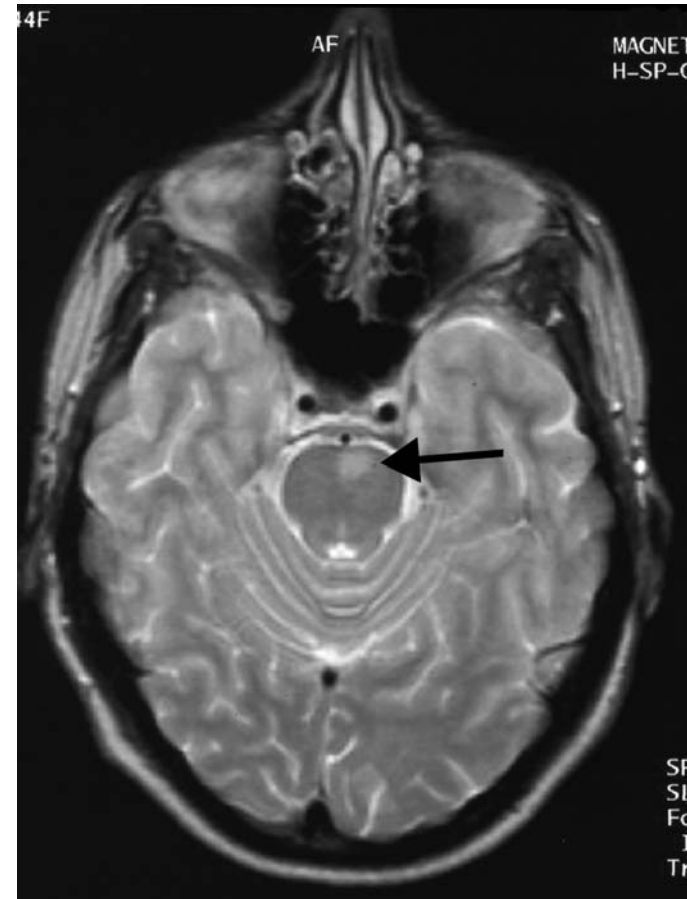
Localization: Retrobulbar optic nerve.

Pathology: Retrobulbar optic neuritis OS.

Confrontation testing with hand motion showed the same characteristics of the defect.

This is the field defect that would occur if an arcuate defect like that in Case 23 widened a bit more temporally to impair half the papillomacular bundle and a bit more nasally to impair the adjacent temporal field wedge. Altitudinal defects are supposed to be more characteristic of ischemic optic neuropathy (see Case 33). However, the patient's young age, lack of vascular risk factors such as diabetes or hypertension, and progression over a few days are unusual for ischemic cases. In addition, most ischemic optic neuropathies involve the disc (anterior ischemic optic neuropathy) and should cause disc edema that persists for at least 1–2 months. It is also clear now that, contrary to neurologic folklore, altitudinal defects make up 30% of focal defects on automated perimetry in optic neuritis, the single largest group (31). In fact, this is more than double the 15% figure for cecocentral and central defects combined.

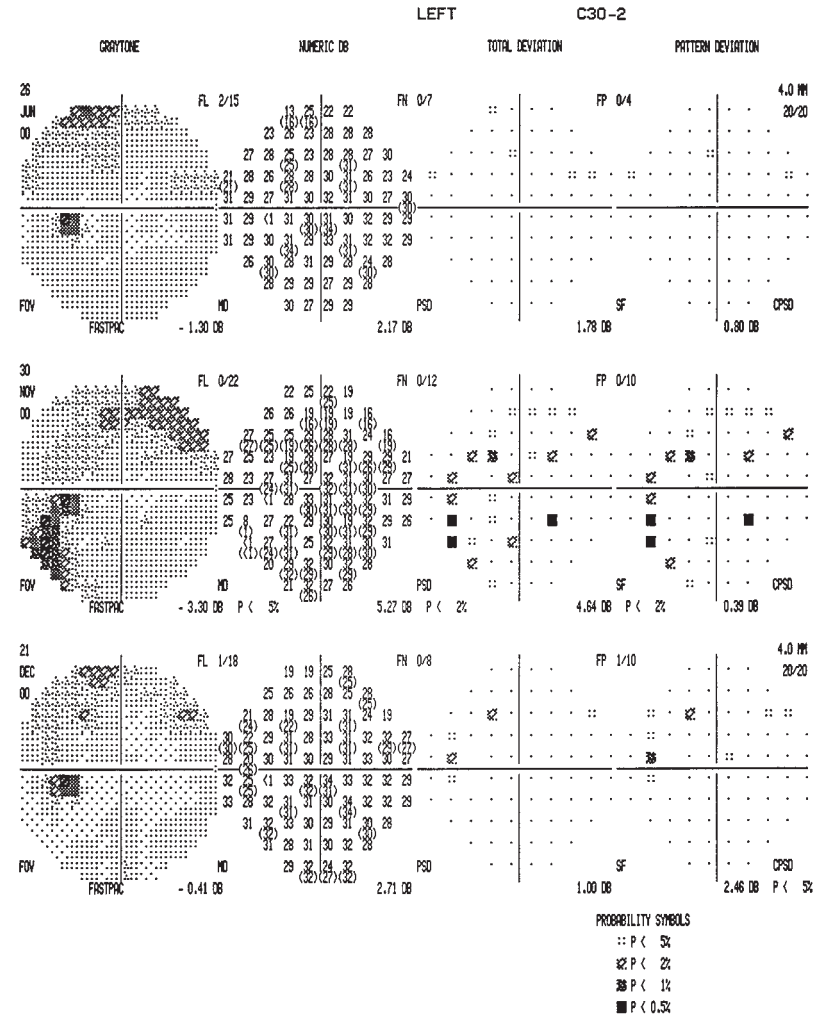
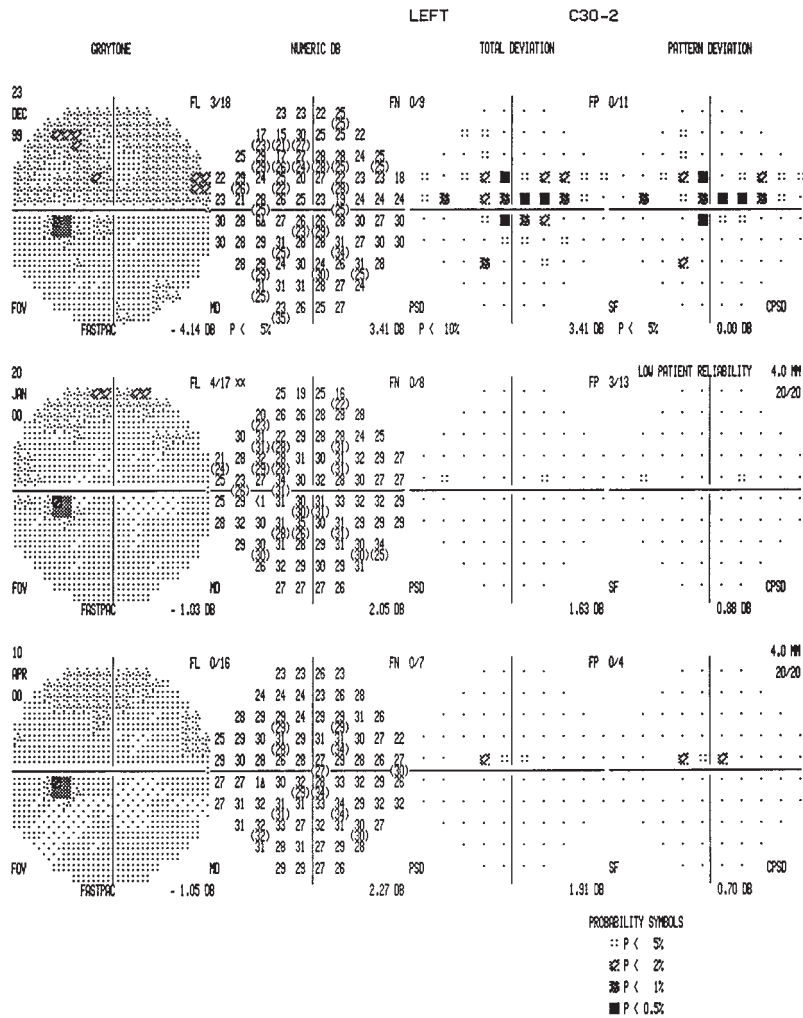
At follow-up the patient's defect had not improved 6 weeks after onset, atypical for optic neuritis, which generally begins to recover in the first month (33). The diagnosis should be questioned when there is progression or failure to improve over more than 1 month. She had an MRI of the orbit and sella, a spinal tap, and testing for vasculitis and Lyme disease. Her only finding was a positive anti-nuclear antibody (ANA), of unclear significance. Her brain MRI did show a hyperintense lesion in the pons (arrow), consistent with demyelination, shown in this T2-weighted axial image.



HISTORY AND EXAM

This 43-yr-old woman developed pain with eye movement and progressive visual loss in the left eye over 10 days, about 3 weeks after a flu-like illness with a facial rash. Initial examination showed visual acuity of 20/20 OD and 20/25 OS, Ishihara color scores of 14/14 OD and 5/14 OS, and an RAPD OS. Maculae and optic discs were normal. Her

condition resolved over one month, but she presented 11 months later with new “foggy vision” OS, without change in acuity or color vision OS on examination. An overview program is presented for this eye. (The right eye remained normal throughout her care.)



DISCUSSION

Field description: Initial cecentral scotoma with superior nasal step OS, with inferotemporal wedge defect 1 year later.

Localization: Retrobulbar optic nerve.

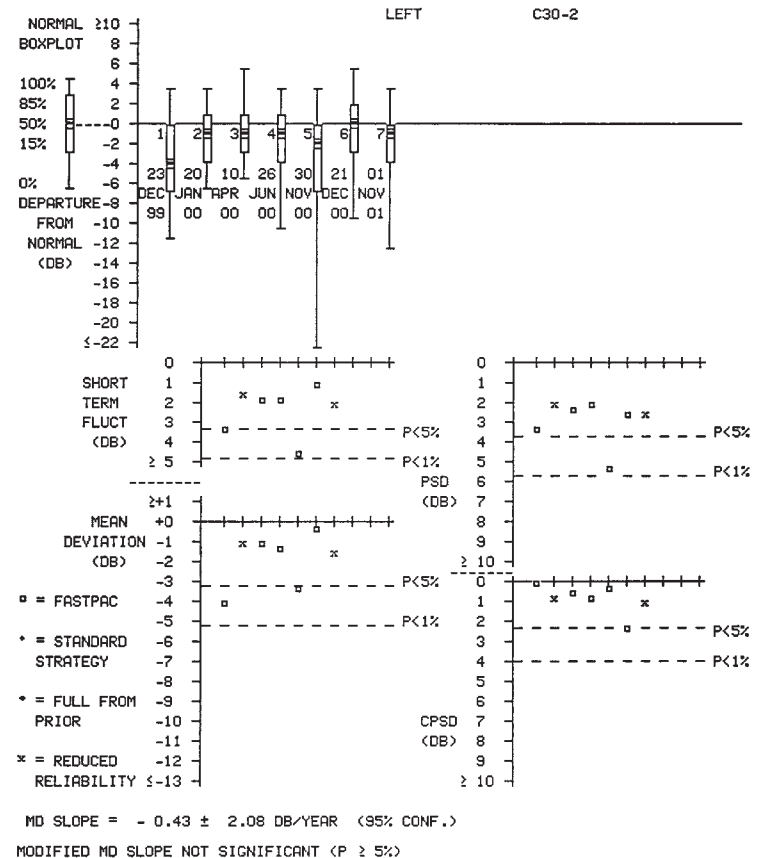
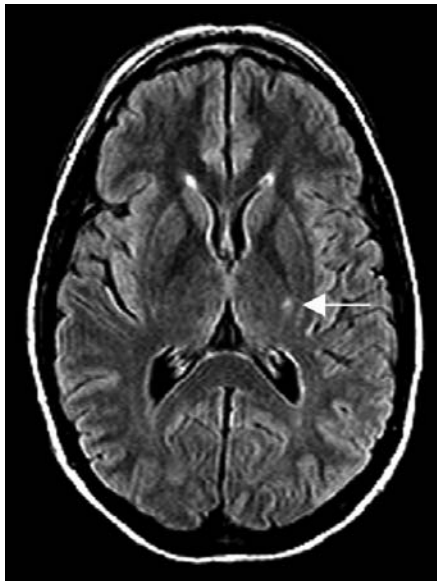
Pathology: Recurrent retrobulbar optic neuritis.

Confrontation testing with red targets at her first visit showed a superonasal step OS.

Note the change over serial perimetry results. The first episode combined a cecentral defect and a superior arcuate defect, manifest as the abnormal points on the deviation plots arrayed just above the nasal horizontal meridian. This represents a combination of damage to the papillomacular bundle and arcuate fibers in the inferior disc. The second episode is clearly different from the first and represents a new inflammatory episode. The change analysis (this page) shows worsening of short-term fluctuation and MD with each episode, seen as dips below the dashed line representing $p < 5\%$, meaning that there is a 95% probability that the field is abnormal. There is also a marked decline in pattern standard deviations (pattern standard deviation and corrected pattern standard deviation) with the second episode, indicating greater distortion of the hill of vision. This is consistent

with the patient's wedge defect, which was more focal than her first, more diffuse central and arcuate depression. Her reliability was excellent during the pathologic events.

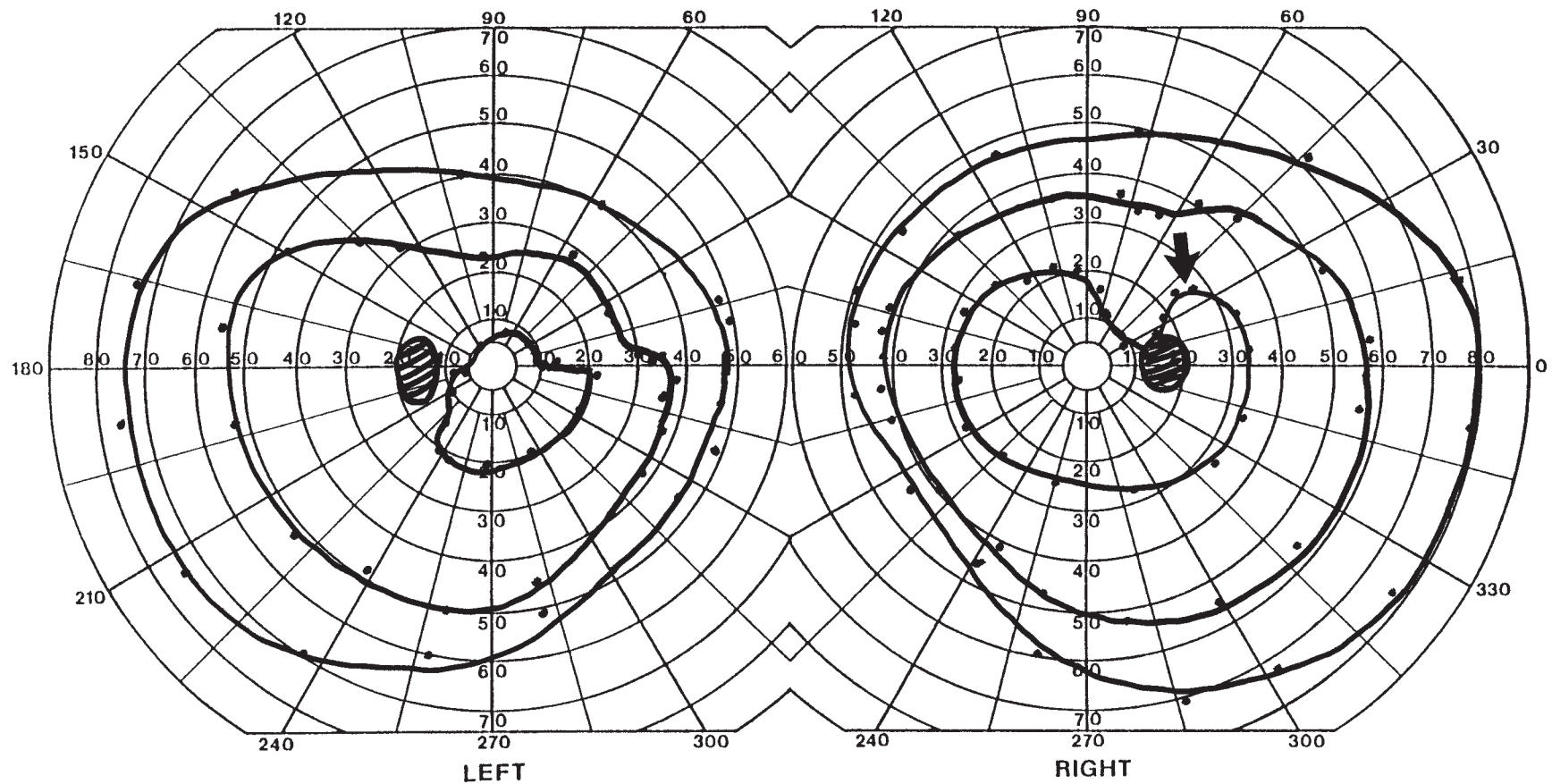
The patient's initial MRI showed two small white matter lesions, one shown on this FLAIR axial image (arrow), which did not change on repeated MRI 2 years later. The ONTT suggests that she has an intermediate risk of about 25% of another demyelinating event over the next 5 years (32). However, her story included a recurrent facial rash and a positive ANA, though she never developed other evidence of connective tissue disease. While the ONTT found little value in testing for vasculitis, syphilis, and sarcoidosis in typical optic neuritis (31), unusual features such as rash, uveitis, or arthritis do require more investigation. In this patient, the second episode of optic neuritis increased the suspicion of MS instead, and, indeed, 1 month later she returned with a right internuclear ophthalmoplegia. β -Interferon treatment was recommended.



HISTORY AND EXAM

This 56-yr-old man had relapsing-remitting MS for 19 years. His only visual episode was a few months of monocular blurry vision 18 years earlier, but he could not recall which eye had been affected. Visual acuity was 20/30 OD and 20/25 OS, and Ishihara

color scores were 13/14 OU. There was no RAPD. He had mild temporal optic disc pallor OD and a normal optic disc OS. He also had spastic quadriparesis and an ataxic left arm.



DISCUSSION

Field description: Superior temporal wedge defect OD, superior arcuate defect with enlarged blind spot OS.

Localization: Retrobulbar optic nerves, bilateral.

Pathology: Retrobulbar optic neuropathy OU.

Confrontation testing found some red desaturation in both inferonasal fields.

Both of the patient's defects are subtle and led to confusing results on confrontation testing (perhaps the darker color in the upper field was the abnormality!). The arcuate defect OS is confirmed by its presence on two isopters. The temporal wedge defect OD differs from physiologic baring of the blind spot by the prominent temporal shoulder (arrow), which clearly defines the narrow path of the defect. In addition, this eye has optic atrophy. Not surprisingly, these peripheral defects of demyelinating optic neuropathy spare central acuity and color vision and, like the defects in early glaucoma, can be hard to find on confrontation testing. Such asymptomatic defects are not uncommon in patients with MS (34) and represent a mild chronic optic neuropathy. When slowly progressive, or asymptomatic and therefore not readily dated, as in this patient, one must also consider the possibility of compressive or other optic neuropathies. Having MS does not immunize one against the other vagaries of life.

HISTORY AND EXAM

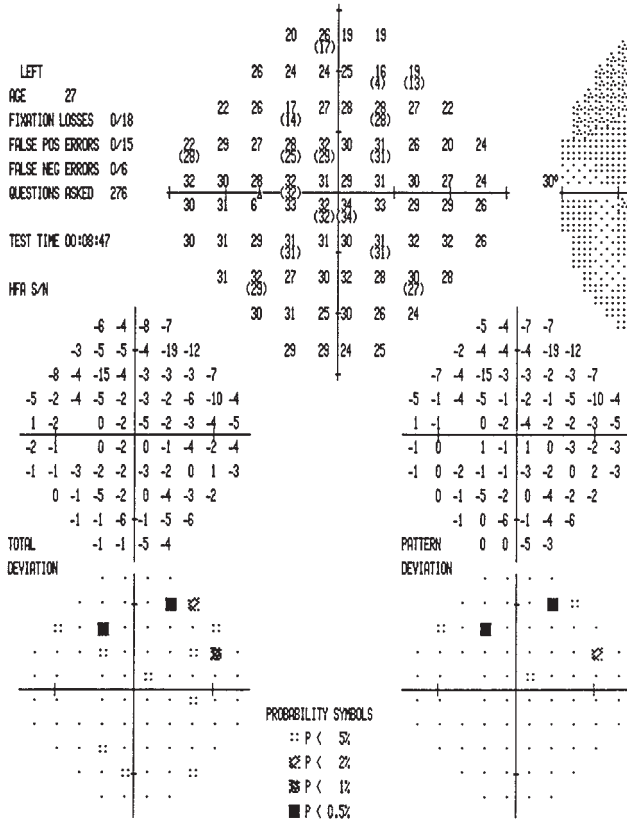
Seven months earlier, this 27-yr-old woman had vertigo, imbalance, and blurred vision OD that recovered with iv methylprednisolone after 3 weeks. Two months later, she had visual blurring OS, was treated with steroids again, with recovery after 1 week. A spinal tap showed oligoclonal bands and MRI showed multiple periventricular white matter lesions. She then presented with 5 days of blurred vision OD along with new tingling in

the left arm and leg, clumsiness of the left hand, and imbalance. With this attack, her acuity was 20/60 OD and 20/20 OS. Ishihara color scores were 12/14 OD and 13/14 OS, but slower OD. There was an RAPD OD and new mild blurring of the optic disc margin OD. She had mild pyramidal weakness in the right arm.

CENTRAL 30 - 2 THRESHOLD TEST

STIMULUS III, WHITE, BCKGND 31.5 ASB BLIND SPOT CHECK SIZE III
 STRATEGY FULL THRESHOLD
 FASTPAC

DATE 10-22-98
 TIME 01:51:39 PM
 FIXATION TARGET CENTRAL
 RX USED ~~PHOSPHOS~~ DCX
 DEG PUPIL DIAMETER 3.0 MM VA 20/20



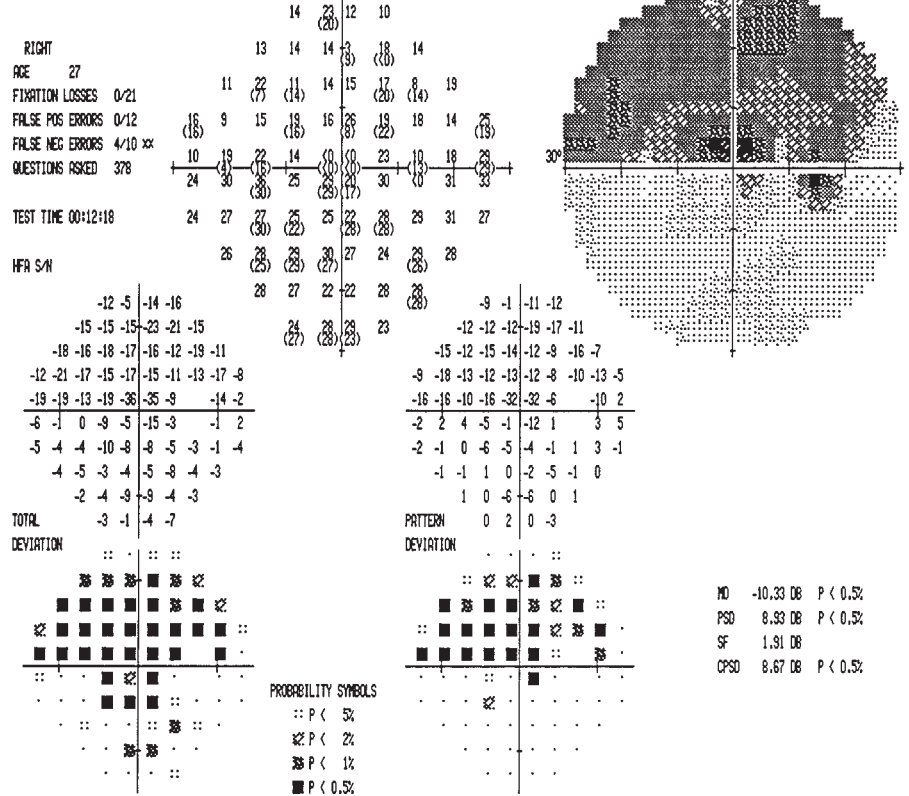
MD -3.00 DB P < 10%
 PSD 3.22 DB
 SF 1.34 DB
 CPSD 2.84 DB P < 5%

CENTRAL 30 - 2 THRESHOLD TEST

STIMULUS III, WHITE, BCKGND 31.5 ASB BLIND SPOT CHECK SIZE III
 STRATEGY FULL THRESHOLD
 FASTPAC

DATE 10-22-98
 TIME 01:41:34 PM
 FIXATION TARGET CENTRAL
 RX USED DS DCX
 DEG PUPIL DIAMETER 3.0 MM VA 20/60

LOW PATIENT RELIABILITY



MD -10.33 DB P < 0.5%
 PSD 8.33 DB P < 0.5%
 SF 1.31 DB
 CPSD 8.67 DB P < 0.5%

DISCUSSION

Field description: Central scotoma and incomplete superior altitudinal defect OD.

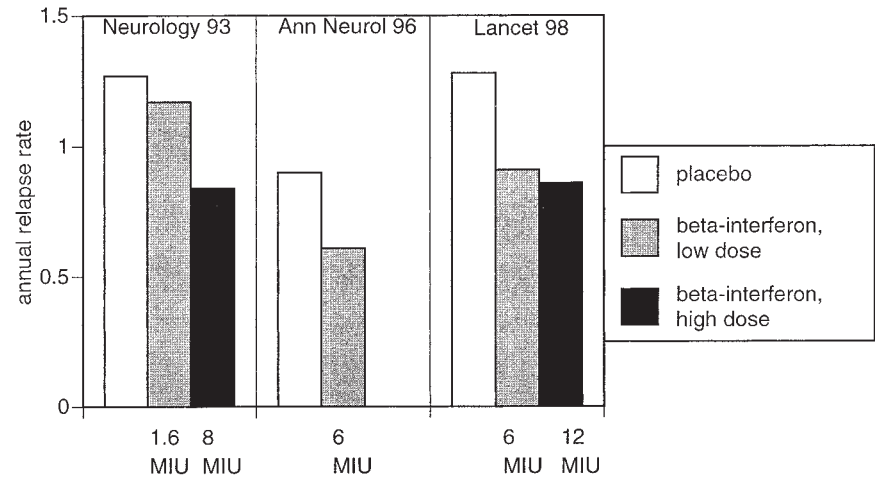
Localization: Anterior optic nerve.

Pathology: Optic neuritis/papillitis.

Confrontation testing showed a superior nasal step to red targets and abnormal hand and face comparison in the superior and temporal paracentral fields.

Perimetry shows almost complete reduction of sensitivity in the superior field, with the exception of a few points just temporal to the optic disc. This could be either a severe arcuate or an incomplete altitudinal defect. Clarification of this point would require examination of the visual field beyond 30°, best with a Goldmann field, but also possible with confrontation testing. The distinction is not necessarily that crucial. Both defects have been described with optic neuritis, and the boundary between the two is more quantitative than qualitative.

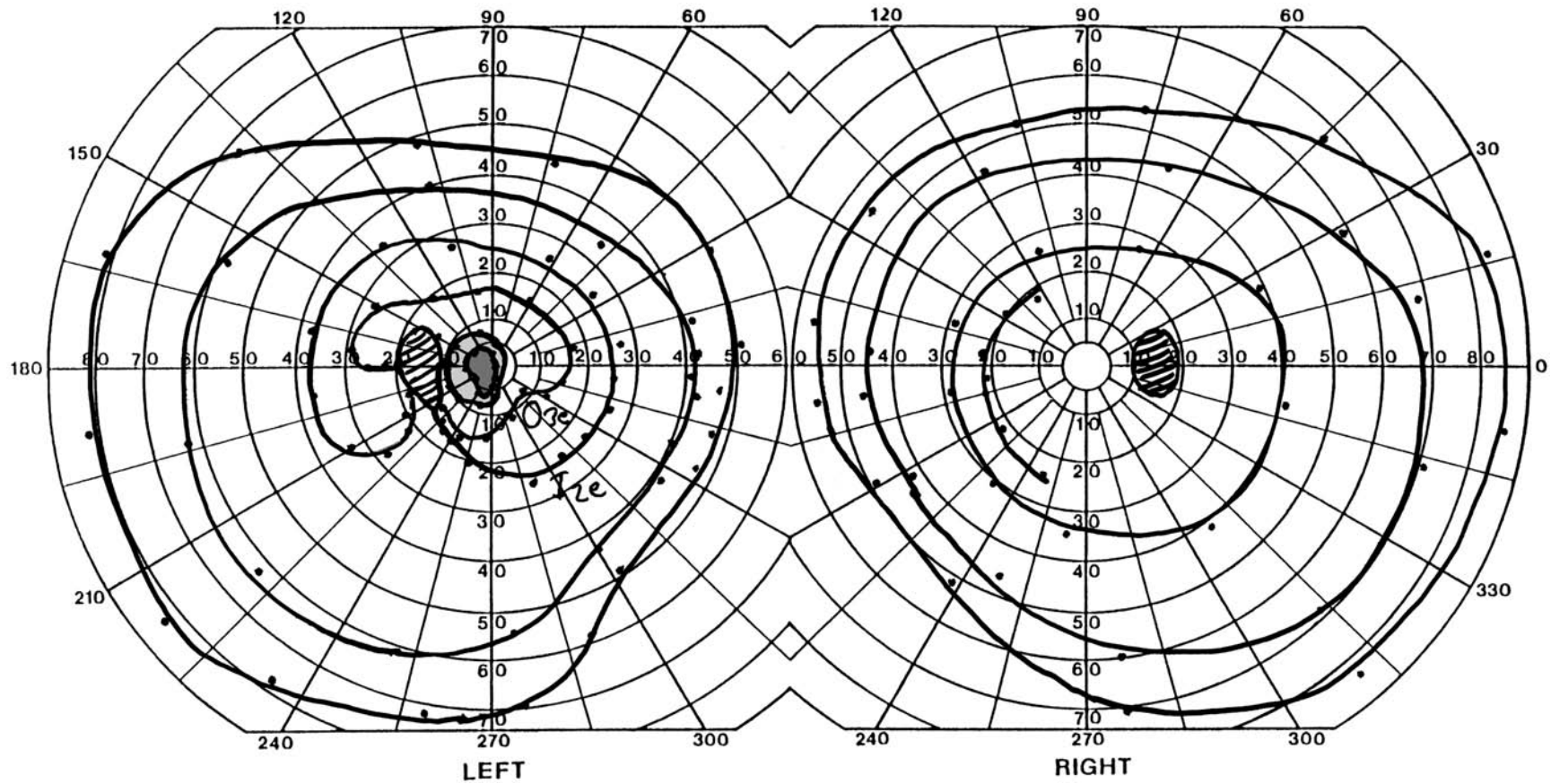
With her prior neurologic episodes and abnormal MRI, the patient meets the criteria for MS. Prospective placebo-controlled trials show that β -interferon reduces the annual relapse rate in MS by approximately 30% (35–37) (figure). There is also some evidence that it slows the rate of accumulation of physical disability. At 2 years, 34% of placebo-treated and 21% of β -interferon-treated patients had developed sustained progression of disability (36). β -Interferon also slows progression of disability in secondary progressive MS, but the effect is less impressive (38).



HISTORY AND EXAM

This 31-yr-old woman with MS for 5 years presented with 1 day of decreased central and inferior vision in the left eye. Visual acuity was 20/20 OD and 20/60 OS. Ishihara color scores were 12/14 OD and 5.5/14 OS. There was an RAPD OS but the optic discs

were normal. She had mild spasticity and hyperreflexia in the left arm and leg, and an action and postural tremor of both hands.



DISCUSSION

Field description: Central scotoma with subtle inferior wedge defect OS.

Localization: Retrobulbar optic nerve.

Pathology: Retrobulbar optic neuritis.

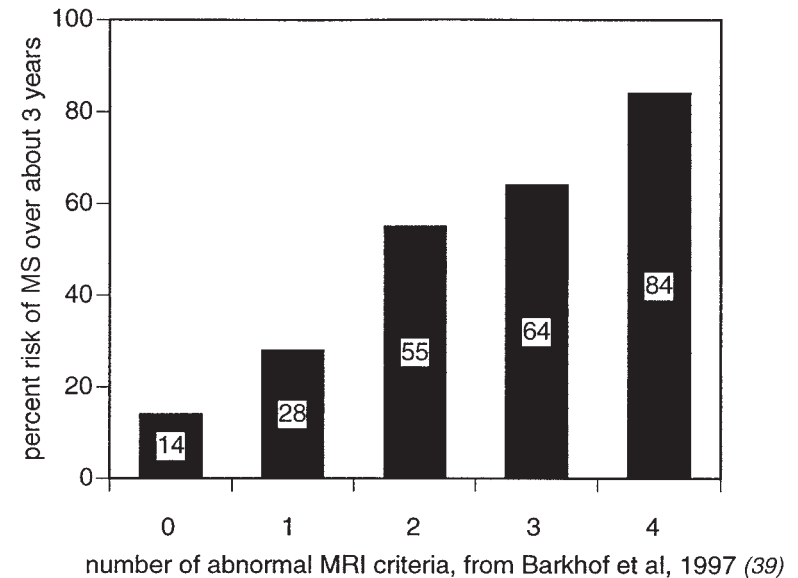
Confrontation testing showed an inferonasal step to a red target and a temporal decrease in the perifoveal field to face comparison.

The central hole in the patient's field is obvious. Inferior to the disc is a wedge defect. While this is fairly narrow with the I2e target, with the smaller 03e isopter it widens to approach the temporal horizontal meridian on one side and arches nearly to the nasal horizontal meridian on the other.



Sagittal FLAIR MRI demonstrated multiple areas of signal hyperintensity that appear to arise from the corpus callosum and extend out radially toward the cortical surface. These are areas of perivenular demyelination (known as Dawson fingers) and are one of the characteristic patterns of demyelination seen in MS.

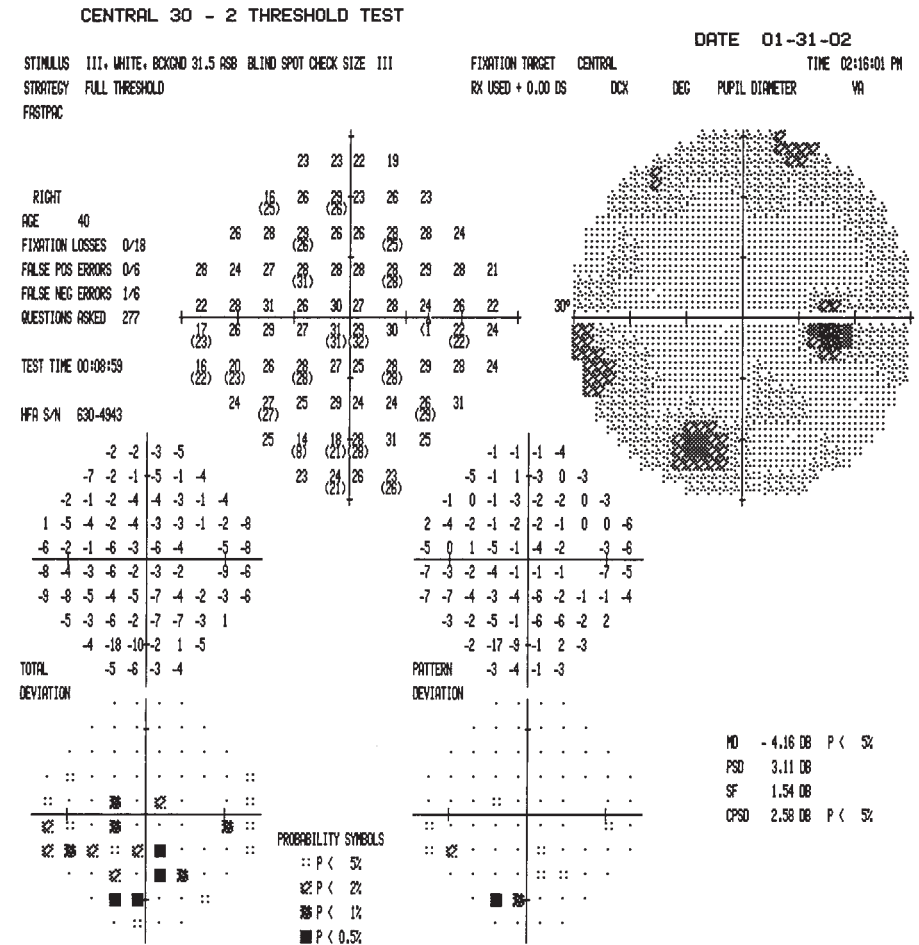
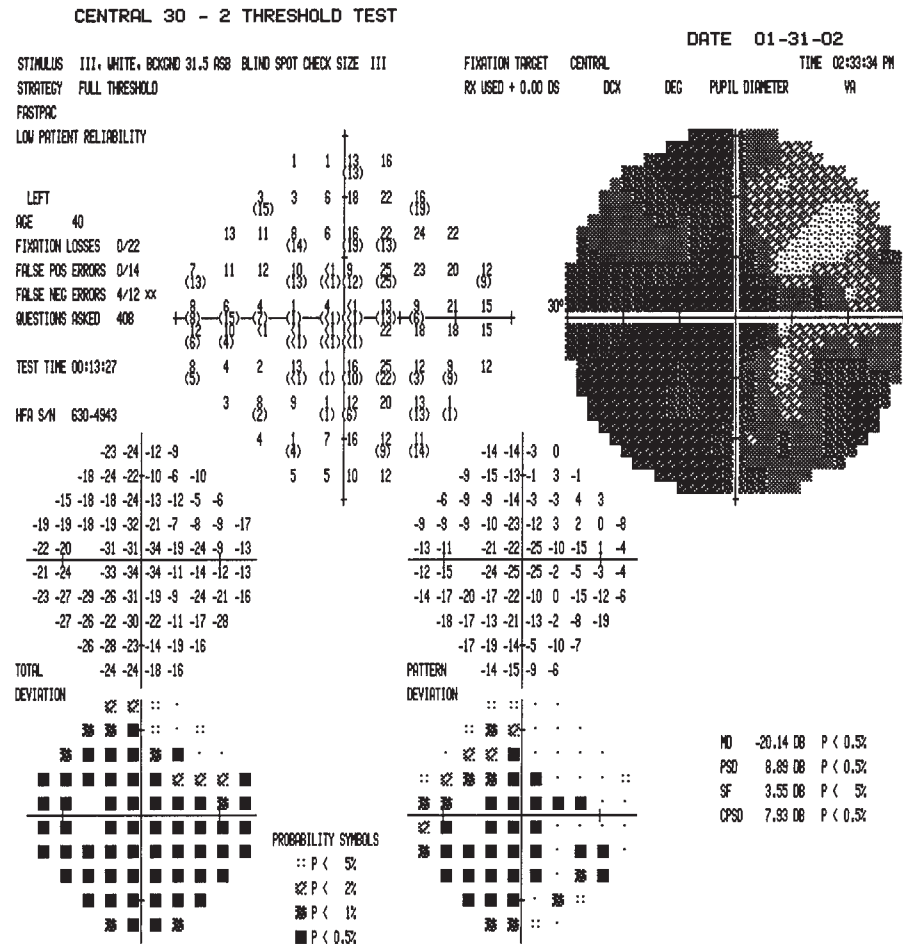
In someone who may be presenting with a first neurologic episode, the location as well as the number of MRI lesions may be helpful in predicting whether the individual will develop MS. One study (39) identified four critical features: gadolinium enhancement of one or more white matter lesions, location of white matter lesions adjacent to the cortical gray matter (i.e., "juxtacortical"), periventricular white matter lesions, and infratentorial lesions, in the brain stem or cerebellum. With no such lesions, the calculated risk of MS in a patient's median follow-up period of about 3 years was only 14%, and with all four criteria met, the risk was 84% (see graph).



HISTORY AND EXAM

This 38-yr-old man had 6 weeks of "decreased contrast" in vision OS, "like a bad photocopy," with fading of colors and darkening. The other eye was fine. Two years earlier he had been hospitalized with numbness progressing from his feet to his buttocks over a few days, which resolved almost completely over several weeks. A year earlier he had

similar temporary numbness of the right face. Acuity was 20/20 OD and 20/40 OS, with Ishihara color scores of 13/14 OD and 2/14 OS. There was a small RAPD OS. Fundi were normal OU. He had a comitant exotropia. The left hand had a mild pronator drift and clumsiness.



DISCUSSION

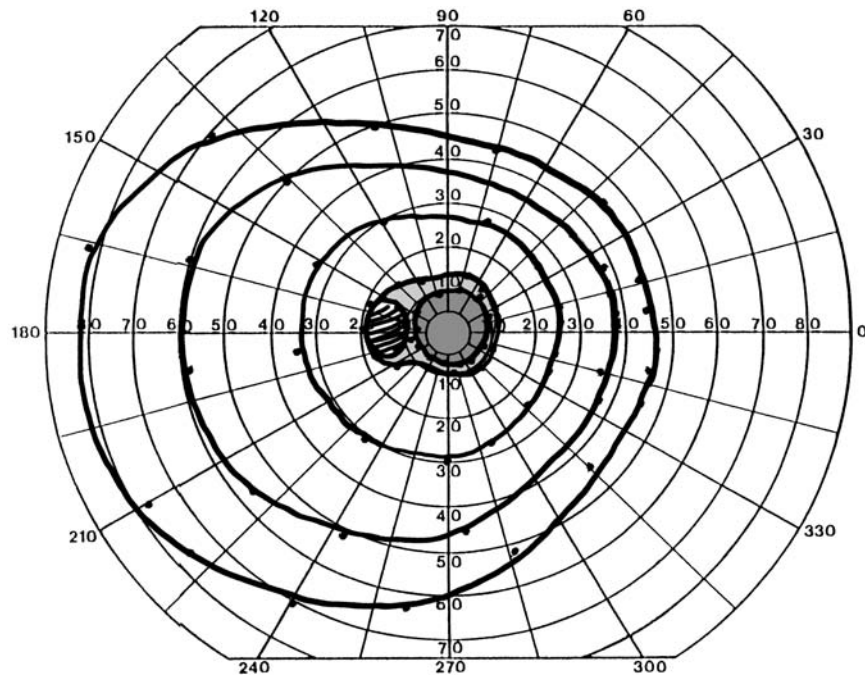
Field description: Generalized depression OS and inferior arcuate defect OD.

Localization: Retrobulbar optic nerves, bilateral.

Pathology: Retrobulbar optic neuritis, MS.

Confrontation fields showed generalized red desaturation OS.

The patient's field in the symptomatic eye shows no particular pattern, just a diffuse variable depression, which was actually the most common finding on automated perimetry in the ONTT, occurring in half the patients (30). However, he has a lot of false negative errors, which implies that his defect is not as severe as his responses indicate on automated perimetry. Indeed, Goldmann perimetry 30 min later showed a less impressive (but more classic) moderate relative central scotoma. (This does raise the question of how many of the diffuse defects on automated perimetry in the ONTT (30) may also have been central defects, if they had been examined with other techniques.) The arcuate defect in the asymptomatic eye cannot be dated, but the ONTT did show that such defects in the fellow eye occur in half or more of patients, with peripheral rim defects and diffuse loss



the most common patterns (30,40). Fellow eye defects are more common in patients with more severe loss in the symptomatic eye (acuity <20/200) but, counter-intuitively, do not correlate with associated clinical or radiologic signs of demyelination (40).

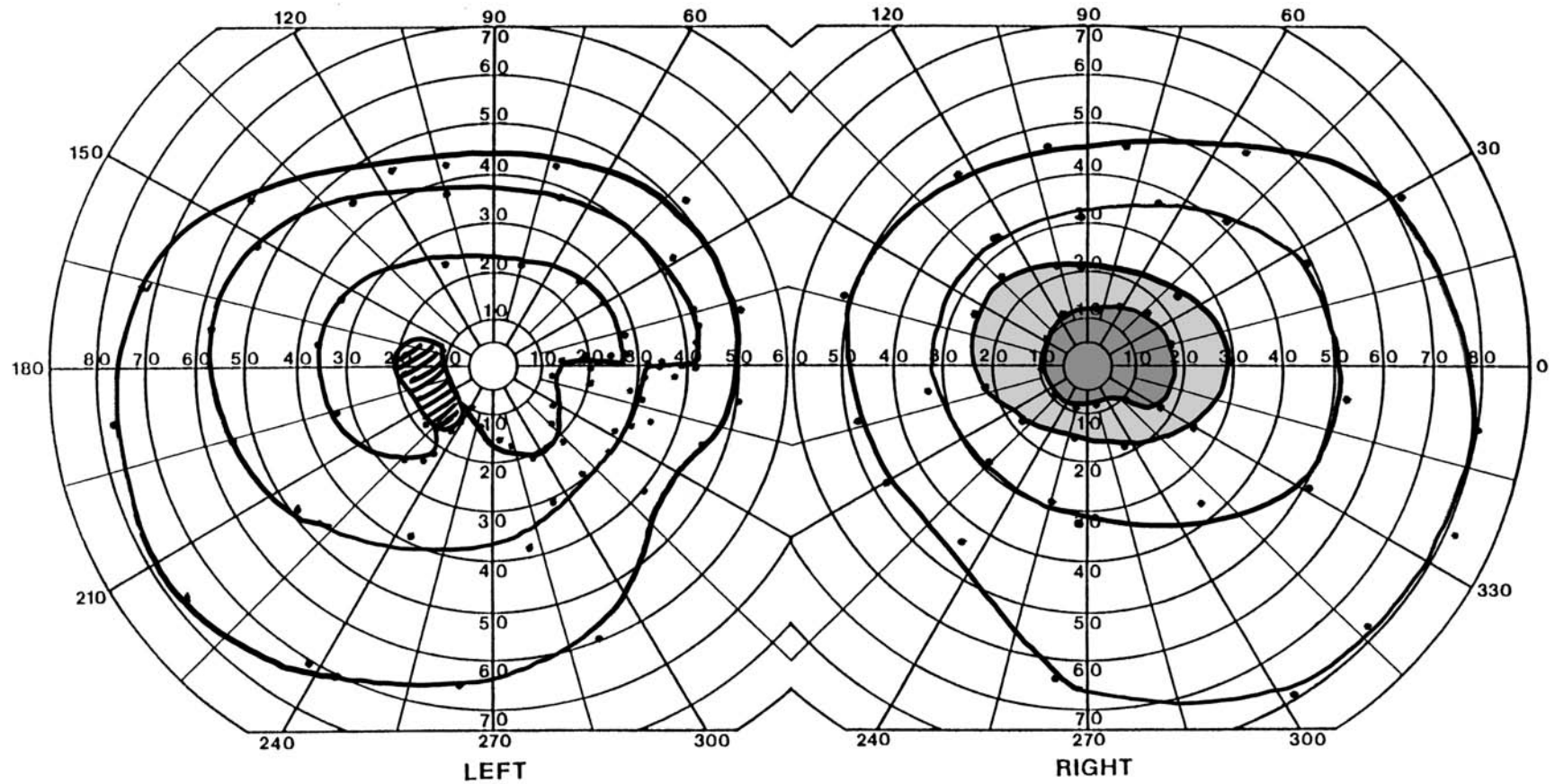
This patient already has a history of relapsing neurologic dysfunction. A thoracic spine MRI done 2 years earlier showed a demyelinating lesion (arrow). Thus, he already has clinically definite MS. The prognostic aspects of MRI and long-term effects of methylprednisolone found by the ONTT in patients with no earlier neurologic history do not apply to him. He was referred for β -interferon treatment.



HISTORY AND EXAM

A 40-yr-old man had 3 weeks of bilateral orbital pain with eye movement and 6 days of progressive deterioration in acuity and color vision in both eyes, the right more than the left. He could see hand motion only with the right eye. Acuity of the left eye was

20/25, and the Ishihara color score with this eye was reduced at 5/14. Optic discs were mildly hyperemic and swollen OU.



DISCUSSION

Field description: Large cecocentral scotoma OD, inferior arcuate defect OS.

Localization: Bilateral anterior optic nerves.

Pathology: Bilateral papillitis.

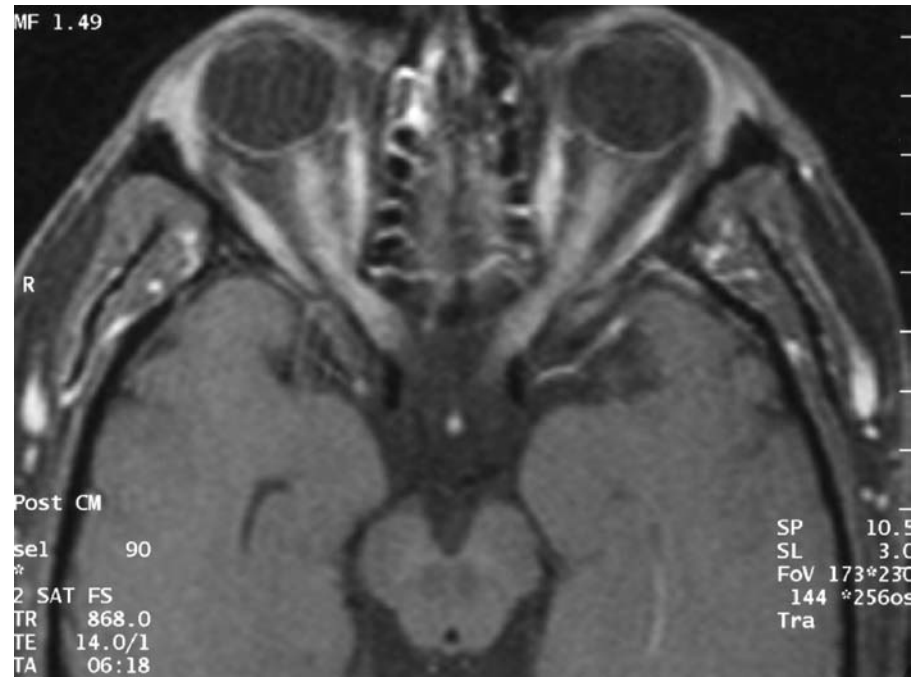
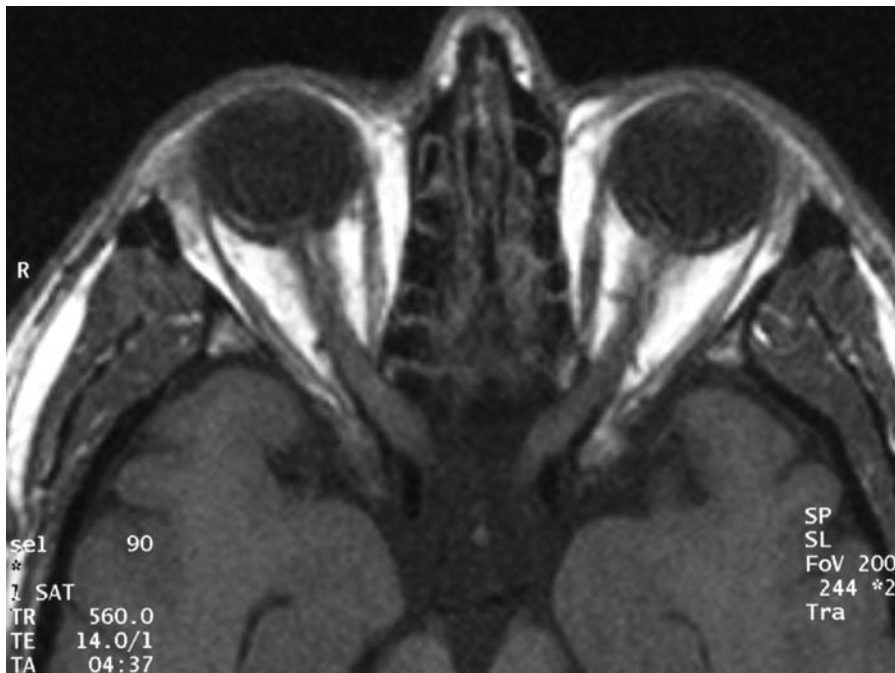
Confrontation testing showed dense central defect to finger motion OD, and inferior arcuate defect to finger counting and red targets OS.

Note how the defect OS arches from the blind spot to form a step at the nasal horizontal meridian. Subacute onset of visual loss and pain with eye movement suggest an inflammatory process. T1-weighted MRI of the orbits showed bilateral optic nerve enhancement with gadolinium (right image is enhanced).

Does enhancement of the optic nerve provide any useful prognostic information? The answer is probably no. Enhancement is common in idiopathic optic neuritis and does

not necessarily indicate a different diagnosis (41). Furthermore, neither the length of enhancement nor the involvement of the intracanalicular nerve predicted degree of recovery or response to steroids (42). This patient had an excellent clinical response to 3 days of iv methylprednisolone. Automated perimetry 2 weeks later demonstrated mild residual central depression on the right and inferior arcuate defect on the left, which resolved completely over the ensuing months.

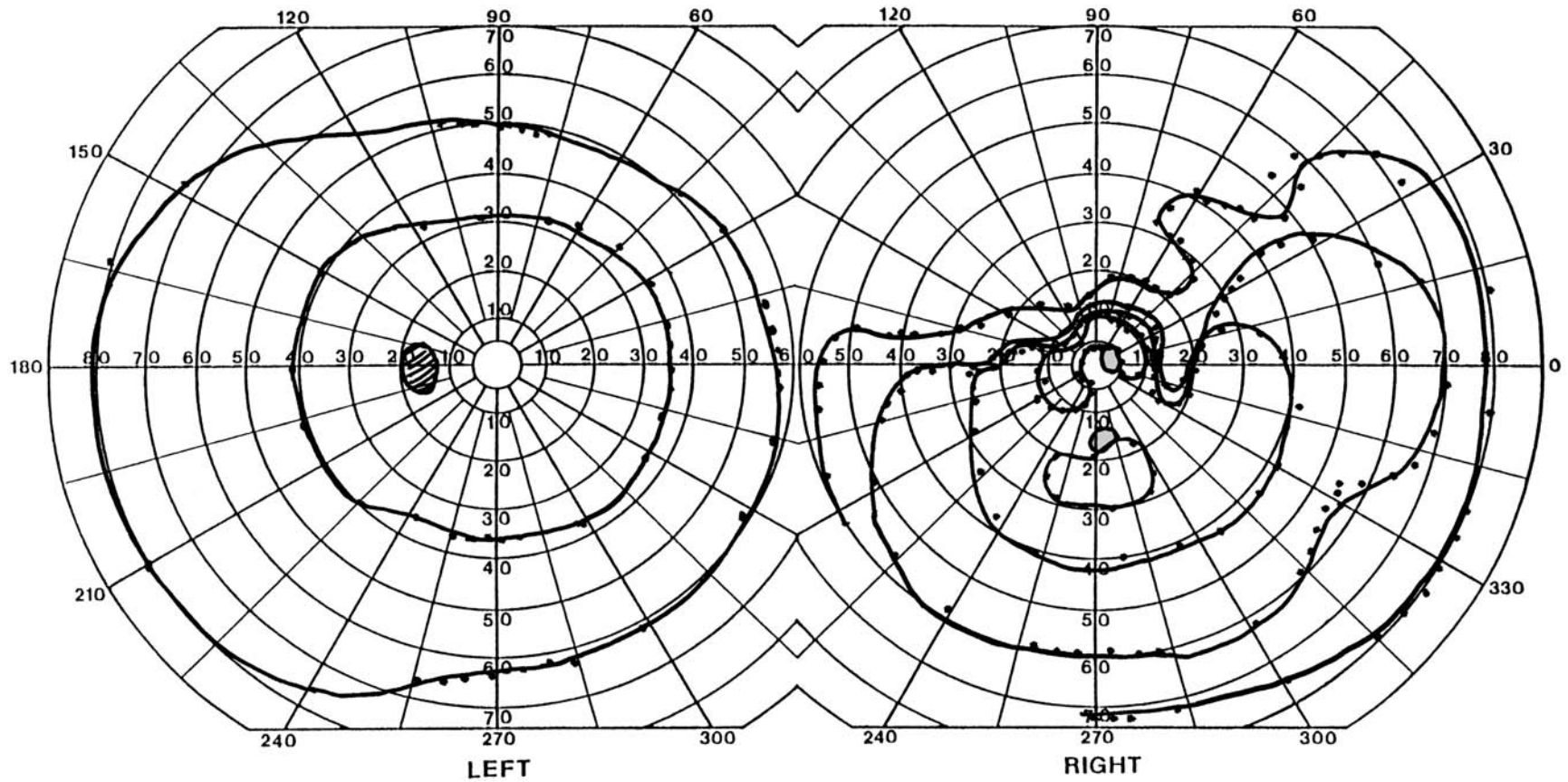
More important, the patient's brain MRI was normal. Bilateral simultaneous optic neuritis carries a low risk of future MS, probably about 20% over 30 years (43,44), in contrast to bilateral sequential optic neuritis. About another 20% of cases can be due to Leber's hereditary optic neuropathy (LHON) (44). In the absence of other inflammatory conditions such as sarcoidosis, one might speculate that this presentation is some post-viral event. Four years later, he remains free of neurologic events.



HISTORY AND EXAM

This 29-yr-old woman with chronic headaches had 2 weeks of blurred vision OD and fever. For 3 weeks she had noted small round lesions on her shins. Acuity was 20/200 OD and 20/20 OS. There was an RAPD OD. Fundoscopy showed disc edema OD with a mac-

ular star. The skin lesions were diagnosed as erythema nodosum. She was treated with 80 mg of prednisone, and 4 months later acuity had improved to 20/50 OD, with the field below.



DISCUSSION

Field description: Superior and inferior arcuate defects with superior nasal step OD.

Localization: Anterior optic nerve.

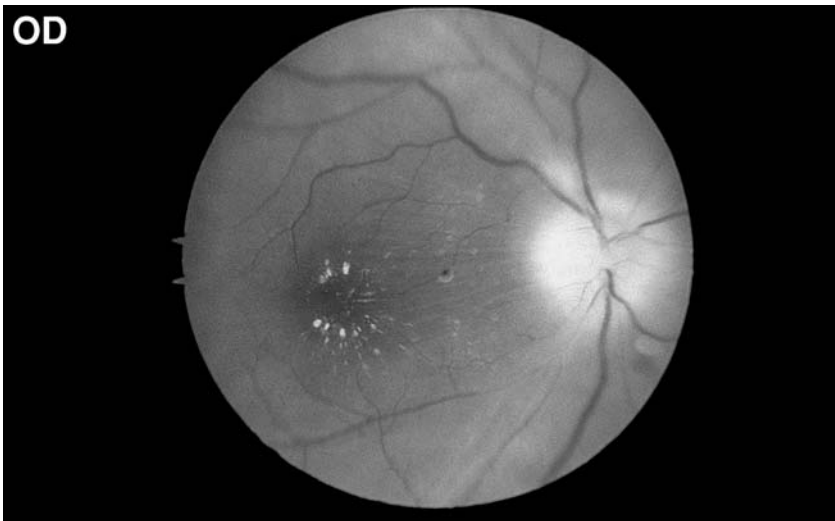
Pathology: Probable sarcoidosis.

Other features: Macular star (see fundus photograph below).

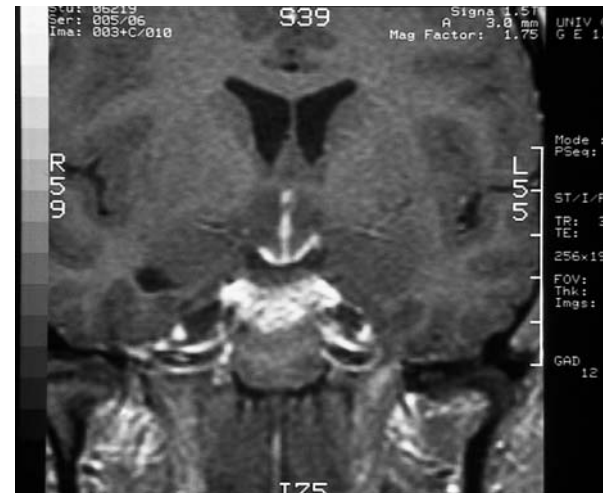
The patient's field OD is complex, with a superior defect that points to the location of the blind spot, and approaches an incomplete altitudinal defect in its extent. The smaller isopters align at the nasal horizontal meridian. Inferiorly there is a scotoma (shaded spot) in the course of the inferior arcuate bundle. There is also a depression in the central 5°, consistent with her reduced acuity.

She had an MRI showing enlargement and enhancement of the right intracranial optic nerve and chiasm, as well as enhancement lining the base of the brain and third ventricle (shown here), all of which resolved after 3 months of steroids. Chest X-ray, bronchoscopy, and cerebrospinal fluid (CSF) were normal.

Optic neuropathy in sarcoidosis can be either a chronic form that responds poorly to steroids or, as here, an acute form with rapid improvement with treatment (45). Features that distinguish acute sarcoid optic neuropathy from idiopathic demyelinating optic neuritis include progression beyond the first week, more extensive peripheral field loss, and "steroid dependency", i.e., relapse of visual loss when steroids are tapered and stopped (45,46). The macular star indicates neuroretinitis and is so unusual for idiopathic optic neuritis that it can be considered evidence against MS (47). Basilar meningeal enhancement on MRI is not a feature of MS but of sarcoidosis (46,48).



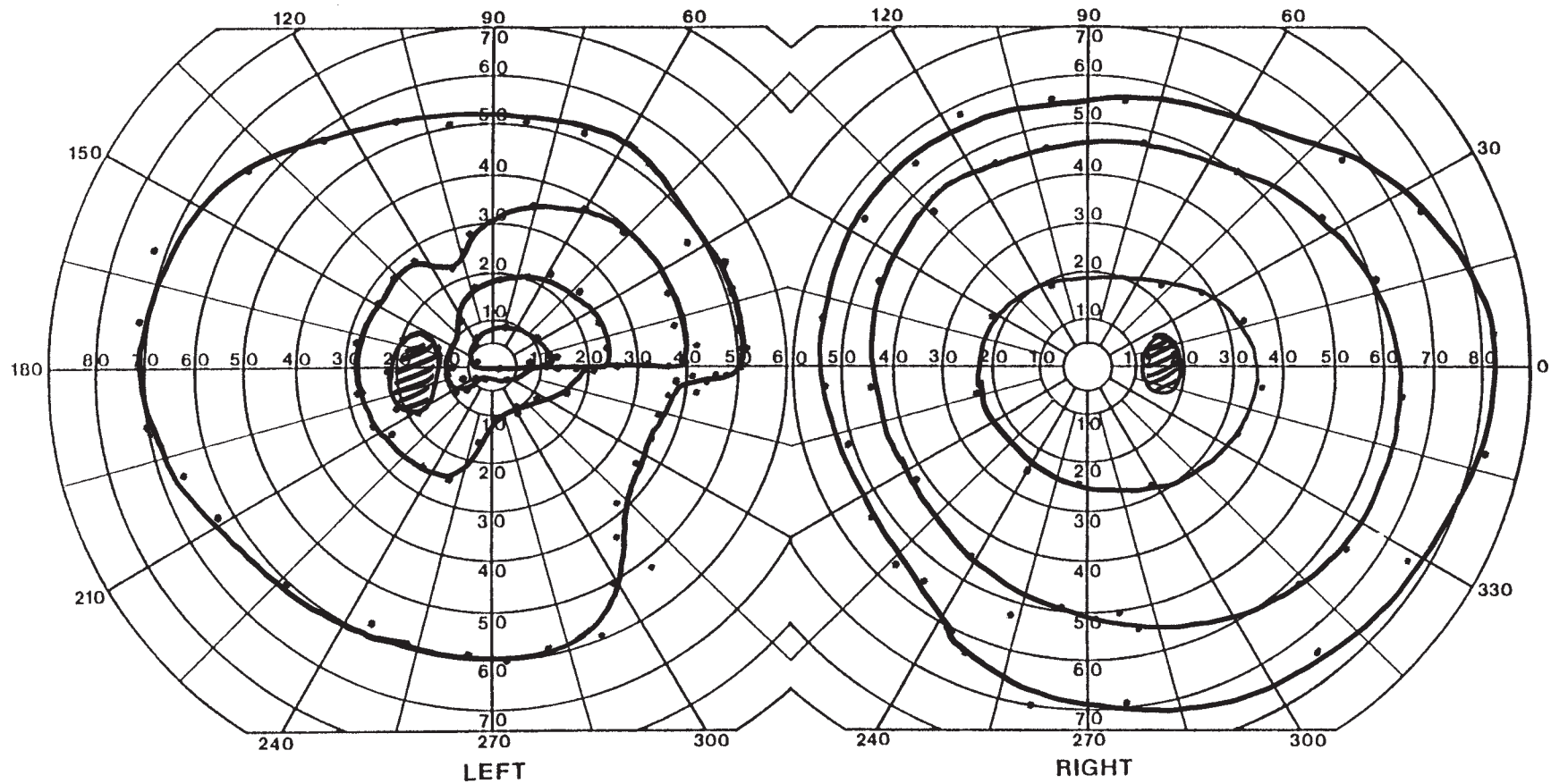
See Color Plate after page 180



HISTORY AND EXAM

This 57-yr-old man noted 1 month of ill-defined decreased vision OS. It seemed stable. He had mild tenderness above the eye but no jaw claudication or scalp tenderness. He had no other illness. Acuity was 20/15 OD and 20/20 OS, with normal color scores

of 13/14 OU. There was an RAPD OS. Fundoscopy showed superior segmental disc edema OS with a peripapillary flame hemorrhage (shown next page).



DISCUSSION

Field description: Inferonasal step OS.

Localization: Anterior optic nerve.

Pathology: Anterior ischemic optic neuropathy (AION) (nonarteritic).

Confrontation testing showed decreased hand and color comparison in the inferior hemifield OS.

The patient presents with a classic inferior arcuate defect and segmental disc edema. The disc edema with sudden nonprogressive visual loss in a man of his age points to ischemia of the optic disc (AION), which is supplied by the posterior ciliary arteries (see Chapter 2). The most important initial step in the evaluation and management of AION is the determination of whether the cause is arteritic (i.e., giant cell arteritis) or nonarteritic (49), the latter usually related to microvascular disease from diabetes, hypertension, or old age. Symptoms in favor of arteritis include preceding amaurosis fugax, headache,

fever, jaw claudication, and scalp tenderness, the latter due to ischemia distal to the external carotid artery (49). Signs suggestive of arteritis are more severe visual loss, with 60% of patients having acuities of less than 20/200 in the affected eye, and a pale chalky color to the swollen disc (49). Less severe loss with segmental rather than diffuse disc edema favors the nonarteritic form, as here. The erythrocyte sedimentation rate (ESR) and C-reactive protein (CRP) are typically elevated in arteritic AION (50), with the ESR usually above 70 mm/h, but normal in up to 16% of biopsy-proven cases. Poor or absent filling of the choroid on fluorescein angiography also points to arteritic AION. Giant cell arteritis is confirmed by positive temporal artery biopsy, but the false negative rate of biopsy has been estimated as between 5 and 8% (50). Diagnosis of arteritic AION needs to be made promptly, in order to begin steroid treatment to prevent possible imminent loss of the second eye's vision.

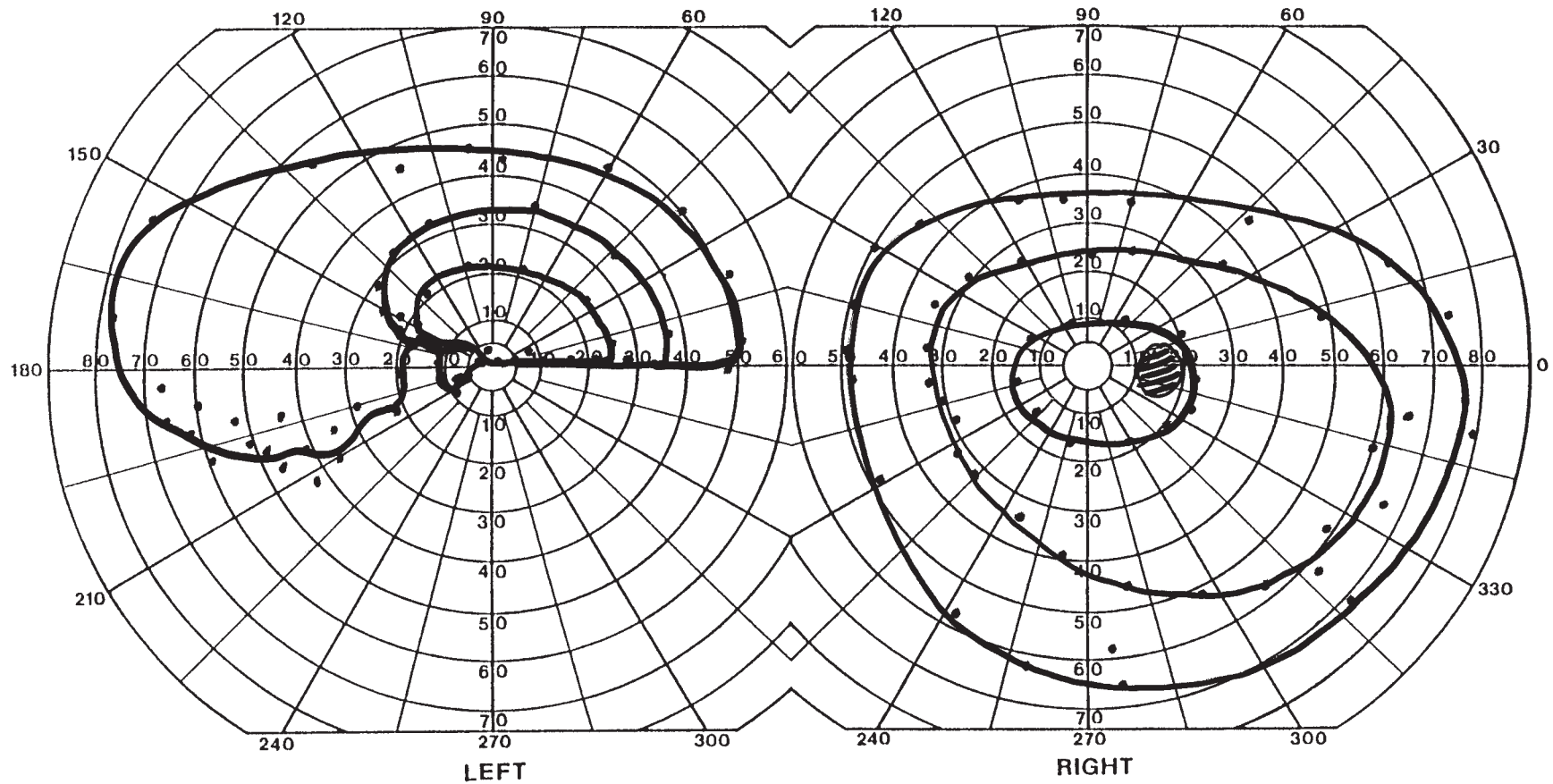


See Color Plate after page 180

HISTORY AND EXAM

This 43-yr-old woman had sudden painless inferior visual loss in the left eye, which did not change over the next month. Visual acuity was 20/20 OD and 20/40 OS. Ishihara color scores were 14/14 OD and 6.5/14 OS, with an RAPD OS. There was a hyperemic

inferior sector on the left optic disc. The right optic disc was small and crowded, with minimal central cup (shown next page).



DISCUSSION

Field description: Inferior altitudinal defect, splitting macula OS.

Localization: Anterior optic nerve.

Pathology: AION, nonarteritic.

Confrontation testing showed near complete inferior altitudinal defect to hand motion.

Altitudinal defects are the classic pattern associated with AION. The patient's defect is typical, with sharp demarcation at the nasal horizontal meridian and some partial sparing of the temporal field of the affected half. Her macula is split in half by the field defect, but this central region can be spared or involved completely by an altitudinal defect (see Case 35).

Disk edema fades over the first 1 to 2 mo, and about 40% of patients may have some mild improvement when this occurs (51). Interestingly, this patient's disc hyperemia was in the normally functioning inferior half (serving the superior field), suggesting that this

may be an unusual luxury hyperperfusion of the remaining disc rather than persistent edema (52). The other disc was small and lacked a central cup; such "crowded" discs are considered a risk factor for AION, the "disk at risk" (53). Indeed, 3 mo later she had a second episode OD, with an inferior altitudinal defect, and then progressive constriction of both eyes that eventually stabilized after a few months. ESR and temporal artery biopsies were normal.

The early course of nonarteritic AION is usually static with little or no change in the initial visual loss. More unusual is a progressive form, in which vision continues to decline over weeks to months before eventual stabilization. Although optic nerve sheath fenestration was once promoted as a treatment for this form, it remains unclear whether there is benefit from the procedure. For AION in general, the procedure worsens vision (51). Progressive AION can sometimes improve spontaneously (54).



See Color Plate after page 180

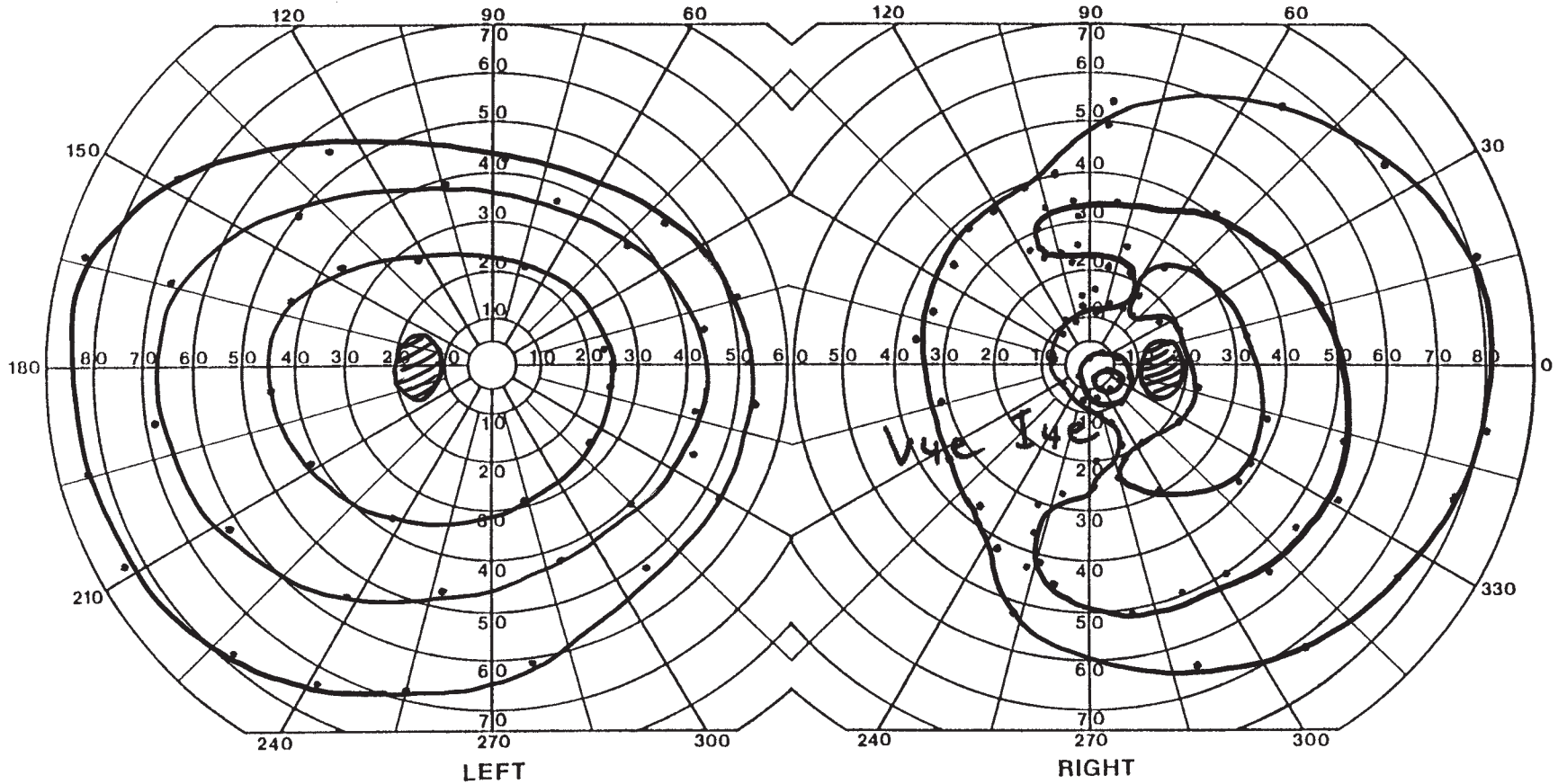


See Color Plate after page 180

HISTORY AND EXAM

This 71-yr-old man awoke one morning and noticed a dark spot in the right eye. There was no change in his symptoms over the following mo. When examined a month after onset, visual acuity was 20/20 OU, but there was an RAPD OD. Ishihara color scores

were 12/14 OD and 11/14 OS. The optic disc OD was diffusely swollen, and the optic disc OS had a minimal central cup. The remainder of the examination was normal.



DISCUSSION

Field description: Inferior and superior arcuate defects OD.

Localization: Anterior optic nerve.

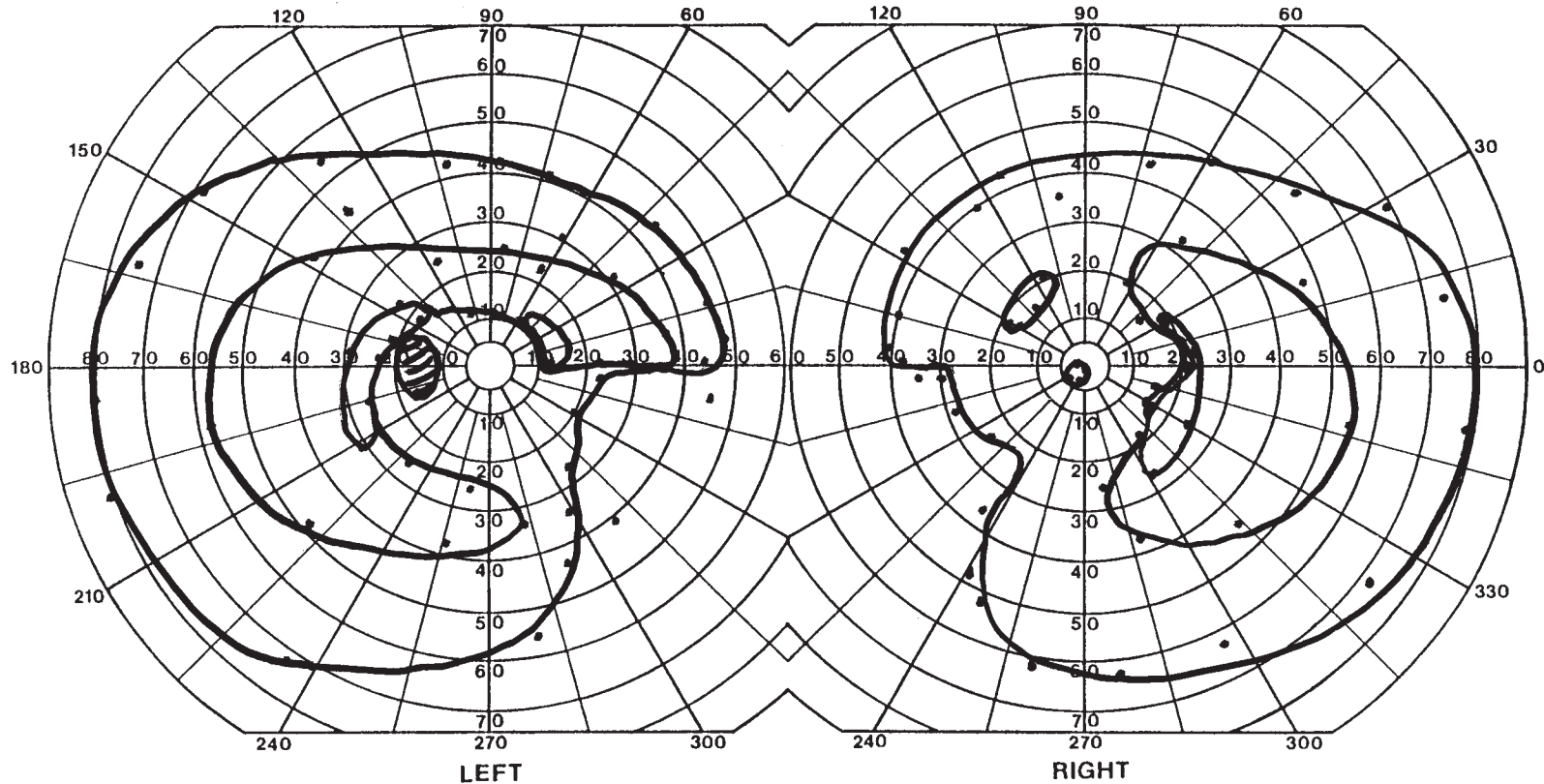
Pathology: AION, nonarteritic.

Confrontation testing showed decreased finger counting in the inferonasal sector and decreased color in all except the superior temporal quadrant OD.

There is a relative nasal constriction to the large (V4e) isopter. Within this, the I4e isopter is indented above and below center, leading to depressed valleys of the smallest isopter that curve into the blind spot, leaving a small central island of better vision. ESR was 32 mm/h and CRP was <0.4 mg/dL, and the patient was diagnosed with a nonarteritic AION. He returned 2 months later and reported that his vision had deteriorated further, but he could not identify any time of sudden worsening. Examination revealed a visual acuity

of 20/40 on the right and 20/100 on the left. Color vision was markedly impaired in both eyes. Fundoscopy demonstrated optic atrophy on the right and mild disc edema on the left. Visual fields, shown below, revealed some minor evolution of the prior arcuate defects on the right as well as a new centrocecal scotoma and inferior arcuate defects on the left.

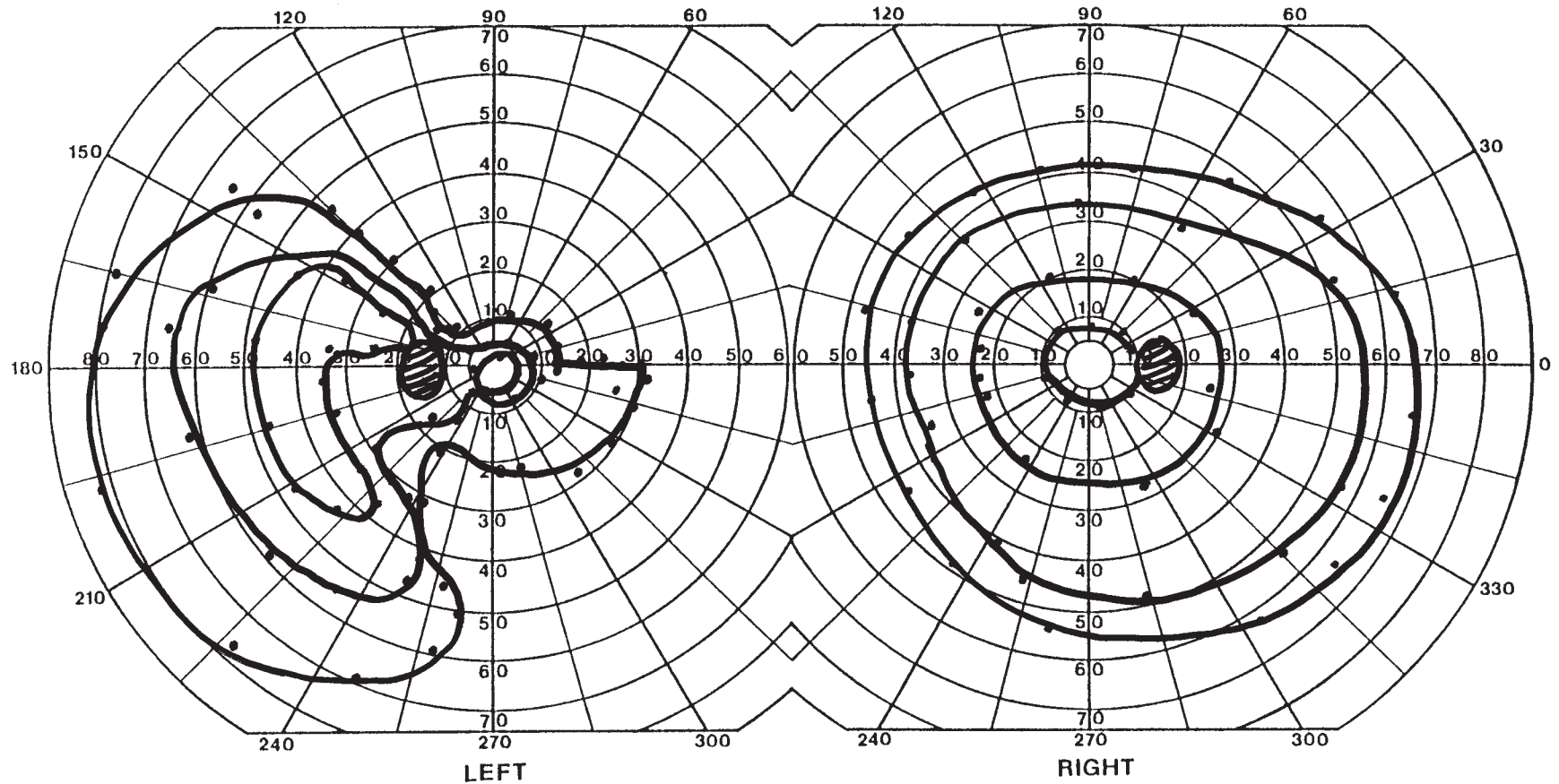
The optic disc in the eye contralateral to that with nonarteritic AION is typically small in diameter and the physiological cup is often either small or absent (53) (see Case 33). This can be associated with a small degree of hyperopia (55). The term *disc at risk* has been used to describe these crowded discs and their risk for AION. Structural crowding of the disc at the level of the cribriform plate may contribute to microvascular compression and render the optic disc vulnerable to ischemia. The finding of such a “disk at risk” in the contralateral eye may, therefore, sometimes assist in making the diagnosis of nonarteritic AION in the affected eye.



HISTORY AND EXAM

This 78-yr-old woman had sudden visual loss in the left eye 4 months earlier. Her ophthalmologist saw disc edema with a nerve fiber layer hemorrhage OS. She denied jaw claudication, headache, or scalp tenderness. ESR was 12 mm/h and CRP was <0.4 mg/dL.

She had 6 years of hypertension, treated with a diuretic. Acuity was 20/20 OU, and Ishihara color scores 13/14 OD and 8/14 OS. There was an RAPD OS. She had a normal optic disc OD but temporal pallor of the disc OS.



DISCUSSION

Field description: Superior incomplete altitudinal and inferior arcuate defects, with superonasal step, OS.

Localization: Anterior optic nerve.

Pathology: AION, nonarteritic.

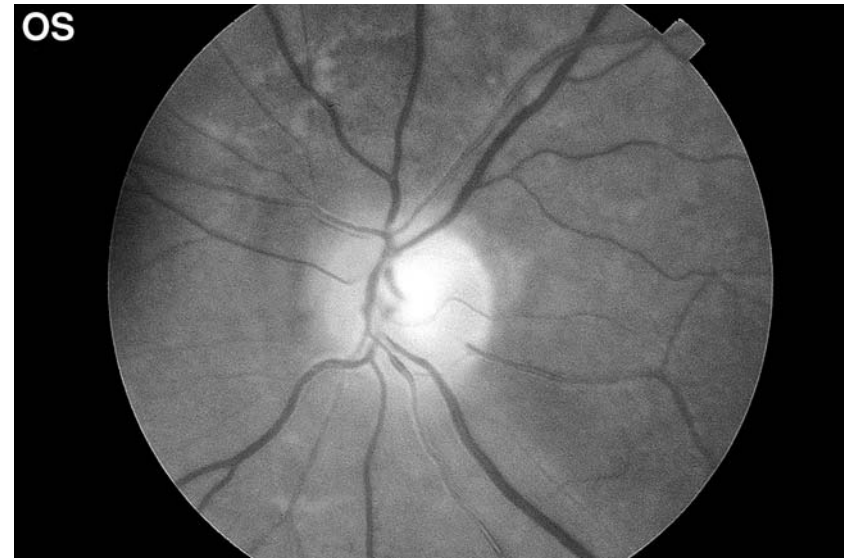
Confrontation testing showed superonasal step defect to a red target.

The best way to approach this patient's complex defect is to divide the field in vertical halves. In the top half, she has an incomplete altitudinal defect, sparing some of the temporal field as well as the macula. Inferiorly there is a less severe arcuate defect arching out of the blind spot toward the nasal field, and also some depression in the temporal field immediately adjacent to the optic disc.

The documentation of disc edema in the acute phase is key to diagnosing AION. At this late stage, the patient has only nonspecific optic atrophy (shown here OS), which is

the end stage of any number of pathologic processes. Without knowledge of her earlier disc edema, one would have to consider other disorders, including the suddenly noted visual loss of a compressive optic neuropathy (see Case 52).

Arteritic AION is an occlusive disease, which is reflected in large areas of choroidal nonperfusion on fluorescein angiogram. Nonarteritic AION is usually a hypoperfusion event affecting the watersheds among different posterior ciliary arteries in the same eye (56). Microvascular disease due to long-standing hypertension or diabetes increases the vulnerability of the discs during episodes of hypotension. The normal nadir of blood pressure in early morning hours may explain why many patients first note visual loss on awakening (57). This nocturnal hypotension can be aggravated by the use of antihypertensive medication in the evening. Unlike the situation with central retinal artery occlusion, carotid atherosclerosis is not a major risk factor for AION (58).

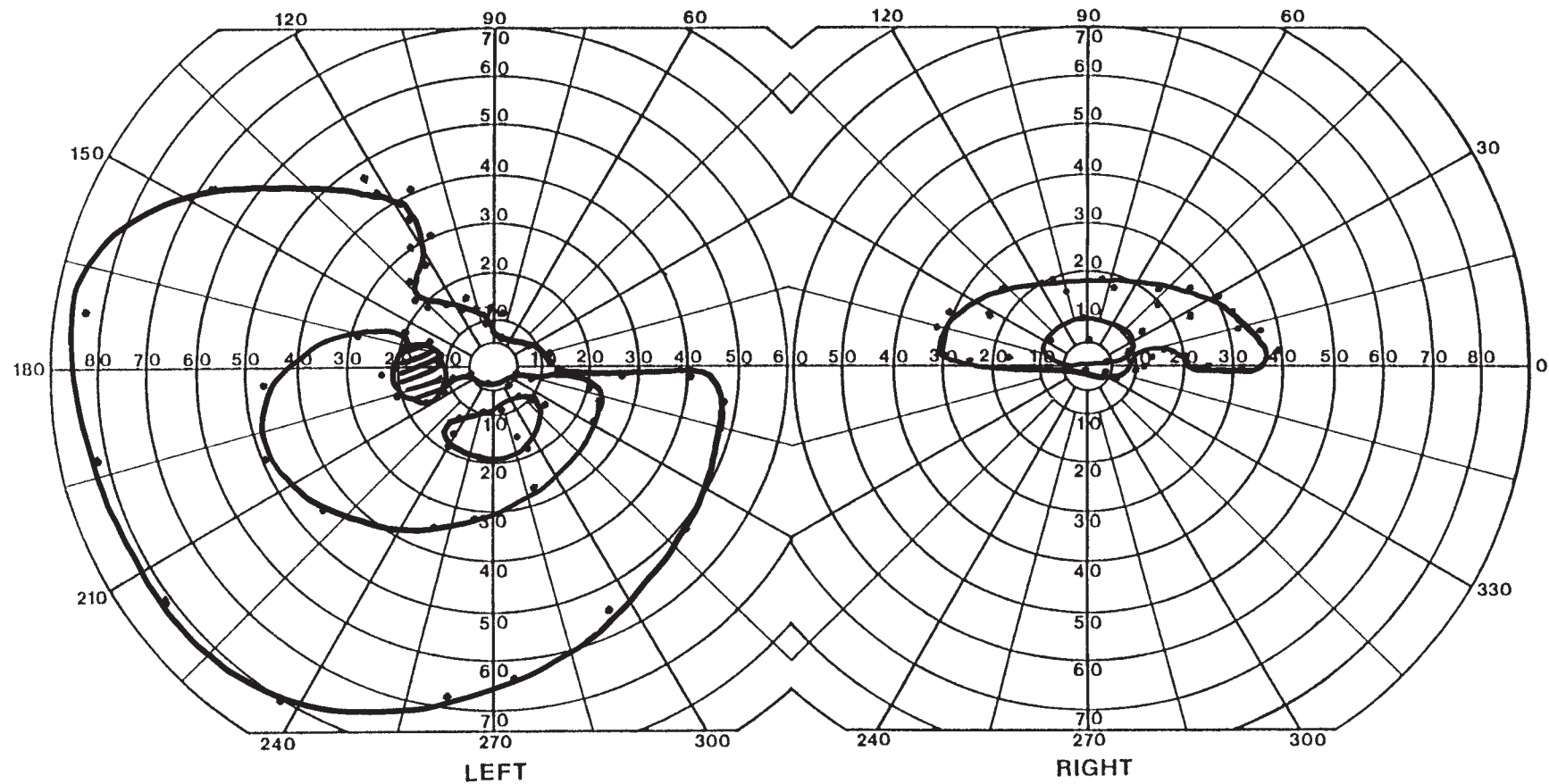


See Color Plate after page 180

HISTORY AND EXAM

This 65-yr-old man had 1 week of painless nonprogressive blurry vision OS. One year earlier he had awakened with painless visual loss OD that persisted. He had hypertension and diabetes for 10 years, and was taking ASA. Acuity was count fingers at 8 ft OD and

20/80 OS with eccentric fixation. There was an RAPD OD. Fundoscopy showed severe optic disc pallor OD and diffuse disc edema OS, with peripapillary nerve fiber layer hemorrhages. His ESR was 10 mm/h and CRP <0.4 mg/dL.



DISCUSSION

Field description: Complete inferior altitudinal defect with general constriction OD; incomplete superior altitudinal defect with central depression OS.

Localization: Bilateral optic nerves, anterior OS.

Pathology: Bilateral sequential nonarteritic AION.

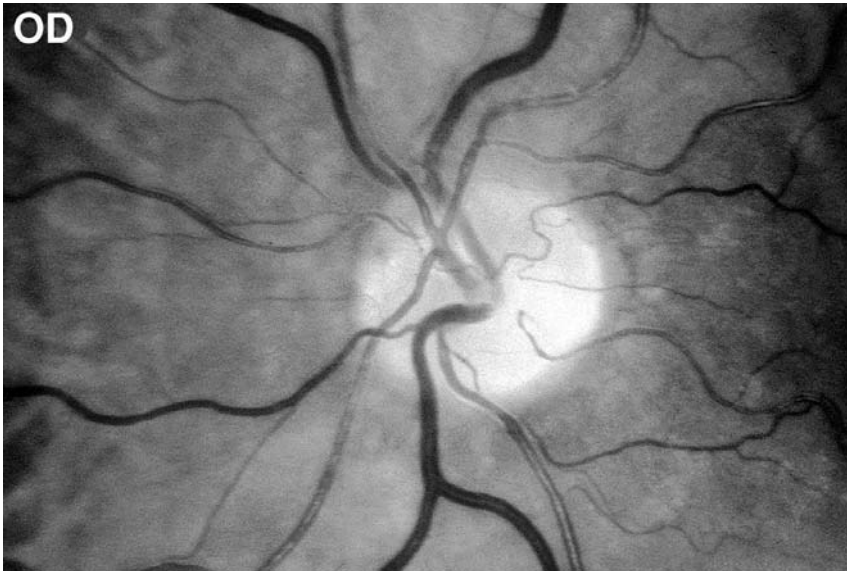
Confrontation testing showed an inferior altitudinal defect for hand motion OD and a superonasal step defect for hand and color comparisons OS.

The patient has only a sliver of remaining superior vision OD, which lies completely above the horizontal meridian. In the other eye, he has lost almost all of the superonasal quadrant, with a relative depression of both the superotemporal quadrant and the central region, so that he can see only the smallest target when it is just below center (this accords with his reduced acuity). Note how the largest V4e isopter “points” to the blind spot, in arcuate fashion.

Foster Kennedy syndrome combines optic atrophy in one eye with papilledema in the other (59). The classic cause is an orbitofrontal mass such as a meningioma causing an ipsilateral compressive optic neuropathy and contralateral papilledema from raised intracranial pressure (not expressed in the ipsilateral eye because of the atrophy). Usually this presents with progressive visual loss in the ipsilateral eye and no visual change other than an enlarged blind spot in the other eye.

Like all classic signs, its mimics are more common than the real thing. Bilateral sequential AION or optic neuritis is more frequent than the neoplastic version of Foster Kennedy syndrome (60). The difference is that the edematous eye in ischemic or inflammatory conditions has significant visual loss, and the deficit in the other eye is static rather than progressive.

In nonarteritic AION, about 20% of patients develop a second episode over the next 5 years (61). There is some marginal evidence that aspirin might reduce this risk by about half.



See Color Plate after page 180

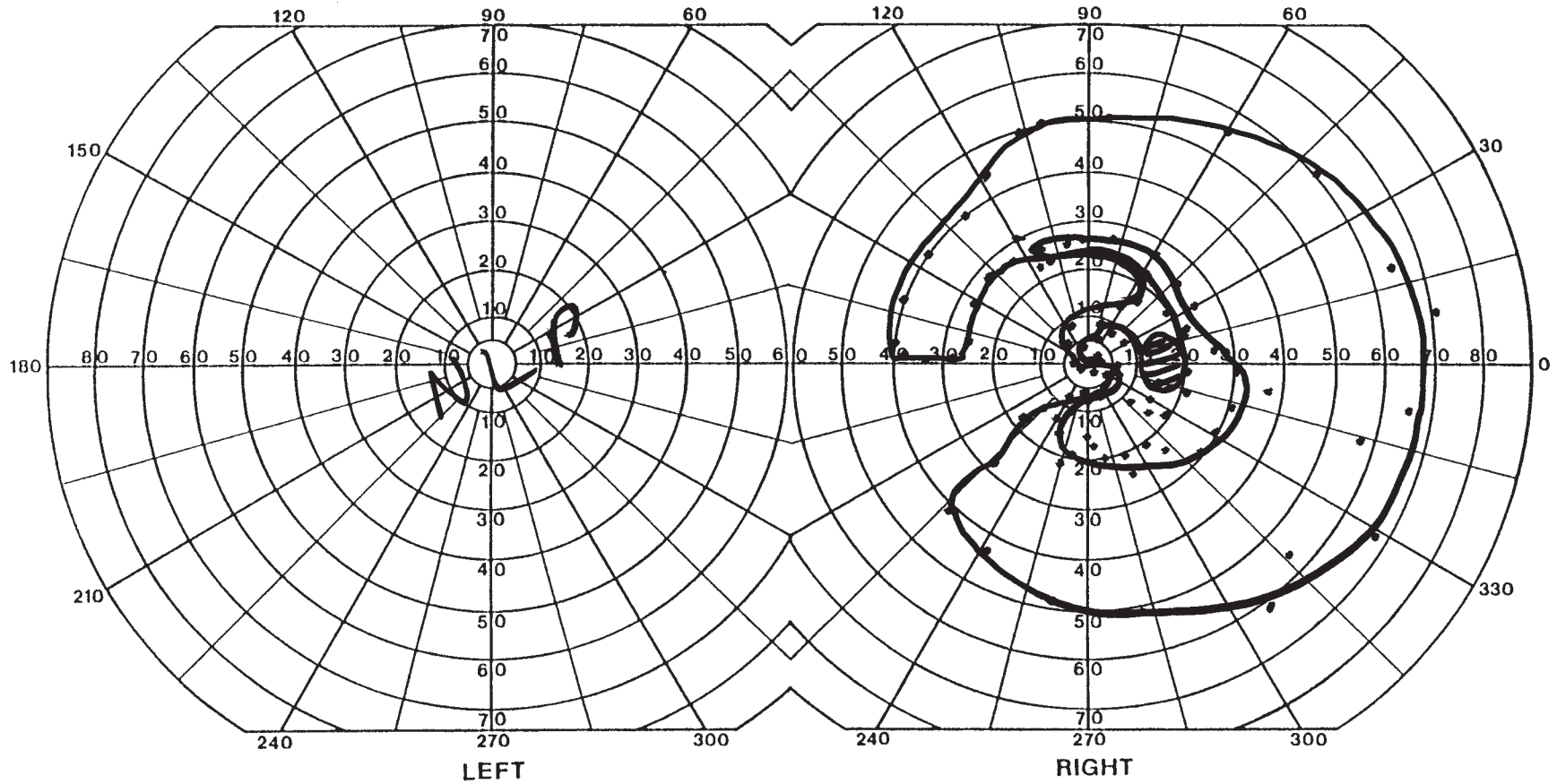


See Color Plate after page 180

HISTORY AND EXAM

This 47-yr-old man with 9 years of known hypertension was hospitalized with a severe hemorrhage from an ulcer, precipitated by the use of ibuprofen and requiring transfusion with 6 units of blood. At this time he rapidly developed bilateral visual loss, which improved slightly 4 days later. When reviewed 6 months later, he had visual acuity of

20/30 OD and no light perception OS. Ishihara color score was 0/14 OD. There was a large RAPD OS, with some weak light reaction still present OS. There was diffuse pallor of both optic discs, worse OS.



DISCUSSION

Field description: Superior arcuate defect and inferior nasal step extending to inferior macula OD, complete loss OS.

Localization: Bilateral optic nerves.

Pathology: Ischemic optic neuropathy.

Confrontation testing showed preserved superior and inferior temporal islands of vision to light OD.

The patient's defect OD is complex. The superior defect begins at the disc as a zone of relative depression but quickly becomes a dense arch heading to the nasal meridian, in which the V4e isopter is not seen in the zone between 10 and 25° eccentricity. Inferiorly there is a dense nasal step defect, merging into an inferior hemimacular hole. Although he cannot see the V4e target OS, confrontation testing shows some residual glimmer of perception when a light is shone into the eye rather than projected onto a screen. This residual vision also explains the persisting weak pupillary light reaction and reminds us that

one cannot conclude total blindness just because a patient cannot see the biggest target in a perimetric test.

Severe hypotension or blood loss can precipitate ischemic optic neuropathy, particularly in patients with hypertension, as here, or atherosclerosis. Ischemia may occur either at the disc (AION) or behind it (posterior ischemic optic neuropathy [PION]) (62,63). The difference is that acutely the former has edematous optic discs, whereas the latter has normal discs. After a few months, both resolve into optic atrophy, as seen here. Since no one bothered to record this patient's fundoscopic findings in the hospital, we do not know which he had.

Besides gastrointestinal bleeding, other high-risk situations for this complication include cardiac surgery and lumbar spine surgery. Bilateral visual loss in the setting of hypotension could also be caused by occipital ischemia but would cause homonymous bilateral hemianopic defects without RAPD or optic atrophy, which is not the pattern in this case.



See Color Plate after page 180

DISCUSSION

Field description: Bilateral cecocentral scotomata.

Localization: Bilateral optic neuropathy.

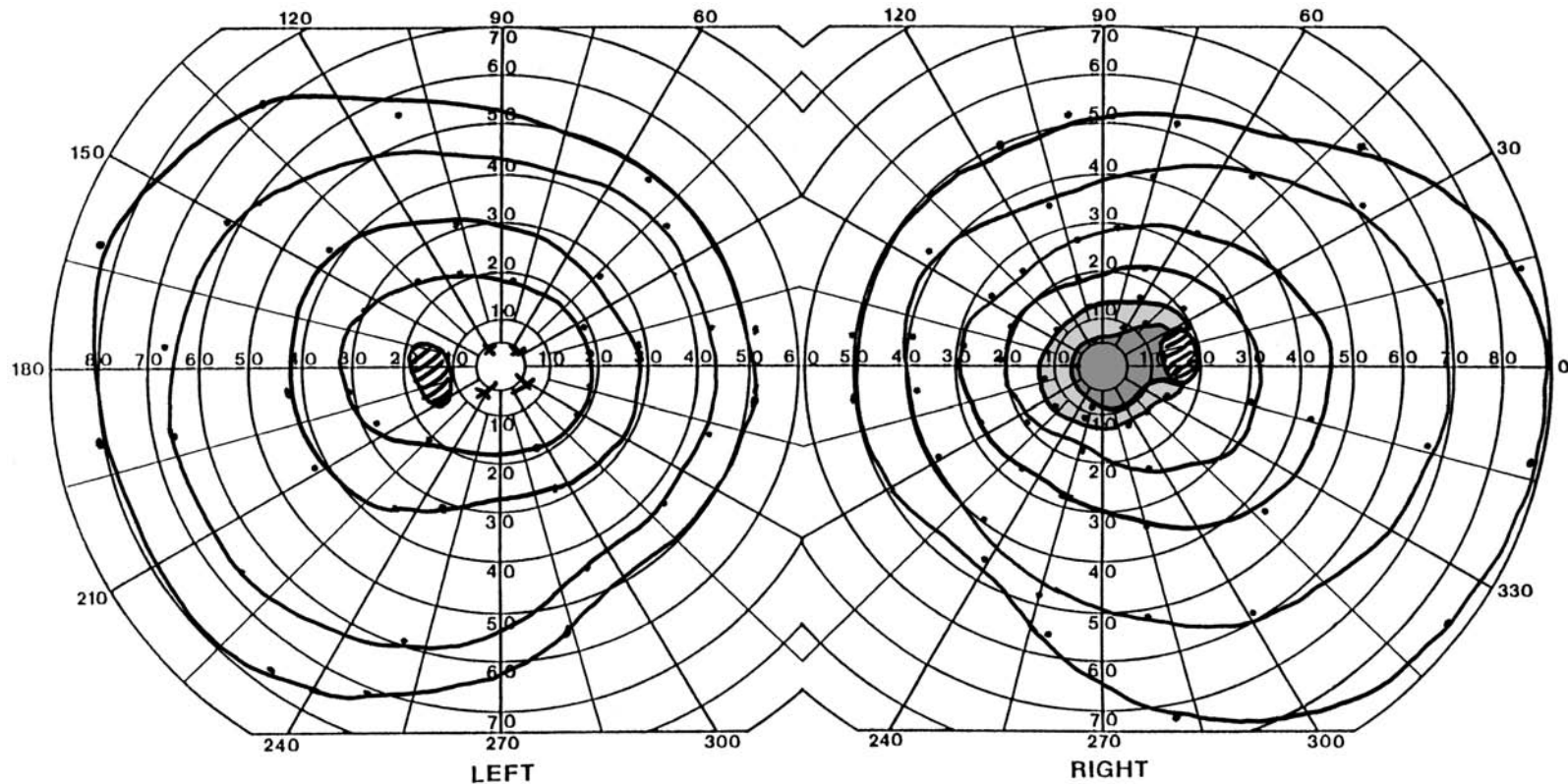
Pathology: B₁₂ deficiency.

Confrontation testing was normal OU.

Although Humphrey 30-2 perimetry clearly shows the central defects in both eyes, Goldmann perimetry showed only the cecocentral scotoma on the right (The 'x' in the central field OS indicate that a flashed O2e target was seen at those locations.) This indicates the superiority of static threshold measurements in the highly sensitive central field (see Chapter 1). Although asymmetric, the slow progression of bilateral central defects over many years is most in keeping with a metabolic or degenerative condition of either

the optic nerves or maculae. The absence of a history of acute/subacute visual loss argues against old (bilateral) inflammatory or ischemic optic neuropathy. This patient had a low-normal serum B₁₂ level and elevated homocysteine and methylmalonic acid (MMA), indicating a mild B₁₂ deficiency.

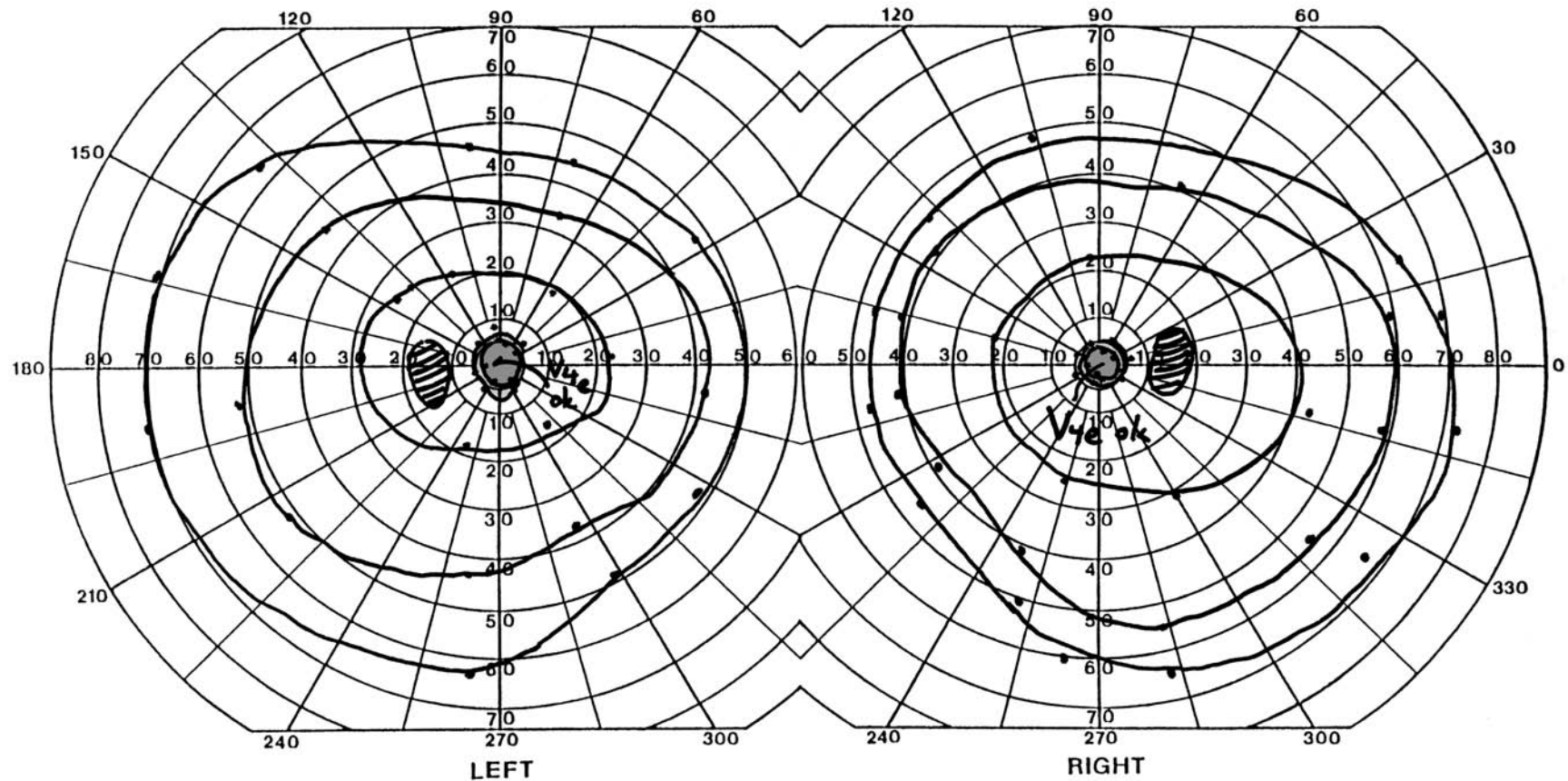
The characteristic clinical features of toxic and nutritional optic neuropathies include slowly progressive, symmetric central visual loss, with dyschromatopsia, cecocentral scotomata, and eventual temporal optic disc pallor, reflecting loss of the papillomacular bundle (64). As in this patient, acuity can remain surprisingly good, but in many it is reduced to 20/200 or less (see Case 39). Apart from B₁₂ deficiency, drugs such as ethambutol and isoniazid can cause a similar disorder. Visual loss may be reversible if the offending toxin is removed or the deficient nutrient replaced.



HISTORY AND EXAM

This 40-yr-old woman presented with bilateral visual loss of about 4 months' duration. She reported having suddenly become aware of the visual loss, which had subsequently progressed gradually to the point where she could not read and struggled to watch television. In addition to heroin addiction, she had smoked a pack of cigarettes each day for

more than 20 years, and although she denied alcohol consumption, her breath smelled of alcohol in the clinic. Visual acuity was 20/200 OU and Ishihara color plates were 10/14 OD and 8/14 OS. There was no RAPD, and funduscopy demonstrated mild temporal pallor OU. The remainder of the examination was normal.



DISCUSSION

Field description: Bilateral central scotomata OU.

Localization: Optic nerves.

Pathology: Tobacco/alcohol and B₁₂ deficiency optic neuropathy.

Confrontation testing showed defects to red targets and face comparison, mainly in the temporal side of central vision OU.

The patient's fields show a classic bilateral central depression. Her confrontation testing suggested bitemporal central defects, which is not an uncommon pattern for cecocentral scotomata of nutritional optic neuropathy to mimic.

MRI did not show a compressive lesion of the optic nerves. Genetic testing for the mitochondrial mutations of Leber's hereditary optic neuropathy (LHON) were negative.

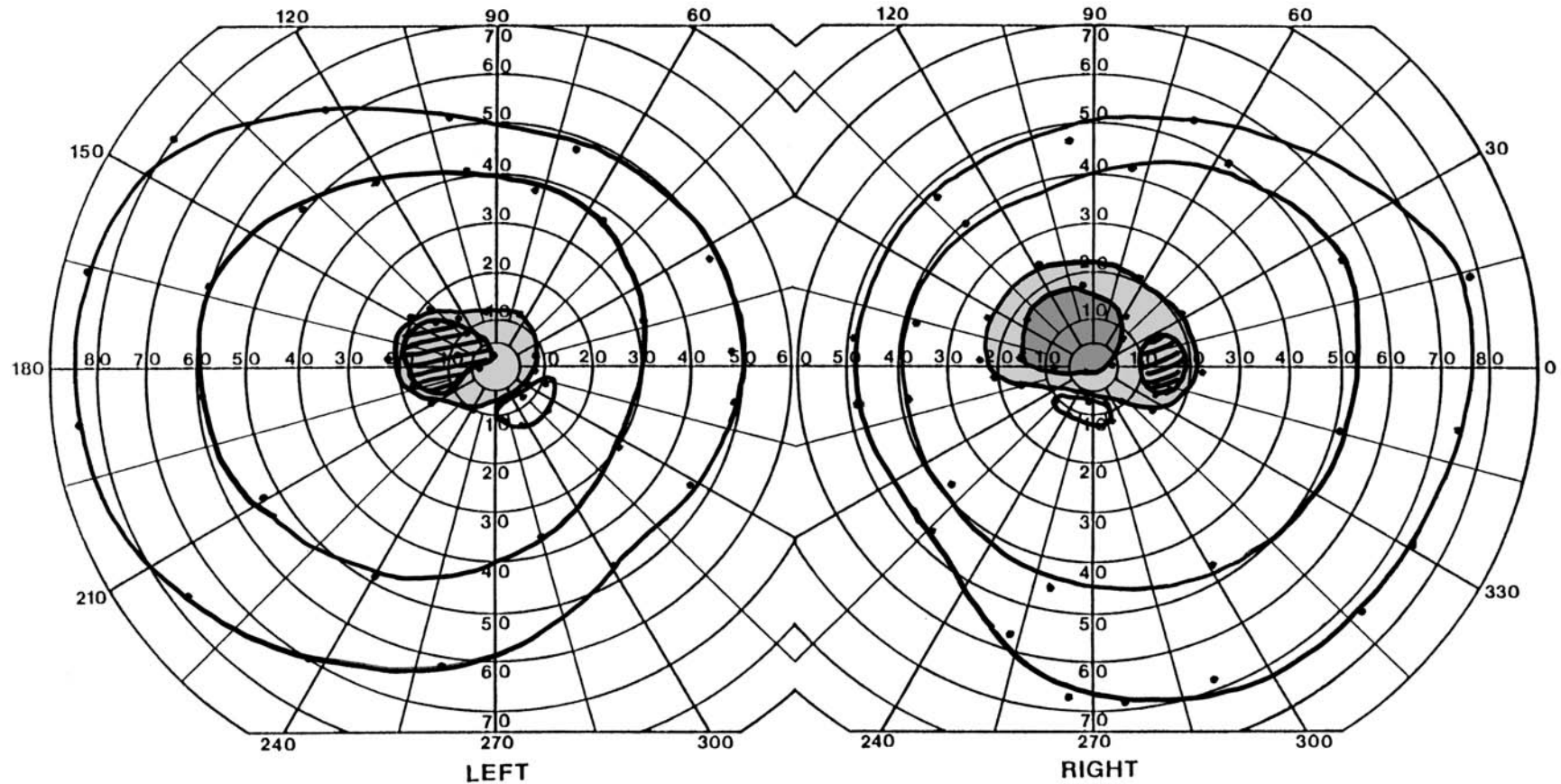
A toxic-metabolic optic neuropathy was considered most likely. She had low serum B₁₂ and elevated homocysteine and methylmalonic acid.

Although B₁₂ deficiency is a recognized cause of optic neuropathy (64), it may also represent a contributing factor in tobacco–alcohol amblyopia, a slowly progressive bilateral optic neuropathy that develops in the context of heavy tobacco and alcohol consumption. The mechanisms involved in tobacco/alcohol optic neuropathy are unclear. Cyanide moieties in tobacco may impair oxidative phosphorylation and lead to demyelination (65). Vitamin B₁₂ binds to and detoxifies cyanide, and its deficiency, aggravated by chronic alcoholism, thus contributes to the pathophysiology of this disorder.

HISTORY AND EXAM

This 35-yr-old woman presented with rapid visual loss in the left eye, accompanied by disc edema. The next year she had blurred vision in the right eye and more visual loss in the left eye. She was diagnosed with Leber's hereditary optic neuropathy (LHON) and placed on Coenzyme Q10 and vitamins. She noted gradual mild improvement in the vision of her left eye over the following months. Approximately 1 year later she developed tingling in her fingers as well as a sensation of tightness and swelling in her knees,

ankles, and back. MRI demonstrated periventricular T2-hyperintensities. She was diagnosed with MS and started on β -interferon treatment. On examination 3 years after onset, visual acuity was 20/200 OD and 20/30 OS. Ishihara color plates were 0/14 OD and 7/14 OS. There was an RAPD OD and funduscopy revealed temporal pallor OU, but worse OD. She had impaired vibration and position sense at the ankles and knees and hyper-reflexia in the legs with bilateral extensor plantar responses.



DISCUSSION

Field description: Bilateral cecocentral scotomata, worse on the right.

Localization: Bilateral optic nerve.

Pathology: LHON.

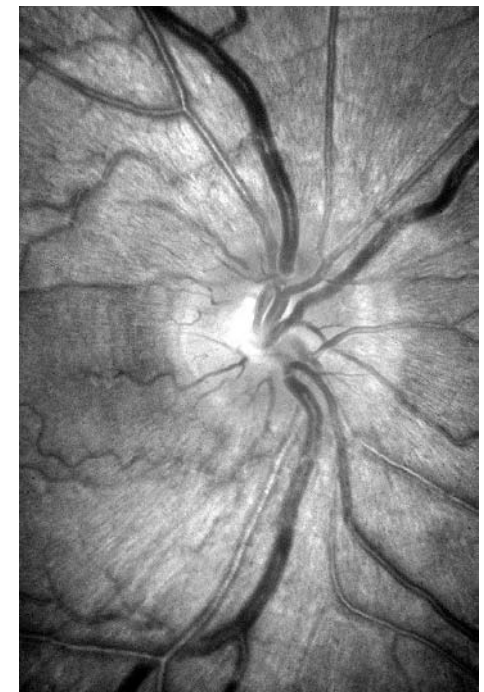
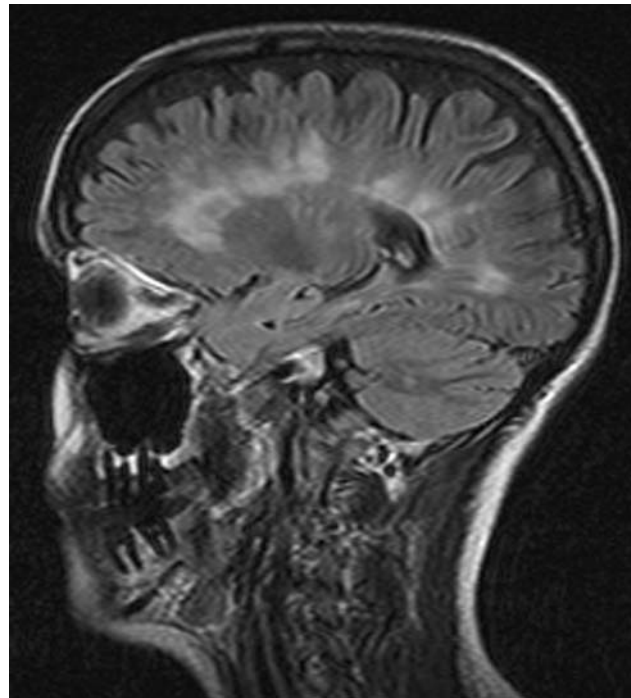
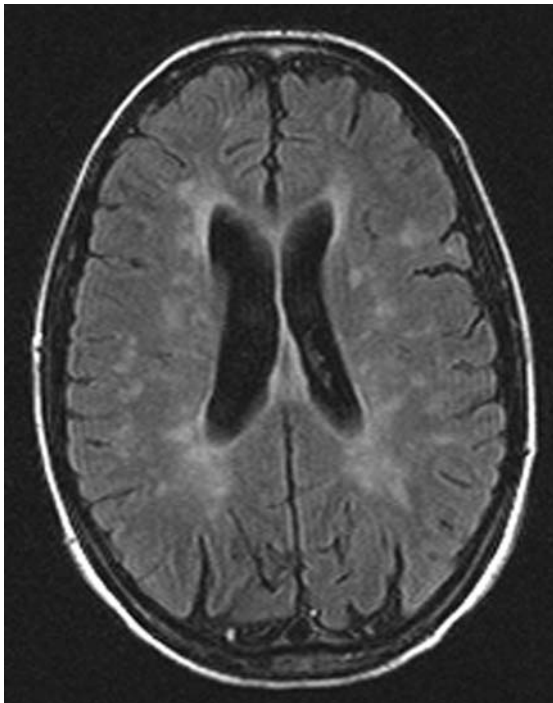
Confrontation testing showed left superior perifoveal scotomata OU to red targets and face comparisons.

The patient's fields show fairly large central depressions, slightly larger OD (deeper shade is an area where even the V4e target cannot be seen). In each eye, the area of highest remaining sensitivity is a small oval-shaped peak in the inferior field, just below the central valleys.

LHON is a maternally inherited optic neuropathy that typically affects men more often than women, usually in young adulthood. The presentation is usually subacute visual loss,

first in one eye and then the second within 6–12 months. The optic disc may appear normal or hyperemic with circumpapillary telangiectasias, as shown in the disc photo from another patient. It is the result of a point mutation in the mitochondrial genome, with mutations at positions 3460, 11778, 14484, and 14459 most frequently reported. The 11778 mutation, which this patient has, accounts for more than 50% of cases. The prognosis for visual recovery is particularly poor for patients with this mutation. Treatment is not effective, but many use Coenzyme Q10.

The patient's other neurologic history and MRI findings (see FLAIR images) are reminiscent of MS. Indeed, others have described patients with LHON who presented with an MS-like illness and periventricular white matter changes on MRI (66,67). Similarly, a study of a large number of patients with a diagnosis of MS found three patients with either the 11778 or 3460 mutation, all with severe bilateral optic neuropathy (68).

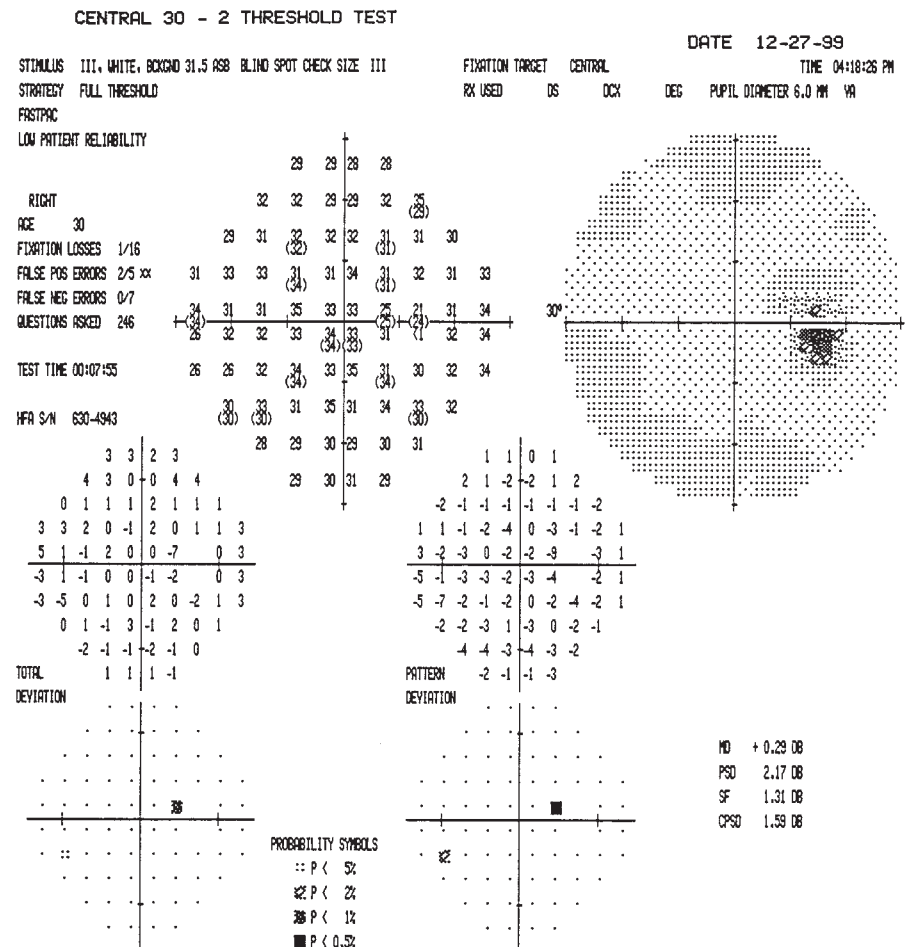
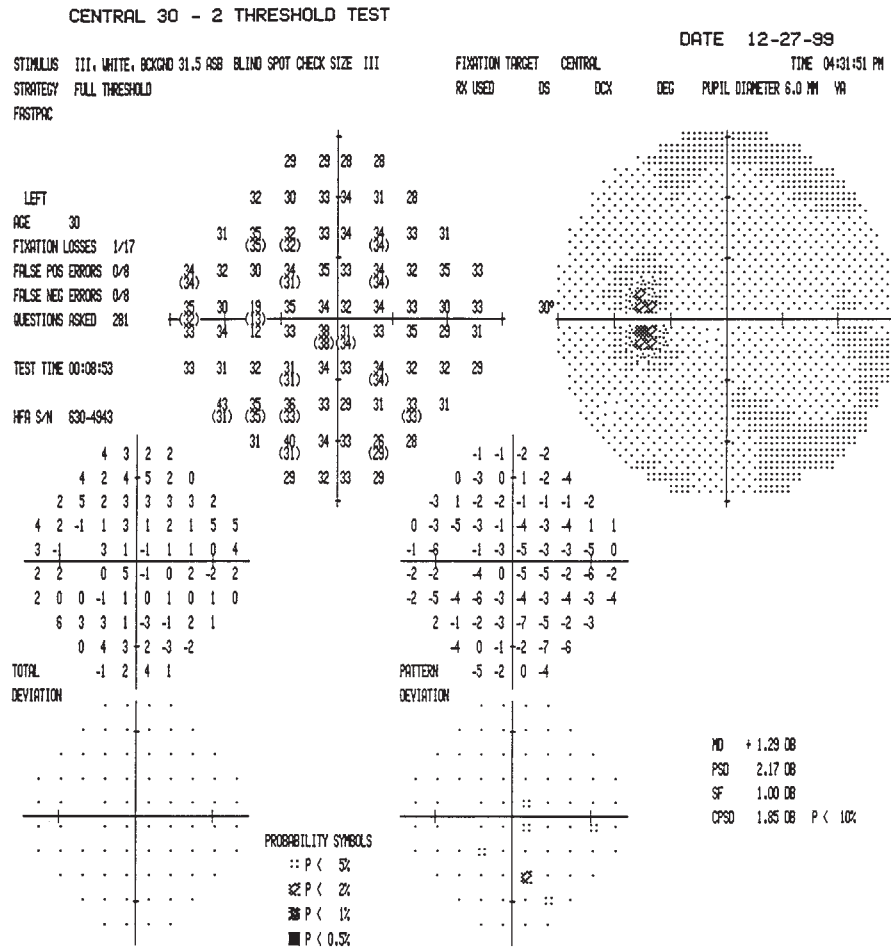


See Color Plate after page 180

HISTORY AND EXAM

This 30-yr-old woman had severe diffuse headaches constantly for a few weeks. Over the 3 days prior to her visit, she noted horizontal diplopia on right gaze and pulsatile tinnitus. Her examination in the emergency room showed papilledema. Computed tomography (CT) scan of her head was normal but the opening pressure on lumbar puncture was

50 cmH₂O, with otherwise normal CSF. Visual acuity was 20/20 OU and color vision was normal. Both optic discs were swollen but more so on the right, which also had peripapillary flame hemorrhages. There was a mild right VI nerve palsy. She weighed 252 lb, with a height of 5 ft., 5 in.



DISCUSSION

Field description: Mild enlargement of blind spot OD.

Localization: Optic disc.

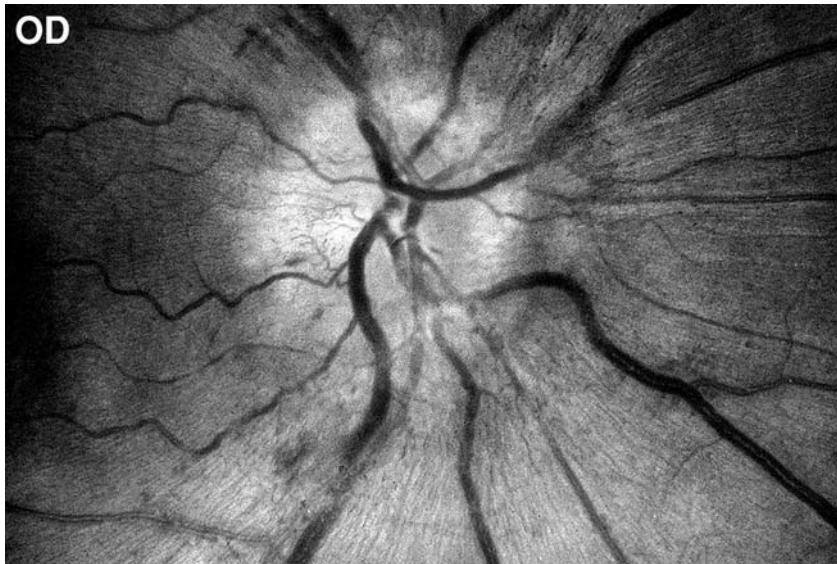
Pathology: Idiopathic intracranial hypertension (IIH), or pseudotumor cerebri.

Confrontation testing was normal.

Automated perimetry shows better reliability on the left than the right eye. This may be because in this, her first perimetric examination ever, the right eye was tested first (note in the upper right corners the time of 04:18, compared with 04:31 for the left eye). The right eye shows a high-responder criterion bias, with a false positive rate of 2/5. Despite this, she shows a depression at a location adjacent and superonasal to the blind

spot (see black square in pattern deviation). There may also be a slight depression just inferonasal to the blind spot on the other eye, but this is less significant, and there are other scattered reductions of a similar magnitude elsewhere in this field.

The diagnosis of IIH requires evidence of increased intracranial pressure with normal brain imaging and normal CSF contents. CSF opening pressure is under 25 cmH₂O in normal and obese subjects (69). The pathogenesis of IIH is unclear but may involve impairment of CSF reabsorption at the level of the arachnoid granulations (70). Weight gain and obesity are the only risk factors convincingly demonstrated in case-control studies (71,72). Vitamin A ingestion and tetracycline-related drugs may exacerbate the condition (73,74).

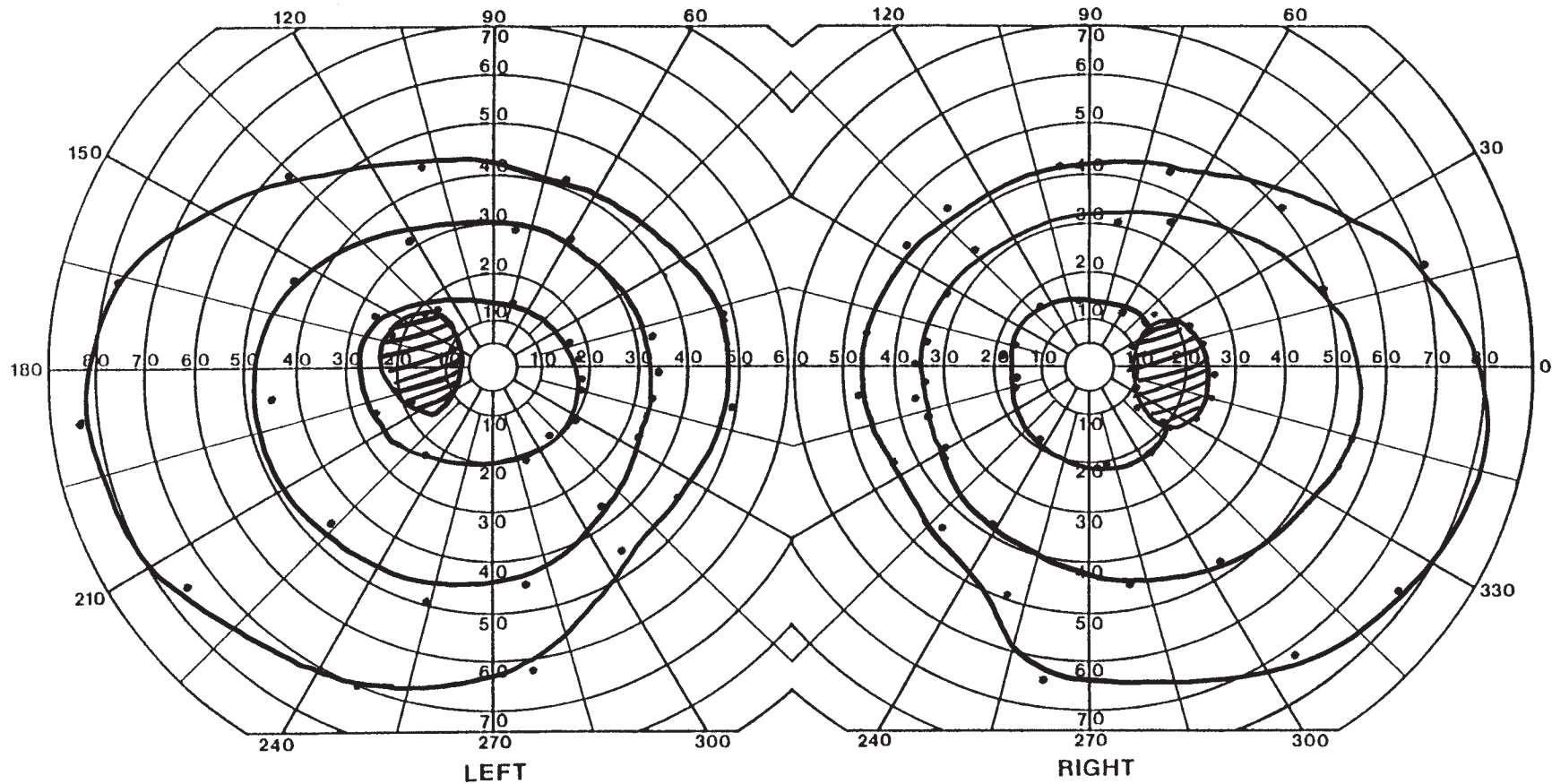


See Color Plate after page 180

HISTORY AND EXAM

This 26-yr-old woman had intractable headaches and was diagnosed with IIH. The headaches persisted despite repeated lumbar punctures and acetazolamide, and a lumbo-peritoneal shunt was inserted. She was referred because of persistent occipital headaches and episodes during which her vision would become hazy or black for 2–5 seconds. These

episodes were precipitated by bending over or standing up. She had gained 60–70 lb, to her current weight of 290 lb, over the preceding few years. On examination, visual acuity and color vision were normal OU. Fundoscopy demonstrated moderately severe chronic papilledema in both eyes.



DISCUSSION

Field description: Bilaterally enlarged blind spots.

Localization: Optic disk.

Pathology: IHH.

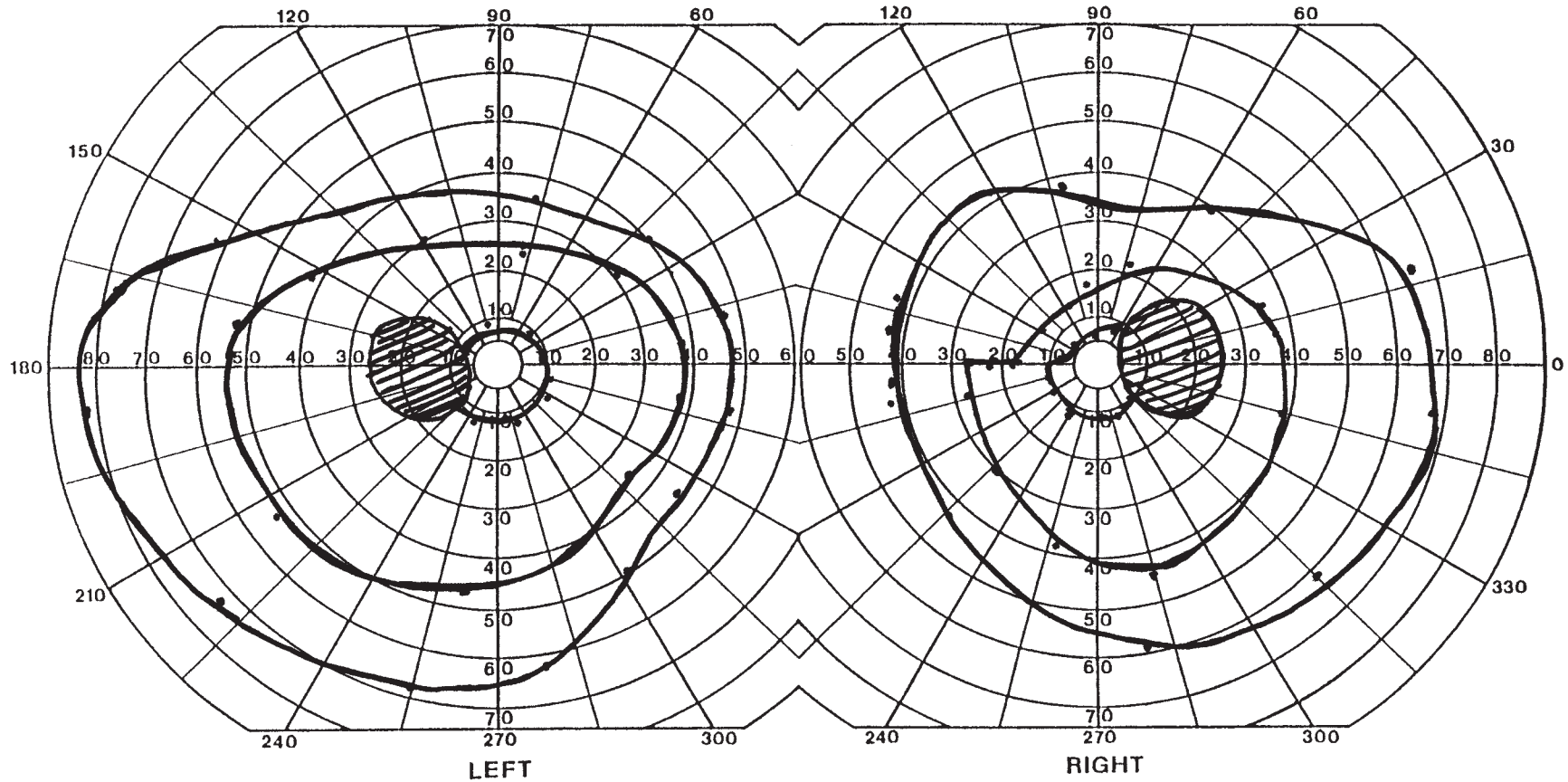
Confrontation fields were normal.

The patient's blind spots are two to three times the size of normal. She was restarted on acetazolamide but defaulted on treatment and returned almost 2 years later, at which time her perimetry was repeated, showing a superonasal step defect on the right (shown here).

Transient visual obscurations (TVOs) occur in 68% of patients with papilledema (71). They are episodes of monocular or binocular visual grayout or blackout lasting a second

or so, rarely minutes, unlike amaurosis fugax, which lasts minutes or more and is monocular. TVOs are likely a manifestation of transient ischemia of an edematous optic disk and are provoked by a postural change half of the time; the temporary drop in blood pressure exacerbates a marginal perfusion situation. TVOs do not occur with congenitally anomalous disk elevations (pseudopapilledema).

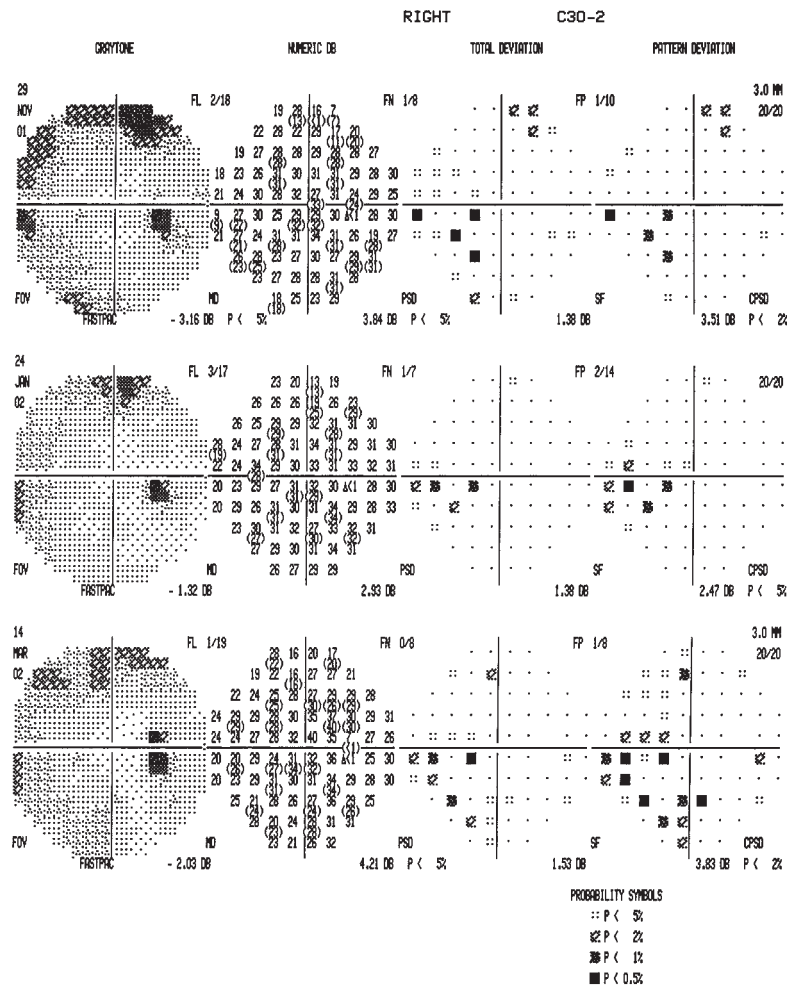
If untreated, chronic intracranial hypertension may cause a compressive optic neuropathy, not unlike the situation in glaucoma, in which it is intraocular pressure rather than transmitted intracranial pressure that is affecting the optic disk. The result is similar, with nerve fiber bundle defects developing, most commonly arcuate defects. The aim of treatment in IHH is the prevention of this visual loss, which can be permanent.



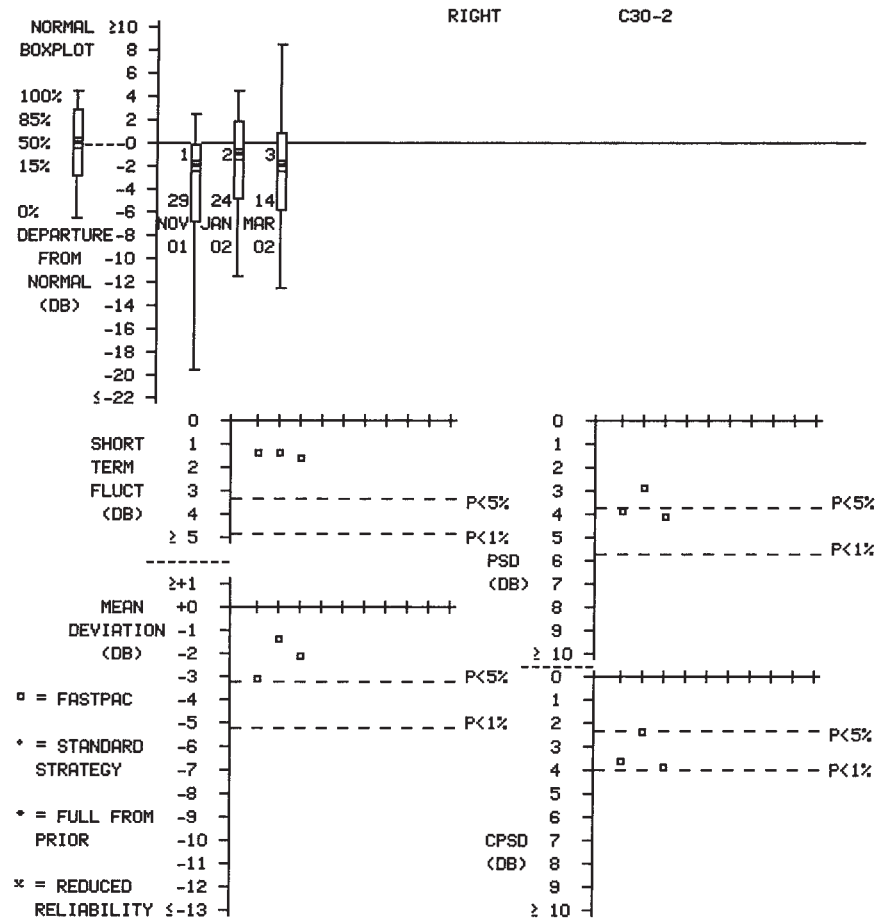
HISTORY AND EXAM

This 42-yr-old woman had 3 weeks of episodes of visual loss in the right eye, lasting 2 to 3 seconds, precipitated by standing up. The visual loss involved either the entire field or just the nasal aspect. She also had pulsatile tinnitus and more frequent headaches. Visual acuity was 20/20 OU and Ishihara color scores 13/14 OD and 14/14 OS. There was

no RAPD. Fundoscopy (next page) showed papilledema OD with circumpapillary hyperemia and vessel obscuration and a milder degree of disk elevation OS. Weight was 139 lb and height 4 ft, 11 in. The remainder of the neurologic examination was normal. An overview and change analysis OD are shown. The fields OS remained normal throughout.



Overview

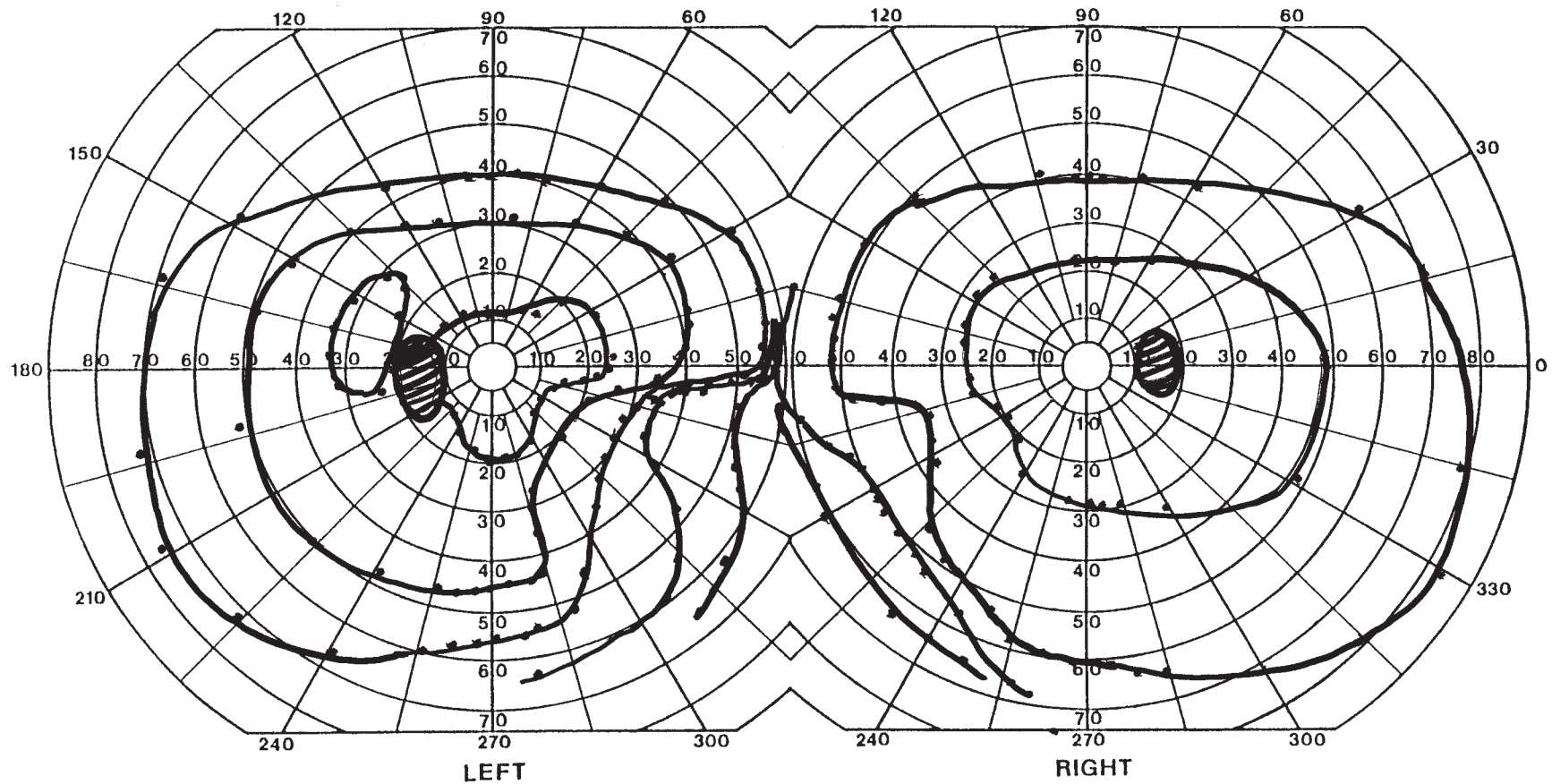


Change analysis

HISTORY AND EXAM

Two months earlier this 39-yr-old woman had been diagnosed with IIH, after presenting with transient visual obscurations OS for 5 months. The opening pressure on spinal tap was 44 cmH₂O. She had a history of recurrent fainting spells. Despite using 500 mg of acetazolamide twice a day, she noted a decrease in the nasal field of vision OS and

increasing occipital headaches in the 2 weeks prior to her visit. Acuity was 20/20 OD and 20/40 OS, with a clear RAPD OS. Ishihara color scores were 9/14 OD and 3/14 OS. Fundoscopy showed asymmetric papilledema, worse OS. There was a subtle esotropia in left gaze, and she had mild postural hypotension.



DISCUSSION

Field description: Inferior arcuate defect OS with enlargement of the blind spot, mild inferonasal step OD.

Localization: Bilateral optic nerve.

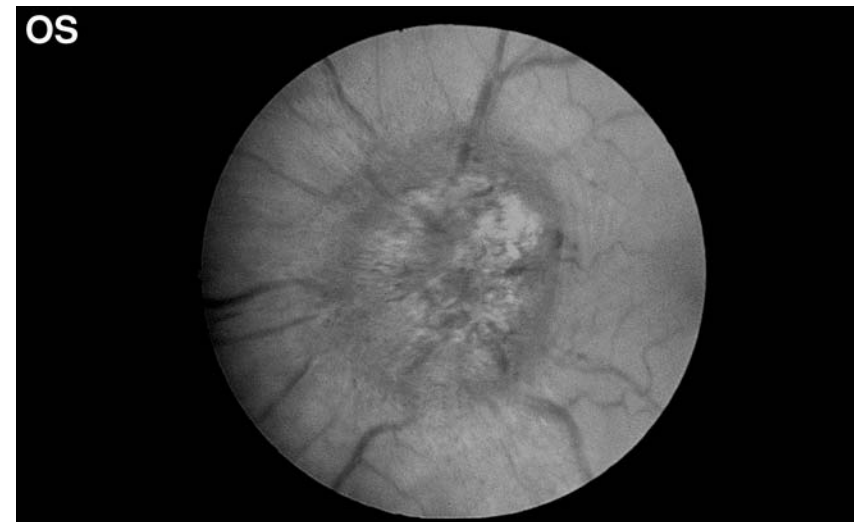
Pathology: IIH.

Added features: Left VI palsy.

While the enlarged blind spot is a minor refractive finding in this condition (see Case 46), the arcuate defect indicates that the swelling at the optic disk is causing axonal dysfunction. Her disks show asymmetric papilledema (76,77), worse on the left, the eye with more nerve fiber bundle loss. The fibrillary pattern of the disk edema in this eye indicates

that the papilledema is chronic. Papilledema is asymmetric in about 8% of cases (76). The asymmetry may be due to variation in the ability of the optic nerve sheaths to transmit intracranial pressure to the optic nerve head, given differences in the trabeculation and size of the subarachnoid space from one nerve to another (77).

The main risk in IIH is visual loss, and the goal of treatment is to prevent it. This patient developed visual loss early in the course despite compliance with medical treatment, which points to a need for more aggressive surgical management. The options are lumboperitoneal shunt or optic nerve sheath fenestration (78). Although there are no formal head-to-head trials, retrospective reviews suggest comparable efficacy (79). As with all shunts, the former may require episodic revision.

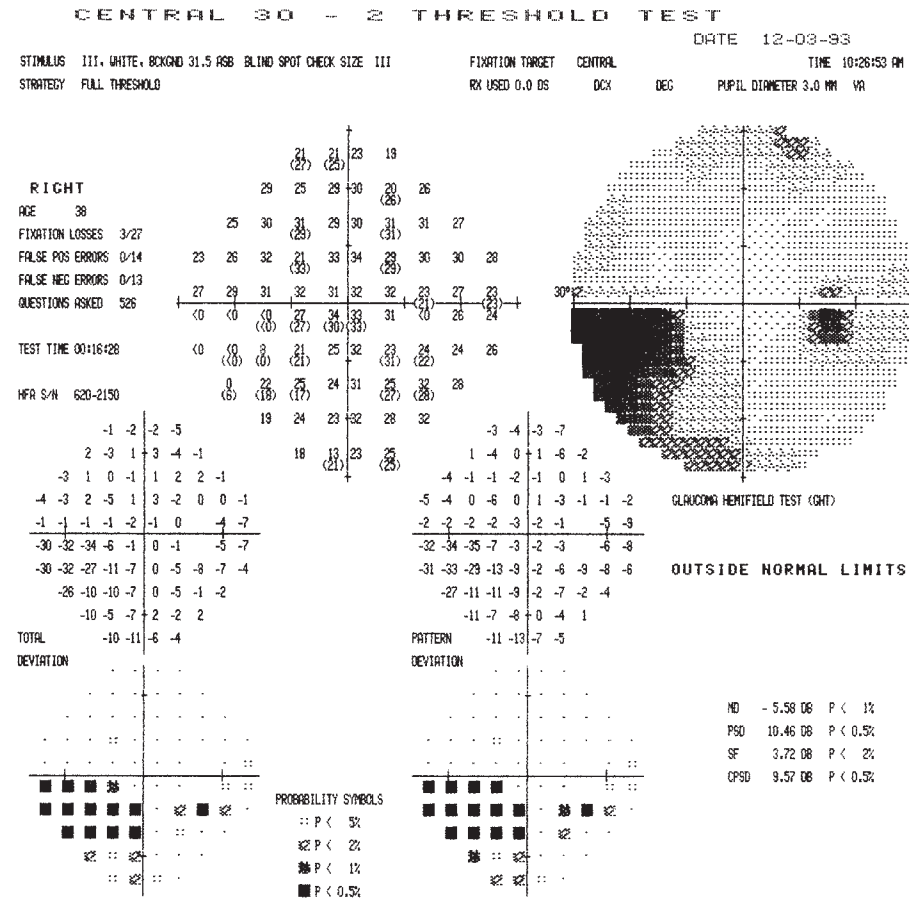
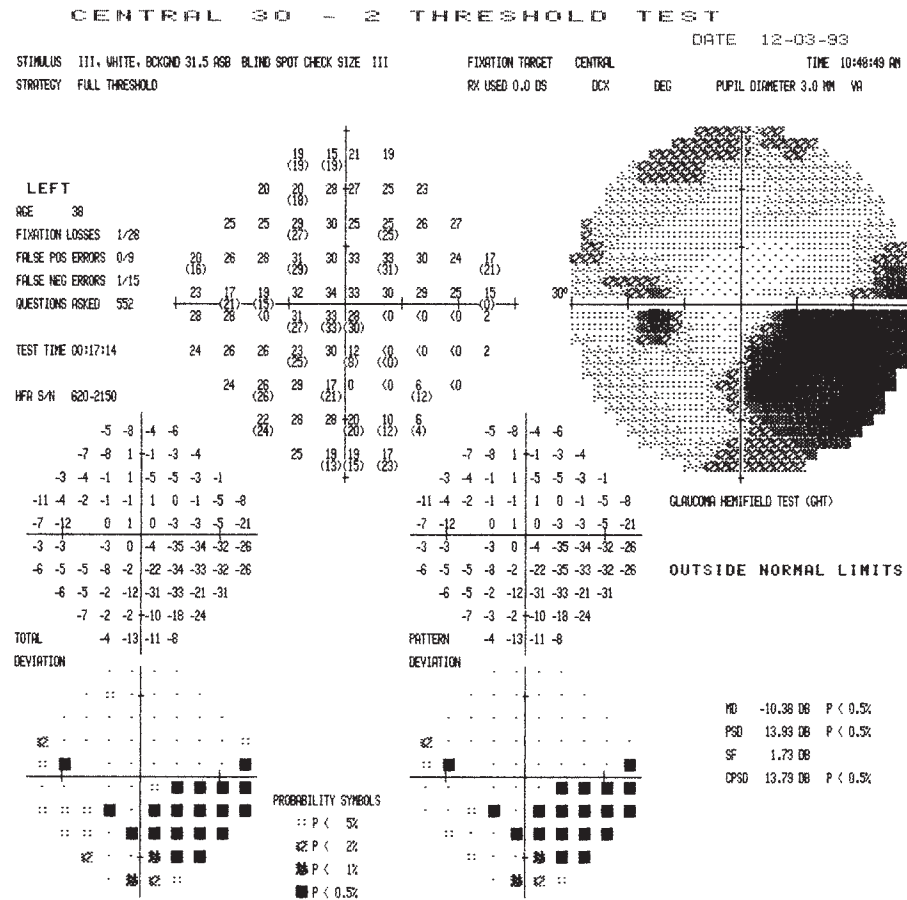


See Color Plate after page 180

CASE

This 37-yr-old woman was admitted with new headaches and recurrent seizures. She had recently had several transfusions and was on hormonal treatment for menorrhagia. She noted new blurred vision OS and horizontal diplopia. Acuity was 20/20 OU, with a

small RAPD OS. Ishihara color scores were 14/14 OU. She had bilateral partial VI nerve palsies.



DISCUSSION

Field description: Bilateral inferonasal step defects with enlarged blind spots OU.

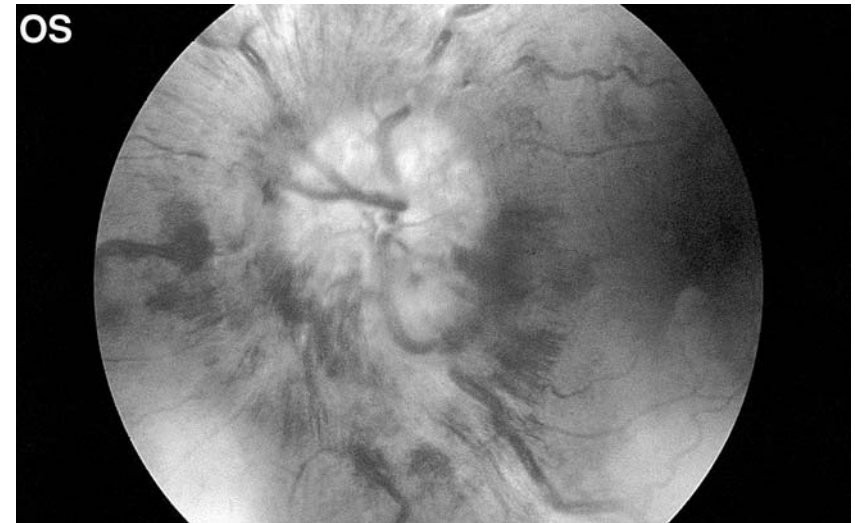
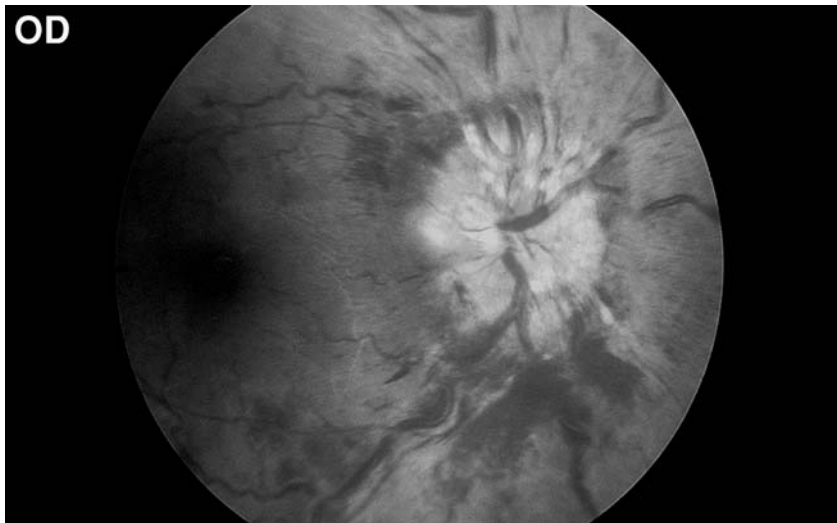
Localization: Optic nerve.

Pathology: Papilledema secondary to sagittal sinus thrombosis.

Tangent screen perimetry showed an inferonasal step defect OS.

The gray-scale images on automated perimetry clearly show the inferior arcuate defects with their nasal steps. The difficulty in showing the nasal step defect OD with tangent screen perimetry illustrates how easily some field defects from optic neuropathy can elude detection at the bedside. What is less apparent from the gray-scale image is the enlargement of the blind spots. This is shown better on the probability maps, which show some depression of test locations adjacent to the blind spots.

VI nerve palsies may occur with increased intracranial pressure of any cause. This patient's gender and age might suggest IIH, but seizures would be very unusual in this condition. Hormonal treatment can cause a hypercoagulable state, increasing the risk for dural sinus thrombosis, in which seizures are common (80). In addition, she had more severe papilledema and more hemorrhages than are seen in typical IIH. This likely reflects a more acute rise in intracranial pressure (81) from her sagittal sinus thrombosis. The best treatment of this condition is debatable, although there are some data in favor of anticoagulation (82). Her disk edema and fields improved over 4 months without treatment, and she remained seizure-free on phenytoin.

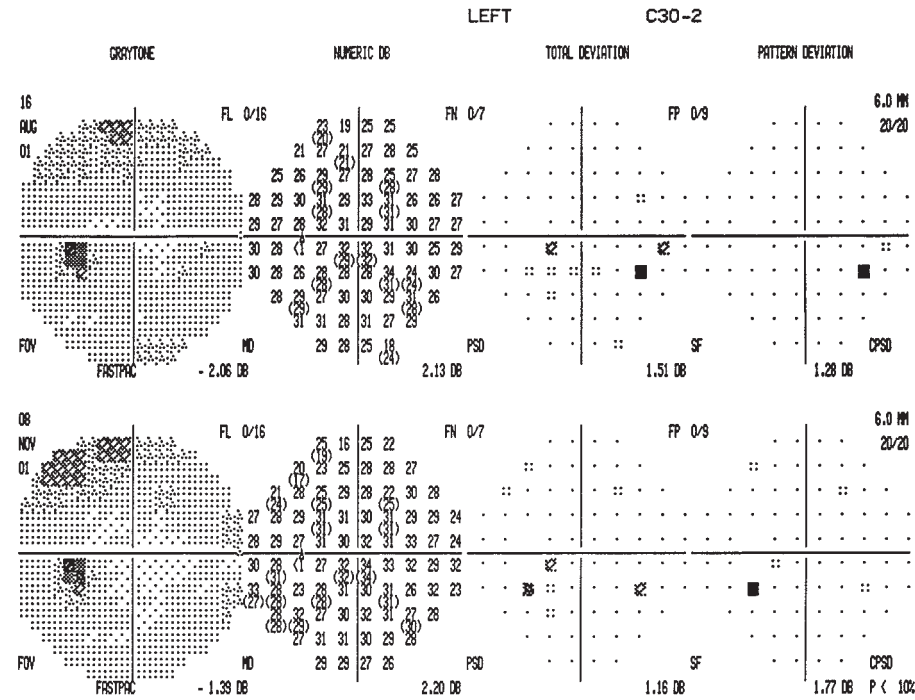


See Color Plate after page 180

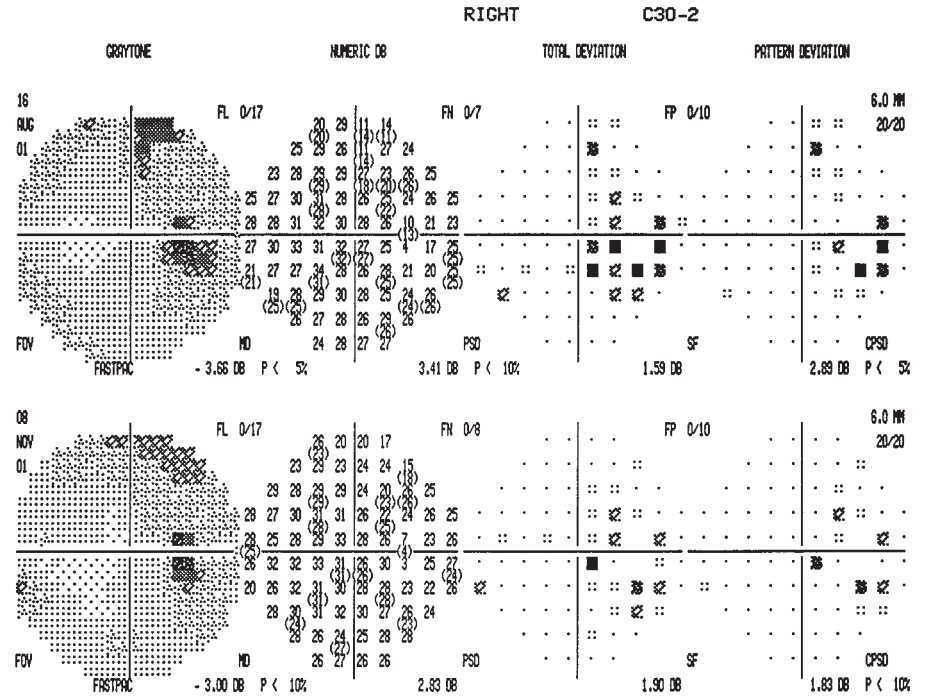
HISTORY AND EXAM

After a few days of flu-like illness, this 39-yr-old man was brought to the emergency room because of confusion. An MR venogram showed a cerebral venous thrombosis. Hematologic investigations uncovered a platelet count of 700,000 and a prothrombin gene mutation. He was started on coumadin. On evaluation 6 months later, his acuity was 20/20

OU, and he had evidence of congenital dyschromatopsia. There was no RAPD. Fundoscopy (shown next page) showed papilledema, worse OD, with choroidal folds OD. He had a mild left VI nerve palsy. He weighed 160 lb and height was 6 ft. An overview shows fields at this time and 3 months later.



PROBABILITY SYMBOLS
 :: P < 5%
 ☞ P < 2%
 ☛ P < 1%
 ■ P < 0.5%



PROBABILITY SYMBOLS
 :: P < 5%
 ☞ P < 2%
 ☛ P < 1%
 ■ P < 0.5%

DISCUSSION

Field description: Enlarged blind spot OD, improving on follow-up.

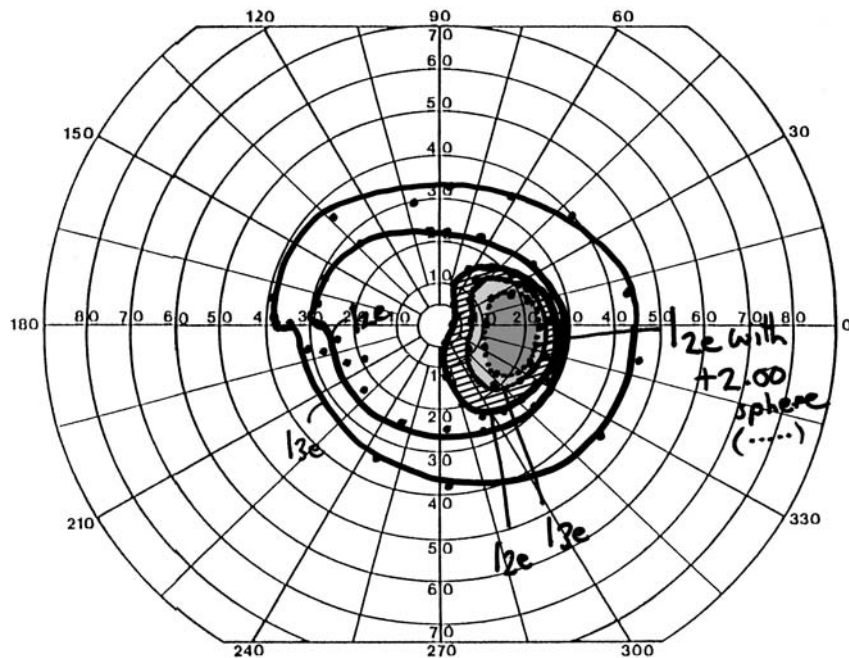
Localization: Optic disk.

Pathology: Papilledema from increased intracranial pressure due to venous sinus thrombosis.

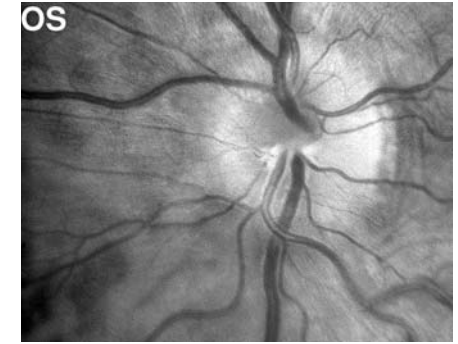
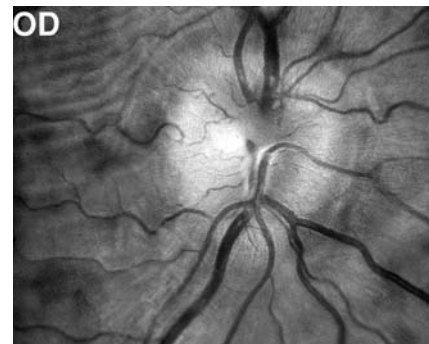
Confrontation fields were normal.

On Goldmann perimetry the marked enlargement of the patient's blind spot is less with the brighter I3e target than with the I2e target, indicating a relative defect. In addition, the enlargement on the I2e isopter shrinks when retested with a +2.00 spherical lens, showing that it is partly the result of elevation of the peripapillary retina out of the plane of focus, a phenomenon also suggested by the choroidal folds shown on his fundus pictures (83). The plus lens restores focus on this retinal zone and the faint small target becomes visible (84).

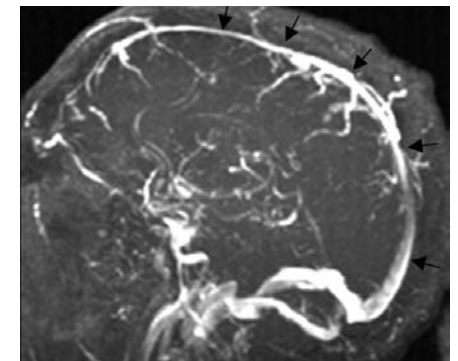
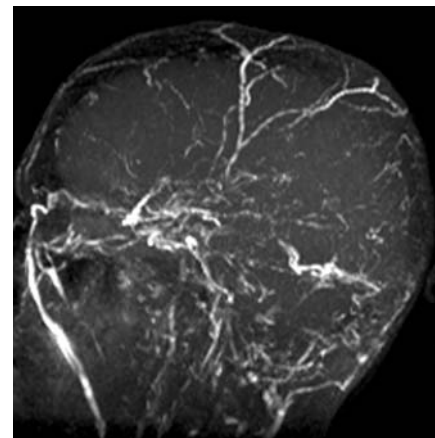
Three months later his disk edema had resolved nearly completely and his fields normalized.



IIH is not the only cause of papilledema in the absence of a mass lesion. Venous occlusion by a small sinus mass or thrombosis can increase intracranial pressure; usually the posterior third of the sagittal sinus and/or the lateral sinuses are affected (85). The patient's MR venogram shows absence of the sagittal sinus (contrasted with a normal MR venogram on the right, arrows). The presentation with confusion in a nonobese man clearly indicates that IIH is unlikely. However, venous thrombosis can present like IIH, with headache as the sole symptom and CSF contents normal (85). Hence, MRI and MR venography are being used more frequently to exclude sinus thrombosis in the work-up of IIH. Risk factors for thrombosis include systemic inflammatory diseases such as Behçet or lupus, the postpartum state, coagulopathies, and cancer.



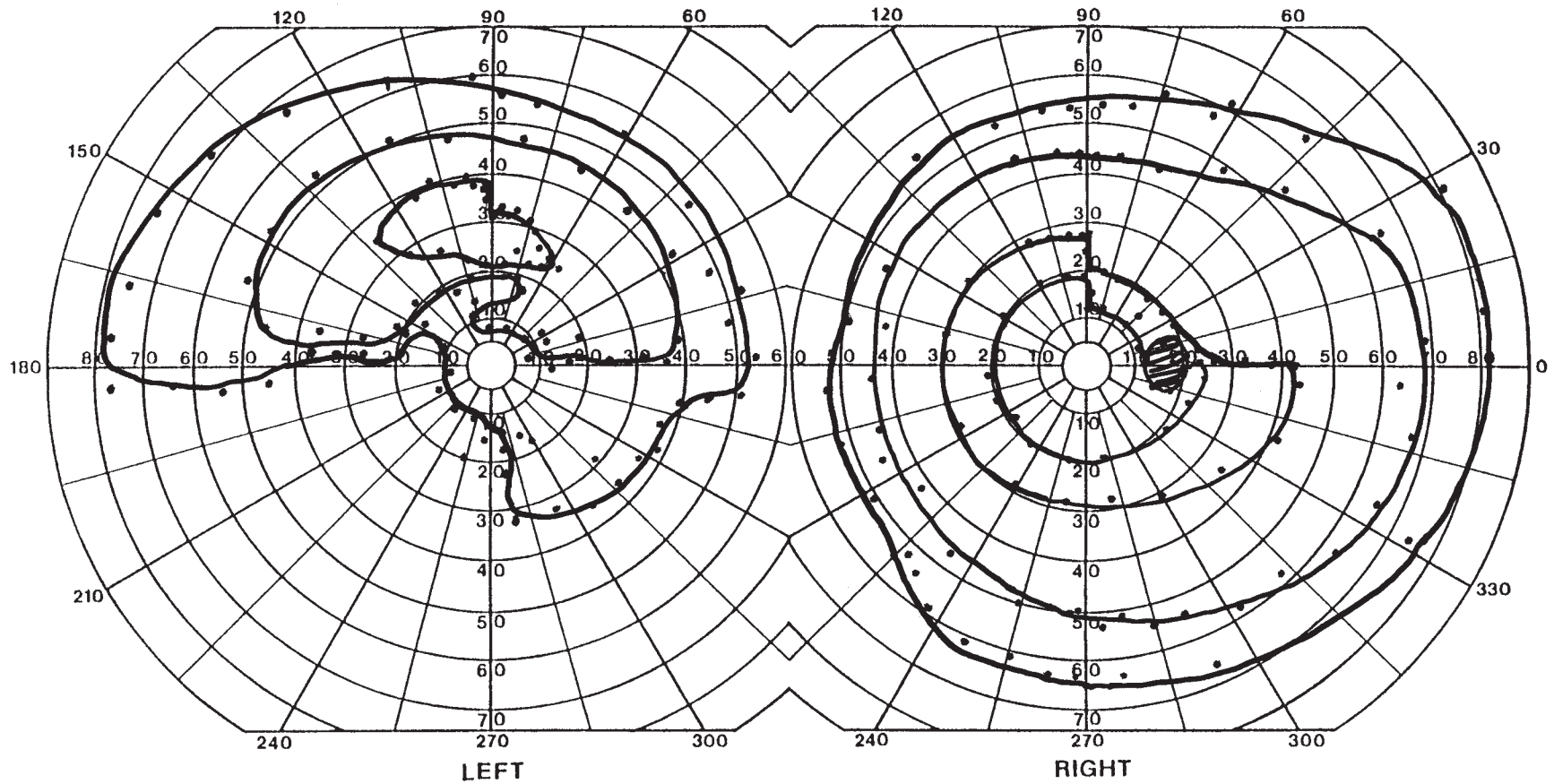
See Color Plate after page 180



HISTORY AND EXAM

This 48-yr-old man had 4 days of blurred vision OS. He had an aggressive neuroendocrine tumor of his colon resected 9 months earlier, treated with VP-16, carboplatin, and radiation, but with a metastasis to the pedicle of the T9 vertebral body 5 months later. For

2 weeks he had noted pulsatile tinnitus. He had recently tapered off dexamethasone. Acuity was 20/20 OU, with a small RAPD OS. Fundoscopy showed unilateral papilledema OS with engorged veins, but no hemorrhages. His legs were areflexic.



DISCUSSION

Field description: Partial inferior altitudinal and superior arcuate defect OS, with homonymous right superior quadrantic depression, respecting vertical meridian.

Localization: Left occipital lobe, left optic nerve.

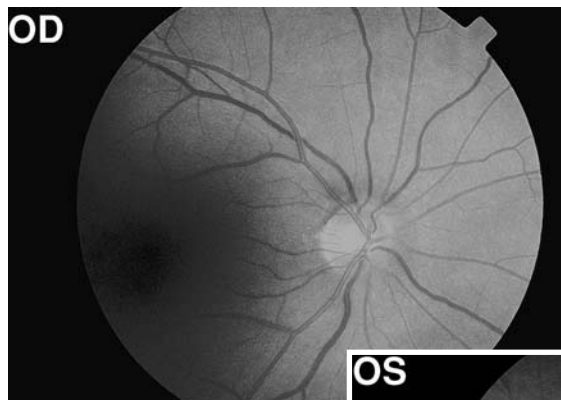
Pathology: Sagittal sinus metastasis and thrombosis causing increased intracranial pressure.

Confrontation testing showed an inferior field decrease to red comparison OS, sparing the macular region.

The Goldmann field shows a subtle vertical meridian effect in both eyes, raising suspicion of a homonymous postchiasmal defect. If this had not been documented, one might have erroneously concluded that the patient also had a relative superior temporal wedge defect OD.

The significant subacute visual field loss OS with disk edema suggested first a compressive or infiltrative optic neuropathy, given his metastatic cancer. However, this would

not explain the mild homonymous defects. Instead, he had an occipital metastasis (arrow) causing both striate dysfunction and sagittal sinus thrombosis (arrow-heads). The latter led to acutely raised intracranial pressure and rapid asymmetric papilledema with visual loss.



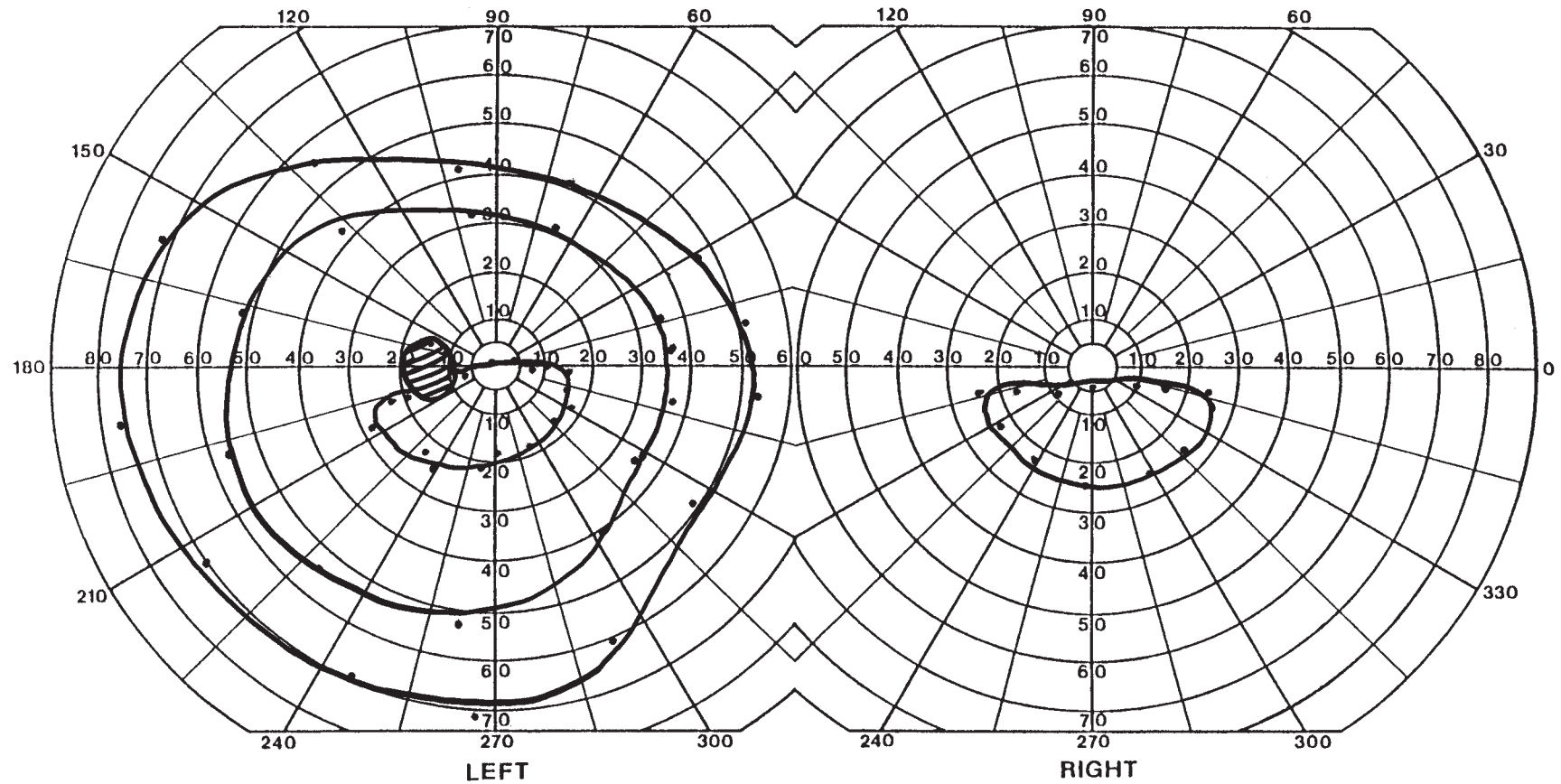
See Color Plate
after page 180



HISTORY AND EXAM

This 74-yr-old woman reported that for 2 weeks the top half of vision in the right eye was missing. She was uncertain about its tempo but had no eye pain or headache. She had hypertension and breast cancer, treated with mastectomy 3 years earlier, but complicated

by local recurrence and a solitary cerebellar metastasis that had been resected 7 months earlier. Visual acuity was count fingers OD and 20/25 OS. There was an RAPD OD and fundi were normal.



DISCUSSION

Field description: Superior altitudinal loss and marked constriction OD, superior parafoveal relative scotoma OS.

Localization: Retrobulbar optic nerves, bilateral.

Pathology: Metastatic cancer.

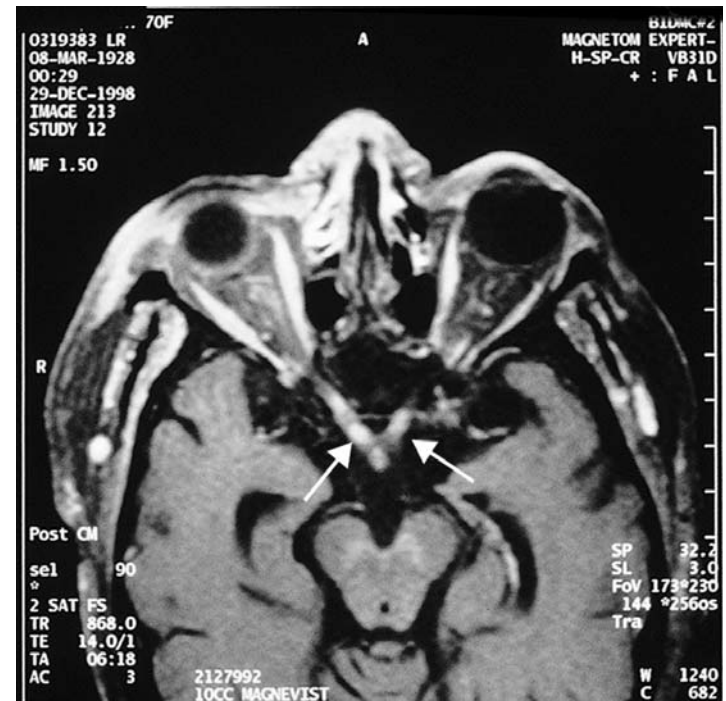
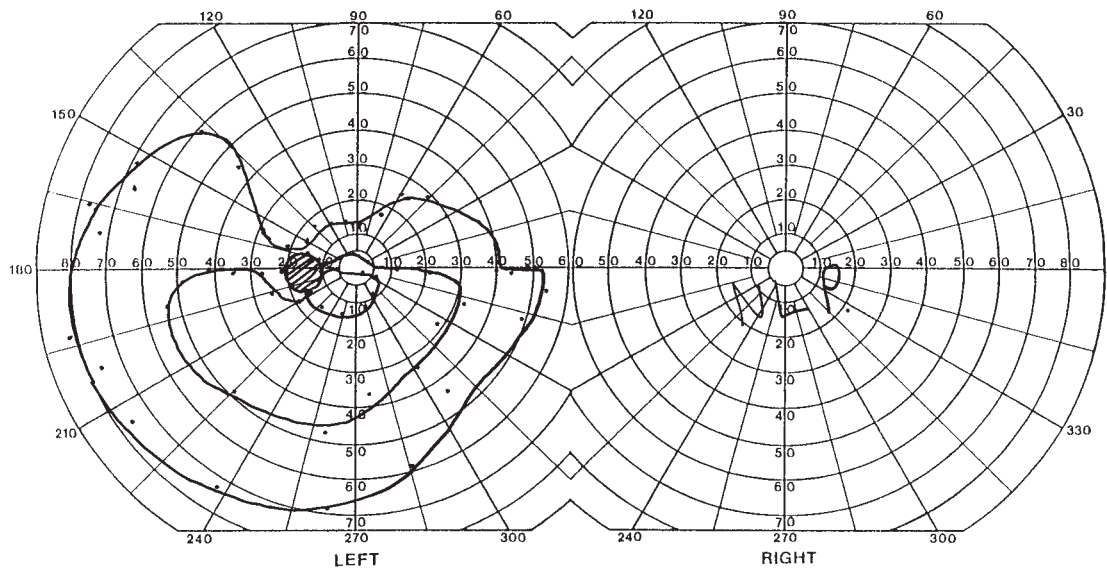
Confrontation testing showed a superior altitudinal defect OD to hand motion, with only hand motion left in the inferior field. OS was normal.

There is severe visual loss OD, with only an island of inferior vision. The apparent displacement of this from the horizontal meridian may be an artifact of displaced fixation of an eye with severely reduced acuity. More important, the other eye has a subtle problem, with depression of the superior central field, on testing with the smallest I2e target.

A unilateral altitudinal defect would suggest ischemic optic neuropathy, for which the patient's hypertension is a risk factor, but ischemia usually causes optic disk edema acutely. Without edema, with some defect in the other eye, and her cancer history, carci-

nomatous optic neuropathy was suspected instead. However, her initial MRI was normal, as were two CSF examinations. Her vision continued to worsen to no light perception OD and increased superior field loss OS 2 weeks later (shown here). Repeat MRI showed enhancement of the intracranial optic nerves (arrows), consistent with leptomeningeal carcinomatosis. She was treated with cranial irradiation, but died 3 months later.

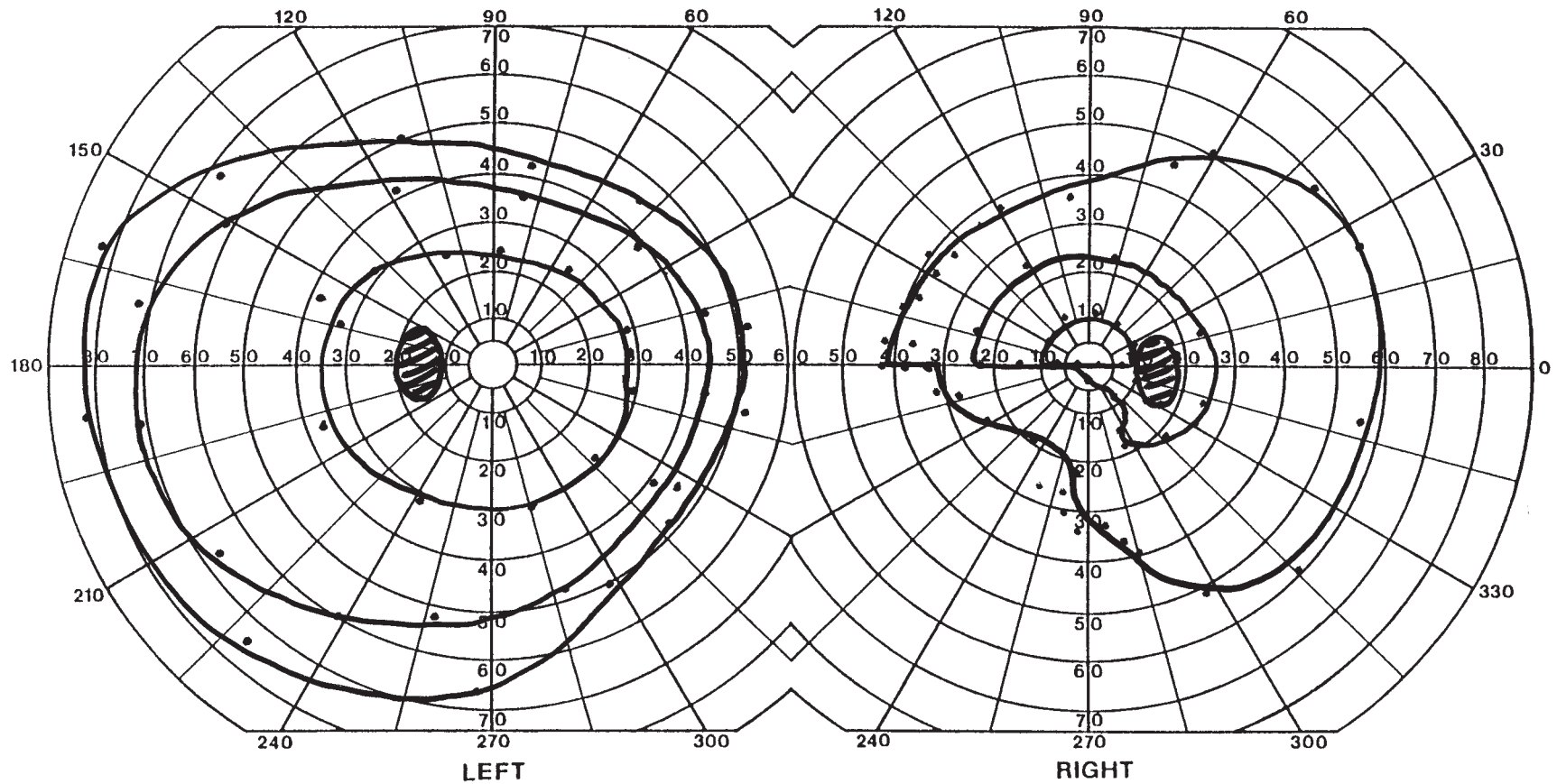
Meningeal spread is most common with breast and lung cancer, melanoma, non-Hodgkin lymphoma, and leukemia. Although the setting and subsequent course in this case made cancer likely, it illustrates the difficulty in confirming meningeal carcinomatosis. With solid tumors, a single CSF examination has positive cytology only 50% of the time (86). Three or more spinal taps are recommended to increase the yield to about 90% in suspicious cases. The value of maintaining a high index of suspicion and repeating initially negative investigations is evident. The life expectancy with meningeal cancer is about 4–6 months, with current therapy having a very modest impact on survival (86,87).



HISTORY AND EXAM

This 55-yr-old man suddenly noted decreased vision in the right eye when he incidentally covered his left eye one day a month earlier. Over this time, the vision in the right eye became progressively more blurry and he was bumping into people on his right side.

Visual acuity was 20/25 OD and 20/15 OS, and color vision was 12/14 OD and 13.5/14 OS. There was an RAPD OD. Fundoscopy demonstrated optic disk drusen OU. There was a slight proptosis OD.



DISCUSSION

Field description: Inferior arcuate defect with inferonasal step OD.

Localization: Right optic nerve.

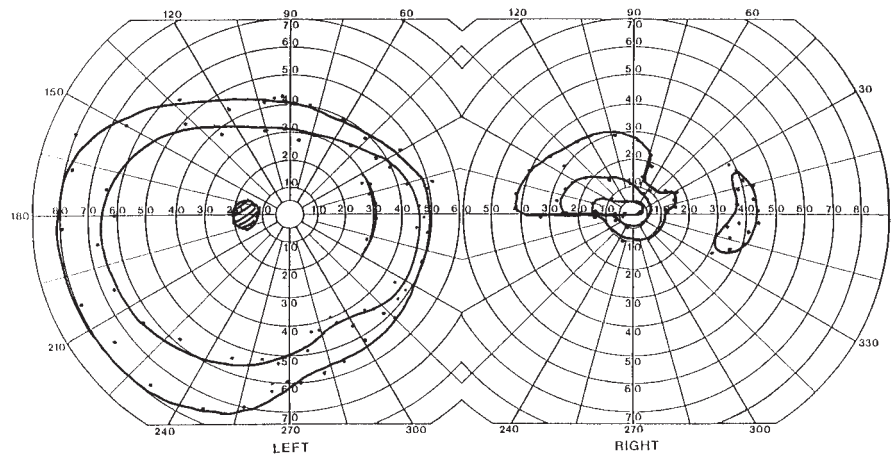
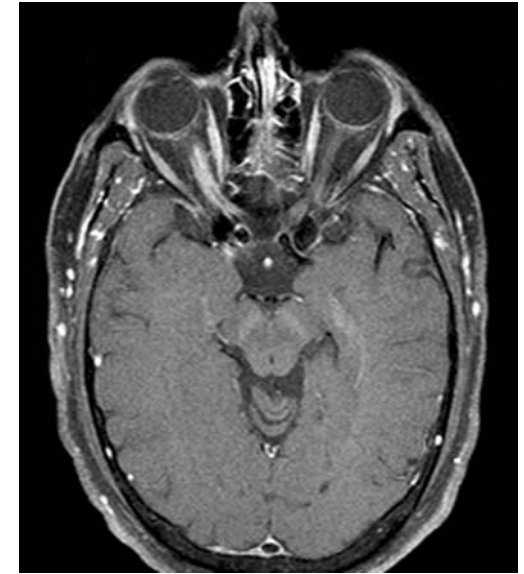
Pathology: Drusen, optic nerve sheath meningioma.

Confrontation testing showed inferior altitudinal defect for hand motion and comparison.

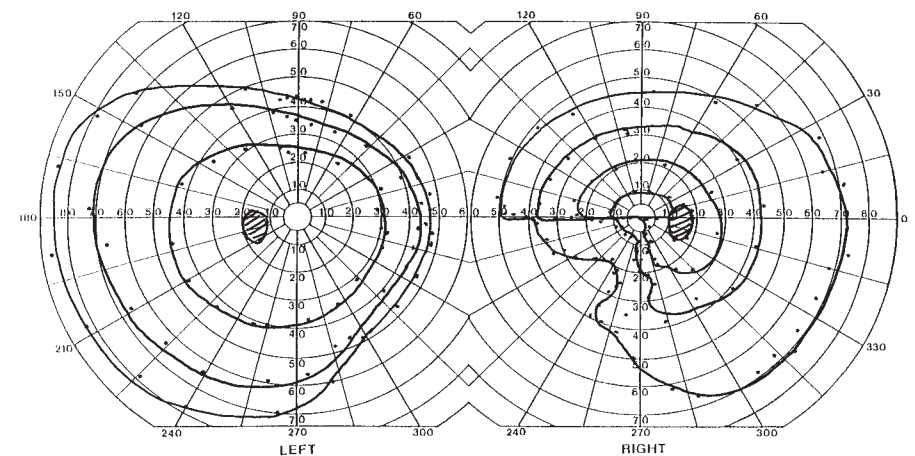
The patient's inferior field loss is a complete altitudinal defect for the smallest target, but for the largest it is mainly an inferonasal step defect. The predominant fibers affected would thus be the superior arcuate fibers.

He has an optic neuropathy, and a visible candidate for cause in the optic disk drusen (see Case 56). However, the question of slight proptosis and his insistence that the field loss had progressed over a month led to further investigations. T1-weighted MRI showed "tram-track" enhancement and enlargement of the intraorbital optic nerve, persisting in repeated imaging over 2.5 years, consistent with optic nerve sheath meningioma. His vision continued to deteriorate over the next 2 years, to an acuity of hand motions only OD (field A, this page).

The goals of treatment are to improve vision and prevent intracranial spread. Traditional surgery usually results in loss of all vision of the eye, and since these tumors are rarely aggressive, there has been controversy over whether they should be resected and, if so, when (88,89). Stereotactic radiosurgery is a recent potential advance on this dilemma (90,91). This patient subsequently had stereotactic radiosurgery, with dramatic improvement in his visual acuity to 20/25 OD and expansion in his field (field B, this page).



Field A

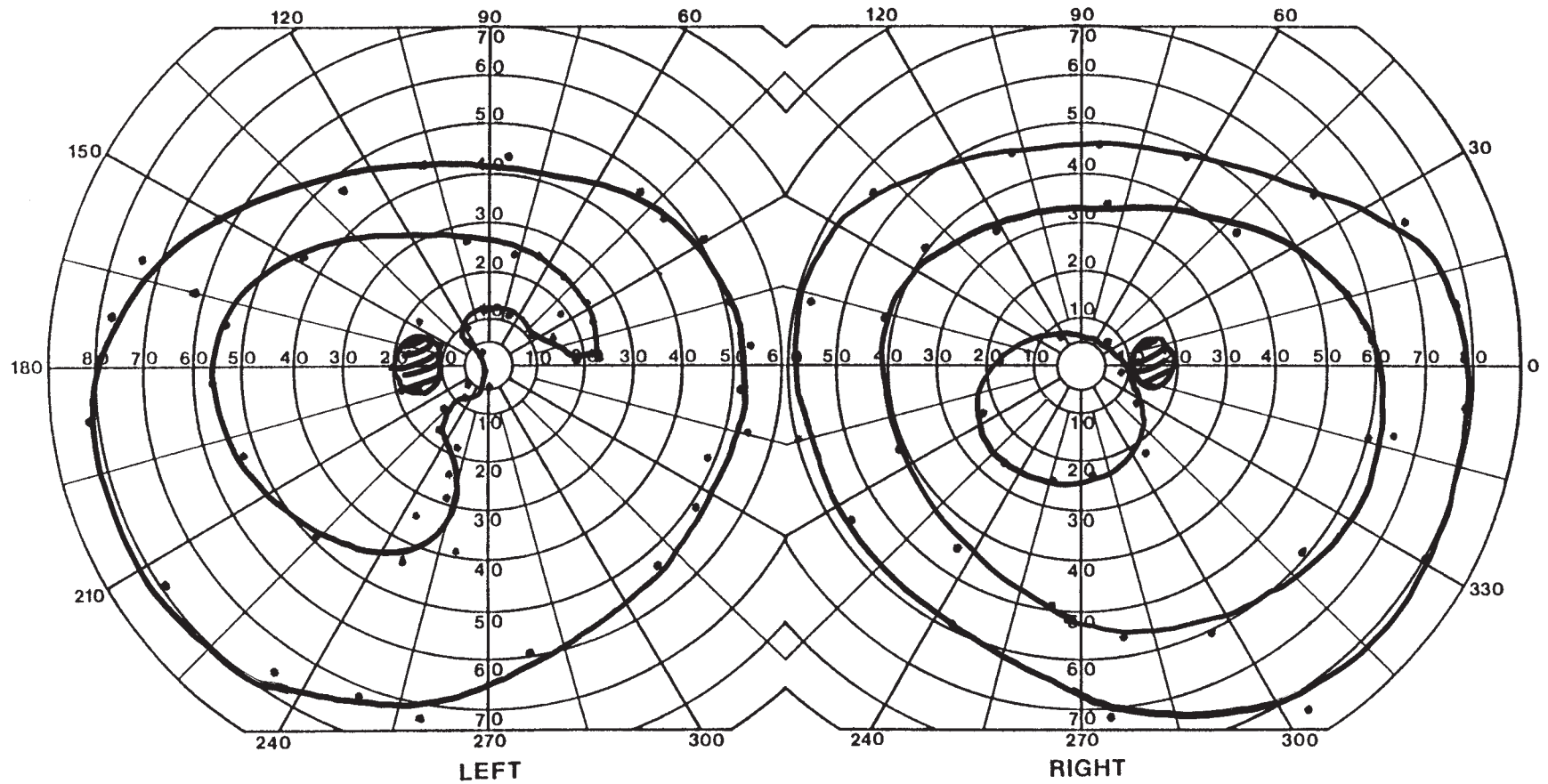


Field B

HISTORY AND EXAM

This 79-yr-old woman fell down a flight of stairs. In the emergency room, she reported flashes of light in her left eye but no visual loss. She had facial bruising. Visual acuity was 20/25 OD and 20/50 OS. Ishihara color plates were 12.5/14 OD and 11/14 OS. There was

an RAPD OS. Optic disks and retina appeared normal OU. The left eye also had severely limited adduction and depression, without anisocoria or ptosis.



DISCUSSION

Field description: Inferonasal defect as well as a small superior nasal arcuate defect OS.

Localization: Left intraorbital optic nerve.

Pathology: Orbital fracture.

Other features: Ophthalmoparesis.

Confrontation testing was normal.

The left eye shows an extensive inferonasal defect, and a milder superior arcuate defect, with some reduction in the central field as well.

CT scan confirmed a blowout fracture of the medial and inferior walls of the orbit. The axial section shown depicts the resulting opacification of the ethmoid sinuses, air within the orbit, and orbital edema, causing proptosis. The patient's visual dysfunction is likely the result of a traumatic optic neuropathy. The limited range of adduction and depression indicate medial and inferior rectus paresis due to either intraorbital third nerve damage or injury to the muscles, with or without entrapment by the orbital wall fractures.

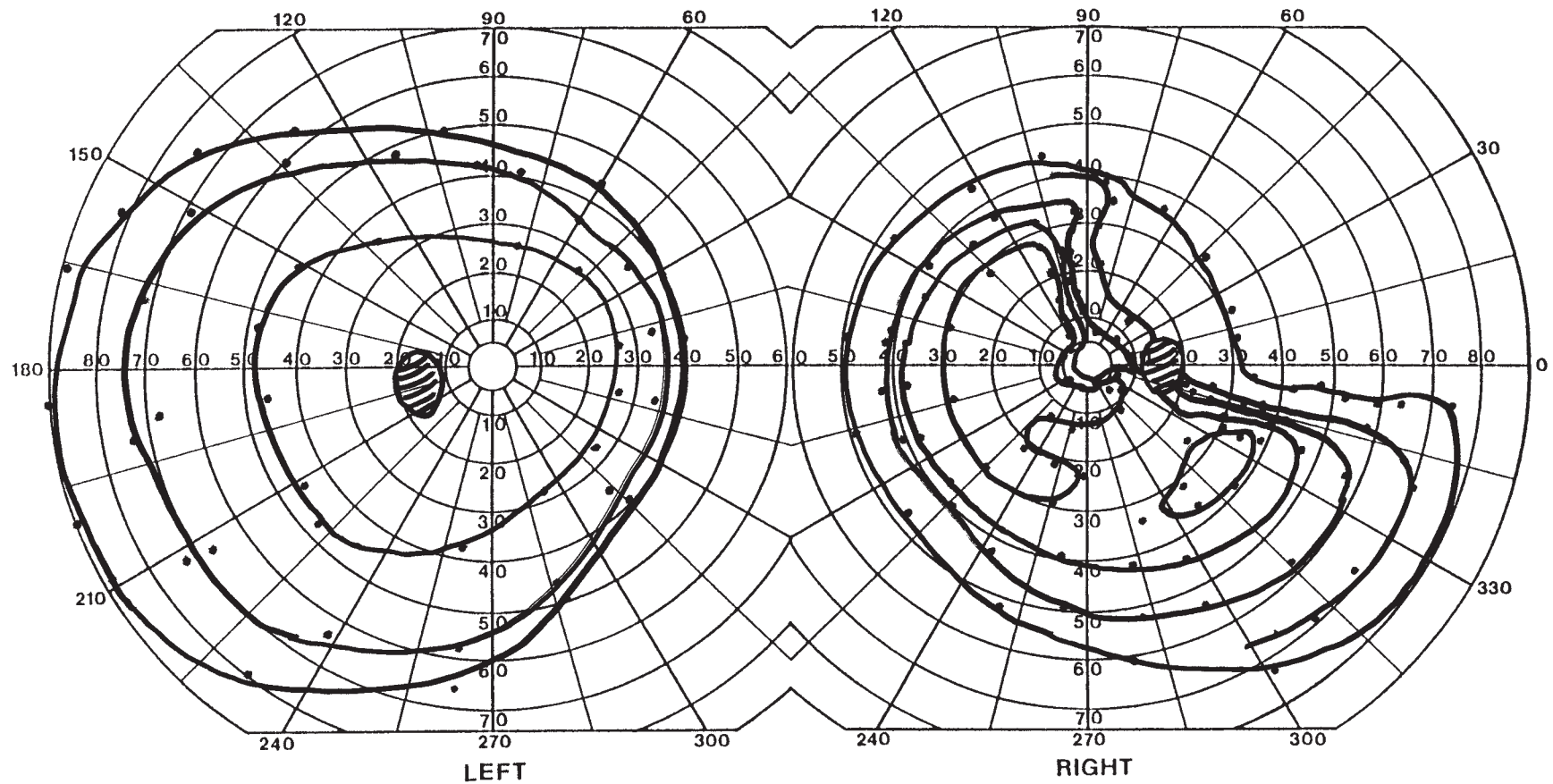
Traumatic optic neuropathy should be suspected in any patient with a severe head injury or periorbital trauma. With midfacial fractures, the likelihood of visual loss correlates with the extent and severity of bony damage (92). Most often, the optic nerve is injured indirectly as a result of the concussive forces to the head that produce both mechanical and ischemic insult. Surgery is indicated if imaging reveals compression of the nerve by bony fragments or an optic nerve sheath hematoma, which usually presents with delayed worsening of vision (93).



HISTORY AND EXAM

This 23-yr-old man suffered an accident while bicycling without a helmet. He had a severe closed head injury with loss of consciousness and a post-traumatic amnesia spanning a period of a few days. On regaining consciousness, he noted visual loss and was

treated with iv steroids for 2 days. Six days after the head injury, visual acuity was 20/40 OD and 20/20 OS with Ishihara color scores of 13/14 OD (slow responses) and 14/14 OS. There was RAPD OD. Fundoscopy was normal.



DISCUSSION

Field description: Combination of a superotemporal wedge defect, a central scotoma, and a mild relative inferior arcuate defect OD.

Localization: Optic nerve.

Pathology: Trauma.

Confrontation fields showed a decrease in the superior temporal quadrant OD.

The patient has lost much of the superotemporal quadrant, extending to a relative depression of the central field. Inferiorly, the smallest isopter shows a temporal peak and a notch between 10 and 20° in the inferior nasal quadrant, both marking a depression in the course of an arcuate nerve fiber bundle. Head CT was normal, showing no evidence of bony fracture.

In at least one series, bicycle accidents were the most common cause of indirect optic nerve injury (94). Fractures through the optic canal were seen in a minority, but the visual

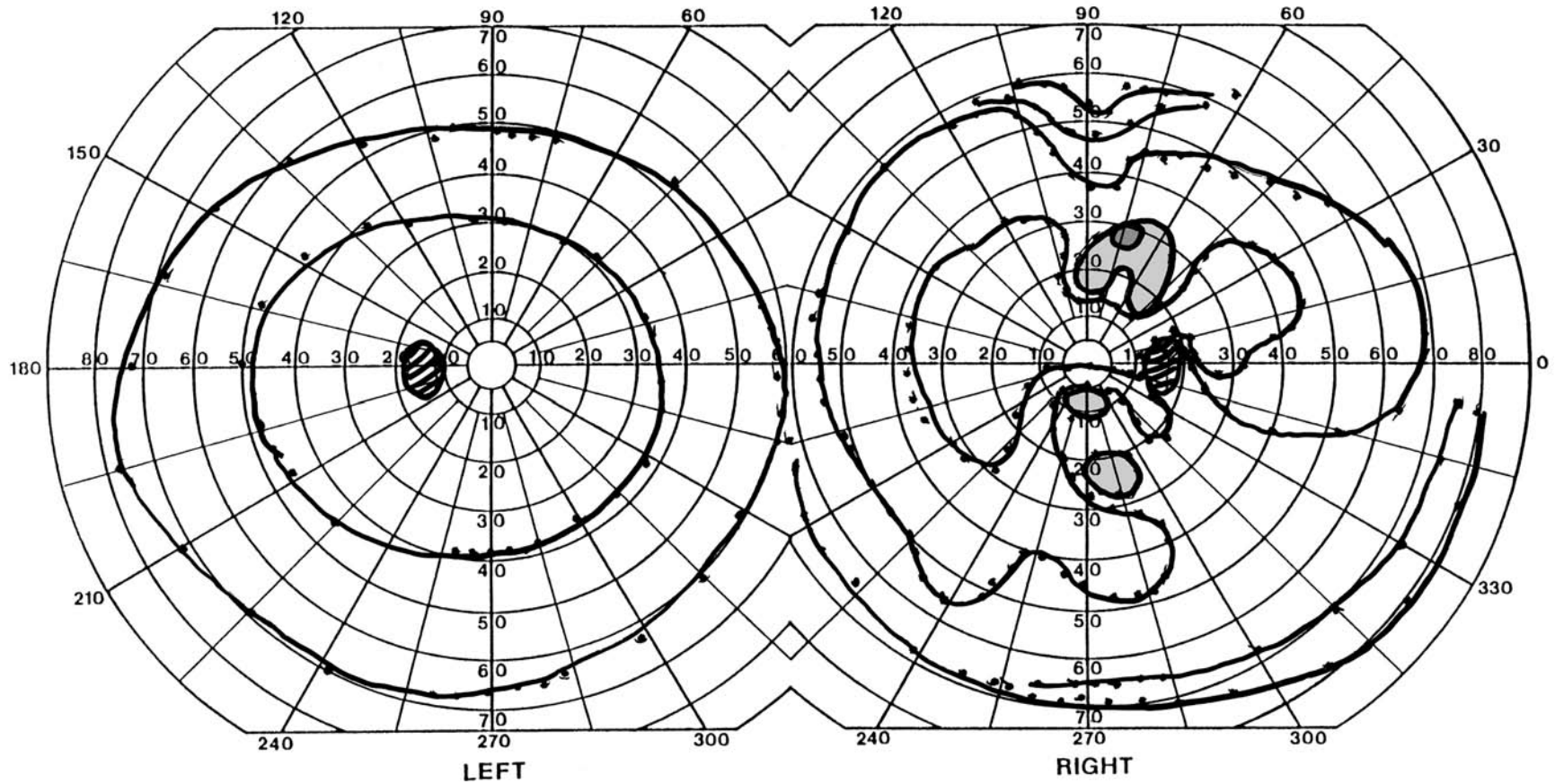
prognosis did not differ between those with and without such fractures, nor did it correlate with the state of consciousness at injury, unlike other neurologic sequelae. The treatment options are high-dose iv steroids and/or optic canal decompression. While a meta-analysis suggested potential benefit with these (95), the International Optic Nerve Trauma Study did not find convincing evidence of efficacy for either treatment over observation alone (96).

There is no specific visual field defect for traumatic optic neuropathy, although some clinicians have noted that isolated involvement of the superior visual field is rare (97). This is thought to reflect the fact that the inferior optic nerve is less tightly bound than the superior nerve to the optic canal, which is presumed to be the most likely site of transmission of shearing and compressive forces to the optic nerve (98).

HISTORY AND EXAM

This 54-yr-old woman suddenly noticed blurred vision and impaired reading OD 6 months earlier. Vision was impaired centrally and inferiorly, like a “clear mesh.” Two months after onset, an optometrist noted optic atrophy OD. Her acuity then was 20/60

OD. Over the next few months her vision worsened, and she had a continuous dull retro-orbital ache. Acuity was now 20/100 OD and 20/20 OS. Ishihara color scores were 0/14 OD and 13/14 OS. There was a moderate RAPD OD, with temporal disk pallor OD.



DISCUSSION

Field description: Superior paracentral scotoma, inferior scotoma in the Bjerrum area, and inferior temporal defect extending to the blind spot OD.

Localization: Optic nerve OD.

Pathology: Optic canal meningioma.

This is a complex defect in one eye, with patchy involvement of multiple nerve fiber groups. The inferior temporal field is most affected, with deep paracentral and central scotomata. In addition, there is a superior paracentral U-shaped defect, with depression of the isopters peripheral to this spot.

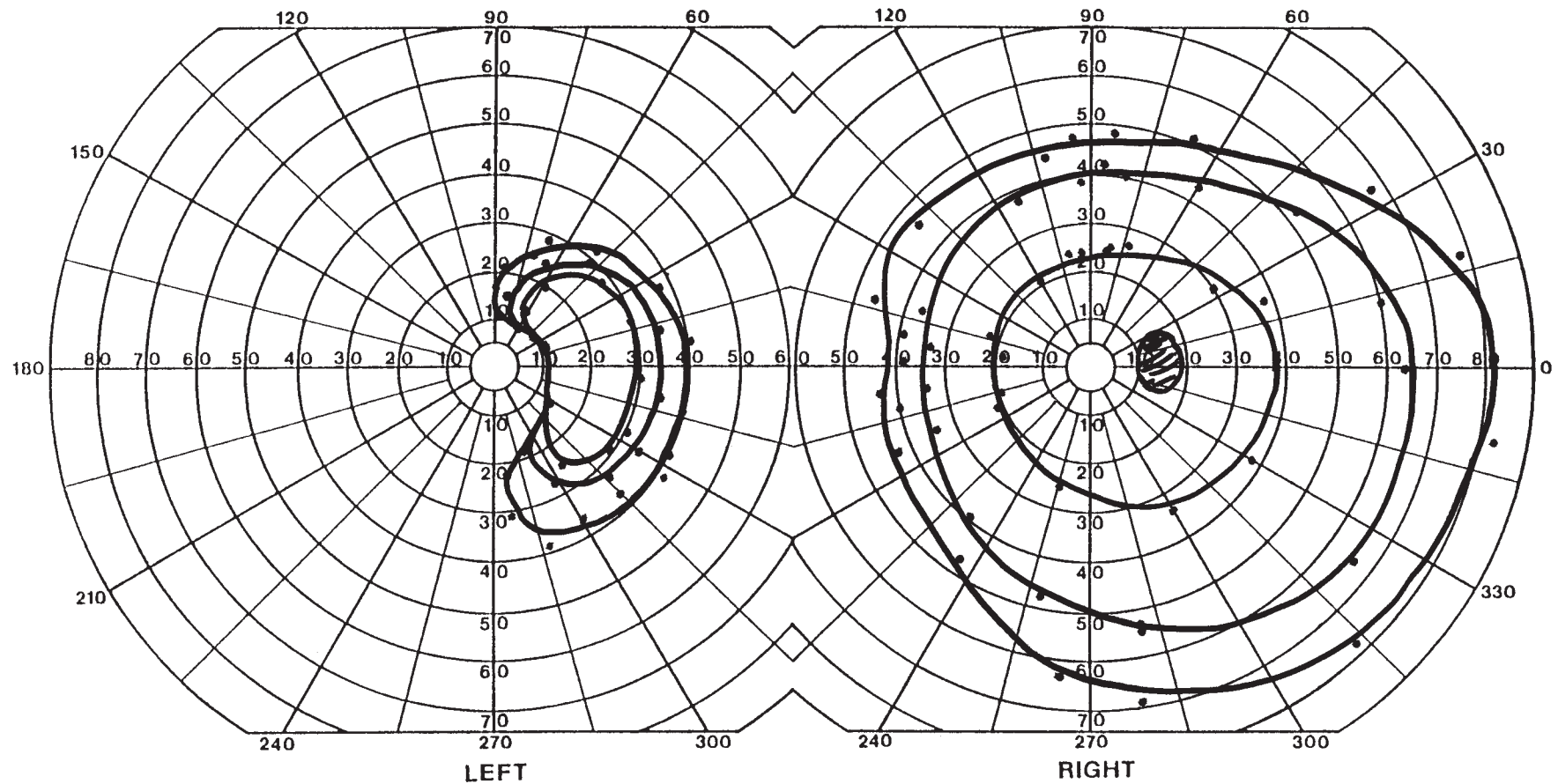
AION was initially suspected at the patient's optometric assessment, which is possible since the disk edema of AION usually resolves into optic atrophy over a few months. (The same can be said of the retinal pallor of CRAO.) Without documentation of disk edema in the acute phase, however, the diagnosis of AION cannot be confirmed. Sudden (ischemic) visual loss may then be confused with suddenly noticed (compressive) loss, as was the case here. The subsequent progression of visual loss by symptoms and measurements over some months raised the suspicion of a compressive lesion. This small optic canal meningioma (arrow) could easily have been missed on routine MRI of the brain and illustrates the value of MRI focused on the orbit, with coronal views, as shown here on the T1-weighted image.



HISTORY AND EXAM

This 51-yr-old woman first noted 2 months earlier that her left eye could not see to the left during a driver's license test. This defect gradually enlarged to eliminate the temporal half and lower nasal field of vision in that eye alone, without pain or proptosis. She had had a left VII nerve palsy 22 years earlier, which partially recovered, leaving chronic

facial pain. A brain MRI 12 years earlier was normal. Acuity was 20/20 OD and count fingers at 4' OS eccentrically. Ishihara color score was 14/14 OD. There was a large RAPD OS and severe optic disk pallor OS. She had mild left facial weakness with aberrant regeneration, and decreased hearing on the left.



DISCUSSION

Field description: Nasal island of vision OS.

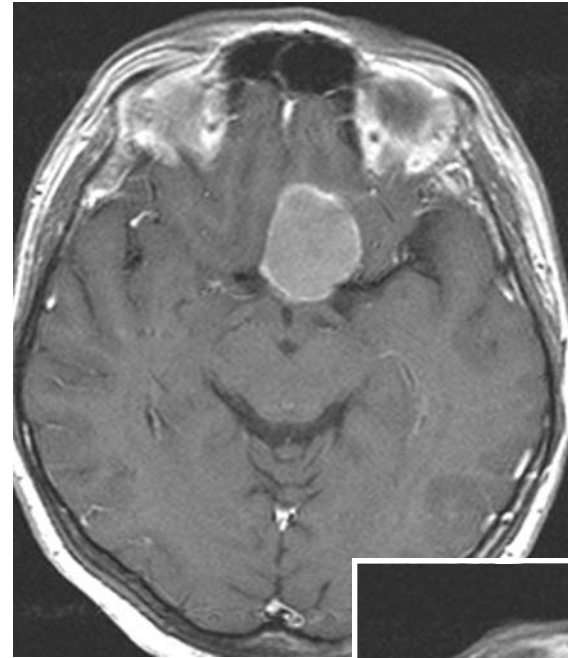
Localization: Optic nerve.

Pathology: Meningioma with optic nerve compression.

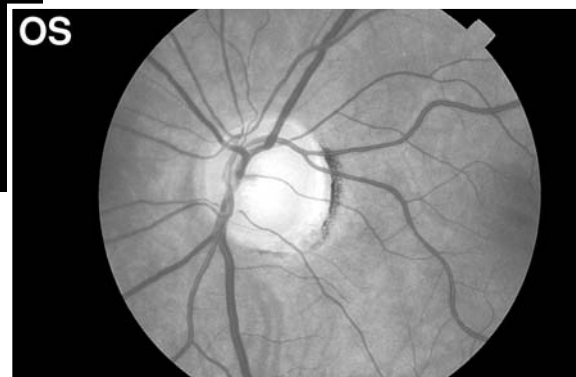
Confrontation testing showed a nasal island of vision OS to finger counting.

This is a severe optic neuropathy, with a nondescript island of residual vision. Its extent and location are a bit imprecise given that accurate fixation was limited by the patient's poor central acuity.

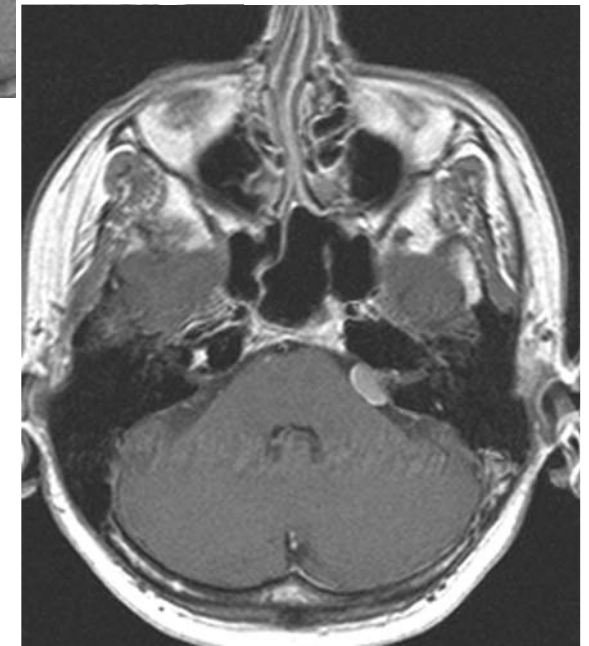
The story of prior facial weakness and new visual loss may have initially suggested MS. However, aberrant regeneration is more likely with a peripheral lesion. The chronic facial pain and hearing loss are both highly unusual for either MS or a Bell's palsy. Rather, a mass in the internal auditory canal is suspected. The progression of visual loss also suggests a mass compressing the optic nerve. The optic nerve and internal auditory canal are relatively far apart, so two lesions are probable. Multiple meningiomas (99) or neurofibromatosis type 1 and 2 (100) are the main suspects. T1-weighted MRI with gadolinium showed two meningiomas, a large suprasellar one compressing the left intracranial optic nerve, and a smaller one in the left internal auditory canal, missed on her imaging 12 years earlier.



See Color Plate after page 180



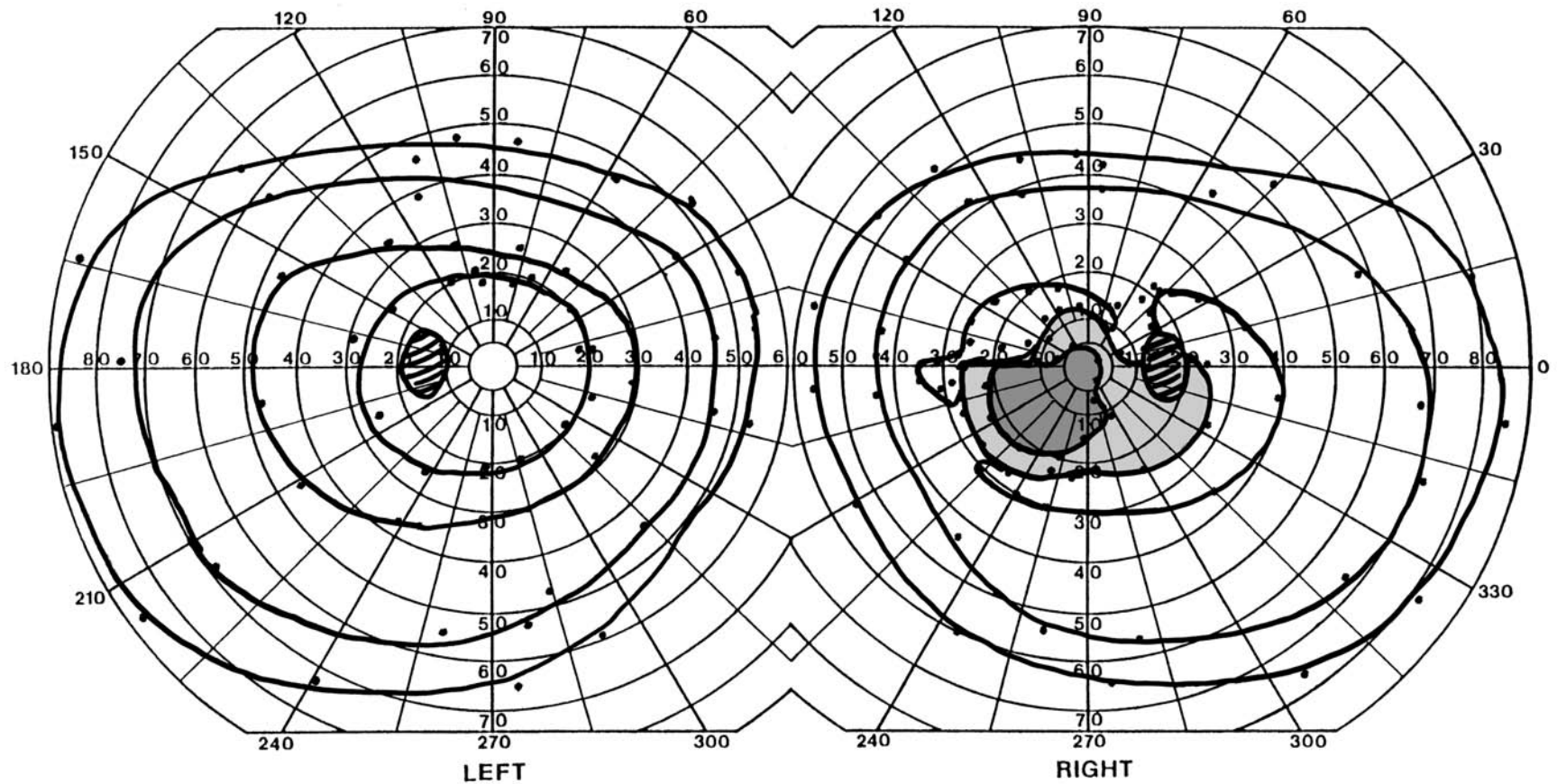
See Color Plate after page 180



HISTORY AND EXAM

After a seizure causing a single-car accident, a right frontal oligodendroglioma was found in this 38-yr-old trucker. He complained of “purple haze” to his vision OD after biopsy. Acuity was slightly reduced at that time, but imaging did not show optic nerve compression. Over the next 18 months, his vision became more persistently blurry OD,

but the purple haze disappeared. Acuity was 20/400 OD and 20/20 OS. There was a large RAPD and temporal optic disk pallor OD. His behavior was disinhibited with a cheerful lack of concern about his problems.



DISCUSSION

Field description: Central scotoma with inferior nasal step and superior arcuate defect OD.

Localization: Optic nerve.

Pathology: Compressive optic neuropathy.

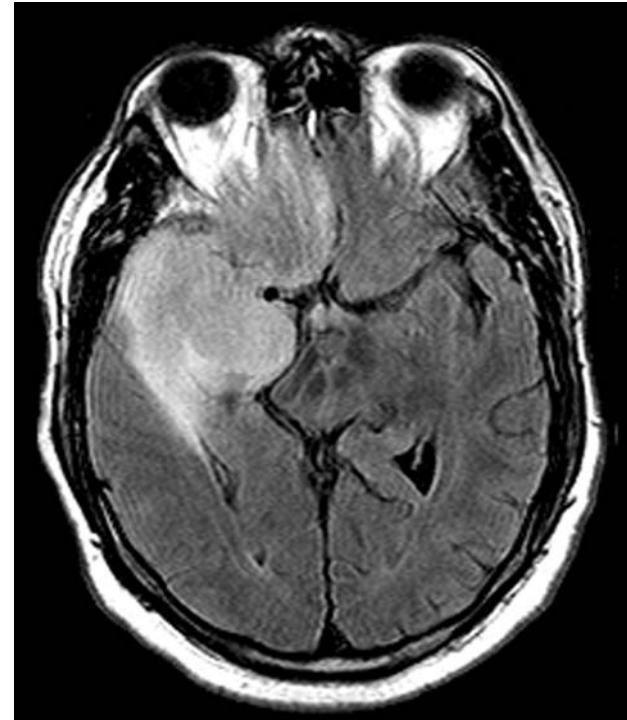
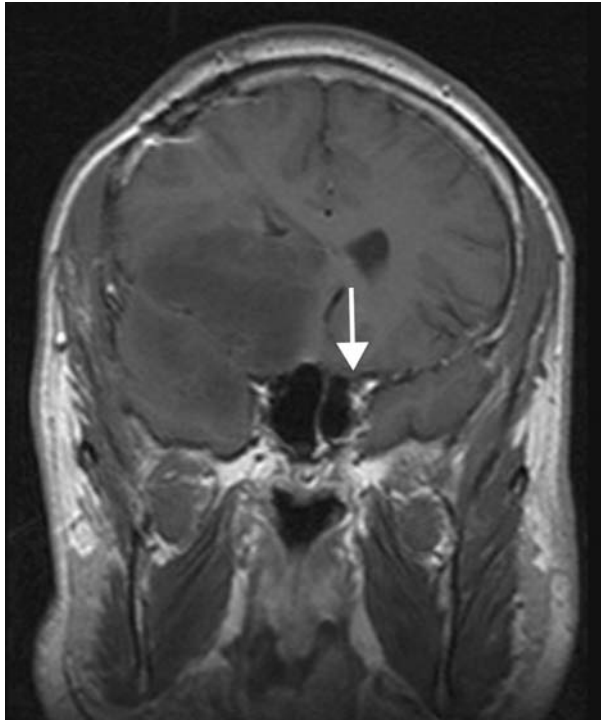
Confrontation testing showed a central scotoma OD to finger motion.

Other features: Frontal disinhibition.

The patient has a large central defect above the horizontal meridian merged with a large inferior scotoma that respects the nasal horizontal meridian. In addition, there is a subtle superior arcuate defect that arches more peripherally than the inferior defect to gen-

erate a second nasal step defect at the 30° mark, and creating a shallow superior valley above the blind spot to the I2e isopter. Thus, he has damage to the papillomacular and both superior and inferior arcuate nerve fiber bundles.

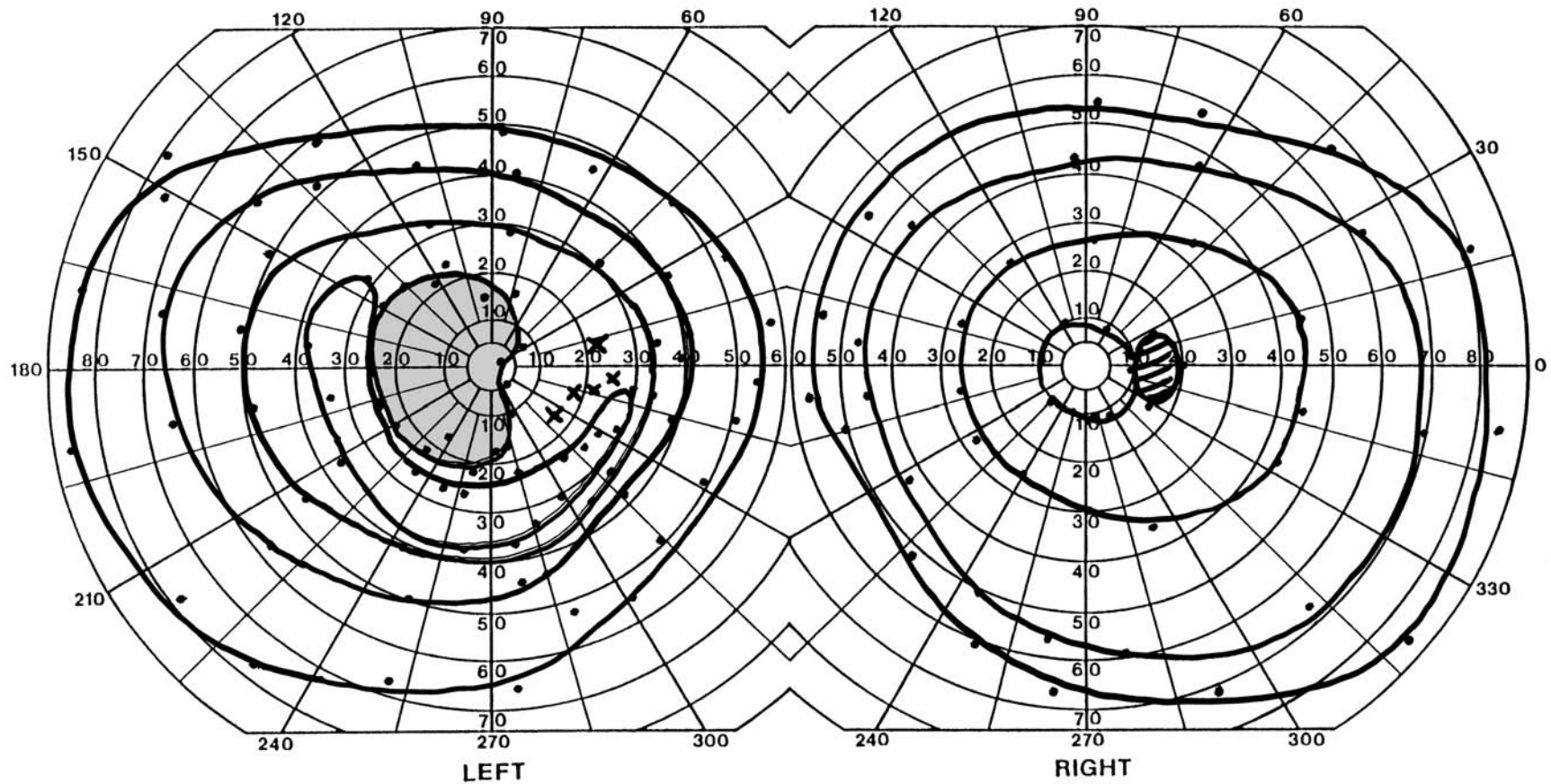
MRI showed a large frontal tumor (see axial FLAIR image) with inferior mass effect, seen on the coronal T1-weighted image (note the location of the normal optic nerve on the other side, arrow). Although intracranial compression of the optic nerve is often from below by parasellar tumors, compression from cerebral tumors above can also occur. Alterations in behavior with either social disinhibition or abulic states may be present, due to frontal lobe dysfunction.



HISTORY AND EXAM

For 3 years this 44-yr-old woman had proptosis and progressive visual loss OS. She had occasional bifrontal or retro-orbital headaches. Acuity without correction was 20/20 OD and count fingers OS, improving with +.62 sphere to 20/200 and with pinhole to

20/70. There was an RAPD OS. Ishihara color scores were 14/14 OU. Fundoscopy showed choroidal folds and mild optic disk pallor OS. She had 7 mm of proptosis, without lateral displacement of the globe. There was mild limitation of abduction OS.



DISCUSSION

Field description: Cecocentral scotoma OS.

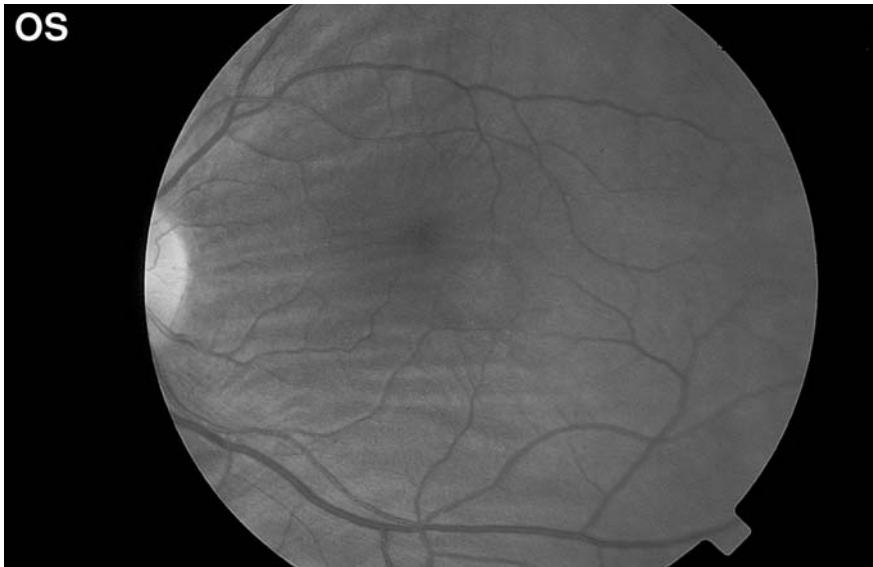
Localization: Intraorbital optic nerve.

Pathology: Compressive optic neuropathy and refractive change.

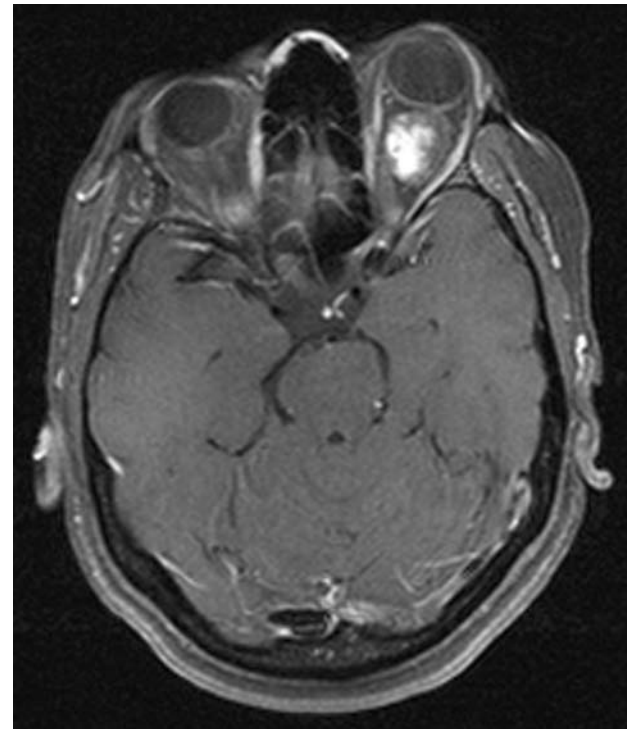
Confrontation fields were full to finger counting.

The patient has a large central field defect with reduced acuity. While she has an RAPD and disk pallor, suggesting some element of compressive optic neuropathy, she has impressive choroidal folds, much like this fundus picture from another patient. These

findings, along with the improved acuity with plus lenses and pinhole, indicate that part of her visual defect is refractive in origin (101). This is due to compression of the posterior globe by a mass pushing the retina anterior to the plane of focus, inducing a hyperopia. This is typical of intraconal tumors, whereas extraconal tumors induce an astigmatism related to their asymmetric distortion of the globe. Her T1-weighted MRI showed a large enhancing intraconal mass, which resection confirmed to be a cavernous hemangioma (102). She recovered well with improvement in acuity to 20/40 (20/30 with pinhole) and marked shrinkage of the scotoma.

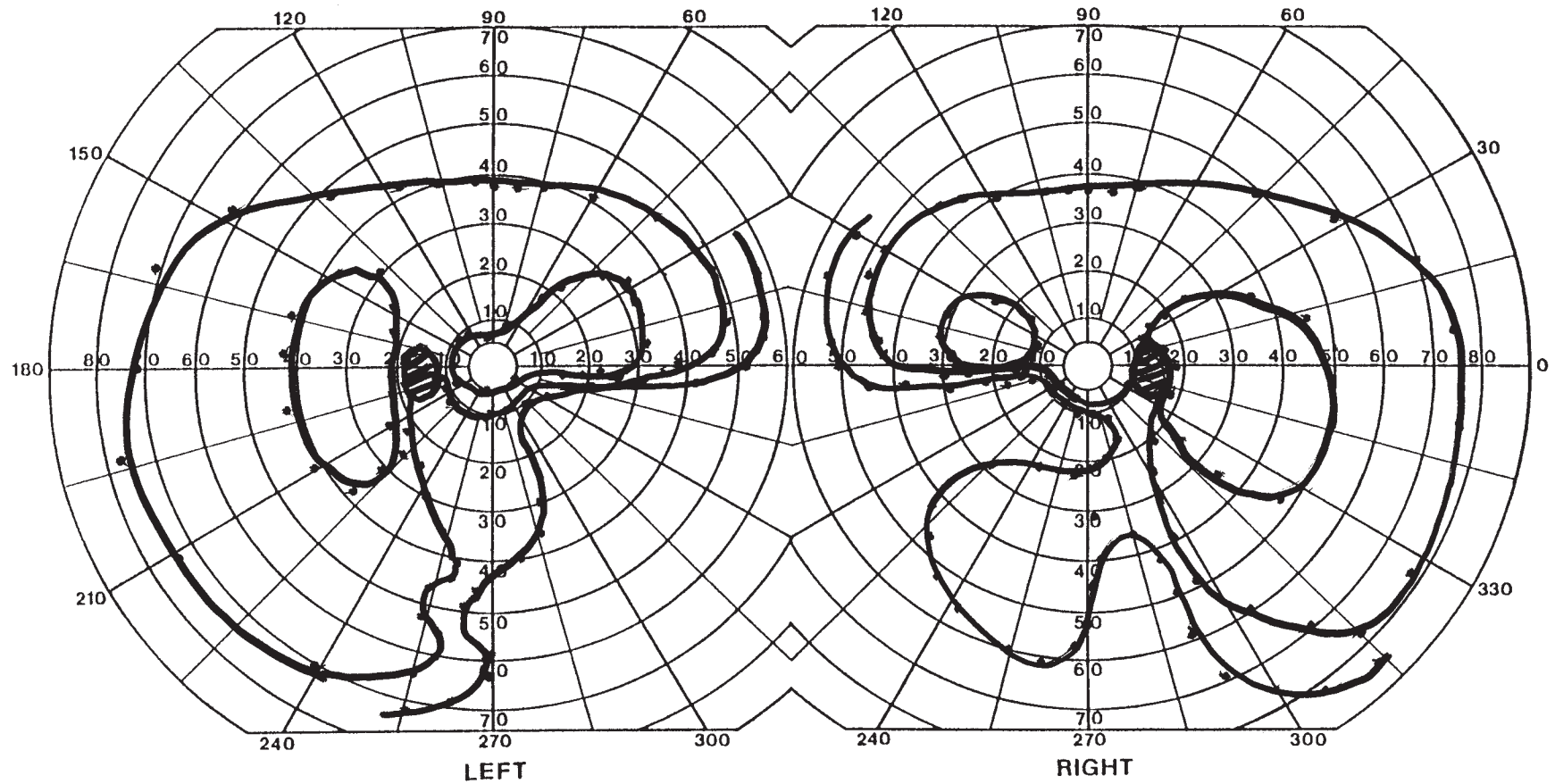


See Color Plate after page 180



HISTORY AND EXAM

A routine ophthalmologic examination of this 15-yr-old boy uncovered asymptomatic nasal field defects. Visual acuity was 20/25 OU, and Ishihara color scores were 9/14 OD and 8/14 OS. There was no RAPD.



DISCUSSION

Field description: Bilateral inferior nasal defects OU.

Localization: Bilateral optic nerve.

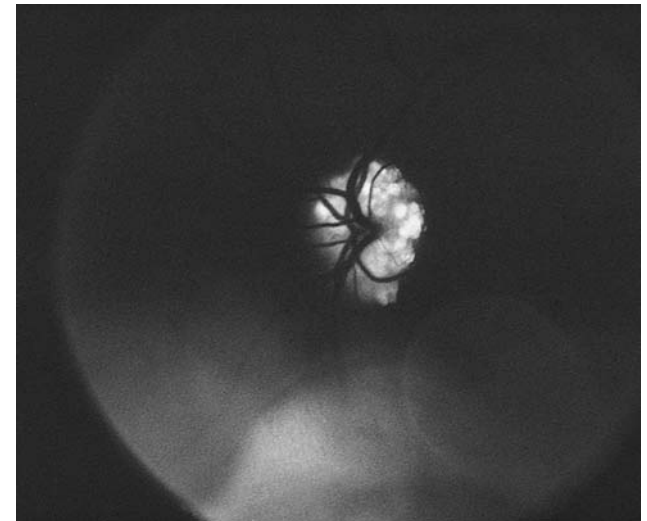
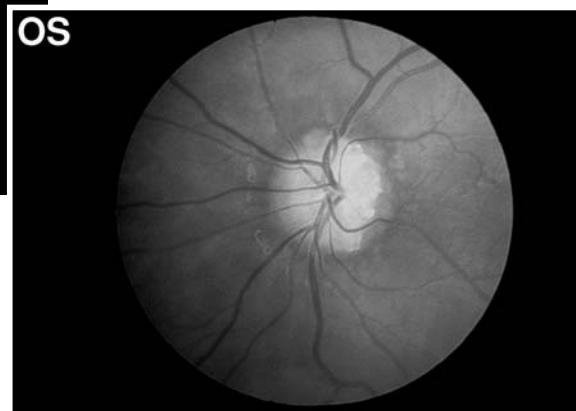
Pathology: Superficial optic disk drusen.

Disk drusen are hyaline concretions that either aggregate on the surface of the disk or are buried beneath its surface. Superficial drusen appear as irregular, shiny, yellowish white clusters of granules that autofluoresce (103), as shown in the photo taken using the filters for fluorescein angiography (but without injection of fluorescein). Buried drusen may be confused with papilledema, but differ in the following ways:

1. The central portion of the disk is most elevated, with lack of a central cup.
2. The disk is not hyperemic, and the elevation does not involve the surrounding retina.
3. The vessels overlying the disk are not obscured but, rather, may have anomalous branching patterns.

Orbital ultrasound or CT scan can help confirm buried drusen by showing the calcifications at the optic disk.

Visual field defects are noted in 70% of patients with optic disk drusen, most frequently enlargement of the blind spot and inferior nasal defects (104), as in this patient. These defects tend to be static or slowly worsen over months to years (105), suggesting a compressive mechanism of visual loss, but some patients have sudden onset of defects with superimposed disk edema or retinal pallor, indicating an ischemic effect. Optic disk drusen may make the disk vulnerable to vascular compromise, much as the crowded “disk at risk” does (see Case 34).



With filters

See Color Plate after page 180

HISTORY AND EXAM

This 35-yr-old woman came to the emergency room after 3 days of episodic diplopia. With reading, letters would suddenly double, and at other times they seemed to disappear. While looking across the room, sudden vertical steps would appear in windowsills and

door frames. She denied any visual loss. Acuity was 20/20 OU, but she often omitted the right half of lines with her right eye and the left half with her left eye. Ishihara color scores were 12/14 OU. There was no RAPD. Fundoscopy showed bilateral optic disk pallor.

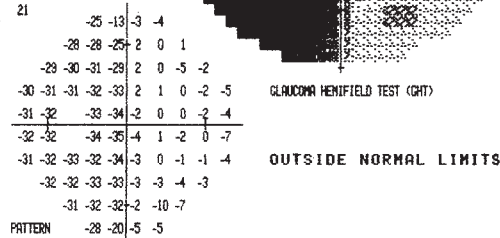
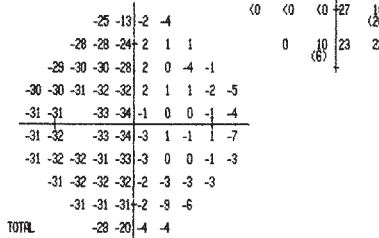
CENTRAL 30 - 2 THRESHOLD TEST

DATE 01-18-93

STIMULUS III, WHITE, BKXGND 31.5 ASB BLIND SPOT CHECK SIZE III
 STRATEGY FULL THRESHOLD
 FIXATION TARGET CENTRAL ID 200-96-83 TIME 04:29:33 PM
 RX USED +3.0 DS DCX DEG PUPIL DIAMETER 3.0 MM VA

LEFT

AGE 51
 FIXATION LOSSES 0/20
 FALSE POS ERRORS 0/11
 FALSE NEG ERRORS 0/9
 QUESTIONS ASKED 361
 TEST TIME 00:11:08
 HFA S/N 620-2150



GLAUCOMA HEMIFIELD TEST (GHT)
 OUTSIDE NORMAL LIMITS

MD -14.87 DB P < 0.5%
 PSD 17.30 DB P < 0.5%
 SF 1.56 DB
 OPSD 17.21 DB P < 0.5%

PROBABILITY SYMBOLS
 :: P < 3%
 :: P < 2%
 :: P < 1%
 ■ P < 0.5%

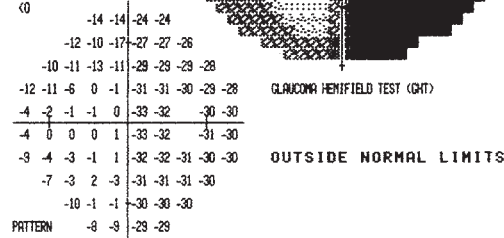
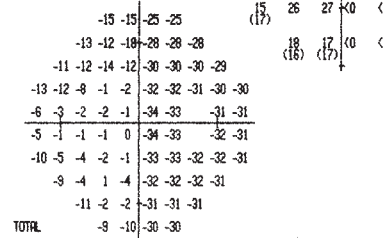
CENTRAL 30 - 2 THRESHOLD TEST

DATE 01-18-93

STIMULUS III, WHITE, BKXGND 31.5 ASB BLIND SPOT CHECK SIZE OFF
 STRATEGY FULL THRESHOLD
 FIXATION TARGET CENTRAL ID 200-96-83 TIME 04:16:03 PM
 RX USED +3.0 DS DCX DEG PUPIL DIAMETER 3.0 MM VA

RIGHT

AGE 51
 FIXATION LOSSES 0/0
 FALSE POS ERRORS 0/8
 FALSE NEG ERRORS 0/10
 QUESTIONS ASKED 337
 TEST TIME 00:12:42
 HFA S/N 620-2150



GLAUCOMA HEMIFIELD TEST (GHT)
 OUTSIDE NORMAL LIMITS

MD -16.80 DB P < 0.5%
 PSD 16.09 DB P < 0.5%
 SF 2.61 DB P < 5%
 OPSD 15.81 DB P < 0.5%

PROBABILITY SYMBOLS
 :: P < 3%
 :: P < 2%
 :: P < 1%
 ■ P < 0.5%

DISCUSSION

Field description: Complete bitemporal hemianopia.

Localization: Optic chiasm.

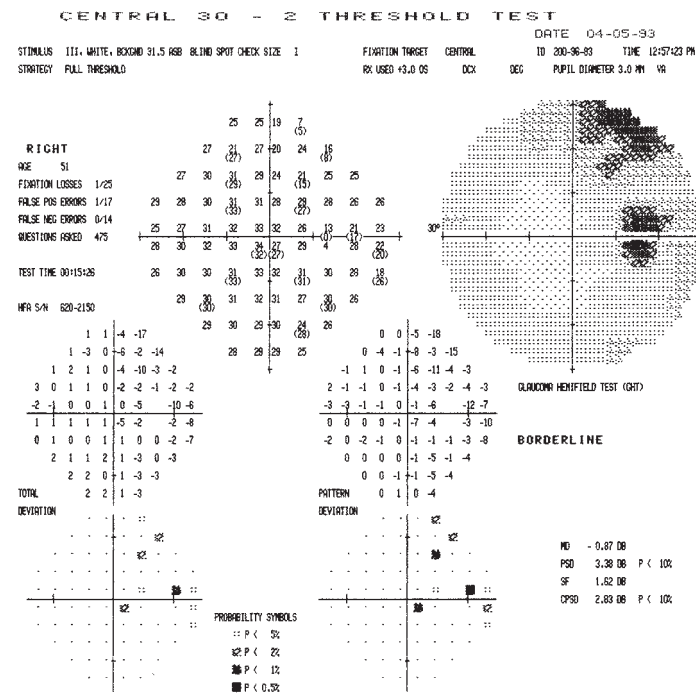
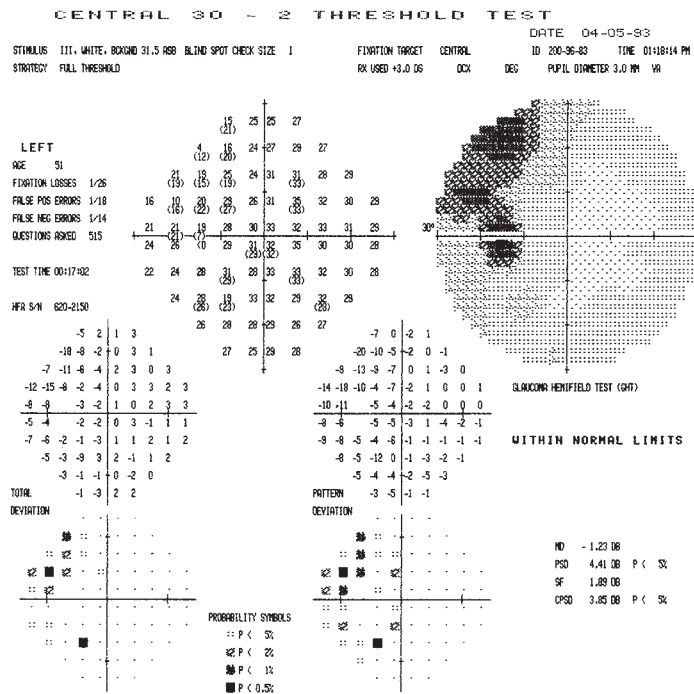
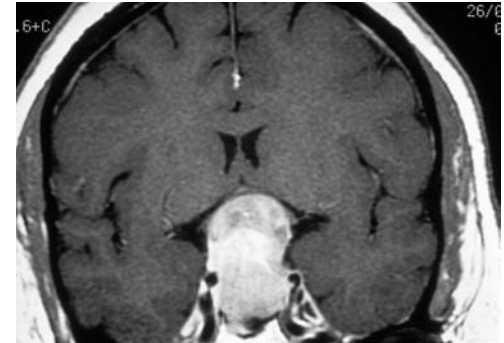
Pathology: Pituitary macroadenoma.

Other features: Hemifield slide.

The patient's fields correspond to the classic cartoon of complete loss of both temporal fields, which, like all classic signs, is the exception rather than the rule, as partial temporal field loss is more common than complete hemianopia. Coronal T1-weighted MRI showed a large enhancing pituitary adenoma that was nonsecreting. Three months after surgery her fields had improved to nearly normal with mild residual depression in the superior temporal fields (shown this page).

Her visual complaints represent an unusual phenomenon called *hemifield slide* (106). Normally, apart from the monocular temporal crescents, all points in the visual field of one eye have a corresponding location in the field of the other eye. This visual corre-

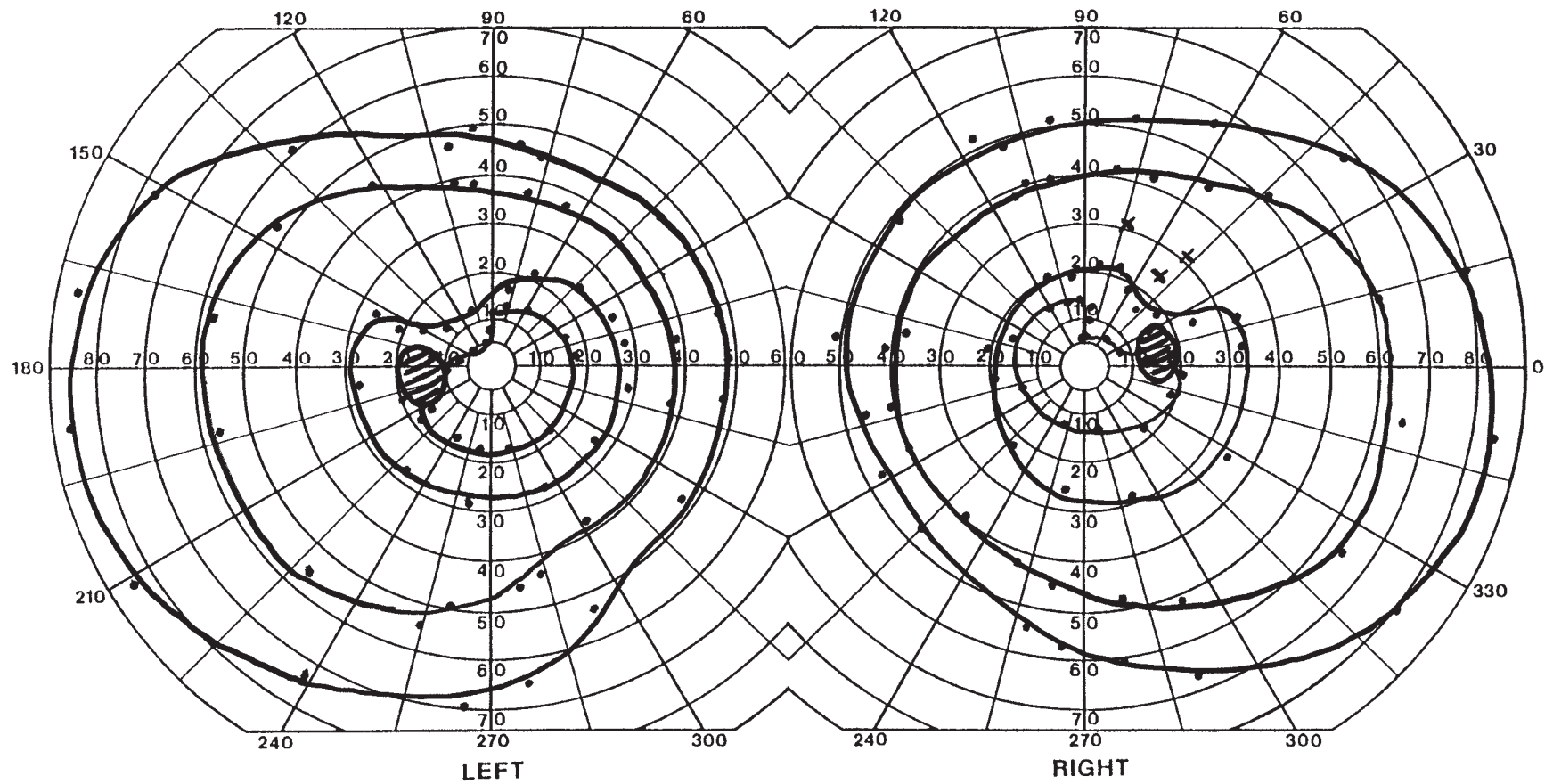
spondence can serve to anchor the eyes together, to maintain a stable fused single image of the world. With complete bitemporal hemianopia, no point in the visual field has binocular representation. Slight drifts in eye alignment may emerge. If they cross transiently, a vertical gap in the middle will develop, causing letters and stimuli in the midline to disappear. If they drift apart, in an exotropic direction, the remaining nasal fields will overlap in the midline, causing a temporary doubling for stimuli at the midline. If they drift vertically, a step defect will appear. One can easily imagine the resulting confusion during reading.



HISTORY AND EXAM

This 50-yr-old man came to the emergency room 2 months earlier with a sudden severe headache. MRI showed a tumor, which was resected. Afterward he noted blurred vision OD and vertical diplopia, from a right III nerve palsy. Visual acuity was 20/25 OU

and color vision was normal. There was no RAPD and optic disks were normal. He had an exotropia worse in left gaze and a small right hypertropia. The rest of the neurologic examination was normal.



DISCUSSION

Field description: Subtle superior bitemporal hemifield depression in paracentral region.

Localization: Optic chiasm.

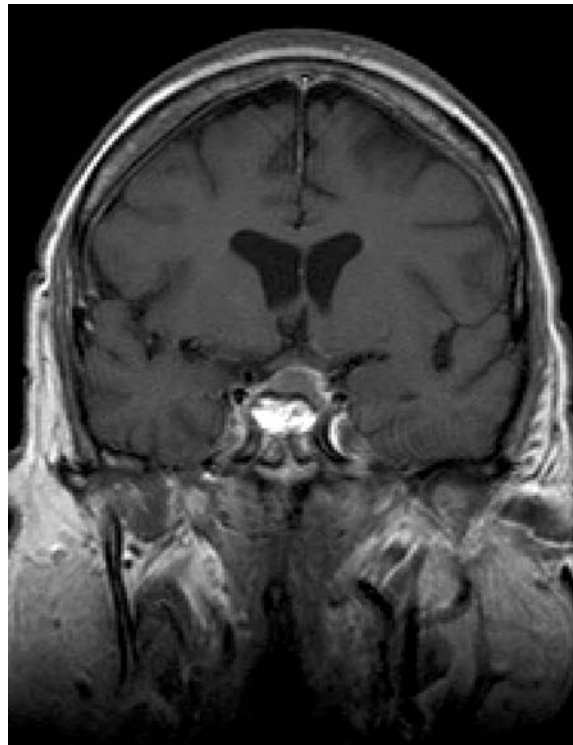
Pathology: Pituitary adenoma with apoplexy.

Confrontation testing was normal.

The patient's bitemporal defects are subtle and only apparent near the center of vision. Nevertheless, the perimetrist has been careful to document clear vertical steps in the smallest (03e) isopter.

Coronal T1-weighted MRI (below) revealed a pituitary tumor with hemorrhage (pituitary apoplexy). The optic chiasm is bowed upward above the bright enhancing rim of the tumor. Fibers from the inferior nasal retina (superior temporal visual fields) cross in the inferior aspect of the optic chiasm. Compression of the chiasm from below, as by pituitary masses, will tend to produce superior bitemporal defects first.

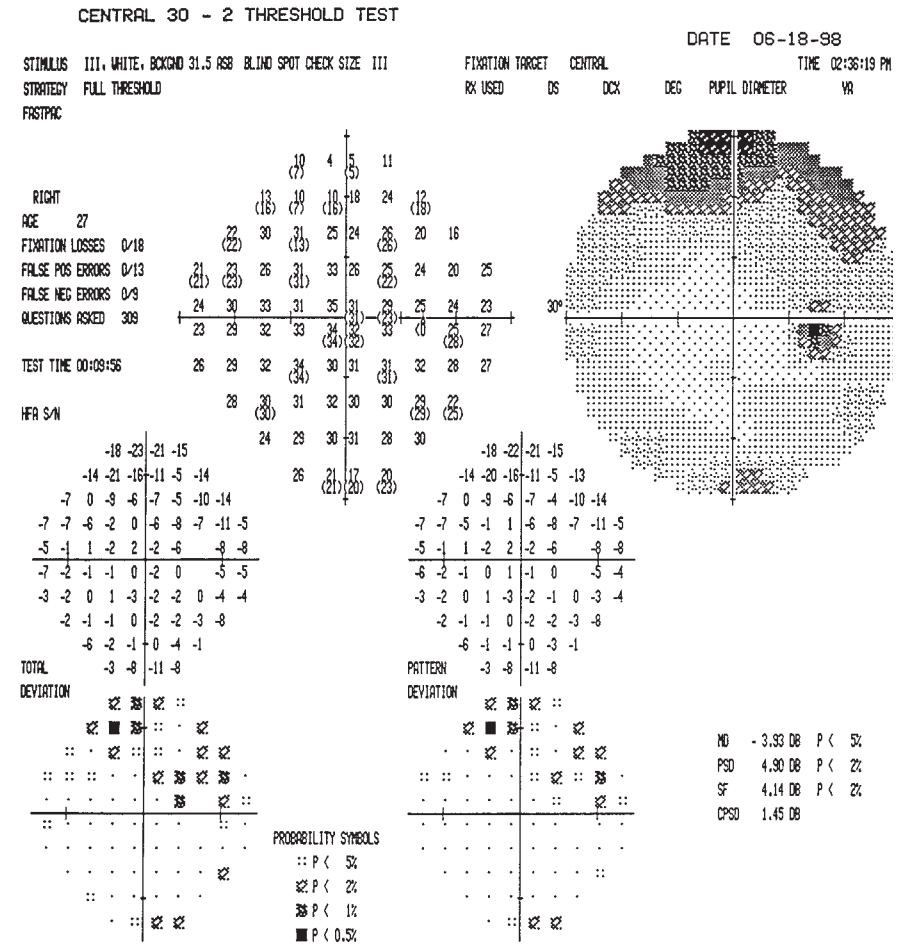
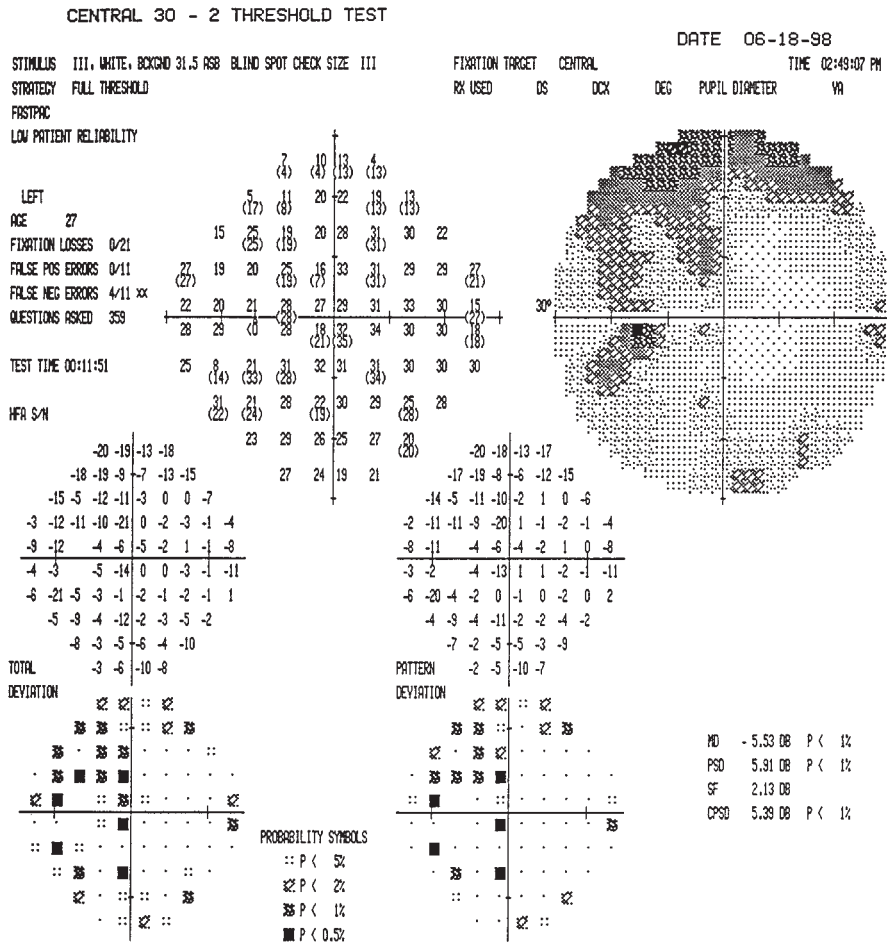
Pituitary apoplexy is the sudden expansion of the pituitary gland from hemorrhage, infarction, or edema. Typically, these are complications of an underlying pituitary tumor. Infarction or hemorrhage in a normal gland can occur in the postpartum state (Sheehan syndrome) but less frequently affects vision than apoplexy related to a tumor (107). Pituitary apoplexy presents with sudden severe headache, nausea and vomiting, and a variable degree of hypopituitarism, a major threat being acute adrenal insufficiency. Other symptoms depend on the direction of expansion (107,108). Extension into the cavernous sinus causes acute ophthalmoplegia of one or both eyes, as in this patient. Downward extension causes epistaxis with the risk of exsanguination. Upward extension impairs vision. Rupture into the subarachnoid space causes meningismus and stupor.



HISTORY AND EXAM

This 27-yr-old man had not been able to wear his hats or gloves for a year or two, and his shoe size had increased from 13 to 14-wide over this time. He had occasional headaches but no visual symptoms. Visual acuity was 20/20 OU and color vision was

normal. There was no RAPD. Optic disks were normal. He was clearly acromegalic, with large spade-shaped hands and a prominent brow and jaw.



DISCUSSION

Field description: Subtle bitemporal defects; also probably a supraorbital artifact from his enlarged brow.

Localization: Optic chiasm.

Pathology: Pituitary adenoma, growth hormone (GH) secreting.

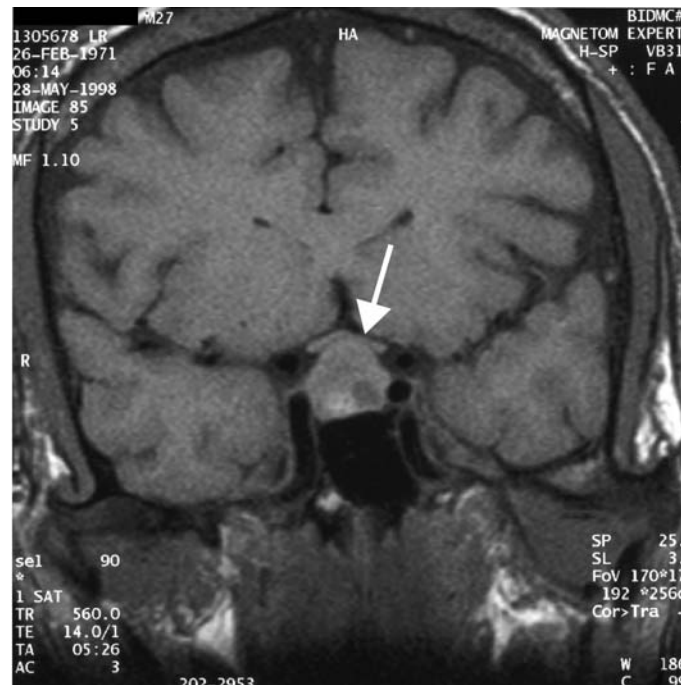
Other features: Acromegaly.

Confrontation testing was normal.

The patient's fields show some mild superior depression that does not respect the vertical meridian. This is likely lid or brow artifact. However, there are clearly defects that line up at the meridian OS. It is less clear whether there is a chiasmal defect OD, although there may be more superior field depression temporally than nasally. Coronal

T1-weighted MRI showed a moderately large pituitary lesion with a cystic component, bowing the optic chiasm upward (arrow).

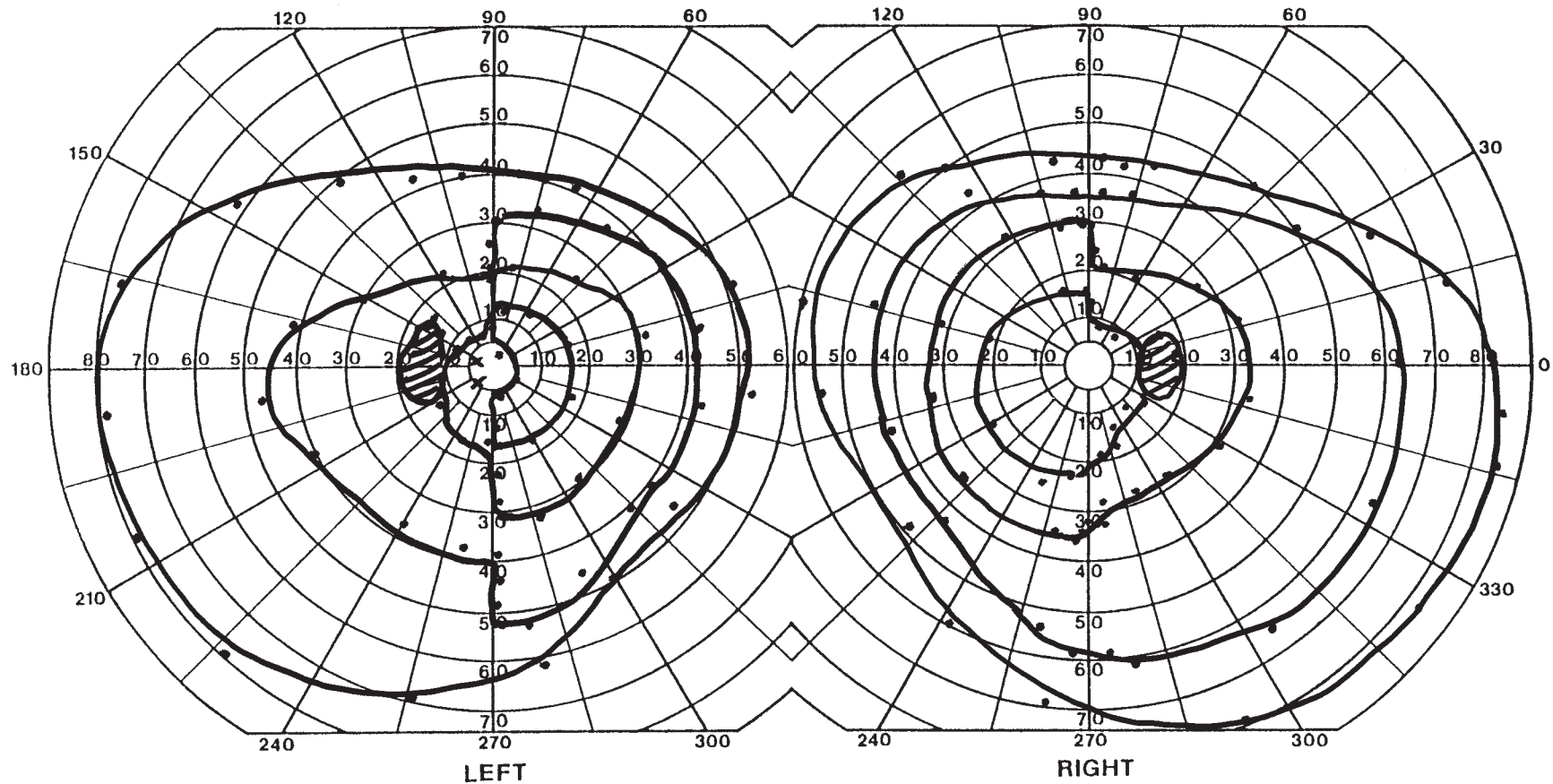
Acromegaly results from excess secretion of GH during adulthood (109,110). This causes bone and soft-tissue enlargement (especially of the face, hands, and feet), visceromegaly, and glucose intolerance. Not surprisingly, these clinical symptoms mean that pituitary adenomas associated with acromegaly present at a smaller size than do nonsecreting adenomas. Therefore, visual field defects arise less frequently with GH-secreting tumors than with other pituitary adenomas. This patient's field defects are clearly more subtle than many of the others in this atlas. Automated perimetry was chosen because no defect was evident on confrontation testing, despite knowing that such a tumor was likely. Transsphenoidal resection is the treatment of choice.



HISTORY AND EXAM

This 67-yr-old man, on anticoagulants for earlier deep venous thrombosis, went to an emergency room for a sudden severe headache. He was confused and drowsy with meningismus and a mild left inferior rectus paresis. INR was 2.2. CT of his brain showed an enlarged sella with hemorrhage in the interhemispheric fissure. He developed acute adrenal insufficiency and hydrocephalus, requiring an intraventricular drain. He was dis-

charged without surgery and returned 2 months later for assessment. Acuity was 20/15 OD and 20/40 OS, and Ishihara color scores were 12/14 OD and 11/14 OS. There was no RAPD. Optic disks were normal but there was (known) macular degeneration OS. Ductions were full.



DISCUSSION

Field description: Relative bitemporal depression, greater OS, with relative central scotoma OS.

Localization: Optic chiasm and retina.

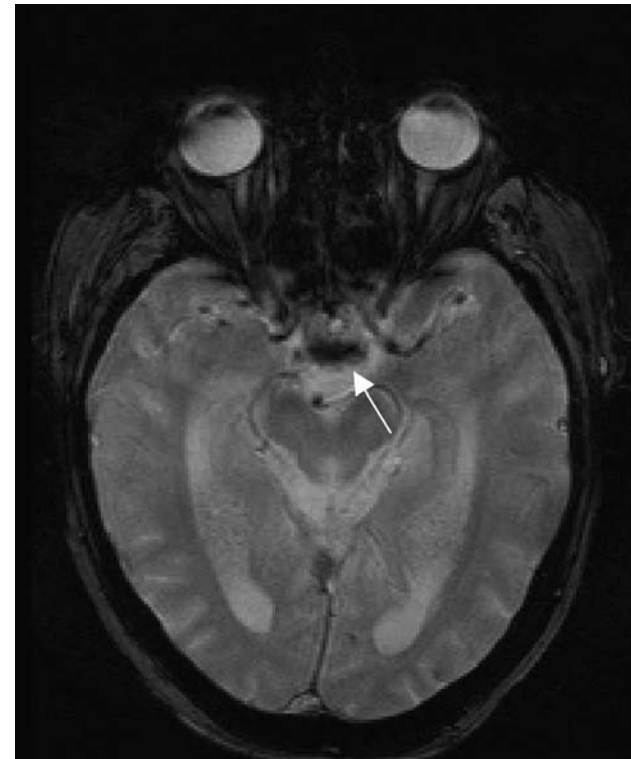
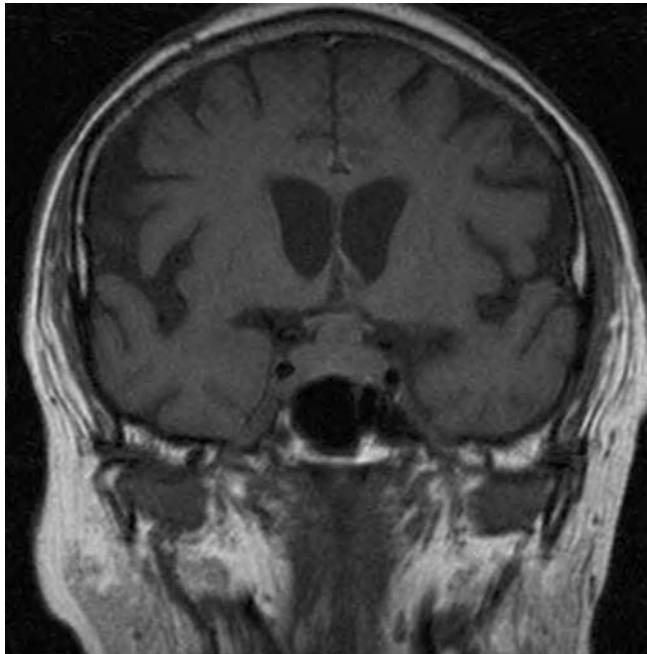
Pathology: Pituitary adenoma with apoplexy, macular degeneration.

Confrontation testing was normal OU.

The patient's bitemporal defects again affect mainly the central fields. On the left, there is also a shallow central scotoma for the smallest isopter. While this might raise the question of added compression of the left intracranial optic nerve, this is probably explained by his known macular degeneration, which is worse OS.

The sudden headache suggests subarachnoid hemorrhage or pituitary apoplexy. The subarachnoid blood explains the meningismus and stupor, but the enlarged pituitary

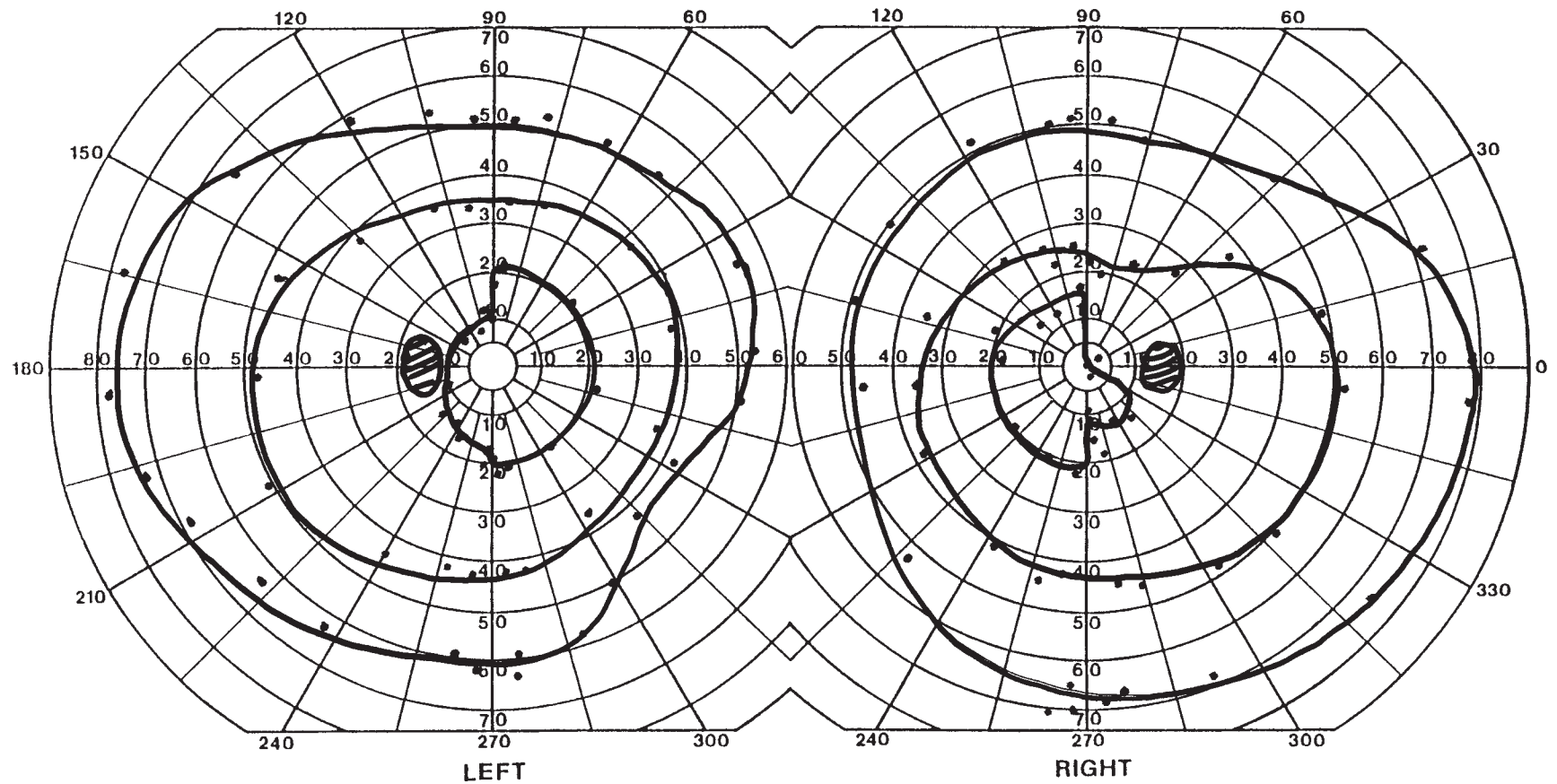
suggests that the subarachnoid hemorrhage is secondary to apoplexy, as confirmed on these coronal T1-weighted and axial susceptibility MRI images (note the dark spot on the latter indicating blood; see arrow). Misdiagnosis as meningitis or subarachnoid hemorrhage frequently delays the diagnosis of pituitary apoplexy. The importance of the early diagnosis of apoplexy lies in the need to recognize the potential for life-threatening hypoadrenalism requiring immediate iv steroid replacement. Risk factors for apoplexy include diabetes; atherosclerosis; earlier pituitary irradiation; use of bromocriptine; and use of anticoagulants, as in this man (107,111). Surgical treatment is not always necessary and is mainly indicated for altered consciousness, visual loss, and progressive enlargement of the pituitary (107).



HISTORY AND EXAM

This 48-yr-old woman had a brain tumor at age 14, treated with partial resection and radiation. A routine eye examination found decreased color vision in her left eye, and she was referred for further evaluation. Visual acuity was 20/30 OU and Ishihara color plates

were 13/14 OU. There was no RAPD. Optic disks were normal. The remainder of the neurologic examination was normal.



DISCUSSION

Field description: Mild relative bitemporal hemifield defects.

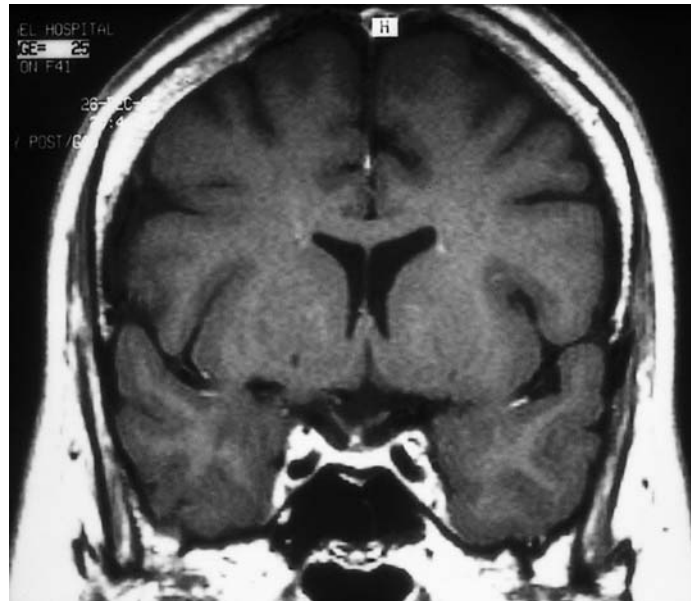
Localization: Optic chiasm.

Pathology: Descent of the optic chiasm, post-radiation/surgery.

Confrontation testing showed red desaturation in the temporal paracentral fields OU, with sudden steps at the vertical meridians.

On perimetry, the patient's bitemporal defect is a relative depression evident only in the central field, with testing using the smallest (I2e) isopter. On confrontation, a subtle bitemporal reduction in color was the only clue to this mild field defect.

Old charts eventually revealed that her earlier brain tumor had been a craniopharyngioma. In the absence of knowledge of her visual fields in the past, tumor recurrence must be considered, although it is rare when this type of tumor is treated with both resection and radiation (112). Instead of recurrence, her coronal T1-weighted MRI shows "descent of the optic chiasm" (113). The middle of the chiasm is drawn down toward the sella, causing a V-shaped configuration on coronal images. This has been reported to worsen preexisting bitemporal defects, presumably via a traction mechanism. In this woman, is the visual defect a remnant from her prior tumor and surgery, or is it due to her current chiasmatal descent? Without earlier visual fields, one cannot know for sure.



HISTORY AND EXAM

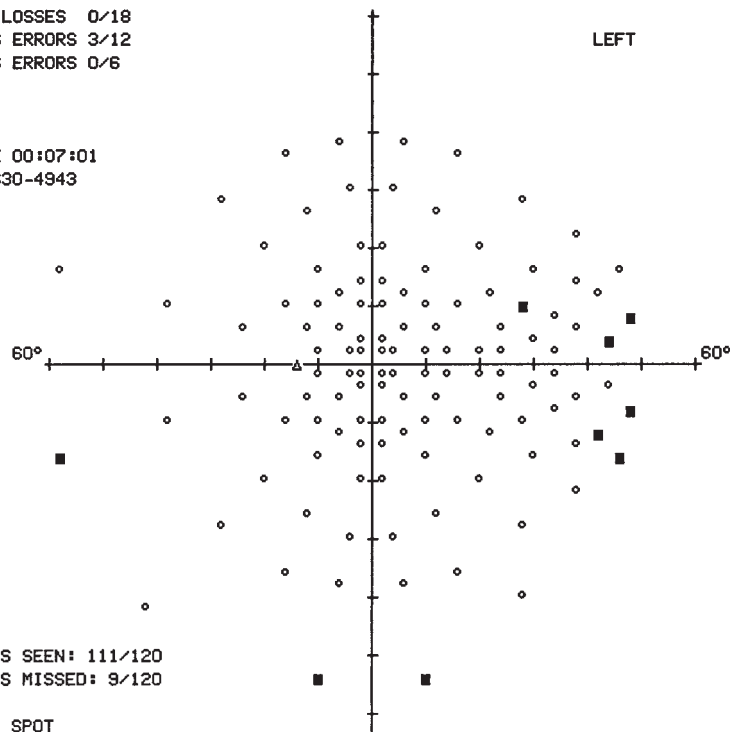
This 49-yr-old woman with symptoms of polyuria and polydipsia was diagnosed with diabetes insipidus. MRI demonstrated a pituitary mass, which partial resection showed to consist of lymphocytic infiltration, without tumor. Visual field screening showed a defect,

and she was referred for evaluation. Visual acuity was 20/20 OD and 20/30 OS, and Ishihara color plates were 13/14 OD and 14/14 OS. There was no RAPD. Optic disks appeared normal. The remainder of the neurologic examination was normal.

FULL FIELD 120 POINT SCREENING TEST
 STIMULUS III, WHITE, BCKGND 31.5 ASB
 BLIND SPOT CHECK SIZE III
 FIXATION TARGET CENTRAL
 STRATEGY THRESHOLD RELATED
 CEN 36 DB PER 30 DB
 DATE 08-08-00 TIME 01:13:30 PM
 PUPIL DIAMETER VA 20/25
 RX USED + 2.00 DS DCX DEG

FIXATION LOSSES 0/18
 FALSE POS ERRORS 3/12
 FALSE NEG ERRORS 0/6

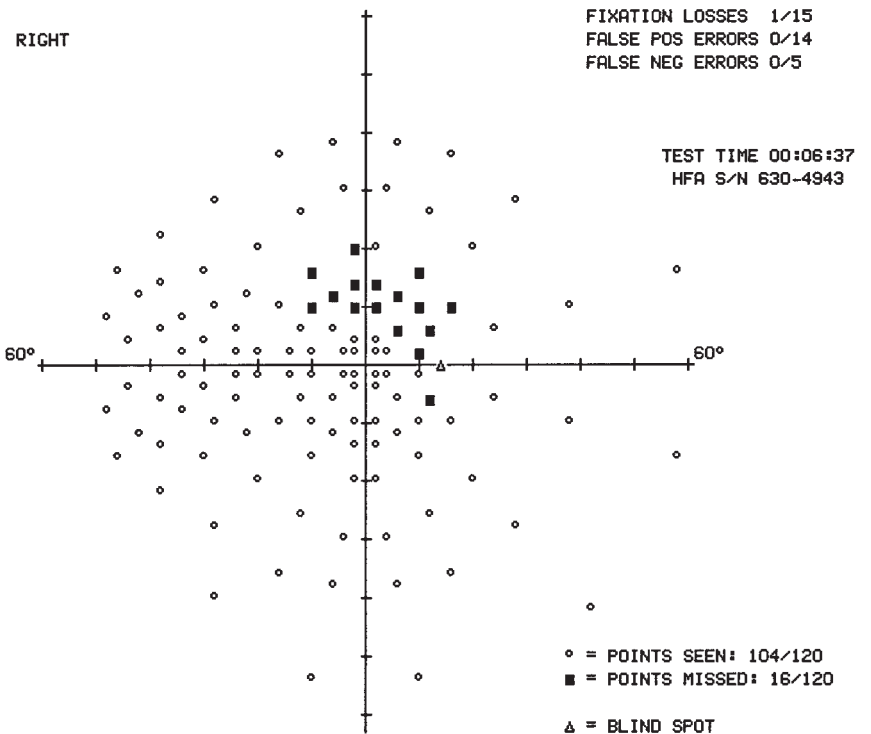
TEST TIME 00:07:01
 HFA S/N 630-4943



○ = POINTS SEEN: 111/120
 ■ = POINTS MISSED: 9/120
 △ = BLIND SPOT

FULL FIELD 120 POINT SCREENING TEST
 STIMULUS III, WHITE, BCKGND 31.5 ASB
 BLIND SPOT CHECK SIZE III
 FIXATION TARGET CENTRAL
 STRATEGY THRESHOLD RELATED
 CEN 37 DB PER 32 DB
 DATE 08-08-00 TIME 12:59:01 PM
 PUPIL DIAMETER VA 20/25
 RX USED + 2.00 DS DCX DEG

FIXATION LOSSES 1/15
 FALSE POS ERRORS 0/14
 FALSE NEG ERRORS 0/5

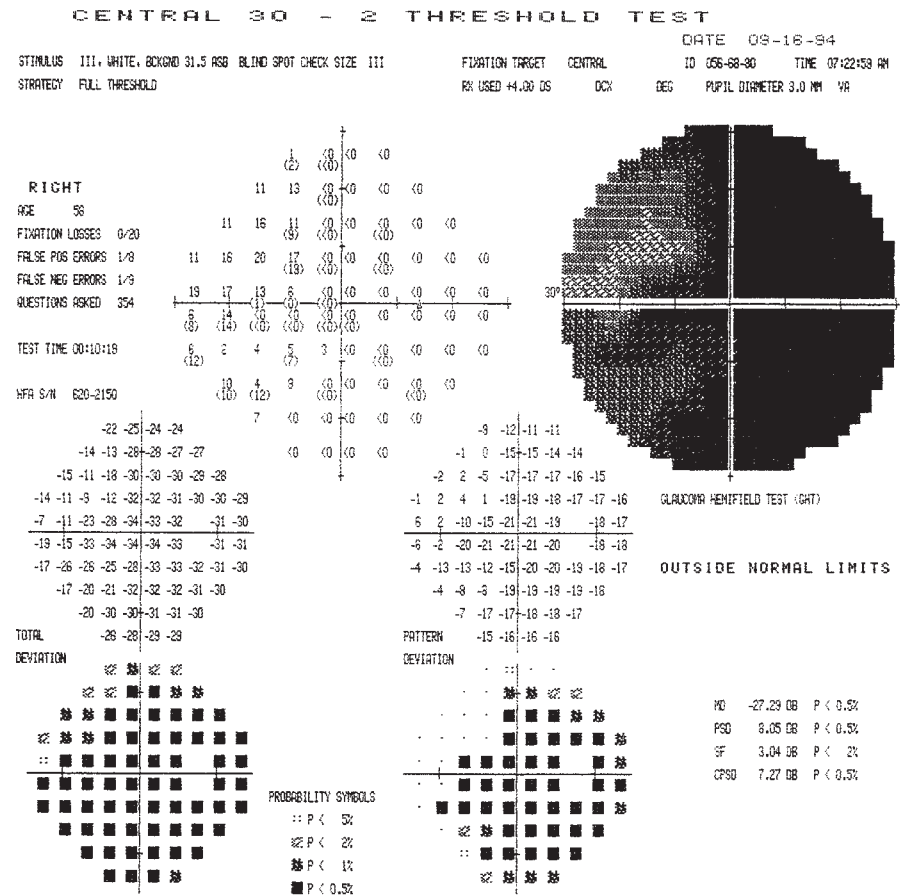
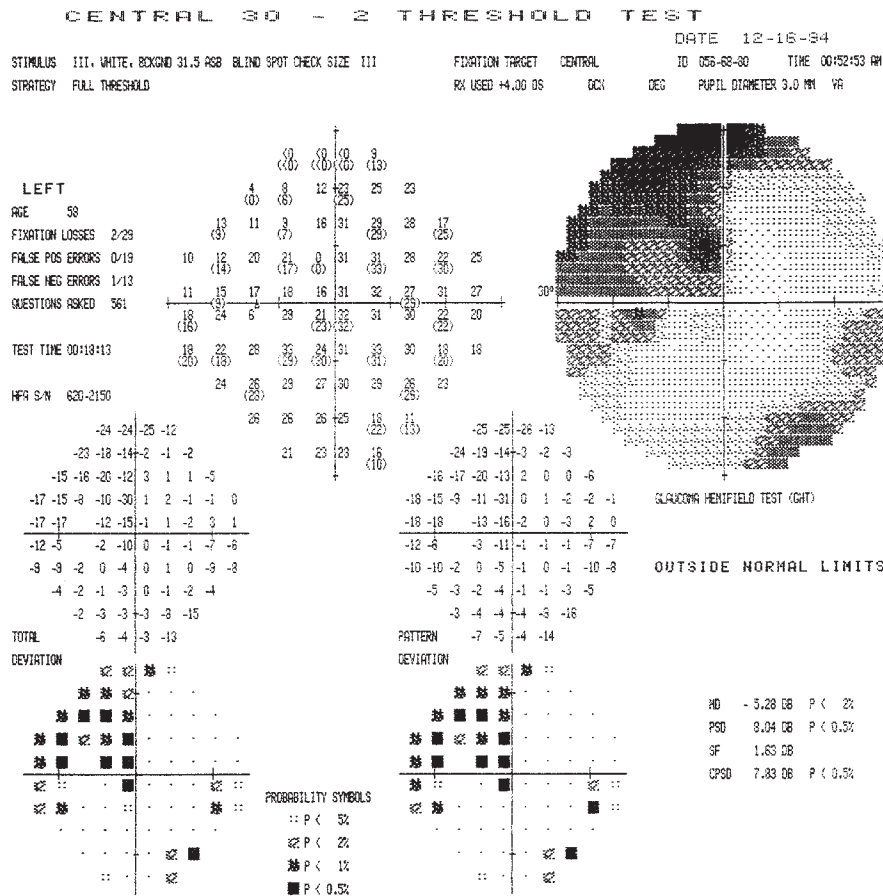


○ = POINTS SEEN: 104/120
 ■ = POINTS MISSED: 16/120
 △ = BLIND SPOT

HISTORY AND EXAM

This 50-yr-old woman had a known right anterior communicating artery aneurysm, discovered and treated 14 years earlier because of visual loss in the right eye. A few weeks prior to evaluation, she had noted new worsening of vision in the right eye as well as in the left upper field of the left eye, accompanied by episodic hallucinations of colors in this

left upper quadrant. Visual acuity was counting fingers at 6' OD and 20/20 OS. She read 13/14 Ishihara color plates OS. There was a prominent RAPD OD and optic disk pallor, more severe OD than OS.



DISCUSSION

Field description: Junctional scotoma, with diffuse loss OD and superior temporal quadrantanopia OS.

Localization: Junction of right intracranial optic nerve and optic chiasm.

Pathology: Compression by anterior communicating artery aneurysm.

Tangent screen perimetry showed similar findings.

The patient has severe visual loss OD on perimetry (note, however, that even in this eye the loss as depicted on the sensitivity plot is more severe temporally). In the other eye, there is a superior temporal hemifield defect that respects the vertical meridian. These are the essential features of a junctional scotoma.

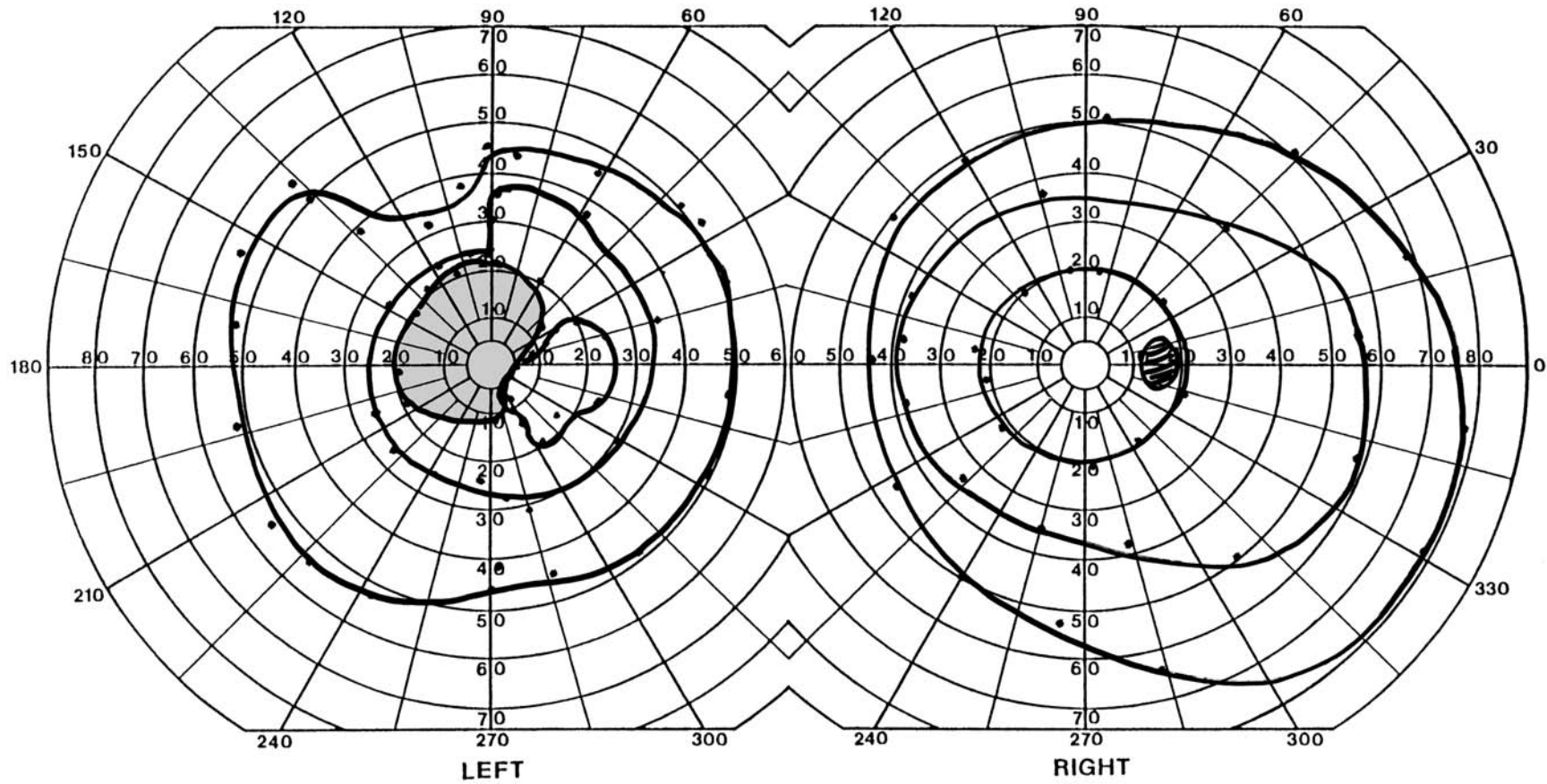
Coronal CT scan showed the large aneurysm in a location appropriate to compress the right optic chiasm and nerve anteriorly. Traditionally, a junctional scotoma is ascribed to compression of the termination of the optic nerve, where decussating fibers from the superior temporal field of the other eye were supposed to loop forward before passing posteriorly into the optic tract (115). Recent work has argued that this is an artifact (116). The combination may result instead from compression of both the terminal optic nerve and the adjacent inferior optic chiasm. The clinical implication remains the same, however. Perimetry in all cases of optic neuropathy should examine the superior temporal field of the opposite eye, because a defect there changes the differential diagnosis from one of optic neuropathy to that of lesions of the optic chiasm. Most lesions of the chiasm are masses, which is not true of optic neuropathy.



HISTORY AND EXAM

During the last week of her pregnancy, this 20-yr-old woman had bitemporal headache and blurred and decreased color vision in the left eye. When seen 2 days following deliv-

ery, the headaches were much improved. Visual acuity was 20/20 OD and 20/40 OS with an RAPD OS. There was red desaturation OS. Optic disks were normal.



DISCUSSION

Field description: Central scotoma in the left eye with a superotemporal vertical step.

Localization: Intracranial left optic nerve and chiasm.

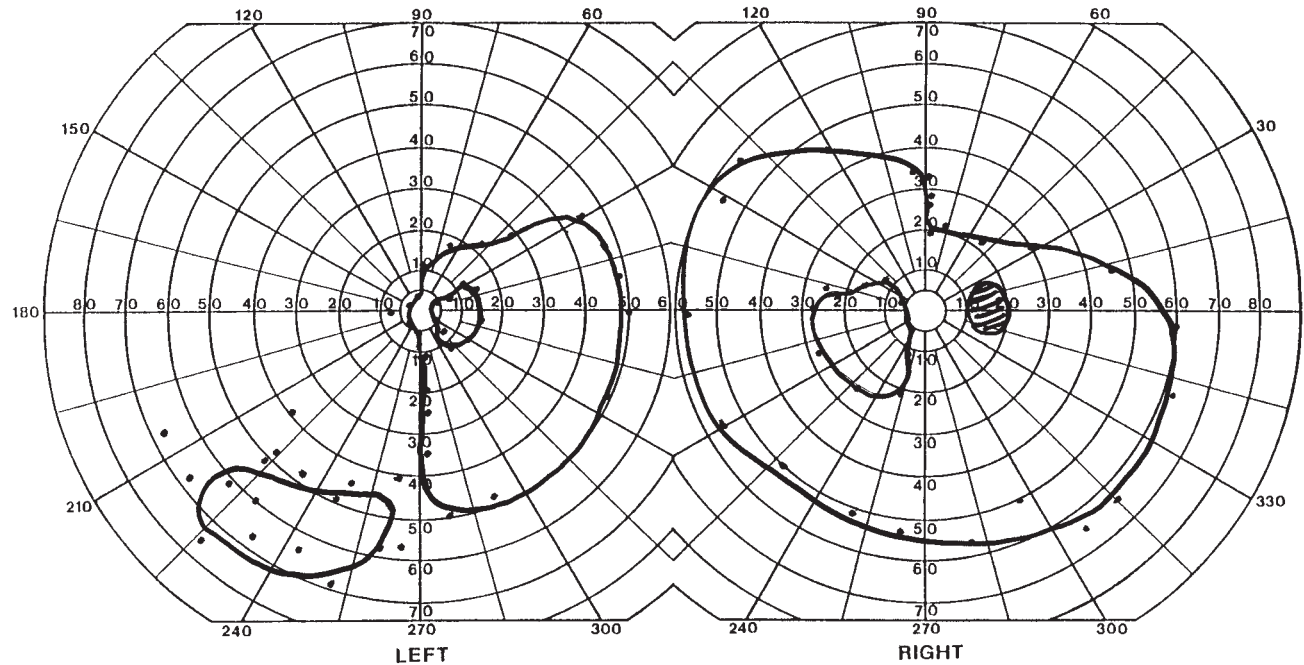
Pathology: Lymphocytic hypophysitis.

The initial field showed a large central scotoma, which might suggest an optic neuritis in a young woman. However, the key finding is the vertical step in the I4e isopter superiorly. No optic neuropathy does this.

T1-weighted coronal MRI showed a moderately enlarged pituitary gland abutting the optic chiasm (arrow), with homogeneous enhancement. Over the next 2 weeks, the vision OS worsened to count fingers and repeated visual field testing (this page) showed temporal hemifield defect OD and only a remaining nasal and inferior temporal islands of vision OS. This clearly indicated a lesion of the chiasm and left intracranial optic nerve. CSF was normal. Endocrine testing revealed low thyroid-stimulating hormone (TSH)

(<0.1) and low luteinizing hormone (LH) (<0.6). The patient was diagnosed with lymphocytic hypophysitis and treated with iv methylprednisolone, with visual fields returning to normal 1 month later.

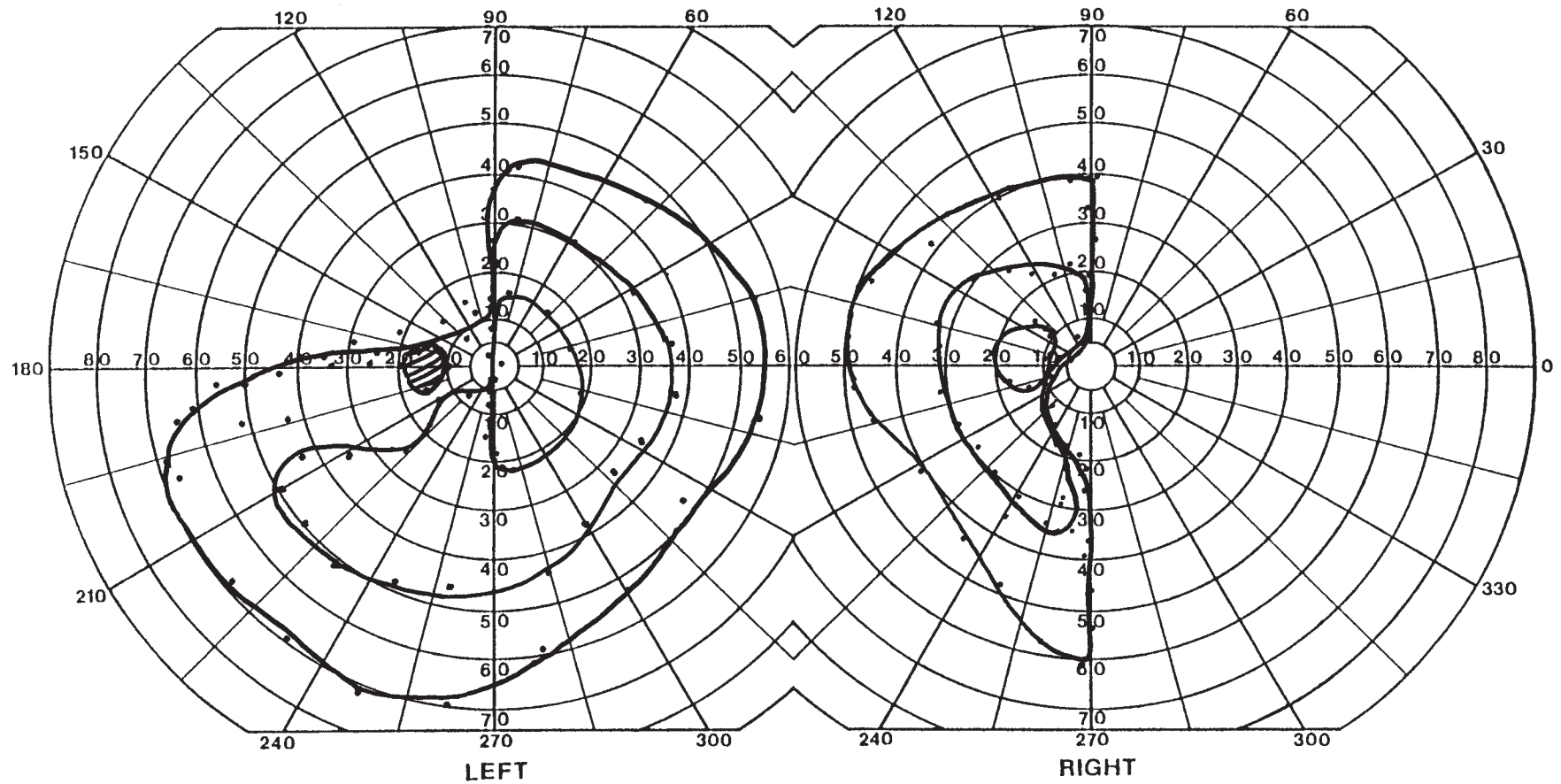
A chiasmal lesion in late pregnancy or the postpartum period suggests lymphocytic hypophysitis, postpartum pituitary necrosis (Sheehan syndrome), or pituitary adenoma. The lack of mass effect or hemorrhage on MRI is against the latter two, and more consistent with an inflammatory process. The management of lymphocytic hypophysitis is not well established (114). If headache and visual symptoms are mild, close observation is appropriate. Progressive visual loss should prompt trans-sphenoidal biopsy. If this shows lymphocytic infiltration without tumor, decompression without removal of the pituitary gland should be performed. The efficacy of corticosteroids is unproven. Hormone replacement may be needed.



HISTORY AND EXAM

This 51-yr-old man with hypercholesterolemia had gradual deterioration over a few years in the vision of the right eye, affecting the central and temporal field. More recently, he occasionally missed words on the left side of the page when reading with both eyes

open. Visual acuity was 20/400 OD and 20/25 OS, and there was a prominent RAPD OD. There was marked diffuse optic disk pallor OD and bowtie optic atrophy OS. The remainder of the neurologic examination was normal.



DISCUSSION

Field description: Bitemporal hemifield loss, more superior OS, with additional central scotoma OD.

Localization: Optic chiasm and right intracranial optic nerve.

Pathology: Prolactin (PRL)-secreting pituitary macroadenoma.

Other features: Bowtie atrophy.

The patient has dense superior loss with lesser inferior central depression OS (note that the smallest I2e isopter is only a semicircle, missing its left hemifield portion). There is complete loss of the temporal hemifield OD with extension into the nasal field centrally, indicating an added central scotoma OD from compression of the distal right optic nerve.

As with Case 58, the more severe superior loss in the temporal defect OS suggests compression of the decussating fibers in the inferior optic chiasm, from a mass below.

T1-weighted coronal MRI demonstrated a huge enhancing multilobulated tumor with cystic components, arising from the pituitary with lateral extension into the cavernous sinus, encasement of the left internal carotid, and downward extension into the sphenoid sinus. Serum PRL was markedly elevated at 2500 (normal: <25). Follicle-stimulating hormone, LH, and TSH were normal. The patient was started on cabergoline, a dopamine agonist similar to bromocriptine, but he developed a sudden severe headache from pituitary apoplexy, necessitating surgical decompression.

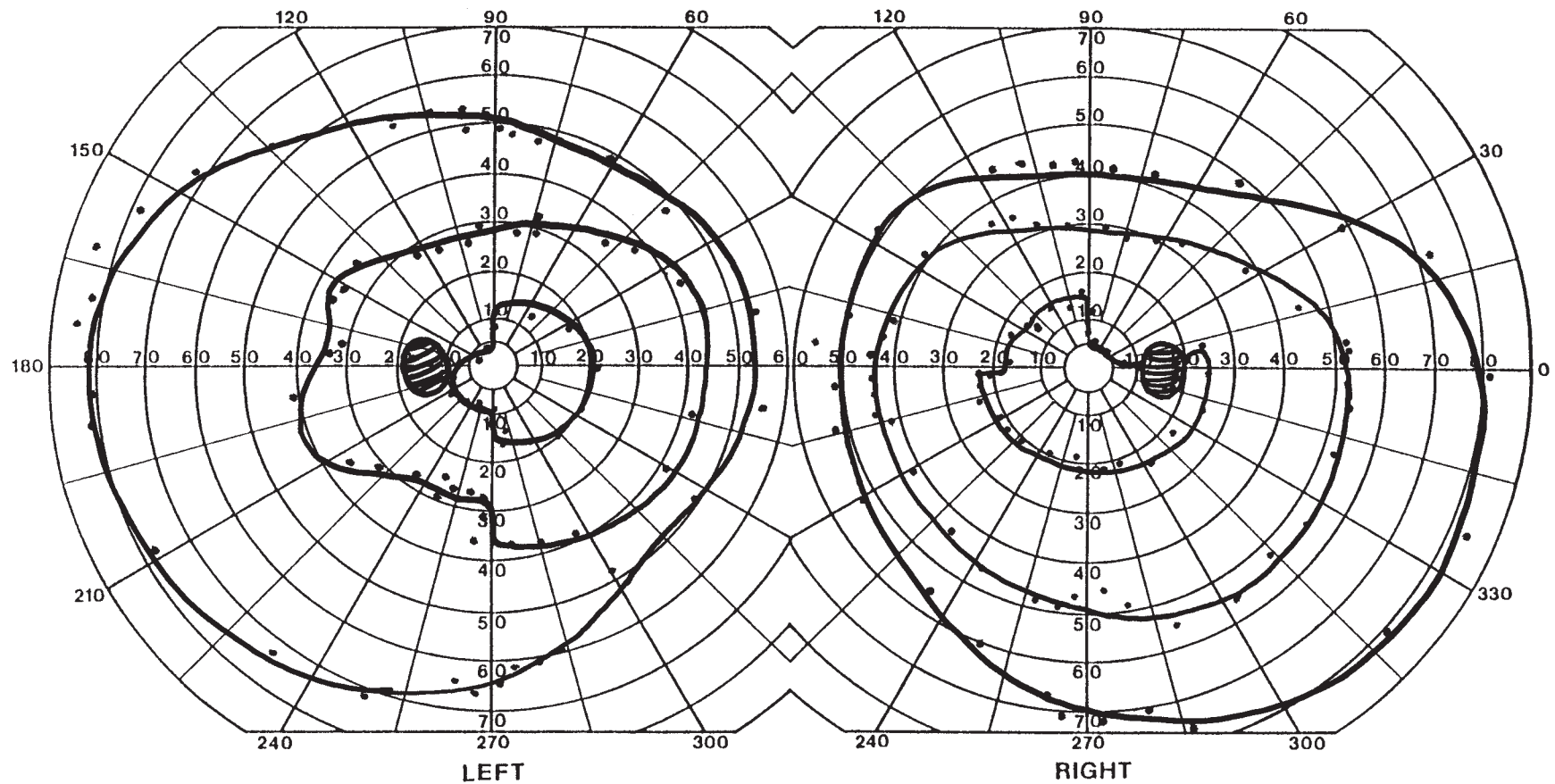
Bowtie (band) optic atrophy (see case 69) is a classic finding with long-standing compression of fibers from the nasal hemiretina (temporal hemifield), in either the optic chiasm or the optic tract (117). The superior and inferior aspects of the optic disk are spared the atrophy, because they are occupied by the arcuate fibers arching in from the temporal hemiretina, around the papillomacular bundle (see Chapter 2).



HISTORY AND EXAM

This 61-yr-old woman reported gradually progressive visual loss in the left eye over 5 months. In the days prior to presentation, she could not read the numbers on her bedside clock. Vision was worst in the center and in the temporal field. She had glaucoma in the right eye and an iatrogenic peripheral neuropathy following cisplatin treatment for

ovarian cancer. Acuity was 20/20 OD and 20/40 OS. Ishihara color plates were 13/14 OD and 9/14 OS. Fundoscopy showed normal disks. The remainder of the neurologic examination was normal, apart from the peripheral neuropathy.



DISCUSSION

Field description: Bitemporal hemifield defects with superior nasal step OD.

Localization: Optic chiasm and optic nerve OD.

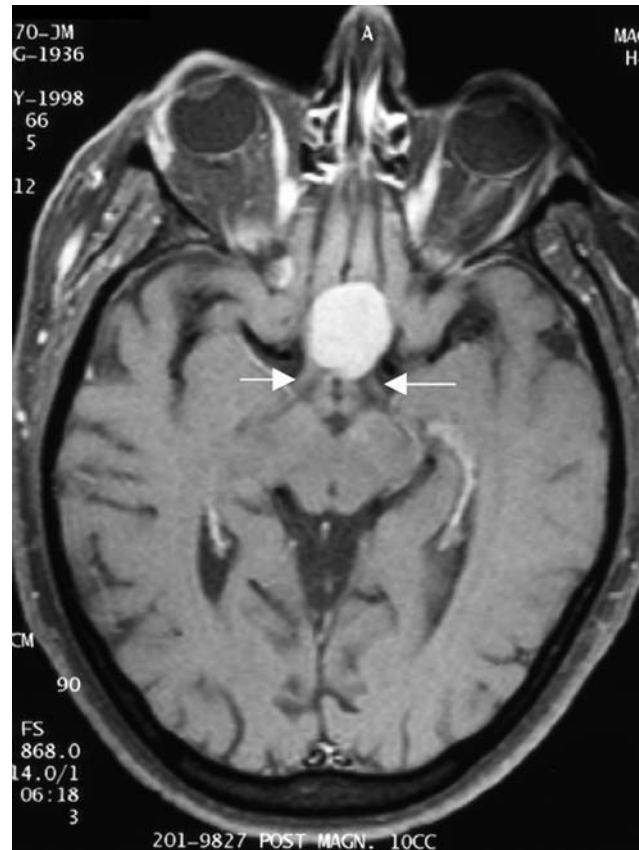
Pathology: Meningioma.

Confrontation testing was normal OD and showed decreased color and hand comparisons temporally OS.

In addition to the by-now familiar bitemporal depressions in the central field that align along the vertical meridian, the patient has a curious superior nasal step respecting the horizontal meridian OD, indicating damage to the right optic nerve (which could be from her glaucoma too). Enhanced axial T1-weighted MRI demonstrated a parasellar menin-

gioma with compression of the optic chiasm (note the optic tracts emerging just behind the bright mass, arrows).

Visual loss with or without nonspecific headaches is the most common presentation of patients with meningiomas of the sella or medial sphenoid ridge. Gradually progressive asymmetric visual field loss is the rule. However, acute onset with fluctuations over weeks or months may also occur, mimicking optic neuritis (see Case 67). Surgery remains the mainstay of therapy for patients with meningiomas involving the intracranial optic nerve and chiasm. Radiotherapy reduces the risk of recurrence when surgical removal has been incomplete. The visual outcome is related primarily to the duration of symptoms.



DISCUSSION

Field description: Diffuse depression with temporal hemifield defect OD, inferior arcuate defect OS.

Localization: Intracranial optic nerves and chiasm.

Pathology: Compression by meningioma (shown below).

Note that on May 24, 1991, the patient has thresholds of 0 dB in almost the entire temporal hemifield and inferonasal quadrant OD, with the defect aligning along the vertical meridian in the superior field. On the same day, the field OS shows a typical inferior arcuate defect arching out of the blind spot on the gray-scale image and ending in a nasal step at the horizontal meridian, best seen on the total deviation plot. Five days later, on May 29, with her menstrual period ending, there is already evident improvement in both eyes, with the mean deviation (MD) of both eyes improving by about 3–4 db, confirming her own observations.

The history of acute visual loss with improvement suggested optic neuritis. In retrospect, she had probably suddenly noticed a visual loss that had been present for some

time. Recurrence of optic neuritis does occur (see Case 25), but frequent predictable relapses timed to the menstrual cycle are definitely odd. This history, verified by perimetry, suggests a hormonally sensitive tumor. Some meningiomas contain estrogen receptors and can fluctuate in this manner.

Suprasellar meningiomas frequently express estrogen and progesterone receptors and may enlarge under the influence of these hormones, particularly during the second half of pregnancy (118). Cyclical enlargement and shrinkage of these hormone-sensitive meningiomas may also occur concurrent with the hormonal fluctuations that accompany menstrual cycles. In a similar vein, the pituitary gland enlarges slightly during pregnancy principally because of hypertrophy of the PRL-secreting cells. However, under normal circumstances, the chiasm is situated about 4–10 mm above the diaphragm sella, so visual symptoms due to changes in the size of the pituitary should not occur in the absence of an underlying macroadenoma (119).



HISTORY AND EXAM

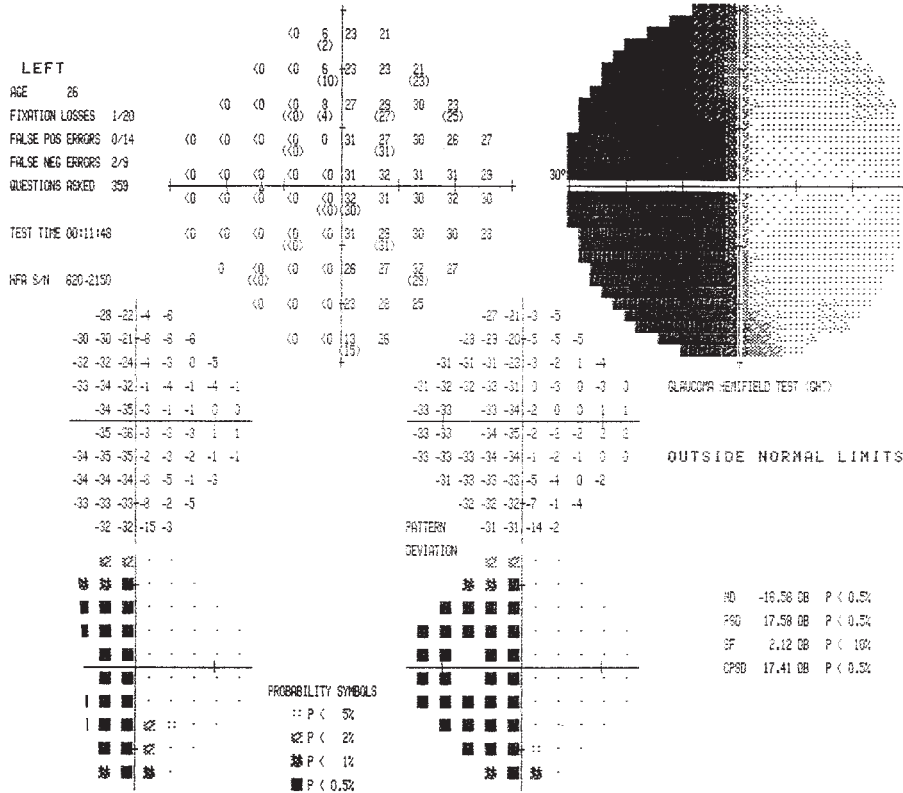
This 26-yr-old man had 1 year of unusual persistent headaches and 3 months of blurry peripheral vision in both eyes that had gradually encroached on central vision. He then found that letters disappeared or doubled vertically or horizontally when he tried to read. His doctor discovered hypothyroidism with a low TSH and obtained brain imaging. He

was treated surgically a few days prior to evaluation and the reading disturbance resolved, but his peripheral vision to the left seemed worse. His acuity was 20/20 OU and there was an RAPD OS. Optic disks showed temporal pallor OU. Eye movements were normal.

CENTRAL 30 - 2 THRESHOLD TEST

DATE 08-26-93

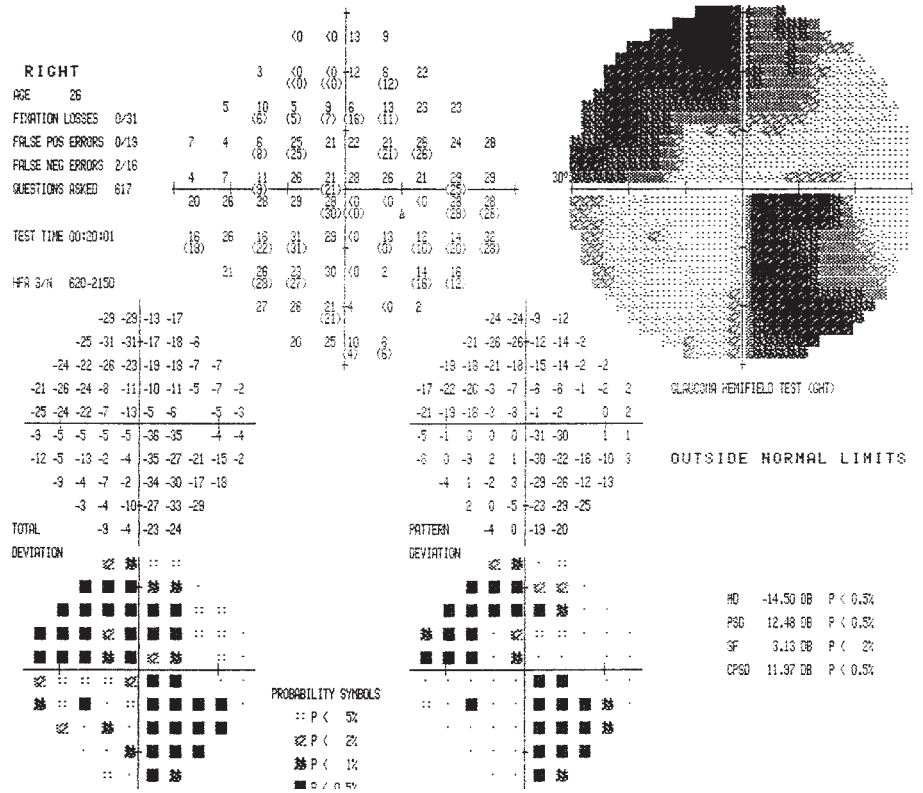
STIMULUS III, WHITE, BCKGND 31.5 ASB BLIND SPOT CHECK SIZE III
 STRATEGY FULL THRESHOLD
 FIXATION TARGET CENTRAL
 RX USED OS DCK DEG PUPIL DIAMETER 3.0 MM VR
 TIME 01:14:21 PM



CENTRAL 30 - 2 THRESHOLD TEST

DATE 08-26-93

STIMULUS III, WHITE, BCKGND 31.5 ASB BLIND SPOT CHECK SIZE III
 STRATEGY FULL THRESHOLD
 FIXATION TARGET CENTRAL
 RX USED OS DCK DEG PUPIL DIAMETER 3.0 MM VR
 TIME 01:06:43 PM



DISCUSSION

Field description: Bitemporal partial hemifield loss with superior arcuate defect OD.

Localization: Optic chiasm, superior aspect, and right intracranial optic nerve.

Pathology: Craniopharyngioma (MRI shown below).

Other features: Hemifield slide, central hypothyroidism.

Tangent screen perimetry with a 3-mm white target showed a complete temporal defect OD and nasal and inferotemporal defects OS. Hand motion was preserved except in the far temporal periphery OD.

The patient's bitemporal defects line up at the vertical meridian, with complete temporal hemianopia OS and inferotemporal loss OD; the latter suggests that it is the superior aspect of the optic chiasm that is being compressed. In addition, he has a nasal field defect that respects the horizontal nasal meridian and arches across the vertical merid-

ian—a typical superior arcuate defect, indicating compression of the right intracranial optic nerve as well. The resulting pattern on the plot is not unlike the BMW logo.

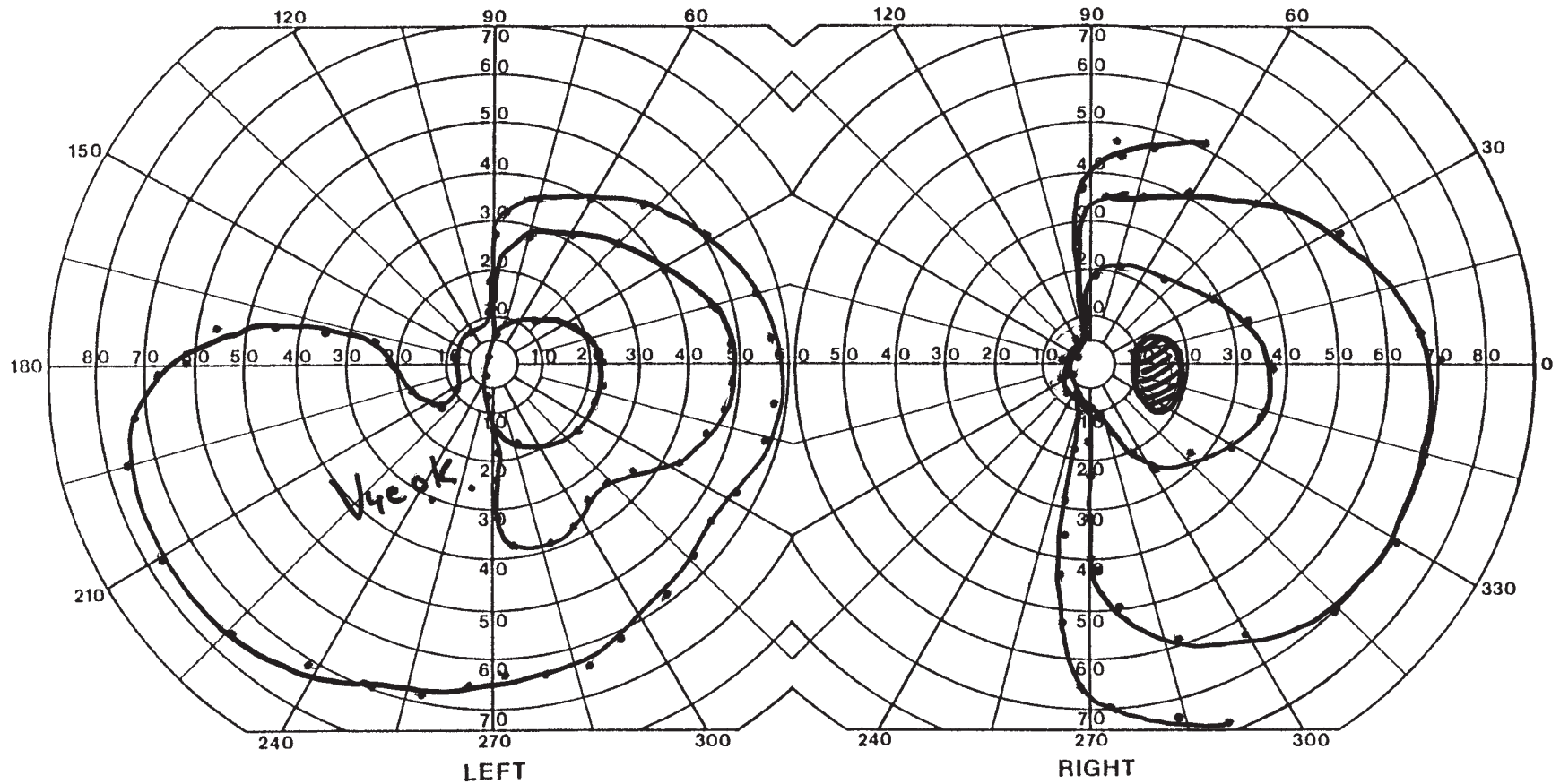
Craniopharyngiomas likely arise from the remnants of the Rathke pouch, nests of squamous cells scattered along the infundibular stem and posterior pituitary gland. The direction of compression of visual structures is more variable than with pituitary adenomas. These tumors are heterogeneous, with cystic areas and regions of dystrophic calcification. They can occur at any age from infancy onward. Children often do not complain of visual loss and present instead with hydrocephalus and pituitary insufficiency with, e.g., growth failure, retarded sexual development, and diabetes insipidus. Treatment is difficult. Complete surgical resection is rarely possible, but radiation usually given after subtotal resection reduces the risk of tumor recurrence (112).



HISTORY AND EXAM

This 51-yr-old woman had a generalized tonic-clonic seizure. MRI demonstrated multiple lesions in the right temporal lobe, which a biopsy showed to be due to sarcoidosis. She had a left upper quadrantanopia, thought to be a complication of her biopsy. She was

maintained on low-dose prednisone for many years. On examination 7 years later, visual acuity was 20/40 OU and color vision was 9/14 OD and 8/14 OS. There was an RAPD OS, and funduscopy showed diffuse pallor OD and bowtie atrophy OS.



DISCUSSION

Field description: Incongruous partial left homonymous hemianopia.

Localization: Right optic tract.

Pathology: Sarcoidosis.

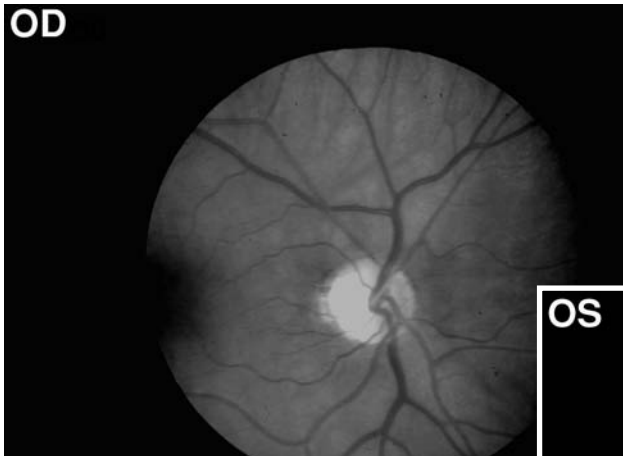
Other features: Bowtie optic atrophy OS (arrowheads).

Confrontation testing showed a left upper quadrantanopia more pronounced in the right eye to hand motions.

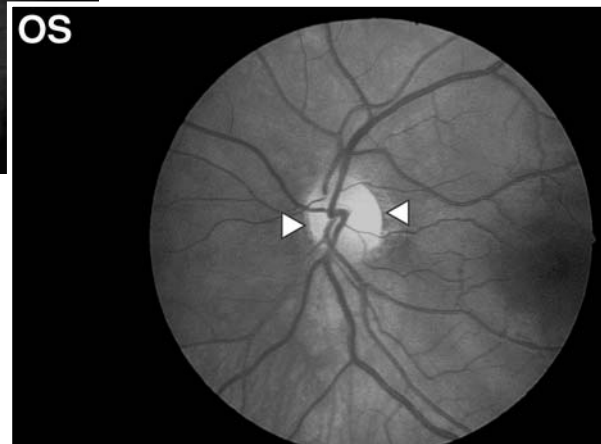
The dramatic incongruity appears mainly in the V4e isopter, where there is a virtually complete hemianopia OD, yet preserved perception of this target in the entire left inferior quadrant OS. Marked incongruity of the field defect (120,121), the left RAPD (122), and the presence and pattern of the patient's optic atrophy indicate that her visual loss is due

to damage to the optic tract, not the optic radiation. T1-weighted axial MRI showed basilar enhancement that included not only the right temporal lobe (the cause of her seizures), but also the right optic tract, hypothalamus, and pituitary stalk. Thus, her field loss is from her disease, not the biopsy.

In a series of 68 patients with neurosarcoidosis, 38% had involvement of the optic chiasm or nerve (46). The disease can also affect the brain stem, spinal cord, and meninges, with some CSF abnormality (pleocytosis or elevated protein) in 81%. MRI of the brain can show either multiple white matter lesions (43%) or meningeal enhancement (38%) (46). Chest X-ray had poor sensitivity, being normal in two-thirds of the patients in this series. Biopsy of tissue from the brain or elsewhere is usually required to make the diagnosis.



See Color Plate after page 180



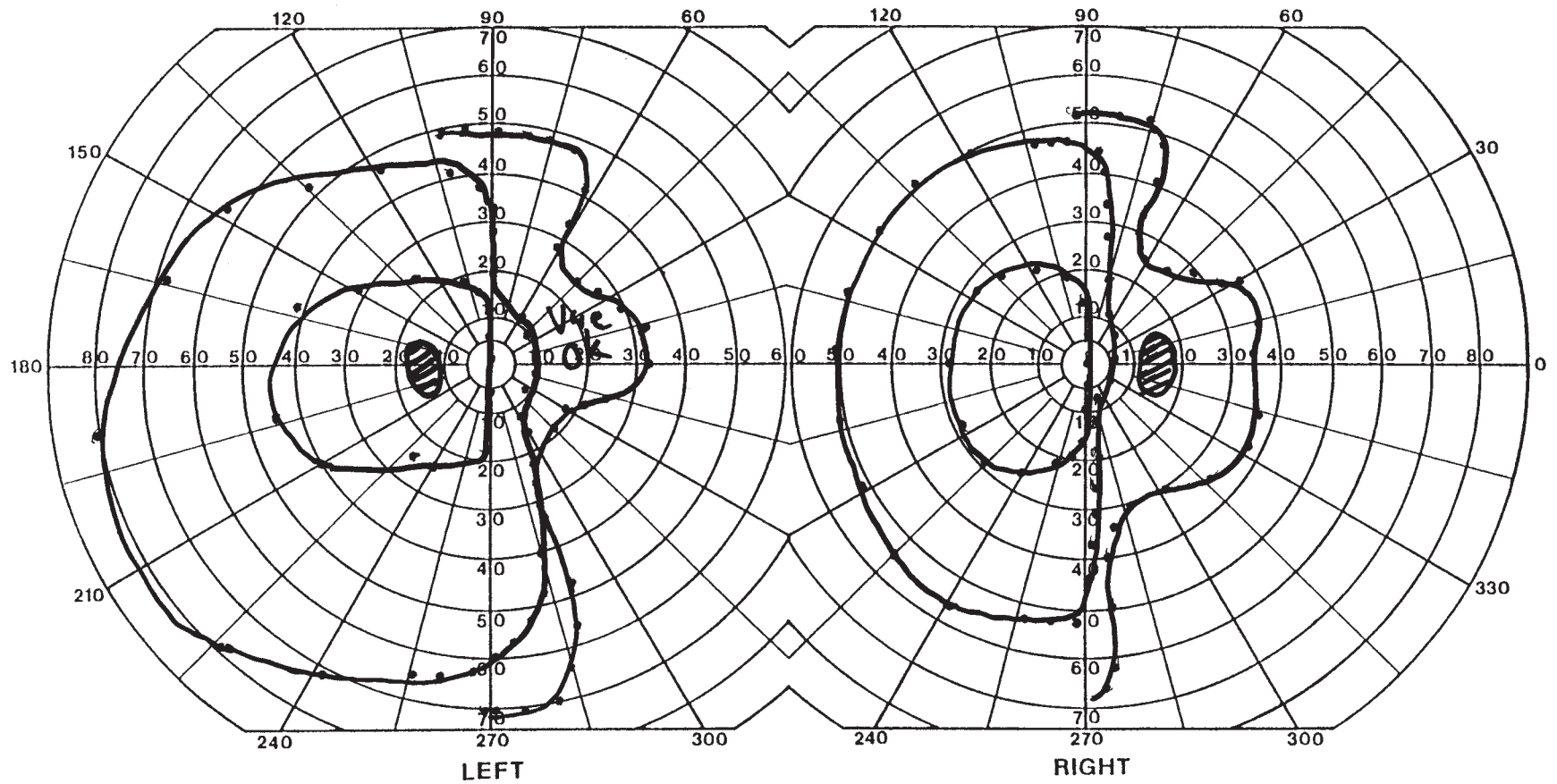
See Color Plate after page 180



HISTORY AND EXAM

This 7-yr-old girl presented with 1 month of worsening frontal headaches. She also had double vision on rightward gaze. Visual acuity was normal OU, but there was a right

RAPD and fundoscopy demonstrated papilledema bilaterally. There was also a partial right VI nerve palsy. The remainder of the neurologic examination was normal.



DISCUSSION

Field description: Incongruous partial right homonymous hemianopia.

Localization: Left optic tract.

Pathology: Hypothalamic glioma.

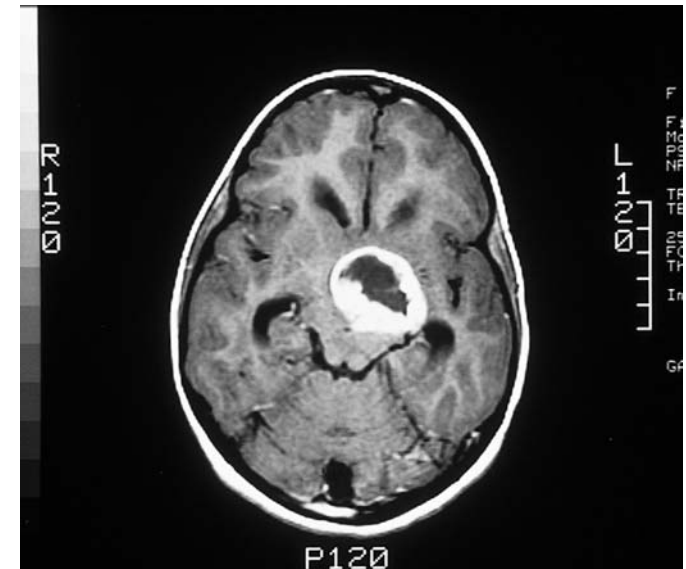
Other features: Twin peaks papilledema OD.

The patient's partial hemianopia respects the vertical meridian only for the smallest (I2e) target. There is more sparing near the meridian with the larger targets, which differs in outline between the two eyes. Some of the irregularity along the vertical midline may be the result of poor fixation in a young patient, but the variability in the partial sparing with the largest (V4e) isopter seems more than attributable to fixation shift. This sparing may obscure the vertical step of the hemianopia at the bedside if only large targets such as hand motion are used. T1-weighted axial MRI showed an enhancing left hypothalamic mass with hydrocephalus. She had ventriculostomy, and histology of the resected tumor showed a glioma.

Her right optic disk showed a special "twin peaks" form of papilledema (123). This provides a vivid demonstration of the pattern of optic atrophy with optic tract lesions. The eye with temporal field loss has some atrophy of the temporal disk, where fibers from the retina just nasal to the fovea enter the nerve, and also of the nasal disk, which is occupied by fibers from the more peripheral nasal retina. The superior and inferior disk are not atrophic because they contain the arcuate fibers from the temporal retina (the good nasal hemifield). The eye with nasal field loss has atrophy of the superior and inferior disk as well as the temporal disk, because this also contains fibers from the temporal half of the macula. The result is a bowtie pattern of optic atrophy in the eye with temporal hemianopia and a more generalized temporal atrophy in the eye with nasal hemianopia, after a tract lesion has been present for several months. Most tract lesions are masses. When such a mass causes increased intracranial pressure, only the nonatrophic portions of the optic disks can express the papilledema—hence, the edema of the upper and lower disk only in this patient's right eye.

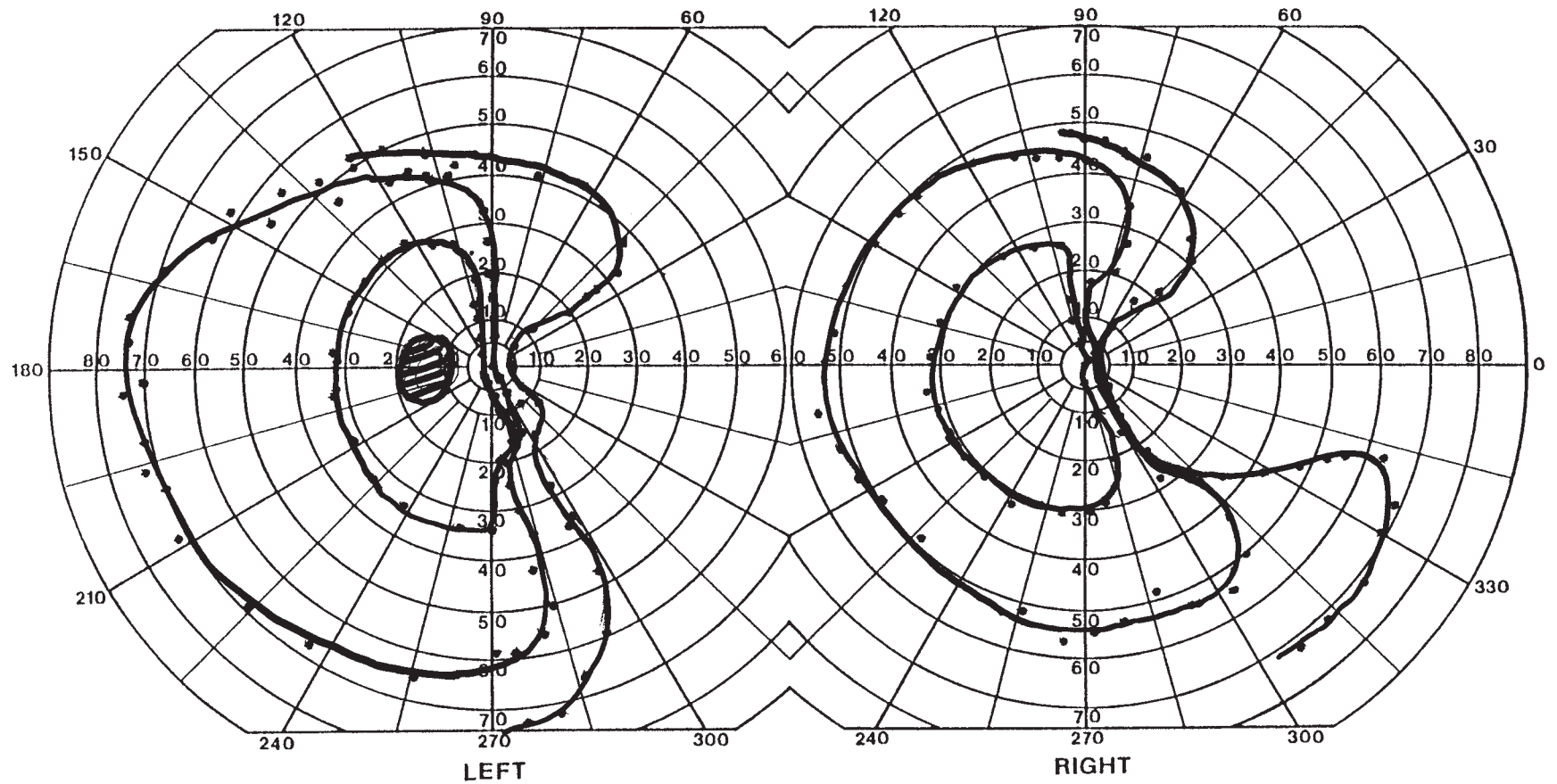


See Color Plate after page 180



HISTORY AND EXAM

A 60-yr-old man had sudden headache and right-sided visual loss. He had a history of hypertension. When assessed 1 week later, visual acuity was 20/25 OU, and there was no RAPD or optic atrophy. Eye movements were normal.



DISCUSSION

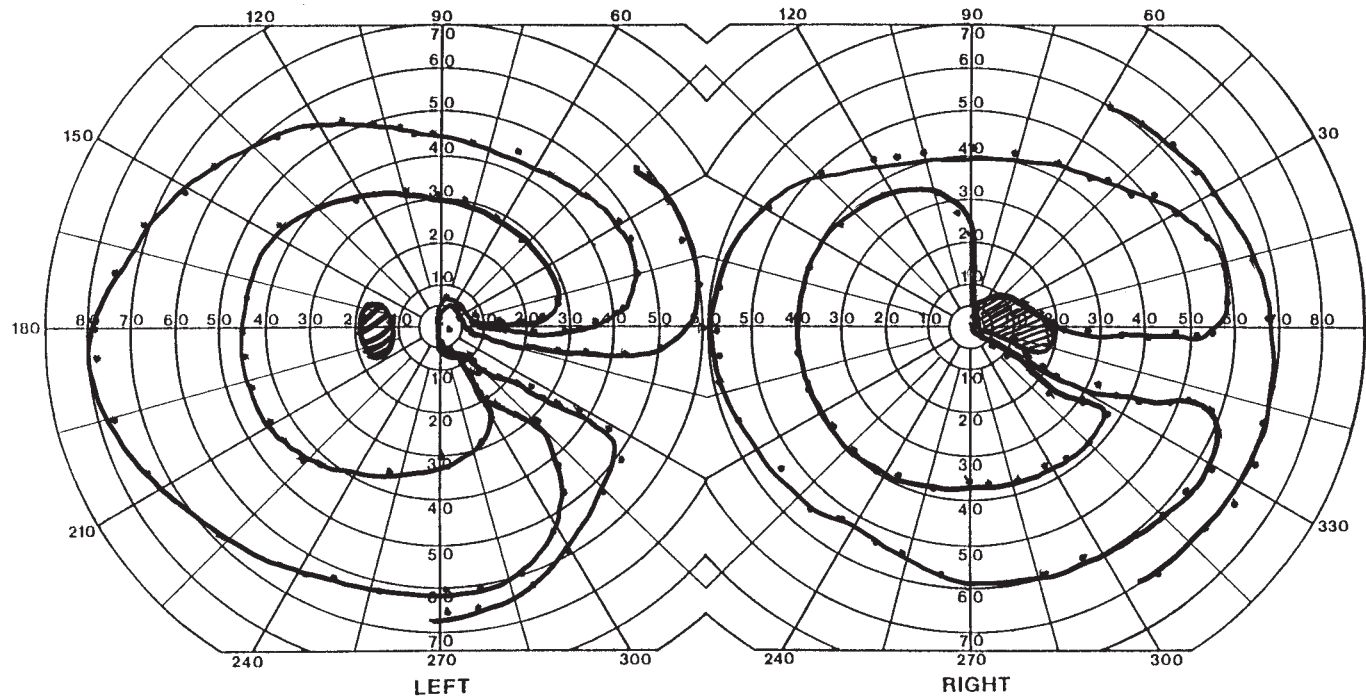
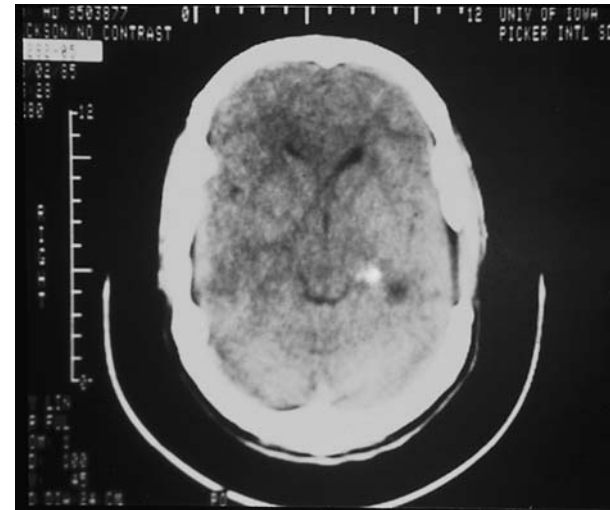
Field description: Incongruous homonymous right horizontal sectoranopia.

Localization: Left lateral geniculate nucleus, central/hilar zone.

Pathology: Hypertensive cerebral hemorrhage.

The initial field shows a sectoranopia, with sparing of the field adjacent to the vertical meridians, most prominent OD and with the largest V4e target. This indicates that the region most affected is the zone surrounding the horizontal meridian.

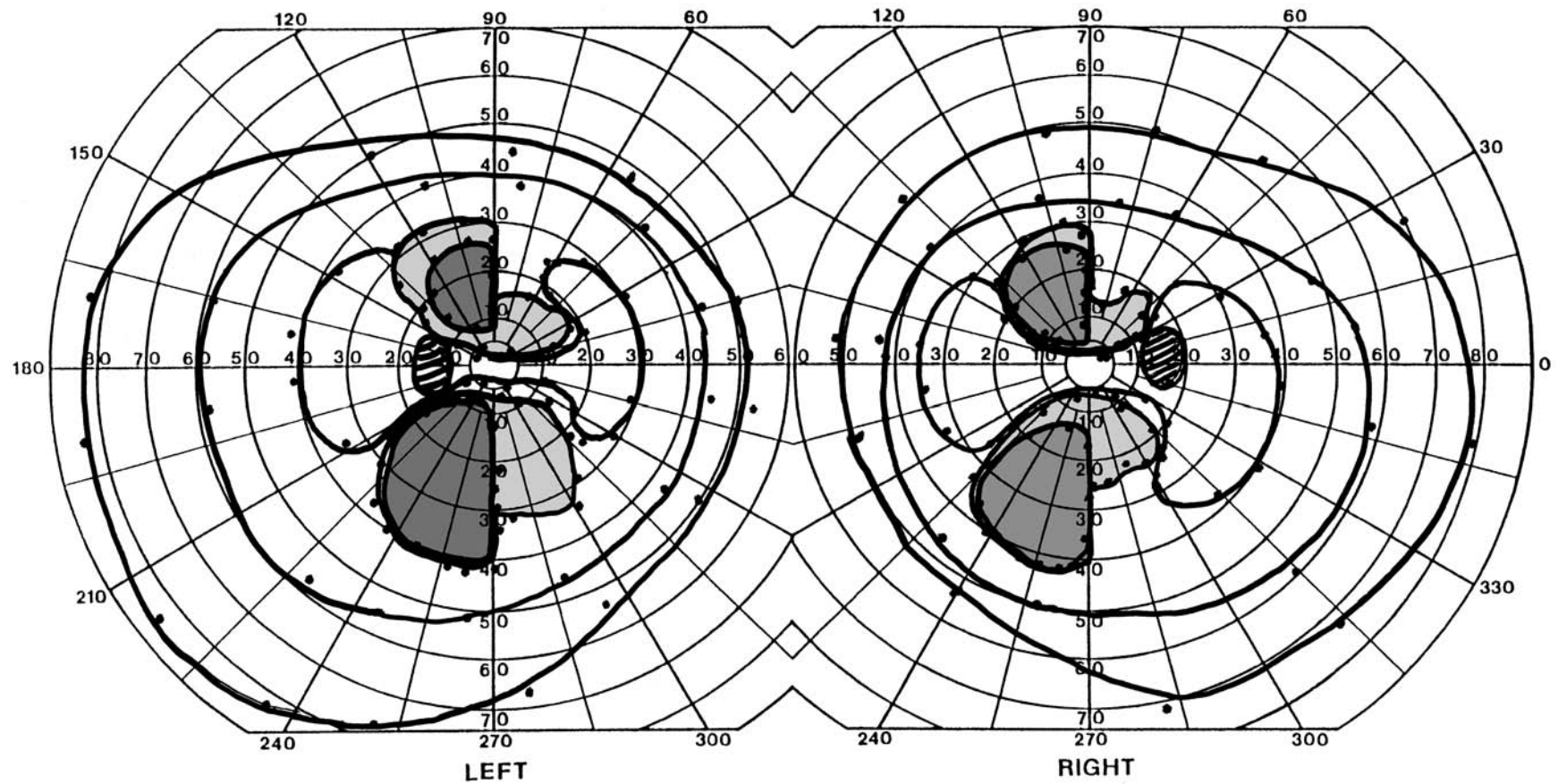
The middle portion of the lateral geniculate nucleus (LGN) is supplied by the posterior choroidal artery, and an infarct of this zone will cause a wedge field defect straddling the horizontal meridian (124). In this case, the pathology is not an infarct but a small deep hemorrhage, as shown on axial CT scan. Over time the sectoranopia improved partially, with narrowing of the wedge to a keyhole defect, shown here.



HISTORY AND EXAM

A 65-yr-old woman with cryptogenic hepatic failure and portal hypertension underwent a liver transplant. It was difficult to wean her off the respirator, and she was in prolonged coma. When she regained consciousness, her vision was not clear and she had trouble reading. She also had dysarthria, incoordination, increased forgetfulness, and gen-

eralized limb weakness. When assessed 4 months later, visual acuity was 20/25 OD and 20/75 OS. She had no RAPD or optic atrophy. Verbal memory was impaired. She had signs of critical care myopathy.



DISCUSSION

Field description: “Hourglass” field defects—bilateral, slightly incongruous homonymous sectoranopias abutting the upper and lower vertical meridians, sparing the field around the horizontal meridians.

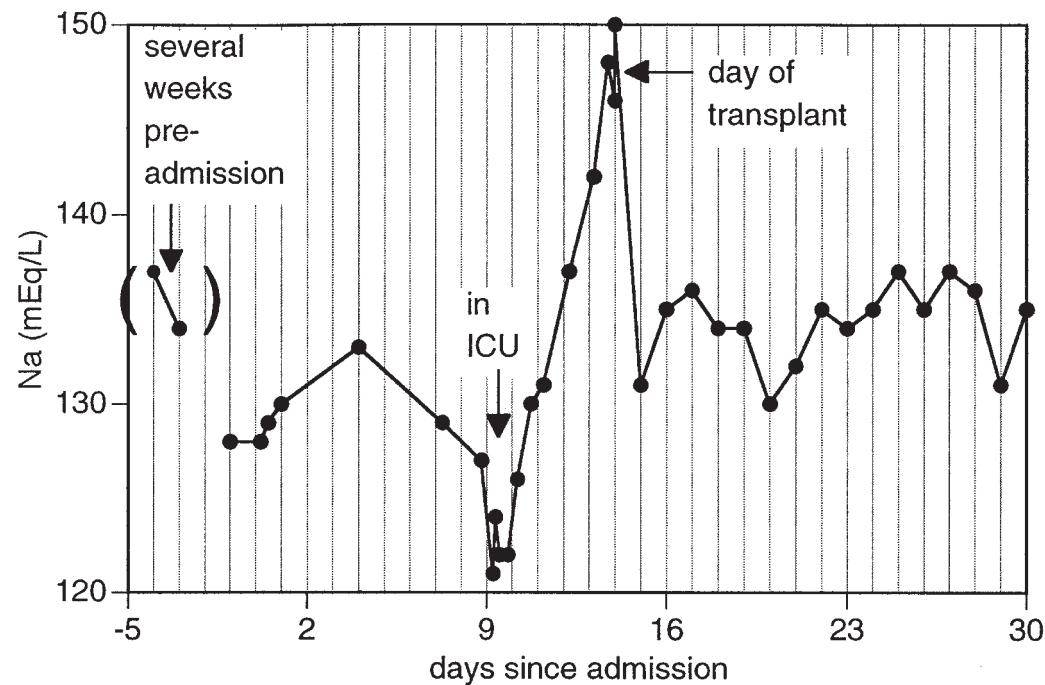
Localization: Bilateral lateral geniculate nuclei, medial and lateral zones.

Pathology: Central pontine myelinolysis.

Confrontation testing showed left superior quadrant central defects OU to red targets and face comparison.

These unusual “hourglass” field defects (125) represent the converse of the sectoranopia of the previous case, in bilateral combination. The similarity between the two eyes

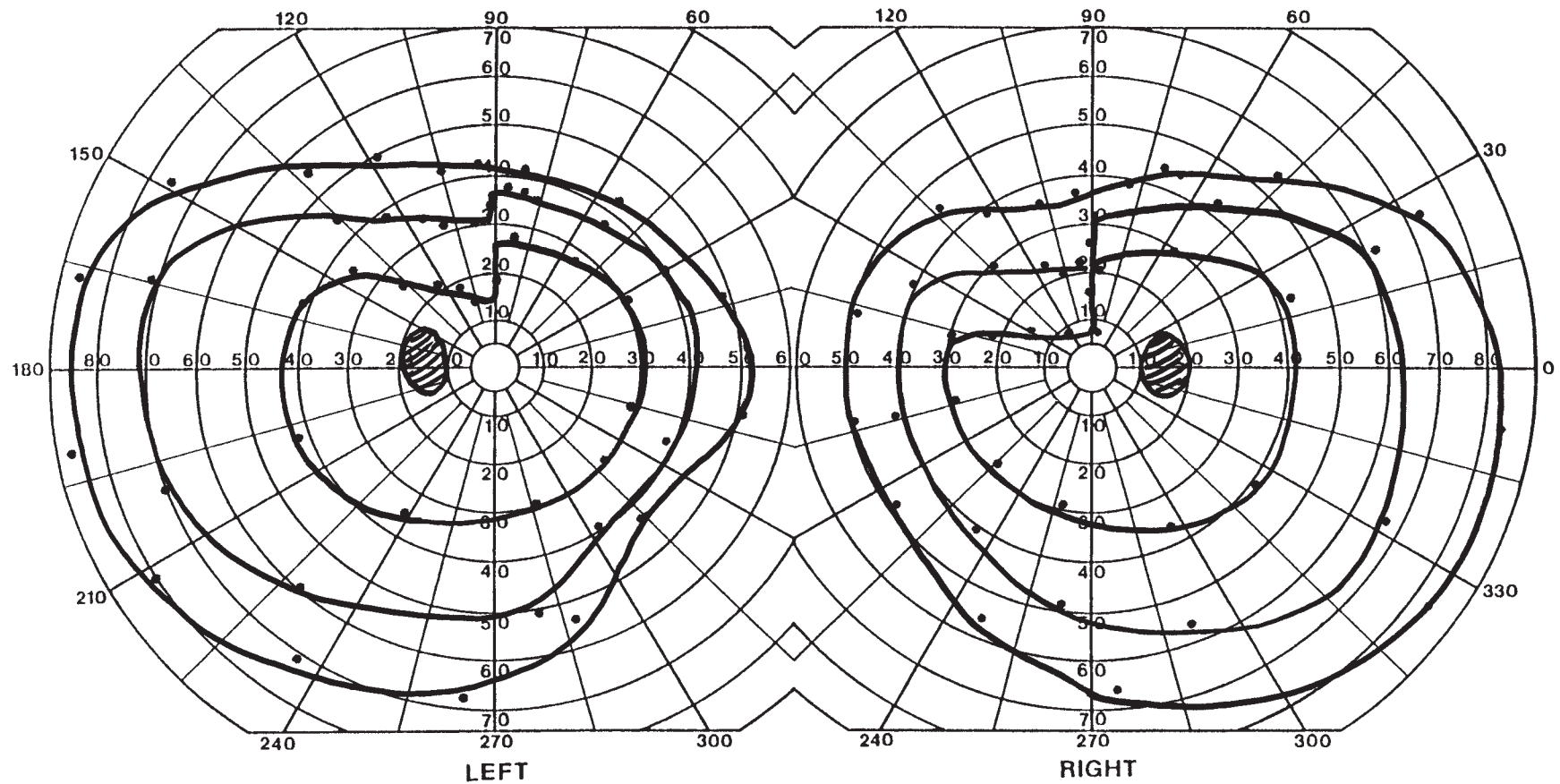
and the steps at the vertical meridian confirm that there are bilateral postchiasmal lesions. These sectoranopias stem from dysfunction of the lateral and medial zones of the lateral geniculate nuclei. The anterior choroidal artery supplies these zones. However, here the most likely cause is myelinolysis (125). A chart review revealed a preoperative hyponatremia of 121 meq/L, which was overcorrected to 150 meq/L on the day of transplantation. Myelinolysis, or osmotic demyelination, is related to this rapid overcorrection. Pathologic studies have confirmed the vulnerability of the LGN to this disorder (126). Among transplantation procedures, myelinolysis is a risk unique to liver transplants, in which patients often run a preoperative hyponatremia related to ascites and portal hypertension (127). The patient’s field defects remained stable 1 year after surgery.



HISTORY AND EXAM

This 32-yr-old man had complex partial seizures since childhood. These were refractory to medical therapy, and at age 20 he had a right anterior temporal lobectomy, which

initially improved seizure control. He did not have any visual symptoms. On assessment for a drug study, his acuity was 20/20 OU and fundi were normal.



DISCUSSION

Field description: Mildly incongruous left homonymous partial superior quadrantanopia.

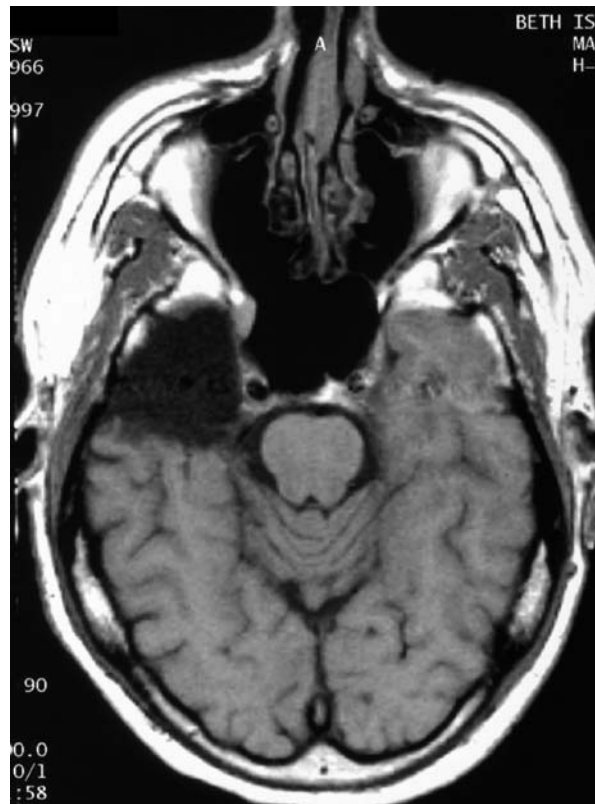
Localization: Right temporal optic radiation.

Pathology: Resection.

Confrontation fields were normal OU.

The patient has a subtle relative depression of the superior field, more OD, and not extending close to the horizontal meridian or fixation.

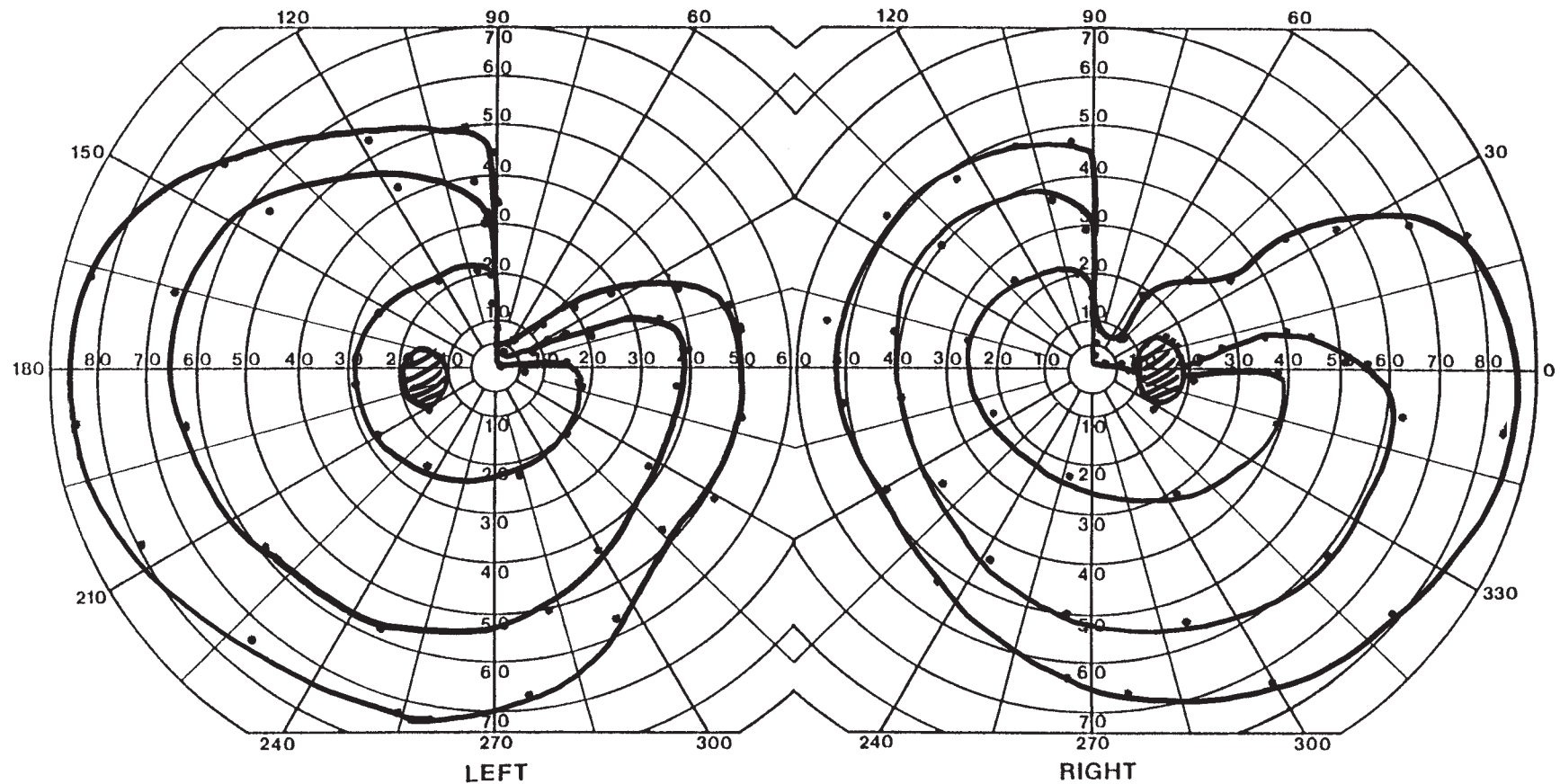
Field defects from temporal lobe resections are homonymous and always begin at the vertical meridian. The degree to which they spread toward the horizontal meridian varies with the posterior extent of the resection. Hence, the vertical meridian is the area to concentrate field testing in these patients. This subtle defect was missed on confrontation testing, but careful probing of the vertical meridian with Goldmann perimetry shows the defect. MRI shows the resection, which extends about 4 cm from where the anterior temporal pole had been. The classic neurosurgical series reported that field defects were produced when resections extended at least 4 cm posteriorly from the temporal pole (128,129). Lesions extending beyond 8 cm tend to produce complete hemianopia (128,130).



HISTORY AND EXAM

This 40-yr-old man had complex partial seizures since age 19, sometimes followed by a period of postictal psychosis. There was a history of complex febrile seizures as a child. video-electroencephalogram (EEG) telemetry showed that the seizures arose from the left temporal lobe. MRI demonstrated scarring in the white matter lateral to the temporal horn

of the lateral ventricle, and the left temporal lobe was smaller than the right. His visual fields at that time were normal. He had a left anterior temporal lobectomy, which showed hippocampal (mesial temporal) sclerosis. Acuity was 20/20 OU and fundoscopy was normal.



DISCUSSION

Field description: Mildly incongruous right homonymous partial superior quadrantanopia.

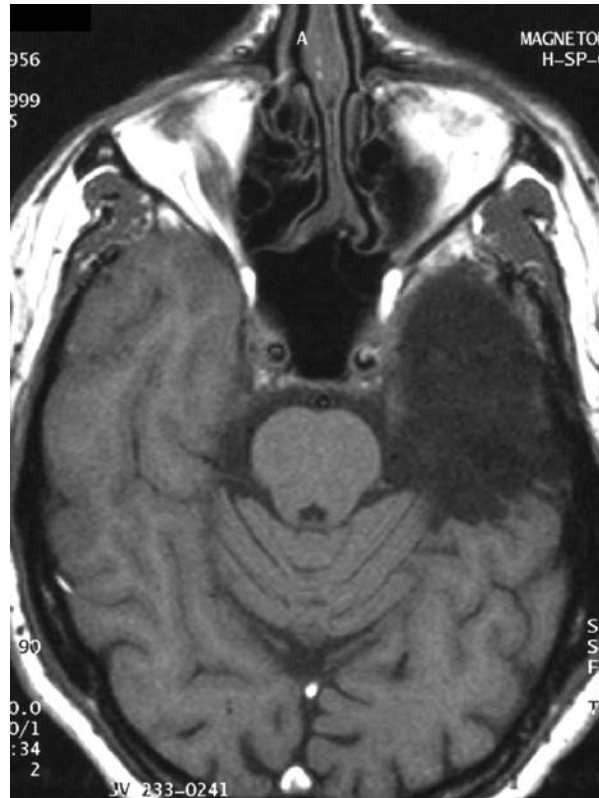
Localization: Left temporal optic radiation.

Pathology: Resection.

Confrontation testing with hand motion did not show the defect, but careful searching with a moving finger along the vertical meridian did.

The patient's defect is more extensive than that of Case 73. It extends to fixation in the smaller isopters but still does not quite reach the horizontal meridian with the larger isopters. Postoperative MRI shows a resection of about 5.5 cm, consistent with the degree

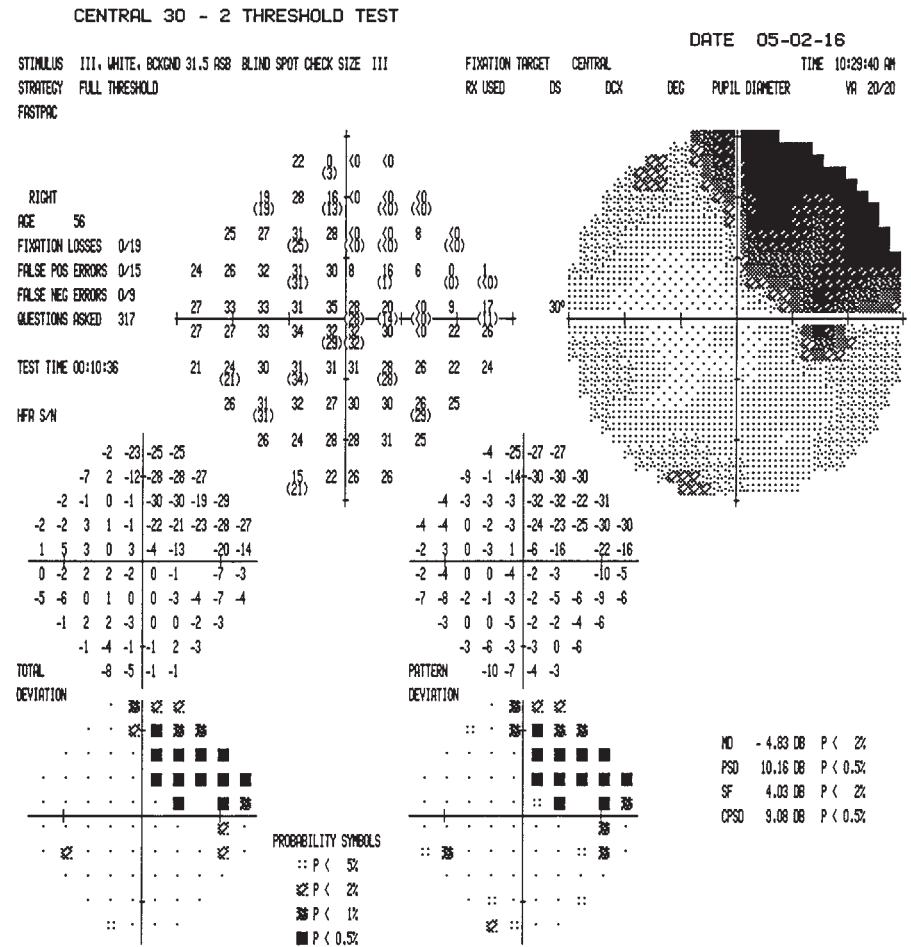
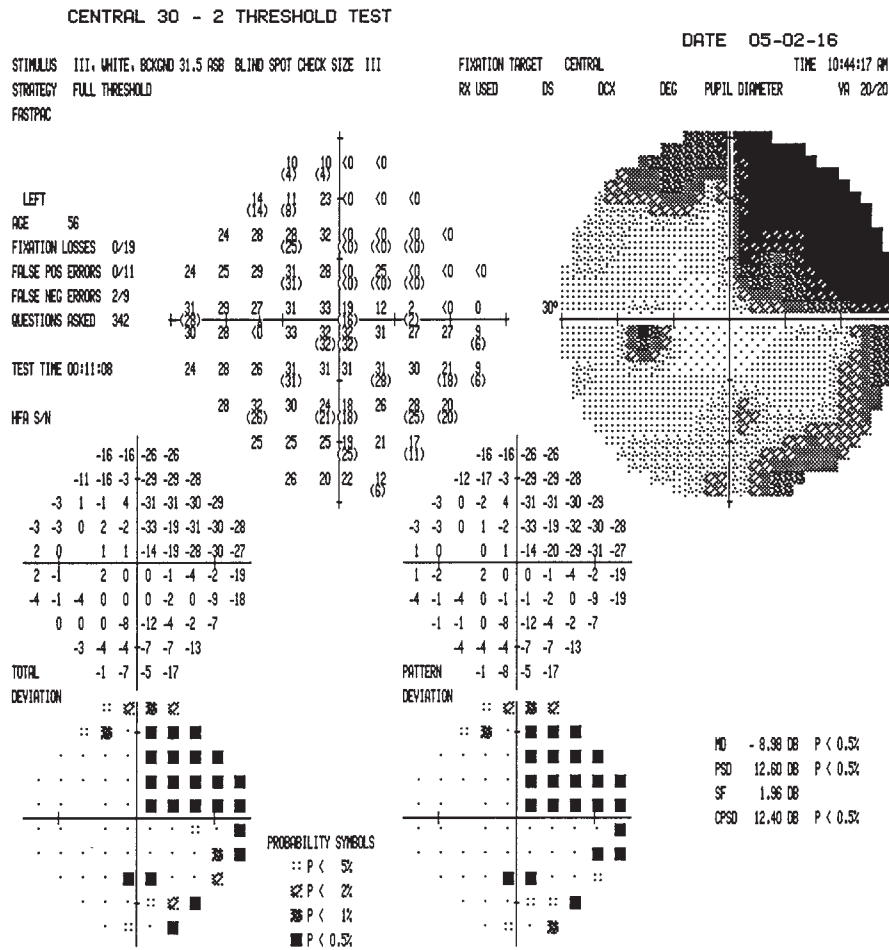
of resection thought to encroach on Meyer's loop. The preoperative MRI abnormality is consistent with mesial temporal sclerosis, the most common pathologic finding in patients with refractory temporal lobe epilepsy who undergo surgical resection for seizure control. The exact relation of mesial temporal sclerosis to seizures is still debated. Childhood complex febrile seizures may injure the medial temporal lobe, or the medial temporal lobe injury may occur first and cause subsequent seizures. The pathogenetic story may be even more complicated; a subtle brain anomaly may predispose to febrile seizures, which themselves may induce further injury and cause hippocampal sclerosis and, ultimately, adult complex partial seizures (131–133).



HISTORY AND EXAM

This 36-yr-old woman had long-standing seizures refractory to anticonvulsants. At age 26, she had a right anterior temporal lobectomy, which rendered her free of seizures without medication. Postoperatively she had a visual field defect that has remained stable.

Visual acuity and color vision were normal. There was no RAPD and the optic disks were normal.



DISCUSSION

Field description: Moderately incongruous, nearly complete homonymous right superior quadrantanopia.

Localization: Left temporal optic radiation.

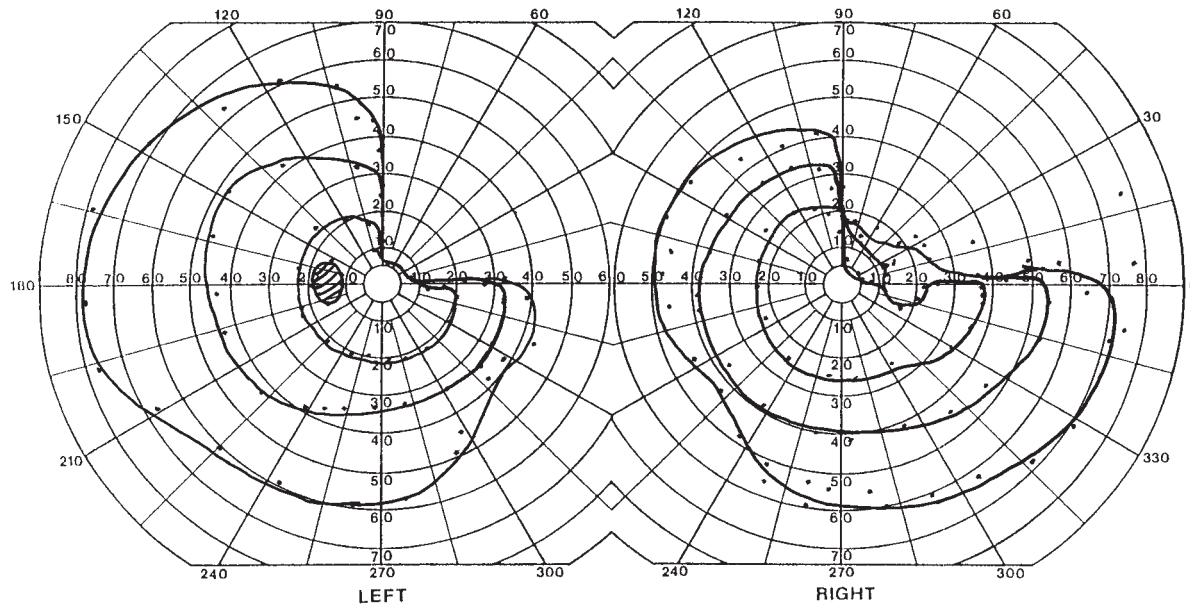
Pathology: Resection.

Confrontation fields showed greater incongruity, with no hand motions seen in the whole upper quadrant OS, but some preserved finger counting ability in this quadrant OD.

Automated perimetry shows a quadrantic defect that aligns at the horizontal meridian, with perhaps slight sparing at the macula. The incongruity is best appreciated in the sensitivity plot and gray scale, where more scattered locations with some residual sensitivity

(i.e., >0 dB) are found OD than OS. There are scattered reductions in sensitivity inferiorly, more so on the right eye, but these do not respect the vertical meridian and are not confluent with the quadrantanopia, and thus are not likely due to the resection, which MRI showed to be extensive, involving the anterior 5.3 cm of the temporal lobe. Goldmann perimetry confirmed normal inferior fields (shown here).

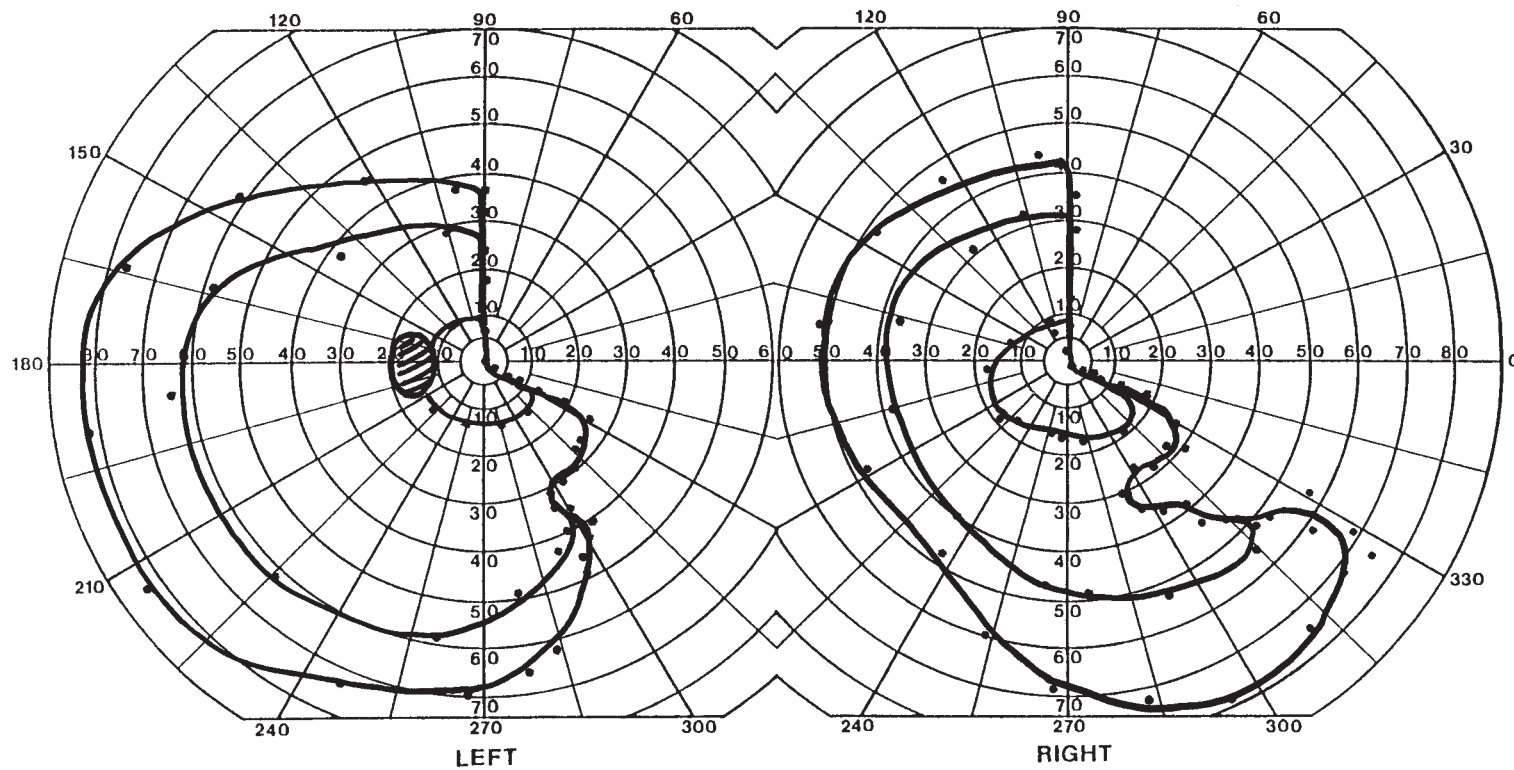
Surgery is being used more frequently in the treatment of epilepsy. A recent randomized trial (134) of 80 patients showed that 58% of surgical patients remained free of complex partial seizures at 1 year of follow-up, compared with 8% of patients treated medically. Evaluation for surgery should probably not be delayed by prolonged and numerous trials of drugs if seizures are poorly controlled.



HISTORY AND EXAM

This 74-yr-old woman suddenly lost vision on the right while at the circus with her grand-daughter. She found her reading slow, often having to re-read lines. She reported no problems with face or object recognition. Examination in the emergency room showed a right hemifield defect, normal acuity, no RAPD, and normal color scores with Ishihara

plates. However, within the remaining seeing regions of the right hemifield, she was unable to distinguish one color from another. She was in atrial fibrillation, which was treated with amiodarone and anticoagulation with coumadin.



DISCUSSION

Field description: Congruous right homonymous superior quadrantanopia plus.

Localization: Left striate cortex.

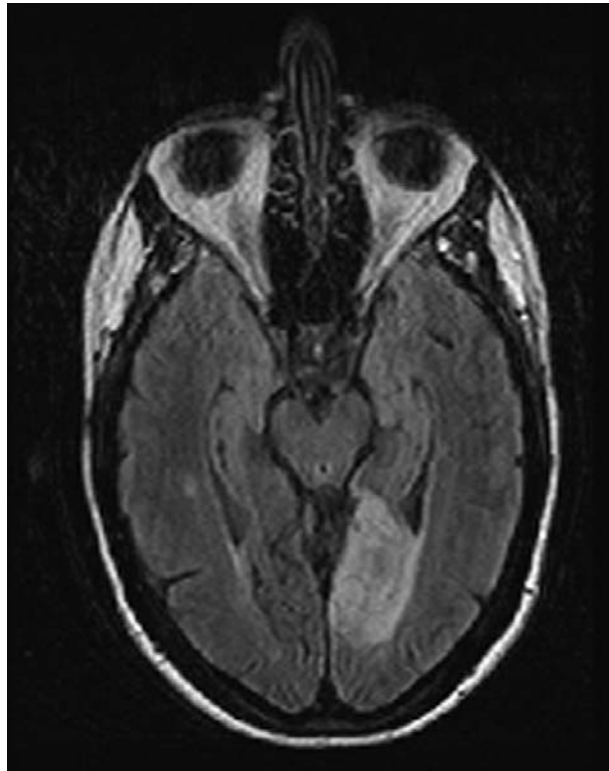
Pathology: Posterior cerebral arterial infarct, cardioembolic.

Other features: Right hemidyschromatopsia.

Confrontation testing with hand motions showed the same defect, involving the macula and upper part of the inferior quadrant.

Hemi-dyschromatopsia is impaired color vision in the hemifield contralateral to the lesion. It is often not spontaneously noticed by patients (135,136). The diagnosis requires an inability to discriminate among colors. Color naming may or may not be impaired,

depending on the severity of the color defect. Lesions of the lingual and fusiform gyri in the ventromedial occipital lobe are responsible (137). Achromatopsia affecting the entire visual field is always apparent to the patient and requires bilateral occipital lesions. FLAIR axial MRI demonstrates a left posterior cerebral artery territory infarction that involves the fusiform gyrus. This patient's stroke is likely due to emboli from her atrial fibrillation. The risk of stroke with this disorder is high. It is one of the few scenarios for which a prospective double-blind, placebo-controlled trial (138) has proven that coumadin reduces the annual risk of recurrent stroke from 12 to 4%. The target INR in the study was 2.5–4.0.



DISCUSSION

Field description: Incongruous right homonymous superior quadrantic defects, with possible extension into lower field OS, complicated by poor reliability.

Localization: Distal optic radiation.

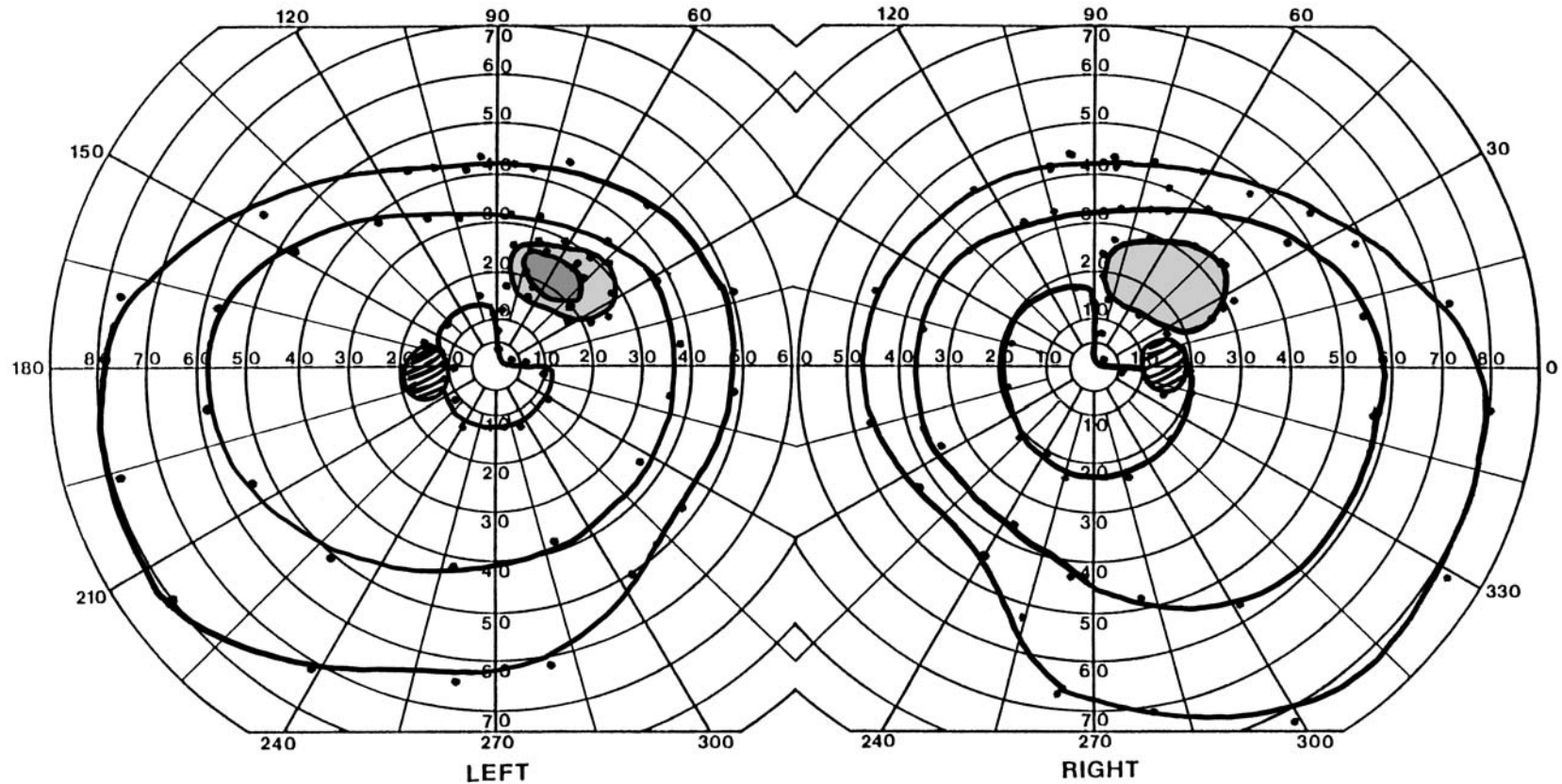
Pathology: Subcortical infarction.

Confrontation fields were normal, even though the results of perimetry were known.

Both right and left fields clearly show in the upper right quadrant a zone in which no target is seen at all (values of 0 dB on visual sensitivity plot). The rest of the right eye's field is normal, and the three reliability indices are excellent. In the left eye, which was tested second, the first thing to note is the poor fixation index of "6/21 xx," and the comment of

"low patient reliability," in the upper left part of the printout. This makes the patchy, less severe reductions in threshold flagged in the lower quadrants (both left and right!) more dubious. Poor fixation may have been related to the patient's macular disease. Goldmann perimetry 2 weeks later (see Goldmann field below) showed a congruous homonymous right superior quadrant scotoma, confirming that the inferior field defects were factitious.

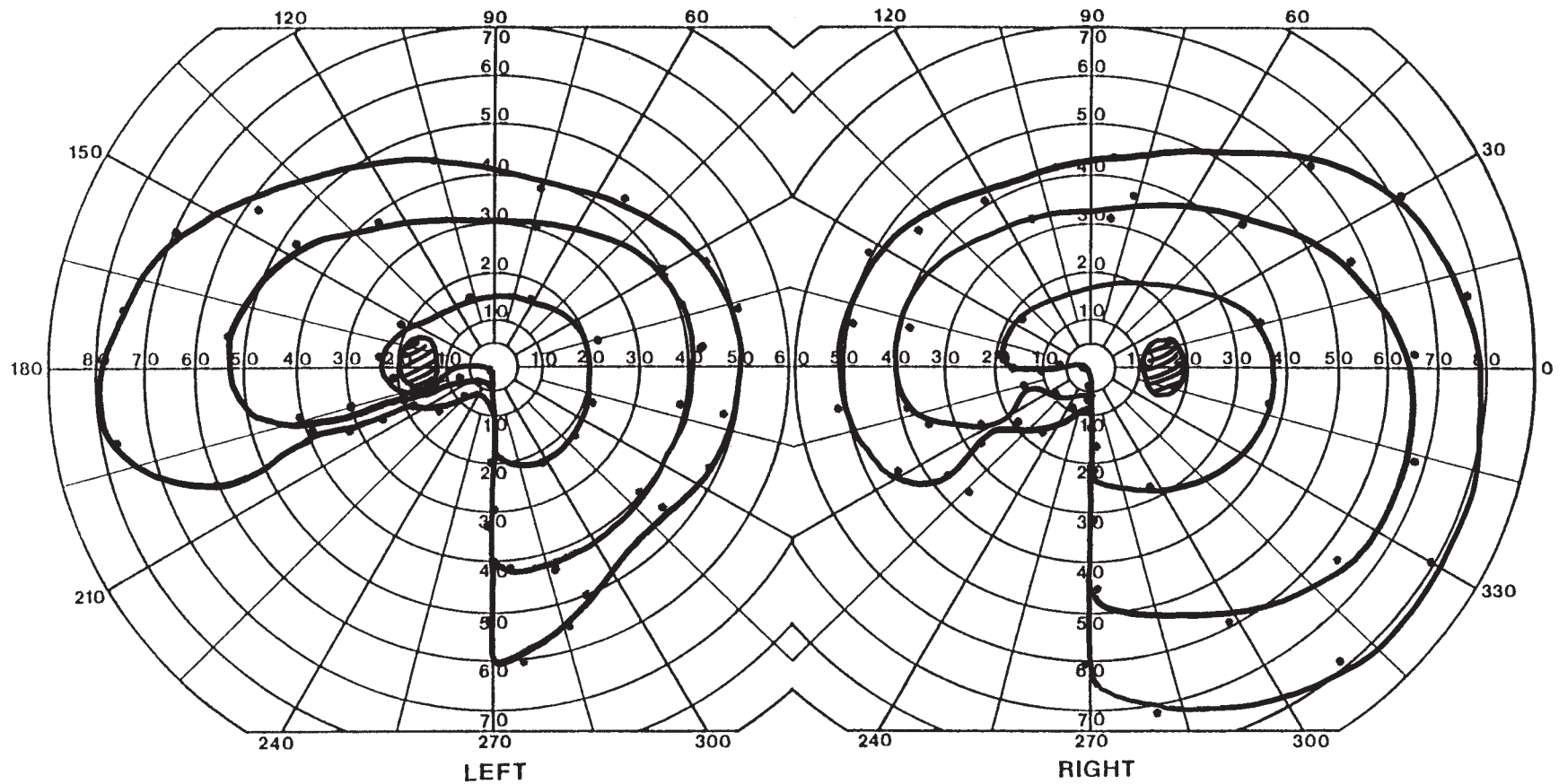
MRI showed scattered white matter T2 hyperintensities with one large lesion near the trigone of the left lateral ventricle, likely involving the optic radiation. Patients with isolated quadrantanopic defects are most likely to have lesions in the occipital lobe. Isolated superior quadrantanopia may also result from a temporal lobe lesion (139), as in cases 73 to 75.



HISTORY AND EXAM

This 60-yr-old man with long-standing hypertension had sudden frontal headache with left-sided visual loss. Over the ensuing week images in the left field of vision appeared to be moving or jumping. Findings on neurologic examination included visual acuity of

20/20 OU, Ishihara color scores of 13/14 OU, and preserved recognition of famous faces. Optic disks were normal. Saccadic eye movements to the left were hypometric.



DISCUSSION

Field description: Mildly incongruous left inferior quadrantanopia, partial.

Localization: Right parietal optic radiation.

Pathology: Primary lobar hemorrhage.

Confrontation testing with hand motion showed the quadrantic defect.

The patient has almost complete loss of the inferior quadrant, not quite reaching the horizontal meridian. This is much like an inversion of the defect in Case 74.

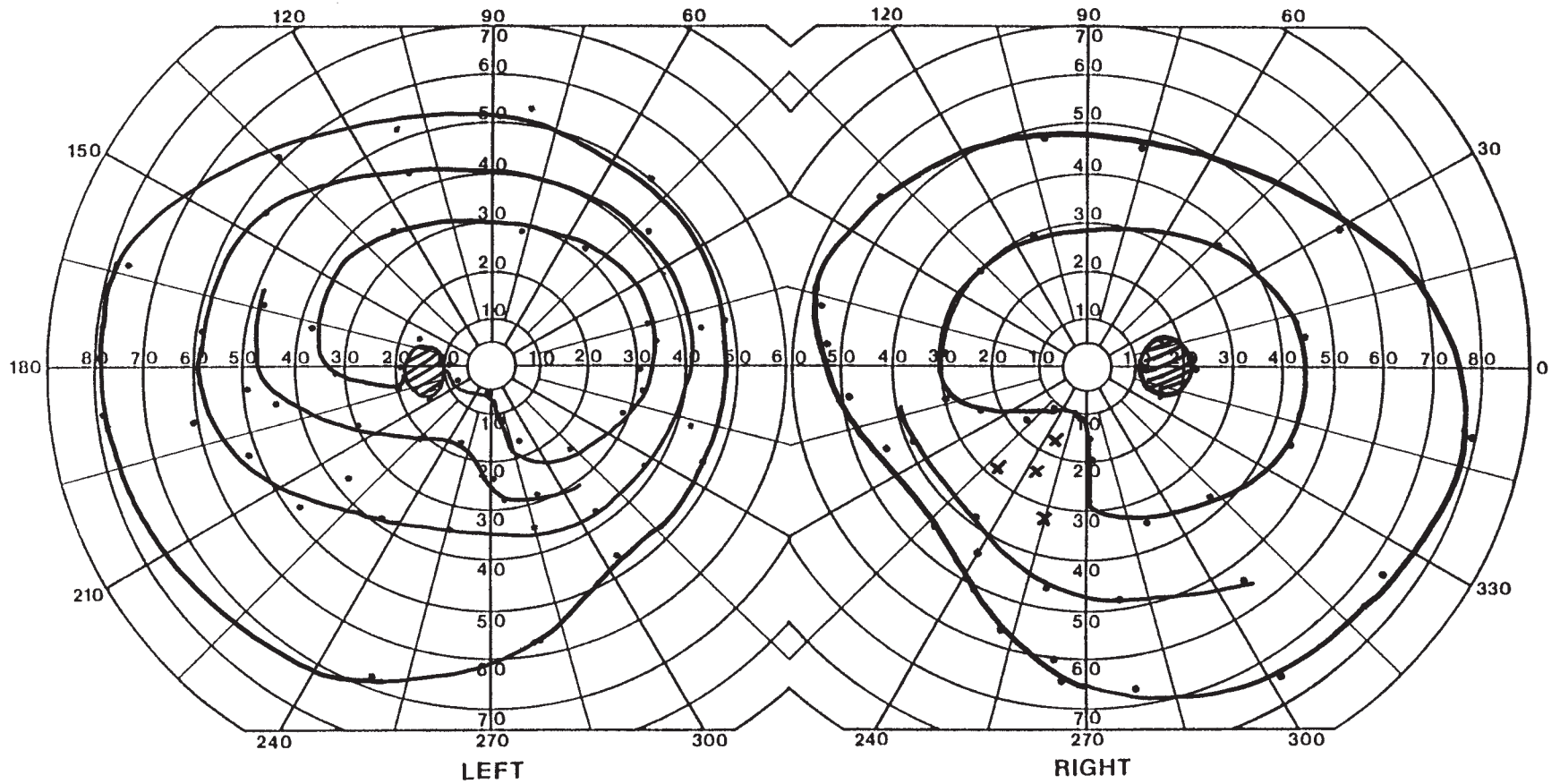
A CT scan showed a large right parietal lobe hemorrhage with a small amount of surrounding edema. Lobar hemorrhage is typically the result of either coagulopathy (most often iatrogenic from the use of coumadin) or an underlying amyloid angiopathy (140). Hypometria of contralateral saccades is sometimes reported with posterior parietal lesions (141) but is usually mild and hard to detect. It may indicate loss of the human homologue of the lateral intraparietal area studied in monkeys (142).



HISTORY AND EXAM

This 84-yr-old woman was referred to determine whether her vision was contributing to a problem with recurrent falls over the preceding 5 months. Visual acuity was 20/25 on

the right and 20/80 on the left, but the latter improved with pinhole to 20/25. Color vision was normal and there was no RAPD. Optic disks were normal.



DISCUSSION

Field description: Congruous relative left inferior quadrantanopia.

Localization: Right parietal optic radiation.

Pathology: Infarct.

Confrontation testing showed a subtle mildly incongruous quadrantic defect, but only with a moving red target.

The patient's field defect is less dense and extensive than that of Case 78, even though the size of her old, large, right parietotemporal infarct on CT is similar to that patient's hemorrhage. Clearly the bulk of her lesion narrowly avoided most of her optic radiation, a stroke of luck not afforded to Case 78. In the brain, as in real estate, location is everything.

With an indeterminate history of onset of the visual problem and its subsequent course, one cannot exclude a neoplasm from the clinical information. A lesion of the superior bank of the calcarine sulcus is also possible.

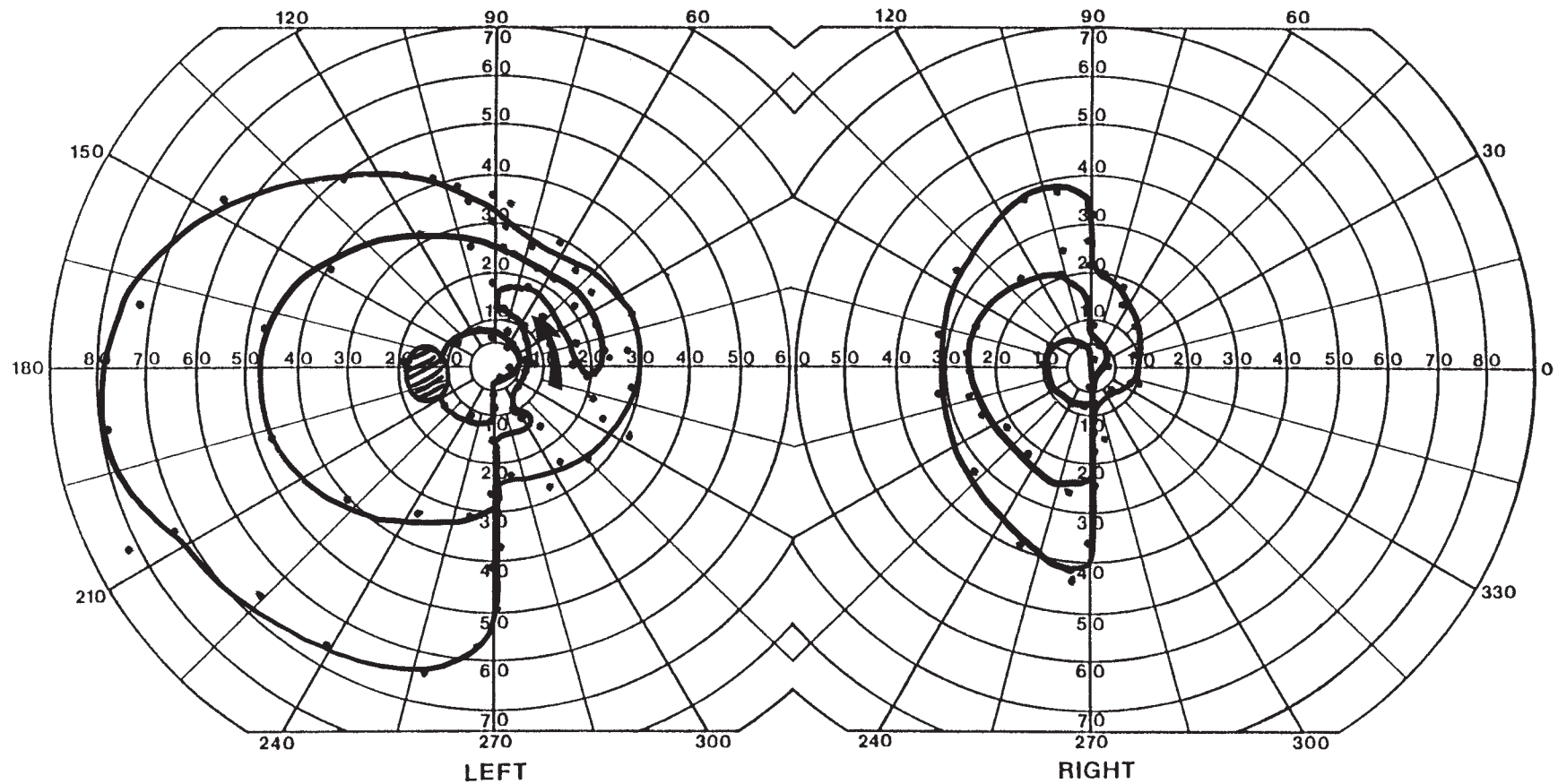
Inferior quadrantanopia is often more troubling than superior quadrant defects. It obscures the view of the floor, and patients will stumble over objects. When driving, we fixate on the horizon, so that the road, sidewalks, pedestrians, and other cars are located more in the lower field than the upper. Since we read lines from the top to the bottom of the page, an inferior quadrantanopia obscures the coming text more than a superior defect does.



HISTORY AND EXAM

This 38-yr-old woman reported decreased vision in the right eye. She had a 10-year history of MS, treated with β -interferon injections. She had one distant episode of optic neuritis but could not recall in which eye. She was treated with steroids and apparently had a full recovery. Visual acuity was 20/100 OD and 20/25 OS. Ishihara color plates

were 0/14 OD and 4/14 OS. There was an RAPD OD. The right eye had diffuse optic atrophy and the left had temporal disk pallor. There was a mild spastic quadraparesis and diminished vibration sense in the hands and feet. She had left-right confusion and mild finger agnosia, but her writing and arithmetical performance were normal.



DISCUSSION

Field description: Incongruous right partial homonymous hemianopia, with general constriction OD and superior arcuate defect OS.

Localization: Right optic radiation, parietal lobe, and previous bilateral optic nerve.

Pathology: Demyelination.

Confrontation fields showed decreased hand motion in the right hemifield and left superior quadrant OU.

This is a complex field. Part of the incongruity may stem from the patient's prior optic neuropathies. From her color vision scores, acuity, RAPD, and optic disk appearance, the optic neuropathy is worse in the right eye and likely causes the general constriction of the nasal field, the side not affected by the cerebral hemifield defect. The curving arcuate

defect in the left eye (arrow) does respect the vertical meridian but its shape and location are much more suggestive of a nerve fiber defect. The optic atrophy in both eyes suggests that the nerve damage is old. Her new complaint is probably of decreased vision in the right hemifield, not the right eye, although the confusion and the false conclusion are common among new patients, let alone someone who has experienced visual loss in one eye.

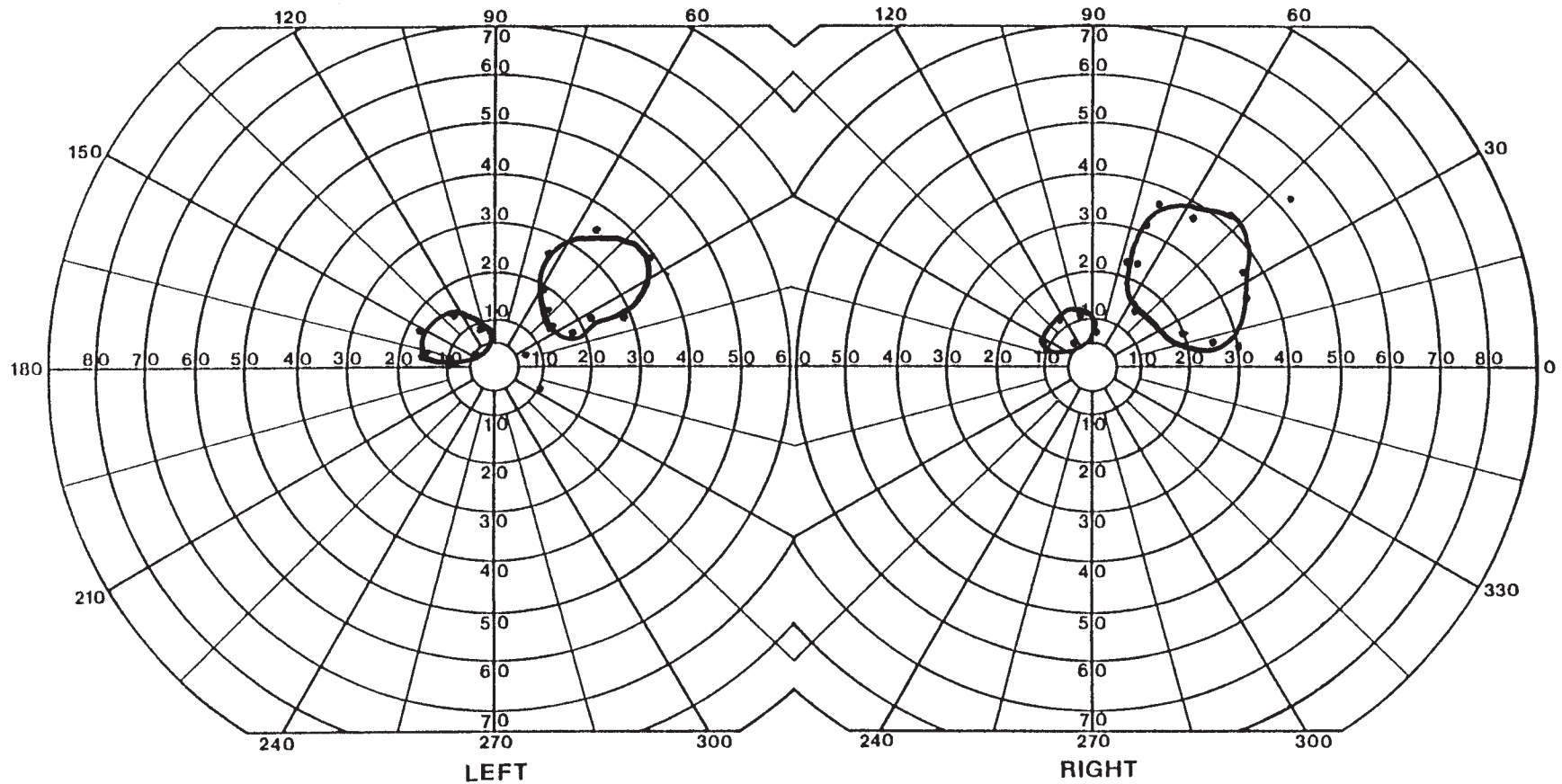
Her MRI revealed a new large lesion of the left parieto-occipital area and extensive loss of occipital white matter, shown on this axial T1-weighted image (arrows). Finger agnosia and left-right confusion are two of the four features of Gerstmann syndrome (acalculia and agraphia being the other two), which is characteristic of damage to the left parietal region (143).



HISTORY AND EXAM

This 72-yr-old man described his vision immediately following a right carotid endarterectomy as “scrambled,” with the parts of objects spatially disjointed (e.g., hair displaced left of the eyes, and eyes placed one above the other). While reading he saw

words as blurred and fragmented. He saw four images of objects, even with either eye closed. He could not reach accurately for objects with his left hand. Visual acuity was light perception only OU. Fundi were normal, although he had a severe cataract OS.



DISCUSSION

Field description: Homonymous visual islands in right superior quadrant and left superior paracentral field.

Localization: Bilateral occipitoparietal radiations.

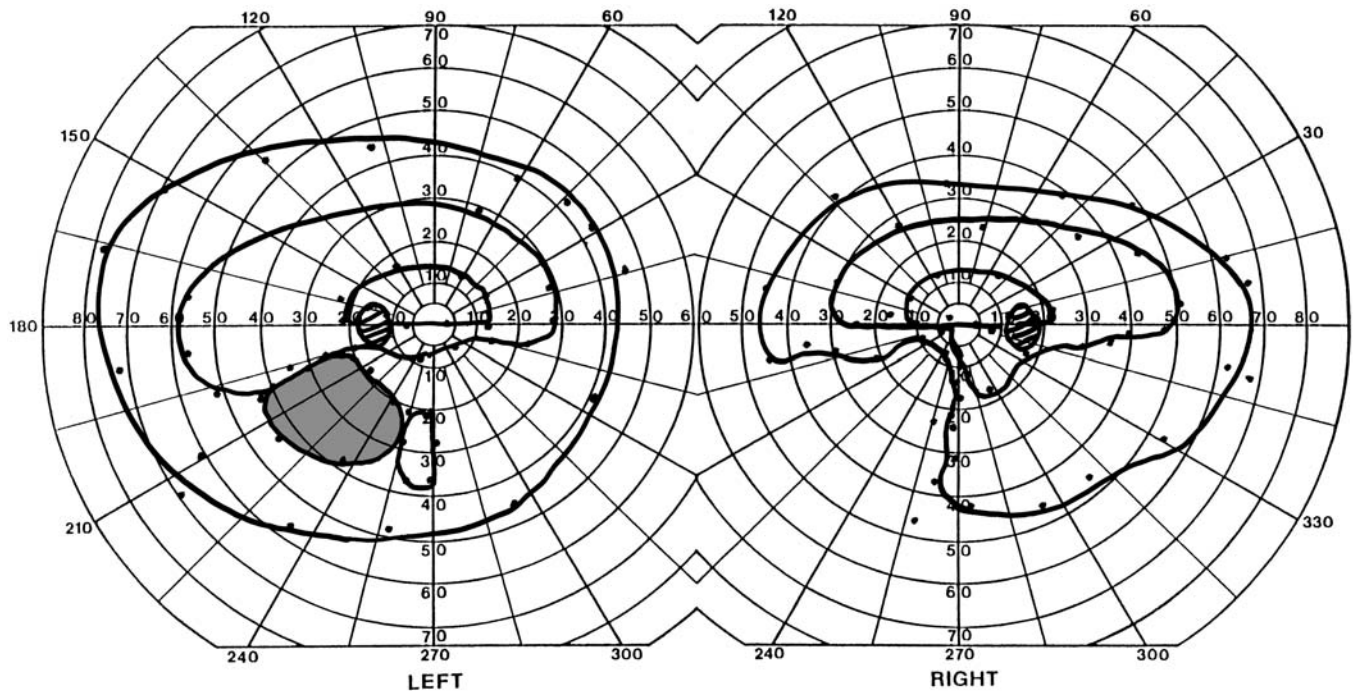
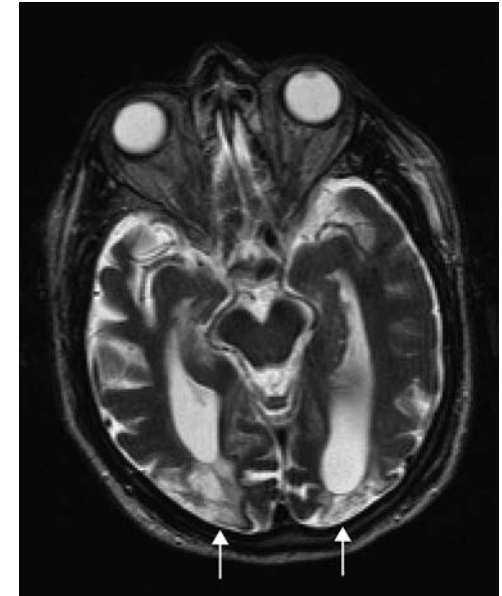
Pathology: Watershed infarctions.

Confrontation fields showed the larger superior island OU with hand motion testing.

Axial T2-weighted MRI demonstrated bilateral watershed infarcts (arrows) with sparing of the striate cortex. His devastating visual loss is the result of bilateral optic radiation injury. Fortunately, 1 month later his vision had substantially recovered, with acuity of 20/40 OD and 20/200 OS. His improved fields (shown here) show mainly homonymous inferior losses in both hemifields, worse on the left side.

Cerebral diplopia or polyopia refers to the perseveration of a visual image in space (144). The number of images perceived may range from two to hundreds, and the multiple images persist with monocular vision irrespective of which eye is closed. Palinopsia refers to the temporal perseveration of an image (i.e., an image, or component thereof,

continues to be perceived, even though it is no longer present) (145). There is overlap between these two symptoms, and at times they may be difficult to distinguish. Polyopia may be accompanied by other signs including visual field defects, achromatopsia, or impaired visually guided reaching. This patient reported the latter. His report of fractured and disoriented vision may reflect a combination of preserved islands of vision and polyopia but may also indicate spatial disorientation secondary to his parietal lesions.



DISCUSSION

Field description: Congruous homonymous right horizontal sectoranopia.

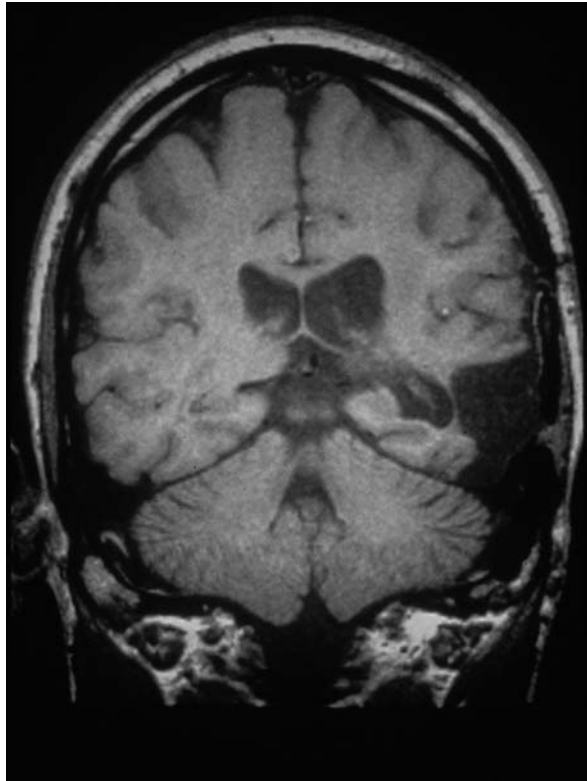
Localization: Left optic radiations, midzone.

Pathology: Infarct, secondary to head trauma.

Confrontation fields did not show a defect, but tangent screen perimetry with a 3-mm white target showed a right hemifield wedge defect extending to 20° on either side of the horizontal meridian OU.

The predominant feature of the patient's defect from the gray scale and visual sensitivity plots is a severe reduction in thresholds in a zone straddling the horizontal meridian. There is also some depression along the inferior vertical meridian (which helps to

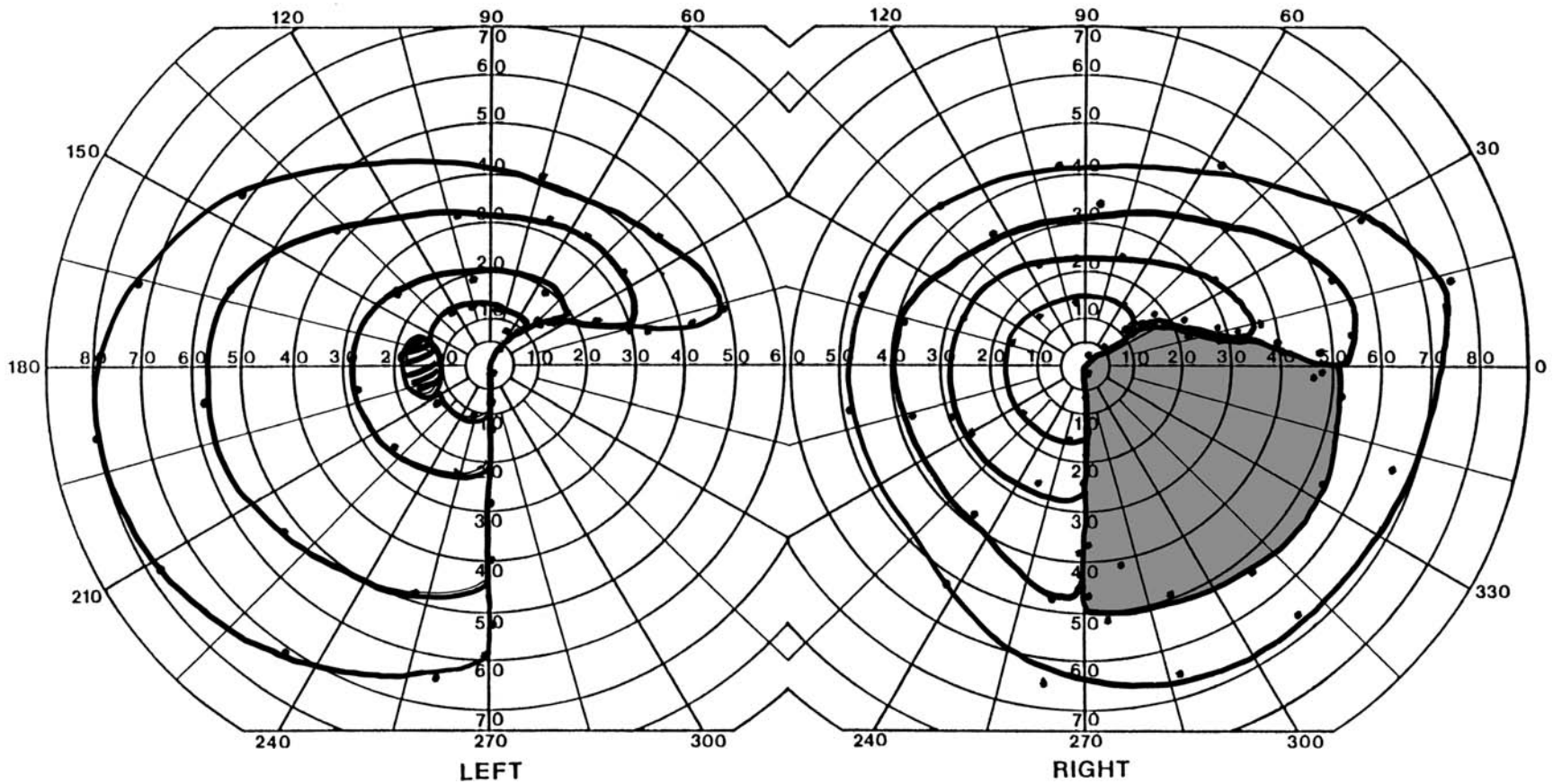
confirm a retrochiasmal location), but this is much milder compared to the sector defect. The sectoranopia in this patient resembles that seen with posterior choroidal arterial infarction affecting the LGN (124). However, geniculate lesions of this duration are usually accompanied by a pattern of optic atrophy not unlike that seen with lesions of an optic tract. Admittedly, such atrophy may be subtle with partial geniculate lesions (124). Damage to the middle of the optic radiations, at the converging boundary between the parietal and temporal fibers, can also create a sectoranopia without optic atrophy (146). Coronal T1-weighted MRI in this patient reveals a wedge defect fanning from the ventricular to the cortical surface, intersecting the optic radiations.



HISTORY AND EXAM

This 53-yr-old woman with diabetes, hypertension, and hypercholesterolemia had a blurry “smudge” on the right side of vision OD that had increased in size over the first few days or weeks. Three months after onset, her acuity was 20/20 OD and 20/25 OS, and

Ishihara color scores were 13/14 OD and 14/14 OS. There was no RAPD. There was mild nonproliferative diabetic retinopathy.



DISCUSSION

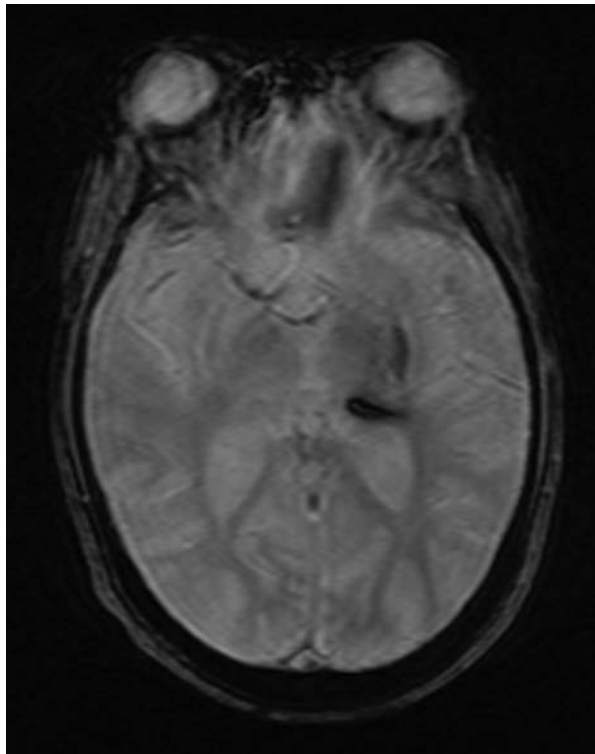
Field description: Congruous right inferior quadrantanopia plus, with sparing of the monocular temporal crescent.

Localization: Proximal optic radiation.

Pathology: Hypertensive hemorrhage.

Confrontation fields showed the quadrantanopia extending into the upper quadrant, for hand and finger motion.

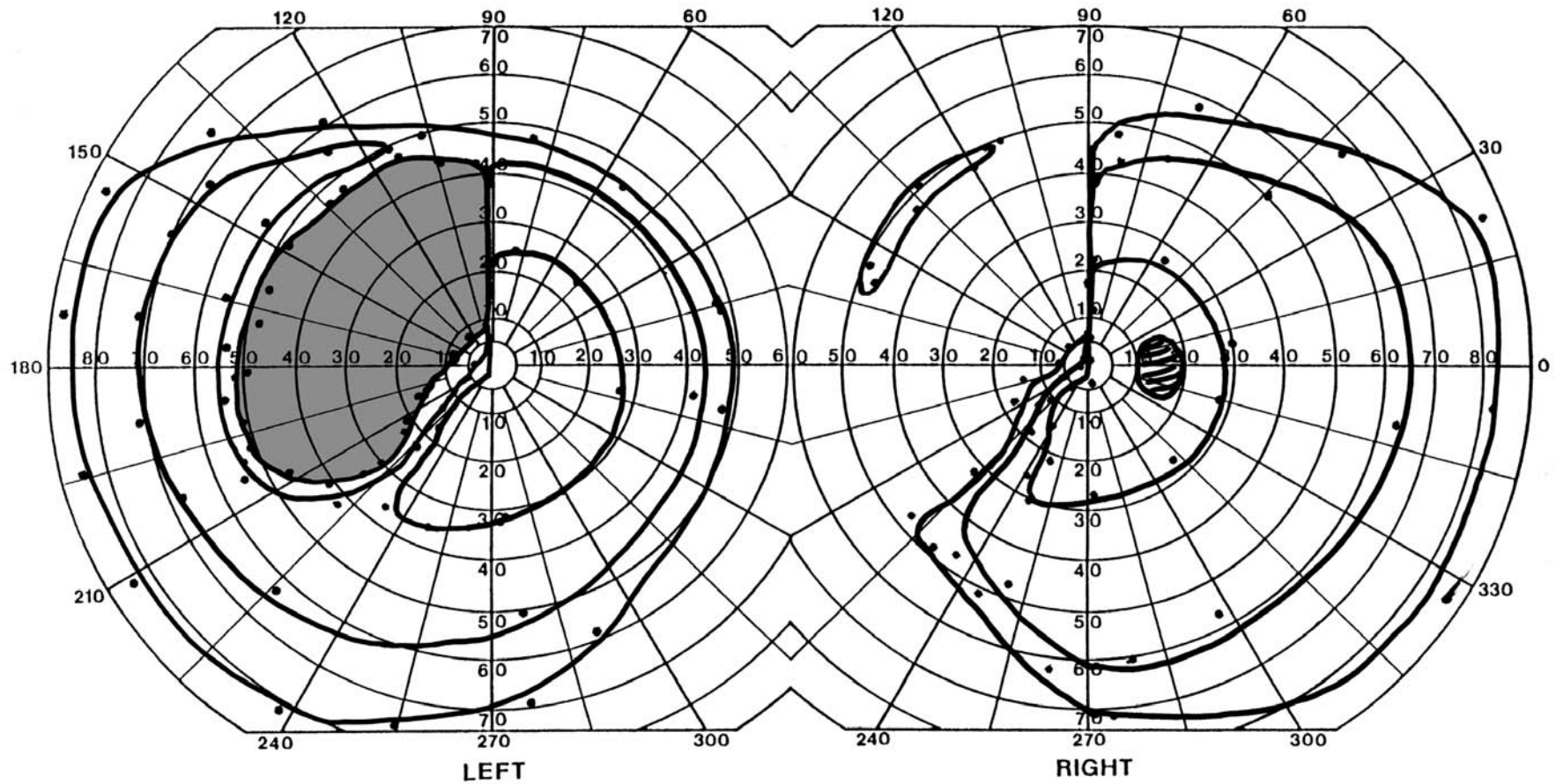
The field shows high congruity along the superior border of the defect, and clear sparing of the monocular temporal crescent, both features that pointed to a striate lesion (see Case 84). However, MRI (susceptibility sequence) showed a left putaminal/capsular hemorrhage, seen here as the black streak, and thin coronal cuts through the occipital lobe were normal. While striate lesions are probably the most common cause of hemifield defects sparing the monocular temporal crescent, isolated lesions of the optic radiations did cause a similar finding in 3 of 16 patients in a recent series (147).



HISTORY AND EXAM

This 58-yr-old man developed sudden blurred vision during a bowel movement. This gradually improved over the following weeks, but he still had difficulty reading because he could not see the left side of pages. He also intermittently noted dark vague shapes like

butterflies in the left field of vision. Visual acuity and fundi were normal and there was no RAPD.



DISCUSSION

Field description: Congruous partial left homonymous superior quadrantanopia with sparing of the macula and monocular temporal crescent.

Localization: Right striate cortex, inferior bank.

Pathology: Posterior cerebral arterial infarct, posterior temporal branch.

Other features: Release hallucinations (see Case 94).

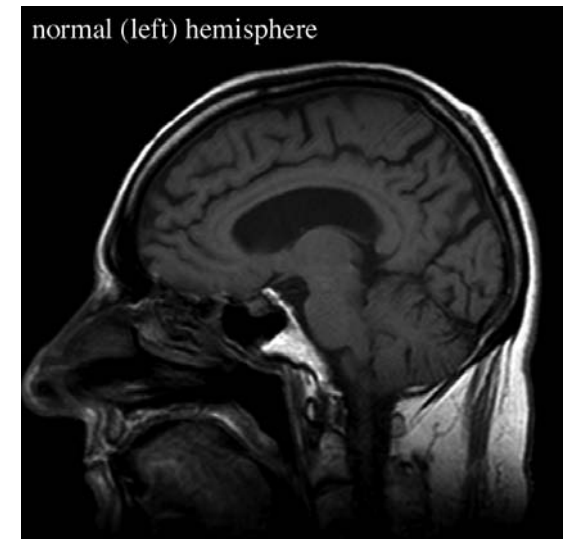
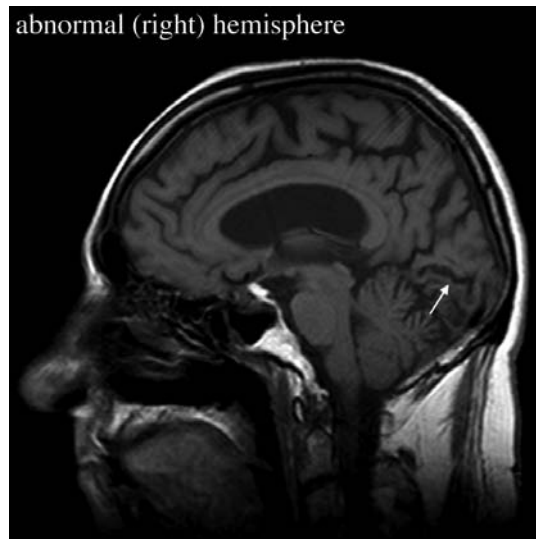
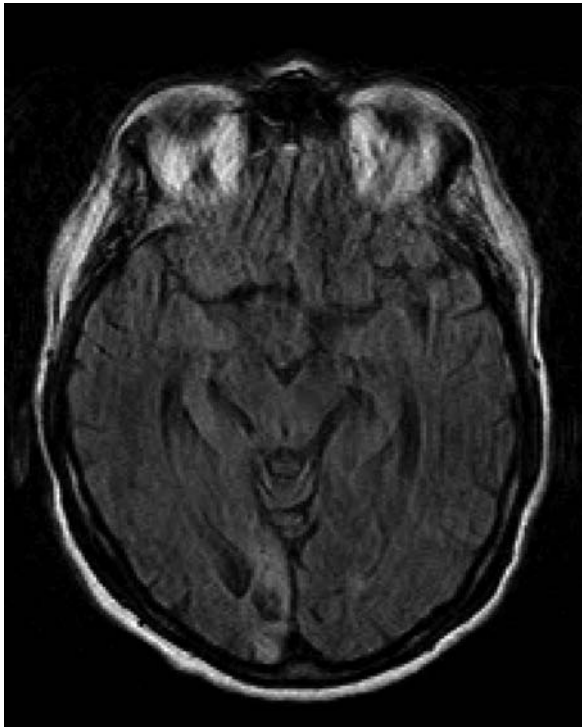
Confrontation fields using hand motion showed a left hemianopia, with sparing of the macula, temporal crescent, and a zone adjacent to the lower vertical meridian.

Since the temporal field extends over 90° while the nasal field stops at 60°, each hemifield has a region that is seen only by the ipsilateral eye—the monocular temporal crescent. This region is represented in the most anterior 10% of striate cortex. The inferior temporal crescent is spared more often than the superior crescent, implying more frequent selective sparing of the superior rostral calcarine bank (147). The most commonly ordered programs in automated perimetry do not detect sparing of the crescent. A special thresh-

old program that tests only the crescent is needed. Goldmann perimetry, however, provides the best comprehensive picture. Preservation of the temporal crescent most often implies a striate lesion, although it can occur less frequently with lesions of the optic radiations (147) (see Case 83).

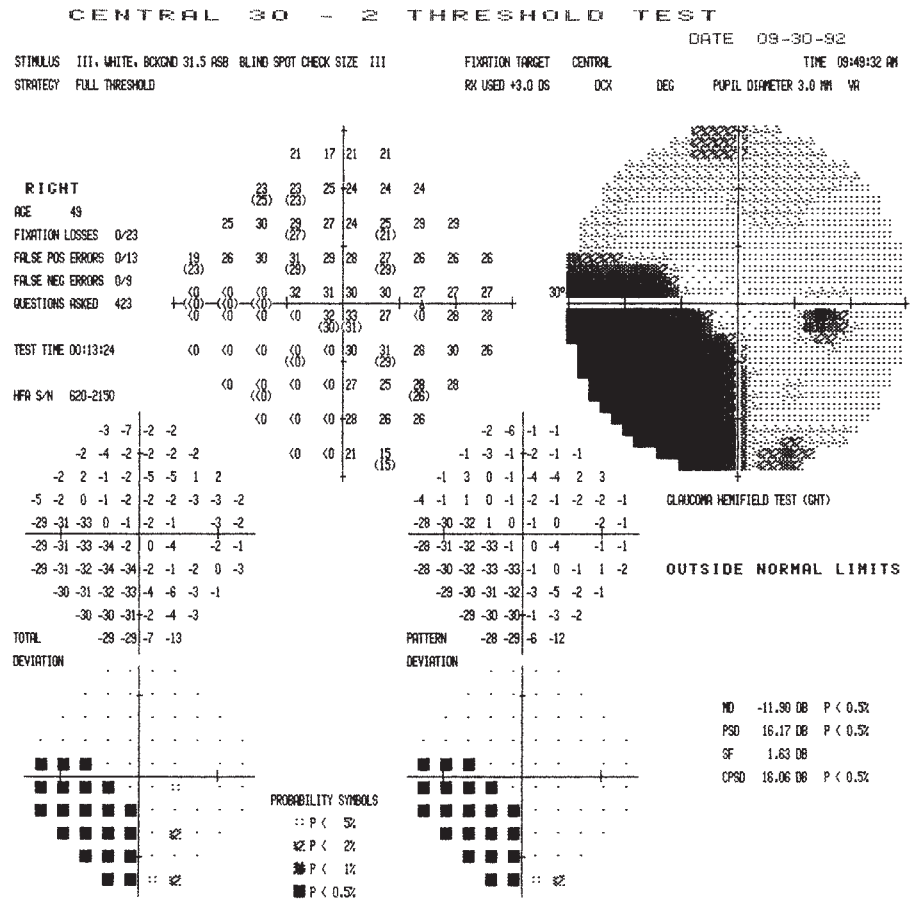
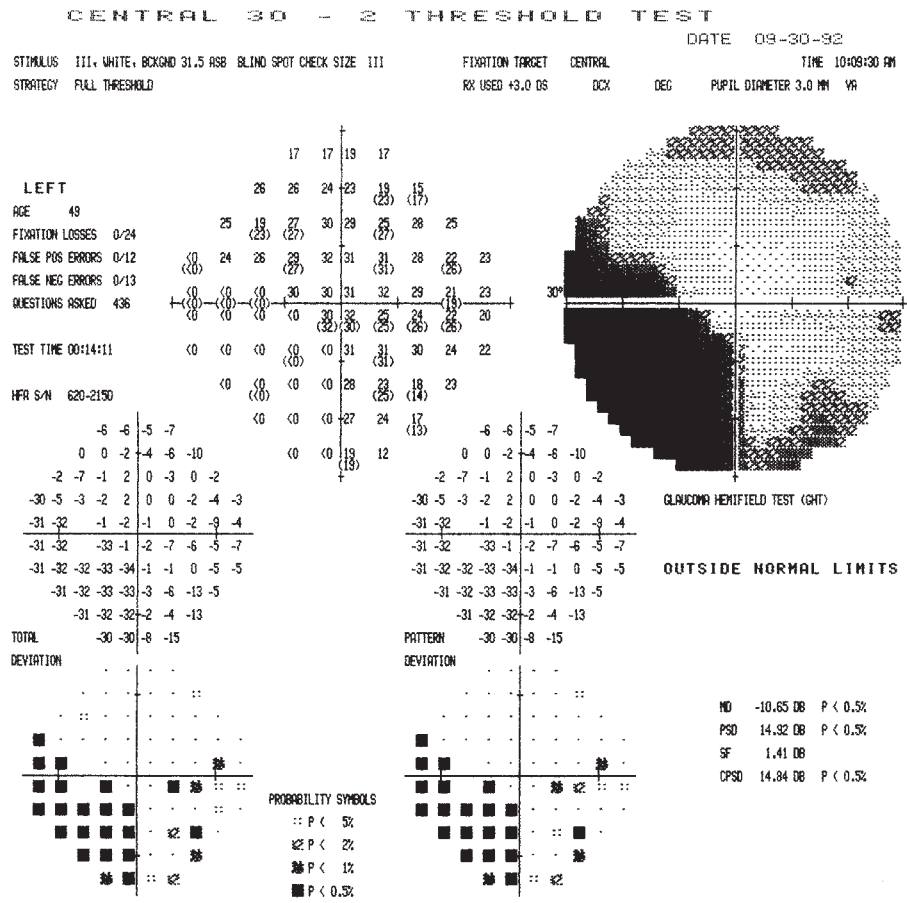
The axial FLAIR MRI showed an infarct of the right striate cortex (pale area) sparing the anterior retrosplenial portion within the territory of the posterior cerebral artery. The sagittal T1-weighted image 6 weeks later demonstrates atrophy of the inferior bank of the calcarine cortex (arrow, compare with similar image through other hemisphere).

Onset during straining suggests paradoxical cardiac embolism (148). A transient increase in right-sided pulmonary pressure during a Valsalva maneuver may expose a right-to-left cardiac shunt, allowing a clot to migrate from the venous to the systemic arterial circulation and on to the cerebral arteries. Echocardiography with a saline bubble study will document the shunt, while tests for deep venous thrombosis of the legs or pulmonary embolism may provide evidence of a clot.



HISTORY AND EXAM

This 49-yr-old woman woke up one morning and found that she could not see objects to her left. Acuity was 20/20 OU and Ishihara color scores were 9/14 OU. There was no RAPD. Optic disks were normal, as were cardiac investigations.



DISCUSSION

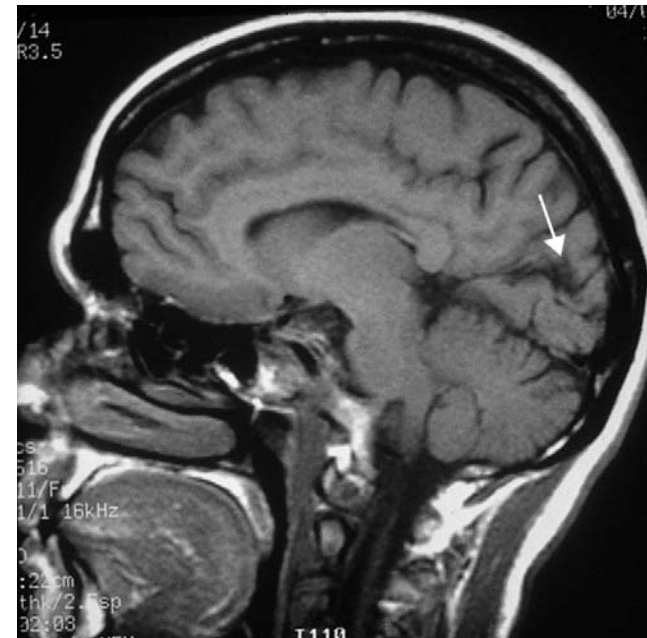
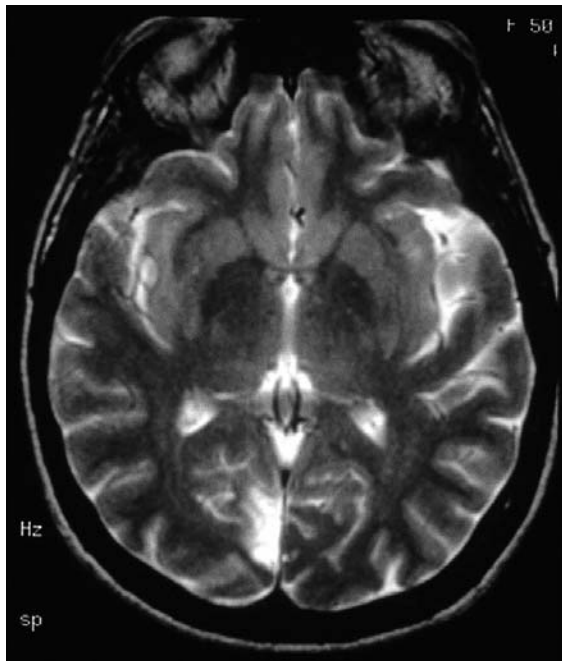
Field description: Congruous homonymous left inferior quadrantanopia plus, sparing the macula.

Localization: Right superior striate cortex, sparing the occipital pole.

Pathology: Posterior cerebral arterial infarct, parieto-occipital branch.

Tangent screen perimetry with a 3-mm white target showed a left inferior quadrantic defect with macular sparing.

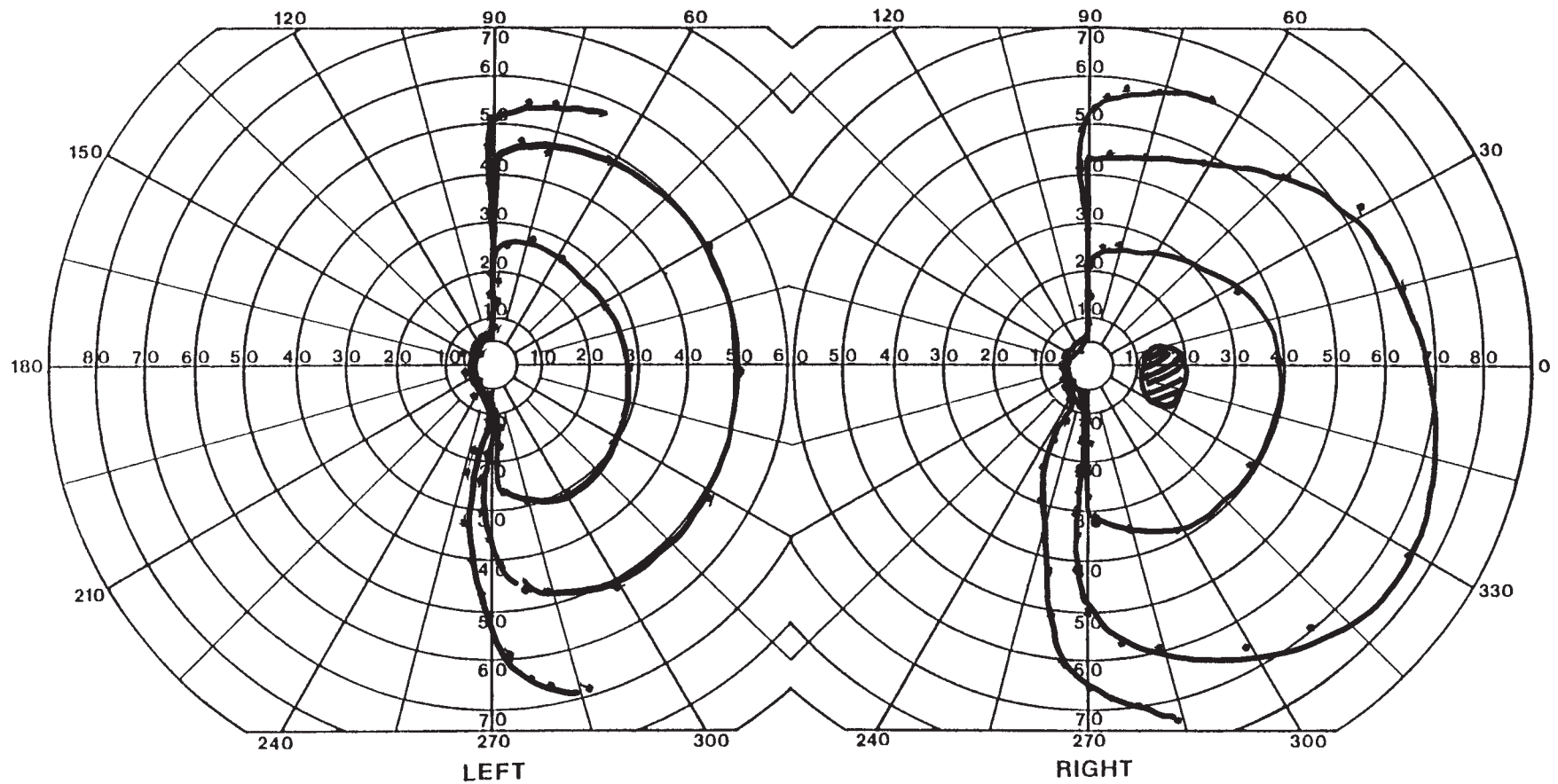
The automated fields show very congruous defects: the same perifoveal test spot is spared in the lower left quadrant, and the defect extends just above the horizontal meridian beyond the 10° mark in both eyes. Such congruity points to striate cortex as the most likely site of damage. MRI shows the well-demarcated infarct restricted to striate cortex, and providing precise anatomic correlation with the functional deficit: sparing of the occipital pole (see both axial T2 and sagittal T1 images) and involvement of cortex above the calcarine fissure (seen on sagittal T1 image, arrow).



HISTORY AND EXAM

This 49-yr-old woman with non-insulin-dependent diabetes mellitus awoke one morning with a severe right-sided occipital headache and difficulty seeing things on the left. Visual acuity was 20/20 OU and Ishihara color scores were 10/14 OU. She was able to

name colors normally. Fundi were normal apart from a mild nonproliferative diabetic retinopathy.



DISCUSSION

Field description: Congruous left homonymous hemianopia with macular sparing.

Localization: Right striate cortex, sparing occipital pole.

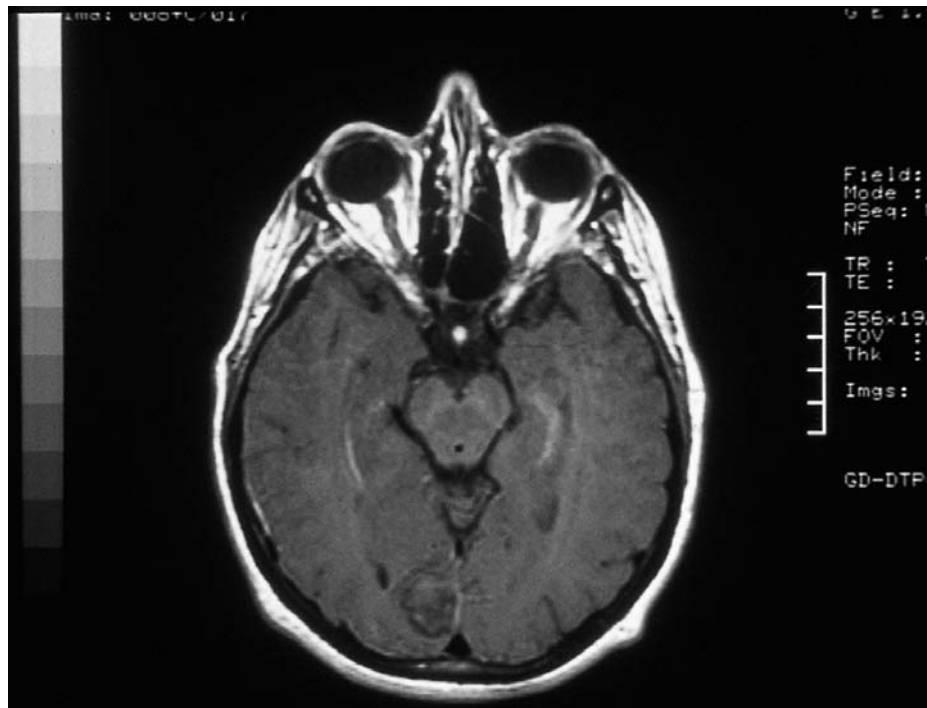
Pathology: Posterior cerebral arterial infarct.

Confrontation fields showed congruous left homonymous hemianopia to hand motion.

Hemianopia with sparing of the central 5° is far more common with striate infarction than damage to other retrochiasmal structures. The macular representation lies at the occipital pole, which is a watershed zone between the vascular territories of the posterior and middle cerebral arteries. The exact location of the boundary varies among individu-

als. In those in whom the pole is perfused more by the middle cerebral artery, a posterior cerebral infarct will spare the macula. Because there is so much cortex devoted to central vision, a slight variation in the boundary at the pole will not greatly affect the amount of central vision spared; it always seems to span about 5°.

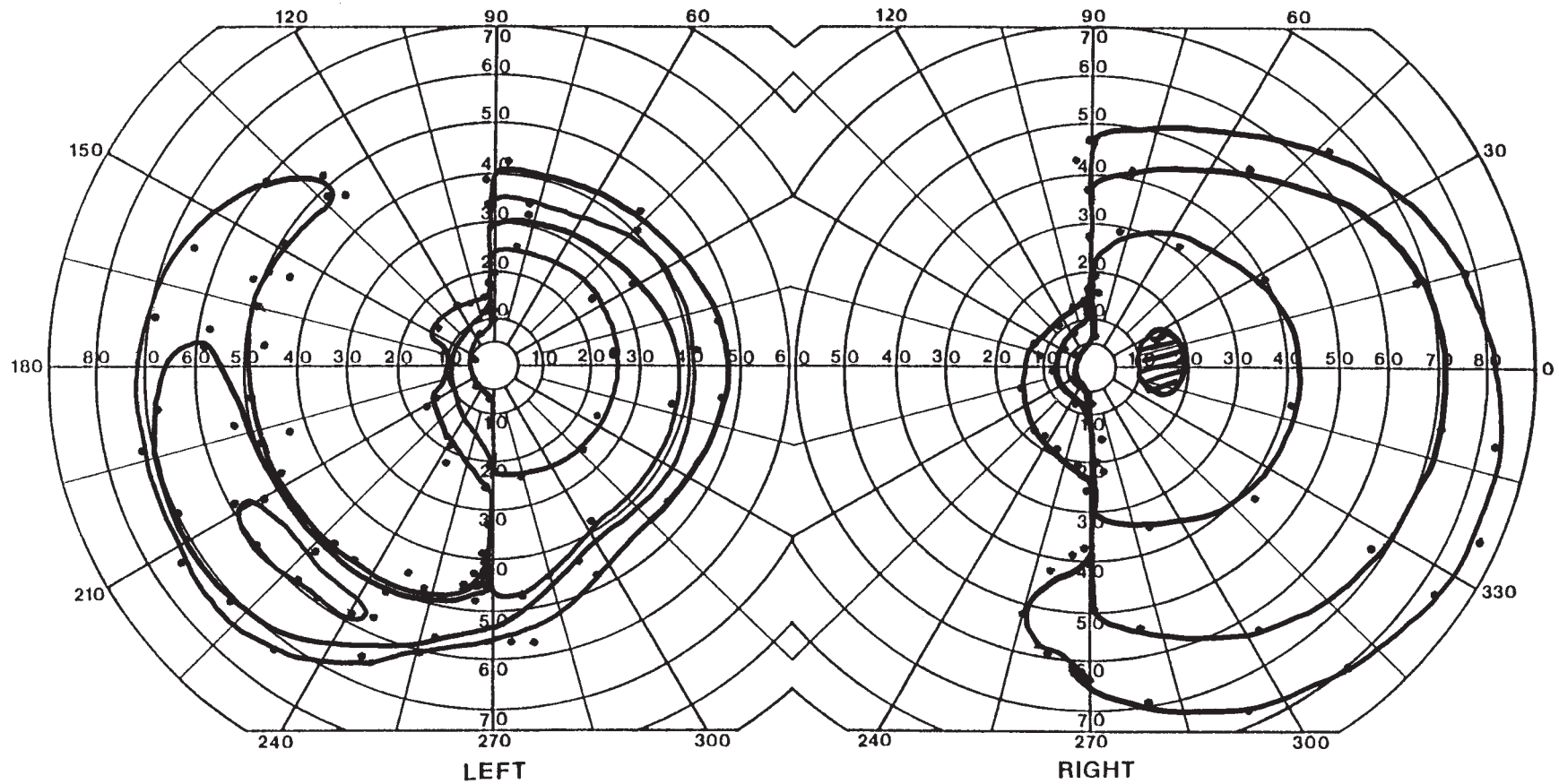
Previously, macular sparing had been considered an artifact of poor fixation (which it may be with sloppy perimetry) or a result of overlapping receptive fields in the retina (149), but modern neuroimaging has placed the occipital pole watershed explanation at the fore (150,151).



HISTORY AND EXAM

An optometrist found a hemifield defect on a routine examination of this 27-yr-old man. Even on direct questioning, he recalled no symptoms that might have dated its onset.

He had normal visual acuity and color vision. Fundoscopy was normal OD but demonstrated band (bowtie) atrophy OS.



DISCUSSION

Field description: Left homonymous hemianopia with sparing of the central field and monocular temporal crescent.

Localization: Striate cortex, sparing the occipital pole posteriorly and the retrosplenial zone anteriorly.

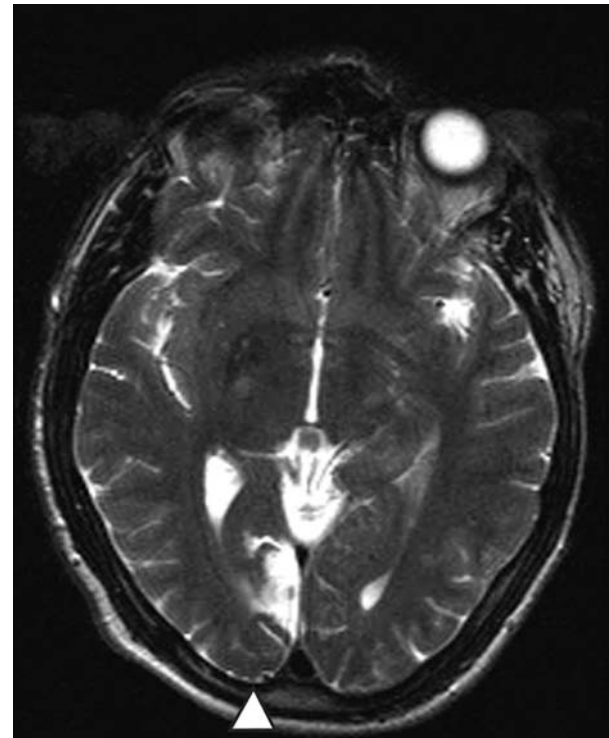
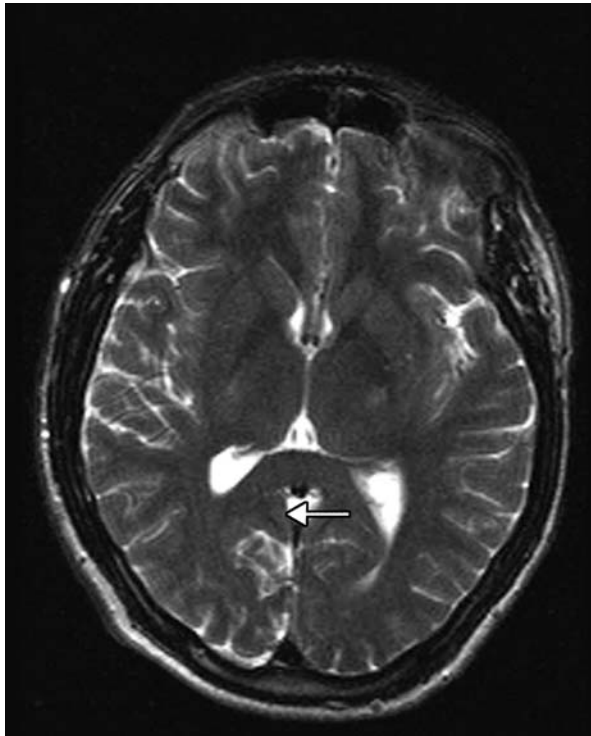
Pathology: Old posterior cerebral arterial infarction.

Confrontation testing showed a left hemianopia with temporal crescent sparing to hand motion.

The sparing of the macula and monocular temporal crescent indicates pathology in the midzone of the striate cortex on the right and likely explains the patient's lack of awareness of the visual field defect. Axial T2-weighted MRI (shown) revealed a lesion in the expected location. Note the sparing of the occipital pole (arrowhead) as well as the most

anterior portion of the striate cortex (arrow). The presence of band atrophy on the left suggests a long-standing injury with retrograde trans-synaptic degeneration (117), creating a fundoscopic appearance more associated with optic tract injury.

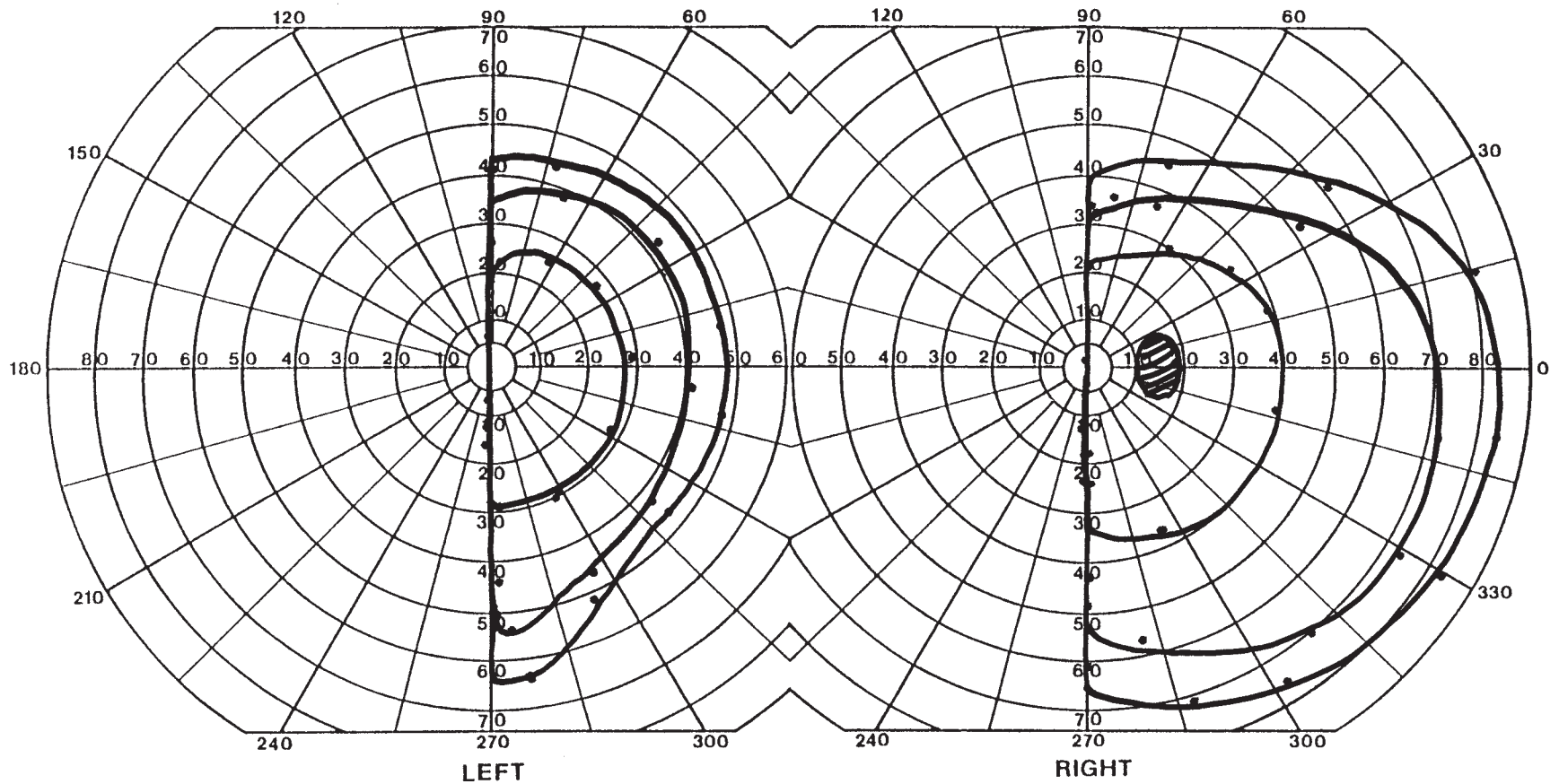
Why did he not notice this sizable hemianopia? Why had he never had a car accident? We have seen several patients with presumed childhood-onset hemianopia and anosognosia—this patient is not unique. It may be that such patients have unconsciously become very proficient at an adaptive strategy of making more saccadic eye movements into their blind hemifield (152,153). It is also postulated that subjects with early onset lesions may have the potential for blindsight (154), a residual visual ability mediated by brain stem and extrastriate regions, without the patient's awareness (155). Blindsight remains somewhat controversial (156–158). Furthermore, it has yet to be shown that blindsight has any practical impact on the daily behavior of patients.



HISTORY AND EXAM

This 52-yr-old man had resection of a right occipital oligodendroglioma. He had presented with sudden headache from hemorrhage into the tumor. Postoperatively he noted difficulty seeing to the left. He was bumping into objects on that side and had trouble keeping his place on the page while reading. He would get lost occasionally when walk-

ing in the town where he had lived for many years. On examination 7 months after surgery, visual acuity was 20/25 OU, there was no RAPD, and color vision and optic disks were normal. His ability to identify famous faces was impaired, despite good general knowledge. The rest of the neurologic examination was normal.



DISCUSSION

Field description: Complete left homonymous hemianopia, macula splitting.

Localization: Right striate cortex, medial occipitotemporal lobe.

Pathology: Oligodendroglioma with surgical resection.

Other features: Prosopagnosia, topographagnosia, hemianopic dyslexia.

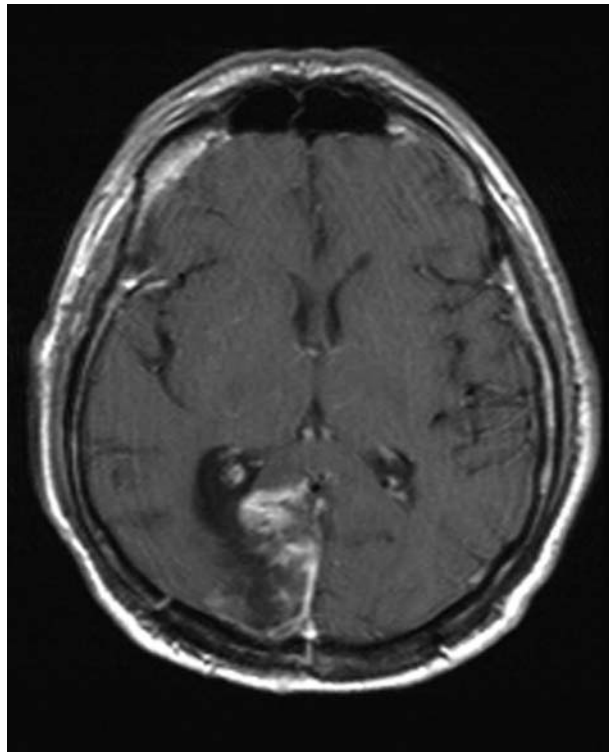
Confrontation testing with hand motion showed complete hemianopia.

Complete macula-splitting hemianopia is the least localizing of all hemifield defects. A large lesion anywhere from the optic tract to striate cortex can do this. Optic radiation lesions with such severe defects tend to be associated with other motor, sensory, attentional, or language deficits, unless close to the LGN or to the termination of the radiations in the striate cortex. This patient has prosopagnosia (impaired recognition of familiar faces) and topographagnosia (getting lost in familiar surroundings), indicating dysfunction

of extrastriate regions in medial occipitotemporal cortex. While it was previously thought that prosopagnosia required bilateral occipital damage (159), modern neuroimaging has shown that at least some cases may occur with only right-sided damage (160–162).

His reading difficulty is a hemianopic dyslexia, which occurs when the central 5° of vision are affected (163). Subjects with left hemifield defects read a single line quickly but struggle to find the beginning of a new line because the left side of the page lies within the hemianopic field (164). As a result, they frequently skip or repeat lines and may begin to read midway through a line. A ruler with a marker to place at the left hand margin of text can be helpful when held under the line being read.

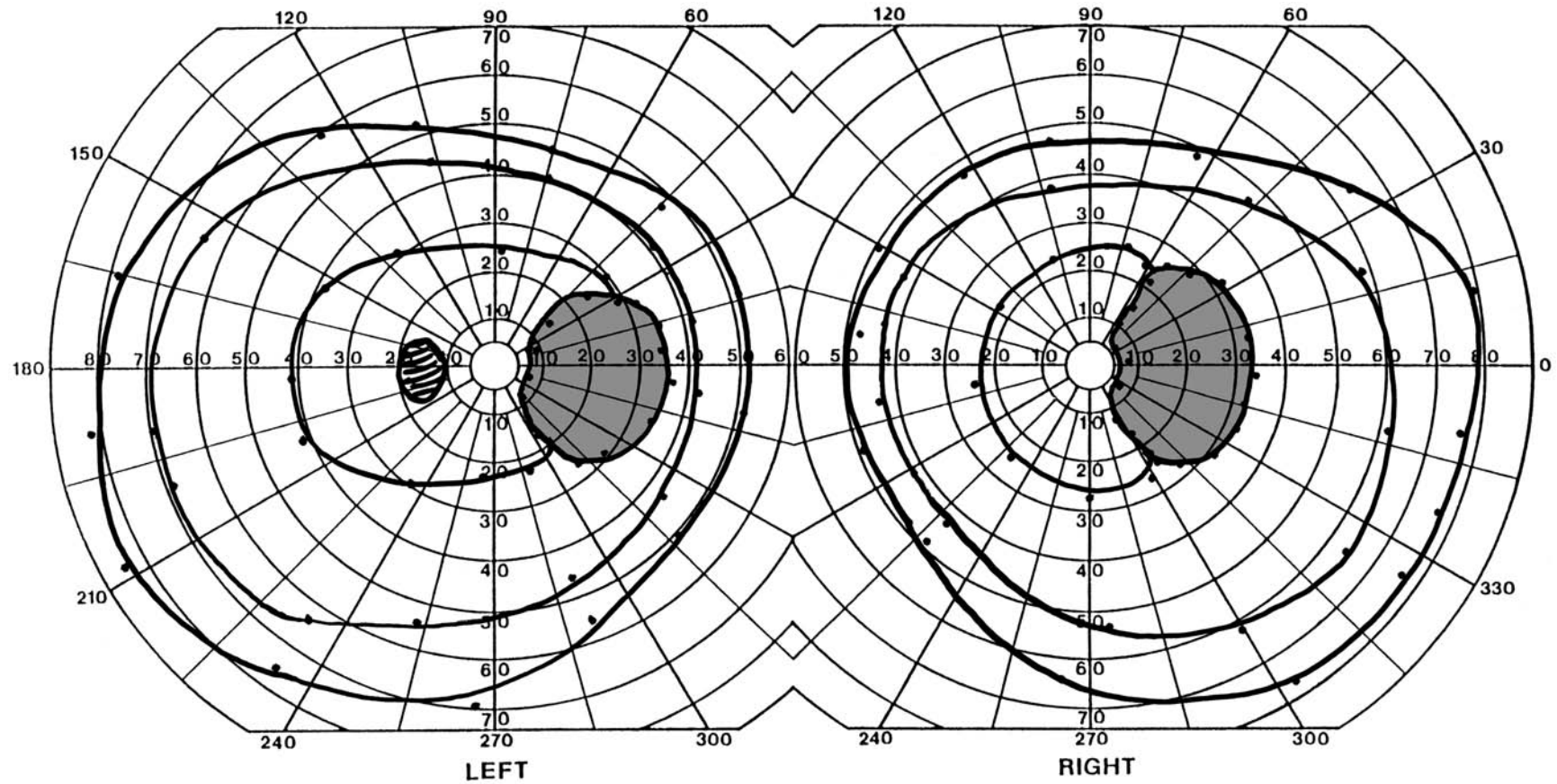
T1-weighted axial MRI with gadolinium showed residual tumor in the right occipital lobe involving the striate cortex and distal optic radiation.



HISTORY AND EXAM

A 22-yr-old woman with a 1-year history of autoimmune hemolytic anemia and thrombocytopenia presented with complaints of decreased vision on the right and right-sided headaches of 10 days duration. She was referred for evaluation of an enlarged blind spot

in the right eye. General and neurologic examinations were normal. Her platelet count was only 9000.



DISCUSSION

Field description: Right homonymous paracentral scotomata.

Localization: Striate cortex, midzone (anteroposteriorly), in depth of calcarine sulcus.

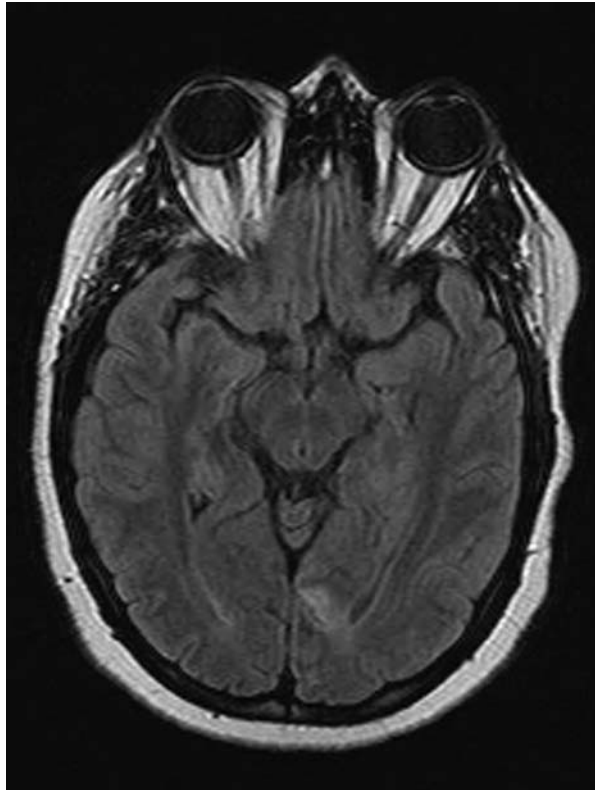
Pathology: Posterior cerebral arterial infarct secondary to platelet dysfunction.

Confrontation testing with finger motion showed the homonymous scotomata.

Although the patient was referred with what was thought to be a unilateral problem, confrontation testing and perimetry both demonstrated that the problem was actually bilateral. This reinforces the point about not evaluating one eye's field without seeing that of the other.

Axial FLAIR MRI (shown) confirms a midzone infarct sparing both the anterior and posterior striate cortex. The topography of the striate cortex proceeds from the macula posteriorly at the occipital pole to the far periphery anteriorly, just behind the splenium and parieto-occipital sulcus. In coronal section, the horizontal meridian lies in the depths of the calcarine sulcus, with the vertical meridians lying on the exposed banks.

She received steroids and plasmapheresis, which improved the thrombocytopenia. Over time the scotomata shrank but still persisted, at least 1 year later. The combination of hemolytic anemia, thrombocytopenia, and stroke makes thrombotic thrombocytopenic purpura the most likely diagnosis (165).



HISTORY AND EXAM

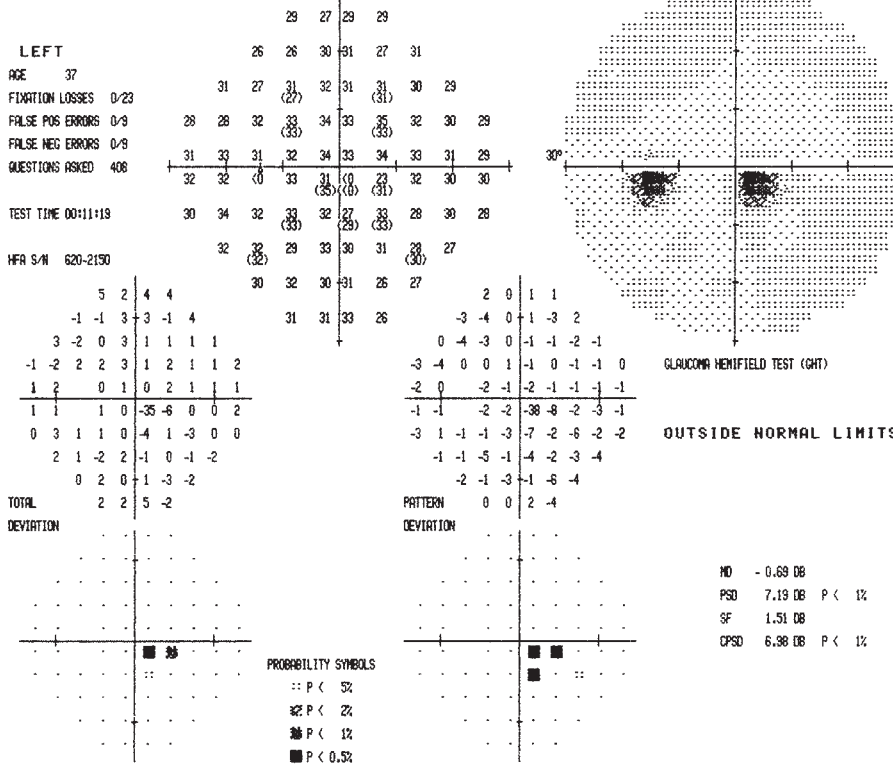
This 37-yr-old man lost consciousness briefly in a car accident but did not have an apparent head injury. Shortly after, he complained of difficulty reading and noted a shadowy fog in the left inferior field of both eyes. Visual acuity and color vision were normal, as was the remainder of the neurologic examination.

owgy fog in the left inferior field of both eyes. Visual acuity and color vision were normal, as was the remainder of the neurologic examination.

CENTRAL 30 - 2 THRESHOLD TEST

DATE 05-11-92

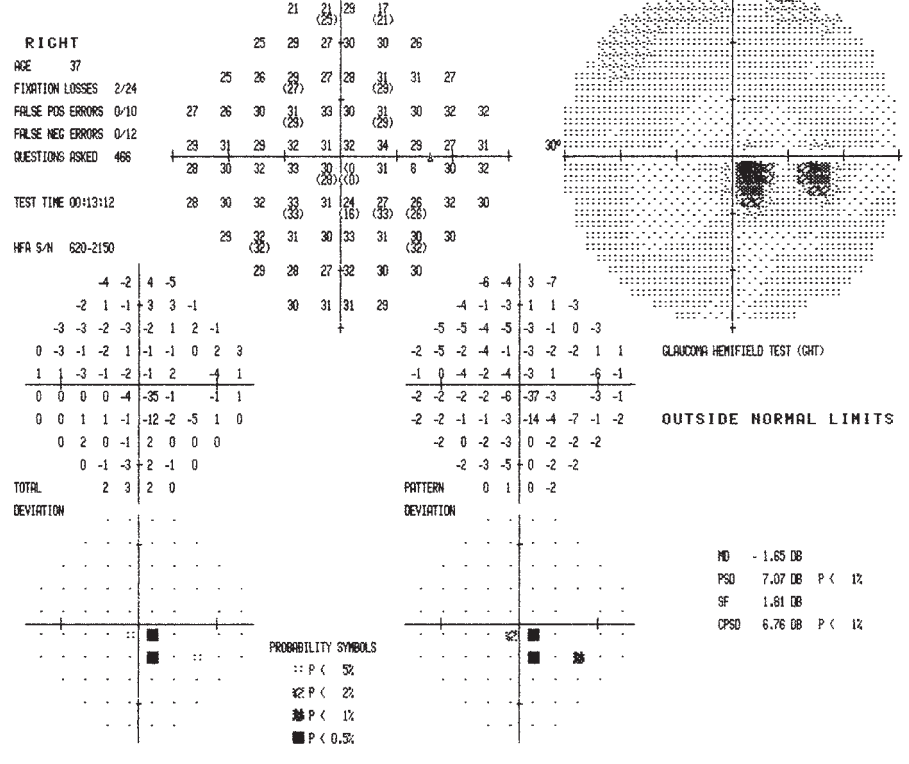
STIMULUS III, WHITE, BCKGND 31.5 ASB BLIND SPOT CHECK SIZE III
 STRATEGY FULL THRESHOLD
 FIXATION TARGET CENTRAL
 RX USED DS DCX DEG PUPIL DIAMETER VA 20/20



CENTRAL 30 - 2 THRESHOLD TEST

DATE 05-11-92

STIMULUS III, WHITE, BCKGND 31.5 ASB BLIND SPOT CHECK SIZE III
 STRATEGY FULL THRESHOLD
 FIXATION TARGET CENTRAL
 RX USED DS DCX DEG PUPIL DIAMETER VA 20/20



DISCUSSION

Field description: Congruous homonymous right inferior perifoveal scotoma.

Localization: Left superior occipital pole.

Pathology: Infarct/contusion.

Other features: Hemianopic dyslexia.

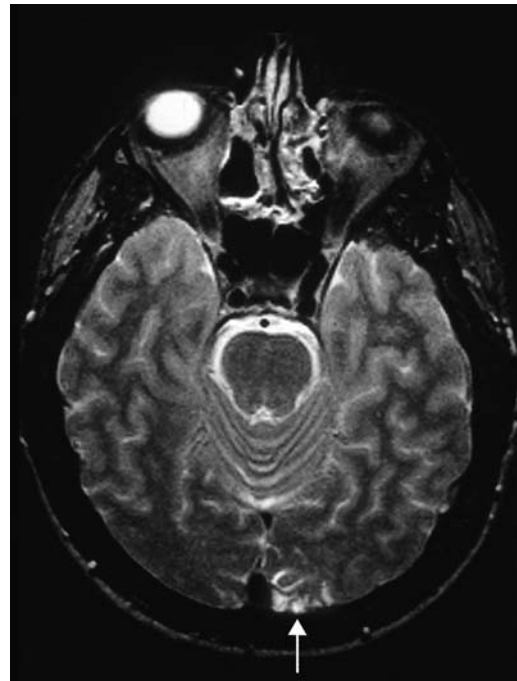
Confrontation fields were normal, but tangent screen perimetry showed a small homonymous left inferior quadrantic defect to finger motion.

The automated perimetry shows central defects in both eyes. Are these central scotomata from bilateral optic nerve injury or from striate injury? In the left eye, the defect clearly respects the vertical meridian, consistent with striate damage. In the right eye, there is a mild depression in the total and pattern deviation maps on the other side of the vertical meridian. However, this is a borderline defect (28–30 dB in the visual sensitivity plot), compared with the drastic reduction to 0 and 16–24 dB for the two locations flagged in the right field. The similarity of the defects in the two eyes and the concentration of the

severe defects within one hemifield must outweigh this slight depression in the left quadrant of the right eye and lead one to conclude that a striate lesion is present. This was confirmed on axial T2 MRI (shown, arrow), as a faint occipital pole lesion.

Patients are frequently aware of defects within the central 5° because they impair tasks requiring high spatial resolution, such as reading. Loss of the right perifoveal field is more disabling to reading than loss of the left side (163,166). Since we read from left to right, the text ahead of fixation is always obscured by a right perifoveal field defect. This is especially vexing because we tend to fixate slightly left of the center of each word we look at. By contrast, subjects with left hemifield defects read quickly but encounter difficulty when they need to move to the next line (see Case 88).

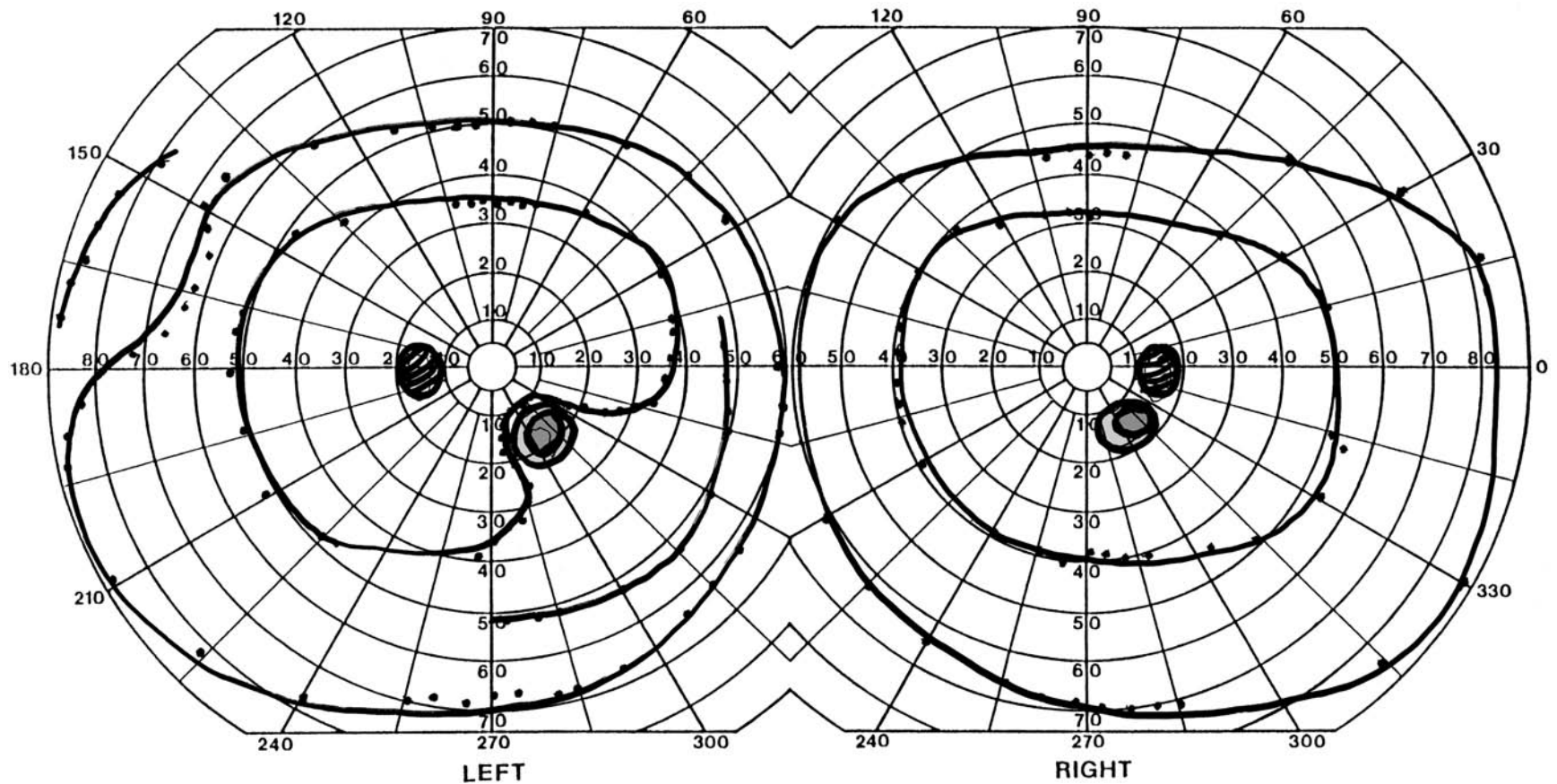
A perifoveal defect may be missed on kinetic perimetry or confrontation fields if done without care. With the normal acuity, this may lead the unsuspecting examiner to the false conclusion that vision is normal. Automated perimetric tests that focus on the central 10 or 30° of vision are best at detecting this visual field defect.



HISTORY AND EXAM

This 14-yr-old girl reported that over the last year there were repeated times when she could not see clearly in the right inferior field. She would be aware of this only briefly, for about a minute. Her birth had been difficult with shoulder dystocia, meconium aspiration, a seizure, and subarachnoid hemorrhage. At age 3 days, an examination had found vitreous hemorrhage OS and retinal and preretinal hemorrhages OD (i.e., a neonatal

Terson's syndrome). She had developed well, though, and only reported occasional headaches, with no other neurologic problems. At evaluation, her acuity was 20/20 OD and 20/25 OS, with normal color scores of 13/14 OD and 12/14 OS. There was no RAPD. Fundoscopy showed normal optic disks and some peripheral pigment clumping OS, consistent with old choroidal infarction. She had a comitant intermittent exotropia.



DISCUSSION

Field description: Congruous homonymous right inferior scotomata OU.

Localization: Striate cortex.

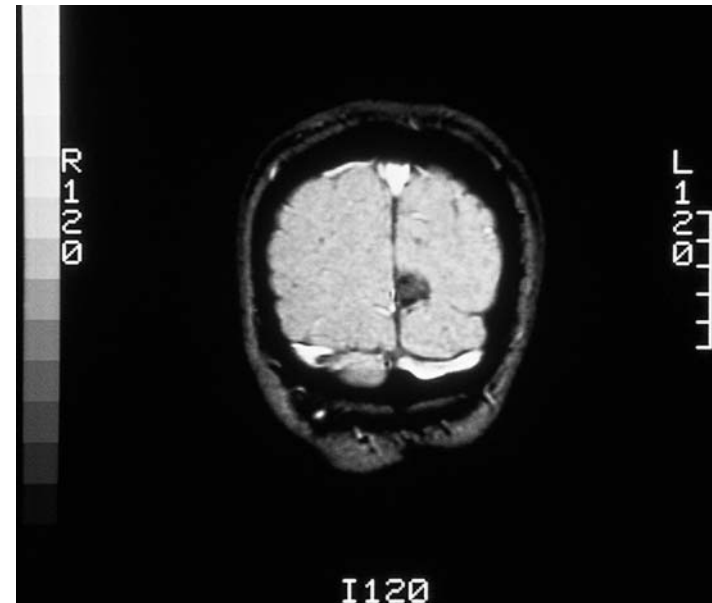
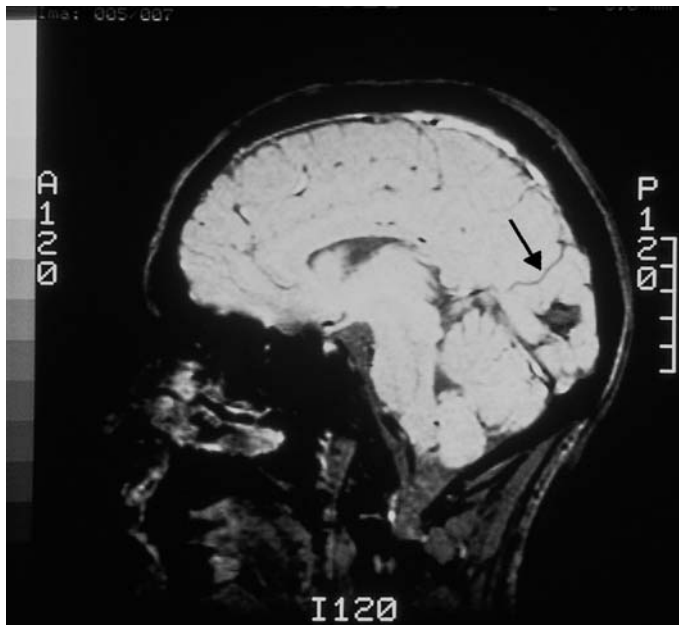
Pathology: Occipital hemorrhage.

Confrontation fields were full, including color comparisons.

Despite the patient's extensive earlier retinal history, her small field defect was present in both eyes and highly congruous. The lesion respected the vertical meridian, insofar as it did not cross it, but it did not abut this to cause a definitive vertical step. Nevertheless, the congruity stamps this as retrochiasmal and most likely striate in origin. Sagittal and coronal T1 MRI (shown) demonstrate the lesion above the calcarine fissure and well anterior to the pole.

Why had she only intermittently noted the scotoma? It is not uncommon for small defects outside of the perifoveal region to go unnoticed. Furthermore, in her case the exotropia may have helped hide the defect. Because of her ocular misalignment, most of the time the defects were not overlapping in her view of the world. Hence, they would come to light only during moments when she was intermittently orthotropic, suppressing the vision of one eye, or just closing one eye.

Note on the sagittal image that the distances from the lesion to the parieto-occipital fissure (arrow) and to the occipital pole are about the same. On the field, this volume of spared striate cortex corresponds to 60° of peripheral vision and a mere 10° of central vision—a graphic illustration of cortical magnification (see Chapter 2).



HISTORY AND EXAM

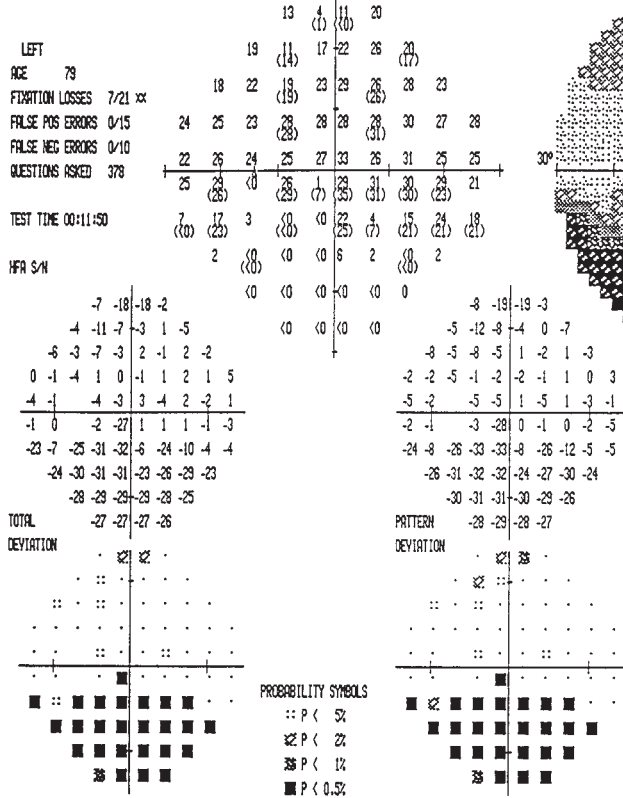
This 77-yr-old man noted the sudden onset of several visual problems. He bumped into things, especially on the right. He had trouble reading newspapers and seeing objects on the floor. He had a history of coronary artery disease, hypertension, diabetes, a previous stroke, and resection of a right occipital meningioma 7 years earlier. On examination 3

weeks after onset, visual acuity was 20/25 OD and 20/20 OS. Ishihara color plates were 6/12 OD and 5/12 OS, with a tendency to miss digits on the right. There was no RAPD and disks appeared normal. The remainder of the neurologic examination was normal.

CENTRAL 30 - 2 THRESHOLD TEST

DATE 12-10-98

STIMULUS III, WHITE, BKGD 31.5 ASB BLIND SPOT CHECK SIZE III
 STRATEGY FULL THRESHOLD
 FIXATION TARGET CENTRAL
 RX USED +1.5 OS DCX DEG PUPIL DIAMETER 4.0 MM VA 20/20
 FASTPAC
 LOW PATIENT RELIABILITY

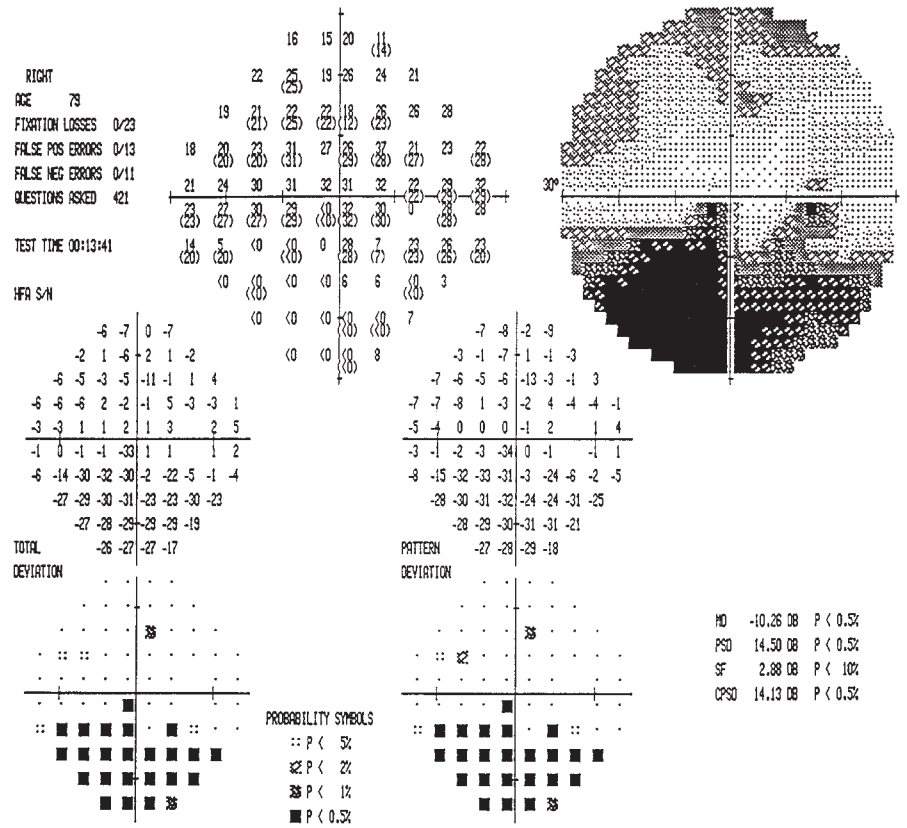


MD -10.11 DB P < 0.5%
 PSD 13.78 DB P < 0.5%
 SF 2.68 DB
 CPSD 13.44 DB P < 0.5%

CENTRAL 30 - 2 THRESHOLD TEST

DATE 12-10-98

STIMULUS III, WHITE, BKGD 31.5 ASB BLIND SPOT CHECK SIZE III
 STRATEGY FULL THRESHOLD
 FIXATION TARGET CENTRAL
 RX USED +1.5 OS DCX DEG PUPIL DIAMETER 4.0 MM VA 20/20
 FASTPAC



MD -10.26 DB P < 0.5%
 PSD 14.50 DB P < 0.5%
 SF 2.88 DB P < 10%
 CPSD 14.13 DB P < 0.5%

DISCUSSION

Field description: Relatively congruous homonymous inferior defects involving the two hemifields asymmetrically, with probable vertical step.

Localization: Occipital cortex bilaterally.

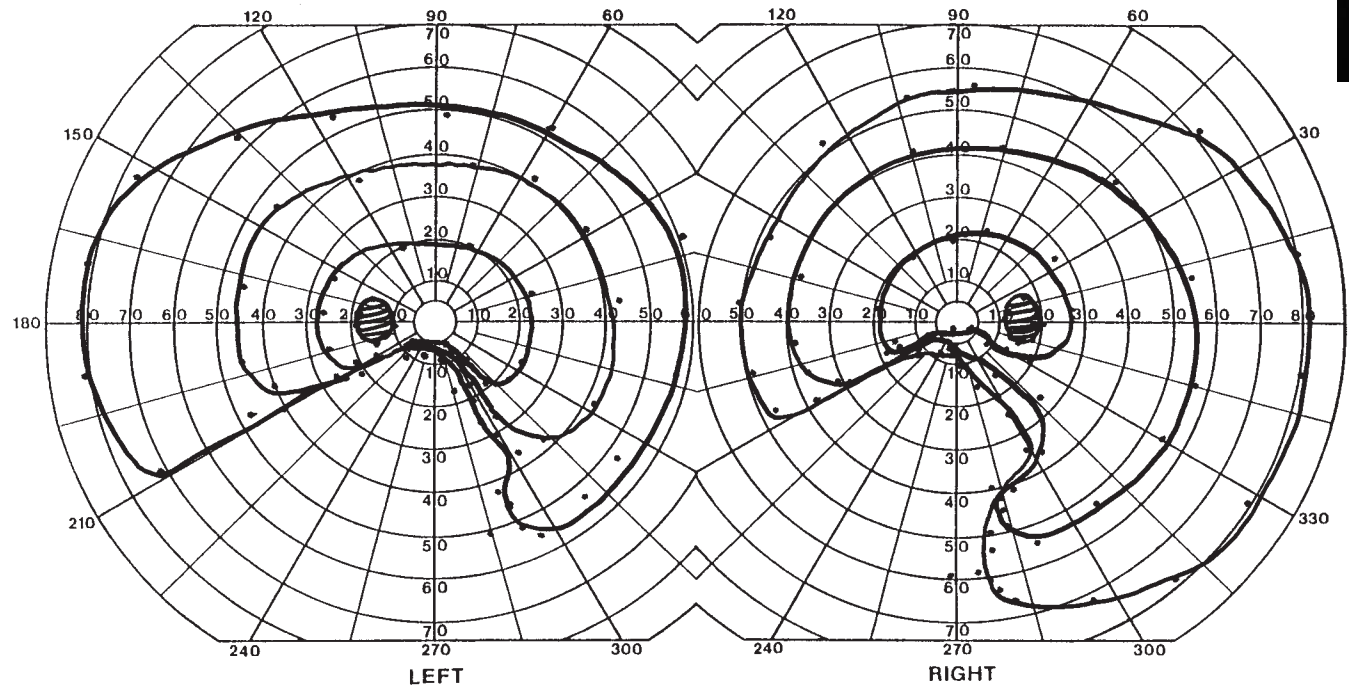
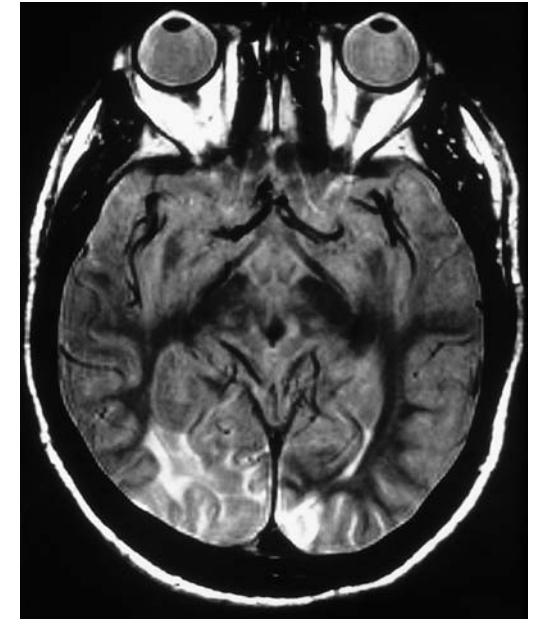
Pathology: New left infarct, old right meningioma resection.

Confrontation testing showed no hand motions in the left lower quadrant and decreased vision to hand comparisons in the right lower quadrant OU.

Bilateral inferior defects might also be the result of bilateral optic neuropathy, particularly AION (see Case 33). However, altitudinal defects from optic nerve disease should always extend to the nasal horizontal meridian in each eye, which is not the case here. In addition, the similarity of the defects in the two eyes and the vertical steps at the center of vision in both eyes here are best explained by a retrochiasmal problem.

While Goldmann perimetry showed the full peripheral extent of the defect, it does not show the central vertical step as well as the automated field did.

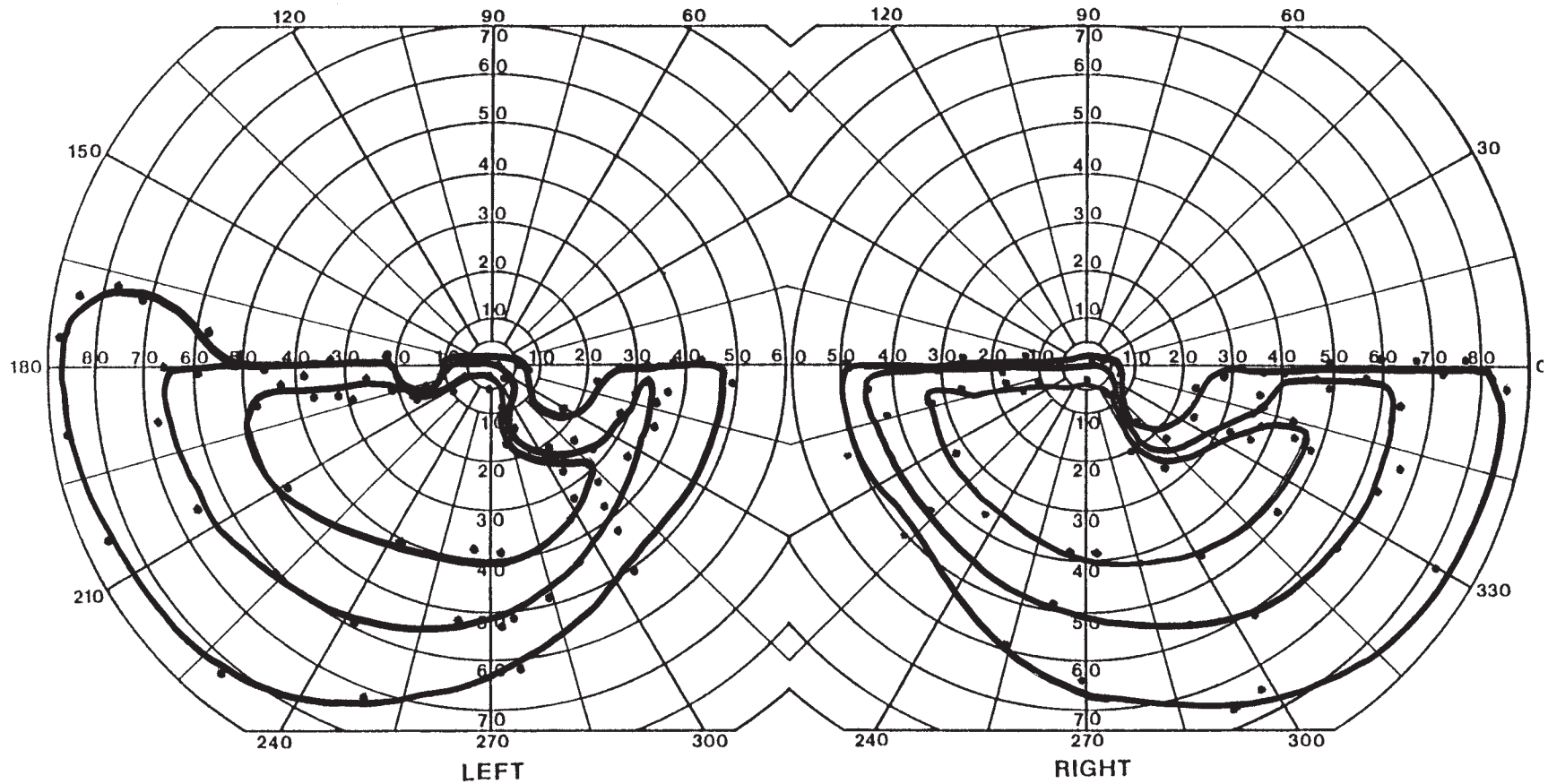
Without knowing whether the left hemifield defect dates to the patient's resection, it is not clear whether his new event is unilateral or bilateral. Tumor recurrence is a possibility, but MRI ruled this out. Rather, T1 and T2 axial MRI showed, in addition to a large area of right occipital encephalomalacia, a new area of abnormal signal in the left occipital lobe.



HISTORY AND EXAM

This 38-yr-old man was shot in the head at age 20, with subsequent evacuation of an intracranial hematoma. Since that time he has been unable to recognize faces, gets lost in familiar surroundings, and notes that colors are faded and grayish. Visual acuity was

20/20 OU. He saw 10/14 Ishihara pseudo-isochromatic plates OU. Eye movements were normal. He had mild difficulty recognizing visual objects, particularly when seen in unusual views. He had a mild verbal memory impairment.



DISCUSSION

Field description: Congruous bilateral superior quadrantanopia, with extension into right inferior quadrant.

Localization: Bilateral striate cortex, inferior calcarine banks.

Pathology: Gunshot wound.

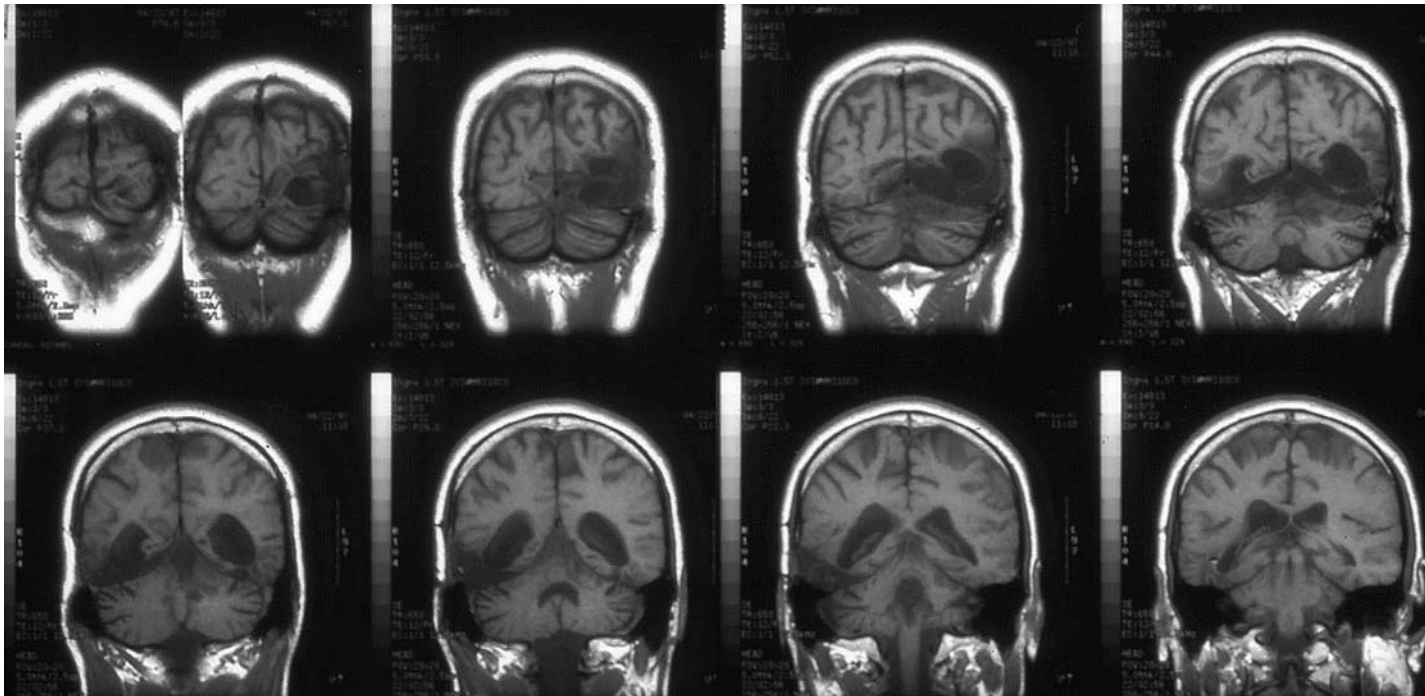
Other features: Prosopagnosia, topographagnosia, partial dyschromatopsia.

Confrontation fields showed no hand motion vision in any superior quadrant, with impaired color discrimination in the lower right quadrant.

Bilateral superior altitudinal defects could also be the result of bilateral optic neuropathy, particularly the ischemic variety. While there is no obvious step at the vertical meridian, the congruous nature of the defect, especially in the right hemifield, stamp this

as bilateral quadrantanopia rather than bilateral altitudinal nerve fiber layer defects. The defect in the left eye is particularly revealing; the defect aligns more along the horizontal meridian on the temporal side and not the nasal side, the opposite of what is seen with optic neuropathy.

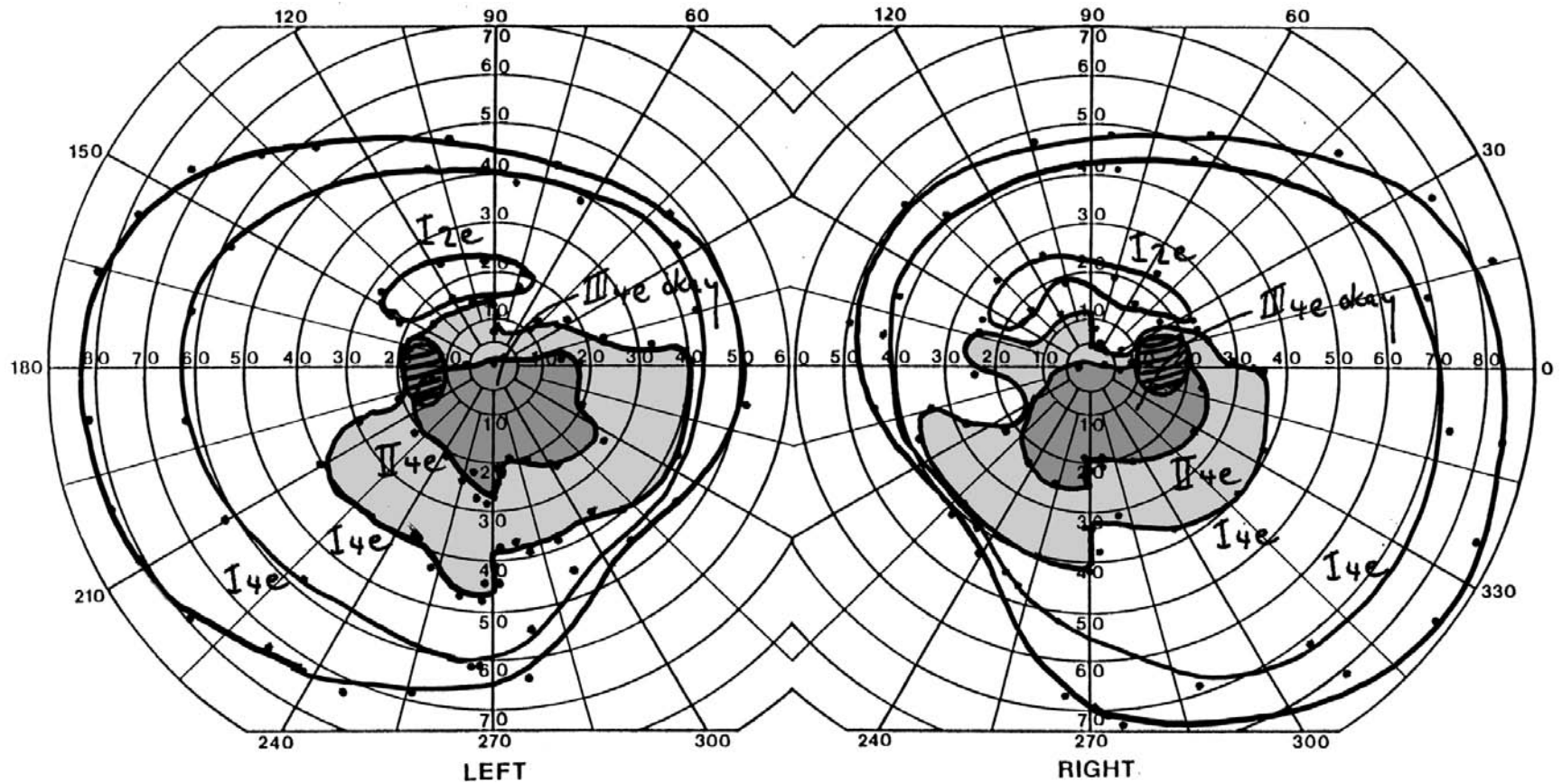
Coronal MRI showed the trajectory of the bullet, causing bilateral posterior ventral occipitotemporal lesions, extending more anteriorly on the right. Bilateral medial occipitotemporal lesions are associated with a classic tetrad of superior field defects, prosopagnosia, topographagnosia, and dyschromatopsia (159). While the patient does not have complete loss of color vision, subsequent testing showed that he was severely impaired on judgments of color saturation.



HISTORY AND EXAM

This 52-yr-old man was resuscitated from a cardiac arrest due to an inferolateral myocardial infarction. Five days later he lost consciousness briefly in the hospital and on recovery was blind in both eyes. Over the following few days vision gradually improved, and he began to experience episodic hallucinations of flashes of light and colors. His

examination 2 years later showed visual acuity at only count fingers OU, without RAPD or optic atrophy. He continued to report hallucinations of colored clouds or people in his central vision, and sometimes saw objects such as television images a few minutes after they had disappeared from view.



DISCUSSION

Field description: Fairly congruous, large bilateral central scotomata with inferior extension and vertical steps.

Localization: Bilateral striate cortex, posterior.

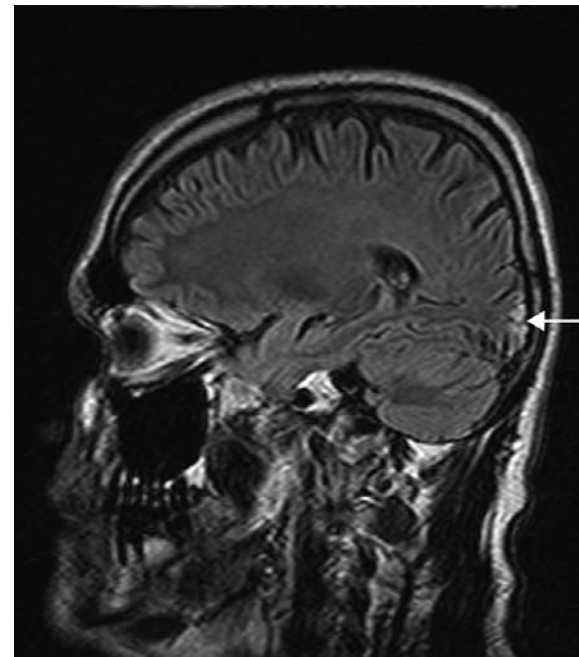
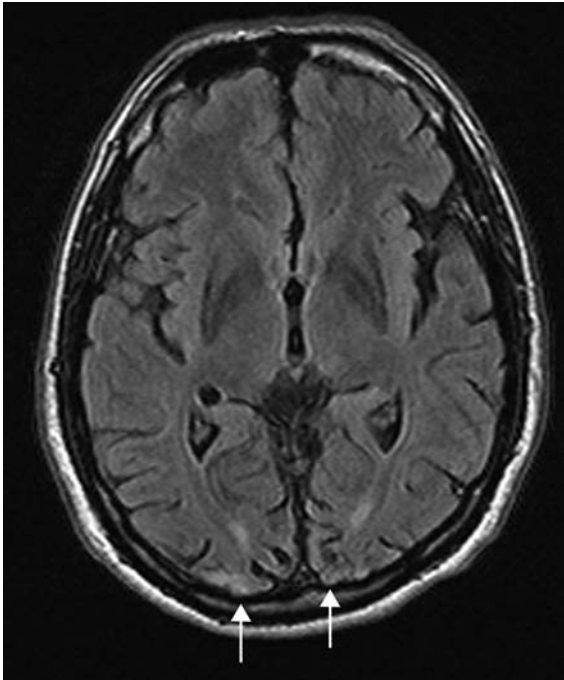
Pathology: Bilateral posterior cerebral arterial infarction, calcarine branches, probably embolic (“top of the basilar” syndrome).

Other features: Release hallucinations, palinopsia, initial cerebral blindness.

These are fairly complex fields at first glance. One starts by visualizing the shape of the holes, which have transformed the hill of vision into a volcano. The deepest part of the valley (dark gray shading) is a central zone in which the II4e target is not seen. (However, the perimetrist has indicated that a III4e target can be seen here; thus, it is a relative, not an absolute, scotoma.) Surrounding this is a shallow slope, with a zone in which the II4e but not the I4e can be seen (light gray shading). The defect is less severe superiorly, where it rises to a preserved crescent in which the I2e target can be seen. This represents

the lip of the volcano’s crater, as it were. Having visualized the overall shape of the defect, the key then is to search for localizing clues. In this example, the two main features are (1) relative congruity of the complex margins of the scotomata (mild incongruity may be due to difficulty maintaining fixation at center, given the patient’s acuity of counting fingers only); and (2) the numerous vertical steps in the isopters defining the central holes, indicating pathology behind the chiasm.

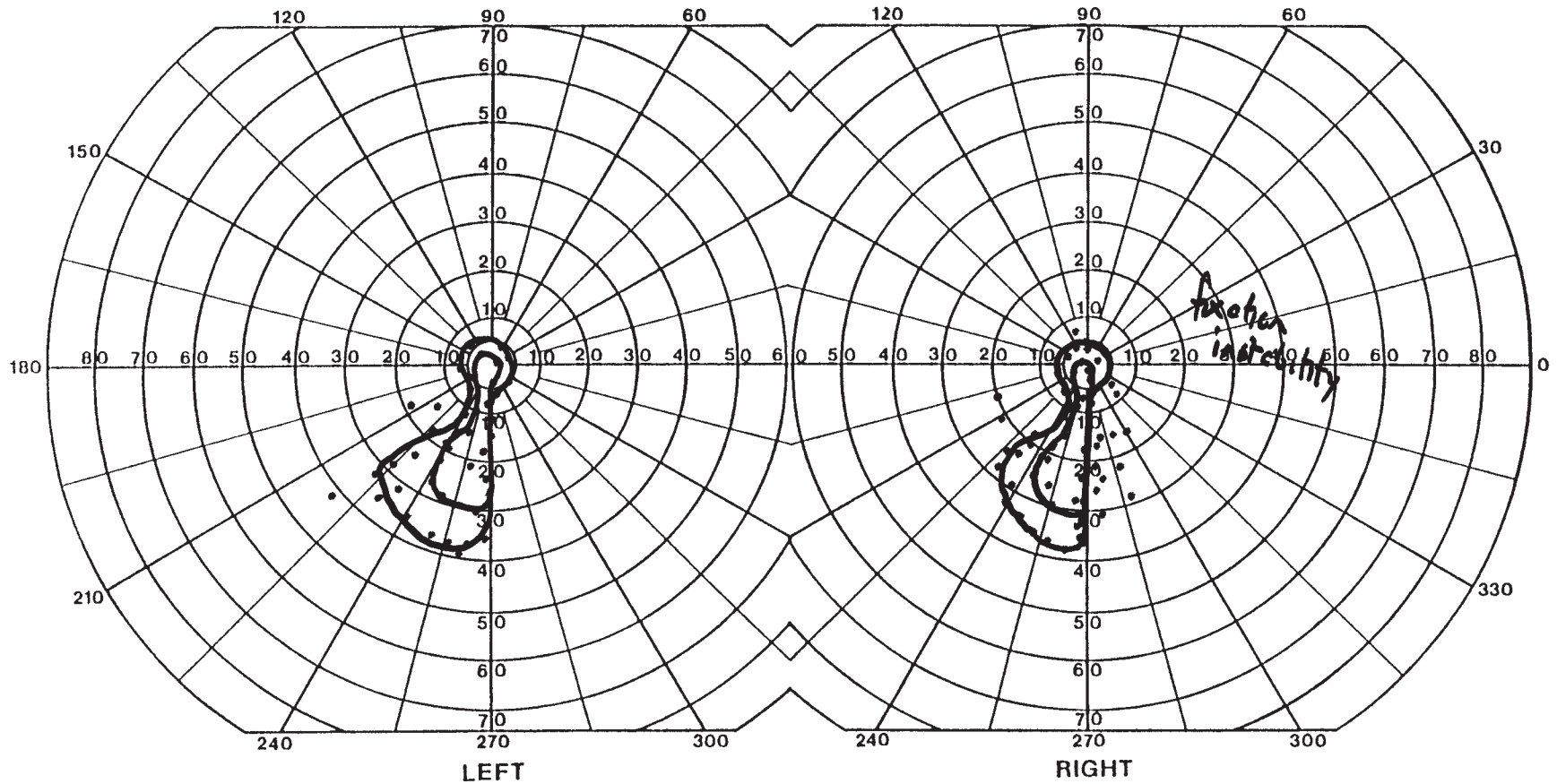
Bilateral central defects can occur with either bilateral cerebral disease (167) or bilateral optic neuropathy. Bilateral striate lesions are more common than bilateral optic radiation damage, especially when simultaneous and in the absence of other neurologic defects. His hallucinations are release phenomena (Charles Bonnet syndrome) and lack localizing value, since they can occur with bilateral visual loss ranging from cataracts to striate lesions. Sagittal and axial FLAIR MRI showed bilateral occipital pole infarcts (arrows), with some change to the white matter also, seen on the axial image.



HISTORY AND EXAM

Immediately after a prostatectomy, this 69-yr-old man with hypertension and asthma was completely blind and had slurred speech, drowsiness, right gaze deviation, and right hemiparesis. He gradually improved to only a mild right-sided weakness and a visual field defect. Visual acuity was 20/30 OU, and Ishihara color scores were 11/14 OD and 13/14

OS. There was no RAPD and optic disks were normal. Pursuit was impaired in all directions and saccades were inaccurate in both fields, requiring multiple saccades to locate a target. He had a right hemiparesis. Reaching for targets with either hand was inaccurate; this improved when the targets were parts of his own body.



DISCUSSION

Field description: Congruous homonymous bilateral hemianopia, with sparing of macula and left inferior island of vision, respecting the vertical meridian.

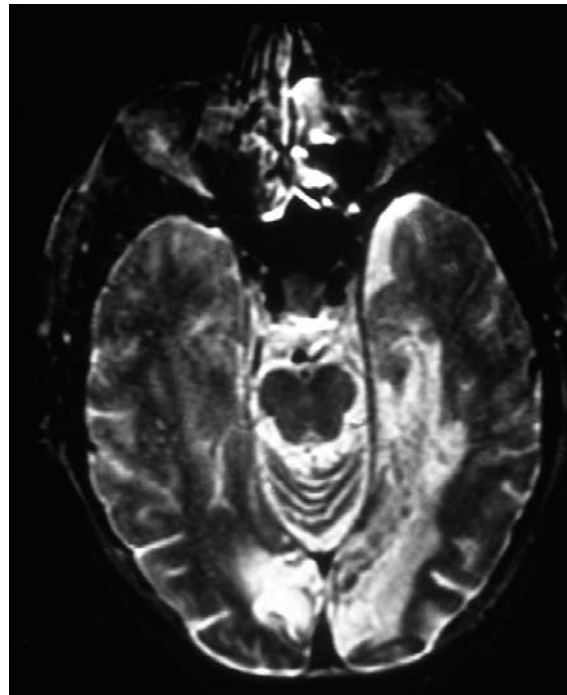
Localization: Bilateral striate cortex, sparing occipital pole.

Pathology: Bilateral posterior cerebral artery infarction.

Confrontation testing with hand motion showed a residual island of vision in the left inferior quadrant OU.

Prostate surgery used to be followed by an acute confusional state in some patients, because the glycine used as a diluent was absorbed and gained access to the CNS, where it is an inhibitory neurotransmitter (168). Glycine is no longer used, however. In this patient, the event was an embolic “top-of-the-basilar” stroke (169). The nonvisual symp-

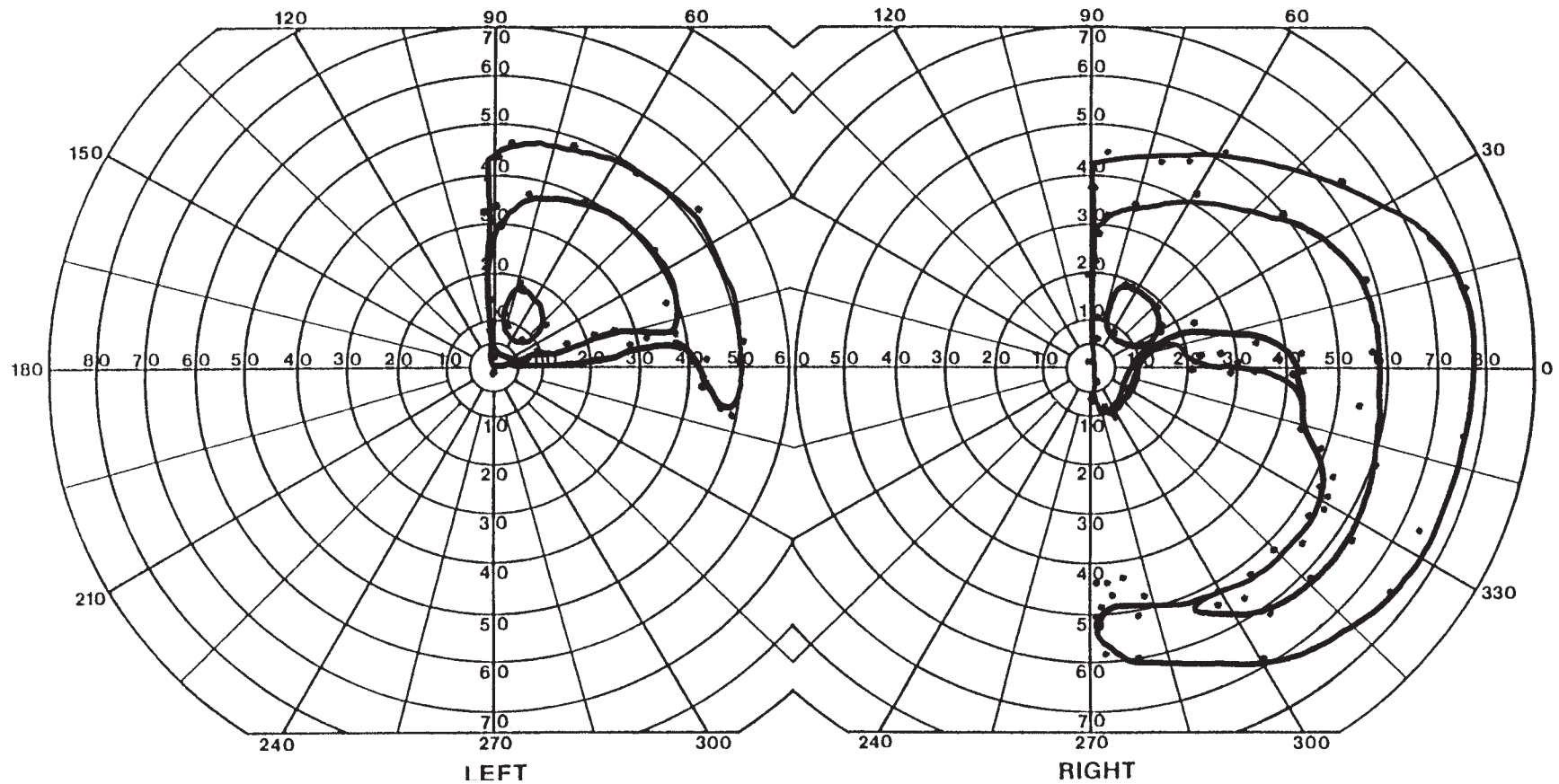
toms were likely due to brain stem ischemia, and the visual symptoms to propagation of emboli into both posterior cerebral arteries at the terminus of the basilar artery. Bilateral blindness with normal fundi after surgery might also represent posterior ischemic optic neuropathies (63), especially when hypotension or significant blood loss occurs, but the pupillary light reflexes would be impaired in PION, whereas they would be normal in cerebral blindness. His partial defects now are clearly congruous and have a step at the vertical meridian, indicating bilateral hemianopias rather than bilateral optic neuropathies. He has inaccurate saccades and misreaching to visual targets, signs reminiscent of the ocular motor apraxia and optic ataxia of Bálint syndrome. However, in this case, these are due to severely limited peripheral vision and not additional parietal damage. Axial T2 MRI shows the bilateral medial occipital infarctions.



HISTORY AND EXAM

This 67-yr-old woman got lost while driving familiar routes and struggled to find her desk at work, only succeeding when she recognized her coat on the chair. She had trouble remembering her daily schedule and began having severe headaches. Two months later a left hemianopia was found by an ophthalmologist, and MRI showed a mass, which was resected. She was stable for the next 4 months, but in the few weeks prior to examination

was having more trouble navigating and finding objects around her. Visual acuity was 20/30 OD and 20/40 OS. Ishihara color plates were 0/14 OU. Optic disks were normal. Line bisection showed left hemineglect and she drew the numbers on a clock face in reverse order. Cube construction was poor. The remainder of the neurologic examination was normal.



DISCUSSION

Field description: Complete left homonymous hemianopia and right inferior quadrantanopia with sparing of the monocular temporal crescent.

Localization: Bilateral occipitotemporal and right occipitoparietal lobes.

Pathology: Tumor.

Other features: Topographagnosia, achromatopsia, left hemineglect.

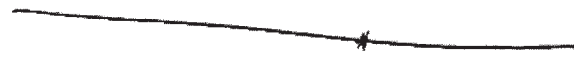
Confrontation fields showed no hand motion in the left hemifield and hand motion but not count fingers vision in the right inferior quadrant.

The homonymous nature and the vertical step at the meridian confirm that the patient's fields represent bilateral hemifield defects. Achromatopsia indicates damage to the lingual and fusiform gyri in the occipitotemporal cortex, while the left hemineglect suggests right parietal involvement. The reverse ordering and scattering of left-sided numbers in her

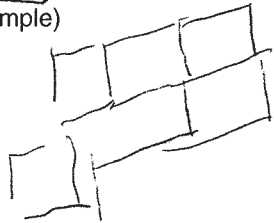
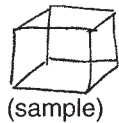
clock drawing reveal severe spatial disorganization, again attributable to a right parietal lesion (170) and borne out in her attempt to copy a cube. The lesion must be bilateral and extensive. MRI showed enhancing tumor in the right occipital lobe with edema spreading into the temporal lobe on the right as well as faint enhancement in the left temporo-occipital white matter, (arrows), seen on these axial and coronal T1-weighted images.

Bilateral tumors are bad news, and are usually glioblastoma multiforme (GBM) or primary CNS lymphoma. The pathology from her partial resection showed GBM and she was treated with cranial irradiation. Factors predicting a better prognosis include: Grade III (anaplastic astrocytoma) rather than Grade IV (GBM), age under 50 yr, normal mental state examination, gross total surgical resection, and Karnofsky performance score over 70 (i.e., the patient is independent in his or her activities of daily living) (171). This patient died 2 months after her visit.

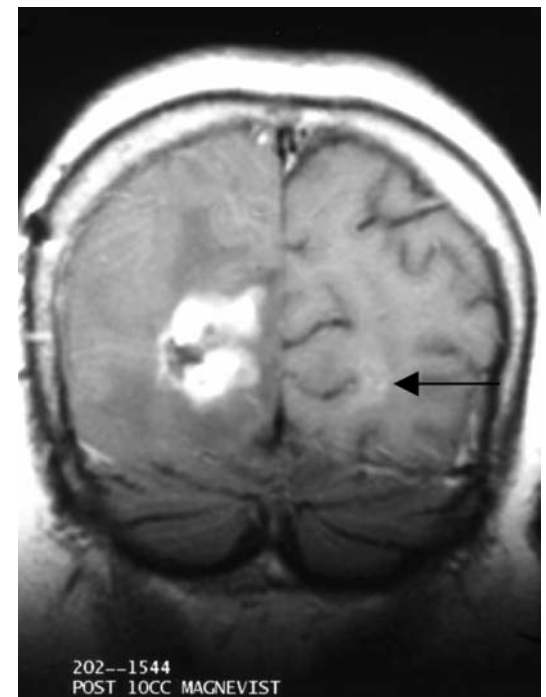
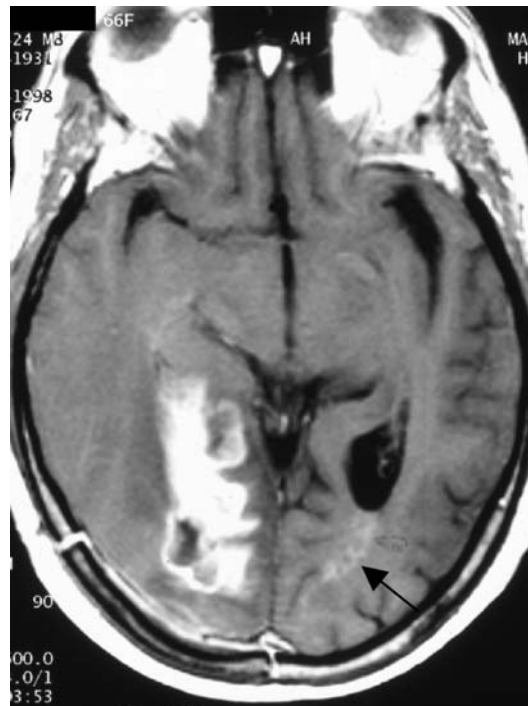
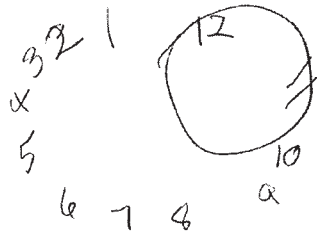
line bisection



cube copying



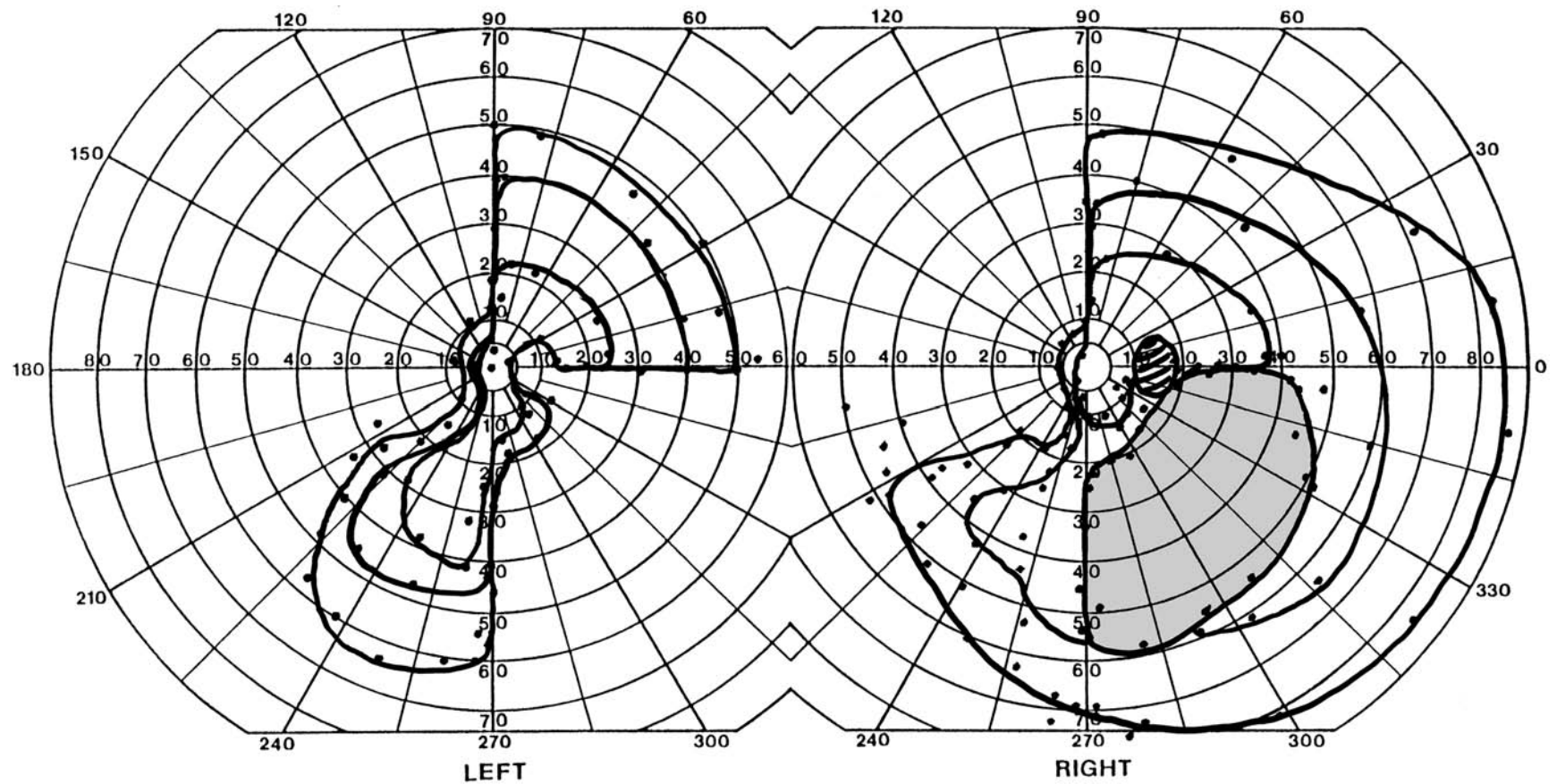
clock drawing



HISTORY AND EXAM

This 66-yr-old man noted blurred vision and difficulty seeing to the left after a coronary artery bypass graft (CABG). This interfered with reading, and he noted swirls of colors in his vision for 3 days. Repeated evaluation 2 weeks later showed acuity of 20/25

OU and good color vision scores of 12/14 OD and 13/14 OS. There was no RAPD. He also had a right Horner's syndrome, but no other neurologic deficits.



DISCUSSION

Field description: Congruous homonymous left upper and right lower quadrantanopias, with sparing of right temporal crescent.

Localization: Bilateral striate cortex.

Pathology: Bilateral partial posterior cerebral arterial infarctions, involving left parieto-occipital branch and right posterior temporal branch.

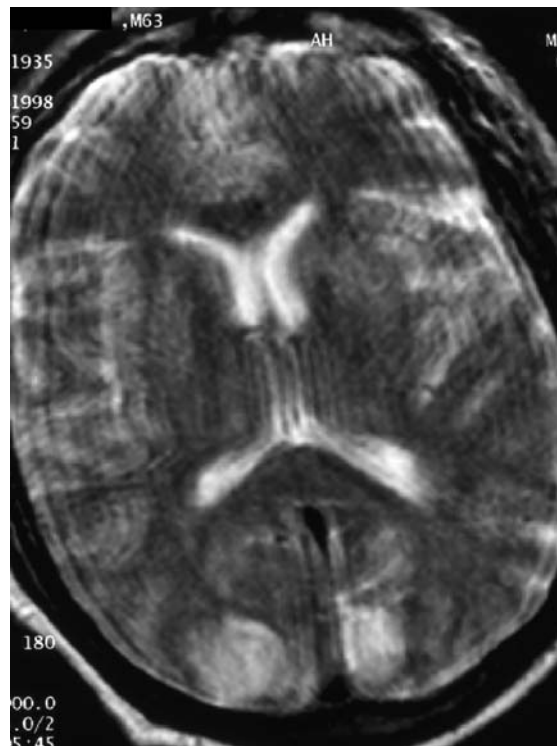
Other features: Charles Bonnet syndrome (release hallucinations).

Confrontation fields showed a superior quadrantic defect extending into the lower quadrant to hand motion, but no defect apparent in the right hemifield.

The bilateral vertical meridian steps clearly stamp this as bilateral occipital rather than bilateral optic disease. T2-weighted axial MRI shows these lesions, despite the motion artifact.

Stroke after CABG is common, occurring in 2–6% of patients. A prospective study of 456 patients undergoing CABG identified five factors associated with an increased risk of intraoperative stroke: previous stroke, carotid bruit, hypertension, diabetes, and old age (172). Most strokes in this setting involve multiple vascular territories, as might be expected with emboli from the heart or aortic arch. Showers of emboli may result from manipulation of an atherosclerotic aorta. The deleterious effects of these emboli on the brain may be compounded by concurrent hypoperfusion from low mean arterial pressure or lack of pulsatile blood flow while on cardiac bypass (173).

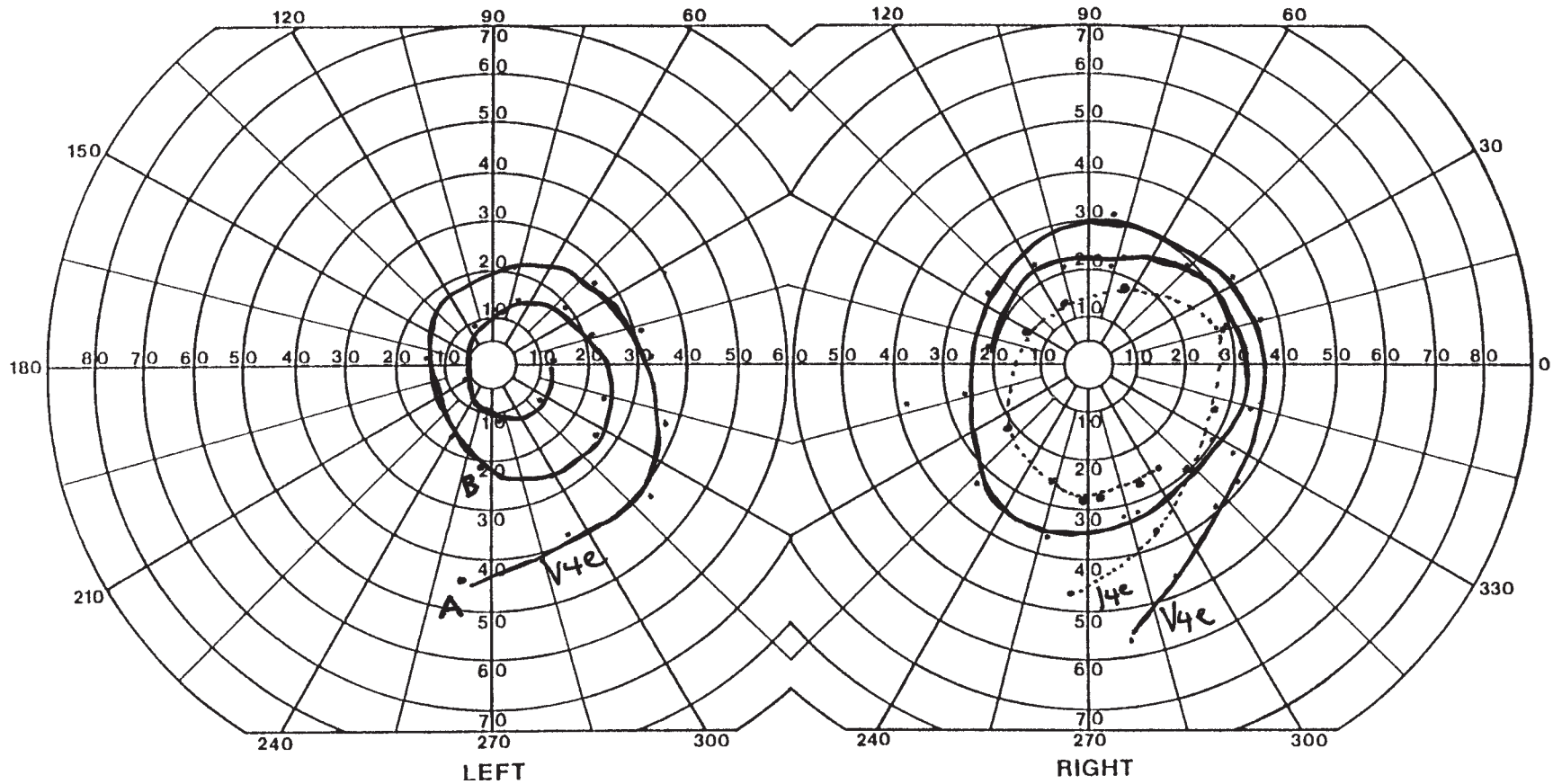
The patient's Horner's syndrome is probably due to intrathoracic surgical manipulation (174). Vertebrobasilar brain stem ischemia could also cause a Horner's syndrome, but he lacked other signs of midbrain or lateral medullary damage.



HISTORY AND EXAM

This 40-yr-old woman had decreased vision OS, trouble looking to the left, left-sided weakness, and fatigue 3 years earlier. An MRI showed a few spots in her white matter. Over the following year she continued to experience fatigue, blackouts, and “straining to see.” In the past 10 days, she had had intermittent diplopia and total body numbness and was given iv methylprednisolone for a presumed MS attack. Acuity was 20/80 OD and

20/50 OS, improving with pinhole and encouragement to 20/40 OD and 20/30 OS. There was no RAPD. Ishihara color scores were 7/14 OD and 10/14 OS. Optic disks were normal. Eye movements were normal, and she was orthotropic in all positions of gaze. Neurologic examination showed give-way weakness diffusely, and reduction of all sensory modalities in all body parts tested.



DISCUSSION

Field description: Spiraling.

Localization: Functional deficit.

Pathology: Psychogenic.

Confrontation fields with varying viewing distance showed cylindrical tunnel vision OU.

The patient displays two classic functional patterns on visual field testing: cylindrical tunnel vision on confrontation testing (see Chapter 3), and functional spiraling on kinetic perimetry. In spiraling, the first test location is usually seen in the midperiphery (point A). If the examiner maintains an orderly test sequence, moving, say, in a counterclockwise direction (as in her field), the eccentricity at which the target is seen gradually decreases. The result is that when the examiner has completed a full circle and is back testing at the first location, the target cannot be seen until it is much closer to fixation (point B) than when it was perceived at the start of the test. As the examiner continues in a second

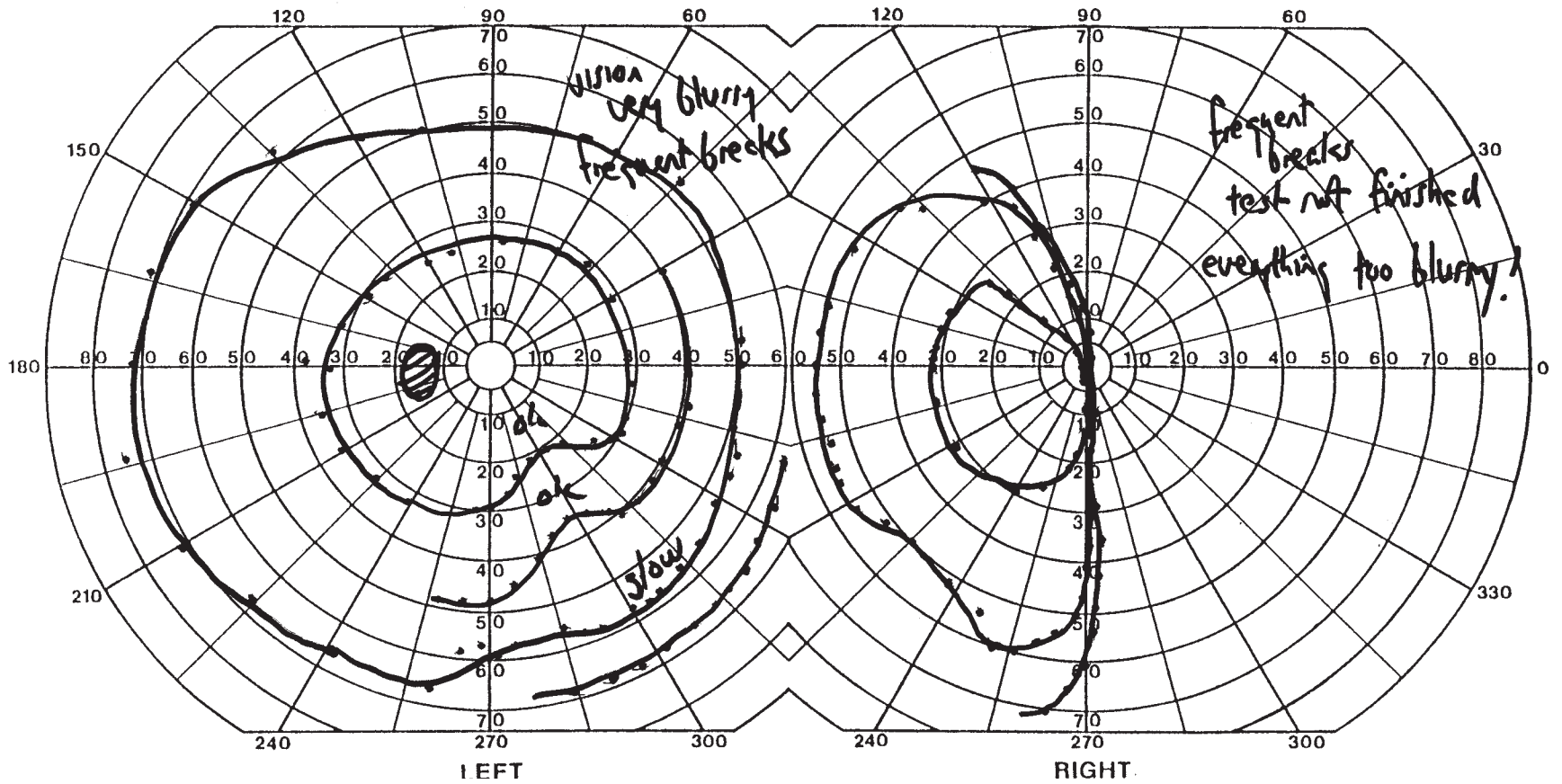
counterclockwise circle, this can be shown for the rest of the points as well. It is as if the patient is losing vision during the actual test!

So what does this mean about her vision? Clearly, at least part of her deficit is functional, but given her history she could still have a mild optic neuropathy with some nerve fiber layer field defect. It is just that the functional defect makes it that much harder to discern any signs of true pathology that might be present. Functional and organic defects can coexist and often do in other neurologic arenas, the combination of pseudo-seizures and seizures being one such example (175). At the least, in this patient the lack of optic atrophy argues against a severe neuropathy. Evoked potentials may or may not help; it is possible to create artifactual abnormalities on such testing by poor fixation or defocusing one's eyes (176). Evidence that this patient has MS will have to come from avenues other than the eye clinic. Unfortunately, the rest of her neurologic examination also shows functional elements.

HISTORY AND EXAM

This 47-yr-old school bus driver had an accident, hitting her head, but without loss of consciousness. Since then she had been unable to see to the right with her right eye. Acuity

was 20/20 OU, Ishihara color scores were 13/14 OU, and there was no RAPD. Fundoscopy was normal OU.



DISCUSSION

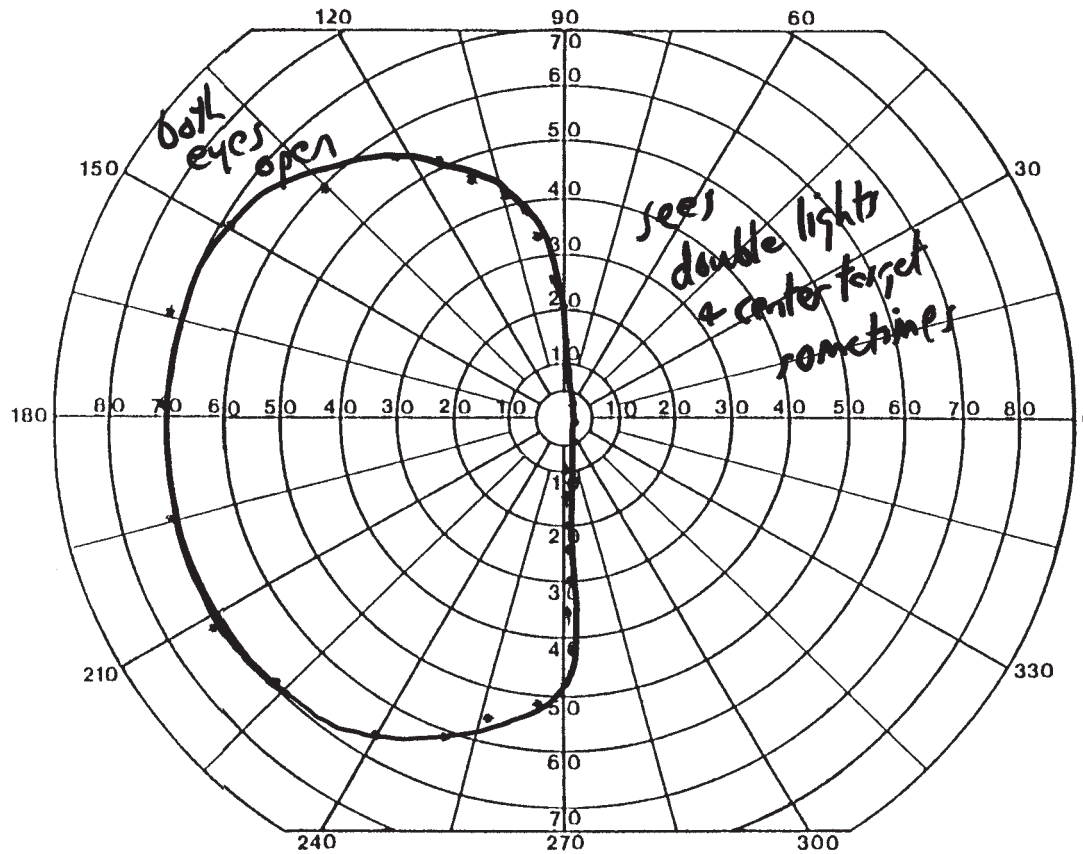
Field description: Monocular temporal hemianopia.

Localization: Functional.

Pathology: Psychogenic (“hysterical hemianopia”).

The patient’s monocular visual fields suggest a unilateral temporal hemianopia in the right eye, respecting the vertical meridian. This is a puzzling defect—rare monocular nasal hemianopias have been described with lateral chiasmal compression; however, it is

virtually impossible for lesions affecting the crossing fibers to eliminate one temporal hemifield entirely and spare the other temporal hemifield. This raises suspicion of a functional hemianopia, which is one of the few clinical settings in which perimetry with both eyes open is useful. When tested with both eyes viewing, as shown on this page, the patient still fails to see in the right hemifield, despite the fact that her normal left eye is now open. Some call this the “missing half” field defect (177). Not surprisingly, she was applying for disability after 25 years of ferrying screaming children to and from school.



HISTORY AND EXAM

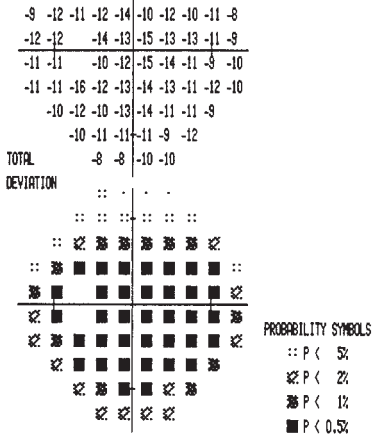
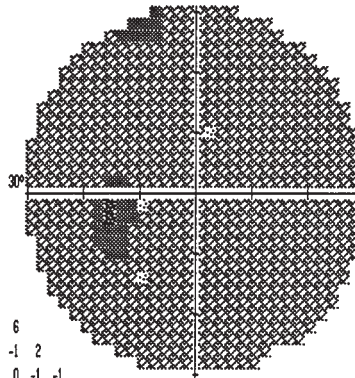
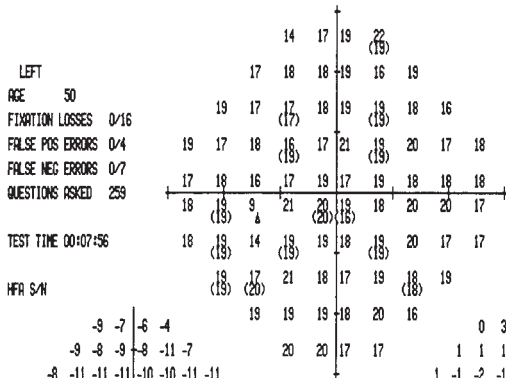
This 49-yr-old woman had 20 years of "eye strain" impairing reading, shopping, and looking at people. A prior examination had found latent hyperopia, and her symptoms had responded 16 years before to clonazepam. She had a long history of depression.

Acuity was 20/20 OU with correction, and Ishihara color scores were 14/14 OU. There was no RAPD. She had small optic disks with minimal cups. Neurologic examination was normal.

CENTRAL 30 - 2 THRESHOLD TEST

STIMULUS III, WHITE, BKGD 31.5 ASB BLIND SPOT CHECK SIZE III
 STRATEGY FULL THRESHOLD
 FASTPAC

DATE 05-20-99
 TIME 03:22:11 PM
 FIXATION TARGET CENTRAL
 RX USED +4.5 DS DCX DEG PUPIL DIAMETER 5.0 MM VA 20/20



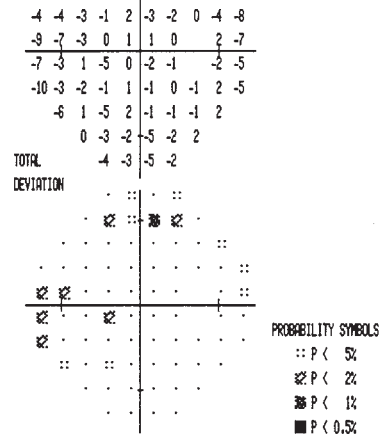
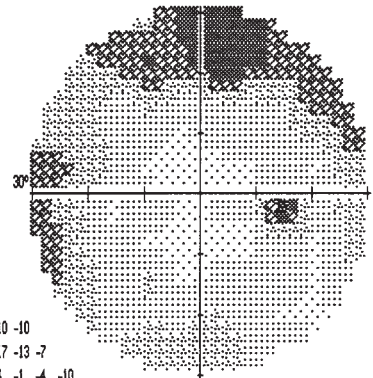
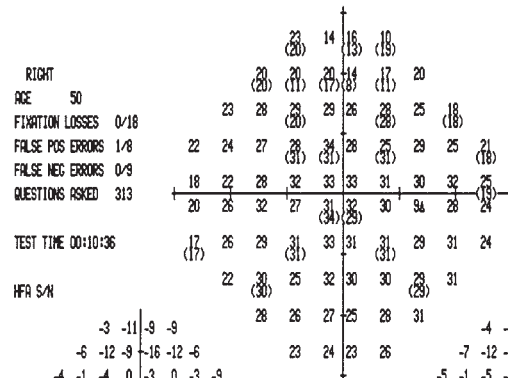
MD -11.22 DB P < 0.5%
 PSD 2.08 DB
 SF 1.20 DB
 CPSP 1.58 DB

PROBABILITY SYMBOLS
 :: P < 5%
 ☒ P < 2%
 ☐ P < 1%
 ■ P < 0.5%

CENTRAL 30 - 2 THRESHOLD TEST

STIMULUS III, WHITE, BKGD 31.5 ASB BLIND SPOT CHECK SIZE III
 STRATEGY FULL THRESHOLD
 FASTPAC

DATE 05-20-99
 TIME 02:56:41 PM
 FIXATION TARGET CENTRAL
 RX USED +5 DS DCX DEG PUPIL DIAMETER 5.0 MM VA 20/20



MD -2.31 DB
 PSD 3.63 DB P < 5%
 SF 2.74 DB
 CPSP 1.87 DB P < 10%

PROBABILITY SYMBOLS
 :: P < 5%
 ☒ P < 2%
 ☐ P < 1%
 ■ P < 0.5%

DISCUSSION

Field description: Flat thresholds across entire field, OS.

Localization: Functional defect.

Pathology: Depression.

Confrontation field were normal.

Note that the patient's entire field has nearly the same thresholds, 17–20 dB, which correspond to fairly bright lights of 100–200 asb. Apart from being a tour de force of functional consistency, this performance is physiologically implausible. A global reduc-

tion from physiologic causes should still preserve a hill-like shape to the visual field, with decreasing sensitivity in more eccentric retina.

This patient has a history of depression. However, serious psychopathology is unusual among patients with functional visual loss, with only half meriting a psychiatric diagnosis on follow-up (178). Unfortunately, visual complaints resolve in only about a quarter, despite reassurance and encouragement. Nevertheless, the social and functional consequences of the visual aspect of their problems are minimal (179).

DISCUSSION

Field description: Inferior arcuate defect, with dense inferonasal scotoma OS.

Localization: Optic nerve.

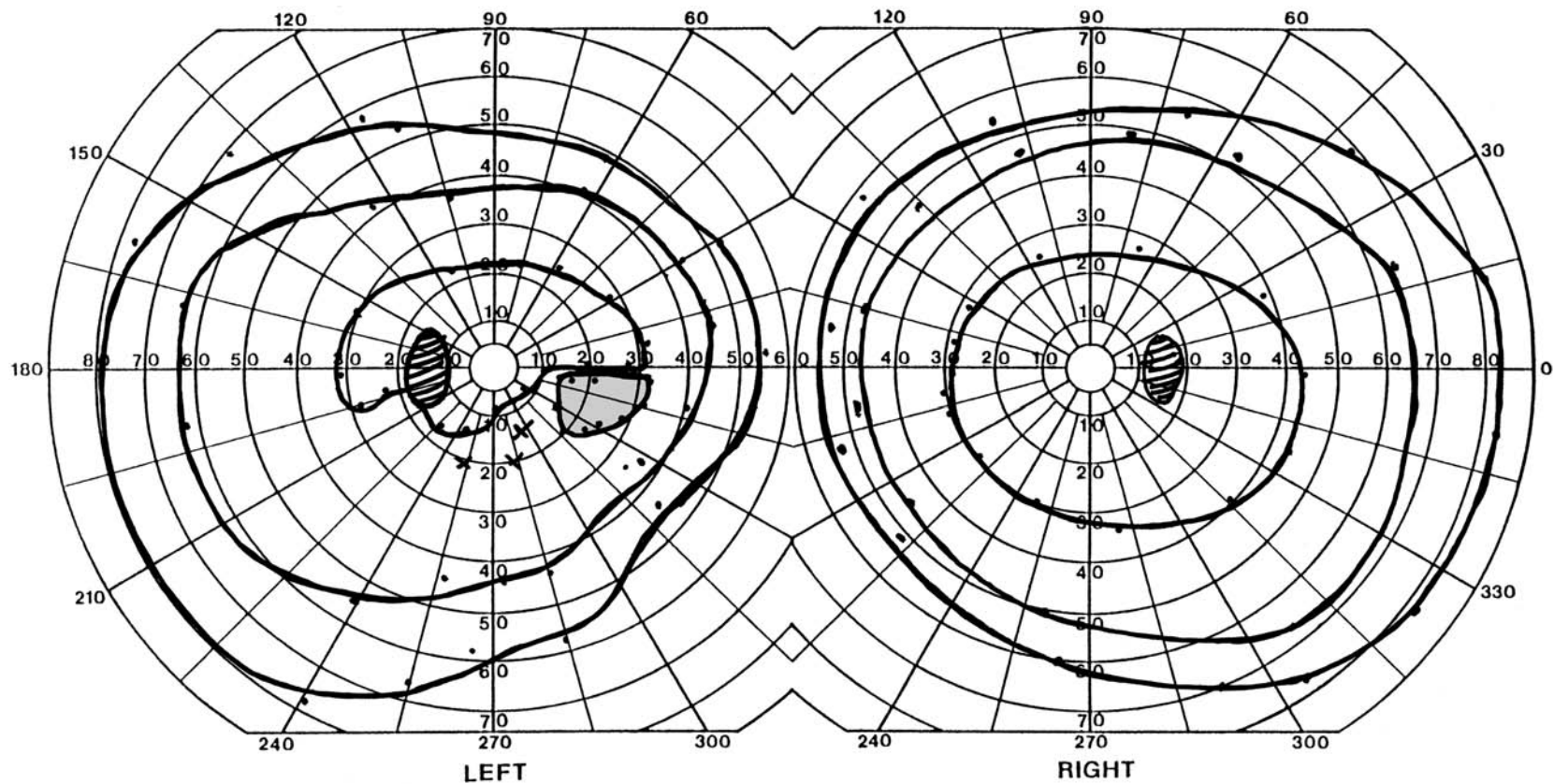
Pathology: Sarcoidosis.

Confrontation testing showed inferior paracentral scotoma to color and hand comparisons.

Automated perimetry shows a defect that arches out of the blind spot to end in a dense defect just below the nasal horizontal meridian—note that the visual sensitivities in this region are very low (2–6 dB). Goldmann perimetry done 10 months earlier showed exactly the same arcuate defect, with the same dense hole between 15 and 30° eccentric-

ity nasally, a nice example of the correlation of the two techniques. The presence of optic disk pallor implies that the optic neuropathy is not new.

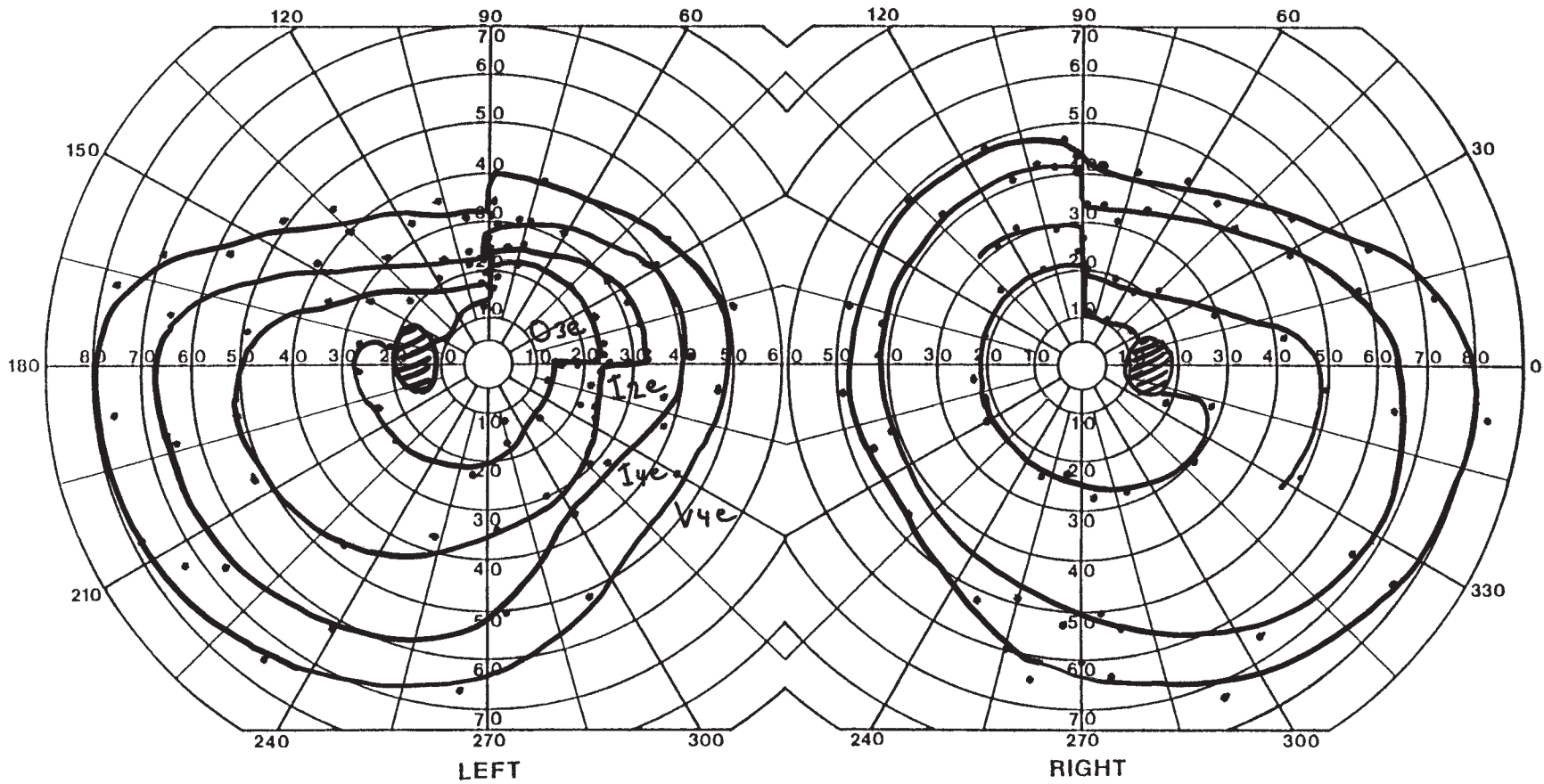
After the facial nerve, the optic nerve is the second most commonly affected cranial nerve in sarcoidosis, being involved in about 5% of patients with this disorder (180). Although unusual, this disease can present as an isolated optic neuritis (45,181). In this patient, an atypical optic neuritis must have been suspected initially, given the unusually long course of steroids. The subsequent development of erythema nodosum and hilar lymphadenopathy confirmed the diagnosis. While this patient did well with steroids, some cases can relapse when steroids are withdrawn—“steroid-dependent” optic neuropathy (182). Immunosuppression with azathioprine may be required in such cases.



HISTORY AND EXAM

While having a CT scan of his chest 1 month prior to evaluation, this 58-yr-old man had a sudden severe headache. Two weeks later a coronary artery bypass was complicated postoperatively by hyponatremia, confusion, and transient blurring of vision, possibly in

both eyes. Acuity 2 weeks after this was 20/20 OU, and Ishihara color scores were 13/14 OU. There was an RAPD OS. Optic disks appeared normal.



DISCUSSION

Field description: Superior temporal hemifield defects OU, with inferior arcuate defect and nasal step OS.

Localization: Optic chiasm and left intracranial optic nerve.

Pathology: Pituitary macroadenoma complicated by apoplexy.

Confrontation fields showed a mild temporal step defect to red comparison in the upper fields of both eyes.

The superior temporal field depressions OU point to a lesion of the inferior chiasm. The inferior nasal step defect OS, seen in both the I2e and O3e isopters, indicates left optic

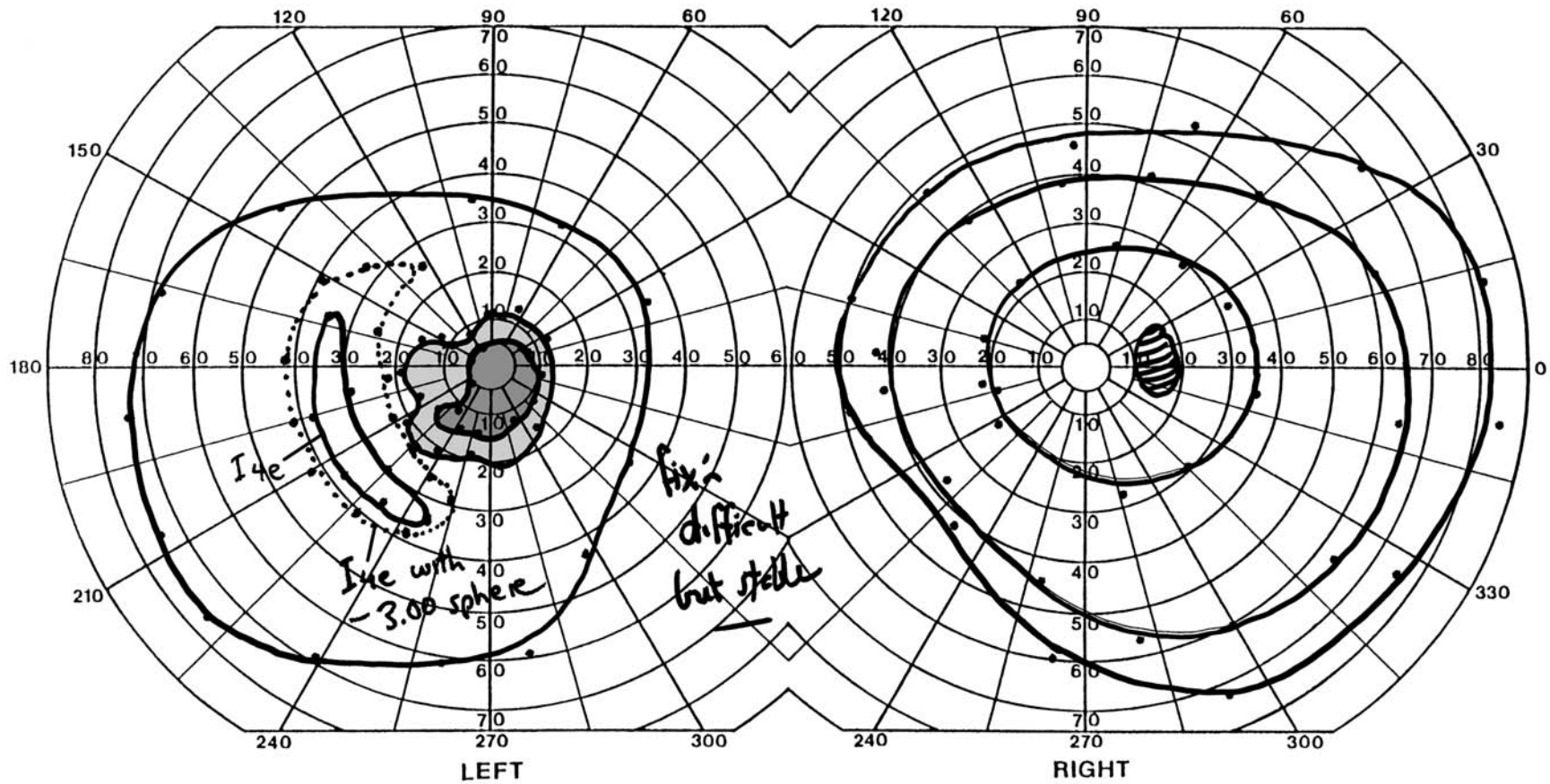
neuropathy. This combination has an inverted resemblance to the right eye of Case 68, in which the compression was from above the chiasm.

The sudden severe headache should have been a red flag for some intracranial bleed, such as a subarachnoid hemorrhage or pituitary apoplexy. Acute hypopituitarism is a medical emergency (108). Fortunately, the patient survived until its belated discovery and responded well to replacement with desmopressin, cortisone, thyroid hormone, and testosterone patch. He had resection of the tumor with no change in his fields over the next 2 years.

HISTORY AND EXAM

This 36-yr-old woman, seen for headache, had long-standing poor vision OS. Previous neurologists had also questioned a left VI nerve palsy because of esotropia with limited

abduction OS. Acuity was 20/20 OD and hand motion at 6' OS. Ishihara color score was 14/14 OD. There was a large RAPD OS and mild limitation of abduction OS.



DISCUSSION

Field description: Large relative cecocentral scotoma, with refractive border.

Localization: Retina.

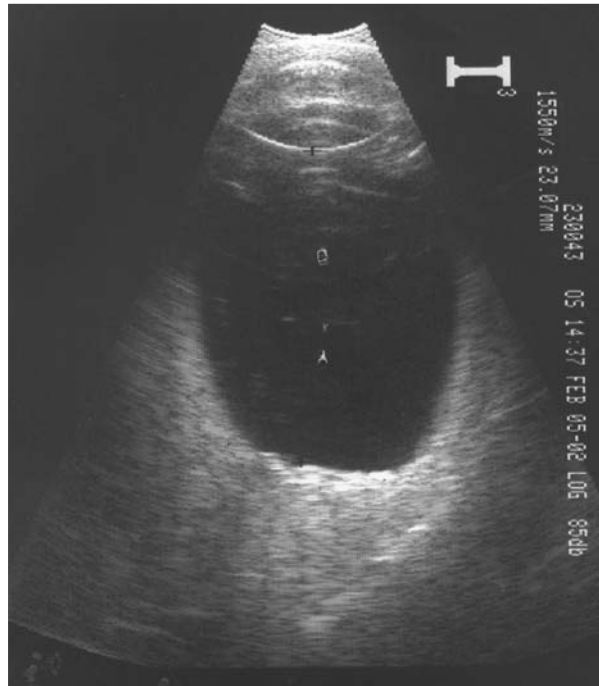
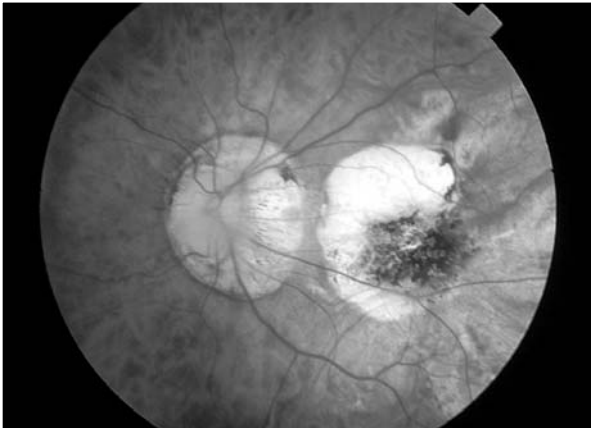
Pathology: Posterior staphyloma.

Confrontation fields showed a large central defect to hand motion OS.

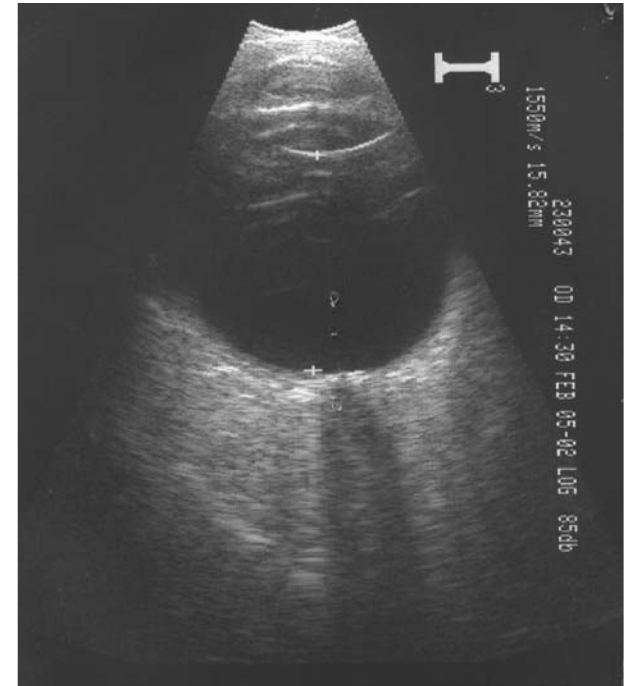
The patient has a depression of the central field, resulting in peak sensitivity being found in a small crescent-shaped hilltop in her temporal field. This crescent enlarges with the addition of a -3.00 spherical lens, indicating that at least part of the defect is refrac-

tive in origin, from retina displaced posterior to the plane of focus.

Funduscopy showed a large staphylomatous defect occupying the macula, with peripapillary atrophy (see Case 6). Orbital ultrasound (shown here) and MRI orbit showed a markedly elongated globe OS with a bulging defect at the pole, consistent with a posterior staphyloma (rather than congenital toxoplasmosis). This finding explains her limited abduction. Rotating a long grape-shaped eyeball within a spherical orbit is mechanically difficult. Limited abduction has been described in previous cases of myopia with similar high-axial globe lengths (183).



Left eye

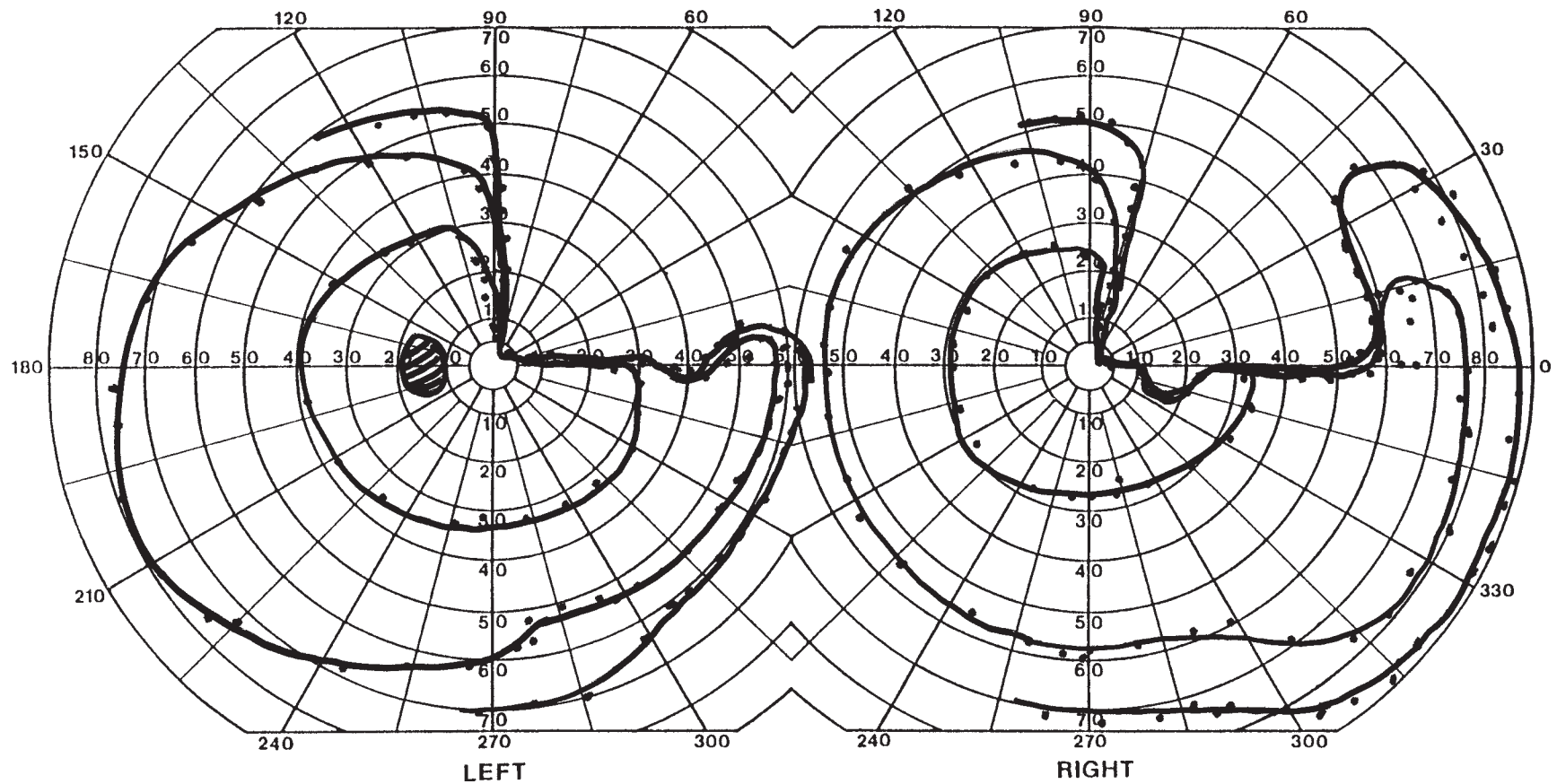


Right eye

HISTORY AND EXAM

This 77-yr-old woman was admitted for a transient ischemic attack, with tingling of the right arm and impaired speech. She reported a stroke about 1 year earlier, presenting with "blurred vision," but was unable to provide more details. Visual acuity was 20/20 OU

and color vision was normal. There was no RAPD and fundi were normal. The remainder of the neurologic examination was normal.



DISCUSSION

Field description: Congruous right homonymous superior quadrantanopia with partial sparing of the temporal crescent.

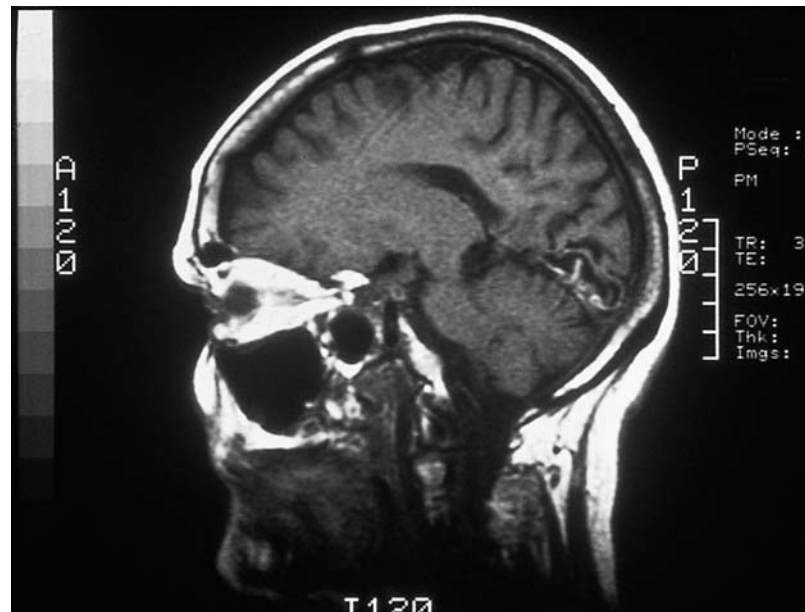
Localization: Left inferior calcarine cortex, sparing retrosplenial portion.

Pathology: Posterior cerebral arterial infarct, posterior temporal branch.

Confrontation fields showed homonymous right superior quadrantanopia to hand motion, with the crescent not detected.

Quadrantanopias that are precisely aligned at the horizontal meridian (167) are less common than those that are not. With superior field loss, such perfect quadrant defects

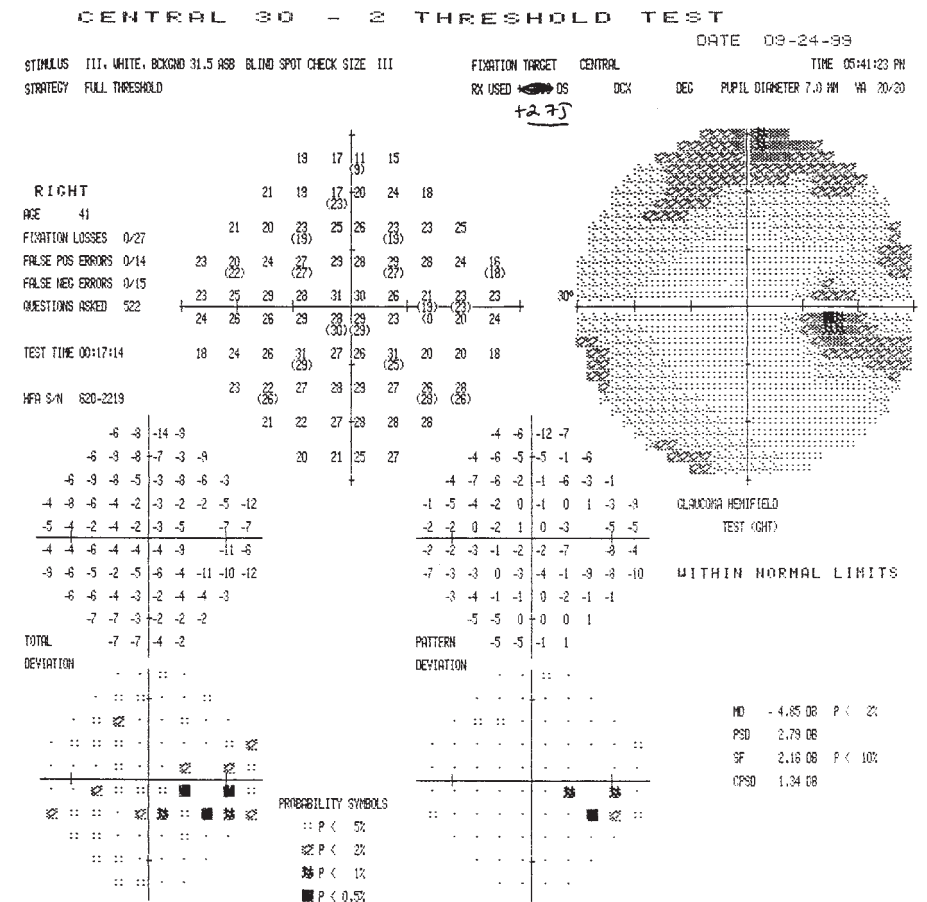
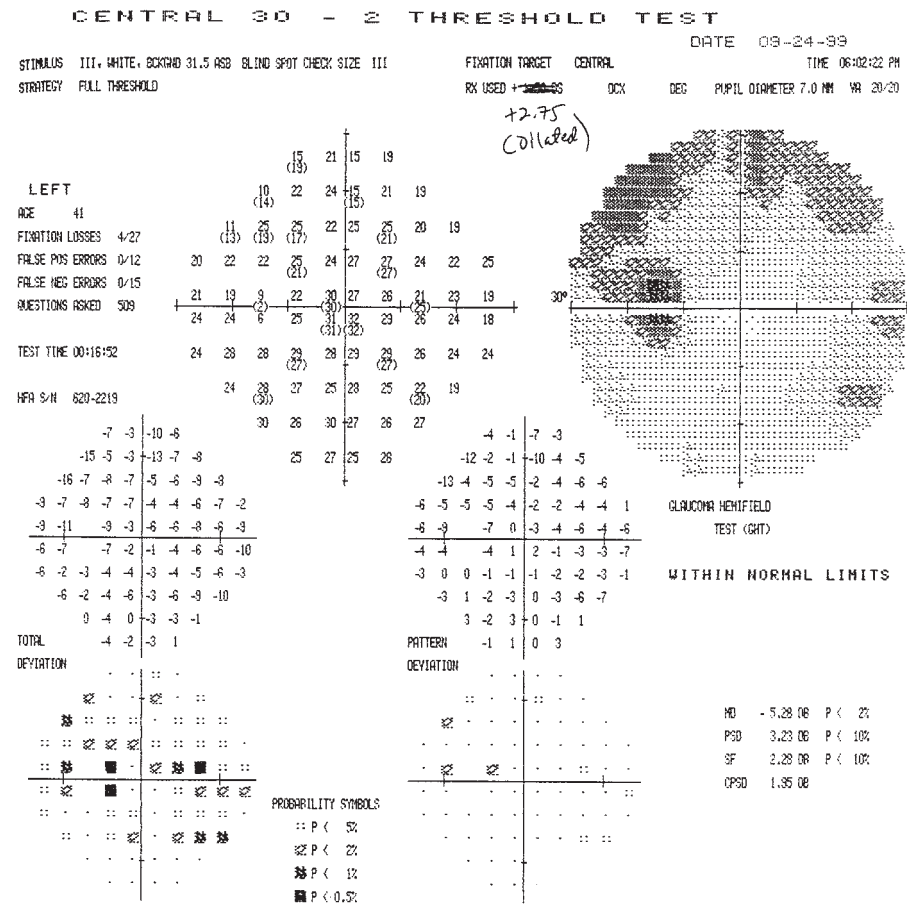
can result from lesions of the temporal optic radiations (Meyer's loop) as well as striate cortex (139). However, in striate cortex there is no distinct separation between the upper and lower fields, which meet in the depths of the sulcus. This has led some to propose that complete quadrantanopia from occipital damage may actually result from damage to V2, the functional zone surrounding striate (V1) cortex, where there is a clear separation between upper and lower fields (184). This hypothesis remains controversial. This patient's stroke is confined to the inferior striate cortex on T1 sagittal MRI.



HISTORY AND EXAM

This 41-yr-old woman had 3 weeks of episodes of visual distortion lasting 30–45 seconds. In the preceding year, she had gained 50 lb, to her current weight of 250 lb (height: 5 ft, 7 in). Visual acuity was 20/20 OU and Ishihara color scores were 14/14 OU. She

had swollen disks with circumpapillary hyperemia, flame-shaped hemorrhages, and retinal folds bilaterally (see arrows, next page).



DISCUSSION

Field description: Bilaterally enlarged blind spots.

Localization: Optic disk.

Pathology: IHH.

Confrontation testing was normal.

Perimetry shows bilateral enlargement of the blind spots, more prominent than in Case 41. This is obscured a bit in the left eye, where there were fixation losses as well as a generalized reduction in sensitivity (compare the total deviation with the pattern deviation). The latter may be due to refractive error, since the patient was tested after mydriasis and with the addition of plus lenses (see the hand-written annotation at the top of the print-out). The pattern deviation in the right eye shows the blind spot enlargement best.

Papilledema is disk swelling secondary to elevated intracranial pressure. This pressure is transmitted down through the CSF space contained within the optic nerve sheath, to the cribriform plate at the optic nerve head, where it retards axoplasmic flow in the optic nerve. The earliest signs are circumpapillary hyperemia and obscuration of the vessels crossing the disk surface. The disk enlarges most in its periphery, sparing the central cup and resembling a doughnut, whereas pseudopapilledema causes central protrusion, like a champagne cork or umbilicus, without the other signs (79,185).

Enlargement of the blind spot with papilledema is not due to nerve fiber loss, but to elevation of the retina surrounding the optic disk. Light in this retinal zone is therefore poorly focused, reducing sensitivity. This can be proven by repeating perimetry with a plus correction, which will reduce the size of the enlarged blind spot (84) (see case 46).

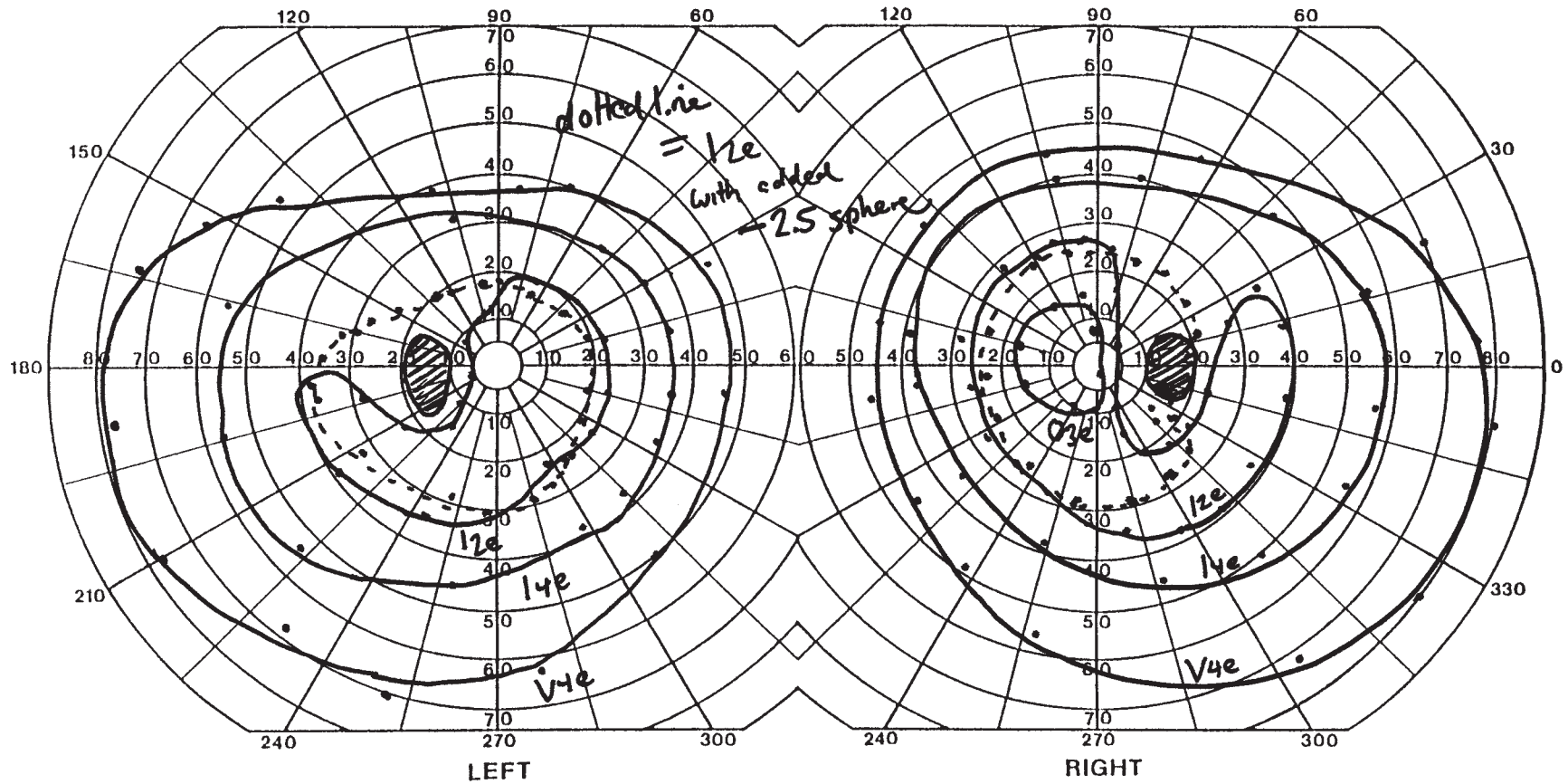


See Color Plate after page 180

HISTORY AND EXAM

This 47-yr-old man was seen for new migraines with visual aura and was incidentally found to have a field defect OU. Visual acuity was 20/25 OD and 20/20 OS with normal color vision. There was no RAPD. He was a high myope, with a refraction of -22.25

sphere, $-1.50 \times 60^\circ$ cylinder OD and -21.50 sphere, $-1.75 \times 100^\circ$ cylinder OS (the cylinder measures indicate a degree of astigmatism). The remainder of the neurologic examination was normal.



DISCUSSION

Field description: Relative defects in the upper temporal fields bilaterally, without respect for the vertical or horizontal meridians, reducible with minus lenses.

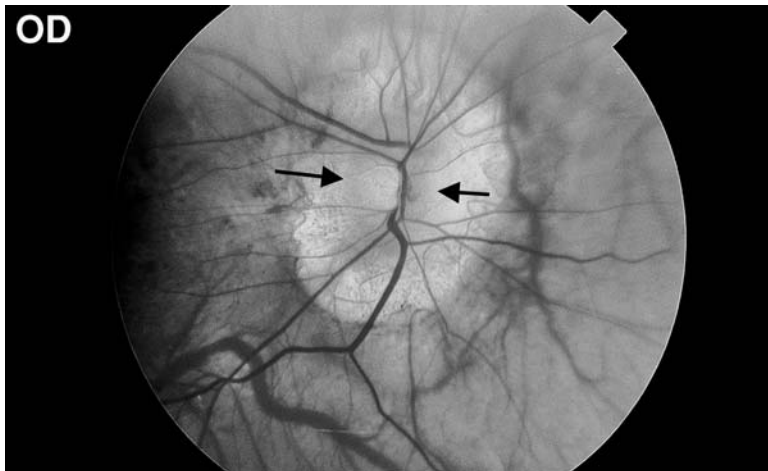
Localization: Globe.

Pathology: Nasal fundus ectasia.

Confrontation testing showed decreased red and hand comparison in lower temporal quadrant OD.

The patient has superotemporal field defects that do not show a sharp demarcation at the vertical meridian. In addition, repeating the I2e isopter with a -2.5 diopter spherical lens eliminates the temporal defects. Dilated funduscopy showed small optic discs (between arrows) and pale, hypopigmented nasal fundi OU.

Nasal fundus ectasia is associated with myopia in 90% and astigmatism of more than one diopter in 70% of cases (17). Pallor is typical of the ectatic region, occurring in 90%. The ectasia is a posterior bulge that lies four to eight diopters more posterior than the rest of the retina, creating a relative temporal depression in the visual field that can be refracted away with a negative-diopter lens. This case is quite similar to Riise's Case 23 (17). Although generally benign, nasal fundus ectasia can be complicated by retinal detachment, likely related to the high myopia. The other complication, before the advent of CT and MRI, was unnecessary neurosurgical exploration of the sella region.

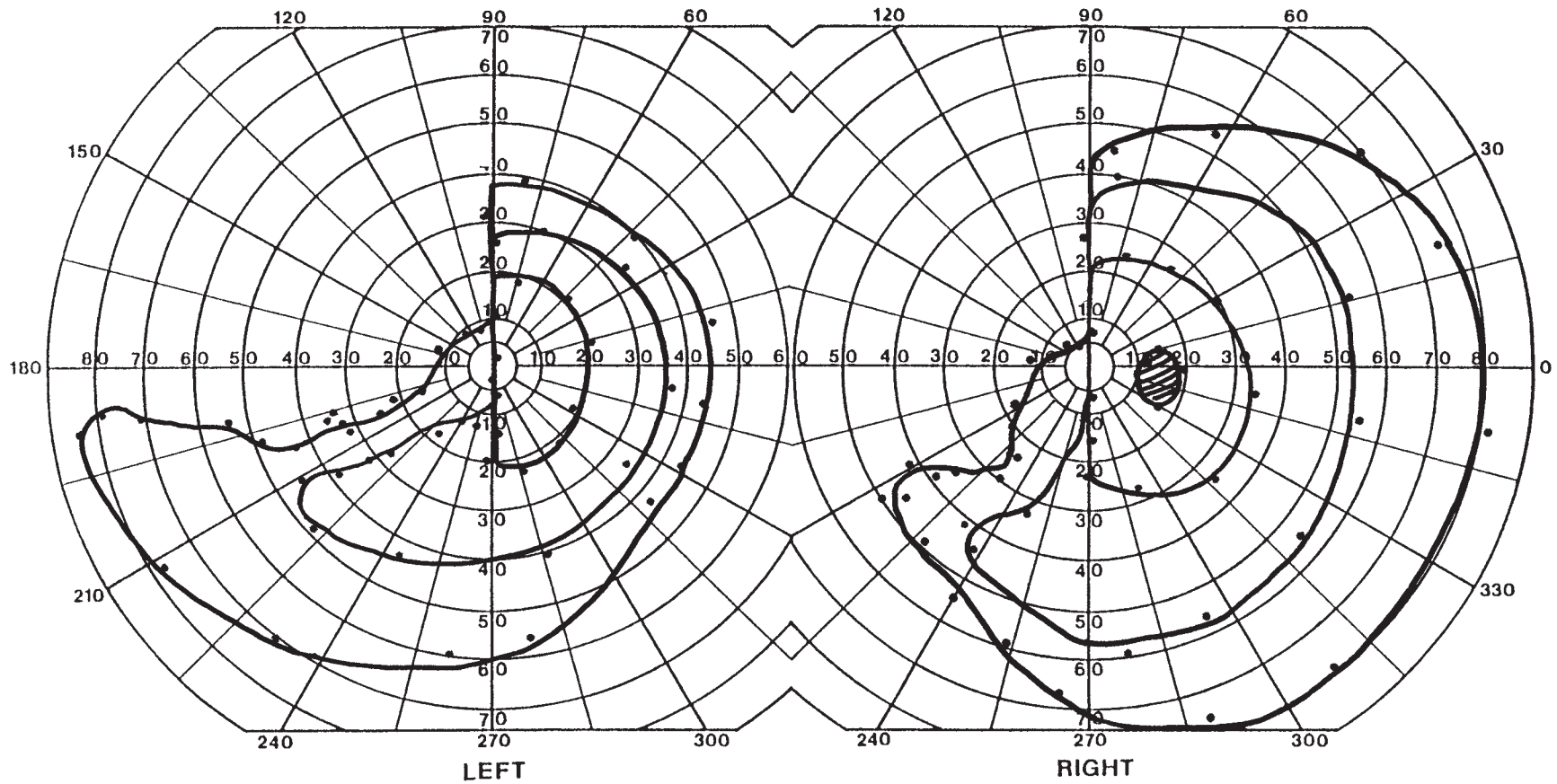


See Color Plate after page 180

HISTORY AND EXAM

This 79-yr-old woman presented with sudden numbness of the left thumb and adjacent two fingers, lasting 30 minutes. A transient ischemic attack was diagnosed, and she was anticoagulated with heparin and coumadin. A few days later she developed headache,

nausea, and vomiting, with numbness of the left hand and face. Examination showed decreased sensation in the left hand. INR was 4.7.



DISCUSSION

Field description: Mildly incongruous left superior quadrantanopia plus.

Localization: Right temporal optic radiation, in medial occipitotemporal cortex.

Pathology: Cerebral hemorrhage, secondary to excessive anticoagulation.

Confrontation testing showed decreased finger counting in the same region.

CT scan demonstrated an intracerebral hemorrhage involving the medial occipitotemporal cortex. This may involve the most anterior portions of the striate cortex, but it is

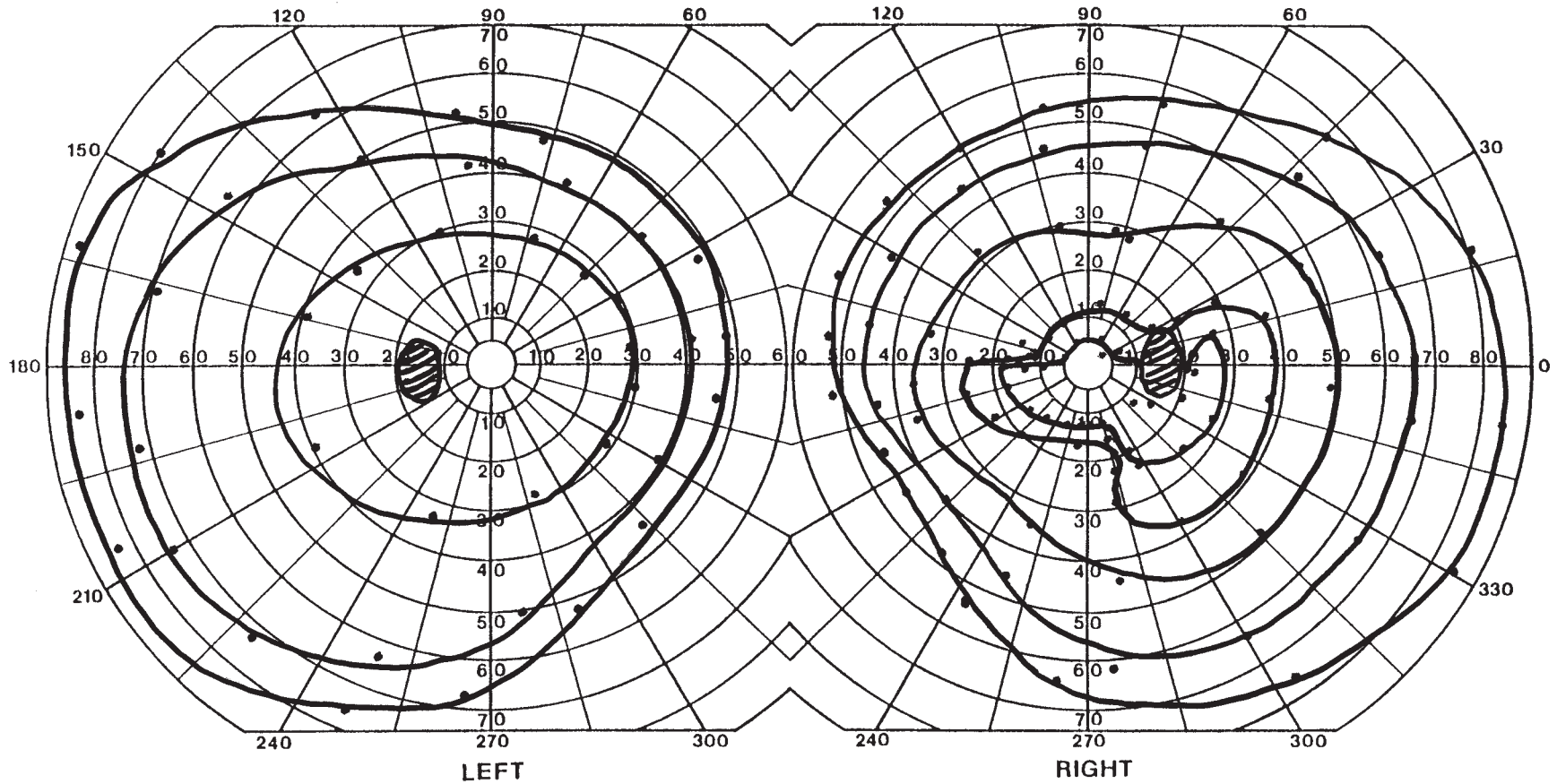
clear that the posterior regions and the occipital pole are spared, even though the field defect extends into the macular region. Thus, the most relevant aspect of the patient's lesion to her visual fields must be the extensive damage to occipitotemporal white matter, affecting the optic radiations in their course to the striate cortex.



HISTORY AND EXAM

Unilateral papilledema was found incidentally in this 48-yr-old woman 8 years earlier. Visual acuity and fields were normal at that time and at successive visits every 6–12 months. Routine check-up 2 weeks prior to evaluation found a slight reduction in visual acuity of 20/25 OD compared with 20/15 OS. Ishihara color scores were 13/14 OU. There

was an RAPD OD. Fundoscopy confirmed the papilledema OD, but the disk was normal OS. There was also mild 3-mm proptosis OD. The remainder of the examination was normal.



DISCUSSION

Field description: Superior and inferior arcuate defects OD, more severe superiorly.

Localization: Optic nerve.

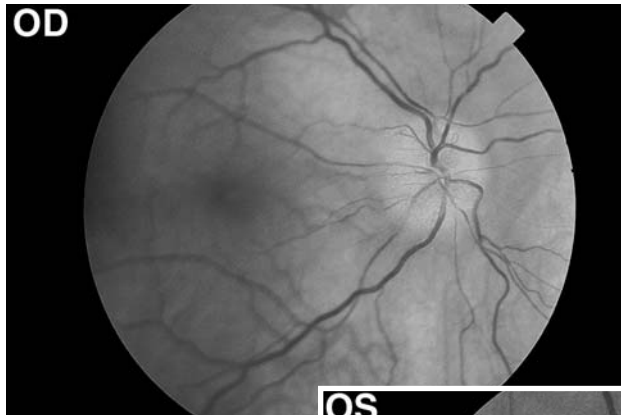
Pathology: Intraorbital cavernous hemangioma compressing optic nerve.

Confrontation fields were normal.

The patient has a prominent superior arcuate defect with a nasal step. Inferiorly there is a depression that points toward the blind spot, indicating a milder arcuate defect there also. Axial T1-weighted orbital MRI showed a soft-tissue mass in the right orbit, with marked speckled gadolinium enhancement on the fat-saturated image, and lateral displacement of the optic nerve (this aspect not shown). These findings are consistent with

an orbital cavernous hemangioma, which was confirmed on resection a month later. Over the ensuing months, her visual acuity remained 20/20 OU and her visual field defects resolved.

Cavernous hemangiomas of the orbit are benign vascular growths. They may remain asymptomatic or present with slowly progressive proptosis and/or visual loss due to compression of the optic nerve. Those with asymptomatic cavernous hemangiomas, discovered incidentally during neuroimaging, can be safely followed without surgery (186). Surgery should be considered once there is visual compromise but should be undertaken with caution, given that preexisting visual deficits may worsen following apparently uncomplicated surgical excision (102,187).



See Color Plate
after page 180



without gadolinium

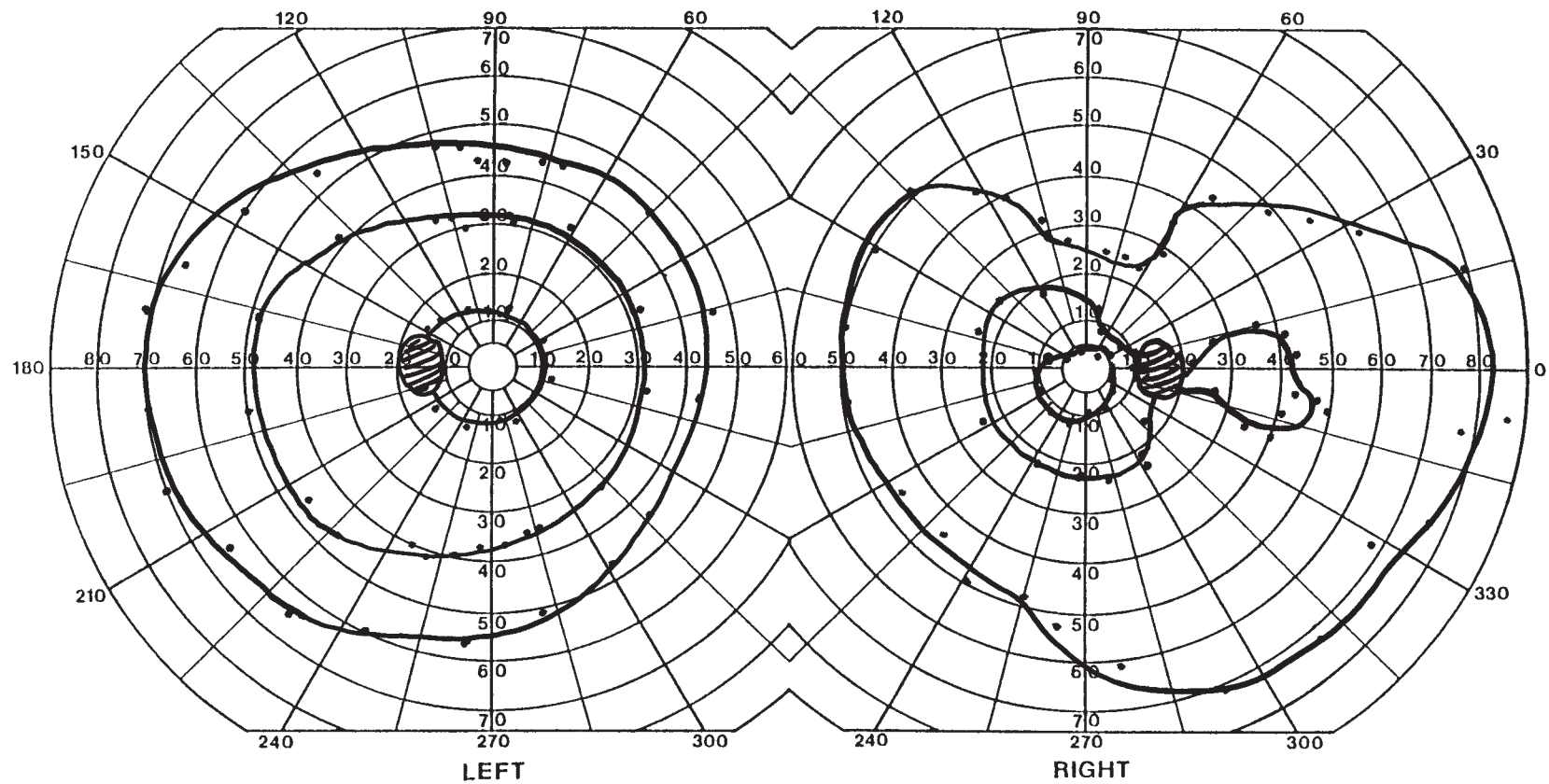


with gadolinium

HISTORY AND EXAM

This 47-yr-old woman had presented with 4 months of increasing blurry vision in the right eye. Approximately 6 months prior she had resection of a right sphenoid wing meningioma that presented with headaches. Visual acuity at far was 20/30 OD and 20/25

OS. Ishihara color plates were 10.5/14 OD and 12/14 OS. There was an RAPD OD. Fundoscopy showed mild temporal optic disk pallor OD. She had mild limitation of elevation and adduction OD.



DISCUSSION

Field description: Right superior and inferior temporal wedge defects.

Localization: Right intracranial optic nerve.

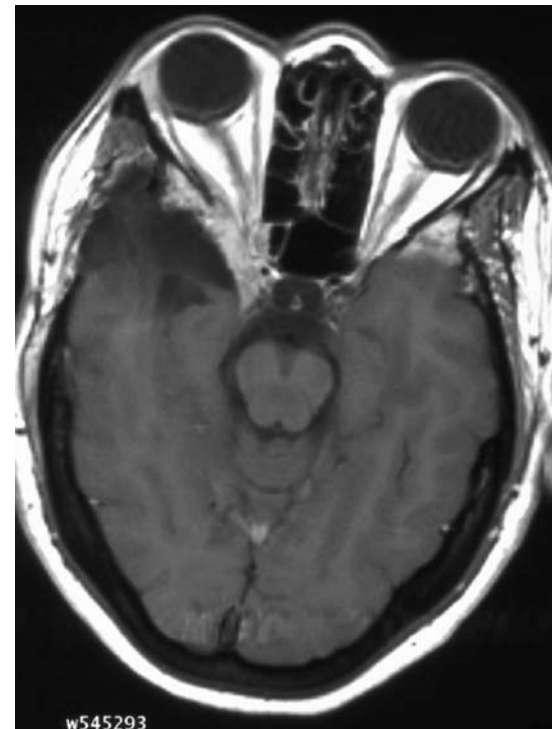
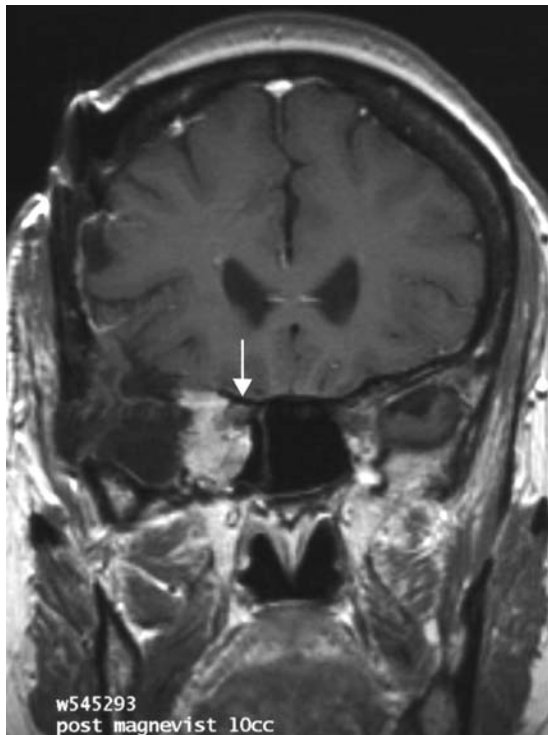
Pathology: Compression by residual sphenoid wing meningioma.

Confrontational field testing showed hesitancy to finger count in the inferotemporal paracentral region OD, but colored stimuli and hand appearance were normal.

The wedge defects pointing at the blind spot indicate loss of superior and inferior wedges of nerve fiber layer. The combination of a compressive optic neuropathy and a partial III nerve palsy points to a lesion at the superior orbital fissure or cavernous sinus. Enhanced T1-weighted coronal and axial MRI showed a mass at the cavernous sinus

tracking along the lateral wall of the orbit, and encasing the right optic nerve (arrow).

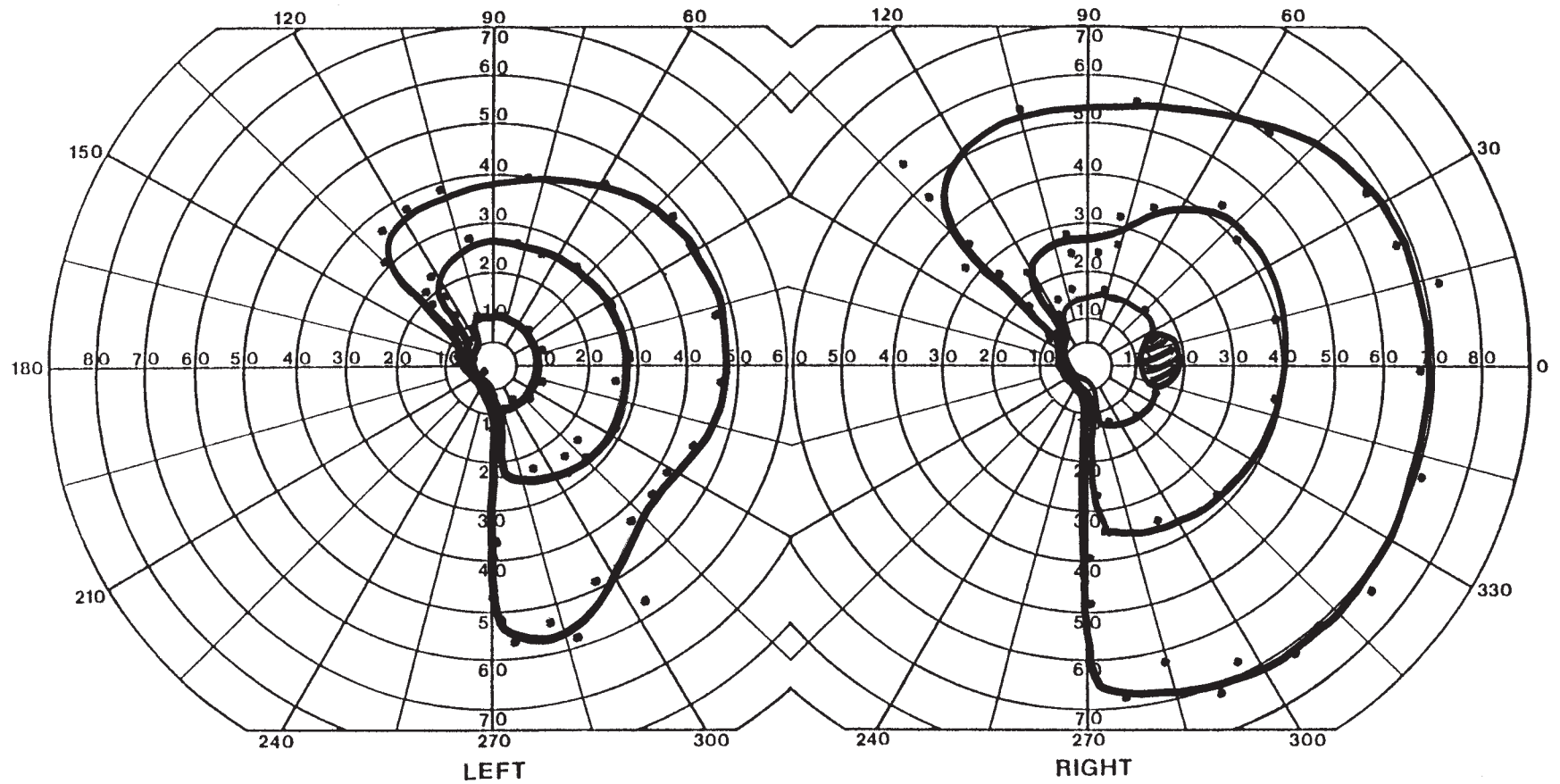
Medial sphenoid wing meningiomas disturb vision by compressing the intracranial optic nerve or chiasm. They arise from a number of structures, including the anterior clinoid process, medial sphenoid ridge, tuberculum sellae, and diaphragma sellae. They can extend into the cavernous sinus or the superior orbital fissure, causing cranial nerve palsies and/or Horner's syndrome. Tumors from the diaphragma sellae and medial sphenoid ridge are least often completely removed and most commonly associated with post-operative visual deterioration (188). Worsening may be due to slow progression or malignant transformation of the meningioma. The latter is a rare event, occurring in 1.7% of cases (189).



HISTORY AND EXAM

This 68-yr-old woman with diabetes, congestive heart failure, and moderate left carotid stenosis had a right occipital stroke that left her with a left hemifield defect 3 years previously. Three days prior to evaluation, she noted a grayness in the far periphery of her

right lower field, which gradually improved over the next few days. Visual acuity was 20/25 OU and there was no RAPD. Optic disks were normal, as was the rest of the neurologic examination.



DISCUSSION

Field description: Congruous left inferior quadrantanopia plus, macula sparing.

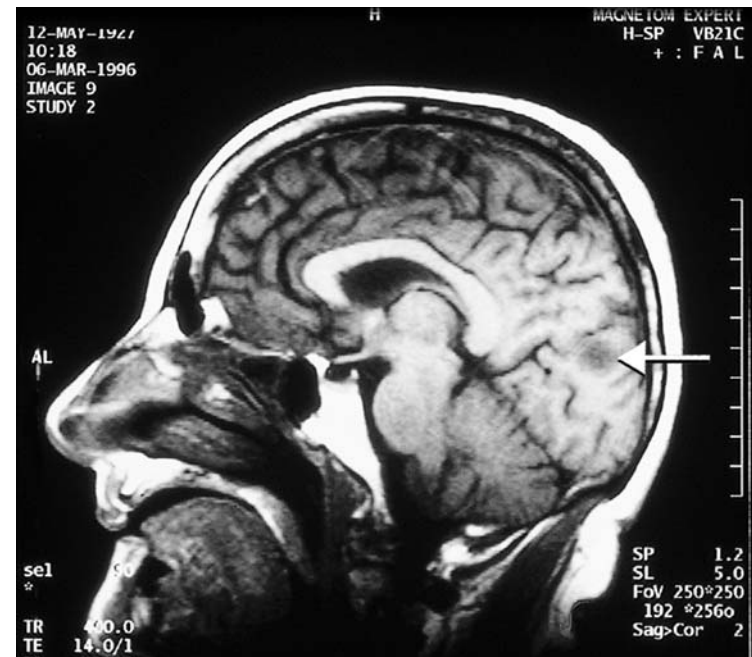
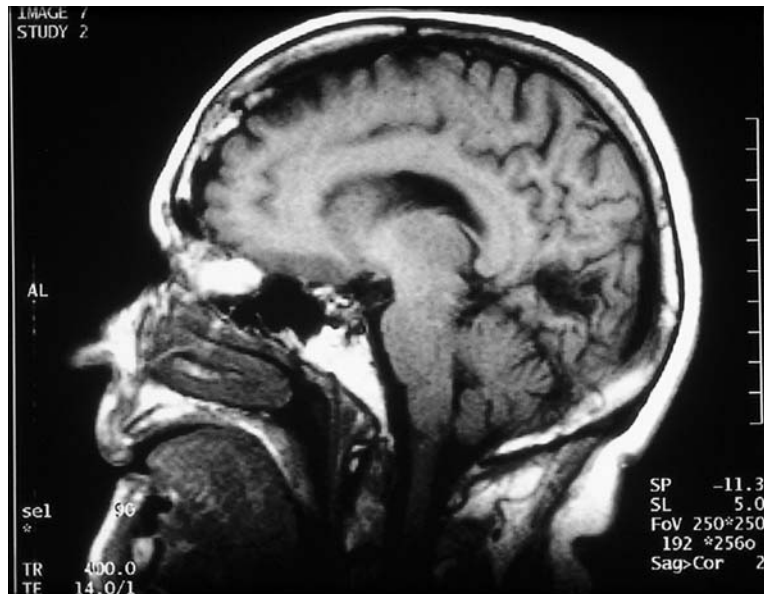
Localization: Right striate cortex, superior bank of calcarine sulcus, sparing occipital pole.

Pathology: Posterior cerebral arterial infarct, parieto-occipital branch.

Confrontation field showed left inferior quadrantanopia extending into the superior field to hand motion.

T1-weighted sagittal MRI showed the old right striate infarct (left image), causing the patient's field defect. There was also a new left medial parieto-occipital infarct (arrow,

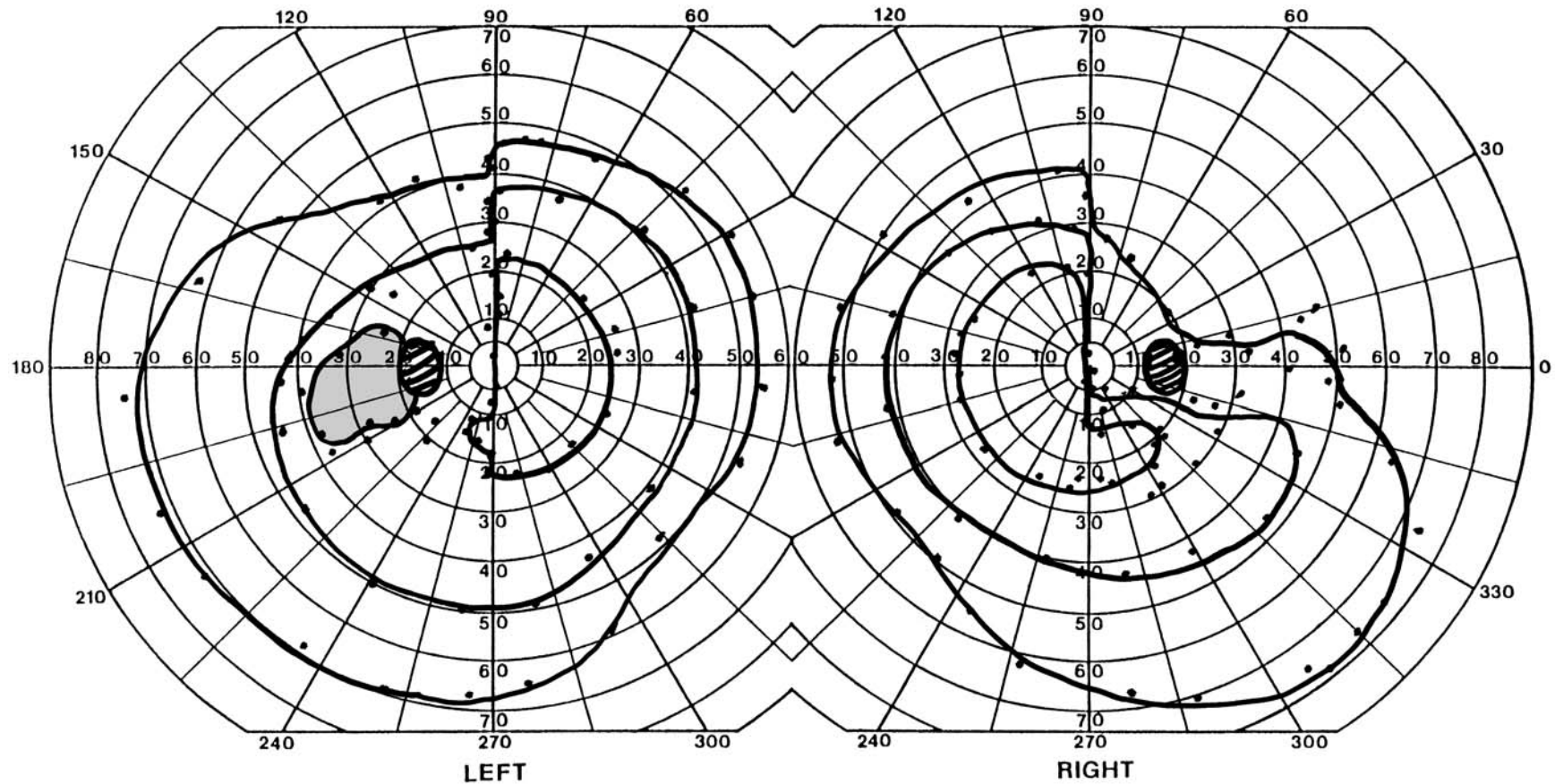
right image) just above the anterior extent of the striate cortex. There is no current field defect corresponding to this new lesion. The transient field defect she had noticed may have been due to edema or compression surrounding the infarct, which may have had secondary effects on the adjacent striate cortex. This lesion, which probably affects human homologues of areas V2 and V3, does not cause a field defect on conventional perimetry. It is possible that other specific visual functions such as perception of motion or illusory contours may be affected contralaterally by this lesion. The old and the new lesions in this patient nicely illustrate the difference between striate and extrastriate lesions in relation to perimetry.



HISTORY AND EXAM

Over the week prior to his visit, this 52-yr-old man with mild hypertension noted that the midportion of license plates in front of him would disappear transiently. He then became aware that car bumpers would intermittently develop a vertical discontinuity or step. He had some blurry vision in both eyes, more to the temporal sides. He recalled

bifrontal headaches present for a few months. Visual acuity was 20/30 OD and 20/20 OS. Ishihara plates were 10/14 OU, and he missed the temporal digits of the plates with two-digit numbers. There was no RAPD. Optic disks showed mild temporal pallor OU. The remainder of the neurologic examination was normal.



DISCUSSION

Field description: Bitemporal superior and central hemifield defects.

Localization: Optic chiasm, inferior aspect.

Pathology: Pituitary adenoma.

Other features: Hemifield slide.

Confrontation testing showed blurred images in the upper and lower temporal fields OU.

Every isopter tested shows a sharp demarcation at the vertical midline, with normal nasal hemifields. The vertical steps are predominantly in the superior fields, consistent

with compression of the inferior optic chiasm. Enhanced sagittal T1-weighted MRI demonstrated a homogeneously enhancing mass arising from the sella and compressing the optic chiasm from below. This proved to be a nonsecreting pituitary adenoma on resection 3 weeks later.

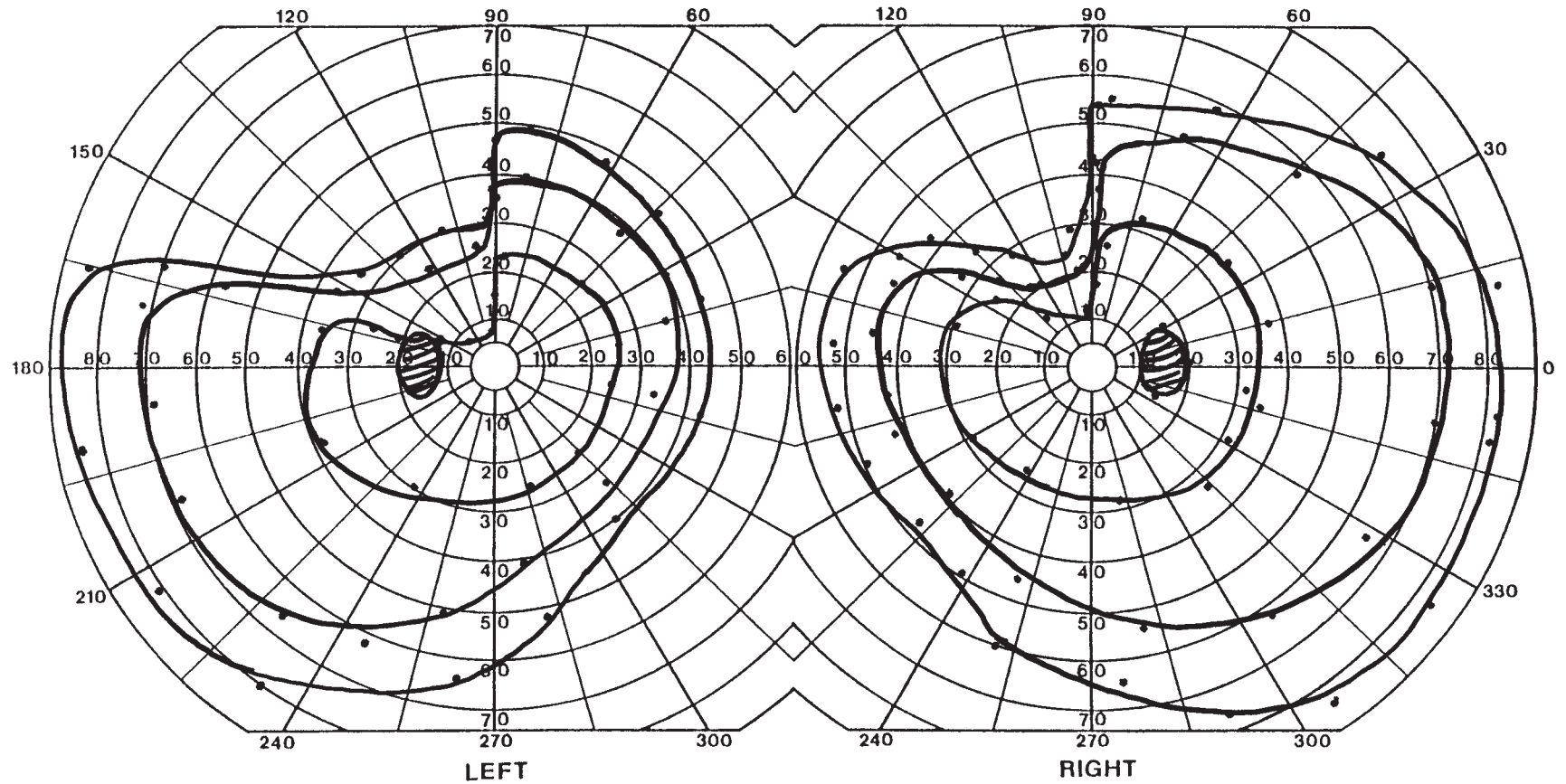
The patient's hemifield slide resembles that of Case 57. Unlike that patient, his defect was not a complete bitemporal hemianopia, which is the defect typically associated with hemifield slide. This case shows that even partial loss of temporal fields can weaken the fusional registration of one eye's field with the other.



HISTORY AND EXAM

This 40-yr-old woman with a 6-year history of seizures was found to have a right temporal lobe lesion. The lesion was resected with histology demonstrating a dysembryoplastic neuroepithelial tumor. Seizure control was improved following surgery. Visual

acuity and color vision were normal. There was no RAPD and funduscopy showed normal optic disks. The visual fields are shown.



DISCUSSION

Field description: Incongruous left homonymous superior quadrantanopia.

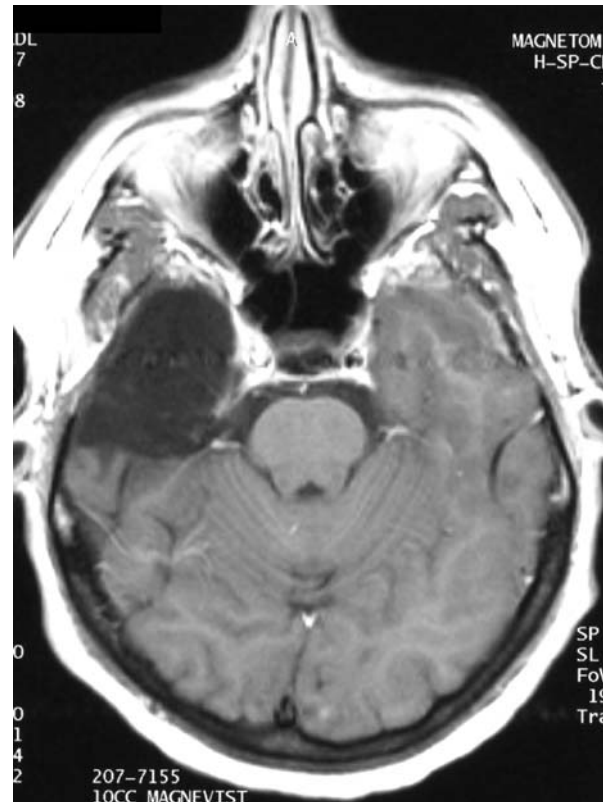
Localization: Right anterior temporal optic radiations.

Pathology: Resected dysembryoplastic neuroepithelial tumor.

Confrontation testing showed very incongruous left superior quadrantanopia to hand motion, worse OD.

In general, the resections involved in temporal lobectomies begin at the anterior pole and extend a variable degree posteriorly. The retinotopy in Meyer's loop is such that the

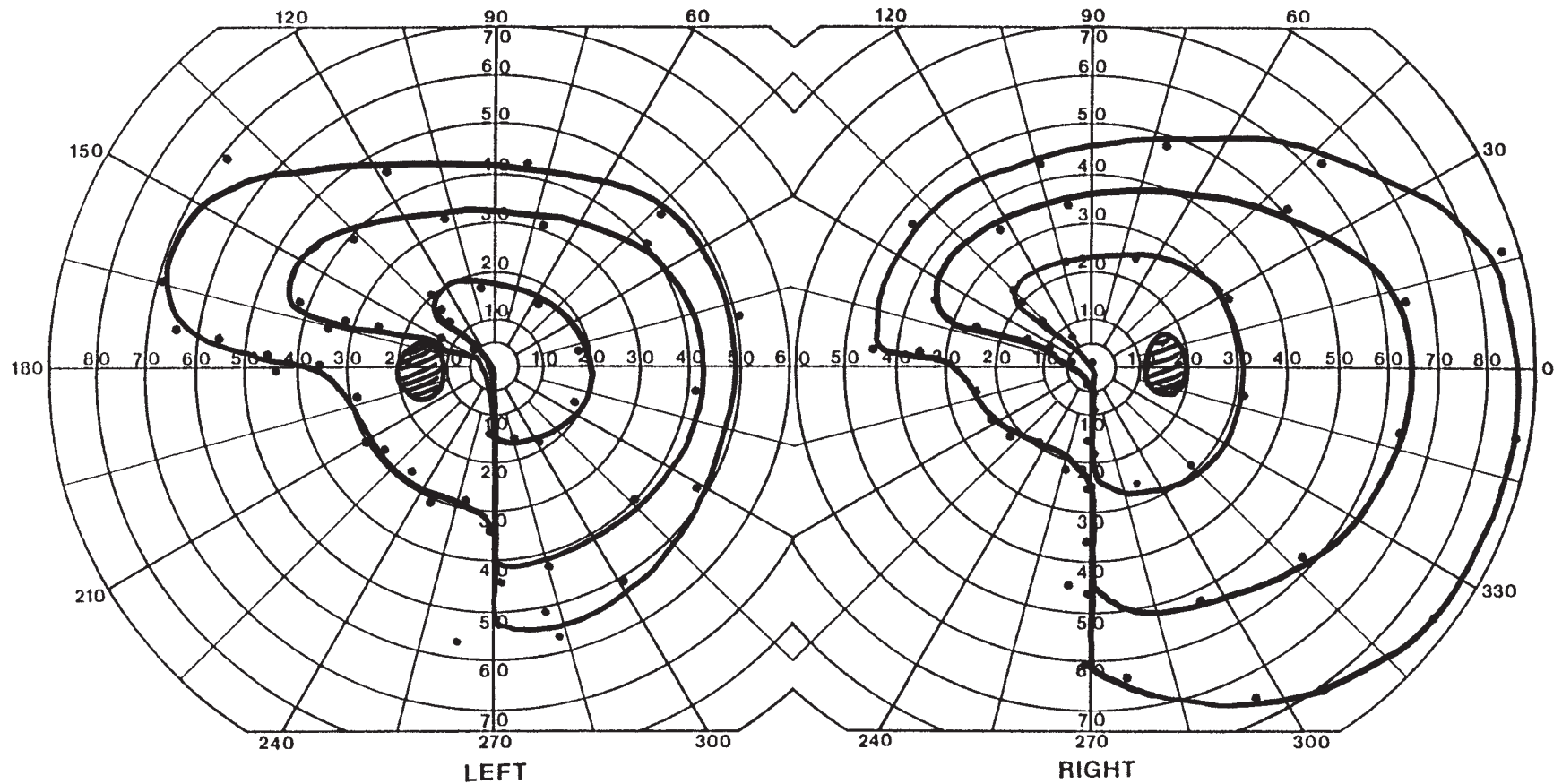
fibers representing the vertical meridian are most anterior, and those near the horizontal meridian most posterior (where they eventually merge with the parietal radiations). The consequence of these two facts is that the field defects associated with lobectomy always begin at the vertical meridian and extend a variable degree toward the horizontal meridian, likely depending on the extent of resection. In this patient's case, the resection of 4.2 cm is consistent with some sparing of field near the horizontal meridian.



HISTORY AND EXAM

This 68-yr-old woman had a known glioblastoma multiforme diagnosed 1 year earlier and treated with surgery and radiation. In the week prior to evaluation, she had unusual morning headaches and then a single, generalized tonic-clonic seizure. Her family also reported that she was getting lost on routes around her home. Visual acuity was 20/20 OU,

Ishihara color scores were 13/14 OU, and there was no RAPD. Neurologic examination in the emergency room showed a visual field defect as well as left hemineglect, extinction of left-sided stimuli when touched simultaneously on both sides of her body, and a dressing apraxia.



DISCUSSION

Field description: Mildly incongruous homonymous left inferior quadrantanopia involving the macula.

Localization: Right parietal lobe.

Pathology: GBM.

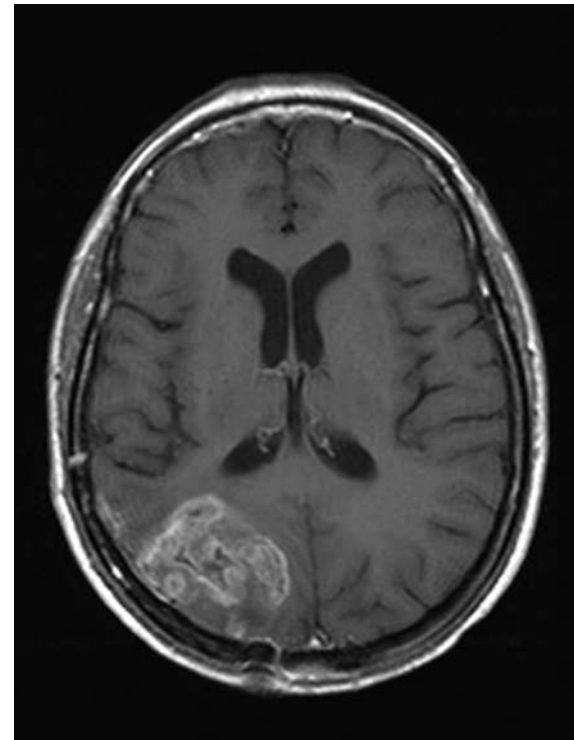
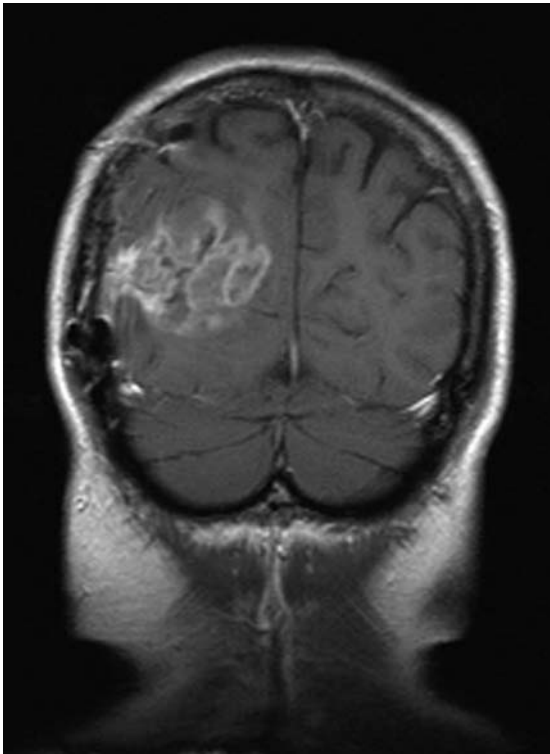
Other features: left hemineglect, topographagnosia, dressing apraxia.

Confrontation testing showed a relative left inferior quadrantic defect, with slower responses to targets here and extinction of stimuli in this quadrant when counting fingers.

The incongruity is seen mainly in the largest (V4e) isopter inferiorly, where it extends to 30° OS but only to 20° OD. The slight incongruity suggests that the pathology is more likely in the optic radiations than in the striate cortex, and involvement of the inferior

quadrant implies dysfunction of parietal rather than temporal optic radiations. The hemineglect, dressing apraxia, and topographagnosia all indicate dysfunction of the right parietal lobe. Axial and coronal gadolinium-enhanced T1-weighted MRI (shown) demonstrated a complex and irregularly enhancing space-occupying lesion involving the parietal optic radiation, and also extending toward the superior striate cortex.

Patients with topographagnosia get lost in familiar environments (190). There are two forms. In one, associated with lesions of the medial occipitotemporal cortex, patients cannot identify familiar landmarks, a problem that is often part of a broader visual agnosia, including prosopagnosia. In the other, associated with right parietal dysfunction, topographagnosia is a function of impaired spatial processing and patients are unable to describe, follow, or memorize a route.

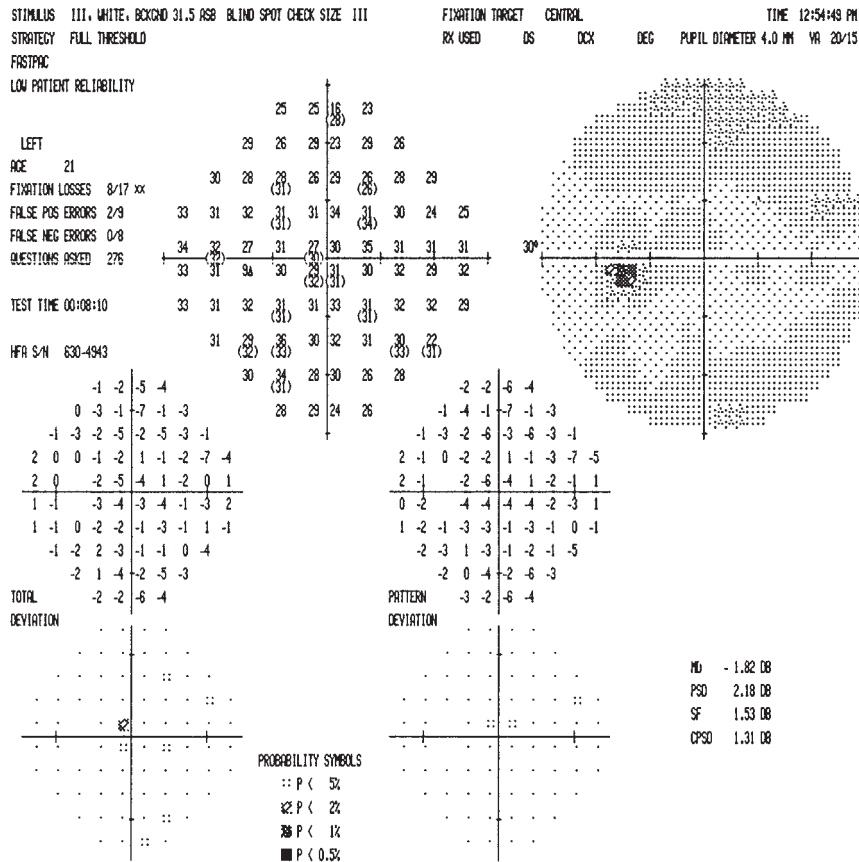


HISTORY AND EXAM

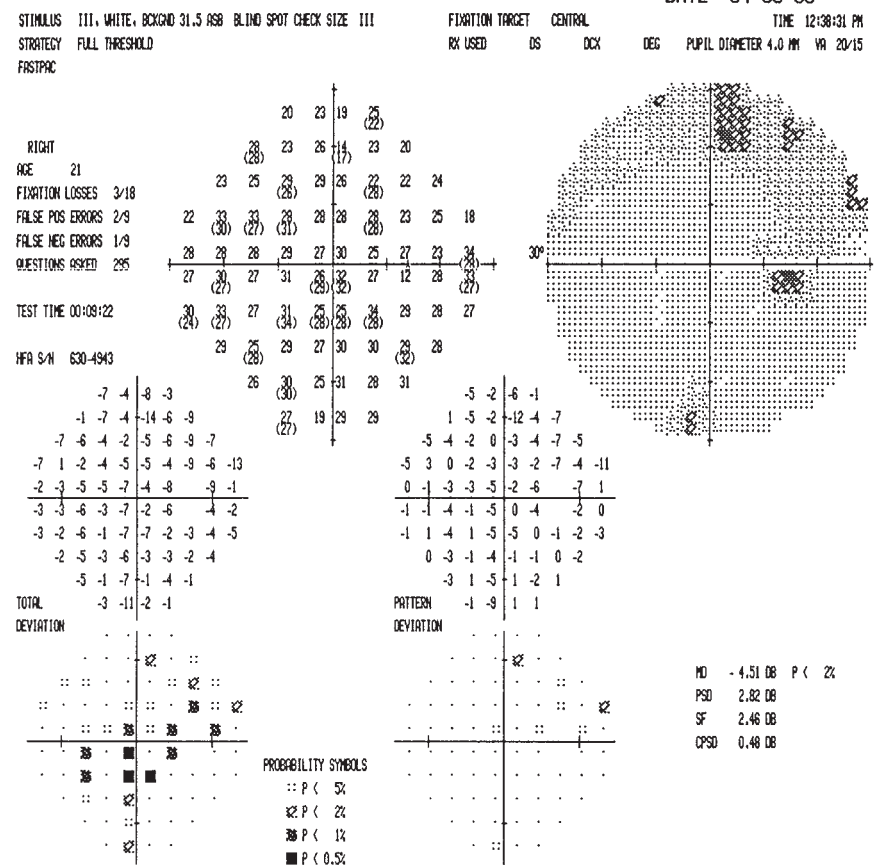
This 20-yr-old man had horizontal diplopia in left gaze, left facial weakness, and left arm ataxia. MRI showed multiple periventricular white matter lesions, consistent with MS. He was treated with iv methylprednisolone. Two weeks later he noted darker vision

in the right eye, with blurring and decreased color vision worsening over the next 2 days. Visual acuity was 20/10 OD and 20/15 OS. Ishihara color plates were 13/14 OD and 12/14 OS. There was no RAPD.

CENTRAL 30 - 2 THRESHOLD TEST



CENTRAL 30 - 2 THRESHOLD TEST



DISCUSSION

Field description: Mild relative cecocentral depression OD.

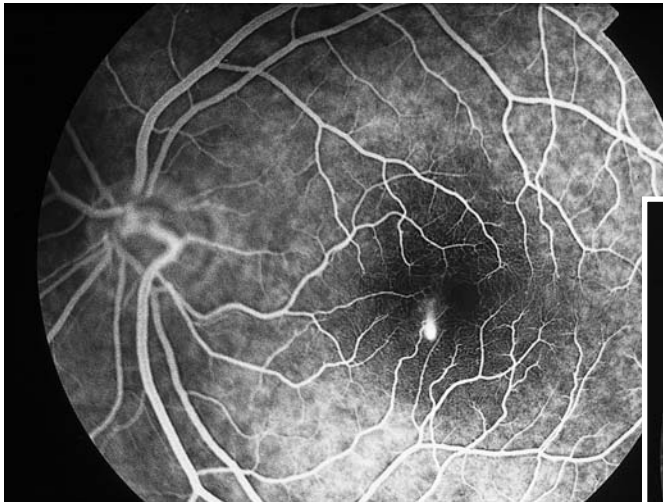
Localization: Macula.

Pathology: Central serous retinopathy.

Confrontation testing was full OU.

In view of the recent diagnosis of MS, the patient was thought to have optic neuritis even though there was no definitive evidence of an optic neuropathy. The differential diagnosis, however, included a central serous retinopathy, and therefore he underwent a fluorescein angiogram, which confirmed the diagnosis.

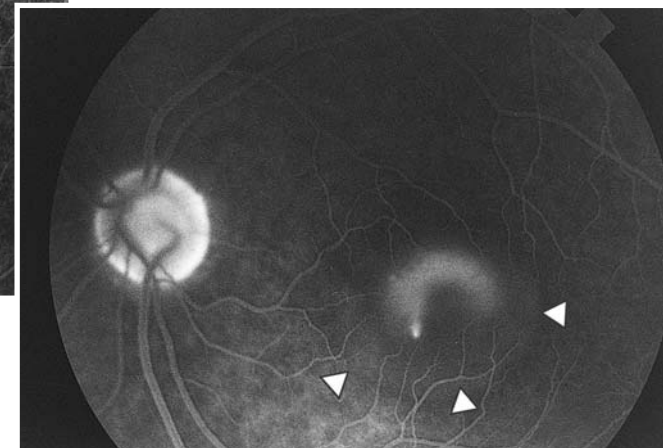
Central serous retinopathy (or choroidopathy) is an idiopathic disorder characterized by the accumulation of serous fluid between the sensory retina and the retinal pigment epithelium. The serous fluid originates from a breakdown of the blood-retina barrier because of inflammation of the choroidal capillaries. The effect is a focal retinal detachment at the macula. Clinically, central serous retinopathy manifests with mildly reduced visual acuity (blurred vision), micropsia, and metamorphopsia (5). It is a disorder that typically affects young men. Spontaneous recovery is the norm. Fluorescein angiography, as shown in this example from another patient (courtesy of Tim Murtha), shows early a minute area of hyperfluorescence at the level of the retinal pigment epithelium where dye begins to leak into the subretinal space (between the sensory retina and the retinal pigment epithelium), eventually delineating the area of detachment in the 'late' image.



early



mid

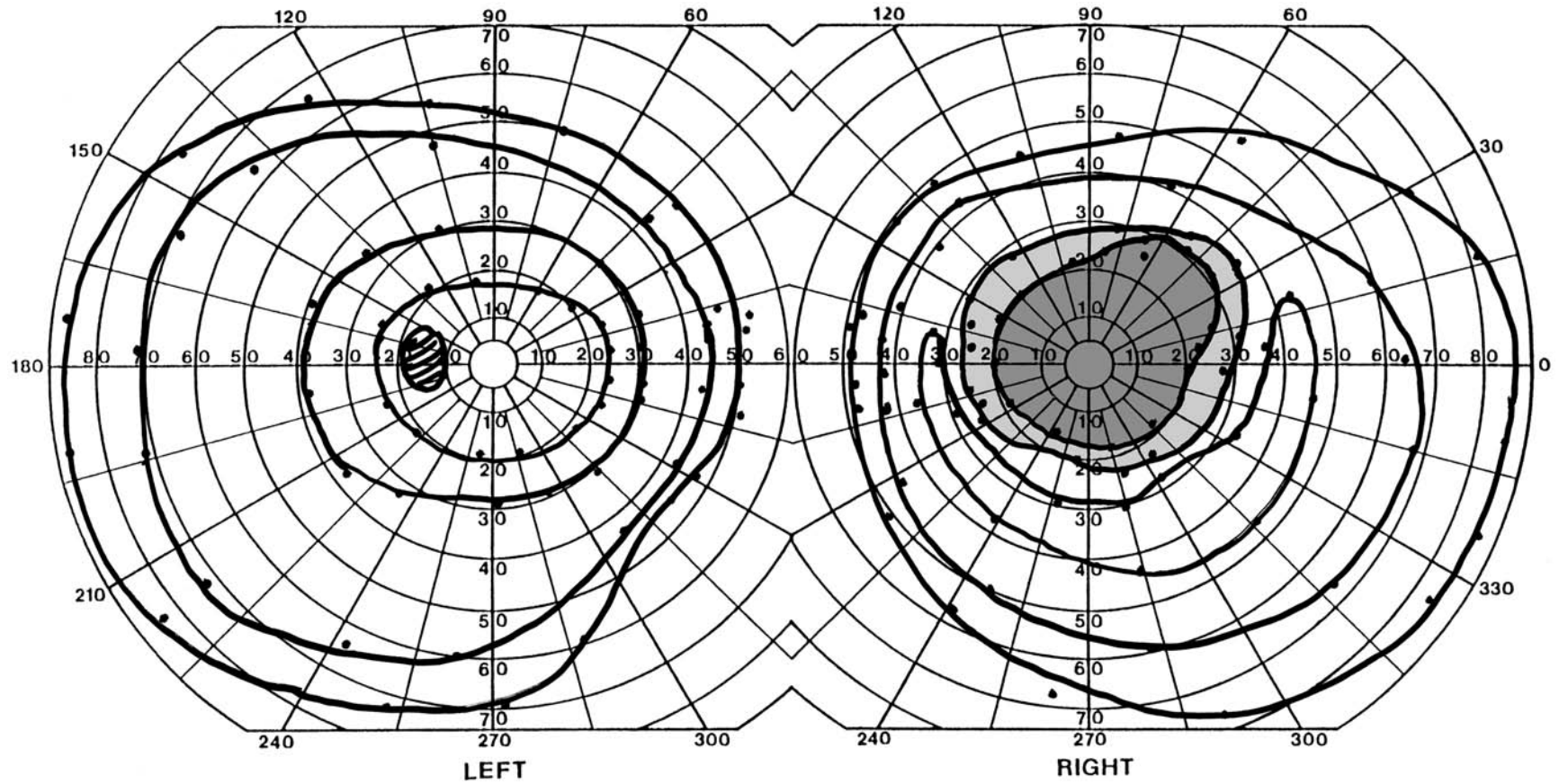


late

HISTORY AND EXAM

While driving to work one morning, this 35-yr-old woman became aware of a brown rectangle just temporal to fixation in the right eye. This central hole became darker and larger over the following week. She also reported that 6 weeks earlier, for a few days,

objects pressed against the back of her thigh felt hot, after which she had a persistent coldness and numbness over the front of the left thigh. Visual acuity was count fingers OD and 20/15 OS. There was a large RAPD OD. Optic disks were normal.



DISCUSSION

Field description: Large cecocentral scotoma OD.

Localization: Optic nerve.

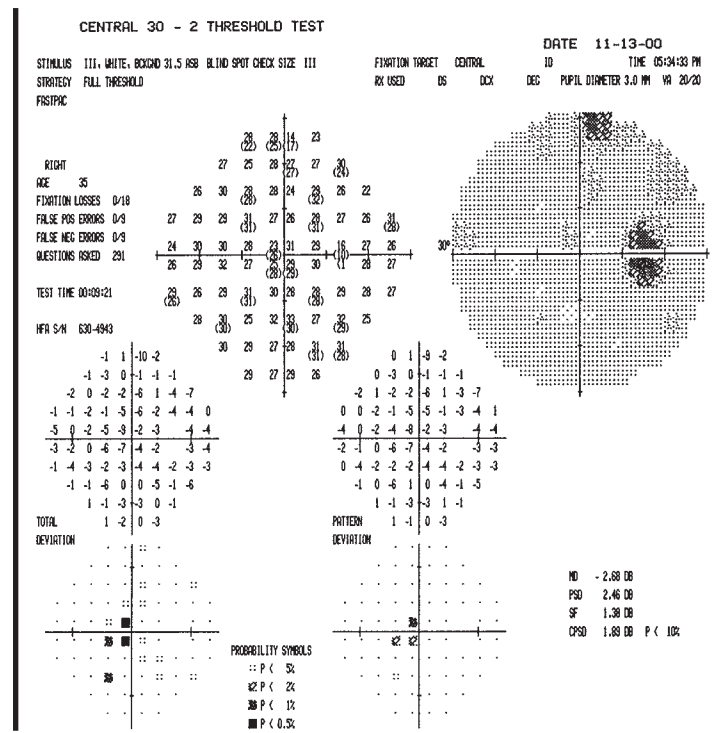
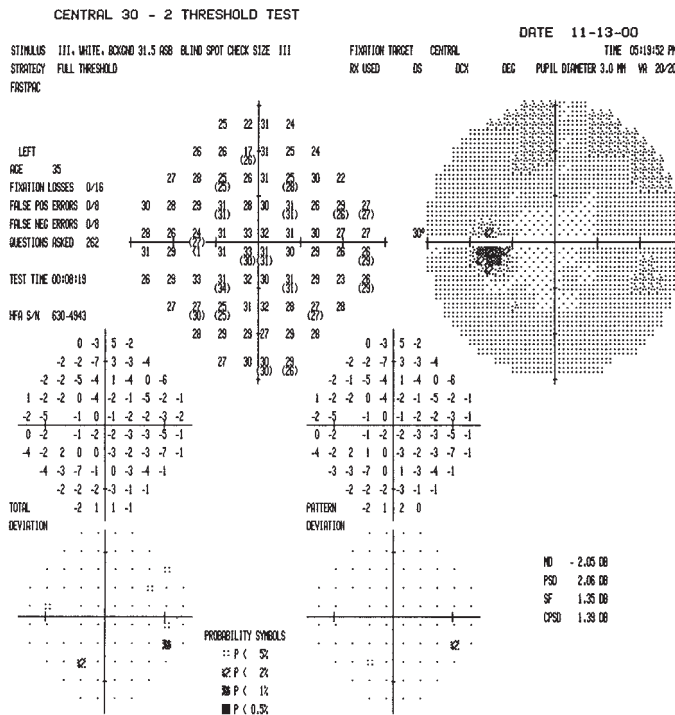
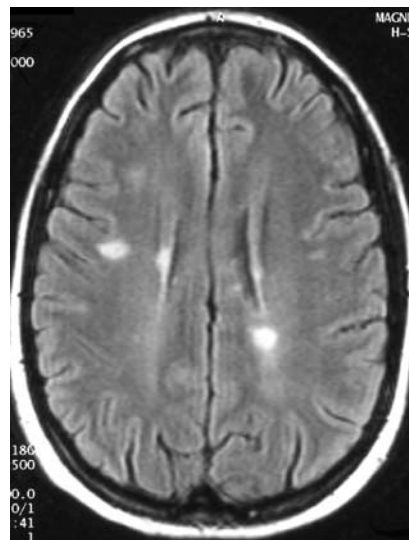
Pathology: Retrobulbar optic neuritis.

Confrontation testing showed the large central defect OD with only light perception within it.

The patient's MRI showed many T2-hyperintense lesions in the periventricular white matter bilaterally and in the inferior cerebellar peduncle. She was treated with steroids and her vision gradually improved over 7 weeks to 20/20 OD. Humphrey visual fields at this time demonstrated a residual central scotoma OD (shown here). Although the gray-scale plot does not show the defect well, both the deviation plots show that the central field is depressed nevertheless. This is consistent with a subtle central scotoma, despite her excellent acuity.

Acute visual loss in a 35-yr-old with a cecocentral scotoma and normal fundus is most consistent with optic neuritis. The prognosis for visual recovery is good. Approximately

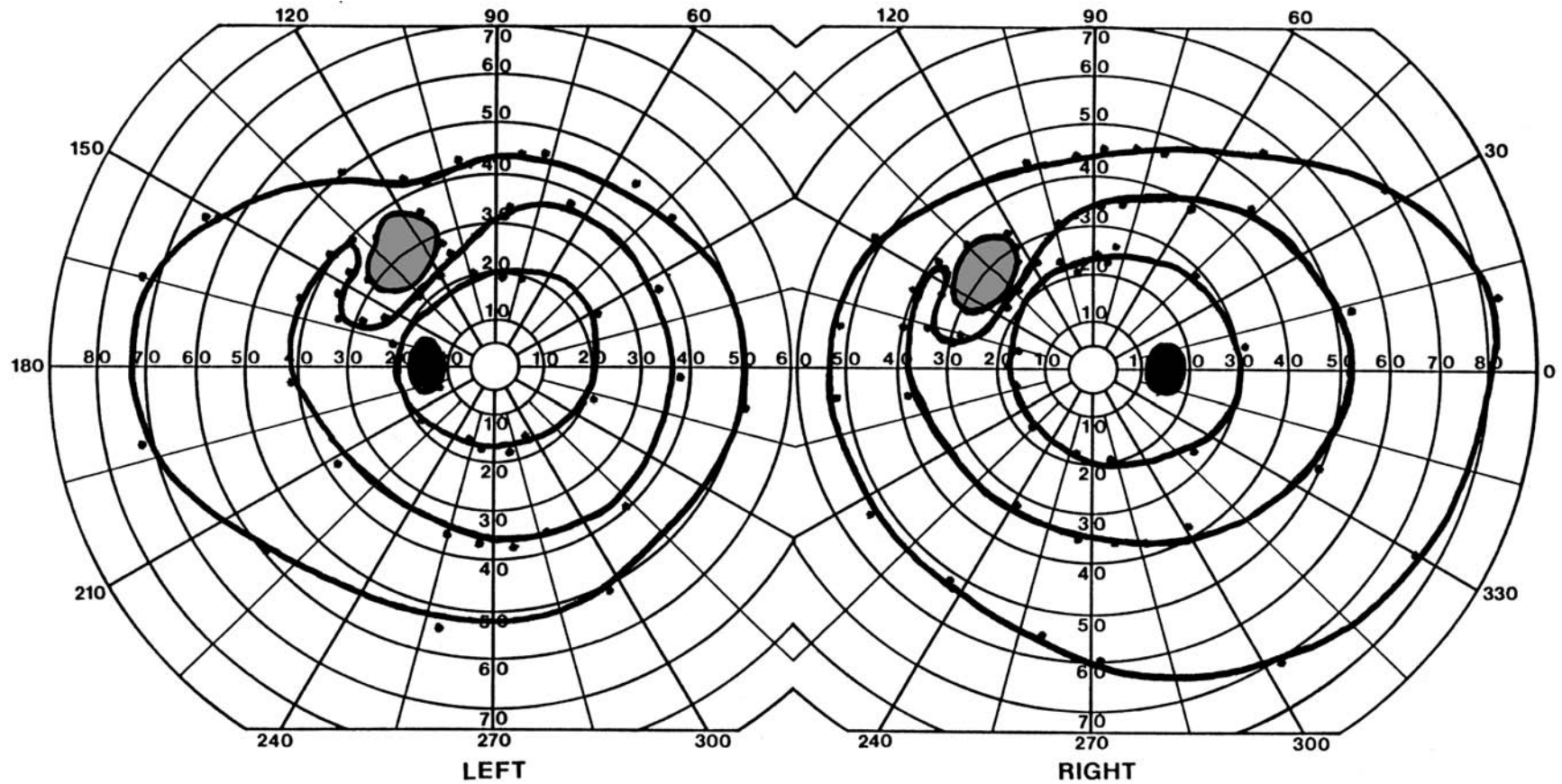
95% of patients are at least 20/40 and 70% are 20/20 12 months later (191). Intravenous methylprednisolone hastens visual recovery but has no effect on ultimate visual function. Apart from visual prognosis, this patient will wish to know her risk of developing MS. Independent of MRI findings (see Case 28), a history of prior nonspecific neurologic symptoms (predominantly paresthesiae, as she had) is also associated with an increased risk of MS (192). Among the patients with optic neuritis and no lesions on brain MRI, the risk of subsequent MS over 5 yr was 44% in those with such symptoms and 15% in those without. The combination of earlier neurologic symptoms and three or more white matter lesions on MRI increases the risk even further to 66%. Should she start on β -interferon or wait until a second episode confirms the diagnosis of MS? The CHAMPS (193) and ETOMS (194) studies indicate that early treatment with β -interferon of patients with MRI scans indicating a high risk of MS (as in this patient) delays the onset of a second neurologic event. What is unclear, however, is whether early treatment has any effect on the more important outcome measure of later disability.



HISTORY AND EXAM

A 32-yr-old woman developed her typical migraine aura of zigzag lines followed by headache, but on this occasion she also had right-sided numbness and weakness. The latter resolved within a few hours but she was left with a permanent hazy area in the upper

quadrant of the left eye. She had had a myocardial infarction at age 29, suffered from Raynaud's phenomenon, and smoked 1.5 packs of cigarettes per day. Three months later visual acuity and color vision were normal, as were the fundi.



DISCUSSION

Field description: Highly congruous homonymous peripheral scotomata in left upper quadrant.

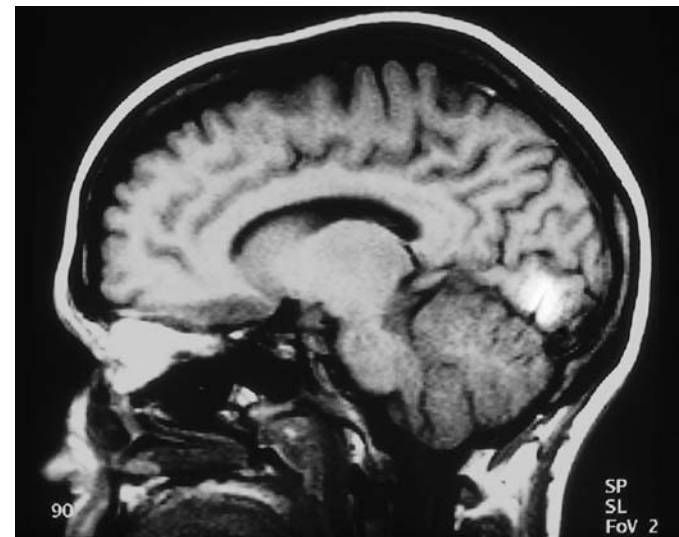
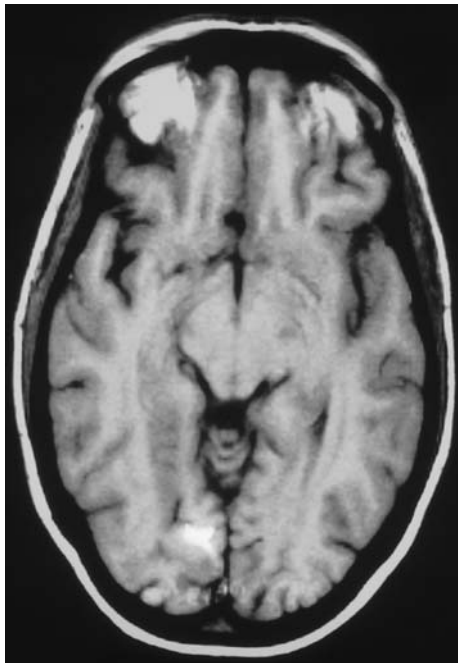
Localization: Right inferior calcarine cortex, midzone.

Pathology: Migrainous infarction.

Tangent screen perimetry showed a homonymous small defect in the upper left quadrant approaching the horizontal but not the vertical meridian.

Axial and sagittal T1 MRI showed an infarct in the midportion of the inferior calcarine cortex. Even though the scotomata are not aligned along the vertical meridians, they are highly congruous, indicating cerebral disease. Damage to optic radiations is also possible.

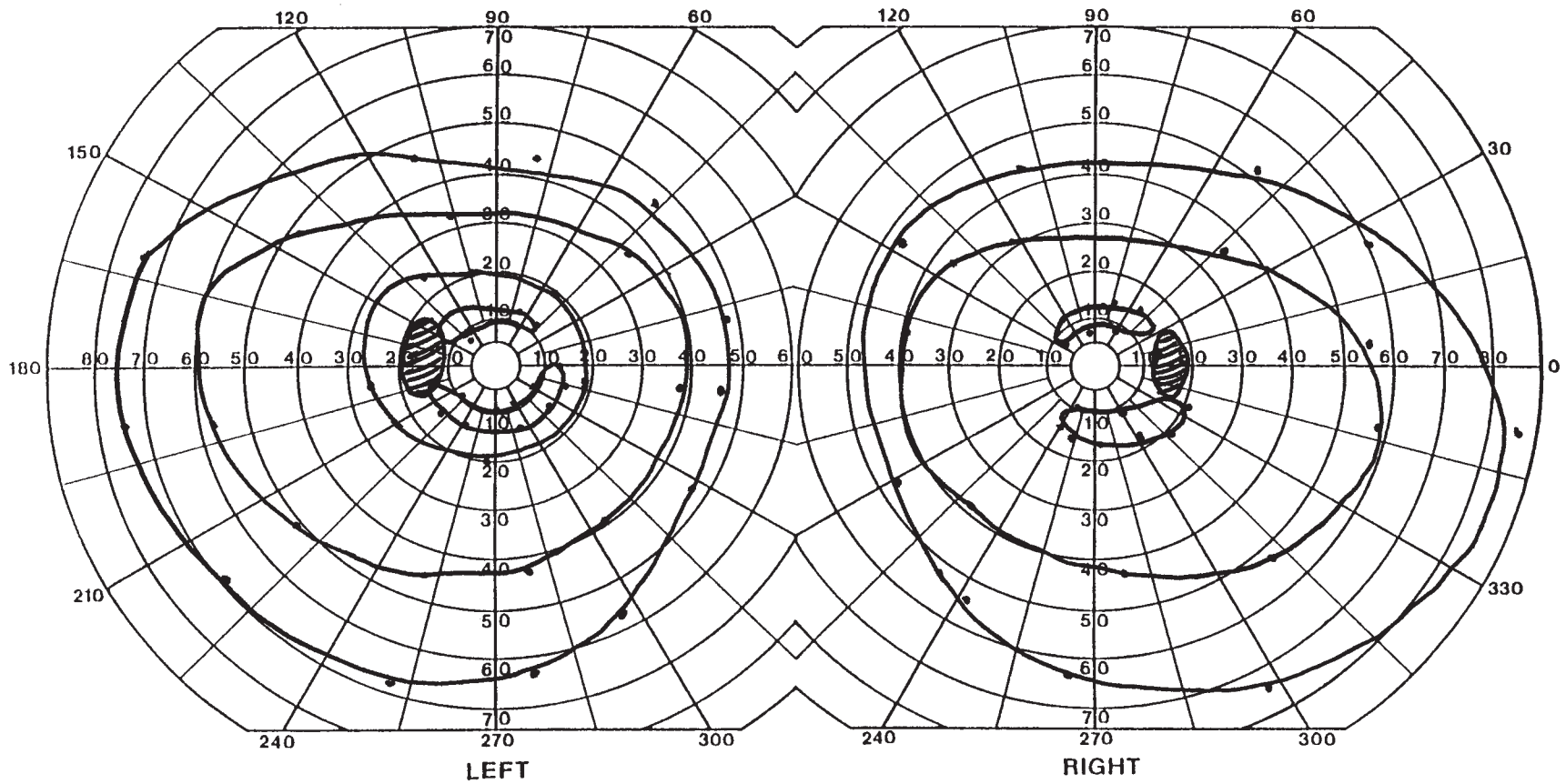
Ischemic stroke is a rare complication of migraine with aura (195,196). The International Headache Society (197) suggests that the diagnosis of migrainous stroke requires a history of migraine with aura and that the attack in question is typical of prior attacks with the exception that the neurologic deficit fails to resolve. Other possible causes of infarction must be excluded. Migraine may increase the risk for stroke in general in women under age 45 (198), especially if they smoke or use oral contraceptives.



HISTORY AND EXAM

This 74-yr-old woman had slowly progressive bilateral visual loss over about 9 years. She had a 15-year history of diabetes mellitus and hypertension. She was also a lifelong vegan, although she had recently started eating meat at the prompting of her daughter. On examination her visual acuity was 20/100 OD and 20/60 OS. Ishihara color plates were

7.5/14 OD and 4/14 OS. There was a small RAPD OS. Fundoscopy revealed bilateral temporal pallor of the optic disks and no diabetic retinopathy. The remainder of the examination was normal.



DISCUSSION

Field description: Bilateral shallow relative central scotomata.

Localization: Optic nerve.

Pathology: B₁₂ deficiency optic neuropathy.

Confrontation fields were full OU.

The two sausage-shaped zones surrounding each central area are peaks of sensitivity, indicating that there is a relative depression between them, affecting central vision. The gradually progressive visual decline with evidence of bilateral optic neuropathy (decreased color vision, optic atrophy, and central scotomata) is most consistent with a toxic-metabolic optic neuropathy. The long-standing history of veganism without vitamin

supplementation makes vitamin B₁₂ deficiency most likely. Serum B₁₂ was normal (note that she recently started eating meat), but homocysteine was elevated at 14 (normal: <12.4) and methylmalonic acid (MMA) markedly elevated at 430 (normal: <279 nmol/L).

Cobalamin (B₁₂) is a cofactor for a number of enzymatic reactions, including the conversion of homocysteine to methionine (in which a methyl group is donated from methyl-tetrahydrofolate) by methionine synthase, and the conversion of methylmalonic-CoA to succinyl-CoA. B₁₂ deficiency, therefore, results in the accumulation of both homocysteine and MMA. Elevated serum concentrations of homocysteine and MMA are thus useful markers of more subtle vitamin B₁₂ deficiency.

DISCUSSION

Field description: Mildly incongruous left homonymous horizontal sectoranopia.

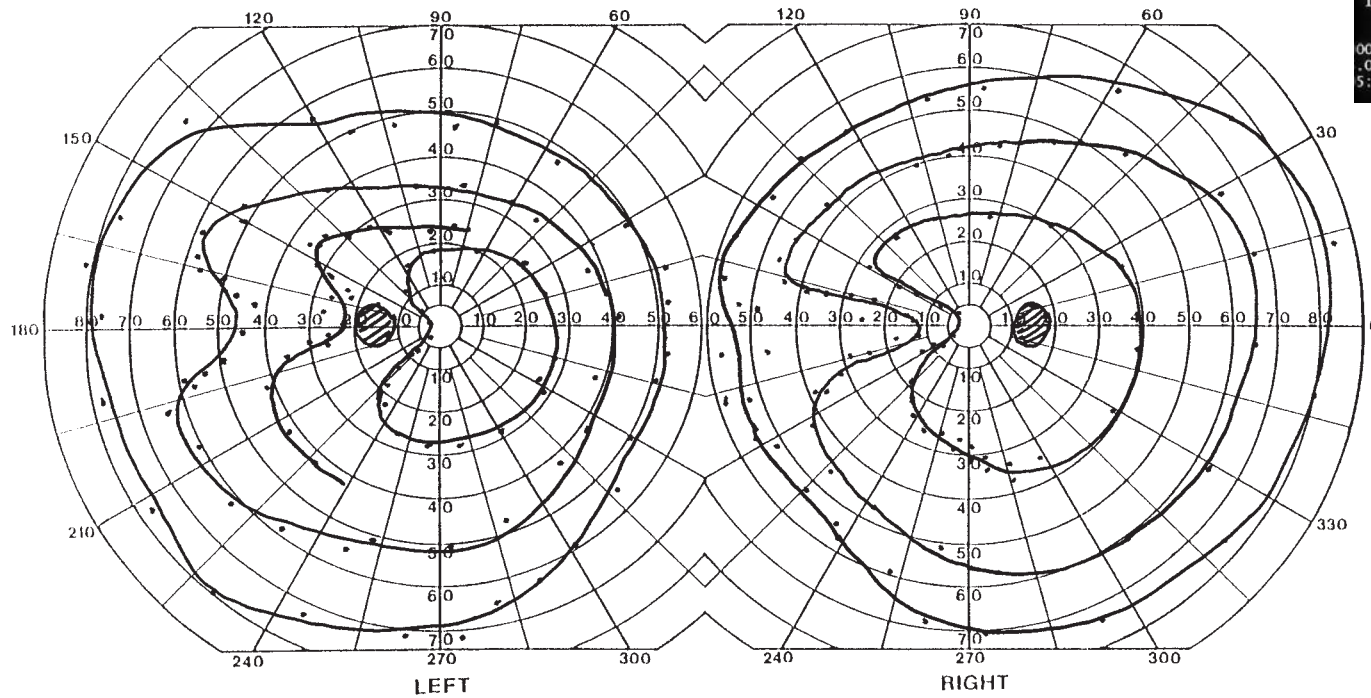
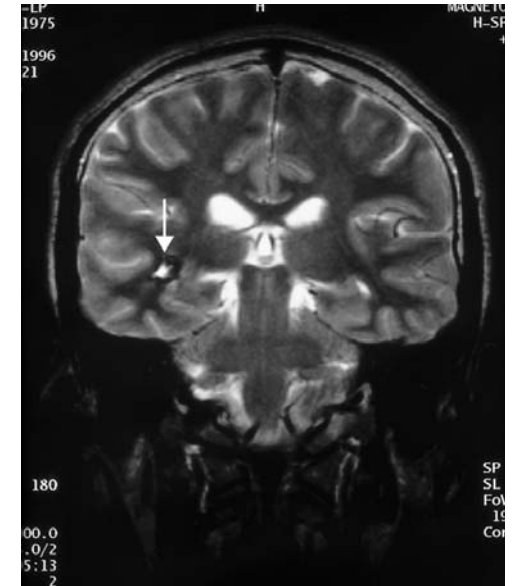
Localization: Right optic radiations, midzone.

Pathology: Venous angioma.

Confrontation testing with all modalities was normal.

The patient's defect is reminiscent of that of Case 82, only with a more focal defect. In both eyes, this clearly straddles the horizontal meridian, most evident in probability plot of the pattern deviation, and to some extent in the gray-scale OS. The area affected is similar in both eyes. Compare his automated perimetry with the Goldmann fields shown on this page.

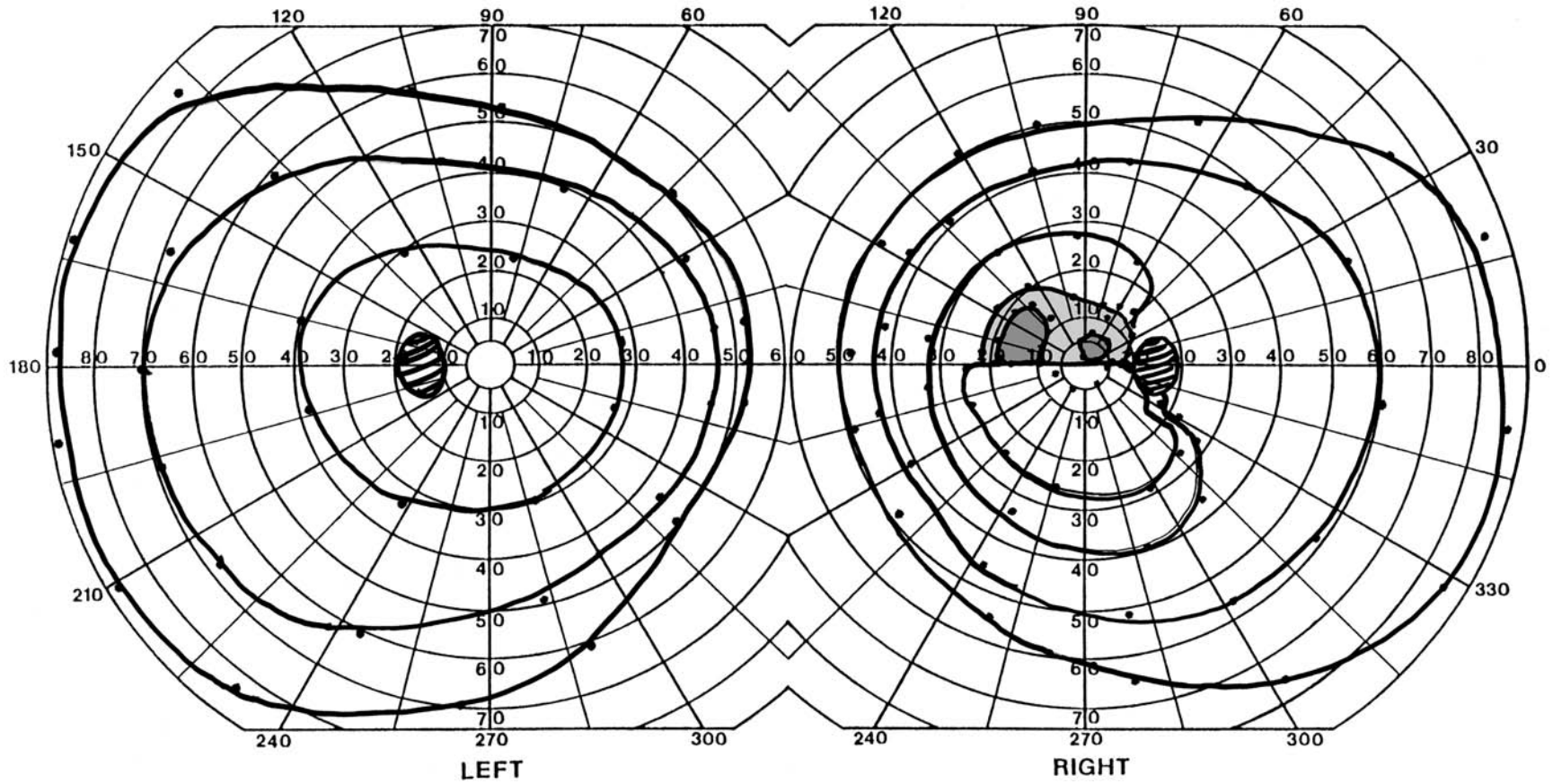
The lack of optic atrophy is against a lesion of the LGN, and his coronal T2-weighted MRI shows that the lesion (arrow) is definitely not in the thalamus, where the LGN resides. Rather, it is in the cerebral white matter, located in the approximate location of the midzone of the optic radiations (146).



HISTORY AND EXAM

This 78-yr-old man with metastatic prostate cancer had two episodes of transient visual loss lasting minutes in the right eye, 16 and 2 months before presentation. The day prior, he had total loss of vision in the right eye that after 20 min resolved into a superior

defect. Acuity was 20/25 OU. Ishihara color scores were 11/14 OD and 14/14 OS. There was an RAPD OD.



DISCUSSION

Field description: Superior central and paracentral scotoma in the right eye that obeys the horizontal meridian, but not the vertical.

Localization: Retinal nerve fiber layer.

Pathology: Branch retinal arterial occlusion (BRAO).

Confrontation testing showed impaired finger counting in the superior field, sparing a small zone around the macula.

The arcuate defect with demarcation at the nasal meridian indicates damage to retinal ganglion cells, either at the disk or in the retinal nerve fiber layer. Sudden onset with earlier transient attacks points to ischemia. The fundus showed a stripe of pale ischemic

retina (arrows) corresponding to the patient's field defect, indicating a BRAO. Retinal ischemia in this age range usually implies an embolic stroke, from cardiac or carotid sources. Carotid stenosis of more than 50% is only found in about a third of patients, however (199). His carotid ultrasound and cardiac echocardiogram were normal. Giant cell arteritis is another cause that must be considered.

Studies of carotid stenosis have shown that emboli to the central retinal arterial territory, causing either a CRAO/BRAO or amaurosis fugax, carry less risk for future cerebral ischemia when compared with cerebral transient ischemic attacks, such as those causing arm or leg weakness.

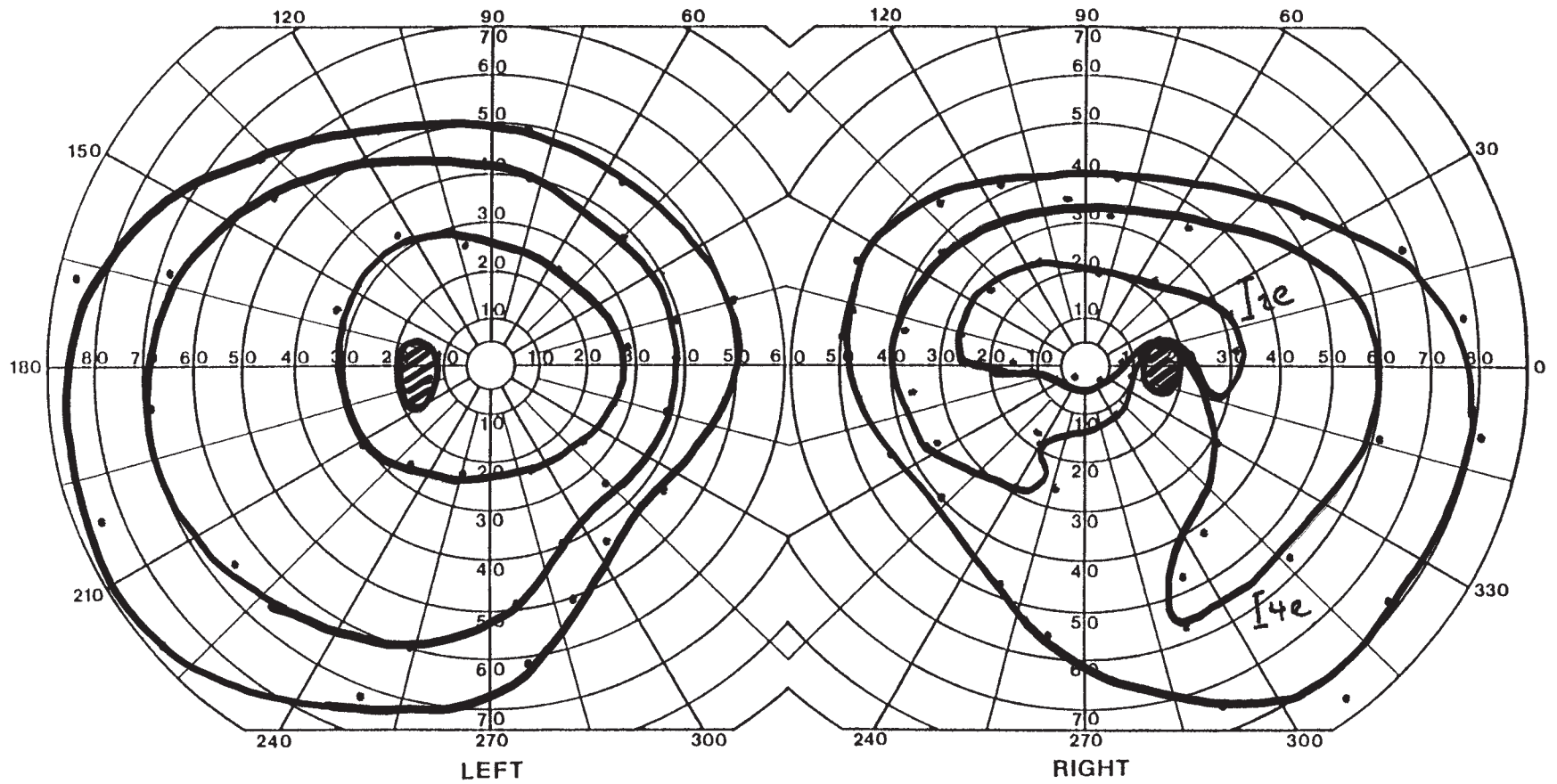


See Color Plate after page 180

HISTORY AND EXAM

This 58-yr-old man noted a blurred gray spot inferotemporally in his right eye, remaining stable over the next 2 d. Visual acuity was 20/20 OU, but Ishihara color scores were 0/10 OD and 8/10 OS. There was an RAPD OD. Fundoscopy showed segmental disk

edema superiorly with a peripapillary white patch OD. Examination was otherwise normal.



DISCUSSION

Field description: Inferior arcuate defect OD.

Localization: Anterior optic nerve.

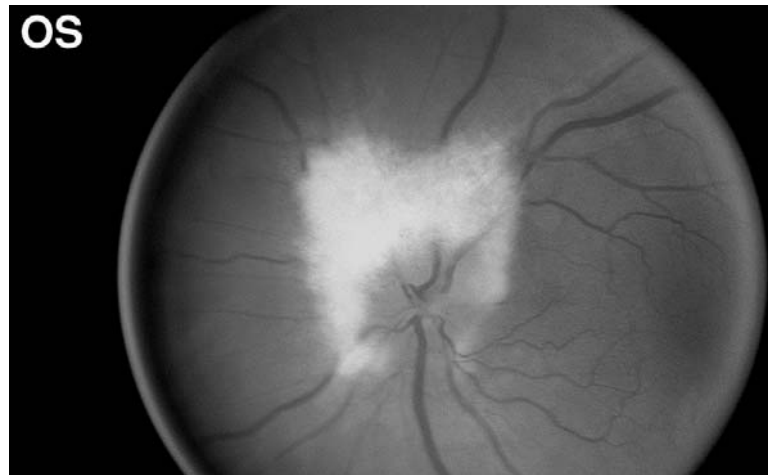
Pathology: AION, nonarteritic.

Other features: Myelinated nerve fibers.

Confrontation testing showed a small inferior defect in both nasal and temporal fields, not respecting the meridian OD.

The patient has a large inferior wedge defect emerging from the blind spot in the I4e isopter, but this also begins to curl nasally, and with the I2e target the defect ends in a shallower depression aligned along the nasal horizontal meridian, marking this as an arcuate defect.

The “white patch” is a collection of myelinated nerve fibers, which are impressive in the fundus picture. These are distinguished from exudates by their feathery appearance, with texture running parallel to the nerve fiber layer (contrast this with the exudate in Case 8). They differ from a macular star in their density (see Case 31). Myelinated nerve fibers are benign variants and are not related to visual loss. Somewhat obscured by these fibers is the mild segmental swelling of the superior aspect of his optic disk, which is consistent with his relatively modest inferior field defect. The rapid onset with segmental disk edema is consistent with ischemia of the optic disk. His defect proved to be stable over the next 3 years.



REFERENCES

1. Allen L. *The Hole in My Vision: An Artist's View of His Own Macular Degeneration*. Iowa City: Penfield Press, 2000.
2. Fine SL, Berger JW, Maguire MG, Ho AC. Age-related macular degeneration. *N Engl J Med* 2000;342:483–492.
3. Rabiah P, Bateman J, Demer J, Perlman S. Ophthalmic findings in patients with ataxia. *Am J Ophthalmol* 1997;123:108–117.
4. Glaser J, Savino P, Summers K. The photostress recovery test: a practical adjunct in the clinical assessment of visual function. *Am J Ophthalmol* 1977;83:255–260.
5. Folk JC, Thompson HS, Han DP, Brown CK. Visual function abnormalities in central serous retinopathy. *Arch Ophthalmol* 1984;102:1299–1302.
6. Chuang EL, Sharp DM, Fitzke FW, Kemp CM, Holden AL, Bird AC. Retinal dysfunction in central serous retinopathy. *Eye* 1987;1:120–125.
7. Smith R, Ganley J. An epidemiologic study of presumed ocular histoplasmosis. *Trans Am Acad Ophthalmol Otolaryngol* 1971;75:994–1005.
8. Beck R, Sergott R, Barr C, et al. Optic disk edema in the presumed ocular histoplasmosis syndrome. *Ophthalmology* 1984;91:183–185.
9. Mets MB, Holfels E, Boyer KM, et al. Eye manifestations of congenital toxoplasmosis. *Am J Ophthalmol* 1997;123:1–16.
10. Hayreh S. Optic disk vasculitis. *Br J Ophthalmol* 1972;56:652–670.
11. Appen R, de Venecia G, Ferwerda J. Optic disk vasculitis. *Am J Ophthalmol* 1980;90:352–359.
12. Greven C, Slusher M, Weaver R. Retinal arterial occlusions in young adults. *Am J Ophthalmol* 1995;120:776–783.
13. Appen R, Wray S, Cogan D. Central retinal artery occlusion. *Am J Ophthalmol* 1975;79:374–381.
14. Qualman SJ, Mendelsohn G, Mann RB, Green WR. Intraocular lymphomas: natural history based on a clinicopathologic study of eight cases and review of the literature. *Cancer* 1983;52:878–886.
15. Phelan JK, Bok D. A brief review of retinitis pigmentosa and the identified retinitis pigmentosa genes. *Mol Vis* 2000;6:116–124.
16. Shastri BS. Retinitis pigmentosa and related disorders: phenotypes of rhodopsin and peripherin/RDS mutations. *Am J Med Genet* 1994;52:467–474.
17. Riise D. The nasal fundal ectasia. *Acta Ophthalmol Suppl* 1975;126:3–108.
18. Miller N, Johnson M, Paul S, et al. Visual dysfunction in patients receiving vigabatrin: clinical and electrophysiologic findings. *Neurology* 1999;53:2082–2087.
19. Malmgren K, Ben-Menachem E, Frisen L. Vigabatrin visual toxicity: evolution and dose dependence. *Epilepsia* 2001;42:609–615.
20. Johnson MA, Krauss GL, Miller NR, Medura M, Paul SR. Visual function loss from vigabatrin: effect of stopping the drug. *Neurology* 2000;55:40–45.
21. Kitazawa Y, Yamamoto T. Glaucomatous visual field defects: their characteristics and how to detect them. *Clin Neurosci* 1997;4:279–283.
22. Caprioli J, Spaeth G. Comparison of visual field defects in the low-tension glaucomas with those in the high-tension glaucomas. *Am J Ophthalmol* 1984;97:730–737.
23. Araie M, Yamagami J, Suziki Y. Visual field defects in normal-tension and high-tension glaucoma. *Ophthalmology* 1993;100:1808–1814.
24. Coleman AL. Glaucoma. *Lancet* 1999;354:1803–1810.
25. Liesegang TJ. Glaucoma: changing concepts and future directions. *Mayo Clin Proc* 1996;71:689–694.
26. Kramer S. The peripheral visual field in glaucoma: re-evaluation in the age of automated perimetry. *Survey Ophthalmol* 1991;36:59–69.
27. Marshall D. Ocular manifestations of multiple sclerosis and relationship to retrobulbar optic neuritis. *Trans Am Ophthalmol Soc* 1950;48:487–525.
28. Sanders E, Vollkers A, van der Poel J, van Lith G. Estimation of visual function after optic neuritis: a comparison of clinical tests. *Br J Ophthalmol* 1986;70:918–924.
29. Wall M. Loss of P retinal ganglion cell function in resolved optic neuritis. *Neurology* 1990;40:649–653.
30. Keltner J, Johnson C, Spurr J, Beck R. Baseline visual field profile of optic neuritis: the experience of the optic neuritis treatment trial. *Arch Ophthalmol* 1993;111:231–234.
31. Optic Neuritis Study Group. The clinical profile of optic neuritis: experience of the Optic Neuritis Treatment Trial. *Arch Ophthalmol* 1991;109:1673–1678.
32. Optic Neuritis Study Group. The 5-year risk of MS after optic neuritis: experience of the Optic Neuritis Treatment Trial. *Neurology* 1997;49:1404–1413.
33. Beck RW, Cleary PA, Backlund JC. The course of visual recovery after optic neuritis: experience of the Optic Neuritis Treatment Trial. *Ophthalmology* 1994;101:1771–1778.
34. Meienberg O, Flammer J, Ludin HP. Subclinical visual field defects in multiple sclerosis: demonstration and quantification with automated perimetry, and comparison with visually evoked potentials. *J Neurol* 1982;227:125–133.
35. Anonymous. Interferon beta-1b is effective in relapsing-remitting multiple sclerosis. I. Clinical results of a multicenter, randomized, double-blind, placebo-controlled trial. The IFNB Multiple Sclerosis Study Group. *Neurology* 1993;43:655–661.
36. Jacobs LD, Cookfair DL, Rudick RA, et al. Intramuscular interferon beta-1a for disease progression in relapsing multiple sclerosis. The Multiple Sclerosis Collaborative Research Group (MSCRG). *Ann Neurol* 1996;39:285–294.

37. Anonymous. Randomised double-blind placebo-controlled study of interferon beta 1a in relapsing/remitting multiple sclerosis. PRISMS (Prevention of Relapses and Disability by Interferon beta-1a Subcutaneously in Multiple Sclerosis) Study Group. *Lancet* 1998;352:1498–1504.
38. Anonymous. Placebo-controlled multicentre randomised trial of interferon beta-1b in treatment of secondary progressive multiple sclerosis. European Study Group on interferon beta-1b in secondary progressive MS. *Lancet* 1998;352:1491–1497.
39. Barkhof F, Filippi M, Miller DH, et al. Comparison of MRI criteria at first presentation to predict conversion to clinically definite multiple sclerosis. *Brain* 1997;120:2059–2069.
40. Beck R, Kupersmith M, Cleary P, Katz B, et al. Fellow eye abnormalities in acute unilateral optic neuritis: experience of the Optic Neuritis Treatment Trial. *Ophthalmology* 1993;100:691–698.
41. Miller DH, Newton MR, van der Poel JC, et al. Magnetic resonance imaging of the optic nerve in optic neuritis. *Neurology* 1988;38:175–179.
42. Kapoor R, Miller DH, Jones SJ, et al. Effects of i.v. methylprednisolone on outcome in MRI-based prognostic subgroups in acute optic neuritis. *Neurology* 1998;50:230–237.
43. Parkin P, Hierons R, McDonald W. Bilateral optic neuritis: a long term follow-up. *Brain* 1984;107:951–964.
44. Morrissey S, Borruat F, Miller D, et al. Bilateral simultaneous optic neuropathy in adults: clinical, imaging, serological, and genetic studies. *J Neurol Neurosurg, Psychiatry* 1995;58:70–74.
45. Graham E, Ellis C, McDonald W. Optic neuropathy in sarcoidosis. *J Neurol Neurosurg Psychiatry* 1986;49:756–763.
46. Zajicek JP, Scolding NJ, Foster O, et al. Central nervous system sarcoidosis—diagnosis and management. *QJM* 1999;92:103–117.
47. Parmley VC, Schiffman JS, Maitland CG, Miller NR, Dreyer RF, Hoyt WF. Does neuroretinitis rule out multiple sclerosis? *Arch Neurol* 1987;44:1045–1048.
48. Khaw K, Manji H, Britton J, Schon F. Neurosarcoidosis—demonstration of meningeal disease by gadolinium enhanced magnetic resonance imaging. *J Neurol Neurosurg Psychiatry* 1991;54:499–502.
49. Hayreh S. Anterior ischemic optic neuropathy: differentiation of arteritic from nonarteritic type and its management. *Eye* 1990;4:25–41.
50. Hayreh S, Podhajsky P, Raman R, Zimmerman B. Giant cell arteritis: validity and reliability of various diagnostic criteria. *Am J Ophthalmol* 1997;123:285–296.
51. The Ischemic Optic Neuropathy Decompression Trial Research Group. Optic nerve decompression surgery for nonarteritic anterior ischemic optic neuropathy (AION) is not effective and may be harmful. *JAMA* 1995;273:625–632.
52. Friedland S, Winterkorn J, Burde R. Luxury perfusion following anterior ischemic optic neuropathy. *J Neuroophthalmol* 1996;16:163–171.
53. Burde R. Optic disk risk factors for nonarteritic anterior ischemic optic neuropathy. *Am J Ophthalmol* 1993;116:759–764.
54. Aiello A, Sadun A, Feldon S. Spontaneous improvement of progressive anterior ischemic optic neuropathy: report of two cases. *Arch Ophthalmol* 1992;110:1197–1199.
55. Katz B, Spencer W. Hyperopia as a risk factor for nonarteritic anterior ischemic optic neuropathy. *Am J Ophthalmol* 1993;116:754–758.
56. Arnold A, Hepler R. Fluorescein angiography in acute nonarteritic anterior ischemic optic neuropathy. *Am J Ophthalmol* 1994;117:222–230.
57. Hayreh S, Zimmerman M, Podhajsky P, Alward W. Nocturnal arterial hypotension and its role in optic nerve head and ocular ischemic disorders. *Am J Ophthalmol* 1994;117:603–624.
58. Fry C, Carter J, Kanter M, Tegeler C, Tuley M. Anterior ischemic optic neuropathy is not associated with carotid artery atherosclerosis. *Stroke* 1993;24:539–542.
59. Massey EW, Schoenberg B. Foster Kennedy syndrome. *Arch Neurol* 1984;41:658–659.
60. Shatz N, Smith J. Non-tumor causes of the Foster Kennedy syndrome. *J Neurosurg* 1967;27:37–44.
61. Beck R, Hayreh S, Podhajsky P, Tan E-S, Moke P. Aspirin therapy in nonarteritic anterior ischemic optic neuropathy. *Am J Ophthalmol* 1997;123:212–217.
62. Connolly S, Gordon K, Horton J. Salvage of vision after hypotension-induced ischemic optic neuropathy. *Am J Ophthalmol* 1994;117:235–242.
63. Johnson MW, Kincaid MC, Trobe JD. Bilateral retrobulbar optic nerve infarctions after blood loss and hypotension: a clinicopathologic case study. *Ophthalmology* 1987;94:1577–1584.
64. Hamilton H, Ellis P, Sheets R. Visual impairment owing to optic neuropathy in pernicious anemia: report of a case and review of the literature. *Blood* 1959;14:378–385.
65. Wilson J. Cyanide in human disease: a review of clinical and laboratory evidence. *Fundam Appl Toxicol* 1983;3:397–399.
66. Harding AE, Sweeney MG, Miller DH, et al. Occurrence of a multiple sclerosis-like illness in women who have a Leber’s hereditary optic neuropathy mitochondrial DNA mutation. *Brain* 1992;115:979–989.
67. Nikoskelainen EK, Marttila RJ, Huoponen K, et al. Leber’s “plus”: neurologic abnormalities in patients with Leber’s hereditary optic neuropathy. *J Neurol Neurosurg Psychiatry* 1995;59:160–164.

68. Kellar-Wood H, Robertson N, Govan GG, Compston DA, Harding AE. Leber's hereditary optic neuropathy mitochondrial DNA mutations in multiple sclerosis. *Ann Neurol* 1994;36:109–112.
69. Corbett JJ, Mehta MP. Cerebrospinal fluid pressure in normal obese subjects and patients with pseudotumor cerebri. *Neurology* 1983;33:1386–1388.
70. Johnston I, Hawke S, Halmagyi M, Teo C. The pseudotumor syndrome: disorders of cerebrospinal fluid circulation causing intracranial hypertension without ventriculomegaly. *Arch Neurol* 1991;48:740–747.
71. Giuseffi V, Wall M, Siegel PZ, Rojas PB. Symptoms and disease associations in IIH (pseudotumor cerebri): a case-control study. *Neurology* 1991;41:239–244.
72. Ireland B, Corbett JJ, Wallace RB. The search for causes of idiopathic intracranial hypertension: a preliminary case-control study. *Arch Neurol* 1990;47:315–320.
73. Chiu AM, Chuenkongkaew WL, Cornblath WT, et al. Minocycline treatment and pseudotumor cerebri syndrome. *Am J Ophthalmol* 1998;126:116–121.
74. Lombaert A, Carton H. Benign intracranial hypertension owing to A-hypervitaminosis in adults and adolescents. *Eur Neurol* 1976;4:340–350.
76. Wall M, White W. Asymmetric papilledema in idiopathic intracranial hypertension: prospective interocular comparison of sensory visual function. *Invest Ophthalmol Visual Sci* 1998;39:134–142.
77. Maxner C, Freeman M, Corbett J. Asymmetric papilledema and visual loss in pseudotumor cerebri. *Can J Neurol Sci* 1987;14:593–596.
78. Corbett J, Thompson H. The rationale management of idiopathic intracranial hypertension. *Arch Neurol* 1989;46:1049–1051.
79. Digre K, Corbett J. IIH (Pseudotumor cerebri): a reappraisal. *Neurologist* 2001;7:2–67.
80. Cantu C, Barinagarrementeria F. Cerebral venous thrombosis associated with pregnancy and puerperium: review of 67 cases. *Stroke* 1993;24:1880–1884.
81. Hayreh S. Pathogenesis of edema of the optic disk (papilledema). *Br J Ophthalmol* 1964;48:522–543.
82. de Bruijn SF, Stam J. Randomized, placebo-controlled trial of anticoagulant treatment with low-molecular-weight heparin for cerebral sinus thrombosis. *Stroke* 1999;30:484–488.
83. Jacobson D. Intracranial hypertension and the syndrome of acquired hyperopia with choroidal folds. *J Neuroophthalmol* 1995;15:178–185.
84. Corbett J, Jacobson D, Mauer R, Thompson H. Enlargement of the blind spot caused by papilledema. *Am J Ophthalmol* 1988;105:261–265.
85. Biousse V, Ameri A, Bousser M. Isolated intracranial hypertension as the only sign of cerebral venous thrombosis. *Neurology* 1999;53:1537–1542.
86. Wasserstrom W, Glass J, Posner J. Diagnosis and treatment of leptomeningeal metastases from solid tumors: experience with 90 patients. *Cancer* 1982;49:759–772.
87. Bleyer W, Byrne T. Leptomeningeal cancer in leukemia and solid tumors. *Curr Problems Cancer* 1988;12:185–238.
88. Arbit E, Wise J, Brem H. Optic nerve meningioma: a case for expectant therapy. *Neuroophthalmology* 1986;6:129–135.
89. Alper M. Management of primary optic nerve meningiomas: current status—therapy in controversy. *J Clin Neuroophthalmol* 1981;1:101–117.
90. Klink DF, Miller NR, Williams J. Preservation of residual vision 2 years after stereotactic radiosurgery for a presumed optic nerve sheath meningioma. *J Neuroophthalmol* 1998;18:117–120.
91. Lee A, Woo S, Miller N, Safran A, Grant W, Butler E. Improvement in visual function in an eye with presumed optic nerve sheath meningioma after treatment with three-dimensional conformal radiation therapy. *J Neuroophthalmol* 1996;16:247–251.
92. Ashar A, Kovacs A, Khan S, Hakim J. Blindness associated with midfacial fractures. *J Oral Maxillofac Surg* 1998;56:1146–1150.
93. Guy J, Sherwood M, Day AL. Surgical treatment of progressive visual loss in traumatic optic neuropathy: report of two cases. *J Neurosurg* 1989;70:799–801.
94. Lessell S. Indirect optic nerve trauma. *Arch Ophthalmol* 1989;107:382–386.
95. Cook M, Levin L, Joseph M, Pinczower E. Traumatic optic neuropathy: a meta-analysis. *Arch Otolaryngol Head Neck Surg* 1996;122:389–392.
96. Levin LA, Beck RW, Joseph MP, Seiff S, Kraker R. The treatment of traumatic optic neuropathy: the International Optic Nerve Trauma Study. *Ophthalmology* 1999;106:1268–1277.
97. Turner J. Indirect injury of the optic nerve. *Brain* 1943;66:140–151.
98. Steinsapir K, Goldberg R. Traumatic optic neuropathy. *Survey Ophthalmol* 1994;38:487–518.
99. O'Neill P, Booth A. Multiple meningiomas: case report and review of the literature. *Surg Neurol* 1984;21:80–82.
100. Evans DG, Sainio M, Baser ME. Neurofibromatosis type 2. *J Med Genet* 2000;37:897–904.
101. Friberg T, Grove A. Choroidal folds and refractive errors associated with orbital tumors. *Arch Ophthalmol* 1983;101:598–603.
102. Acciarri N, Giulioni M, Padovani R, Gaist G, Pozzati E, Acciarri R. Orbital cavernous angiomas: surgical experience on a series of 13 cases. *J Neurosurg Sci* 1995;39:203–209.
103. Kelley J. Autofluorescence of drusen of the optic nerve head. *Arch Ophthalmol* 1974;92:263, 264.

104. Savino P, Glaser J, Rosenberg M. A clinical analysis of pseudopapilledema: II. Visual field defects. *Arch Ophthalmol* 1979;97:71–75.
105. Lansche R, Rucker C. Progression of defects in visual fields produced by hyaline bodies in optic disks. *Arch Ophthalmol* 1957;58:115–121.
106. Kirkham T. The ocular symptomology of pituitary tumors. *Proc R Soc Med* 1972; 65:517, 518.
107. Reid R, Quigley M, SSC Y. Pituitary apoplexy: a review. *Arch Neurol* 1985; 42:712–719.
108. Rusnak R. Adrenal and pituitary emergencies. *Emerg Clin North Am* 1989; 7:903–925.
109. Molitch ME. Clinical manifestations of acromegaly. *Endocrinol Metab Clin North Am* 1992;21:597–614.
110. Melmed S, Ho K, Klibanski A, Reichlin S, Thorner M. Clinical review 75: recent advances in pathogenesis, diagnosis, and management of acromegaly. *J Clin Endocrinol Metab* 1995;80:3395–3402.
111. Mohr G, Hardy J. Hemorrhage, necrosis and apoplexy in pituitary adenomas. *Surg Neurol* 1982;13:181–189.
112. Sorva R, Heiskanen O. Craniopharyngioma in Finland: a study of 123 cases. *Acta Neurochir* 1986;81:85–89.
113. Kosmorsky G, Straga J. A descent thing to do for the chiasm. *J Neuroophthalmol* 1997;17:53–56.
114. Cosman F, Post KD, Holub DA, Wardlaw SL. Lymphocytic hypophysitis: report of 3 new cases and review of the literature. *Medicine (Baltimore)* 1989;68: 240–256.
115. Wilbrand H. Schema des Verlaufs der Sehnervenfasern durch das Chiasma. *Z Augenheilkd* 1926;59:135–144.
116. Horton J. Wilbrand's knee of the primate optic chiasm is an artefact of monocular enucleation. *Trans Am Ophthalmol Soc* 1997;95:579–609.
117. Unsöld R, Hoyt WF. Band atrophy of the optic nerve: the histology of temporal hemianopsia. *Arch Ophthalmol* 1980;98:1637, 1638.
118. Wan WL, Geller JL, Feldon SE, Sadun AA. Visual loss caused by rapidly progressive intracranial meningiomas during pregnancy. *Ophthalmology* 1990; 97:18–21.
119. Kupersmith M, Rosenberg C, Kleinberg D. Visual loss in pregnant women with pituitary adenomas. *Ann Intern Med* 1994;121:473–477.
120. Newman S, Miller N. Optic tract syndrome: neuro-ophthalmologic considerations. *Arch Ophthalmol* 1983;101:1241–1250.
121. Savino PJ, Paris M, Schatz NJ, Orr LS, Corbett JJ. Optic tract syndrome: a review of 21 patients. *Arch Ophthalmol* 1978;96:656–663.
122. Bell R, Thompson H. Relative afferent pupillary defect in optic tract hemianopias. *Am J Ophthalmol* 1978;85:538–540.
123. Czarnecki J, Weingeist T, Burton J, Thompson H. “Twin peaks” papilledema: the appearance of papilledema with optic tract atrophy. *Can J Ophthalmol* 1976;11: 279–281.
124. Frisèn L, Holmegaard L, Rosenkrantz M. Sectoral optic atrophy and homonymous horizontal sectoranopia: a lateral choroidal artery syndrome? *J Neurol Neurosurg Psychiatry* 1978;41:374–380.
125. Donahue S, Kardon R, Thompson H. Hourglass shaped visual fields as a sign of bilateral lateral geniculate myelinolysis. *Am J Ophthalmol* 1995;119:378–380.
126. Goldman J, Hoiroupiou D. Demyelination of the lateral geniculate nucleus in central pontine myelinolysis. *Ann Neurol* 1981;9:185–189.
127. Patchell R. Neurologic complications of organ transplantation. *Ann Neurol* 1994;36:688–703.
128. Falconer M, Wilson J. Visual field changes following anterior temporal lobectomy: their significance in relation to “Meyer’s loop” of the optic radiation. *Brain* 1958;81:1–40.
129. Marino RJ, Rasmussen T. Visual field changes after temporal lobectomy in man. *Neurology* 1968;18:825–835.
130. van Buren J, Baldwin M. The architecture of the optic radiation in the temporal lobe of man. *Brain* 1958;81:15–40.
131. Cendes F, Andermann F, Gloor P, et al. Atrophy of mesial structures in patients with temporal lobe epilepsy: cause or consequence of repeated seizures? *Ann Neurol* 1993;34:795–801.
132. Sutula TP, Pitkanen A. More evidence for seizure-induced neuron loss: is hippocampal sclerosis both cause and effect of epilepsy? *Neurology* 2001;57: 169, 170.
133. Davies KG, Hermann BP, Dohan FC, et al. Relationship of hippocampal sclerosis to duration and age of onset of epilepsy, and childhood febrile seizures in temporal lobectomy patients. *Epilepsy Res* 1996;24:119–126.
134. Wiebe S, Blume WT, Girvin JP, Eliasziw M. A randomized, controlled trial of surgery for temporal-lobe epilepsy. *N Engl J Med* 2001;345:311–318.
135. Paulson HL, Galetta SL, Grossman M, Alavi A. Hemichromatopsia of unilateral occipitotemporal infarcts. *Am J Ophthalmol* 1994;118:518–523.
136. Kölmel HW. Pure homonymous hemichromatopsia: findings with neuroophthalmologic examination and imaging procedures. *Eur Arch Psychiatr Neurol Sci* 1988;237:237–243.
137. Damasio A, Yamada T, Damasio H, Corbett J, McKee J. Central achromatopsia: behavioral, anatomic and physiologic aspects. *Neurology* 1980;30:1064–1071.

138. EAFT (European Atrial Fibrillation Trial) Study Group. Secondary prevention in non-rheumatic atrial fibrillation after transient ischaemic attack or minor stroke. *Lancet* 1993;342:1255–1262.
139. Jacobson D. The localizing value of a quadrantanopia. *Arch Neurol* 1997;54:401–404.
140. Vinters H. Cerebral amyloid angiopathy. In: Barnett H, Mohr J, Stein B, Yatsu F, eds. *Stroke: Pathophysiology, Diagnosis, and Management*. New York: Churchill Livingstone, 1998, pp. 821–858.
141. Heide W, Blankenburg M, Zimmerman E, Kömpf D. Cortical control of double-step saccades: implications for spatial orientation. *Ann Neurol* 1995;38:739–748.
142. Andersen R, Brotchie P, Mazzoni P. Evidence for the lateral intraparietal area as the parietal eye field. *Curr Biol* 1992;2:840–846.
143. Benton AL. Gerstmann's syndrome. *Arch Neurol* 1992;49:445–447.
144. Bender M. Polyopia and monocular diplopia of cerebral origin. *Arch Neurol Psychiatry* 1945;54:323–338.
145. Critchley M. Types of visual perseveration: "palinopsia" and "illusory visual spread." *Brain* 1951;74:267–299.
146. Carter J, O'Connor P, Shacklett D, Rosenberg M. Lesions of the optic radiations mimicking lateral geniculate nucleus visual field defects. *J Neurol Neurosurg Psychiatry* 1985;48:982–988.
147. Lepore F. The preserved temporal crescent: the clinical implications of an "endangered" finding. *Neurology* 2001;57:1918–1921.
148. Loscalzo J. Paradoxical embolism: clinical presentation, diagnostic strategies, and therapeutic options. *Am Heart J* 1986;112:141–145.
149. Huber A. Homonymous hemianopia after occipital lobectomy. *Am J Ophthalmol* 1962;54:623–629.
150. Gray L, Galetta S, Siegal T, Schatz N. The central visual field in homonymous hemianopia: evidence for unilateral foveal representation. *Arch Neurol* 1997;54:312–317.
151. McAuley D, Russell R. Correlation of CAT scan and visual field defects in vascular lesions of the posterior visual pathways. *J Neurol Neurosurg Psychiatry* 1979;42:298–311.
152. Barton J, Behrmann M, Black S. Ocular search during line bisection: the effects of hemi-neglect and hemianopia. *Brain* 1998;121:1117–1131.
153. Behrmann M, Watt S, Black S, Barton J. Impaired visual search in patients with unilateral neglect: an oculographic analysis. *Neuropsychologia* 1997;35:1445–1458.
154. Payne B, Lomber S, Macneil M, Cornwell P. Evidence for greater sight in blind-sight following damage of primary visual cortex early in life. *Neuropsychologia* 1996;34:741–774.
155. Stoerig P, Cowey A. Blindsight in man and monkey. *Brain* 1997;120:535–559.
156. Campion J, Latto R, Smith YM. Is blindsight an effect of scattered light, spared cortex, and near-threshold vision? *Behav Brain Sci* 1983;6:423–486.
157. Scharli H, Harman A, Hogben J. Blindsight in subjects with homonymous visual field defects. *J Cogn Neurosci* 1999;11:52–66.
158. Kasten E, Wuest S, Sabel B. Residual vision in transition zones in patients with cerebral blindness. *J Clin Exp Neuropsychol* 1998;20:581–598.
159. Damasio A, Damasio H, van Hoessen G. Prosopagnosia: anatomic basis and behavioral mechanisms. *Neurology* 1982;32:331–341.
160. Michel F, Perenin M-T, Sieroff E. Prosopagnosie sans hémianopsie après lésion unilatérale occipito-temporale droite. *Rev Neurol* 1986;142:545–549.
161. de Renzi E. Prosopagnosia in two patients with CT scan evidence of damage confined to the right hemisphere. *Neuropsychologia* 1986;24:385–389.
162. Landis T, Cummings J, Christen L, Bogen J, Imhof H-G. Are unilateral right posterior lesions sufficient to cause prosopagnosia? Clinical and radiological findings in six additional patients. *Cortex* 1986;22:243–252.
163. Trauzettel-Klosinski S, Brendler K. Eye movements in reading with hemianopic field defects: the significance of clinical parameters. *Graefes Arch Clin Exp Ophthalmol* 1998;236:91–102.
164. Zihl J. Eye movement patterns in hemianopic dyslexia. *Brain* 1995;118:891–912.
165. Bakshi R, Shaikh Z, Bates V, Kinkel P. Thrombotic thrombocytopenic purpura: brain CT and MRI findings in 12 patients. *Neurology* 1999;52:1285–1288.
166. de Luca M, Spinelli D, Zoccolotti P. Eye movement patterns in reading as a function of visual field defects and contrast sensitivity loss. *Cortex* 1996;32:491–502.
167. Heller-Bettinger I, Kepes J, Preskorn S, Wurster J. Bilateral altitudinal anopia caused by infarction of the calcarine cortex. *Neurology* 1976;26:1176–1179.
168. Hahn RG, Sandfeldt L, Nyman CR. Double-blind randomized study of symptoms associated with absorption of glycine 1.5% or mannitol 3% during transurethral resection of the prostate. *J Urol* 1998;160:397–401.
169. Caplan LR. "Top of the basilar" syndrome. *Neurology* 1980;30:72–79.
170. Freedman M, Leach L, Kaplan E, Winocur G, Shulman K, Delis D. *Clock Drawing: A Neuropsychological Analysis*. Oxford: Oxford University Press, 1994.

171. Curran WJ, Scott CB, Horton J, et al. Recursive partitioning analysis of prognostic factors in three Radiation Therapy Oncology Group malignant glioma trials. *J Natl Cancer Inst* 1993;85:704–710.
172. McKhann GM, Goldsborough MA, Borowicz LM, et al. Predictors of stroke risk in coronary artery bypass patients. *Ann Thorac Surg* 1997;63:516–521.
173. Caplan L, Hurst J, Chimowitz M. *Clinical Neurocardiology: Fundamental and Clinical Cardiology*. Vol. 37. New York: Marcel Dekker, 1999.
174. Loewenfeld I. Impairment of Sympathetic Pathways in: *The Pupil*. Vol. I. Ames: Iowa State University Press, 1993:1146, 1147.
175. Benbadis SR, Agrawal V, Tatum WO. How many patients with psychogenic nonepileptic seizures also have epilepsy? *Neurology* 2001;57:915–917.
176. Morgan R, Nugent B, Harrison J, O'Connor P. Voluntary alteration of pattern visual evoked responses. *Ophthalmology* 1985;92:1356–1363.
177. Keane J. Hysterical hemianopia: the 'missing half' field defect. *Arch Ophthalmol* 1979;97:865, 866.
178. Kathol R, Cox T, Corbett J, Thompson H, Clancy J. Functional visual loss: I. A true psychiatric disorder? *Psychol Med* 1983;13:307–314.
179. Kathol R, Cox T, Corbett J, Thompson H. Functional visual loss. Follow up of 42 cases. *Arch Ophthalmol* 1983;101:729–735.
180. Sharma O, Sharma A. Sarcoidosis of the nervous system. *Arch Intern Med* 1991; 151:1317–1321.
181. Jordan D, Anderson R, Nerad J, Patrinely J, Scrafford D. Optic nerve involvement as the initial manifestation of sarcoidosis. *Can J Ophthalmol* 1988;23:232–237.
182. Gelwan M, Kellen R, Burde R, Kupersmith M. Sarcoidosis of the anterior visual pathway: successes and failures. *J Neurol Neurosurg, Psychiatry* 1988;51: 1473–1480.
183. Aydin P, Kansu T, Sanac A. High myopia causing bilateral abduction deficiency. *J Clin Neuroophthalmol* 1992;12:163–165.
184. Horton JC, Hoyt WF. Quadrantic visual field defects: a hallmark of lesions in extrastriate (V2/V3) cortex. *Brain* 1991;114:1703–1718.
185. Brodsky M. Congenital anomalies of the optic disk. In: Miller N, Newman N, eds. *Walsh and Hoyt's Clinical Neuroophthalmology*. Vol. 1. Baltimore: Williams & Wilkins, 1998:775–823.
186. Orcutt JC, Wulc AE, Mills RP, Smith CH. Asymptomatic orbital cavernous hemangiomas. *Ophthalmology* 1991;98:1257–1260.
187. Missori P, Tarantino R, Delfini R, Lunardi P, Cantore G. Surgical management of orbital cavernous angiomas: prognosis for visual function after removal. *Neurosurgery* 1994;35:34–38.
188. Andrews BT, Wilson CB. Suprasellar meningiomas: the effect of tumor location on postoperative visual outcome. *J Neurosurg* 1988;69:523–528.
189. Mahmood A, Caccamo DV, Tomecek FJ, Malik GM. Atypical and malignant meningiomas: a clinicopathological review. *Neurosurgery* 1993;33:955–963.
190. Aguirre GK, D'Esposito M. Topographical disorientation: a synthesis and taxonomy. *Brain* 1999;122:1613–1628.
191. Beck RW, Cleary PA, Anderson MM, et al. A randomized, controlled trial of corticosteroids in the treatment of acute optic neuritis. The Optic Neuritis Study Group. *N Engl J Med* 1992;326:581–588.
192. Beck RW, Cleary PA, Trobe JD, et al. The effect of corticosteroids for acute optic neuritis on the subsequent development of multiple sclerosis. The Optic Neuritis Study Group. *N Engl J Med* 1993;329:1764–1769.
193. Jacobs LD, Beck RW, Simon JH, et al. Intramuscular interferon beta-1a therapy initiated during a first demyelinating event in multiple sclerosis. CHAMPS Study Group. *N Engl J Med* 2000;343:898–904.
194. Comi G, Filippi M, Barkhof F, et al. Effect of early interferon treatment on conversion to definite multiple sclerosis: a randomised study. *Lancet* 2001;357: 1576–1582.
195. Rothrock J, Walicke P, Swenson M, Lyden P, Logan W. Migrainous stroke. *Arch Neurol* 1988;45:63–67.
196. Bogousslavsky J, Regli F, Van Melle G, Payot M, Uske A. Migraine stroke. *Neurology* 1988;38:223–227.
197. Classification and diagnostic criteria for headache disorders, cranial neuralgias and facial pain. Headache Classification Committee of the International Headache Society. *Cephalalgia* 1988;8(Suppl. 7):1–96.
198. Tzourio C, Tehindrazanarivelo A, Iglesias S, et al. Case-control study of migraine and risk of ischaemic stroke in young women. *BMJ* 1995;310:830–833.
199. O'Farrell CM, FitzGerald DE. Ultrasound morphology of carotid lesions in retinal ischaemia. *Br J Ophthalmol* 1992;76:656–659.

Appendix

Basic Concepts Relevant to Perimetry

Almost all of this book is aimed at providing practical information related to the performance and interpretation of perimetry in the clinical setting. This part is not. Rather, this appendix is dedicated to those readers who are curious about the nature of what is actually being done during perimetry. From the reams of information concerning visual physics and psychophysics, we have selected the following three topics that might be illuminating.

1. UNITS OF LIGHT MEASUREMENT

Light or luminous intensity is the energy radiating from a point source. However, the effectiveness of light energy in stimulating human vision varies with the wavelength of light, being maximal around 550 nm, and restricted to a range from about 400 to 700 nm. (Hence, we do not see infrared or ultraviolet light.) Photometric units of luminance correct for the variable efficacy of light at different wavelengths. The main unit of luminance intensity is the *candle (cd)*, which is technically defined as $1/60^{\text{th}}$ of the intensity per square centimeter of a black body radiating at 2046°K .

A point source of light can theoretically emit light in all directions, generating a sphere of luminous energy. Imagine a portion of that sphere shaped like a cone with its tip at that point source. Imagine specifically a cone whose sides (radius) measure 1 m long and whose circular opening encloses an area of 1 m^2 . This cone is a unit solid angle. A *lumen* is the luminance contained in a unit solid angle from a point source emitting 1 cd of light in all directions (Fig. 1). The relation between a candle and a lumen is that $1\text{ lumen} = 1/\pi\text{ cd} = 0.3183\text{ cd}$.

Most perimetric devices do not shine light sources directly at the eye but project light on reflecting surfaces, usually that of a bowl. The light intensity reaching the eye is a product of the intensity of the light falling on the surface and the ability of the surface to reflect the light back, known as the surface's *reflectance*. The reflectance of the perimetric surface is constant, while the projector varies the light falling on it. The intensity of light spread over a given area of the reflecting surface is measured in candles per square meter (cd/m^2) or lumens per square meter. The latter, lumens/m^2 , also goes by the name of an *apostilb (asb)*, or lux. As before, $1\text{ asb} = 0.3183\text{ cd}/\text{m}^2$.

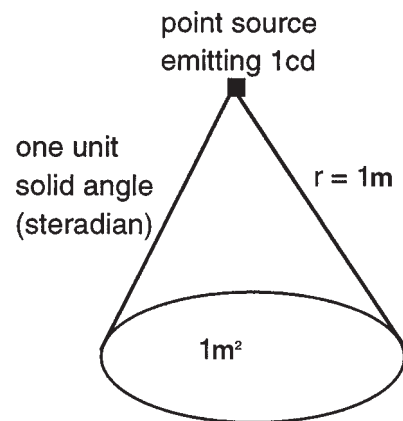


Fig. 1. Lumens and candles. If a point source emits 1 cd of light, the amount of light energy within a steradian (angle whose mouth has an area of 1 m^2 at a radius of 1 m) is a lumen, which thus equals $1/\pi\text{ cd}$.

Another unit worth mentioning is the *Troland*, which attempts to measure *retinal* illumination by correcting stimulus luminance for pupil area. The larger the pupil, the more the amount of light striking the retina, as any subject who has had their eyes dilated can testify. The equation is that a Troland = stimulus luminance (cd/m^2) \times pupil area (mm^2). The fact that retinal illumination is proportional to pupil area has implications mainly for small pupils. Consider the difference between 1- and 2-mm pupils. Since $\text{area} = \pi r^2$, the area of the 1-mm pupil is 0.79 mm^2 and that of the 2-mm pupil is 3.14 mm^2 . Thus, the 2-mm pupil lets in four times as much retinal illumination as the 1-mm pupil. On the other hand, the difference between 4-mm (area = 12.5 mm^2) and 5-mm (area = 19.6 mm^2) pupils is only a factor of 1.5.

2. PERCEPTUAL THRESHOLDS AND SENSITIVITY

2.1. THE CONCEPT OF THRESHOLD

Although it seems obvious, it is worth stating that to be seen an object must differ from its surroundings in some fashion. All current perimeters project bright white spots of light on white backgrounds. The target differs from the background in light intensity alone, as opposed to, say, hue, saturation, texture, or many other visual attributes. Thus, all standard perimeters, automated or

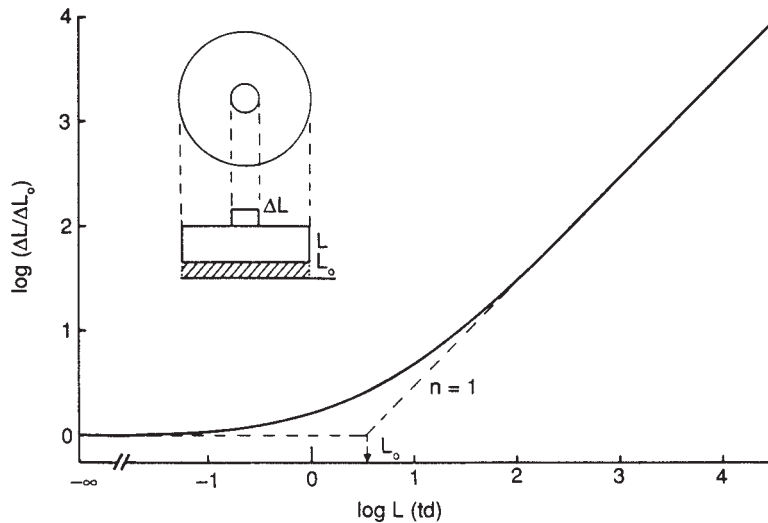


Fig. 2. Threshold-vs-intensity function. The formal equation is $\Delta L/\Delta L_0 = k(L + L_0)^n$, in which L is the background light, ΔL is the increment needed to reach threshold, and ΔL_0 is the threshold in dark light (L_0). At low levels of background light, the threshold is constant. However, with increasing background light, the data approximate the line for $n = 1$. At this point, and when ΔL and L are large relative to ΔL_0 and L_0 , the equation then simplifies to $\Delta L/L = k$, the Weber fraction. The slope of the line equals k . (From (1), with permission.)

manual, measure the *differential light sensitivity threshold*. That is, how much brighter than a standard homogeneously lit background must a target of a given size be before it can be perceived? The answer is highly dependent on retinal location, and the map of this variation is the object of conventional perimetry.

Background luminance has an important influence on threshold. At very dim, low scotopic levels (where rods but not cones are working), the intensity of light needed to reach perceptual threshold is fairly constant. However, with increasing levels of background light, the threshold is no longer a set amount of light but increases in proportion to background luminance. Rather than a fixed level of intensity, threshold (ΔI) is a fixed fraction of background intensity (I). This is known as a *Weber fraction* ($\Delta I/I = k$), where for many sensory functions k is in the range of a few percent (Fig. 2). The standard background of 31.5 asb for both Goldmann and Humphrey is at the low end of photopic vision, where cones operate, which is important because the Weber rule depends on gain control in the cone system (1). The importance of this is that it minimizes the effect of variations in retinal illumination from differences in the ocular media or pupil area. Because these factors affect the intensity of both target and background to the same degree, they should not alter the Weber fraction. (In practice, though, these factors do elevate thresholds, because they have other effects besides reducing illumination, such as diffraction and scattering of light, so that light intensity is less concentrated, being spread over a larger area.)

Ideally, a threshold should be a sharp demarcation between stimuli that are not seen and those that are. However, there is always some random variation in both stimuli and response systems, particularly those involving biologic detectors such as eyes and the shifting criteria typical of human judgment, with all its susceptibility to fatigue, attention, and learning. The result is that thresholds are not sharp boundaries but more gradual shifts in the probability of a stimulus generating a response in the system. In a detection task, the threshold is the value at which a stimulus has a 50% probability of being detected.

2.2. FINDING THRESHOLDS

How does one measure a threshold? The labor-intensive answer is the *frequency-of-seeing* experiment (Fig. 3A). Targets are made with varying levels of difficulty in the property being tested (luminance in our case) and are presented repeatedly in random order to determine how often a subject detects each particular target. The frequency of detection is plotted as a function of the stimulus property and a curve fitted through the data, determining where this line intersects the 50% frequency line.

Because this precision costs time, quicker estimating strategies have evolved. In the *method of adjustment* (Fig. 3B), the value to be changed is set at an invisible level and then gradually increased until the subject sees the stimulus. In other trials, the value is set where the target is clearly visible, then gradually decreased until the subjects says that the stimulus has disappeared. Equal numbers of "up" and "down" trials are usually averaged to give the threshold estimate. (Estimates when moving from unseen to seen tend to be higher than estimates when moving from seen to unseen, because of the tendency of any perceptual system to hold on to the current percept, a phenomenon known as hysteresis.) The precision of this estimate is a function of the number of results being averaged.

A variation of the method of adjustment is the *staircase* strategy (Fig. 3C). The target intensity is set so that it is clearly visible, then decreased stepwise in subsequent trials until the subject no longer sees the target. At this point, direction is reversed and intensity increased until the subject sees the target again. The process of decreasing and increasing is repeated, but with smaller, finer steps, until the reversals oscillate in a narrow range near the threshold. Both staircase and method of adjustment use only a small fraction of trials compared to formal threshold determination, allowing threshold estimation at many more locations in the visual field than would be otherwise possible.

Is method of adjustment used in perimetry? Actually, the stimulus presentations in Goldmann perimetry can be considered truncated forms of this. With static target presentations, one can estimate a luminance threshold by gradually increasing the inten-

sity or size of the stationary target until patients respond that they see it. This is essentially a single method-of-adjustment sequence. With kinetic presentations, the intensity is held constant and the stimulus varies in location instead. Since the normal hill of vision is a smooth slope of gradually increasing sensitivity toward the center, a target moving from the periphery to the center will start as invisible, then strike a region where it reaches threshold and is seen. This, too, then, is a method of adjustment. In clinical practice, one always moves from the unseen to the seen in both static and kinetic strategies, as is standard procedure for testing of all neurologic sensory deficits (hence yielding conservative estimates of threshold), and most perimetrists seldom test a region more than once or twice. The impact of this on precision should always be borne in mind. In cases or regions where there are reasons to doubt reliability, repeated measures should always be done to both improve the threshold estimate and document the variability of the subject's responses.

Threshold estimates in automated perimetry use the staircase strategy. Typical standard protocols use only two reversals. The target intensity is decreased by large steps until it is not seen, then increased in a second reversed sequence by smaller steps until it is seen, and the final intensity at which it was seen is taken as the threshold. This is less accurate than multiple reversals but quicker. Once again, practicality demands some compromises.

2.3. SENSITIVITY

Sensitivity is inversely related to threshold. A high threshold means that a light must be fairly intense to be seen. This indicates that the retinal location in question is relatively insensitive to light. Sensitivities in automated perimetry are given arbitrary units (*decibels* [dB]) but always expressed as the negative of the log of the threshold luminance:

$$s = k - b \log(\Delta I)$$

in which k and b are arbitrary constants. Hence, a sensitivity change of +1 dB equals a threshold change of $-0.1 \log(\text{asb})$. Logarithmic scaling follows from the fact that thresholds obey the proportionality rule expressed in the Weber fraction, since $\log(A/B) = \log(A) - \log(B)$.

For the Humphrey perimeter, the relation is $s = 40 - 10 \log(\Delta I)$, in which s is expressed in dB and ΔI is measured in asb (Fig. 4). This assigns a theoretical maximum sensitivity (when $\Delta I = 0$) a value of 40 dB and declares that for practical purposes, inability to detect a target intensity of 10,000 asb above background implies a sensitivity of 0 dB.

3. SIGNAL DETECTION THEORY

It is worth reviewing a few basic points about detection theory (2), both in terms of understanding how patients detect lights and in terms of how examiners detect defects.

Most detectors, whether biologic or man-made, have a problem with random noise. This noise creates a variable low level of activity in the system even when no stimulus is present and also adds to the variability of the signal generated by a stimulus. This is not a problem when the stimulus's mean signal is much larger than the variations created by noise. If noise is great or the stimulus signal faint or highly variable, however, it can be difficult to judge whether or not the stimulus is present. In this situation, the detector faces two questions: (1) How confidently can I tell absence from presence (discriminative power)? (2) If I have to

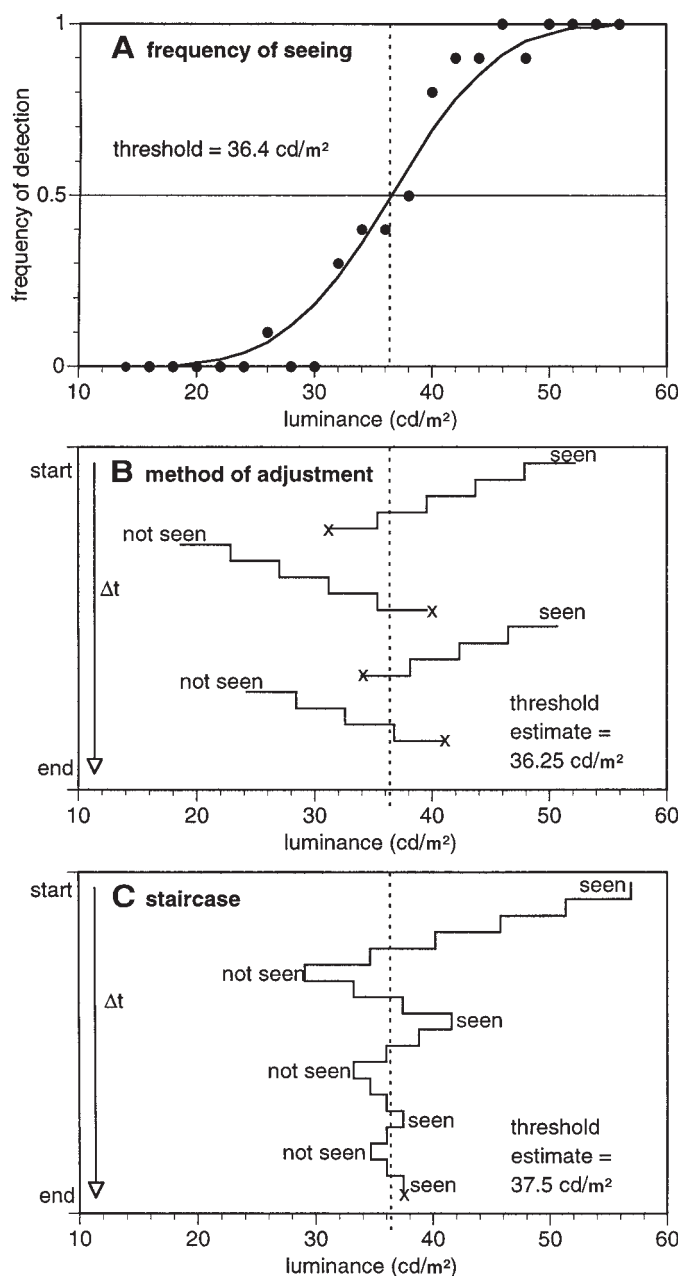


Fig. 3. Threshold determination, three methods. (A) Frequency-of-seeing experiment. The subject is tested 10 times at each of 22 different levels of brightness, to determine how often they report seeing the target at each level. A curve is then fitted to the data, and the point at which it intersects the line representing 50% frequency of seeing is taken as the threshold, which is 36.4 cd/m². (B) Method of adjustment. Time is now depicted on the y-axis. At the start (top), a bright easily seen target is shown, and then its brightness is decreased until the subject says that he cannot see it (first x). This indicates that the threshold has been crossed. A dim invisible target is then shown, and brightness increased until it is seen (next x), indicating crossing of the threshold again. This is repeated until a number of x points are obtained, and these are averaged to estimate the threshold. The number of trials is 22 rather than 220. (C) Staircase. A bright target is chosen and its intensity decreased until the subject says he cannot see it. Brightness is then increased until he can see it, then decreased in smaller steps until he cannot, and so on. After a predetermined number of reversals, the final point (x) is chosen as the threshold. The number of trials is 19.

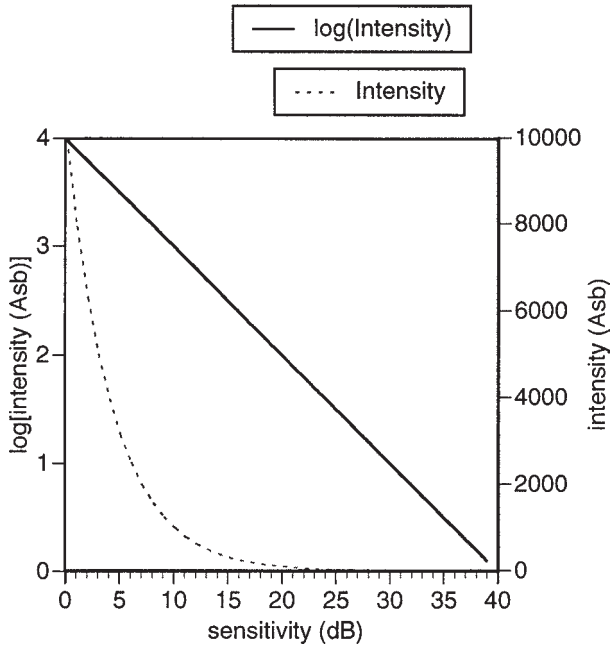


Fig. 4. Sensitivity vs intensity: units used by Humphrey automated perimetry. The equation is $s(\text{dB}) = 40 - 10 \log(\Delta I, \text{asb})$. Plots against both intensity and its logarithm are shown.

choose, is it more important not to miss any stimuli, or not to make any false calls when no stimulus was there—in statistical language, what is the appropriate criterion bias? Signal detection theory gives us a way of characterizing these two issues, discrimination and criterion.

For many situations, one can characterize the random variation in the signal activity related to both the absence and presence of a stimulus as two normally distributed functions. These functions have a mean and a standard deviation (SD). The larger the SD of either, the more noise in the system. For convenience, the curves in Fig. 5A,B show the mean value for the absence of a stimulus as 0, and the SDs of both nonstimulus and stimulus curves as 1 (though in practice there is no requirement that they be equal). The farther apart the curves are *relative to their SDs*, the easier to discriminate the absence from the presence of a stimulus. When the curves are similar in shape (i.e., same SD), this can be most easily expressed as the distance between the mean values divided by the SD, a value called d' . The larger d' is (cf. Fig. 5B with 5A), the more the discriminative power.

A *criterion* is a signal value that one chooses as a cutoff, so that all values above this are classified as positive and all values below as negative. Unfortunately, when curves overlap a lot, there will be both stimuli and nonstimuli that are classified as having a positive signal (lying to the right of the cutoff). That is, there will be both true positives and false positives. In the curves of Fig. 5A,B, imagine calculating for each signal value the corresponding true and false positive rates. Plotting these against each other yields the *receiver operator characteristic* (ROC) curve (Fig. 5C), showing how true positive rates vary with false positive rates as the criterion is moved through the range of data in Fig. 5A,B. The long dashed diagonal line where the true positive rate equals the false positive rate is the hypothetical line where d' equals zero, or no ability to tell whether a stimulus is

present or not. The greater the discriminative power, the farther away from this diagonal a curve will lie, being pulled toward the upper left corner where true positive rates are high and false positive rates low. Compare the dark solid curve for $d' = 3$ with the light solid curve for $d' = 1$.

If the true and false positive rates are plotted not as probabilities but as their z -transform (i.e., in normalized space), the curves become straight lines (Fig. 5D). The advantages of this are that it is easier to see when two points belong to the same d' line, and the calculation of d' becomes trivial, since it equals $z(\text{true positive}) - z(\text{false positive})$.

Knowing what an ROC curve represents, it becomes easier to understand criterion bias. Imagine in Fig. 5A that a first attempt at a criterion is to use a cutoff of +0.5 (dashed vertical line). Here, the amount of the stimulus curve lying to the right of criterion is 69%: this is the true positive rate. The amount of the no-stimulus curve lying to the right of criterion is 31%: this is the false positive rate. (This equals $100 - 69$ because we happened to choose a point where the curves intersect.) In the ROC curve of Fig. 5C, this point is indicated by the intersection of the short dashed diagonal line with the curve for $d' = 1$. If a true positive rate of 69% seems disappointingly low, one could try to boost this by moving (biasing) the criterion downward in Fig. 5A, to the solid vertical line at a signal value of -0.5 . This yields a much better true positive rate of 93%. However, the price is a higher false positive rate of 69%. This is depicted as a rightward move along the ROC curve in Fig. 5C to the intersection with the solid line. The point is that for any given fixed discriminative power, true positive rate cannot be changed without changing the false positive rate. Where one chooses to place one's criterion is determined by need. Is it more important not to miss a true positive (i.e., screening for a treatable cancer) or more important to minimize false positives (i.e., detecting an untreatable dementia)? This is what is referred to as *criterion bias*.

How does signal detection theory apply to perimetry? Consider first the patient attempting to see the bright spot on the lit background. With dimmer and dimmer lights, the distribution of neural signals generated by the target in the patient's visual system will start to overlap that of signals from the background alone with no target—the non-event. Discriminative power decreases as the threshold is approached. At this point, it becomes important how the patient is internally biased. Patients who are determined to see all possible targets will bias their criterion to responding to the slightest hint of a target. Their thresholds will be elevated, but they will probably also have responded on occasions when there was no target at all. This is detected by catch trials on automated perimetry as false positive responses and is analogous to the shift in criterion bias illustrated in Fig. 5C. In Goldmann perimetry, it is reflected in patients who press the button when small kinetic targets are so far in the periphery that they could not possibly see them. On the other hand, patients who are determined to respond only when they are absolutely certain that there was a clear target will have diffusely depressed thresholds—often more so in the periphery—and no false positives. This is not unusual for patients doing perimetry for the first time. Both patients may have the same discriminative ability for targets of equal brightness and are merely shifting themselves up or down on the same ROC curve.

A second application of signal detection theory to perimetry refers not to the way the patient sees the targets but to the manner in which the examiner assesses the perimetric field. It is not just the

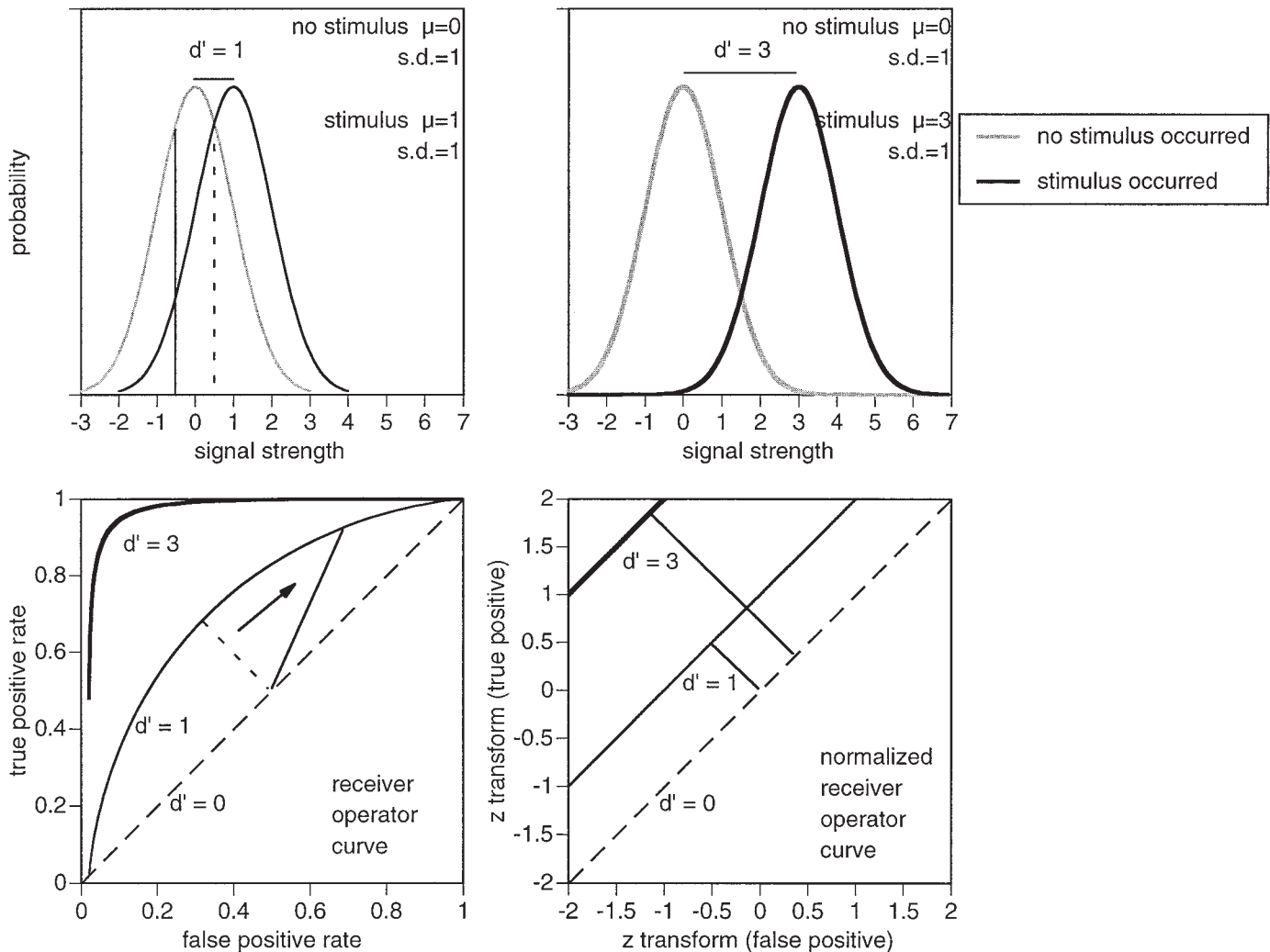


Fig. 5. Signal detection theory. (A) Distribution of some hypothetical signal intensity generated by both the absence (gray curve) and the presence (black curve) of a stimulus. Noise generates normal distributions of both functions. Here the difference between the mean signal strength for the absence and that for the presence of a stimulus is only equivalent to 1 SD ($d' = 1$), and there is significant overlap between the two curves. The vertical lines represent two possible cutoffs, or criteria, above which one might classify signals as being positive. (B) Same plot, but now $d' = 3$, and there is wider separation between the signals of the two different events. (C) ROC curve plotting the false positive rates against the true positive rates from the data of (A) (thin curve) and (B) (thick curve). The long dashed diagonal is where $d' = 0$, and if data fell here, one would not be able to tell the presence from the absence of a stimulus. For the curve belonging to (A) ($d' = 1$), the solid and dashed lines correspond to the criteria represented by the vertical lines in (A). Shifting the criterion in (A) from the dashed line to the solid line causes an increase in the true positive rate, but at the expense of a comitant increase in the false positive rate. (D) ROC curve plotted in normalized space. The curves become straight lines, and it is easier to calculate $d' = z(\text{true positive rate}) - z(\text{false positive rate})$.

patient who is being given a detection test, but also the perimetrist. How many abnormal points are needed to generate confidence that a defect is present? How well does it have to fit a pattern to indicate a certain disease process? The process of learning to interpret visual fields is an exercise in appreciating which signs have excellent discriminative power, how their appearance might be affected by the criterion bias of different patients, and which situations deserve a stricter or a looser interpretive criterion, based to a large degree on the clinical information available. An example of such an application is given in Fig. 3 of Chapter 3, where the discriminative power and criterion bias of testing with colored targets is

contrasted with the use of the examiner's fingers, with results that are not all that intuitive.

For those wishing more information on signal detection theory, see MacMillan and Creelman (2).

REFERENCES

1. Walraven J, Enroth-Cugell C, Hood D, MacLeod D, Schnapf J. The control of visual sensitivity: receptor and postreceptor processes. In: Visual Perception: The Neurophysiological Foundations. Spillman L, Werner J, eds. Boston: Academic, 1990:53–102.
2. MacMillan N, Creelman C. Detection Theory: A User's Guide. Cambridge, UK: Cambridge University Press, 1991.

INDEX

- A**
Acromegaly, *see* Pituitary adenoma, optic chiasm effects
Age-related macular degeneration,
 late stage forms, 72
 perimetry, 71, 72
 risk factors, 72
Aging, luminance sensitivity effects, 2, 3
AION, *see* Anterior ischemic optic neuropathy
Alcoholism, *see* Tobacco/alcohol optic neuropathy
Altitudinal defect,
 cases, 119–120, 125–126,
 137–138, 142–144, 165–168
 definition, 44
Amsler grid,
 central vision testing, 24, 25
 cone dystrophy, 74
Aneurysm, optic chiasm and nerve
 compression,
 computed tomography, 196
 perimetry, 195, 196
Anterior ischemic optic neuropathy (AION),
 arteritic,
 course, 136
 disk at risk, 138
 laboratory tests, 134
 perimetry, 133–138
 differential diagnosis, 174
 nonarteritic,
 bilateral disease, 141, 142
 hypoperfusion, 140
 perimetry, 139–142, 309, 310
Apoplexy (*see* Pituitary apoplexy)
Arcuate defect, *see also specific conditions*,
 cases, 85–90, 103–104, 107–112, 115–118,
 129–134, 141–142, 145–146, 157–160,
 165–166, 169–174, 179–180, 195–196,
 205–208, 231–232, 273–276, 287–288,
 311–312
 chorioretinitis, 83, 84
 definition, 44
 optic disk vasculitis, 86
 papillitis, 116
Automated perimetry, *see* Humphrey field
 analyzer; Short-wavelength automated
 perimetry
- B**
Bedside perimetry
 Amsler grid, 24, 25
 children, 27
 functional visual loss, 26
 hemichromatopsia, 29
 importance, 21
 inattentive/aphasic adults, 26, 27
 macula sparing versus splitting hemianopia, 27
 neglect versus hemianopia, 27–29
 stimuli, 21, 22
 strategy,
 caveats, 22
 central vision, 22
 paracentral vision, 23
 plotting of results, 23
 validation,
 color confrontation, 24
 false positives, 24
 sensitivity, 23, 24
Bjerrum
 scotoma, 106–107, 175–176
 screen, *see* Tangent screen perimetry
Blindspot enlargement, 79–80, 123–124, 153–164,
 281–282
Branch retinal arterial occlusion (BRAO),
 causes, 88, 308
 electroretinography, 90
 perimetry, 87–90, 307, 308
BRAO, *see* Branch retinal arterial occlusion
- C**
CABG, *see* Coronary artery bypass graft

- Cancer, *see* Glioblastoma multiforme;
Hypothalamic glioma; Metastasis;
Meningioma
- Carotid-cavernous fistula,
magnetic resonance imaging, 110
secondary glaucoma,
perimetry, 109, 110
treatment, 110
- Central field, divisions, 42, 43
- Central pontine myelinolysis,
perimetry, 213, 214
risk factors, 214
- Central retinal vein occlusion (CRVO),
etiology, 78
perimetry, 77, 78
- Central scotoma, 73–76, 127–128, 173–174,
179–180, 191–192, 199–202, 305–306
- Central serous retinopathy,
fluorescein angiography, 298
optic neuritis differentiation, 76
perimetry, 75, 76, 297, 298
- Centrocecal scotoma, 79–80, 113–116, 121–122,
131–132, 147–152, 181–192, 277–278
- Children, bedside perimetry, 27
- Chorioretinitis,
perimetry, 83, 84
toxoplasmosis in etiology, 84
- Choroidal metastasis,
lymphoma types, 92
perimetry, 91, 92
treatment, 92
ultrasound, 92
- Clinical examination, *see* Bedside perimetry
- Color comparison, bedside perimetry, 21, 24
- Color vision, *see* hemiachromatopsia and
hemidyschromatopsia
- Computed tomography (CT),
aneurysm, 196
anticoagulation excess and cerebral
hemorrhage, 284
hypertensive cerebral hemorrhage, 212
orbital fracture, optic neuropathy, 170
parietotemporal infarction, 228
primary lobar hemorrhage, 226
- Cone,
distribution, 7, 8
dystrophy,
associated conditions, 74
electroretinography, 74
perimetry, 73, 74
- Confrontation testing, *see* bedside perimetry
- Coronary artery bypass graft (CABG), stroke
association, 263, 264
- Corrected pattern standard deviation (CPSD),
Humphrey field analyzer, 55
- Coumadin, excess and cerebral hemorrhage,
283, 284
- CPSD, *see* Corrected pattern standard
deviation
- Craniopharyngioma,
hemifield slide, 206
magnetic resonance imaging, 206
perimetry, 205, 206
- CRVO, *see* Central retinal vein occlusion
- CT, *see* Computed tomography
- E**
- Electroretinography (ERG),
a-waves and b-waves, 75, 91, 101
branch retinal arterial occlusion, 90
cone, 74
dystrophy, 74
vigabatrin toxicity, 100
- ERG, *see* Electroretinography
- Extrastriate cortex,
hemiachromatopsia, 29
lesions, 17, 18
retinal topography, 16, 17
- F**
- FASTPAC, Humphrey field analyzer, 50, 51
- Finger counting/mimicry, bedside perimetry, 21
- Finger motion, bedside perimetry, 21, 24
- Fixation loss (FL), Humphrey field analyzer
reliability assessment, 54
- FL, *see* Fixation loss
- Foster Kennedy syndrome, features, 142
- Frequency doubling perimetry,
advantages and limitations, 5
principles, 5
- Functional visual field defects
spiraling, 267–268
cylindrical tunnel vision, 271–272

monocular temporal hemianopia, 270–271

G

GBM, *see* Glioblastoma multiforme

Glaucoma, *see* Carotid-cavernous fistula;
Normal tension glaucoma; Primary
open-angle glaucoma

Glioblastoma multiforme (GBM),
magnetic resonance imaging, 262, 296
perimetry, 261, 262, 295, 296
prognostic factors, 262
right parietal lobe, 295, 296

Goldmann perimetry,
Armaly–Drance screening technique, 37, 39
artifacts,

baring of blind spot, 41
general constriction, 40
lens rim artifact, 40
lid artifact, 40
solitary wobble, 41

calibration,
patient, 31
perimeter, 31

controls, 34

indications and contraindications, 4

interpretation, 39–44

island of Traquair, 2

isopter mapping, 36, 37

lens correction by age, 31

nomenclature,
field conventions, 70
location, 42–44
shape, 44

normal visual field, 35

operator functions, 3

optic neuropathy, 37–39

placement of subject, 33, 34

retinal disease, 37

sequential field analysis, 44

targets,

presentation, static versus kinetic, 34, 36
selection, 34
sizes, 34

vertical meridian mapping, 39

H

Hand/face comparison, bedside perimetry, 21

Hand motion, bedside perimetry, 21

Hemangioma, optic nerve compression,
history, 179, 285

magnetic resonance imaging, 180, 286
perimetry, 179, 180, 285, 286

Hemichromatopsia, bedside perimetry, 29

Hemianopia,

bitemporal, 183–184, 187–194, 201–204,
207–208, 217–218

definition, 44

dyslexic, 249, 250

homonymous, 209–212, 231–232, 243–248,
261–264

hysterical hemianopia, 267, 268

macula sparing versus splitting hemianopia, 27
neglect differentiation from, 27–29

posterior cerebral arterial infarction, 244

Hemidyschromatopsia,

perimetry, 221, 222

stroke association, 221, 222

Hemifield slide,

craniopharyngioma, 206

pituitary adenoma, 184, 292

High-pass resolution perimetry,

advantages and limitations, 5

principles, 5

Histoplasmosis, *see* Presumed ocular
histoplasmosis

Horner's syndrome, etiology, 264

Humphrey field analyzer,

advantages of automated perimetry, 3, 4

algorithm selection,

FASTPAC, 50, 51

SITA, 50, 51

calibration, 45

comparison with other devices, 45

data entry, 46

duration of test, 48, 50

grids of test points, 45, 46

indications and contraindications, 4

patient,

instructions, 47, 48

placement, 46, 47

printout, 54

relation of intensity, Humphrey sensitivity,
and Goldmann brightness, 45

screening strategies,
 single intensity, 48, 49
 three zone, 48
 threshold related, 48
 sequential analysis of fields, 64, 68, 69
 single-field analysis,
 global indices,
 corrected pattern standard deviation, 55
 mean deviation, 55
 pattern standard deviation, 55
 short-term fluctuation, 55
 interpretation,
 central scotomata, 55, 57
 gray scale, 55
 high responders, 58
 lens holder artifact, 60-62
 lid artifact, 64-67
 low responders, 59
 optic neuritis, 63, 64
 probability maps, 55, 58
 pseudo-superior defect, 55, 56
 maps,
 pattern deviation, 55
 total deviation, 54, 55
 visual sensitivity, 54
 reliability indices,
 duration of test, 54
 false negatives, 54
 false positives, 54
 fixation loss, 54
 threshold strategies,
 fast threshold, 48
 full threshold, 48, 50
 full threshold from prior data, 48
 zone of target presentation,
 central zone, 52, 53
 full field, 53, 54
 peripheral zone, 53
 specialized zones, 54
 Hypothalamic glioma,
 bowtie optic atrophy, 210
 magnetic resonance imaging, 210
 perimetry, 209, 210

I

Idiopathic intracranial hypertension (IIH),
 papilledema, 154, 156, 280
 perimetry, 151–158, 279, 280
 risk factors, 152
 transient visual obscurations, 154
 treatment, 154
 IIH, *see* Idiopathic intracranial hypertension
 Ischemic optic neuropathy, *see also* Anterior
 ischemic optic neuropathy,
 hypotension, 144
 perimetry, 143, 144
 posterior ischemic optic neuropathy, 144
 risk factors, 144
 Island of Traquair, normal visual field, 2
 Isopter,
 definition, 2
 factors affecting, 2
 Goldmann perimetry mapping, 36, 37

J

Junctional scotoma, 197–198

L

Lateral geniculate nucleus (LGN),
 central pontine myelinolysis, 213, 214
 function, 12, 13
 head trauma, 233, 234
 hypertensive cerebral hemorrhage,
 perimetry, 211, 212
 layers, 13, 14
 lesions,
 optic atrophy, 14
 retinopathy, 14
 optic radiations,
 bundles, 14
 temporal lobectomy effects, 14
 vascular supply, 14, 15
 vascular supply, 14
 Leber's hereditary optic neuropathy (LHON),
 clinical presentation, 150
 magnetic resonance imaging, 150
 papillitis association, 130
 perimetry, 149, 150

- Lens holder artifact, Humphrey field analyzer, 60–62
- Lens rim artifact, Goldmann perimetry, 40
- LGN, *see* Lateral geniculate nucleus
- LHON, *see* Leber's hereditary optic neuropathy
- Lid artifact,
Goldmann perimetry, 40
Humphrey field analyzer, 64–67
- Lymphocytic hypophysitis,
magnetic resonance imaging, 194, 198
perimetry, 193, 194, 197, 198
pregnancy, 198
symptoms, 194
- Lymphoma, *see* Choroidal metastasis
- M**
- Macular degeneration, age-related
late stage forms, 72
perimetry, 71, 72
risk factors, 72
- Macula sparing,
definition, 27
macula-splitting hemianopia comparison, 27
testing, 27, 28
- Magnetic resonance imaging (MRI),
carotid-cavernous fistula, 110
craniopharyngioma, 206
glioblastoma multiforme, 262, 296
gunshot wound, 256
head trauma, 234, 250
hypertensive hemorrhage, 236
hypothalamic glioma, 210
Leber's hereditary optic neuropathy, 150
lymphocytic hypophysitis, 194, 198
meningioma,
occipital meningioma resection followed
by infarction, 254
optic canal meningioma, 174
optic nerve compression, 176
optic nerve sheath meningioma, 168
parasellar, 202
sphenoid wing, 288
suprasellar, 204
migrainous infarction, 302
multiple sclerosis risk assessment, 112, 114,
118, 120, 124, 126, 128, 230
nasal fundus ectasia, 96
occipital hemorrhage, 252
oligodendroglioma resection, 246
optic canal meningioma, 174
optic chiasm, 11
optic chiasm descent, 192
optic nerve, 10
optic nerve compression, 176, 178, 180
optic tract, 13
papillitis, 124, 130
parasellar meningioma, 202
pituitary adenoma, 184, 186, 188, 190, 200, 292
posterior cerebral arterial infarction,
bilateral infarction, 258, 260, 264
parieto-occipital branch, 240, 290
posterior temporal branch, 238, 278
right striate cortex with occipital pole
sparing, 242
thrombotic thrombocytopenic purpura,
247, 248
retrobulbar optic neuritis, 112, 114, 118,
120, 126, 128, 300
sagittal sinus metastasis and thrombosis, 164
sarcoidosis, 132, 208
striate cortex, 16
subcortical infarction, 224
temporal lobectomy, 216, 218, 220
venous angioma, 306
venous sinus thrombosis, 162
watershed infarction, 232
- Manual perimetry, *see* Bedside perimetry;
Goldmann perimetry
- MD, *see* Mean deviation
- Mean deviation (MD), Humphrey field
analyzer, 55
- Meningioma, *see* Magnetic Resonance
Imaging, meningioma, Occipital
meningioma; Optic canal meningioma;
Optic nerve sheath meningioma;
Parasellar meningioma; Sphenoid wing

meningioma; Suprasellar meningioma

Metastasis,
 choroidal metastasis,
 lymphoma, 92
 perimetry, 91, 92
 treatment, 92
 ultrasound, 92
 meningeal metastasis,
 perimetry, 165, 166
 primary tumors, 166
 prognosis, 166
 sagittal sinus metastasis and thrombosis,
 magnetic resonance imaging, 164
 perimetry, 163, 164

Meyer's loop, retinopathy, 294

Migrainous infarction,
 magnetic resonance imaging, 302
 perimetry, 301, 302

Monocular temporal crescent, cases, 245–246,
 263–266, 279–280

Motion perimetry,
 advantages and limitations, 5
 principles, 5

MRI, *see* Magnetic resonance imaging

MS, *see* Multiple sclerosis

Multiple sclerosis (MS),
 Humphrey field analyzer, analysis of sequential
 fields with optic neuritis, 64, 68, 69
 magnetic resonance imaging risk assessment,
 112, 114, 118, 120, 124, 126, 128, 230
 optic neuritis, *see* Optic neuritis
 perimetry, 229, 230

Myelinolysis, *see* Central pontine myelinolysis

N

Nasal fundus ectasia,
 magnetic resonance imaging, 96
 perimetry, 95, 96, 281, 282
 tilted disk syndrome association, 96

Nasal retinal fibers, lesions, 9, 11

Nasal step, definition, 44

Neglect, hemianopia differentiation, 27–29

Normal tension glaucoma, *see also* Primary
 open-angle glaucoma,
 perimetry, 103, 104
 progression, 104

O

Occipital hemorrhage,
 magnetic resonance imaging, 252
 perimetry, 251, 252

Occipital meningioma, resection followed by
 infarction,
 magnetic resonance imaging, 254
 perimetry, 253, 254

Oligodendroglioma resection,
 magnetic resonance imaging, 246
 perimetry, 245, 246

Optic canal meningioma,
 differential diagnosis, 174
 magnetic resonance imaging, 174
 perimetry, 173, 174

Optic chiasm,
 aneurysm compression, 196
 compression, *see specific tumors*
 decussating fiber lesions, 10, 11
 descent following radiation/surgery,
 magnetic resonance imaging, 192
 perimetry, 191, 192
 magnetic resonance imaging, 11
 nasal retinal fiber lesions, 9, 11
 pituitary adenoma effects, 12, 183–190
 vascular supply, 11
 visual field defects, 10
 Wilbrand's knee, 10

Optic disk
 anatomy, 9
 drusen,
 papilledema differentiation, 182
 perimetry, 181, 182
 vasculitis,
 history, 85
 perimetry, 85, 86
 treatment, 86

Optic nerve,
 anatomy, 9
 compression,
 aneurysm, 196
 bilateral, 201, 202
 hemangioma, 179, 180, 285, 286
 magnetic resonance imaging, 176, 178,
 180, 286

- perimetry, 175–180, 195, 196
- sphenoid wing meningioma, 287, 288
- field defects with disorders,
 - nasal retinal fiber lesion, 9
 - papillomacular bundle lesion, 8
 - temporal retinal fiber lesion, 8, 9
- magnetic resonance imaging, 10
- trauma, *see also* Orbital fracture, optic neuropathy,
 - causes, 172
 - perimetry, 171, 172
- vascular supply, 9
- Optic nerve sheath meningioma,
 - magnetic resonance imaging, 168
- optic nerve compression,
 - magnetic resonance imaging, 176
 - perimetry, 175, 176
- perimetry, 167, 168
- treatment, 168
- Optic neuritis,
 - automated perimetry, 63, 64, 68, 69
 - central serous retinopathy differentiation, 76
 - demyelinating retrobulbar optic neuritis,
 - magnetic resonance imaging, 112
 - perimetry, 111, 112
 - papillitis,
 - bilateral disease, 129, 130
 - magnetic resonance imaging, 124, 130
 - perimetry, 115, 116, 123, 124, 129, 130
 - retrobulbar optic neuritis,
 - bilateral disease, 121, 122
 - magnetic resonance imaging, 114, 118, 120, 126, 128, 300
 - perimetry, 113, 114, 117–122, 125–128, 299, 300
 - recurrent disease, 119, 120
 - types, 116
- Optic tract,
 - fibers and defects, 12
 - magnetic resonance imaging, 13
 - patterns of visual losses, 11, 12
 - vascular supply, 12
- Orbital fracture, optic neuropathy,
 - computed tomography, 170
 - management, 170
 - perimetry, 169, 170
- P**
- Papilledema,
 - blind spot enlargement, 155–158, 280
 - hypothalamic glioma, 210
 - idiopathic intracranial hypertension, 154, 158, 162, 280
 - optic disk drusen differentiation, 182
 - sagittal sinus thrombosis,
 - perimetry, 159, 160
 - risk factors, 160
 - transient visual obscurations, 154
 - venous sinus thrombosis,
 - magnetic resonance imaging, 162
 - perimetry, 161, 162
- Papillitis,
 - bilateral disease, 129, 130
 - Leber’s hereditary optic neuropathy association, 130
 - magnetic resonance imaging, 124, 130
 - perimetry, 115, 116, 123, 124, 129, 130
- Papillomacular bundle, lesions, 8
- Paracentral field, definition, 44
- Parasellar meningioma,
 - magnetic resonance imaging, 202
 - management, 202
 - perimetry, 201, 202
- Pattern standard deviation (PSD), Humphrey field analyzer, 55
- Peripheral field, definition, 44
- Pituitary adenoma, optic chiasm effects,
 - acromegaly,
 - magnetic resonance imaging, 188
 - perimetry, 187, 188
 - apoplexy,
 - magnetic resonance imaging, 186
 - perimetry, 185, 186, 273, 274
 - risk factors, 190
 - apoplexy and macular degeneration,
 - magnetic resonance imaging, 190
 - perimetry, 189, 190
 - hemifield slide, 184, 292
 - magnetic resonance imaging, 184, 292
 - overview, 12

- perimetry, 183, 184, 291, 292
- prolactinoma,
 magnetic resonance imaging, 200
 perimetry, 199, 200
- POAG, *see* Primary open-angle glaucoma
- POHS, *see* Presumed ocular histoplasmosis
- Posterior cerebral arterial infarction, *see* Stroke
- Pregnancy, lymphocytic hypophysitis, 198
- Presumed ocular histoplasmosis (POHS),
 etiology, 80
 perimetry, 79, 80
- Primary open-angle glaucoma (POAG),
 automated versus manual perimetry, 108
 normal tension glaucoma, 106
 perimetry, 101, 102, 105-108
 prevalence, 106
 progression, 102
 risk factors, 108
- PSD, *see* Pattern standard deviation
- Pseudotumor cerebri, *see* Idiopathic
 intracranial hypertension
- Psychogenic deficits,
 hysterical hemianopia, 267, 268
 perimetry, 265-268
- Q**
- Quadrantanopia,
 cases, 197-198, 217-230, 237-242, 257-258,
 265-266, 279-280, 285-286, 291-292,
 295-298
 definition, 44
 parietotemporal infarction and inferior
 quadrantanopia, 227, 228
- R**
- Records, perimetry, 2
- Reproducibility, perimetry assessment, 1
- Retina,
 arterial occlusion, *see* Branch retinal arterial
 occlusion
 cones, 7, 8
 ganglion cell types, 9
 lesions, 8
 nerve fiber layer, 8, 9
 rods, 7, 8
 topographic arrangement, 7
 vascular supply, 8, 9
- Retinal detachment,
 perimetry, 97, 98
 progression, 98
- Retinitis pigmentosa,
 heredity, 94
 perimetry, 93, 94
- Retrolubar optic neuritis, *see* Optic neuritis
- Rod, distribution, 7, 8
- S**
- Sagittal sinus thrombosis, papilledema (*see*
 also metastasis),
 perimetry, 159, 160
 risk factors, 160
- Sarcoidosis,
 bowtie optic atrophy, 208
 cranial nerve types, 272
 diagnosis, 208
 magnetic resonance imaging, 132, 208
 optic nerve involvement, 271, 272
 optic nerve localization, 271, 272
 perimetry, 131, 132, 207, 208, 271, 272
- Scotomata, *see also specific conditions*,
 cecocentral scotomata, 112
 central serous retinopathy, 75, 76
 definition, 44
 homonymous scotomata, 44
- Sectoranopia, definition, 44
 cases, 213-216, 235-236, 307-308
- SF, *see* Short-term fluctuation
- Short-term fluctuation (SF), Humphrey field
 analyzer, 55
- Short-wavelength automated perimetry
 (SWAP),
 advantages and limitations, 4, 5
 principles, 4
- SITA, Humphrey field analyzer, 50, 51
- Smoking, *see* Tobacco/alcohol optic
 neuropathy
- Sphenoid wing meningioma,
 history, 287
 magnetic resonance imaging, 288
 perimetry, 287, 288

- Standardization, perimetry assessment, 1
- Staphyloma,
differential diagnosis, 82
perimetry, 81, 82, 275, 276
ultrasound, 82, 276
- Striate cortex,
anatomy, 15
magnetic resonance imaging, 16
optic radiation input, *see* Lateral geniculate nucleus
posterior cerebral arterial bilateral infarction, 257–260
retinotopic map, 15, 16
vascular supply, 16
- Stroke,
anticoagulation excess,
computed tomography, 284
perimetry, 283, 284
hemidyschromatopsia, 221, 222
hypertensive hemorrhage,
magnetic resonance imaging, 236
perimetry, 235, 236
migrainous infarction, 301, 302
occipital hemorrhage,
magnetic resonance imaging, 252
perimetry, 251, 252
parietotemporal infarction and inferior quadrantanopia, 227, 228
posterior cerebral arterial infarction,
bilateral infarction, 257–260, 263, 264
old infarction, 243, 244
parieto-occipital branch,
magnetic resonance imaging, 240, 290
perimetry, 239, 240, 289, 290
posterior temporal branch,
magnetic resonance imaging, 238, 278
perimetry, 237, 238, 277, 278
right striate cortex with occipital pole sparing, 241, 242
thrombotic thrombocytopenic purpura, 247, 248
primary lobar hemorrhage,
computed tomography, 226
perimetry, 225, 226
subcortical infarction and distal optic radiation,
magnetic resonance imaging, 224
perimetry, 223, 224
venous angioma, 305, 306
- Suprasellar meningioma,
hormone secretion and sensitivity, 204
perimetry, 203, 204
- SWAP, *see* Short-wavelength automated perimetry
- T**
- Tangent screen perimetry, paracentral vision testing, 25, 26
- Temporal lobectomy,
epilepsy management, 220
left temporal optic radiation, 217–220
magnetic resonance imaging, 216, 218, 220, 294
perimetry, 215–220, 293, 294
right anterior optic radiation, 294
right temporal optic radiation, 215, 216
- Temporal retinal fibers, lesions, 8, 9
- Thrombotic thrombocytopenic purpura,
posterior cerebral arterial infarction,
magnetic resonance imaging, 248
perimetry, 247, 248
- Tilted disk syndrome,
perimetry, 95, 96
- Tobacco/alcohol optic neuropathy,
pathogenesis, 148
perimetry, 147, 148
- Toxoplasmosis, *see* Chorioretinitis
- Transient visual obscurations (TVOs), features, 154
- TVOs, *see* Transient visual obscurations
- U**
- Ultrasound,
choroidal metastasis, 92
staphyloma, 82, 276
- V**
- Venous angioma,
magnetic resonance imaging, 306
perimetry, 305, 306

Venous sinus thrombosis, papilledema,
magnetic resonance imaging, 162
perimetry, 161, 162

Vigabatrin toxicity,
electroretinogram, 100
perimetry, 99, 100

Visual cortex, *see* Striate cortex

Vitamin B₁₂ deficiency,
clinical features, 146
functions of vitamin B₁₂, 304
perimetry, 145–148, 303, 304

tobacco and alcohol exacerbation, 147, 148

W

Watershed infarction,
magnetic resonance imaging, 232
perimetry, 231, 232

Wedge

definition, 44

temporal wedge defect cases, 81–82, 105–106,
121–124, 127–128, 173–174, 289–290

Wilbrand's knee, 10

ABOUT THE AUTHORS



Jason J. S. Barton, MD, PhD, FRCP(C)

Jason Barton is a clinical neuro-ophthalmologist and director of the human vision and ocular motor research laboratory at Harvard Medical School and Beth Israel Deaconess Medical Center. He received education at the University of British Columbia, University of Iowa, and University of Toronto.



Michael Benatar, MBChB, DPhil

Michael Benatar is a clinical neurologist at Harvard University, Boston, MA. His clinical and research interests are in neuro-ophthalmology, neuromuscular disease and evidence-based medicine.

FIELD OF VISION

A MANUAL AND ATLAS OF PERIMETRY

Jason J. S. Barton, MD, PhD, FRCP(C)

*Departments of Neurology and Ophthalmology, Beth Israel-Deaconess Medical Center, Harvard Medical School;
and Department of Bioengineering, Boston University, Boston, MA*

Michael Benatar, MBChB, DPhil

Department of Neurology, Beth Israel-Deaconess Medical Center, Harvard Medical School, Boston, MA

Foreword by

Martin A. Samuels, MD

Neurologist-in-Chief, Brigham and Women's Hospital, Boston, MA

From the Foreword

"...a welcome addition to the basic texts for all those who practice clinical neurology, as well as those training in the area...I enjoyed reading it from beginning to end and will undoubtedly refer back to it in the future."

Although the visual field provides clinicians with important diagnostic information for many neurologic and ophthalmologic conditions, its evaluation is often perceived as difficult or mysterious. In *Field of Vision: A Manual and Atlas of Perimetry*, neuro-ophthalmologist Jason J.S. Barton, MD, PhD, FRCP(C), and neurologist Michael Benatar, MBChB, DPhil, provide a comprehensive overview of the use of both perimetric devices and bedside testing, and how to interpret the results. The authors focus on the clinically relevant points, providing enough technical detail and anatomic knowledge for the physician to competently examine patients with a perimeter. To develop the clinician's skill in interpretation, the authors include an atlas of 100 real-life cases arranged in anatomic order from retina to striate cortex. Each case contains a brief clinical vignette, a visual field, and a description of the field and its causal lesion, most with photographs of the pathology. The accompanying discussion addresses the nuances of the field and considers some of the clinical issues relevant to each case. An additional quiz section of 20 randomly arranged visual fields provides readers with an opportunity to test newly acquired skills in detecting the abnormalities, describing them, localizing them, and making a reasonable guess at their pathology.

Simply written and clinically focused, *Field of Vision: A Manual and Atlas of Perimetry* brings together in an accessible format the specialist knowledge and skills needed by today's clinicians to successfully measure and interpret the visual fields of patients.

- Concise tutorial on how to measure the visual field and interpret the results
- One hundred real-life case studies to perfect interpretive skills
- Twenty exercises to test the ability to interpret visual fields
- Review of key perimetric concepts and visual anatomy

CONTENTS

An Introduction to Perimetry and the Normal Visual Field. Functional Visual Anatomy. Perimetry at the Bedside and Clinic. Goldmann Perimetry. Automated Perimetry (Humphrey Field Analyzer). Atlas. Color Plates of Selected Cases. Appendix. Index.

